Finite elements and boundary elements – coupling in time domain

Von der Fakultät für Mathematik und Physik
der Gottfried Wilhelm Leibniz Universität Hannover
zur Erlangung des Grades
Doktor der Naturwissenschaften
Dr. rer. nat.

genehmigte Dissertation

von

Ceyhun Özdemir

24. September 2019

Referent:	Prof. Dr. Ernst P. Stephan, Leibniz Universität Hannover, DE
Korreferent:	Dr. Heiko Gimperlein, Heriot-Watt University Edinburgh, UK
Korreferent:	Prof. Dr. Dirk Praetorius, TU Wien, AT
Tag der Einreichung:	18.07.2019
Tag der Promotion:	24.09.2019

Abstract

This thesis considers the treatment of the wave equation given outside of a bounded, orientable Lipschitz domain with the boundary element method (BEM). Beginning with a scattering problem the retarded (potential) boundary integral operators are defined. These operators are discretized with a tensor product ansatz. For the retarded Poincaré-Steklov operator and the inverse counterpart, numerical experiments are presented using the marching-on-in time (MOT) scheme.

The coupling of the finite element method (FEM) and the boundary element method (BEM) provide an analysis of a fluid-structure interaction (FSI) problem with given transmission conditions and the wave propagation interface problem with corresponding transmission conditions. For the FSI problem two approaches are addressed. The symmetric FEM-BEM coupling are discretized such that the MOT-scheme is applicable. Numerical experiments demonstrate the reliability of the implementation. The other approach uses a retarded boundary integral operator as a test function, which leads to major challenges in the discretization and the performing of numerical experiments. The wave propagation interface problem is adressed with a symmetric coupling. Here the discretization is chosen such that a MOT-scheme may applied. Numerical results are demonstrated as well. A prori and a posteriori error estimates for conforming Galerkin approximation are derived in all these cases, motivating adaptive mesh refinement procedures.

The remaining chapters consider the results of time domain boundary element discretizations for screen problems, unilateral contact and a real-world application on tyres. Numerical experiments achieve optimal approximation rates on graded meshes for screen problems, resolving the edge and corner singularities. As a first step towards high-order methods p and $hp-$versions of time domain boundary element method are presented for quasi-uniform meshes. Further crack and punch problems, as two examples of dynamic contact problems in time domain, are analyzed. While an error analysis is done for flat contact areas, numerical experiments show convergence even for non-flat contact areas. The sound emission of tyres, where noise emitting from the contact of the tyre with the pavement, are discussed. Numerical experiments illustrate the applicability of the boundary element method to real-world problems.

Keywords: FEM-BEM coupling, wave equation, finite elements, boundary elements, a posteriori error estimates, graded meshes, hp method, dynamic contact, sound emission

Erklärung

Hiermit versichere ich, dass ich die vorliegende Arbeit selbständig verfasst und keine anderen als die angegebenen Quellen und Hilfsmittel benutzt habe, dass alle Stellen der Arbeit, die wörtlich oder sinngemäß aus anderen Quellen übernommen wurden, als solche kenntlich gemacht sind und dass die Arbeit in gleicher oder ähnlicher Form noch keiner Prüfungsbehörde vorgelegt wurde.

Hannover, den 18.07.2019 Ceyhun Özdemir

Acknowledgements

In the name of Allah, the most gracious, the most merciful.

First I would like to thank God for giving me the circumstances to be able to write this thesis.

Next I express my utmost gratitude for my supervisors Prof. Dr. E. P. Stephan and Dr. Heiko Gimperlein for accepting me as their student and benefitting from their knowledge. It was an honour to work under them, publishing numerical results, which contributes to research in general.

Further I am grateful to Prof. Dr. D. Praetorius, for his great willingness to examine my thesis, even though this thesis became quite long.

Furthermore I am also thankful to Prof. Dr. T. Wick for his readiness and PD Dr. Michael J. Gruber for taking charge of the commision.

Next I am also grateful to Fabian Meyer and Jakub Stocek, whom I wish the best of luck for their PhD thesis, and David Stark for an outstanding collaborative work.

I wish for all of them the best and a lot of fun in their future researches/works.

Then I would like to express my gratitude to PD Dr. M. Maischak and the whole institute of applied mathematics, i.e. Mrs. Behrens, Mr. and Mrs. Gatzen, Mrs. Fleischhauer, Mrs. Krienen, Mrs. Günther, Dr. F. S. Attia, Dr. F. Leydecker, Sebastian Bohlmann and all the Professors and PhD students for creating a comfortable work atmosphere and for supporting me with the capacities I needed to get this thesis done.

In the next part of my ackknowledgement, I would like to express my deepest gratitude to my parents, Recep and Ayten Özdemir. If they didn't support me I would never be as far as I am today. I can't even put in words on how much they helped me. Then I would like to thank my brother, Mehmet Özdemir. Further I thank my whole family in Turkey (especially my grand parents), in Germany, in the Netherlands and in France. I will mention especially: Mevlit Özdemir, Hüseyin Özdemir and Erhan Bugöl.

I can't continue without mentioning: Muhittin Yılmaz, Batuhan Çelik, Emran Altınöz, Enes Doğan, Oğuzhan Ağaç and Alper Aykul.

Then I would like to show my sincere gratitude to the members of J-Zeiten: Ali Junnur (aka Pyro), Виктор Niedens, Ha$an Agah Turcinho, Burak Mehmet-Ali Aydin Ibn Atila Abu Macit, Furkan Aydin (aka hab gesehen), Furkan Polat, Tolga カイム .

Last but by far not least I am greatful to Abdussamet Balci and the Avicenna study agency for mental and financial support, in particular the regional group Niedersachsen coached by Fatih Kozan. I wish for all of them to be succesful in their PhD or their undergraduate program.

Hannover, den 18.07.2019 Ceyhun Özdemir

Contents

1 Introduction **1**

2 Wave equation and boundary integral formulations **5**
2.1 Introduction to scattering problems 5
2.2 Retarded integral operators 6
2.2.1 A retarded single layer potential ansatz 12
2.2.2 A retarded double layer potential ansatz 16
2.3 Boundary element discretization 18
2.3.1 The retarded single layer potential 19
2.3.2 The retarded adjoint double layer potential 23
2.3.3 The retarded double layer potential 26
2.3.4 The retarded hypersingular integral operator 29
2.3.5 Retarded Poincaré-Steklov operator 31
2.3.6 Retarded inverse Poincaré-Steklov operator 38

3 FEM-BEM coupling in time domain I: retarded single layer potential as test function **41**
3.1 Introduction 41
3.2 Preliminaries and discretization spaces 42
3.3 An a priori error estimate 44
3.4 An a posteriori error estimate 47
3.5 Discretization via generalized light cones 50
3.6 Discretization via an L^2-projection method in space and time 58
3.7 First numerical experiments with V as test function 64
3.8 Derivation of a numerical example for a fluid-strucuture interaction problem 68
3.9 Numerical experiments 72

4 FEM-BEM coupling in time domain II: FSI with symmetric coupling **77**
4.1 Introduction 77
4.2 Preliminaries 79
4.3 A priori error estimate 83
4.4 A posteriori error estimate 87
4.5 Discretization and MOT-Algorithm 90
4.6 Numerical results 95

5 FEM-BEM coupling in time domain III: wave-wave coupling 105
5.1 Introduction . . . 105
5.2 Symmetric wave-wave coupling . . . 106
5.2.1 A priori error estimate . . . 109
5.2.2 A posteriori error estimate . . . 111
5.2.3 Discretization of the symmetric wave-wave coupling . . . 113
5.2.4 Derivation of a numerical example for the wave wave coupling . . . 116
5.3 Numerical results . . . 117

6 Time domain BEM: graded meshes and hp-version on quasi-uniform meshes 123
6.1 Introduction . . . 123
6.2 β-graded meshes . . . 124
6.3 Asymptotic expansions and numerical approximation . . . 125
6.3.1 Singularities for circular screens and approximation for graded meshes . . . 125
6.3.2 Singularities for circular screens and approximation for hp-version 126
6.3.3 Singularities for polygonal screens and approximation for graded meshes . . . 127
6.3.4 Singularities for polygonal screens and approximation for hp-version 128
6.4 Numerical experiments . . . 129
6.4.1 Single layer potential for graded meshes . . . 129
6.4.2 Single layer potential for p-version . . . 138
6.4.3 Hypersingular operator for graded meshes . . . 141
6.4.4 Dirichlet-to-Neumann operator for graded meshes . . . 148

7 Unilateral contact problems: Punch problems / Crack problems 153
7.1 Introduction . . . 153
7.2 Boundary integral formulation and well-posedness for the crack problem 155
7.3 Discretization and a priori error estimates for the crack problem . . . 157
7.4 Mixed formulation of the crack problem . . . 159
7.5 A variational inequality for the punch problem . . . 162
7.6 Algorithmic considerations and space time Uzawa algorithm . . . 170
7.7 Numerical experiments . . . 171
7.7.1 Numerical experiments for the crack problem . . . 172
7.7.2 Numerical experiments for the punch problem . . . 175

8 Applications to sound emission of tyres 179
8.1 Introduction . . . 179
8.2 Boundary integral formulation . . . 180
8.3 Numerical experiments . . . 181
8.3.1 Numerical experiments on a sphere . . . 181
8.3.2 Numerical experiments on a tyre . . . 183
8.3.3 Numerical experiments on a graded tyre . . . 186

9 Appendix **189**
9.1 The computation of the retarded time integrals 189
9.2 Important theorems 195
9.3 Road map with spaces and norms 197
9.4 Computation of the retarded single layer potential with $\sigma > 0$ 200
9.5 A documentation of the operators used in maiprogs 203
9.5.1 A bcl-script for the retarded single layer potential 203
9.5.2 A bcl-script for the retarded double layer potential 206
9.5.3 A bcl-scriot for the adjoint double layer potential 209
9.5.4 A bcl-script for the retarded hypersingular integral operator . . . 211
9.5.5 A bcl-script for the retarded Poincaré-Steklov operator 214
9.5.6 A bcl-script for the retarded inverse Poincaré-Steklov operator . . 218
9.5.7 A bcl-script for a time dependent Lame problem with finite elements 222
9.5.8 A bcl-script for a time dependent wave equation with finite elements 224
9.5.9 A bcl-script for the fluid-structure interaction problem with the retarded Poincare-Steklov operator 227
9.6 Explanation of the Code for the *hp*-version 232

Bibliography **235**

List of Figures

2.1 Sparsity of the retarded matrices for plane triangles 20
2.2 $L^2(\Gamma)$-norm of the solution to $\mathcal{S}v = f$ for fixed CFL ratio $\frac{\Delta t}{h} \approx 0.6$. Figure 1 in [47] 37
2.3 Absolute error of the exact solution and the numerical solution for the L^2 norm in space as a function of time for fixed $\frac{\Delta t}{h}$. Figure 2 in [47] . . . 37
2.4 $L^2([0,T]\times\Gamma)$-error vs. degrees of freedom of the solution to $\mathcal{S}v = f$ for fixed $\frac{\Delta t}{h}$. Figure 3 in [47] 38
2.5 $L^2(\Gamma)$-norm of the solution to $\mathcal{S}^{-1}\lambda = f$ for fixed CFL ratio $\frac{\Delta t}{h} \approx 0.6$. . . . 40
2.6 Absolute error of the exact solution and the numerical solution for the L^2 norm in space as a function of time for fixed $\frac{\Delta t}{h}$. 40
2.7 $L^2([0,T]\times\Gamma)$-error vs. degrees of freedom of the solution to $\mathcal{S}^{-1}\lambda = f$ for fixed $\frac{\Delta t}{h}$. 40

3.1 Generalized light cones after the use of a projection onto the same plane for $t_{k-l} = t_{n-m} = 2(\Delta t)$. For x, y as in this Figure the integral over z exists only on the intersection of the blue ring with the triangles. 57
3.2 Generalized light cones after the use of a projection onto the same plane. The intersection of the blue ring with the triangles is, where a nonzero integral may exists for x, y as in this Figure. This is contained in A_0. The intersection of the first ring beneath the blue ring with the triangles for the same x, y is a subset of A_{-1} and the intersection of the second triangle beneath the first ring with the triangles for the same x, y ia a subset of A_{-2}. 57
3.3 The solution and the right hand side for the computation of (3.21) for Example 3.1. 65
3.4 Results of the Example 3.2. 66
3.5 Results of the Example 3.2 zoomed at time 1.5. 67
3.6 Results of the Example 3.2 zoomed at time 3.1. 67
3.7 Results of the Example 3.2 without $V^T = \tilde{V}^T$ at the right hand side. . . 67
3.8 Results of the Example 3.2, without $V^T = \tilde{V}^T$ at the right hand side, zoomed at time 1.9. 68
3.9 Mesh of the unit cube for (a) $N = 1$, (b) $N = 2$,(c) $N = 4$ and (d) $N = 8$. 73
3.10 Value of $\mathbf{u}$ at $(-1,-1,-1)$ for $N = 2$, i.e. 40 tetrahedrals and $\Delta t = 0.2$ of the Example 3.3, where different solvers where used. 74
3.12 Error plot of the Example 3.3. 74
3.11 L^2-norm of the Example 3.3 for CFL 0.1414 75

3.13 Convergence plot of the Example 3.3. 75
3.14 Result of **u** for the FSI problem in the corner $(-1,-1,-1)$ for Example 3.4. 76

4.1 L2-Norm of the numerical solution of Example 4.1 96
4.2 Error of the L2-Norm of the numerical solution of Example 4.1 96
4.3 The complete error of the fluid-structure interaction problem as function of DOF, Example 4.1 97
4.4 The complete error of the fluid-structure interaction problem as function of h, Example 4.1 97
4.5 L2-Norm of the numerical solution of Example 4.2 98
4.6 Error of the numerical solution of Example 4.2 99
4.7 Figure 4.6 zoomed, error of the numerical solution of Example 4.2 99
4.8 The complete error of the fluid-structure interaction problem as function of DOF, Example 4.2 100
4.9 The complete error of the fluid-structure interaction problem as function of h, Example 4.2 100
4.10 Numerical solutions of the interior against the exact solution of the interior at $(-1,-1,-1)$, Example 4.3 101
4.11 L2-Norm of the numerical solution of Example 4.3 102
4.12 Error of the numerical solution of Example 4.3 102
4.13 The L^2-error in space and time of the fluid-structure interaction problem as function of DOF, Example 4.3 103
4.14 The L^2-error in space and time of fluid-structure interaction problem as function of h, Example 4.3 103

5.1 L^2-norm of the numerical solutions for Example 5.1. 118
5.2 L^2-norm of the numerical solutions for Example 5.1 (zoomed). 118
5.3 L^2-error of the numerical solutions for Example 5.1. 119
5.4 Convergence plot of the Example 5.1 for $N = 4, 8, 16, 32, 64$. 119
5.5 L^2-norm in space of the numerical solutions for the exterior, the normal derivative of the exterior, and the interior, Example 5.2. 120
5.6 Absolute difference of the L^2-norm in space of the numerical solutions against the L^2-norm in space of the exact solutions for the exterior, the normal derivative of the exterior, and the interior, Example 5.2. 121
5.7 Convergence plot of Example 5.2. 121

6.1 β-graded meshes for (a) square and (b) circular screens, with $\beta = 2$. Figure 1 in [46] 124
6.2 Solution of the single layer equation at $T = 0.5$ along $y = 0$ on the circular screen, Example 6.1. Figure 3 in [46] 130
6.3 Asymptotic behavior of the solution to the single layer equation near edge along $y = 0$, Example 6.1, Figure 4 in [46] 131
6.4 Energy error for single layer equation on circular screen, Example 6.1, Figure 5 [46] 131

6.5 Solution of the single layer equation at $T = 0.5$ along $y = x$ on the square screen, Example 6.2, Figure 6 in [46] . . . 132
6.6 Solution of the single layer equation at $T = 0.5$ along $y = 0$ on the square screen, Example 6.2, Figure 7 in [46] . . . 132
6.7 Numerical computation of the corner singularity along diagonal from $(-1,-1)$ to $(1,1)$ at time $T = 0.5$, Example 6.2, Figure 8 in [46] . . . 133
6.8 Asymptotic behavior of the solution to the single layer equation near corner along $y = x$, Example 6.2, Figure 9 in [46] . . . 133
6.9 Asymptotic behavior of the solution to the single layer equation near edge along $y = 0$, Example 6.2, Figure 10 in [46] . . . 134
6.10 Relative energy error for the single layer equation on square screen, Example 6.2, Figure 11 in [46] . . . 134
6.11 $L_2([0,T])$-error for the sound pressure in three points outside square screen, computed from single layer equation, Example 6.2, Figure 12 in [46] . . . 135
6.12 Solution of the single layer equation at $T = 0.5$ along $y = x$ on the L-shaped screen, Example 6.3 . . . 136
6.13 Asymptotic behavior of the solution to the single layer equation near the corner (0,0) along $y = x$, Example 6.3 . . . 136
6.14 Asymptotic behavior of the solution to the single layer equation near the corner (-1,-1) along $y = x$, Example 6.3 . . . 137
6.15 Energy error norm for single layer equation on L-shaped screen, Example 6.3 . . . 137
6.16 Mesh of a square screen . . . 138
6.17 Energy as a function of time for time-singular f_4, Example 6.4. Figure 5 in [49] . . . 138
6.18 Relative error in energy norm for the single-layer equation on a square screen, Example 6.4. Figure 4 in [49] . . . 139
6.19 Relative error in the square of the energy norm for the single-layer equation on a square screen, h-version for $p = 1,2,3$, Example 6.5. Figure 6 in [49] . . . 140
6.20 Solution of the hypersingular equation at $T = 2$ along $y = 0$ on the circular screen, Example 6.6, Figure 13 in [46] . . . 141
6.21 Asymptotic behavior of the solution to the hypersingular equation near edge along $y = 0$, Example 6.6, Figure 14 in [46] . . . 142
6.22 $L_2([0,T], L_2(\Gamma))$ and energy error for hypersingular equation on circular screen, Example 6.6, Figure 15 in [46] . . . 142
6.23 Solution of the hypersingular equation at $T = 2$ along $y = x$ on the square screen, Example 6.7, Figure 16 in [46] . . . 143
6.24 Solution of the hypersingular equation at $T = 2$ along $y = 0$ on the square screen, Example 6.7, Figure 17 in [46] . . . 144
6.25 Asymptotic behavior of the solution to the hypersingular equation near corner along $y = x$, Example 6.6, Figure 18 in [46] . . . 144

6.26 Asymptotic behavior of the solution to the hypersingular equation near edge along $y = 0$, Example 6.6, Figure 19 in [46] . . . 145
6.27 $L_2([0,T], L_2(\Gamma))$ and energy error for hypersingular equation on square screen, Example 6.7, Figure 20 in [46] . . . 145
6.28 Solution of the hypersingular equation at $T = 2$ along $y = x$ on the L-shaped screen, Example 6.8 . . . 146
6.29 Asymptotic behavior of the solution to the hypersingular equation near the corner (0,0) along $y = x$, Example 6.8 . . . 147
6.30 Asymptotic behavior of the solution to the hypersingular equation near the corner (-1,-1) along $y = x$, Example 6.8 . . . 147
6.31 Energy error for the hypersingular equation on the L-shaped screen, Example 6.8 . . . 148
6.32 Solution of the Dirichlet-to-Neumann equation at $T = 0.65$ along $y = x$ on the square screen, Example 6.9, Figure 21 in [46] . . . 149
6.33 Solution of the Dirichlet-to-Neumann equation at $T = 0.65$ along $x = -0.8754$ on the square screen, Example 6.9, Figure 22 in [46] . . . 149
6.34 Asymptotic behavior of the solution to the Dirichlet-to-Neumann equation near corner along $y = x$, Example 6.9, Figure 23 in [46] . . . 150
6.35 Asymptotic behavior of the solution to the Dirichlet-to-Neumann equation near edge along $x = -0.8754$, Example 6.9, Figure 24 in [46] . . . 150
6.36 Error in $L_2([0,T], L_2(\Gamma))$ norm for Dirichlet-to-Neumann equation on square screen, Example 6.9, Figure 25 in [46] . . . 151

7.1 Evolution of u and λ in $G = [-1,1]^2 \times \{0\}$ for the contact problem, Example 7.1. Figure 4 in [47] . . . 172
7.2 Relative $L^2([0,T] \times G)$-error vs. degrees of freedom of the solutions to the contact problem for fixed $\frac{\Delta t}{h}$, Example 7.1. Figure 5 in [47] . . . 173
7.3 Evolution of u and λ in $[-2,2]^2 \times \{2\}$ for the contact problem on $[-2,2]^3$, Example 7.2. Figure 7 in [47] . . . 174
7.4 Relative $L^2([0,T] \times G)$-error vs. degrees of freedom for the contact problem for fixed $\frac{\Delta t}{h} \approx 0.53$, Example 7.2. Figure 8 in [47] . . . 174
7.5 Evolution of u and λ for the punch problem on $G = [-1.2, 1.2]^2 \times \{0\}$, Example (7.3). Figure 9 in [47] . . . 175
7.6 Relative energy error for the punch problem for fixed $\frac{\Delta t}{h}$, Example 7.3. Figure 10 in [47] . . . 176
7.7 Evolution of u and λ in $[-2,2]^2 \times \{2\}$ for the punch problem on $[-2,2]^3$, Example 7.4. Figure 11 in [47] . . . 177
7.8 Relative error of the energy for the punch problem for fixed $\frac{\Delta t}{h}$, Example 7.4. Figure 12 in [47] . . . 177

8.1 Sound pressure at $(\frac{1}{\sqrt{2}}, 0, \frac{1}{\sqrt{2}})$ in $\mathbb{R}^3_+$ as a function of the reflectivity α. Figure 5.7 in [51] . . . 182
8.2 Mesh of the passenger car tire, Figure 5.9 in [51] . . . 183

8.3 Visualization of the density for Δt=0.01, time step: 100 (a), 200 (b), 300 (c). Figure 5.10 in [51] 184
8.4 Sound pressure at $(2.8m, 0, 1.0m)$ as emitted by a car tire, Dirichlet or Neumann boundary conditions on the street. Figure 5.8 in [51] 184
8.5 Sound pressure at $(2.8m, 0, 1.0m)$ in frequency domain, as emitted by a car tire. Figure 5.11 in [51] 185
8.6 A-weighted sound pressure for Dirichlet and Neumann conditions, averaged over 321 points., Figure 5.12 in [51] 185
8.7 Mesh of (a) slick 205/55R16 tire and (b) graded refinement. Figure 27 in [46] 186
8.8 Amplification due to horn effect: Graded mesh approximations for different Δt, compared to a uniform mesh approximation. Figure 28 in [46] 187
8.9 Differences of amplification factors in dB between graded and uniform meshes for fixed Δt. Figure 29 in [46] 187
8.10 Differences of amplification factors in dB within graded meshes for different Δt. Figure 29 in [46] 188

9.1 L2-Norm of the numerical solution of Example 9.1 203

1 Introduction

Variational methods for partial differential equations (PDE) have a long history. They have been established in mathematics as well as in engineering [27, 65, 28]. The boundary element method (BEM) needs the knowledge of a fundamental solution for the considered PDE. The strength of the boundary element method lies in the reduction of a problem given inside or outside of a closed Lipschitz area into the boundary of that area. In particular we are able to reduce problems of an unbounded domain to the compact boundary via a representation formula or an adequate ansatz. The BEM requires the discretization of integral equations.

In this thesis we are interested in an inital boundary value problem with the wave equation given at the outside of a closed Lipschitz area $\Omega \subset \mathbb{R}^3$ as the PDE, homogenous initial conditions at time zero and a Dirichlet, Neumann or Robin boundary conditions at the boundary $\partial\Omega$. This is the scattering problem. The corresponding time-dependent Galerkin boundary element methods go back to Bamberger, Ha-Duong [11, 12] and Ha-Duong [55]. We solve the appearing boundary integral equations via a tensor product ansatz in space time as in [84, 45, 57]. For piecewise constant test functions in time the space time equation reduces to a time stepping scheme, the marching-on-in-time (MOT) scheme, see [97] and [104] for fast methods developed in the engineering literature. For higher test functions in time, e.g piecewise linear test functions in time, we are forced to solve a large space time system. Hence it gives rise to an analysis of a suitable preconditioner, which is in interest of future research. For some first works on preconditioning time domain BEM, see [52, 32, 6, 98]. The work group of Aimi considered an energetic Galerkin approach in space time with a tensor product ansatz in [5, 3, 4]. An alternative to the space time discretization is the convolution quadrature time stepping method, which is done and analyzed in [14, 90].

In the current thesis we also consider transmission problems which couple the wave equation in the exterior domain to an elastic scatterer described by the Lame equation from elasticity at the interior domain. This fluid-structure interaction (FSI) problem is solved by coupled finite elements (FE) and boundary elements (BE) in time domain. In time independent cases an analysis of the coupling method may found in Stephan [92, 54], while previous works on the time dependent case include [64, 63, 1, 44, 13].

In addition to the FSI problem we consider unilateral contact problems for the wave equation. While the analysis of elliptic and parabolic contact problems are well understood, see [54, 103], the dynamic contact for the wave equation requires a numerical analysis. First results are [30, 61]. We propose a time domain boundary element

method, see [47].

Furthermore in [46] and [49], the asymptotic behaviour of the solution of the wave equation in a polyhedral domain in $\mathbb{R}^3$ is studied. In this thesis we briefly show the main results and present numerical experiments for graded meshes and the hp-version on screens.

A modeling of the sound radiation of tyres requires studying the wave equation on a half-space. Therefore we need a Green's function in $\mathbb{R}^3_+$, which is given by Ochmann [83]. Further analysis and numerical experiments for the sound radiation of tyres are given in [15, 82, 48, 100]. In this thesis we present the results based on [51, 46].

All numerical experiments are done in Maiprogs. Maiprogs is a batch control language developed by Matthias Maischak, see [76, 77, 85], which contains amongst other things the implementation of finite elements and boundary elements [78]. We still needed to implement our own code in addition to Maiprogs in Fortran in order to run the numerical experiments, but it gives a great background. The implementation of the boundary elements for the wave equation in Maiprogs has been developed with the support of Matthias Maischak by Elke Ostermann, Matthias Gläfke, Zouhair Nezhi, David Stark for their Phd thesis [84, 53, 82, 91], Fabian Meyer and myself. An implementation of parallelized code becomes a lot easier, since Maiprogs gives the option of using OpenMP and/or MPI. For more information on OpenMP and MPI, see [74, 75].

In Chapter 2 we introduce the scattering problem together with the boundary integral operators. We discretize the corresponding boundary integral equations and show numerical experiments.

In Chapter 3 we consider the bilinearform used by Filipe [44] to solve the FSI problem. This bilinearfom leads to the usage of the retarded single layer potential as a test function. The boundary element part gives the retarded adjoint double layer potential tested with the retarded single layer potential, which lead to a geometrical structure still in need to be analyzed. For the discretization of these operators we use an L^2-projection to get the corresponding boundary element matrices for the already known case in Chapter 2. We discretize the interior part as well. We derive an a priori and a posteriori error estimates for the Galerkin scheme and perform numerical experiments.

In Chapter 4 we take advantage of the bilinearform, used in [64, 63] to solve the same FSI problem. This bilinearform leads to a symmetric coupling of finite and boundary elements. We repeat the discretization, since we need other ansatz and test functions. Again, we derive an a priori and a posteriori error estimates for the Galerkin scheme and perform numerical experiments.

In Chapter 5 we consider for the wave wave interface problem the coupling of the finite element method together with the boundary element method, where we couple the wave equation at the exterior domain together with the wave equation on the interior domain with transmission conditions via a symmetric coupling. We derive an a priori and an a

posteriori error estimates and present numerical experiments.

In Chapter 6 we consider the behaviour of the retarded potential boundary integral operators on screens, based on the joint work with H. Gimperlein, F. Meyer, D. Stark and E. P. Stephan [46] and H. Gimperlein, D. Stark and E. P. Stephan, [49]. We present the main results of these works. Furthermore we demonstrate numerical experiment on a circular screen, an L-shaped screen, and a square screen for a graded mesh with grading parameter $\beta = 2$ as well as an *hp*-version on a uniform square screen.

In Chapter 7 we will have a look at contact problems, based on the joint work with H. Gimperlein, F. Meyer and E. P. Stephan [47]. Here as well we show the main results and present numerical experiments as well.

In Chapter 8 we refer to the joint work with H. Gimperlein and E.P. Stephan [51] and consider the sound radiation of tires on a half-space. Here we consider absorbing conditions on a half-space and present numerical experiments.

In the Appendix there is a detailed computation of time integrals, a listing of some important theorems, used in this thesis, together with a road-map of spaces and norms compared with the one in Ha-Duong's lecture notes [57], computations for the single layer integral equation with a parameter $\sigma > 0$ and the bcl-scripts in Maiprogs. These scripts are executed, which gives us the numerical results in this thesis.

Notation: We write $f \lesssim g$ provided there exists a constant C such that $f \leq Cg$. If the constant C is allowed to depend on a parameter σ, we write $f \lesssim_\sigma g$. Further we write $\dot{f}(x,t) \coloneqq \partial_t f(x,t)$ and $\ddot{f}(x,t) \coloneqq \partial_t^2 f(x,t)$ for the first two derivatives in time.

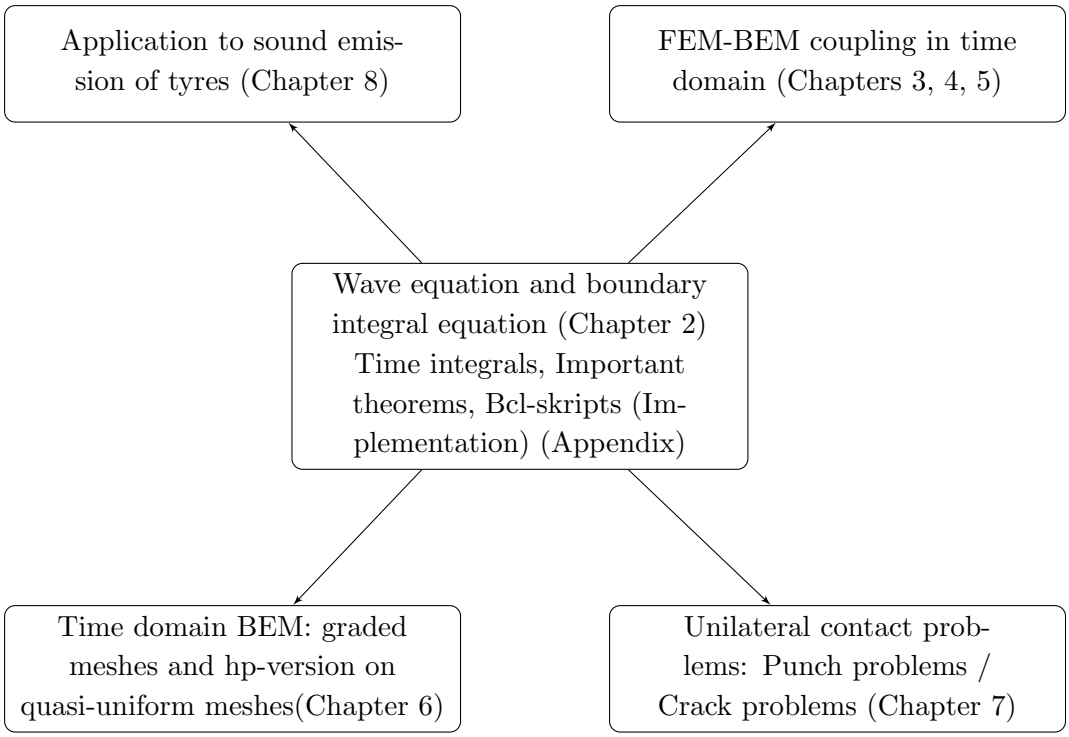

2 Wave equation and boundary integral formulations

2.1 Introduction to scattering problems

Let Ω be a bounded open domain with a connected complement $\Omega^c = \mathbb{R}^3 \backslash \overline{\Omega}$. We consider the transient sound radiation of the body Ω, where the acoustic pressure $v(x,t)$ satisfies

$$\begin{aligned} c^{-2}\frac{\partial^2 v}{\partial t^2} - \Delta v &= 0 \quad (x,t) \in \Omega^c \times \mathbb{R}_+ \\ v(x,0) = \dot{v}(x,0) &= 0 \quad \text{in } \Omega^c \\ Bv &= f \quad \text{in } \Gamma \times \mathbb{R}_+ \end{aligned} \tag{2.1}$$

where B is either the exterior trace of the normal derivative (Neumann boundary condition) or the exterior trace on Γ (Dirichlet boundary condition), f is given and c is the wave-velocity. Here we set $c = 1$. If $c \neq 1$ is given, we may substitute $\tau = ct$ and get a wave equation with respect to τ, where the velocity is 1. In this case we just need to adapt the boundary conditions. Furthermore if we have Neumann data we interprete the problem as a hard scattering problem and if we have Dirichlet data we interprete the problem as a soft scattering problem. In Chapter 8, we also consider $Bv = \frac{\partial v}{\partial n} - \frac{\alpha(x)}{c}\frac{\partial v}{\partial t}$ on an acoustic half-space $\mathbb{R}^2 \times \{0\}$ with constant $\alpha \geq 0$, which refers to an absorbing scatterer. The fundamental solution of the wave equation in 3 dimensions is known as:

$$G(x,t) = \frac{1}{4\pi}\frac{\delta(t-|x|)}{|x|} \tag{2.2}$$

where δ is the delta-distribution. Next we can write down the acoustic pressure $v(x,t)$ for $x \in \Omega^c$ as:

$$\begin{aligned} v(x,t) = &\iint_{\Gamma\times\mathbb{R}_+} \frac{\partial G}{\partial n_y}(x-y,t-\tau)v_+(y,\tau)ds_y d\tau \\ &- \iint_{\Gamma\times\mathbb{R}_+} G(x-y,t-\tau)\frac{\partial v_+}{\partial n}(y,\tau)ds_y d\tau \end{aligned} \tag{2.3}$$

where for $x \in \Gamma$, $\gamma^+ v = v_+(x,t) = \lim_{x' \in \Omega^c \to x} v(x',t)$ and analogously $\partial_n^+ v = \frac{\partial v_+}{\partial n}(x,t) = \lim_{x' \in \Omega^c \to x} \frac{\partial v}{\partial n}(x',t) = \lim_{x' \in \Omega^c \to x} n_x \cdot \nabla v(x',t)$, where $n := n_x$ is the unit normal vector on $x \in \Gamma$ always pointing towards Ω^c. Here γ^+ is the exterior trace and ∂_n^+ is the exterior trace of the normal derivative. A proof can be found in i.e. [17, 55]. In (2.3) the first integral is called the retarded double layer potential and the second integral is called the retarded single layer potential. We consider them in the next section.

2.2 Retarded integral operators

We define the retarded single layer potential and the retarded double layer potential.

Definition 2.1. *Let* $(x,t) \in (\mathbb{R}^3 \backslash \Gamma) \times \mathbb{R}_+$, $\tau = t - |x-y|$ *and* $p \in C^2(\Gamma \times \mathbb{R}_+)$, *then the retarded single layer potential is defined as:*

$$Sp(x,t) := \frac{1}{4\pi} \int_\Gamma \frac{p(y,\tau)}{|x-y|} ds_y \ . \tag{2.4}$$

Definition 2.2. *Let* $(x,t) \in (\mathbb{R}^3 \backslash \Gamma) \times \mathbb{R}_+$, $\tau = t - |x-y|$ *and* $\varphi \in C^2(\Gamma \times \mathbb{R}_+)$, *then the retarded double layer potential is defined as:*

$$D\varphi(x,t) := \frac{1}{4\pi} \int_\Gamma \frac{n_y \cdot (x-y)}{|x-y|} \left(\frac{\varphi(y,\tau)}{|x-y|^2} + \frac{\dot{\varphi}(y,\tau)}{|x-y|} \right) ds_y \ . \tag{2.5}$$

We extend the solution v of (2.1) to the interior by zero, i.e. $v_- = 0$ and $\partial_n^- v = 0$, where analogously to v_+ and resp. $\frac{\partial v_+}{\partial n}$, $\gamma^- v = v_- := \lim\limits_{x' \in \Omega \to x} v(x',t)$ and $\partial_n^- v = \frac{\partial v_-}{\partial n} := \lim\limits_{x' \in \Omega \to x} \frac{\partial v}{\partial n}(x',t) = \lim\limits_{x' \in \Omega \to x} n_x \cdot \nabla v(x',t)$ with $x \in \Gamma$ and the unit normal vector $n = n_x$ is pointed towards Ω^c.
Now let us introduce for $x \in \Gamma$ the jump operator $[\cdot]$:

$$\varphi = [v] := v_+ - v_-, \quad p = \left[\frac{\partial v}{\partial n} \right] := \frac{\partial v_+}{\partial n} - \frac{\partial v_-}{\partial n}. \tag{2.6}$$

Now we write down (2.3) as:

$$v(x,t) = D\varphi - Sp \ . \tag{2.7}$$

Now we define the retarded potential operators on the boundary Γ.

Definition 2.3. *a) Let* $x \in \Gamma$, $t \in \mathbb{R}_+$, $\tau = t - |x-y|$ *and* $p \in C^2(\Gamma \times \mathbb{R}_+)$. *Then the retarded single layer potential on the boundary is defined as:*

$$Vp(x,t) := \frac{1}{4\pi} \int_\Gamma \frac{p(y,\tau)}{|x-y|} ds_y \ .$$

b) Let $x \in \Gamma$, $t \in \mathbb{R}_+$, $\tau = t - |x-y|$ *and* $p \in C^2(\Gamma \times \mathbb{R}_+)$. *Then the retarded adjoint double layer potential on the boundary is defined as:*

$$K^T p(x,t) := K' p(x,t) := \frac{1}{4\pi} \int_\Gamma \frac{n_x (x-y)}{|x-y|} \left(\frac{p(y,\tau)}{|x-y|^2} + \frac{\dot{p}(y,\tau)}{|x-y|} \right) ds_y \ .$$

c) Let $x \in \Gamma$, $t \in \mathbb{R}_+$, $\tau = t - |x-y|$ *and* $\varphi \in C^2(\Gamma \times \mathbb{R}_+)$. *Then the retarded double layer potential on the boundary is defined as:*

$$K\varphi(x,t) := \frac{1}{4\pi} \int_\Gamma \frac{n_y (x-y)}{|x-y|} \left(\frac{\varphi(y,\tau)}{|x-y|^2} + \frac{\dot{\varphi}(y,\tau)}{|x-y|} \right) ds_y \ .$$

d) Let $x \in \Gamma$, $t \in \mathbb{R}_+$, $\tau = t - |x-y|$ and $\varphi \in C^2(\Gamma \times \mathbb{R}_+)$. Then the retarded hypersingular integral operator on the boundary is defined as:

$$W\varphi(x,t) := -\lim_{x' \in \Omega_e \to x} n_x \nabla_{x'} \left(\frac{1}{4\pi} \int_\Gamma n_y \nabla_{x'} \frac{\varphi(y, t-|x'-y|)}{|x'-y|} ds_y \right) .$$

With these operators the following jump relation hold:

Theorem 2.1 ([55], Lemma 3, 4a)**.** *Let $x \in \Omega^c$, $t \in \mathbb{R}_+$ and I the identity, then for $\varphi, p \in C^2(\Gamma \times \mathbb{R}_+)$ there holds:*

$$(Sp)_-(x,t) = (Sp)_+(x,t) = Vp(x,t) , \tag{2.8}$$

$$\frac{\partial (Sp)_+}{\partial n}(x,t) = (-\frac{1}{2}I + K')p(x,t) , \tag{2.9}$$

$$\frac{\partial (Sp)_-}{\partial n}(x,t) = (\frac{1}{2}I + K')p(x,t) , \tag{2.10}$$

$$(D\varphi)_+(x,t) = (\frac{1}{2}I + K)\varphi(x,t) , \tag{2.11}$$

$$(D\varphi)_-(x,t) = (-\frac{1}{2}I + K)\varphi(x,t) , \tag{2.12}$$

$$\frac{\partial (D\varphi)_-}{\partial n}(x,t) = \frac{\partial (D\varphi)_+}{\partial n}(x,t) = W\varphi(x,t) . \tag{2.13}$$

The normal derivative of the retarded single layer potential and double layer potential have an additional jump term if we go to the boundary Γ. The proof of this theorem can be found in [55, Lemma 3 and Lemma 4a].

Now we apply the jump relations to $v(x,t) = D\varphi - Sp$.

$$\varphi = \gamma^+ v(x,t) = (K + \frac{1}{2}I)\varphi - Vp , \quad p = \partial_n^+ v(x,t) = W\varphi - (K' - \frac{1}{2}I)p . \tag{2.14}$$

Since the retarded single layer potential is invertible [53], we get:

$$\varphi = (K + \frac{1}{2}I)\varphi - Vp \Leftrightarrow 0 = -Vp + (K - \frac{1}{2}I)\varphi \;\Leftrightarrow\; p = V^{-1}(K - \frac{1}{2})\varphi . \tag{2.15}$$

Using (2.15) on the second equation of (2.14) yields

$$\partial_n^+ v = (W - (K' - \frac{1}{2}I)V^{-1}(K - \frac{1}{2}I))\varphi =: \mathcal{S}\varphi. \tag{2.16}$$

$\mathcal{S}$ is called the exterior Dirichlet-to-Neumann or the retarded Poincaré-Steklov operator. We write down the retarded Poincaré-Steklov operator as a system of linear equations, where we use, equivalently to (2.15), $Vp - (K - \frac{1}{2}I)\varphi = 0$:

$$\begin{pmatrix} W & -(K' - \frac{1}{2}I) \\ -(K - \frac{1}{2}I) & V \end{pmatrix} \begin{pmatrix} \varphi \\ p \end{pmatrix} = \begin{pmatrix} \partial_n^+ v \\ 0 \end{pmatrix} . \tag{2.17}$$

Since W is also invertible (see [55]), one defines the retarded inverse Poincaré-Steklov operator $\mathcal{S}^{-1}$:

$$p = W\varphi - (K' - \frac{1}{2}I)p \Leftrightarrow 0 = W\varphi - (K' + \frac{1}{2}I)p \Leftrightarrow W^{-1}(K' + \frac{1}{2}I)p = \varphi \ ,$$

$$\gamma^+ v = ((K + \frac{1}{2}I)W^{-1}(K' + \frac{1}{2}I) - V)p =: \mathcal{S}^{-1}p \ . \tag{2.18}$$

We write down the retarded inverse Poincaré-Steklov operator as a system of linear equations:

$$\begin{pmatrix} W & -(K' + \frac{1}{2}I) \\ (K + \frac{1}{2}I) & -V \end{pmatrix} \begin{pmatrix} \varphi \\ p \end{pmatrix} = \begin{pmatrix} 0 \\ \gamma^+ v \end{pmatrix} \ . \tag{2.19}$$

The discretization of the retarded Poincaré-Steklov operator (see Subsection 2.3.5) and its inverse (see Subsection 2.3.6) requires a discretization of the retarded single layer potential, adjoint double layer potential, double layer potential and hypersingular integral operator first. An easier approach to the discretization of the retarded single layer potential, adjoint double layer potential and double layer potential are done in Subsections 2.3.1 - 2.3.3. The discretization of the retarded hypersingular integral operator (see Subsection 2.3.4) is used as well for the retarded Poincaré-Steklov operator and its inverse.

The standard procedure of studying (2.1) requires spaces adapted to the Fourier-Laplace transformation. With the help of the Paley-Wiener theorem (see Appendix 9.2, Theorem 9.1) one can define analogously the single layer potential and the double layer potential in frequency domain. A trace theorem (see Appendix 9.2, Lemma 9.1, 9.2, 9.3) and equivalent jump relations on the half-plane $\{\omega = \nu + i\mu \in \mathbb{C} : \mathrm{Im}\omega := \mu > \sigma\}$ hold for some $\sigma > 0$. Therefore one may proof the well-posedness of the Helmholtz equation. At last using an inverse Fourier-Laplace transform with the help of Parseval's theorem (see Appendix 9.2, Theorem 9.3) we obtain the well-posedness for (2.1). This strategy is also used in other cases as well, like in proving existence and uniqueness for the fluid-structure-interaction problem, see [63, 64] or the wave-wave coupling problem, see [70].

We introduce space-time anisotropic Sobolev spaces, which we use in all Chapters of this thesis. We proceed as in [57].

We consider a bounded, orientable Lipschitz domain $\Omega \subset \mathbb{R}^3$ with $\Omega^c = \mathbb{R}^3 \backslash \overline{\Omega}$ and the closed, orientable Lipschitz boundary $\Gamma = \partial\Omega$. Then we use the usual Hilbert spaces $H^0(\Omega) = L^2(\Omega)$ with the norm $\|u\|_{0,\Omega} = (\int_\Omega |u|^2 dx)^{1/2}$ and with $k = (k_1, k_2, k_3) \in \mathbb{N}_0^3$

$$H^1(\Omega) = \{u \in L^2(\Omega) : D^k u \in L^2(\Omega) \ \text{ with } |k| = \sum_{i=1}^{3} k_i \leq 1, \ \text{ and } D^k = \frac{\partial^{k_1}}{\partial x_1^{k_1}} \frac{\partial^{k_2}}{\partial x_2^{k_2}} \frac{\partial^{k_3}}{\partial x_3^{k_3}}\}$$

with the weighted norm

$$\|u\|_{1,\omega,\Omega} = (\int_\Omega |\nabla u|^2 + |\omega u|^2 dx)^{1/2} \ .$$

In this setting Becache and Ha-Duong prove in [18] a trace theorem (Lemma 9.1, 9.2, 9.3), where the norms of the corresponding trace spaces are defined in the following procedure.

We first extend Γ to a closed, orientable manifold $\widetilde{\Gamma}$, if Γ is a screen, i.e. $\partial\Gamma \neq \varnothing$. For $r \in \mathbb{R}$, we define the usual Sobolev space of supported distributions on Γ:

$$\widetilde{H}^r(\Gamma) = \{u \in H^r(\widetilde{\Gamma}) : \operatorname{supp} u \subset \overline{\Gamma}\} \ .$$

Further $H^r(\Gamma)$ is defined as the quotient space $H^r(\widetilde{\Gamma})\backslash\widetilde{H}^r(\widetilde{\Gamma}\backslash\overline{\Gamma})$. Furthermore, we define for a Hilbert space E, with $\sigma \in \mathbb{R}$, values in E and support in $[0,\infty)$:

$$LT(\sigma, E) := \{f \in D'_+(E), e^{-\sigma t} f \in S'_+(E)\} \ ,$$

where $D'_+(E)$ resp. $S'_+(E)$ are the sets of distributions resp. tempered distributions on $\mathbb{R}$ with values in E and support in $[0,\infty)$. For $\sigma < \sigma'$, $LT(\sigma, E) \subset LT(\sigma', E)$, there exists $\sigma(f) = \inf\{\sigma : f \in LT(\sigma, E)\}$. Then the set of Laplace transformable distributions with values in E is denoted by

$$LT(E) = \cup_{\sigma\in\mathbb{R}} LT(\sigma, E),$$

where for $\sigma > \sigma(f)$ and $\omega = \eta + i\sigma$ the Fourier-Laplace transform of $f \in LT(E)$ in the half-plane $\{\omega \in \mathbb{C} : \mathrm{Im}\omega := \sigma \geq \sigma(f)\}$ with $\mathrm{Im}\omega$ denoting the imaginary part of ω is given by

$$\widehat{f}(\omega) = \mathcal{F}(e^{-\sigma t} f)(\eta) = \int_{-\infty}^{\infty} e^{i\omega t} f(t) dt \ .$$

For u with support for positive times and $u(\cdot, 0) = \dot{u}(\cdot, 0) = 0$, we extend u to the whole $\mathbb{R}$ by setting $u(\cdot, t) = 0$ for $t \leq 0$.

We introduce a partition of unity α_i subordinate to a covering of $\widetilde{\Gamma}$ by open sets B_i $1 \leq i \leq s$ covering Ω. We define the diffeomorphisms φ_i which maps each B_i into the unit cube Q, $B_i \cap \Omega$ into $Q^+ = \{x \in Q : x_3 > 0\}$, and $B_i \subset \widetilde{\Gamma}$ into $\Sigma = \{x \in Q : x_3 = 0\}$. For u defined on $\widetilde{\Gamma}$, we get a family of Sobolev norms with $\omega \in \mathbb{C}\backslash\{0\}$:

$$\|u\|_{r,\omega,\widetilde{\Gamma}} = \left(\sum_{i=1}^{s} \int_{\mathbb{R}^2} (|\omega|^2 + |\xi|^2)^r |\mathcal{F}\{(\alpha_i u) \circ \varphi_i^{-1}(\xi)\}|^2 d\xi\right)^{\frac{1}{2}} \tag{2.20}$$

and for $u \in \Omega$

$$\|u\|_{r,\omega,\Omega} = \left(\sum_{i=1}^{s} \int_{\mathbb{R}^3} (|\omega|^2 + |\xi|^2)^r |\mathcal{F}\{(\alpha_i u) \circ \varphi_i^{-1}(\xi)\}|^2 d\xi\right)^{\frac{1}{2}} \ . \tag{2.21}$$

The weighted norms on $H^r(\Gamma)$ are being induced by $\|u\|_{r,\omega,\Gamma} = \inf_{v\in\widetilde{H}^r(\widetilde{\Gamma}\backslash\overline{\Gamma})} \|u + v\|_{r,\omega,\widetilde{\Gamma}}$. We can also define the weighted norms on $H^r(\Gamma)$ via $\|u\|_{r,\omega,\Gamma,*} = \|e_+ u\|_{r,\omega,\widetilde{\Gamma}}$. Here e_+ extends the distribution u by zero from Γ to $\widetilde{\Gamma}$. Since the norm $\|u\|_{r,\omega,\Gamma}$ is being extended by an arbitrary v, the norm on $\|u\|_{r,\omega,\Gamma,*}$ is stronger than $\|u\|_{r,\omega,\Gamma}$ for $r \in \frac{1}{2} + \mathbb{Z}$ [54].

Due to Theorem 9.1, 9.2 and 9.3 we define the space-time anisotropic Sobolev spaces and the corresponding norms:

Definition 2.4. *For $s, r \in \mathbb{R}$ and $\sigma > 0$ we define for Γ and Ω, being a bounded, orientable Lipschitz domain, the Hilbert space*

$$H^s_\sigma(\mathbb{R}_+, H^r(\Omega)) = \{u \in LT(H^r(\Omega)) : \|u\|_{s,r,\sigma,\Omega} < \infty\},$$
$$H^s_\sigma(\mathbb{R}_+, H^r(\Gamma)) = \{u \in LT(H^r(\Gamma)) : \|u\|_{s,r,\sigma,\Gamma} < \infty\},$$
$$H^s_\sigma(\mathbb{R}_+, \widetilde{H}^r(\Gamma)) = \{u \in LT(\widetilde{H}^r(\Gamma)) : \|u\|_{s,r,\sigma,\Gamma,*} < \infty\},$$

equipped with the norm

$$\|u\|_{s,r,\sigma} := \|u\|_{s,r,\Omega} := \|u\|_{s,r,\sigma,\Omega} = \left(\int_{-\infty+i\sigma}^{+\infty+i\sigma} |\omega|^{2s} \ \|\hat{u}(\omega)\|^2_{r,\omega,\Omega} \ d\omega\right)^{\frac{1}{2}},$$
$$\|u\|_{s,r,\sigma} := \|u\|_{s,r,\Gamma} := \|u\|_{s,r,\sigma,\Gamma} = \left(\int_{-\infty+i\sigma}^{+\infty+i\sigma} |\omega|^{2s} \ \|\hat{u}(\omega)\|^2_{r,\omega,\Gamma} \ d\omega\right)^{\frac{1}{2}},$$
$$\|u\|_{s,r,\sigma,*} := \|u\|_{s,r,\Gamma,*} := \|u\|_{s,r,\sigma,\Gamma,*} = \left(\int_{-\infty+i\sigma}^{+\infty+i\sigma} |\omega|^{2s} \ \|\hat{u}(\omega)\|^2_{r,\omega,\Gamma,*} \ d\omega\right)^{\frac{1}{2}}.$$

We note that for $s = r = 0$ we receive the weighted L^2–space. In case of $\sigma = 0$ we skip the index and write $H^s(\mathbb{R}^+, H^r(\Gamma))$. Because Γ, Ω are Lipschitz, like in the case of standard Sobolev spaces [81] these spaces are independent of the choice of α_i and φ_i when $|r| \leq 1$. Due to Parseval's theorem (Theorem 9.3), we get for the norm in $H^0_\sigma(\mathbb{R}, H^1(\Omega))$:

$$\|u\|_{0,1,\Omega} = \Big(\int_{-\infty+i\sigma}^{\infty+i\sigma} \|\hat{u}\|^2_{1,\omega,\Omega} d\omega\Big)^{1/2} = \Big(\int_\infty^\infty e^{-2\sigma t} \int_\Omega |\nabla u(x,t)|^2 + |\dot{u}(x,t)|^2 dx dt\Big)^{1/2}.$$

Therefore $e^{-\sigma t}\nabla u$ and $e^{-\sigma t}\dot{u}$ both need to be square integrable in space and time, where we have $u(\cdot, 0) = \dot{u}(\cdot, 0) = 0$. Hence for $\sigma' > \sigma$, we say $e^{-\sigma t}u$ need to be in "$H^1(\Omega)$ in space" and "$H^1(\mathbb{R})$ in time".

For a finite time interval $[0, T]$ with $\sigma = 0$, we get

$$H^0([0,T], H^1(\Omega)) = \{\nabla u \text{ and } \dot{u} \text{ are square integrable in } \Omega \text{ and } [0,T] \text{ with } u(\cdot, 0) = 0\},$$

where the norm is defined in [72]:

$$\|u\|_{0,1,\Omega\times[0,T]} = \Big(\int_0^T \|u\|^2_{H^1(\Omega)} dt + \int_\Omega \|u\|^2_{H^1([0,T])} dx\Big)^{1/2}. \tag{2.22}$$

We want to use (2.22) in order to get the norms for the trace spaces of $H^0([0, T], H^1(\Omega))$. For $u \in H^0_\sigma(\mathbb{R}, H^{1/2}(\Gamma)) = \{u \in LT(H^{1/2}(\Gamma)) : (\int_{-\infty+i\sigma}^{\infty+i\sigma} \|\hat{u}\|^2_{1/2,\omega,\Gamma})^{1/2} < \infty\}$, we observe for all ω with $\mathrm{Im}\omega \geq \sigma_0 > 0$ and

$$(|\omega|^2 + |\xi|^2) \leq (1 + |\omega|^2)^{1/2} + (1 + |\xi|^2)^{1/2} \leq 2(\frac{1 + \sigma_0^2}{\sigma_0^2})^{1/2}(|\omega|^2 + |\xi|^2)^{1/2}.$$

that $e^{-\sigma t}u$ needs to be in "$H^{1/2}(\Gamma)$ in space" and "$H^{1/2}(\mathbb{R})$ in time".

Similar as before we write for a finite time interval $[0, T]$ that $u \in H^0([0, T], H^{1/2}(\Gamma))$ needs to be "$H^{1/2}(\Gamma)$ in space" and "$H^{1/2}([0, T])$ in time" with $u(\cdot, 0) = 0$. Corresponding trace theorems (see Appendix Lemma 9.4, 9.5) hold for $H^0([0, T], H^{1/2}(\Gamma))$

as well as it's dual space $H^0([0,T],H^{-1/2}(\Gamma))$. With the same idea for the Hilbert space $H^s([0,T],H^r(\Gamma))$ with $s,r\geq 0$ the corresponding norm is defined as:

$$\|u\|_{s,r,\Gamma\times[0,T]}=\Big(\int_0^T\|u\|^2_{H^r(\Gamma)}dt+\int_\Gamma\|u\|^2_{H^{s+r}([0,T])}ds_x\Big)^{1/2}\ .$$

For negative s,r we use the dual space together with the dual norm of $\|u\|_{-s,-r,\Gamma\times[0,T]}$. In this thesis, we will need this norm only for $s\in\mathbb{Z}$ (in particular Chapter 5). A comparison between the Hilbert spaces defined in this thesis and Ha-Duong in [57] is done in the Appendix 9.3. We will use the same setting for Ω. For more details, see [72, Chapter 4].

For real functions u,v we define

$$\langle u,v\rangle_{\Gamma\times\mathbb{R}^+,\sigma}:=\int_0^\infty e^{-2\sigma t}\int_\Gamma uvds_xdt\quad\text{and}\quad\langle u,v\rangle_\Gamma:=\int_\Gamma uvds_x\ . \tag{2.23}$$

Further we define

$$(u,v)_{\Omega\times\mathbb{R}^+,\sigma}:=\int_0^\infty e^{-2\sigma t}\int_\Omega uvdxdt\ . \tag{2.24}$$

For vector valued $\mathbf{u}=(u_1,\dots,u_d)^T\in(H^s_\sigma(\mathbb{R}^+,H^r(\Omega)))^d$ with $d\in\mathbb{N}$ we define the norm:

$$\|\mathbf{u}\|_{s,r,\Omega}:=\sqrt{\sum_{i=1}^d\|u_i\|^2_{s,r,\Omega}}\quad .$$

Furthermore the corresponding norm for a matrix C is defined by

$$\|C(\cdot)\|_{s,r,\Omega}:=\sqrt{\sum_{i,j}\|C_{i,j}(\cdot)\|^2_{s,r,\Omega}}\quad .$$

Then for real vector valued $\mathbf{u},\mathbf{v}$, we define

$$(\mathbf{u},\mathbf{v})_{\Omega\times\mathbb{R}^+,\sigma}:=\int_0^\infty e^{-2\sigma t}\int_\Omega\mathbf{u}\cdot\mathbf{v}dxdt\quad\text{and}\quad\langle\mathbf{u},\mathbf{v}\rangle_{\Gamma\times\mathbb{R}^+,\sigma}:=\int_0^\infty e^{-2\sigma t}\int_\Gamma\mathbf{u}\cdot\mathbf{v}ds_xdt\ . \tag{2.25}$$

In case of $\sigma=0$, we skip the index.

Next we remark for $\partial_t(Vp)$:

$$\begin{aligned}\partial_t(Vp)(x,t)=\partial_t(\int_\Gamma\frac{p(y,t-|x-y|)}{|x-y|}ds_y)&=\int_\Gamma\frac{\partial_t(p(y,t-|x-y|))}{|x-y|}(\partial_t(t-|x-y|))ds_y\\&=\int_\Gamma\frac{\partial_t(p(y,t-|x-y|))}{|x-y|}ds_y=(V\dot{p})(x,t)\ .\end{aligned}$$

The same property holds for K,K',W as well.

Next from [48] we state the mapping properties of the retarded integral operators.

Theorem 2.2 ([48]). *Let $\mathcal{I}=\mathbb{R}_+$. The following operators are continuous for $r\in\mathbb{R}$:*

$$\begin{aligned}V&:H^{r+1}_\sigma(\mathcal{I},\widetilde{H}^{-\frac{1}{2}}(\Gamma))\to H^r_\sigma(\mathcal{I},H^{\frac{1}{2}}(\Gamma))\ ,\\K'&:H^{r+1}_\sigma(\mathcal{I},\widetilde{H}^{-\frac{1}{2}}(\Gamma))\to H^r_\sigma(\mathcal{I},H^{-\frac{1}{2}}(\Gamma))\ ,\\K&:H^{r+1}_\sigma(\mathcal{I},\widetilde{H}^{\frac{1}{2}}(\Gamma))\to H^r_\sigma(\mathcal{I},H^{\frac{1}{2}}(\Gamma))\ ,\\W&:H^{r+1}_\sigma(\mathcal{I},\widetilde{H}^{\frac{1}{2}}(\Gamma))\to H^r_\sigma(\mathcal{I},H^{-\frac{1}{2}}(\Gamma))\ .\end{aligned}$$

Due to Ha-Duong in [55, Chapter 4.4] an analogous result is made for finite times:

Proposition 2.1. *Let $\mathcal{I} = [0,T]$. The following operators are continuous for $r \in \mathbb{R}$:*

$$\begin{aligned} V &: H^{r+1}_\sigma(\mathcal{I}, \widetilde{H}^{-\frac{1}{2}}(\Gamma)) \to H^r_\sigma(\mathcal{I}, H^{\frac{1}{2}}(\Gamma)) \ , \\ K' &: H^{r+1}_\sigma(\mathcal{I}, \widetilde{H}^{-\frac{1}{2}}(\Gamma)) \to H^r_\sigma(\mathcal{I}, H^{-\frac{1}{2}}(\Gamma)) \ , \\ K &: H^{r+1}_\sigma(\mathcal{I}, \widetilde{H}^{\frac{1}{2}}(\Gamma)) \to H^r_\sigma(\mathcal{I}, H^{\frac{1}{2}}(\Gamma)) \ , \\ W &: H^{r+1}_\sigma(\mathcal{I}, \widetilde{H}^{\frac{1}{2}}(\Gamma)) \to H^r_\sigma(\mathcal{I}, H^{-\frac{1}{2}}(\Gamma)) \ . \end{aligned}$$

For the half-space $\Gamma = \mathbb{R}^{n-1}_+$, Fourier methods yield improved estimates for V and W:

Theorem 2.3 ([56], pp. 503-506)**.** *The following operators are continuous for $r, s \in \mathbb{R}$, $\sigma > 0$:*

$$\begin{aligned} V &: H^{r+\frac{1}{2}}_\sigma(\mathbb{R}^+, \widetilde{H}^s(\Gamma)) \to H^r_\sigma(\mathbb{R}^+, H^{s+1}(\Gamma)) \ , \\ W &: H^r_\sigma(\mathbb{R}^+, \widetilde{H}^s(\Gamma)) \to H^r_\sigma(\mathbb{R}^+, H^{s-1}(\Gamma)) \ . \end{aligned}$$

For G, a bounded Lipschitz subset of Γ, we deduce from Theorems 2.2 and 2.3 corresponding mapping properties for the composition with a restriction p_Q to $Q = G \times \mathbb{R}$. For the retarded single layer potential V as an example, we obtain from Theorem 2.2 $p_Q V : H^{r+1}_\sigma(\mathbb{R}^+, \widetilde{H}^{-\frac{1}{2}}(G)) \hookrightarrow H^{r+1}_\sigma(\mathbb{R}^+, \widetilde{H}^{-\frac{1}{2}}(\Gamma)) \to H^r_\sigma(\mathbb{R}^+, H^{\frac{1}{2}}(G))$. Furthermore we denote with $H^r_\sigma(\mathbb{R}^+, \widetilde{H}^s(G))^+$ the set of nonnegative distributions. We will need this setup for unilateral contact problems in Chapter 7. At last we note the continuous embedding

$$H^0_\sigma(\mathbb{R}^+, H^{1/2}(\Gamma)) \subset H^1_\sigma(\mathbb{R}^+, H^{-1/2}(\Gamma)) \quad .$$

2.2.1 A retarded single layer potential ansatz

Alternative to (2.3), we may use a retarded single layer potential ansatz, see [17, 55]. The acoustic pressure is given via

$$v(x,t) = \iint\limits_{\Gamma \times \mathbb{R}_+} G(x-y, t-\tau) p(y,\tau) ds_y d\tau = Sp \tag{2.26}$$

with v is extended to the interior such that $\gamma^+ v = \gamma^- v$ and $p = (\partial_n^- v - \partial_n^+ v) = -[\frac{\partial v}{\partial n}]$. For a Dirichlet problem, where the boundary condition $\gamma^+ v = f$ on $\Gamma \times \mathbb{R}_+$ is given, we get with the jump relation the integral equation

$$Vp = f \text{ on } \Gamma \times \mathbb{R}_+ \ . \tag{2.27}$$

V satisfies a coercivity estimate in the norm $H^0_\sigma(\mathbb{R}^+, \widetilde{H}^{-\frac{1}{2}}(\Gamma))$: $\|\phi\|^2_{0,-\frac{1}{2},\sigma,*} \lesssim_\sigma \langle V\phi, \partial_t \phi \rangle_{\Gamma \times \mathbb{R}^+, \sigma}$. when testing against a time derivate, see Bamberger and Ha-Duong [11]. On the other hand we get the continuity of $\langle V\phi, \partial_t \phi \rangle_{\Gamma \times \mathbb{R}_+, \sigma}$ with the mapping properties of Theorem

2.2 in the bigger norm of $H^1_\sigma(\mathbb{R}^+, \widetilde{H}^{-\frac{1}{2}}(\Gamma))$: $\langle V\phi, \partial_t\phi\rangle \lesssim \|\phi\|^2_{1,-\frac{1}{2},\sigma,*}$. These estimates are a crucial ingredient in the numerical analysis of time-domain boundary integral equations.

Therefore the variational formulation reads:

Find $p \in H^0_\sigma(\mathbb{R}_+, \widetilde{H}^{-1/2}(\Gamma))$ such that forall $q \in H^1_\sigma(\mathbb{R}_+, \widetilde{H}^{-1/2}(\Gamma))$, there hold

$$\int_0^\infty \int_\Gamma (Vp)\dot{q} ds_x \; e^{-2\sigma t} dt = \int_0^\infty \int_\Gamma f(x,t)\dot{q} \; ds_x e^{-2\sigma t} dt. \tag{2.28}$$

The weak formulation (2.28) for the Dirichlet problem is well-posed [48]:

Theorem 2.4. *Let $\sigma > 0$. Assume that $f \in H^2_\sigma(\mathbb{R}^+, H^{\frac{1}{2}}(\Gamma))$. Then there exists a unique solution $p \in H^1_\sigma(\mathbb{R}^+, \widetilde{H}^{-\frac{1}{2}}(\Gamma))$ of (2.28) and*

$$\|p\|_{1,-\frac{1}{2},\Gamma,*} \lesssim_\sigma \|f\|_{2,\frac{1}{2},\Gamma} \; . \tag{2.29}$$

A theoretical analysis requires $\sigma > 0$, but for the ease of implementation we do computations for finite times using $\sigma = 0$ [11, 45]. In the Appendix 9.4 we perform a numerical experiment for the retarded single layer potential for $\sigma > 0$.

For $\tau = t - |x-y|$ we get:

$$\int_0^\infty \int_\Gamma \int_\Gamma \frac{1}{4\pi} \frac{p(y,\tau)}{|x-y|} \dot{q}(x,t) ds_y ds_x e^{-2\sigma t} dt = \int_0^\infty \int_\Gamma f(x,t)\dot{q} \; ds_x e^{-2\sigma t} dt. \tag{2.30}$$

Remark 2.1. *For $\sigma = 0$, integration by parts in time for (2.30) gives the following equivalence*

$$\langle V\dot{p}, q\rangle_{\Gamma\times\mathbb{R}_+} = \langle \dot{f}, q\rangle_{\Gamma\times\mathbb{R}_+} \quad \Leftrightarrow \quad \langle Vp, \dot{q}\rangle_{\Gamma\times\mathbb{R}_+} = \langle f, \dot{q}\rangle_{\Gamma\times\mathbb{R}_+} \; .$$

Next based on Ha-Duong in [57] we consider the following relationship between the energy at time t

$$E(t) = \frac{1}{2}\int_{\mathbb{R}^3\setminus\Gamma} |\nabla v(x,t)|^2 + |\dot{v}(x,t)|^2 dx$$

and the integral equation (2.27). With Green's formula and v satisfying the wave equation we get

$$\begin{aligned}
\frac{\partial E}{\partial t} &= \frac{1}{2}\int_{\mathbb{R}^3\setminus\Gamma} \partial_t(\nabla v\cdot\nabla v) + \partial_t(\dot{v}\dot{v}) dx = \frac{1}{2}\int_{\mathbb{R}^3\setminus\Gamma} 2(\nabla v\cdot\nabla\dot{v}) + 2(\dot{v}\ddot{v}) dx \\
&= \int_{\Omega^c} (\nabla v\cdot\nabla\dot{v}) + (\dot{v}\cdot\ddot{v}) dx + \int_\Omega (\nabla v\cdot\nabla\dot{v}) + (\dot{v}\ddot{v}) dx \\
&= \int_{\Omega^c} -\dot{v}\cdot\Delta v + \dot{v}\ddot{v} dx - \int_\Gamma \frac{\partial v_+}{\partial n}\gamma^+\dot{v} ds_x + \int_\Omega -\dot{v}\cdot\Delta v + \dot{v}\ddot{v} dx + \int_\Gamma \frac{\partial v_-}{\partial n}\gamma^-\dot{v} ds_x \\
&= \int_\Gamma (\frac{\partial v_-}{\partial n}\gamma^-\dot{v} - \frac{\partial v_+}{\partial n}\gamma^+\dot{v}) ds_x \; .
\end{aligned} \tag{2.31}$$

Now with $\gamma^+\dot{v} = \partial_t(Vp)$ with $p = (\partial_n^- v - \partial_n^+ v)$ and $\gamma^+\dot{v} = \gamma^-\dot{v}$, we get

$$\frac{\partial E}{\partial t} = \int_\Gamma (\partial_n^- v - \partial_n^+ v)\gamma^+\dot{v} ds_x = \int_\Gamma p \; \partial_t(Vp) ds_x \; .$$

Hence with integration by parts in time

$$E(t) = \int_0^t \frac{\partial E}{\partial t} dt = \int_0^t \int_\Gamma p\ \partial_t (Vp) ds_x dt = -\int_0^t \int_\Gamma \dot{p}\ (Vp) ds_x dt\ . \tag{2.32}$$

Also in $\mathbb{R}^+$ for $\sigma > 0$ and integrating by parts in time, we get:

$$\int_0^\infty e^{-2\sigma t} E(t) dt = \frac{1}{2\sigma} \int_0^\infty e^{-2\sigma t} \frac{\partial E}{\partial t} dt = \frac{1}{2\sigma} \int_0^\infty e^{-2\sigma t} \int_\Gamma p \partial_t (Vp) ds_x dt\ .$$

Further as in [57] assuming $e^{-\sigma t} E(t) \in L^2(\mathbb{R})$ using the Fourier transform with $\frac{\partial}{\partial t} \to -i\omega$ and the Parseval's theorem:

$$\begin{aligned}\int_0^\infty e^{-2\sigma t} E(t) dt = \frac{1}{2} \int_0^\infty \int_{\mathbb{R}^3 \setminus \Gamma} |\nabla v|^2 + |\dot{v}|^2 dx dt &= \frac{1}{4\pi} \int_{-\infty + i\sigma}^{\infty + i\sigma} (|\nabla \hat{v}|) + |\omega|^2 |\hat{v}|^2 dx d\omega \\ &= \frac{1}{4\pi} \int_{-\infty + i\sigma}^{\infty + i\sigma} \|\hat{v}\|_{1,\omega,\mathbb{R}^3 \setminus \Gamma} d\omega\ .\end{aligned}$$

With the trace theorem, we estimate

$$\int_0^\infty e^{-2\sigma t} E(t) dt \gtrsim \int_{-\infty + i\sigma}^{\infty + i\sigma} \|\hat{p}\|^2_{-1/2,\omega,\Gamma} d\omega \gtrsim \|p\|_{0,-1/2,\sigma,\Gamma}\ .$$

For $\dot{f} \in H^0([0,T], H^{1/2}(\Gamma))$, we extend f to $\widetilde{f}$ into $\mathbb{R}$ in time by $f(\cdot, t) = 0$ for $t \leq 0$ such that for all $\sigma > 0$ and C independent of σ

$$\|\widetilde{f}\|_{1,1/2,\sigma,\Gamma} \leq C \|\dot{f}\|_{0,1/2,\Gamma \times [0,T]}\ .$$

We write a variational formulation for $\partial_t (Vp) = \dot{f}$: Find $p \in H^1_\sigma(\mathbb{R}_+, \widetilde{H}^{-1/2}(\Gamma))$ such that for all $q \in H^1_\sigma(\mathbb{R}_+, \widetilde{H}^{-1/2}(\Gamma))$:

$$\int_0^\infty e^{-2\sigma t} \int_\Gamma \partial_t (Vp) q ds_x dt = \int_0^\infty e^{-2\sigma t} \int_\Gamma \dot{\widetilde{f}} q ds_x dt\ . \tag{2.33}$$

With (2.32), we state a variational formulation for finite times $[0,T]$:
Find $p \in H^1([0,T], \widetilde{H}^{-1/2}(\Gamma))$ such that for all $q \in H^1([0,T], \widetilde{H}^{-1/2}(\Gamma))$:

$$\int_0^T \int_\Gamma \partial_t (Vp) q ds_x dt = \int_0^T \int_\Gamma \dot{f} q ds_x dt\ . \tag{2.34}$$

Since the solution p of (2.33) doesn't depend on $\widetilde{f}$ for times larger than T (due to Theorem 9.2 and the mapping properties of V), the solution p of (2.33) also satisfies (2.34). For p, a solution of (2.34) we multiply $\partial_t (Vp) = \dot{f}$ with $e^{-2\sigma t}$, extending f to $\widetilde{f}$ and integrating on $\Gamma \times \mathbb{R}_+$ the restriction of (2.33) for $[0,T]$ gives the same solution.

With

$$\begin{aligned}\int_0^T E(t) dt = \int_0^T \int_0^t \int_\Gamma (\partial_r (Vp)(x,r)) p(x,r) ds_x dr dt &= \int_0^T \int_0^t \int_\Gamma p(x,r) \dot{f}(x,r) ds_x dr dt \\ &= \int_0^T (T-r) \int_\Gamma p(x,r) \dot{f}(x,r) ds_x dr\end{aligned}$$

and the duality, we estimate

$$\int_0^T E(t)dt \lesssim_T \|p\|_{0,-1/2,\Gamma\times[0,T]} \cdot \|\dot{f}\|_{0,1/2,\Gamma\times[0,T]} \ .$$

Using (3.14) in [55, Chapter 4.3]:

$$\|p\|^2_{0,-1/2,\Gamma\times[0,T]} \lesssim_T \int_0^T E(t)dt \ .$$

Hence, we have proven:

$$\|p\|_{0,-1/2,\Gamma\times[0,T]} \lesssim_T \|\dot{f}\|_{0,1/2,\Gamma\times[0,T]} \ .$$

Proposition 2.2. *Let $p \in H^1([0,T],\widetilde{H}^{-1/2}(\Gamma))$ satisfy for $f \in H^2([0,T],\widetilde{H}^{1/2}(\Gamma))$ $Vp = f$ on $\Gamma\times[0,T]$. Then there hold*

$$\|p\|_{0,-1/2,\Gamma\times[0,T]} \lesssim_T \|\dot{f}\|_{0,1/2,\Gamma\times[0,T]}$$

For a Neumann problem, where the boundary condition $\partial_n^+ v = f$ on $\Gamma\times\mathbb{R}_+$ is given, we get with the jump relation the integral equation

$$(-\frac{1}{2}I + K')p = f \quad \text{on } \Gamma\times\mathbb{R}_+ \ . \tag{2.35}$$

The weak formulation reads as follows: Find $p \in H^1_\sigma(\mathbb{R}_+,\widetilde{H}^{-1/2}(\Gamma))$ such that

$$\int_0^\infty e^{-2\sigma t}\langle(K' - \frac{1}{2}I)p,\dot{q}\rangle_\Gamma \,\mathrm{dt} = \int_0^\infty\int_\Gamma e^{-2\sigma t} f(x,t)\dot{q}(x,t)\mathrm{d}s_x\,\mathrm{dt}, \tag{2.36}$$

holds for all $q \in H^1_\sigma(\mathbb{R}_+,\widetilde{H}^{1/2}(\Gamma))$.

The weak formulation (2.36) for the Neumann problem is well-posed [55, 51]:

Theorem 2.5 ([51])**.** *Let $\sigma > 0$. Assume that $f \in H^3_\sigma(\mathbb{R}^+,H^{-\frac{1}{2}}(\Gamma))$. Then there exists a unique solution $p \in H^1_\sigma(\mathbb{R}^+,\widetilde{H}^{-\frac{1}{2}}(\Gamma))$ of (2.36) and*

$$\|p\|_{1,-\frac{1}{2},\Gamma,*} \lesssim_\sigma \|f\|_{3,-\frac{1}{2},\Gamma} \ . \tag{2.37}$$

For a finite time interval $[0,T]$ the solution p of the retarded integral equation

$$(-\frac{1}{2}I + K')p = f \quad \text{on } \Gamma\times[0,T]$$

is due to Theorem 9.2 and the mapping properties of K' the same for (2.35), where the corresponding solution for times larger than T doesn't depend on $\widetilde{f}$, the extension of f to $\mathbb{R}$.

2.2.2 A retarded double layer potential ansatz

A further alternative to (2.3) gives the retarded double layer potential ansatz

$$v(x,t) = \iint\limits_{\Gamma\times\mathbb{R}^+} \frac{\partial G}{\partial n_y}(x-y,t-\tau)\varphi(y,\tau)ds_x d\tau = D\varphi \tag{2.38}$$

with v extended to the interior such that $\partial_n^+ v = \partial_n^- v$ and $\varphi = \gamma^- v - \gamma^+ v = -[v]$.

For a Dirichlet problem with boundary conditions $\gamma^+ v = f$ on $\Gamma\times\mathbb{R}_+$, we get with the jump relation the integral equation

$$(\frac{1}{2}I + K)\varphi = f \quad \text{on } \Gamma\times\mathbb{R}_+ \ . \tag{2.39}$$

The weak formulation reads as follows: Find $\varphi \in H^1_\sigma(\mathbb{R}_+, \widetilde{H}^{1/2}(\Gamma))$ such that

$$\int\limits_0^\infty e^{-2\sigma t}\langle (K+\frac{1}{2}I)\varphi, \dot{q}\rangle_\Gamma \,\mathrm{d}t = \int\limits_0^\infty \int\limits_\Gamma e^{-2\sigma t} f(t,x)\dot{q}(t,x)\mathrm{d}s_x\,\mathrm{d}t, \tag{2.40}$$

holds for all $q \in H^1_\sigma(\mathbb{R}_+, \widetilde{H}^{-1/2}(\Gamma))$.

The weak formulation (2.40) for the Dirichlet problem is well-posed, see [55].

Theorem 2.6. *Let $\sigma > 0$. Assume that $f \in H^3_\sigma(\mathbb{R}^+, H^{\frac{1}{2}}(\Gamma))$. Then there exists a unique solution $\varphi \in H^1_\sigma(\mathbb{R}^+, \widetilde{H}^{\frac{1}{2}}(\Gamma))$ of (2.40) and*

$$\|\varphi\|_{1,\frac{1}{2},\Gamma,*} \lesssim_\sigma \|f\|_{3,\frac{1}{2},\Gamma} \ . \tag{2.41}$$

For a finite time interval $[0,T]$ the solution φ of the retarded integral equation

$$(\frac{1}{2}I + K)\varphi = f \quad \text{on } \Gamma\times[0,T]$$

is due to Theorem 9.2 and the mapping properties of K the same for (2.39), where the corresponding solution for times larger than T doesn't depend in $\widetilde{f}$, the extension of f to $\mathbb{R}$.

For the Neumann problem, with $\partial_n^+ v = f$ on $\Gamma\times\mathbb{R}_+$, we get with the jump relation the integral equation

$$W\varphi = f \quad \text{on } \Gamma\times\mathbb{R}^+ \ . \tag{2.42}$$

For W we get similar estimates as for V: $\|\psi\|^2_{0,\frac{1}{2},\sigma,*} \lesssim_\sigma \langle W\psi, \partial_t\psi\rangle \lesssim \|\psi\|^2_{1,\frac{1}{2},\sigma,*}$. See [48, 57] for proofs and further information. Then the variational formulation reads: Find $\varphi \in H^1_\sigma(\mathbb{R}^+, \widetilde{H}^{\frac{1}{2}}(\Gamma))$ such that for all $\Psi \in H^1_\sigma(\mathbb{R}^+, \widetilde{H}^{\frac{1}{2}}(\Gamma))$ there holds:

$$\int_{\mathbb{R}^+\times\Gamma} (W\varphi)\ \partial_t\Psi\, e^{-2\sigma t} dt\, ds_x \ = \int_{\mathbb{R}^+\times\Gamma} f\ \partial_t\Psi\, e^{-2\sigma t} dt\, ds_x \ . \tag{2.43}$$

The weak formulation (2.43) for the Neumann problems is well-posed [51]:

Theorem 2.7 ([51]). *Assume that* $f \in H^2_\sigma(\mathbb{R}^+, H^{-\frac{1}{2}}(\Gamma))$. *Then there exists a unique solution* $\varphi \in H^1_\sigma(\mathbb{R}^+, \widetilde{H}^{\frac{1}{2}}(\Gamma))$ *of* (2.43) *and*

$$\|\varphi\|_{1,\frac{1}{2},\Gamma,*} \leq C\|f\|_{2,-\frac{1}{2},\Gamma} \ . \tag{2.44}$$

Analogously as V we derive an energy formulation for W. From (2.31) with $\partial_n^+ v = \partial_n^- v$ and $\partial_n^+ v = W\varphi$ with $\varphi = \gamma^- v - \gamma^+ v = -[v]$, we observe

$$\frac{\partial E}{\partial t} = \int_\Gamma \frac{\partial v^+}{\partial n}(\gamma^- \dot{v} - \gamma^+ \dot{v}) ds_x = \int_\Gamma (W\varphi)\ \dot{\varphi} ds_x \ .$$

Hence

$$E(t) = \int_0^t \frac{\partial E}{\partial t} dt = \int_0^t \int_\Gamma (W\varphi)\ \dot{\varphi} ds_x dt \ .$$

For a finite time interval $[0,T]$ the solution φ of the retarded integral equation

$$W\varphi = f \quad \text{on } \Gamma \times [0,T] \tag{2.45}$$

is due to Theorem 9.2 and the mapping properties of W the same for (2.42), where the corresponding solution for times larger than T, doesn't depend on $\widetilde{f}$, the extension of f to $\mathbb{R}$. Further proceeding similar as in the retarded single layer potential case

$$\begin{aligned}\int_0^T E(t)dt = \int_0^T \int_0^t \int_\Gamma (W\varphi)(x,r)\dot{\varphi}(x,r) ds_x dr dt &= \int_0^T \int_0^t \int_\Gamma f(x,r)\dot{\varphi}(x,r) ds_x dr dt \\ &= \int_0^T (T-r) \int_\Gamma f(x,r)\dot{\varphi}(x,r) ds_x dr \ .\end{aligned}$$

Now using the duality we estimate

$$\int_0^T E(t)dt \lesssim_T \|\dot{\varphi}\|_{-1,1/2,\Gamma\times[0,T]} \|f\|_{1,-1/2,\Gamma\times[0,T]} \ .$$

Using (3.7) in [55, Chapter 4.3]:

$$\|\varphi\|^2_{0,1/2,\Gamma\times[0,T]} \lesssim_T \int_0^T E(t)dt \ ,$$

we get

$$\|\varphi\|_{0,1/2,\Gamma\times[0,T]} \lesssim_T \|f\|_{1,-1/2,\Gamma\times[0,T]} \ .$$

Proposition 2.3. *Let* $\varphi \in H^1([0,T], \widetilde{H}^{1/2}(\Gamma))$ *satisfying for* $f \in H^2([0,T], \widetilde{H}^{-1/2}(\Gamma))$ $W\varphi = f$ *on* $\Gamma \times [0,T]$. *Then there hold*

$$\|\varphi\|_{0,1/2,\Gamma\times[0,T]} \lesssim_T \|f\|_{1,-1/2,\Gamma\times[0,T]} \ .$$

2.3 Boundary element discretization

Now let us define the discretization spaces as in [84]. Let $\mathcal{T}_{h,2}$ be a regular triangulation of Γ into finite $\Gamma_j (j \in \{1,\dots,N_s\})$, where the following properties are statisfied:

1. $\Gamma = \bigcup_{\Gamma_j \in \mathcal{T}_{h,2}} \Gamma_j$
2. every $\Gamma_j \in \mathcal{T}_{h,2}$ is a closed Lipschitz continuous boundary with $int\Gamma_j \neq \varnothing$
3. for $\Gamma_i, \Gamma_j \in \mathcal{T}_{h,2}, i \neq j$, there hold $int\Gamma_i \cap int\Gamma_j = \varnothing$.

Let $T_{ref,2} := \{(z_1,z_2) : 0 \leq z_1 \leq 1 - z_2 \leq 1; 0 \leq z_2 \leq 1\}$ be the reference element, then we define $\Gamma_j \in \mathcal{T}_{h,2}$ by

$$\Gamma_j := \{x = x^j + a^{1,j} z_1 + a^{2,j} z_2 \text{ with } a^{1,j}, a^{2,j} \in \mathbb{R}^3 \ , \ (z_1,z_2) \in T_{ref,2}\} \ .$$

Furthermore we define

$$S_h^{p_s}(T_{ref,2}) := \{\nu : T_{ref,2} \to \mathbb{R} : \nu(z_1,z_2) = \sum_{i+j \leq p_s} \alpha_{i,j} z_1^i z_2^j \text{ with } \alpha_{i,j} \in \mathbb{R}\}$$

the space of polynomials on $T_{ref,2}$ with degree p_s. Therefore we can set the space of splines for $p_s \geq 0$ as follows:

$$S_h^{p_s}(\Gamma_j) := \{\nu : \Gamma_j \to \mathbb{R} : \nu(x) = (\nu \circ F)(x) \ \text{ with } \ (\nu \circ F) \in S_h^{p_s}(T_{ref,2})\} \ ,$$

where $F : T_{ref,2} \to \Gamma_j$.
Let $V_h^p(\Gamma)$ denote the space of piecewise polynomial functions of degree p in Γ. For $p \geq 1$ $V_h^p(\Gamma)$ is continuous. Moreover, we define $\tilde{V}_h^p(\Gamma)$ as the space $V_h^p(\Gamma)$, where the polynomials vanish on $\partial\Gamma$ for $p \geq 1$. For $p = 0$, both spaces coincide. We will need $\tilde{V}_h^p(\Gamma)$ for the discretization of screens, see Chapter 6. For $p = 0$ and $p = 1$ we have:

$$V_h^0(\Gamma) = \{\nu \in L^2(\Gamma) : \nu|_{\Gamma_j} \in S_h^0(\Gamma_j) \ \forall \ \Gamma_j \in \mathcal{T}_{h.2}\} \subset H^{-1/2}(\Gamma) \ ,$$
$$V_h^1(\Gamma) = \{\nu \in C^0(\Gamma) : \nu|_{\Gamma_j} \in S_h^1(\Gamma_j) \ \forall \ \Gamma_j \in \mathcal{T}_{h,2}\} \subset H^{1/2}(\Gamma) \ .$$

We divide the time interval $\mathbb{R}_+ = (0,\infty)$ into Δt equidistant subintervals $I_n = (t_{n-1}, t_n]$ $n \in \mathbb{N}$. Here $t_n = n\Delta t$ and we take the discretization of a finite subinterval $\mathcal{T}_t := \{I_1,\dots,I_{N_t}\}$. We define with $V_{\Delta t}^q$ the space of piecewise polynomial functions of degree q in time. For $q \geq 1$, $V_{\Delta t}^q$ is continuous and vanishes at $t = 0$. We write

$$V_{h,\Delta t}^{p,q} = V_h^p \otimes V_{\Delta t}^q \tag{2.46}$$

as the tensor product of the approximation spaces in space and time associated to the space-time mesh $\mathcal{T}_h \times \mathcal{T}_t$.
Analogously:

$$\tilde{V}_{h,\Delta t}^{p,q} = \tilde{V}_h^p \otimes V_{\Delta t}^q \ . \tag{2.47}$$

In this thesis we use the notation:

- for the basis of piecewise constant functions in time, $\gamma^m_{\Delta t}(t) = H(t-t_{m-1}) - H(t-t_m)$
$$= \begin{cases} 1 \text{ , if } t \in (t_{m-1}, t_m] \\ 0 \text{ , else} \end{cases}$$

- for the basis of piecewise linear functions in time,
$$\beta^m_{\Delta t}(t) = (\Delta t)^{-1}((t - t_{m-1})\gamma^m_{\Delta t}(t) - (t - t_{m+1})\gamma^{m+1}_{\Delta t}(t))$$

- for the basis of piecewise constant functions in space, $\psi^i_h(x) = \begin{cases} 1 \text{ , if } x \in \Gamma_i \\ 0 \text{ , else} \end{cases}$

- for the basis of piecewise linear functions in space, $\xi^i_h(x)$.

2.3.1 The retarded single layer potential

We recapitulate the weak formulation: Find $p \in H^0_\sigma(\mathbb{R}_+, \widetilde{H}^{-1/2}(\Gamma))$ such that forall $q \in H^1_\sigma(\mathbb{R}_+, \widetilde{H}^{-1/2}(\Gamma))$, there hold

$$\int_0^\infty \int_\Gamma (Vp)\dot{q} ds_x \; e^{-2\sigma t} dt = \int_0^\infty \int_\Gamma f(x,t)\dot{q} \; ds_x e^{-2\sigma t} dt.$$

For $\tau = t - |x-y|$, we get

$$\int_0^\infty \int_\Gamma \int_\Gamma \frac{1}{4\pi} \frac{p(y,\tau)}{|x-y|} \dot{q}(x,t) ds_y ds_x e^{-2\sigma t} dt = \int_0^\infty \int_\Gamma f(x,t)\dot{q} \; ds_x e^{-2\sigma t} dt. \tag{2.48}$$

Then the discretized variational formulation reads: Find $p_{h,\triangle t} \in V^{p_1,q_1}_{h,\Delta t}$ such that for all $q_{h,\triangle t} \in V^{p_2,q_2}_{h,\Delta t}$:

$$\int_0^\infty \int_\Gamma \int_\Gamma \frac{1}{4\pi} \frac{p_{h,\Delta t}(y,\tau)}{|x-y|} \dot{q}_{h,\Delta t}(x,t) ds_y ds_x e^{-2\sigma t} dt = \int_0^\infty \int_\Gamma f(x,t)\dot{q}_{h,\Delta t} \; ds_x e^{-2\sigma t} dt \; . \tag{2.49}$$

Set $\sigma = 0$ and use piecewise constant ansatz function in space and in time, i.e.

$$p_{h,\Delta t}(x,t) = \sum_{m=1}^{N_t} \sum_{i=1}^{N_s} p^m_i \gamma^m_{\Delta t}(t)\psi^i_h(x) \quad \in V^{0,0}_{h,\Delta t} \quad . \tag{2.50}$$

We use piecewise constant test functions in space and time, i.e $q_{h,\Delta t}(x,t) \in V^{0,0}_{h,\Delta t}$. We write for $1 \le n \le N_t$ and $1 \le j \le N_s$ $q_{h,\Delta t}(x,t) = \gamma^n_{\Delta t}(t)\psi^j_h(x)$. This yields $\dot{q}_{h,\Delta t}(x,t) = \dot{\gamma}^n_{\Delta t}(t)\psi^j_h(x)$. Now let us compute the retarded single layer potential with this setting:

$$\begin{aligned} &\sum_{m=1}^{N_t} \sum_{i=1}^{N_s} p^m_i \int_0^\infty \int_\Gamma \int_\Gamma \frac{1}{4\pi} \frac{\gamma^m_{\Delta t}(\tau)\psi^i_h(y)}{|x-y|} \dot{\gamma}^n_{\Delta t}(t)\psi^j_h(x) \; ds_x ds_y dt \\ &= \sum_{m=1}^{N_t} \sum_{i=1}^{N_s} p^m_i \int_\Gamma \int_\Gamma \Big[\int_0^\infty \gamma^m_{\Delta t}(\tau)\dot{\gamma}^n_{\Delta t}(t) dt \Big] \frac{\psi^i_h(y)\psi^j_h(x)}{4\pi|x-y|} \; ds_x ds_y \; . \end{aligned} \tag{2.51}$$

The computation of the time integral may be found in the Appendix 9.1 (see (9.2)). It leads to the so-called acoustic lightcones.

$$E_l := \{(x,y) \in \Gamma \times \Gamma : t_l \leq |x-y| \leq t_{l+1}\} \subset \Gamma \times \Gamma$$

Let $\chi_A = \begin{cases} 1, x \in A \\ 0, x \notin A \end{cases}$ be the indicator function of the set A. Altogether we get for (2.51):

$$\begin{aligned} &\sum_{m=1}^{N_t} \sum_{i=1}^{N_s} p_i^m \int_\Gamma \int_\Gamma (\chi_{E_{n-m-1}}(x,y) - \chi_{E_{n-m}}(x,y)) \frac{\psi_h^i(y)\psi_h^j(x)}{4\pi|x-y|} ds_y ds_x \\ &= \sum_{m=1}^{N_t} \sum_{i=1}^{N_s} p_i^m \left[\iint\limits_{E_{n-m-1}} \frac{\psi_h^i(y)\psi_h^j(x)}{4\pi|x-y|} ds_y ds_x - \iint\limits_{E_{n-m}} \frac{\psi_h^i(y)\psi_h^j(x)}{4\pi|x-y|} ds_y ds_x \right] =: \sum_{m=1}^{N_t} V^{n-m} p^m \end{aligned} \tag{2.52}$$

where V^{n-m} is a matrix which has these two integrals as the i,j–th entry and p^m the corresponding vector with $p^m = \begin{pmatrix} p_1^m \\ \vdots \\ p_{N_s}^m \end{pmatrix}$. The integral over E_{n-m} disappears, if $n-m$ is negative. This integral also disappears if we have already passed the mesh, i.e. $n-m > [\frac{\operatorname{diam}\Gamma}{\Delta t}]$. V^{n-m} has only nonzero entries if the lightcone E_{n-m} or E_{n-m-1} intersects with the triangles of the mesh (see Figure 2.1). It is also enough to compute only the integral over E_{n-m} for timestep n, since we can use the integral from the previous timestep $n-1$ and change it's sign. Furthermore we can compute every entry of V^{n-m} in a parallelized fashion.

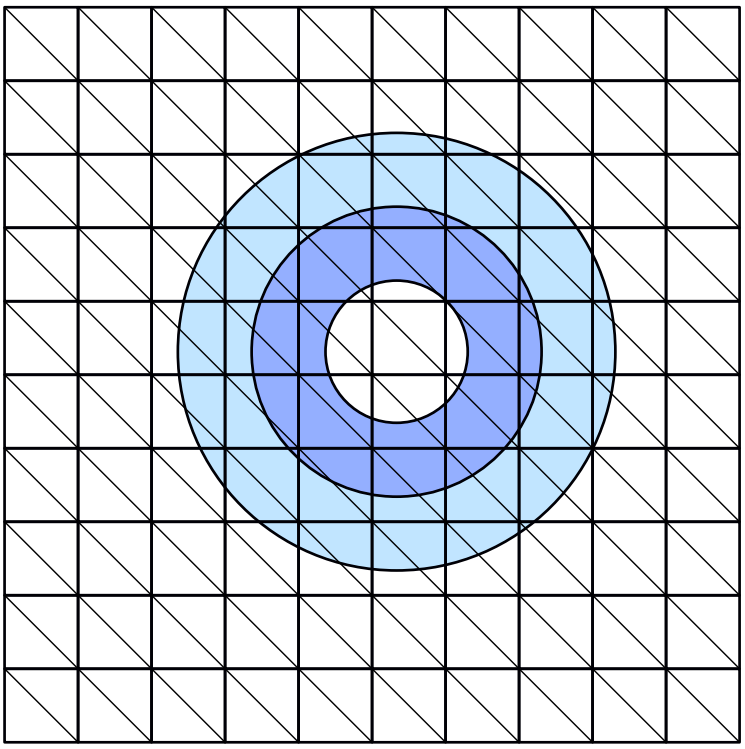

Figure 2.1: Sparsity of the retarded matrices for plane triangles

In the case depicted in Figure 2.1, i.e. for 2 lightcones, we only get entries for triangles intersecting the blue and lightblue colored area. Therefore the corresponding matrix is sparse. We calculate these integrals by using a composite *hp*-graded quadrature rule [84].

Let us consider the right hand side. We approximate f as follows:

$$f_{h,\Delta t}(x,t) = \sum_{m=1}^{N_t} f^m \gamma_{\Delta t}^m(t) \ ,$$

where $f^m = f(x,t_m)$. This yields for the right hand side:

$$\int_0^\infty \int_\Gamma f_{h,\Delta t}(x,t)\dot{\gamma}_{\Delta t}^n(t)\psi_h^j(x)ds_x dt = \sum_{m=1}^{N_t} \int_\Gamma f^m \left[\int_0^\infty \gamma_{\Delta t}^m(t)\dot{\gamma}_{\Delta t}^n(t)dt\right]\psi_h^j(x)ds_x. \tag{2.53}$$

We compute the time integral part in (2.53)

$$\begin{aligned}&\int_0^\infty \gamma_{\Delta t}^m(t)\frac{\partial\left[H(t-t_{n-1})-H(t-t_n)\right]}{\partial t}\,dt = \int_0^\infty \gamma_{\Delta t}^m(t)\left[\delta(t-t_{n-1})-\delta(t-t_n)\right]dt\\ &= \int_0^\infty \gamma_{\Delta t}^m(t)\delta(t-t_{n-1})dt - \int_0^\infty \gamma^m(t)\delta(t-t_n)dt = \gamma_{\Delta t}^m(t_{n-1}) - \gamma_{\Delta t}^m(t_n),\end{aligned}$$

to obtain

$$\int_0^\infty \int_\Gamma f_{h,\Delta t}(x,t)\dot{\gamma}_{\Delta t}^n(t)\psi_h^j(x)ds_x dt = \int_\Gamma \left[\sum_{m=1}^{N_t} f^m\gamma_{\Delta t}^m(t_{n-1}) - \sum_{m=1}^{N_t} f^m\gamma_{\Delta t}^m(t_n)\right]\psi_h^j(x)ds_x.$$

Since $\gamma^m(t_{n-1}) = 1$ if $t_{n-1} \in (t_{m-1}, t_m]$, therefore $t_{n-1} = t_m$ yields $n-1 = m$

$$\sum_{m=1}^{N_t} f^m\gamma_{\Delta t}^m(t_{n-1}) = f^{n-1} \quad \text{and} \quad \sum_{m=1}^{N_t} f^m\gamma_{\Delta t}^m(t_n) = f^n.$$

We get:

$$\int_0^\infty \int_\Gamma f_{h,\Delta t}(x,t)\dot{\gamma}_{\Delta t}^n(t)\psi_h^j(x)ds_x dt = \int_\Gamma \left[f^{n-1} - f^n\right]\psi_h^j(x)\ ds_x =: F^n.$$

We compute the integral in space by using the standard Gauss quadrature. Therefore (2.49) results in a space-time linear system:

$$\begin{pmatrix} V^0 & 0 & 0 & 0 & \cdots \\ V^1 & V^0 & 0 & 0 & \\ V^2 & V^1 & V^0 & 0 & \\ V^3 & V^2 & V^1 & V^0 & \ddots \\ \vdots & & & \ddots & \ddots \end{pmatrix}\begin{pmatrix} p^1 \\ p^2 \\ p^3 \\ p^4 \\ \vdots \end{pmatrix} = \begin{pmatrix} F^1 \\ F^2 \\ F^3 \\ F^4 \\ \vdots \end{pmatrix} .$$

Since we have a block lower triangular matrix this allows us to solve the system via forward substitution. This procedure is called the marching-on-in-time (MOT) algorithm (see Algorithm 1), [97]. We need to solve a linear equation system in every timestep n:

$$\sum_{m=1}^{n} V^{n-m}p^m = F^n \Leftrightarrow V^0 p^n = F^n - \sum_{m=1}^{n-1} V^{n-m}p^m \ . \tag{2.54}$$

We can also compute a discretized energy with (2.32) for $T = N_t(\Delta t)$:

$$\tilde{E}(T) := -\int_0^T \int_\Gamma \dot{p}_{h,\Delta t}(V p_{h,\Delta t}) ds_x dt \ . \tag{2.55}$$

Inserting $p_{h,\Delta t}$:

$$\tilde{E}(T) := -\int_0^T \int_\Gamma \Big(\sum_{n=1}^{N_t}\sum_{j=1}^{N_s} p_j^n \dot{\gamma}_{\Delta t}^n(t)\psi_h^j(x)\Big) \int_\Gamma \Big(\sum_{m=1}^{N_t}\sum_{i=1}^{N_s} p_i^m \frac{\gamma_{\Delta t}^m(t-|x-y|)\psi_h^i(y)}{4\pi|x-y|}\Big) ds_y ds_x dt \ .$$

The integral:

$$\int_{\Gamma\times\Gamma} \frac{\psi_h^i(y)\psi_h^j(x)}{4\pi|x-y|} \int_0^T \gamma_{\Delta t}^m(t-|x-y|)\dot{\gamma}_{\Delta t}^n(t) dt ds_y ds_x$$

gives us the i,j-th entry of the matrix V^{n-m}. Together with the vector $\vec{p} = \begin{pmatrix} p^1 \\ \vdots \\ p^{N_t} \end{pmatrix}$, we get

$$\tilde{E}(T) = -(p^1\ p^2\ \dots\ p^{N_t}) \begin{pmatrix} V^0 & 0 & \dots & 0 \\ V^1 & V^0 & \ddots & \vdots \\ \vdots & & \ddots & 0 \\ V^{N_t} & \dots & \dots & V^0 \end{pmatrix} \begin{pmatrix} p^1 \\ p^2 \\ \vdots \\ p^{N_t} \end{pmatrix} =: -\vec{p}^T \tilde{V} \vec{p} \ . \tag{2.56}$$

for $n = 1, 2, \dots$ **do**
  if $n - 1 > \left[\frac{\operatorname{diam}\Gamma}{\Delta t}\right]$ **then**

$$\frac{1}{4\pi}\int_{E_{n-1}} \frac{\psi_h^i(y)\psi_h^l(x)}{|x-y|}\, ds_x ds_y = 0, \quad \text{for } i,l = 1,\dots,N_s$$

  else
    Compute and store

$$\frac{1}{4\pi}\int_{E_{n-1}} \frac{\psi_h^i(y)\psi_h^l(x)}{|x-y|}\, ds_x ds_y, \quad \text{for } i,l = 1,\dots,N_s$$

  end if
  Construct and store (V_{il}^{n-1}) by using the stored computation in the timestep before, i.e. for $i,l = 1,\dots,N_s$

$$V_{il}^{n-1} = -\frac{1}{4\pi}\int_{E_{n-1}} \frac{\psi_h^i(y)\psi_h^l(x)}{|x-y|}\, ds_x ds_y + \frac{1}{4\pi}\int_{E_{n-2}} \frac{\psi_h^i(y)\psi_h^l(x)}{|x-y|}\, ds_x ds_y,$$

  Compute right hand side $f^{n-1} - f^n - \sum_{m=1}^{n-1} V^{n-m} p^m$
  Solve system of linear equations (2.54)
  Store solution p^n
end for

Algorithm 1: Marching-on-in-time algorithm for the retarded single layer potential with ansatz and testfunctions as in (2.50) and below.

2.3.2 The retarded adjoint double layer potential

We repeat the weak formulation: Find $p \in H^1_\sigma(\mathbb{R}_+, \widetilde{H}^{-1/2}(\Gamma))$ such that

$$\int_0^\infty e^{-2\sigma t}\langle (K' - \frac{1}{2}I)p, \dot{q}\rangle_\Gamma \,\mathrm{d}t = \int_0^\infty \int_\Gamma e^{-2\sigma t} f(x,t)\dot{q}(x,t)\mathrm{d}s_x \,\mathrm{d}t,$$

holds for all $q \in H^1_\sigma(\mathbb{R}_+, \widetilde{H}^{1/2}(\Gamma))$. Then the discretized weak variational formulation reads : Find $p \in V_{h,\Delta t}^{p_1,q_1}$ such that

$$\int_0^\infty e^{-2\sigma t}\langle (K' - \frac{1}{2}I)p_{h,\Delta t}, \dot{q}_{h,\Delta t}\rangle_\Gamma \,\mathrm{d}t = \int_0^\infty \int_\Gamma e^{-2\sigma t} f(t,x)\dot{q}_{h,\Delta t}(t,x)\mathrm{d}s_x \,\mathrm{d}t,$$

holds for all $q_{h,\Delta t} \in V_{h,\Delta t}^{p_2,q_2}$. For our computations we set $\sigma = 0$ and choose ansatz and test functions such that we get a MOT-scheme. For ansatz functions we choose piecewise constants in time and space, i.e.

$$p_{h,\Delta t}(x,t) = \sum_{m=1}^{N_t}\sum_{i=1}^{N_s} p_i^m \gamma_{\Delta t}^m(t)\psi_h^i(x) \in V_{h,\Delta t}^{0,0}. \tag{2.57}$$

For the derivative of the test function we choose piecewise constants in time and space, i.e.

$$\dot{q}_{h,\Delta t}(x,t) = \gamma_{\Delta t}^m(t)\psi_h^i(x) \in V_{h,\Delta t}^{0,0}.$$

We divide the computation into two parts:

$$\begin{aligned}\int_0^\infty \int_\Gamma (K' - \frac{1}{2}I)p_{h,\Delta t}(x,t)\dot{q}_{h,\Delta t}(x,t)ds_x dt &= \int_0^\infty \int_\Gamma K' p_{h,\Delta t}(x,t)\dot{q}_{h,\Delta t}(x,t)ds_x dt \\ &\quad - \frac{1}{2}\int_0^\infty \int_\Gamma I p_{h,\Delta t}(x,t)\dot{q}_{h,\Delta t}(x,t)ds_x dt\ .\end{aligned}$$

Let us consider the retarded adjoint double layer potential first. Inserting the ansatz and test function

$$\begin{aligned}&\int_0^\infty \int_\Gamma K' p_{h,\Delta t}(x,t)\dot{q}_{h,\Delta t}(x,t)ds_x dt \\ &= \sum_{m=1}^{N_t}\sum_{i=1}^{N_s} p_i^m \int_0^\infty \iint_{\Gamma\times\Gamma} \frac{n_x\cdot(x-y)}{4\pi|x-y|}\Big(\frac{\gamma_{\Delta t}^m(\tau)\psi_h^i(y)}{|x-y|^2} + \frac{\dot{\gamma}_{\Delta t}^m(\tau)\psi_h^j(y)}{|x-y|}\Big)\gamma_{\Delta t}^n(t)\psi_h^j(x)ds_y ds_x dt \\ &= \sum_{m=1}^{N_t}\sum_{i=1}^{N_s} p_i^m \iint_{\Gamma\times\Gamma} \frac{n_x\cdot(x-y)}{4\pi|x-y|}\Big(\frac{\psi_h^i(y)\psi_h^j(x)}{|x-y|^2}\int_0^\infty \gamma_{\Delta t}^m(\tau)\gamma_{\Delta t}^n(t)dt \\ &+ \frac{\psi_h^i(y)\psi_h^j(x)}{|x-y|}\int_0^\infty \dot{\gamma}_{\Delta t}^m(\tau)\gamma_{\Delta t}^n(t)dt\Big)ds_y ds_x\end{aligned}$$

The time integrals are computed in the Appendix 9.1, see (9.5) and (9.3). We get

$$
\begin{aligned}
&\int_0^\infty \int_\Gamma K' p_{h,\Delta t}(x,t)\dot{q}_{h,\Delta t}(x,t)ds_x dt \\
&= \sum_{m=1}^{N_t}\sum_{i=1}^{N_s} p_i^m \iint_{\Gamma\times\Gamma} \frac{n_x\cdot(x-y)}{4\pi|x-y|}\Bigg(\frac{\psi_h^i(y)\psi_h^j(x)}{|x-y|^2}\Big((t_{n-m+1}-|x-y|)\chi_{E_{n-m}}(x,y) \\
&+ (-t_{n-m-1}+|x-y|)\chi_{E_{n-m-1}}(x,y)\Big) + \frac{\psi_h^i(y)\psi_h^j(x)}{|x-y|}\Big(\chi_{E_{n-m}}(x,y)-\chi_{E_{n-m-1}}(x,y)\Big)\Bigg) ds_y ds_x \\
&= \sum_{m=1}^{N_t}\sum_{i=1}^{N_s} p_i^m \iint_{\Gamma\times\Gamma} \frac{n_x\cdot(x-y)}{4\pi|x-y|}\Bigg(\frac{\psi_h^i(y)\psi_h^j(x)}{|x-y|^2} t_{n-m+1}\chi_{E_{n-m}}(x,y) - \frac{\psi_h^i(y)\psi_h^j(x)}{|x-y|}\chi_{E_{n-m}}(x,y) \\
&- \frac{\psi_h^i(y)\psi_h^j(x)}{|x-y|^2} t_{n-m-1}\chi_{E_{n-m-1}}(x,y) + \frac{\psi_h^i(y)\psi_h^j(x)}{|x-y|}\chi_{E_{n-m-1}}(x,y) \\
&+ \frac{\psi_h^i(y)\psi_h^j(x)}{|x-y|}\chi_{E_{n-m}}(x,y) - \frac{\psi_h^i(y)\psi_h^j(x)}{|x-y|}\chi_{E_{n-m-1}}(x,y)\Bigg) ds_y ds_x \\
&= \sum_{m=1}^{N_t}\sum_{i=1}^{N_s} p_i^m \Bigg(t_{n-m+1}\iint_{E_{n-m}} \frac{n_x\cdot(x-y)\psi_h^i(y)\psi_h^j(x)}{4\pi|x-y|^3} ds_y ds_x \\
&- t_{n-m-1}\iint_{E_{n-m-1}} \frac{n_x\cdot(x-y)\psi_h^i(y)\psi_h^j(x)}{4\pi|x-y|^3} ds_y ds_x\Bigg) = \sum_{m=1}^{N_t} K'^m p^m \ ,
\end{aligned}
$$

where $t_k = k(\Delta t)$ with $k \in \mathbb{Z}$ and K'^k has entries of the both integral above. Remember that the integral vanishes if $n-m$ is negative. This gives us the following space-time matrix:

$$
\begin{pmatrix}
K'^0 & 0 & 0 & 0 & \cdots \\
K'^1 & K'^0 & 0 & 0 & \\
K'^2 & K'^1 & K'^0 & 0 & \\
K'^3 & K'^2 & K'^1 & K'^0 & \ddots \\
\vdots & & & \ddots & \ddots
\end{pmatrix} .
$$

Next considering the identity part, leading to the mass matrix I:

$$
\begin{aligned}
&\frac{1}{2}\int_0^\infty \int_\Gamma I p_{h,\Delta t}(x,t)\dot{q}_{h,\Delta t}(x,t)ds_x dt = \frac{1}{2}\sum_{m=1}^{N_t}\sum_{i=1}^{N_s} p_i^m \int_0^\infty \int_\Gamma \gamma_{\Delta t}^m(t)\psi_h^i(x)\gamma_{\Delta t}^n(t)\psi_h^j(x)ds_x dt \\
&= \frac{1}{2}\sum_{m=1}^{N_t}\sum_{i=1}^{N_s} p_i^m \int_\Gamma \psi_h^i(x)\psi_h^j(x)ds_x \int_0^\infty \gamma_{\Delta t}^m(t)\gamma_{\Delta t}^n(t)dt \\
&= \frac{1}{2}\sum_{m=1}^{N_t}\sum_{i=1}^{N_s} p_i^m \int_\Gamma \psi_h^i(x)\psi_h^j(x)ds_x \int_{t_{n-1}}^{t_n} H(t-t_{m-1}) - H(t-t_m)dt \\
&= \frac{1}{2}(\Delta t)\sum_{i=1}^{N_s} p_i^n \int_\Gamma \psi_h^i(x)\psi_h^j(x)ds_x = \frac{1}{2}(\Delta t) I p^n \ ,
\end{aligned}
$$

where we used that the time integral is nonzero only if $n = m$. For the right hand side, we approximate f in time with piecewise linear functions:

$$f_{h,\Delta t}(x,t) = \sum_{m=1}^{N_t} f^m \beta^m_{\Delta t}(t),$$

where $f^m = f(x,t_m)$. This gives:

$$\int_0^\infty \int_\Gamma f_{h,\Delta t}(x,t)\gamma^n(t)\xi^j_h(x)ds_x dt = \sum_{m=1}^{N_t} \int_\Gamma f^m \left[\int_0^\infty \beta^m_{\Delta t}(t)\gamma^n_{\Delta t}(t)dt\right]\xi^j_h(x)ds_x. \quad (2.58)$$

We compute the time integral part of (2.58)

$$\begin{aligned}&\int_0^\infty \beta^m_{\Delta t}(t)\gamma^n_{\Delta t}(t)dt = \int_{t_{n-1}}^{t_n} \beta^m_{\Delta t}(t)dt \\ &= \int_{t_{n-1}}^{t_n} (\Delta t)^{-1}(t - t_{m-1})\gamma^m_{\Delta t}(t)dt - \int_{t_{n-1}}^{t_n} (\Delta t)^{-1}(t - t_{m+1})\gamma^{m+1}_{\Delta t}(t)dt\ .\end{aligned}$$

For $n = m$ the second integral vanishes and the first integral is $\frac{(\Delta t)}{2}$. For $n = m+1 \Leftrightarrow n-1 = m$ the first integral vanishes and the second integral is $\frac{(\Delta t)}{2}$. In every other case both integrals vanish. We get:

$$\int_0^\infty \int_\Gamma f_{h,\Delta t}(x,t)\gamma^n_{\Delta t}(t)\xi^j_h(x)ds_x dt = \frac{(\Delta t)}{2}\int_\Gamma (f^n + f^{n-1})\xi^j_h(x)ds_x =: F^n\ .$$

We compute the integral in space:

$$\int_\Gamma (f^n + f^{n-1})\xi^j_h(x)ds_x$$

with a standard Gauss quadrature.

Altogether we get the following space-time linear system:

$$\begin{pmatrix} K'^0 - \frac{1}{2}(\Delta t)I & 0 & 0 & 0 & \cdots \\ K'^1 & K'^0 - \frac{1}{2}(\Delta t)I & 0 & 0 & \\ K'^2 & K'^1 & K'^0 - \frac{1}{2}(\Delta t)I & 0 & \\ K'^3 & K'^2 & K'^1 & K'^0 - \frac{1}{2}(\Delta t)I & \ddots \\ \vdots & & & \ddots & \ddots \end{pmatrix}\begin{pmatrix} p^1 \\ p^2 \\ p^3 \\ p^4 \\ \vdots \end{pmatrix} = \begin{pmatrix} F^1 \\ F^2 \\ F^3 \\ F^4 \\ \vdots \end{pmatrix}.$$

Again we take advantage of the block lower triangular scheme of the space-time matrix. For every timestep n, we solve the system:

$$(K'^0 - \frac{1}{2}(\Delta t)I)p^n = F^n - \sum_{m=1}^{n-1} K'^{n-m}p^m \quad (2.59)$$

Compute and store

$$I_{il} = \frac{\Delta t}{2} \int_\Gamma \phi_h^i(x)\phi_h^l(x) ds_x ds_y, \quad i,l = 1,...,N_s$$

for $n = 1, 2, \dots$ **do**
if $n - 1 > \left[\frac{\operatorname{diam}\Gamma}{\Delta t}\right]$ **then**

$$k'^{n-1}_{i,j} = \frac{1}{4\pi} \int_{E_{n-1}} \frac{n_x \cdot (x-y)\psi_h^i(y)\psi_h^j(x)}{|x-y|^3}\, ds_x ds_y = 0, \quad i,j = 1,\dots,N_s$$

else
Compute and store

$$k'^{n-1}_{i,j} = \frac{1}{4\pi} \int_{E_{n-1}} \frac{n_x \cdot (x-y)\psi_h^i(y)\psi_h^j(x)}{|x-y|^3}\, ds_x ds_y, \quad i,j = 1,\dots,N_s$$

end if
Construct and store (K'^{n-1}) by using the stored computation in the timestep before and multiply with the corresponding time factors, i.e.

$$K'^{n-1} = t_n k'^{n-1} - t_{n-2} k'^{n-2}$$

Compute right hand side $F^n - \sum_{m=1}^{n-1} K'^{n-m} p^m$
Solve system of linear equations (2.59)
Store solution p^n
end for

Algorithm 2: Marching-on-in-time algorithm for the retarded adjoint double layer potential with ansatz and testfunctions as in (2.57) and below.

2.3.3 The retarded double layer potential

The weak formulation reads: Find $\varphi \in H^1_\sigma(\mathbb{R}_+, \widetilde{H}^{1/2}(\Gamma))$ such that

$$\int_0^\infty e^{-2\sigma t} \langle (K + \frac{1}{2} I) p, \dot{q} \rangle_\Gamma \,\mathrm{dt} = \int_0^\infty \int_\Gamma e^{-2\sigma t} f(t,x) \dot{q}(t,x) \mathrm{d}s_x \,\mathrm{dt},$$

holds for all $q \in H^1_\sigma(\mathbb{R}_+, \widetilde{H}^{-1/2}(\Gamma))$. The discretized weak variational formulation reads: Find $\varphi_{h,\Delta t} \in V^{p_1,q_1}_{h,\Delta t}$ such that

$$\int_0^\infty e^{-2\sigma t} \langle (K + \frac{1}{2} I) p_{h,\Delta t}, \dot{q}_{h,\Delta t} \rangle_\Gamma \,\mathrm{dt} = \int_0^\infty \int_\Gamma e^{-2\sigma t} f(t,x) \dot{q}_{h,\Delta t}(t,x) \mathrm{d}s_x \,\mathrm{dt},$$

holds for all $q_{h,\Delta t} \in V^{p_2,q_2}_{h,\Delta}$.

As before we set $\sigma = 0$ and choose ansatz and test functions such that we get a MOT-scheme. We can use the same ansatz and test functions in space and time as in Subsection 2.3.2. For ansatz functions we choose piecewise constant in time and space, i.e.

$$\varphi_{h,\Delta t}(x,t) = \sum_{m=1}^{N_t}\sum_{i=1}^{N_s}\varphi_i^m\gamma_{\Delta t}^m(t)\psi_h^i(x) \in V_{h,\Delta t}^{0,0}. \tag{2.60}$$

For the derivative of the test function we choose piecewise constant in time and space, i.e.

$$\dot{q}_{h,\Delta t}(x,t) = \gamma_{\Delta t}^m(t)\psi_h^i(x) \in V_{h,\Delta t}^{0,0}.$$

We divide the computation into two parts:

$$\begin{aligned}\int_0^\infty\int_\Gamma (K+\frac{1}{2}I)\varphi_{h,\Delta t}(x,t)\dot{q}_{h,\Delta t}(x,t)ds_x dt = &\int_0^\infty\int_\Gamma K\varphi_{h,\Delta t}(x,t)\dot{q}_{h,\Delta t}(x,t)ds_x dt\\ &+\frac{1}{2}\int_0^\infty\int_\Gamma I\varphi_{h,\Delta t}(x,t)\dot{q}_{h,\Delta t}(x,t)ds_x dt\ .\end{aligned}$$

For the identity part I we obtain the same result as in Subsection 2.3.2. Let us consider the retarded double layer potential . Inserting $\varphi_{h,\Delta t}$ and $\dot{q}_{h,\Delta t}$:

$$\begin{aligned}&\int_0^\infty\int_\Gamma K\varphi_{\Delta t,h}\dot{q}_{\Delta t,h}ds_x dt\\ &= \sum_{m=1}^{N_t}\sum_{i=1}^{N_s}\varphi_i^m\int_0^\infty\iint_{\Gamma\times\Gamma}\frac{n_y\cdot(x-y)}{4\pi|x-y|}\Big(\frac{\gamma_{\Delta t}^m(\tau)\psi_h^i(y)}{|x-y|^2}+\frac{\dot{\gamma}_{\Delta t}^m(\tau)\psi_h^j(y)}{|x-y|}\Big)\gamma_{\Delta t}^n(t)\psi_h^j(x)ds_y ds_x dt\\ &= \sum_{m=1}^{N_t}\sum_{i=1}^{N_s}\varphi_i^m\iint_{\Gamma\times\Gamma}\frac{n_y\cdot(x-y)}{4\pi|x-y|}\Big(\frac{\psi_h^i(y)\psi_h^j(x)}{|x-y|^2}\int_0^\infty\gamma_{\Delta t}^m(\tau)\gamma_{\Delta t}^n(t)dt\\ &+\frac{\psi_h^i(y)\psi_h^j(x)}{|x-y|}\int_0^\infty\dot{\gamma}_{\Delta t}^m(\tau)\gamma_{\Delta t}^n(t)dt\Big)ds_y ds_x\end{aligned}$$

The time integrals are computed in the Appendix 9.1, see (9.5) and (9.3). We get

$$\begin{aligned}&\int_0^\infty\int_\Gamma K\varphi_{\Delta t,h}\dot{q}_{\Delta t,h}ds_x dt\\ &= \sum_{m=1}^{N_t}\sum_{i=1}^{N_s}\varphi_i^m\iint_{\Gamma\times\Gamma}\frac{n_y\cdot(x-y)}{4\pi|x-y|}\Bigg(\frac{\psi_h^i(y)\psi_h^j(x)}{|x-y|^2}\Big((t_{n-m+1}-|x-y|)\chi_{E_{n-m}}(x,y)\\ &+(-t_{n-m-1}+|x-y|)\chi_{E_{n-m-1}}(x,y)\Big)+\frac{\psi_h^i(y)\psi_h^j(x)}{|x-y|}\Big(\chi_{E_{n-m}}(x,y)-\chi_{E_{n-m-1}}(x,y)\Big)\Bigg)ds_y ds_x\\ &= \sum_{m=1}^{N_t}\sum_{i=1}^{N_s}\varphi_i^m\iint_{\Gamma\times\Gamma}\frac{n_y\cdot(x-y)}{4\pi|x-y|}\Bigg(\frac{\psi_h^i(y)\psi_h^j(x)}{|x-y|^2}t_{n-m+1}\chi_{E_{n-m}}(x,y)-\frac{\psi_h^i(y)\psi_h^j(x)}{|x-y|}\chi_{E_{n-m}}(x,y)\end{aligned}$$

$$
\begin{aligned}
&- \frac{\psi_h^i(y)\psi_h^j(x)}{|x-y|^2} t_{n-m-1}\chi_{E_{n-m-1}}(x,y) + \frac{\psi_h^i(y)\psi_h^j(x)}{|x-y|}\chi_{E_{n-m-1}}(x,y) \\
&+ \frac{\psi_h^i(y)\psi_h^j(x)}{|x-y|}\chi_{E_{n-m}}(x,y) - \frac{\psi_h^i(y)\psi_h^j(x)}{|x-y|}\chi_{E_{n-m-1}}(x,y)\Bigg) ds_y ds_x \\
&= \sum_{m=1}^{N_t}\sum_{i=1}^{N_s} \varphi_i^m \iint\limits_{\Gamma\times\Gamma} \frac{n_y\cdot(x-y)}{4\pi|x-y|}\Bigg(\frac{\psi_h^i(y)\psi_h^j(x)}{|x-y|^2} t_{n-m+1}\chi_{E_{n-m}}(x,y) \\
&+ \frac{\psi_h^i(y)\psi_h^j(x)}{|x-y|^2} t_{n-m-1}\chi_{E_{n-m-1}}(x,y)\Bigg) ds_y ds_x \\
&= \sum_{m=1}^{N_t}\sum_{i=1}^{N_s} \varphi_i^m \Bigg(t_{n-m+1} \iint\limits_{E_{n-m}} \frac{n_y\cdot(x-y)\psi_h^i(y)\psi_h^j(x)}{4\pi|x-y|^3} ds_y ds_x \\
&- t_{n-m-1} \iint\limits_{E_{n-m-1}} \frac{n_y\cdot(x-y)\psi_h^i(y)\psi_h^j(x)}{4\pi|x-y|^3} ds_y ds_x \Bigg) = \sum_{m=1}^{N_t} K^m\varphi^m \ ,
\end{aligned}
$$

where $t_k = k(\Delta t)$ with $k \in \mathbb{Z}$ and K^k contains entries from both of the integrals above. Remember that the integral vanishes if $n-m$ is negative. This gives us the following space-time matrix:

$$
\begin{pmatrix}
K^0 & 0 & 0 & 0 & \cdots \\
K^1 & K^0 & 0 & 0 & \\
K^2 & K^1 & K^0 & 0 & \\
K^3 & K^2 & K^1 & K^0 & \ddots \\
\vdots & & & \ddots & \ddots
\end{pmatrix} .
$$

With the right hand side as in Subsection 2.3.2, altogether we get the following space-time linear system:

$$
\begin{pmatrix}
K^0 + \frac{1}{2}(\Delta t)I & 0 & 0 & 0 & \cdots \\
K^1 & K^0 + \frac{1}{2}(\Delta t)I & 0 & 0 & \\
K^2 & K^1 & K^0 + \frac{1}{2}(\Delta t)I & 0 & \\
K^3 & K^2 & K^1 & K^0 + \frac{1}{2}(\Delta t)I & \ddots \\
\vdots & & & \ddots & \ddots
\end{pmatrix}
\begin{pmatrix} \varphi^1 \\ \varphi^2 \\ \varphi^3 \\ \varphi^4 \\ \vdots \end{pmatrix} =
\begin{pmatrix} F^1 \\ F^2 \\ F^3 \\ F^4 \\ \vdots \end{pmatrix} .
$$

Taking advantage of the block lower triangular scheme of the space-time matrix the MOT-scheme reads:

$$
(K^0 + \frac{1}{2}(\Delta t))\varphi^n = F^n - \sum_{m=1}^{n-1} K^{n-m}\varphi^m \ . \tag{2.61}
$$

Compute and store

$$I_{il} = \frac{\Delta t}{2} \int_\Gamma \phi_h^i(x)\phi_h^l(x) ds_x ds_y, \quad i,l = 1,...,N_s$$

for $n = 1, 2, \dots$ **do**
if $n-1 > \left[\frac{\operatorname{diam}\Gamma}{\Delta t}\right]$ **then**

$$k_{i,j}^{n-1} = \frac{1}{4\pi} \int_{E_{n-1}} \frac{n_x \cdot (x-y)\psi_h^i(y)\psi_h^j(x)}{|x-y|^3} \, ds_x ds_y = 0, \quad i,j = 1,\dots,N_s$$

else
Compute and store

$$k_{i,j}^{n-1} = \frac{1}{4\pi} \int_{E_{n-1}} \frac{n_x \cdot (x-y)\psi_h^i(y)\psi_h^j(x)}{|x-y|^3} \, ds_x ds_y, \quad i,j = 1,\dots,N_s$$

end if
Construct and store (K^{n-1}) by using the stored computation in the timestep before and multiply with the corresponding time factors, i.e.

$$K^{n-1} = t_n k'^{n-1} - t_{n-2} k'^{n-2}$$

Compute right hand side $F^n - \sum_{m=1}^{n-1} K^{n-m}\varphi^m$
Solve system of linear equations (2.61)
Store solution φ^n
end for

Algorithm 3: Marching-on-in-time algorithm for the retarded double layer potential with ansatz and testfunctions as in (2.60) and below.

2.3.4 The retarded hypersingular integral operator

Recapitulating the variational formulation: Find $\varphi \in H^1_\sigma(\mathbb{R}^+, \widetilde{H}^{\frac{1}{2}}(\Gamma))$ such that for all $\Psi \in H^1_\sigma(\mathbb{R}^+, \widetilde{H}^{\frac{1}{2}}(\Gamma))$ there holds:

$$\int_{\mathbb{R}^+\times\Gamma} (W\varphi)\ \partial_t\Psi\, e^{-2\sigma t} dt\, ds_x \ = \int_{\mathbb{R}^+\times\Gamma} f\ \partial_t\Psi\, e^{-2\sigma t} dt\, ds_x \ .$$

We will need the formula from [55, Lemma 4 b]

$$\begin{aligned}
&\int_{\mathbb{R}^+\times\Gamma} (W\varphi(x,t))\ \partial_t\Psi(x,t)\, e^{-2\sigma t} ds_x dt \\
&= \frac{1}{4\pi} \int_0^\infty \iint_{\Gamma\times\Gamma} \left\{ \frac{-n_x \cdot n_y}{|x-y|} \dot\varphi(y,\tau)\ddot\Psi(x,t) + \frac{(\operatorname{curl}_\Gamma \varphi)(y,\tau) \cdot (\operatorname{curl}_\Gamma \dot\Psi)(x,t)}{|x-y|} \right\} ds_y ds_x e^{-2\sigma t} dt.
\end{aligned}$$

The discretized weak variational formulation reads:

Find $\varphi_{h,\Delta t} \in V_{h,\Delta t}^{p_1,q_1}$ such that for all $\Psi_{h,\Delta t} \in V_{h,\Delta t}^{p_2,q_2}$

$$\int_0^\infty \int_\Gamma (W\phi_{h,\Delta t}(x,t))\partial_t \Psi_{h,\Delta t}(x,t)\, ds_x\, e^{-2\sigma t} dt = \int_0^\infty \int_\Gamma f(x,t)\partial_t \Psi_{h,\Delta t}(x,t)\, ds_x\, e^{-2\sigma t} dt\,. \tag{2.62}$$

Again we set $\sigma = 0$. For our discretization we use piecewise linear ansatz functions in space and time, i.e.

$$\varphi_{h,\Delta t} = \sum_{m=1}^{N_t}\sum_{i=1}^{N_s} \varphi_i^m \beta_{\Delta t}^m(t)\xi_h^i(x) \in V_{h,\Delta t}^{1,1}\,. \tag{2.63}$$

For the test function we choose with $1 \le n \le N_t$ and $1 \le j \le N_s$:

$$\dot{\Psi}_{h,\Delta t}(x,t) = \gamma_{\Delta t}^n(t)\xi_h^j(x) \in V_{h,\Delta t}^{1,0}.$$

We compute

$$\begin{aligned}
&\int_0^\infty \int_\Gamma W\varphi_{h,\Delta t}(x,t)\cdot\dot{\Psi}_{h,\Delta t}(x,t)\; ds_x dt = \frac{1}{4\pi}\int_0^\infty \iint_{\Gamma\times\Gamma} \left\{ \frac{-n_x\cdot n_y}{|x-y|}\dot{\varphi}_{h,\Delta t}(y,\tau)\ddot{\Psi}_{h,\Delta t}(x,t)\right.\\
&\left. + \frac{(\operatorname{curl}_\Gamma \varphi_{h,\Delta t})(y,\tau)\cdot(\operatorname{curl}_\Gamma \dot{\Psi}_{h,\Delta t})(x,t)}{|x-y|}\right\} ds_y ds_x dt\\
&= \sum_{m=1}^{N_t}\sum_{i=1}^{N_s} \varphi_i^m \frac{-1}{4\pi}\int_0^\infty \iint_{\Gamma\times\Gamma} \frac{n_x\cdot n_y}{|x-y|}\left(\dot{\beta}_{\Delta t}^m(\tau)\xi_h^i(y)\right)\cdot\left(\dot{\gamma}_{\Delta t}^n(t)\xi_h^j(x)\right) ds_y ds_x dt\\
&+ \sum_{m=1}^{N_t}\sum_{i=1}^{N_s} \varphi_i^m \frac{1}{4\pi}\int_0^\infty \iint_{\Gamma\times\Gamma} \frac{\beta_{\Delta t}^m(\tau)(\operatorname{curl}_\Gamma \xi_h^i)(y)\cdot\gamma_{\Delta t}^n(t)(\operatorname{curl}_\Gamma \xi_h^j)(x)}{|x-y|} ds_y ds_x dt\\
&= \sum_{m=1}^{N_t}\sum_{i=1}^{N_s} \varphi_i^m \frac{-1}{4\pi}\iint_{\Gamma\times\Gamma} \frac{n_x\cdot n_y}{|x-y|}\left(\xi_h^i(y)\right)\cdot\left(\xi_h^j(x)\right)\int_0^\infty \dot{\beta}_{\Delta t}^m(\tau)\dot{\gamma}_{\Delta t}^n(t) dt ds_y ds_x\\
&+ \sum_{m=1}^{N_t}\sum_{i=1}^{N_s} \varphi_i^m \frac{1}{4\pi}\iint_{\Gamma\times\Gamma} \frac{(\operatorname{curl}_\Gamma \xi_h^i)(y)\cdot(\operatorname{curl}_\Gamma \xi_h^j)(x)}{|x-y|}\int_0^\infty \beta_{\Delta t}^m(\tau)\gamma_{\Delta t}^n(t) dt ds_y ds_x\,.
\end{aligned}$$

The time integrals are computed in the Appendix 9.1 (see (9.4) and (9.9)). We get:

$$\begin{aligned}
&\sum_{m=1}^{N_t}\sum_{i=1}^{N_s} \varphi_i^m \frac{-1}{4\pi}\iint_{\Gamma\times\Gamma} \frac{n_x\cdot n_y}{|x-y|}\left(\xi_h^i(y)\right)\cdot\left(\xi_h^j(x)\right)\int_0^\infty \dot{\beta}_{\Delta t}^m(\tau)\dot{\gamma}_{\Delta t}^n(t) dt ds_y ds_x\\
&= \sum_{m=1}^{N_t}\sum_{i=1}^{N_s} \varphi_i^m \Big[-\frac{1}{(\Delta t)}\iint_{E_{n-m}} \frac{(n_x\cdot n_y)\xi_h^i(y)\xi_h^j(x)}{|x-y|4\pi} ds_y ds_x\\
&+ \frac{2}{(\Delta t)}\iint_{E_{n-m-1}} \frac{(n_x\cdot n_y)\xi_h^i(y)\xi_h^j(x)}{|x-y|4\pi} ds_y ds_x - \frac{1}{(\Delta t)}\iint_{E_{n-m-2}} \frac{(n_x\cdot n_y)\xi_h^i(y)\xi_h^j(x)}{|x-y|4\pi} ds_y ds_x\Big]
\end{aligned}$$

and

$$\begin{aligned}
&\sum_{m=1}^{N_t}\sum_{i=1}^{N_s} \varphi_i^m \frac{1}{4\pi}\iint_{\Gamma\times\Gamma} \frac{(\operatorname{curl}_\Gamma \xi_h^i)(y)\cdot(\operatorname{curl}_\Gamma \xi_h^j)(x)}{|x-y|}\int_0^\infty \beta_{\Delta t}^m(\tau)\gamma_{\Delta t}^n(t) dt ds_y ds_x\\
&= \sum_{m=1}^{N_t}\sum_{i=1}^{N_s} \varphi_i^m \frac{1}{4\pi}\iint_{\Gamma\times\Gamma} \frac{(\operatorname{curl}_\Gamma \xi_h^i)(y)\cdot(\operatorname{curl}_\Gamma \xi_h^j)(x)}{|x-y|}\mathcal{Y}^{n-m}(x,y) ds_y ds_x\,,
\end{aligned}$$

where

$$\begin{aligned}
\mathcal{Y}^{n-m}(x,y) &= \frac{1}{2(\Delta t)}(|x-y|^2 - 2|x-y|(n-m+1)(\Delta t) + ((n-m+1)(\Delta t))^2)\chi_{E_{n-m}}(x,y) \\
&+ \frac{1}{2(\Delta t)}(|x-y|^2 - 2|x-y|(n-m-2)(\Delta t) + ((n-m-2)(\Delta t))^2)\chi_{E_{n-m-2}}(x,y) \\
&+ \frac{1}{2(\Delta t)}(-2|x-y|^2 + 2|x-y|((n-m-1)(\Delta t) + (n-m)(\Delta t)) \\
&- (((n-m-1)(\Delta t))^2 + ((n-m)(\Delta t))^2) + 2(\Delta t)^2)\chi_{E_{n-m-1}}(x,y).
\end{aligned}$$

Altogether we get:

$$\begin{aligned}
&\int_0^\infty \int_\Gamma W\varphi_{\Delta t,h}(x,t)\cdot\dot{\Psi}_{\Delta t,h}(x,t)\; ds_x dt \\
&= \sum_{m=1}^{N_t}\sum_{i=1}^{N_s}\varphi_i^m\Big[-\frac{1}{(\Delta t)}\iint_{E_{n-m}}\frac{(n_x\cdot n_y)\xi_h^i(y)\xi_h^j(x)}{|x-y|4\pi}ds_y ds_x \\
&+ \frac{2}{(\Delta t)}\iint_{E_{n-m-1}}\frac{(n_x\cdot n_y)\xi_h^i(y)\xi_h^j(x)}{|x-y|4\pi}ds_y ds_x - \frac{1}{(\Delta t)}\iint_{E_{n-m-2}}\frac{(n_x\cdot n_y)\xi_h^i(y)\xi_h^j(x)}{|x-y|4\pi}ds_y ds_x\Big] \\
&+ \sum_{m=1}^{N_t}\sum_{i=1}^{N_s}\varphi_i^m\frac{1}{4\pi}\iint_{\Gamma\times\Gamma}\frac{(\mathrm{curl}_\Gamma\,\xi_h^i)(y)\cdot(\mathrm{curl}_\Gamma\,\xi_h^j)(x)}{|x-y|}\mathcal{Y}^{n-m}(x,y)ds_y ds_x = \sum_{m=1}^{N_t}W^{n-m}\varphi^m.
\end{aligned}$$

The right hand side is the same as in Subsection 2.3.2.

Now we can write (2.43) in a space-time linear system:

$$\begin{pmatrix} W^0 & 0 & 0 & 0 & \cdots \\ W^1 & W^0 & 0 & 0 & \\ W^2 & W^1 & W^0 & 0 & \\ W^3 & W^2 & W^1 & W^0 & \ddots \\ \vdots & & & \ddots & \ddots \end{pmatrix}\begin{pmatrix}\varphi^1\\ \varphi^2\\ \varphi^3\\ \varphi^4\\ \vdots\end{pmatrix} = \begin{pmatrix}F^1\\ F^2\\ F^3\\ F^4\\ \vdots\end{pmatrix}.$$

Since we have a block lower triangular matrix we can use the marching-on-in-time (MOT) algorithm as for the retarded hypersingular integral operator. We get for the current timestep n

$$\sum_{m=1}^{n}W^{n-m}\varphi^m = F^n \Leftrightarrow W^0\varphi^n = F^n - \sum_{m=1}^{n-1}W^{n-m}\varphi^m\ . \tag{2.64}$$

2.3.5 Retarded Poincaré-Steklov operator

We begin this subsection with an existence and uniqueness result of the retarded Poincaré-Steklov operator in (2.16). From [88], p. 48:

Set $w^{-1}_{i,curl}, w^{-2}_{i,curl}, w^{-1}_1, w^{-2}_1$ to zero.
for $n = 1, 2, \ldots$ **do**
  if $n - 1 > \left[\frac{\operatorname{diam}\Gamma}{\Delta t}\right]$ **then**
    for $i, j = 1, \ldots, N_s$ **do**

$$w^{n-1}_{1,(i,j)} = \iint_{E_{n-m}} \frac{(n_x \cdot n_y)\xi^i_h(y)\xi^j_h(x)}{|x-y|4\pi} ds_y ds_x = 0$$

$$w^{n-1}_{1,curl,(i,j)} = \frac{1}{4\pi} \iint_{E_{n-1}} \frac{(\operatorname{curl}_\Gamma \xi^i_h)(y) \cdot (\operatorname{curl}_\Gamma \xi^j_h)(x)}{4\pi|x-y|} ds_y ds_x = 0$$

$$w^{n-1}_{2,curl,(i,j)} = \frac{1}{4\pi} \iint_{E_{n-1}} \frac{(\operatorname{curl}_\Gamma \xi^i_h)(y) \cdot (\operatorname{curl}_\Gamma \xi^j_h)(x)}{4\pi} ds_y ds_x = 0$$

$$w^{n-1}_{3,curl,(i,j)} = \frac{1}{4\pi} \iint_{E_{n-1}} \frac{(\operatorname{curl}_\Gamma \xi^i_h)(y) \cdot (\operatorname{curl}_\Gamma \xi^j_h)(x)|x-y|}{4\pi} ds_y ds_x = 0$$

    end for
  else
    Compute and store for $i, j = 1, \ldots, N_s$

$$w^{n-1}_{1,(i,j)} = \iint_{E_{n-m}} \frac{(n_x \cdot n_y)\xi^i_h(y)\xi^j_h(x)}{|x-y|4\pi} ds_y ds_x$$

$$w^{n-1}_{1,curl,(i,j)} = \frac{1}{4\pi} \iint_{E_{n-1}} \frac{(\operatorname{curl}_\Gamma \xi^i_h)(y) \cdot (\operatorname{curl}_\Gamma \xi^j_h)(x)}{4\pi|x-y|} ds_y ds_x$$

$$w^{n-1}_{2,curl,(i,j)} = \frac{1}{4\pi} \iint_{E_{n-1}} \frac{(\operatorname{curl}_\Gamma \xi^i_h)(y) \cdot (\operatorname{curl}_\Gamma \xi^j_h)(x)}{4\pi} ds_y ds_x$$

$$w^{n-1}_{3,curl,(i,j)} = \frac{1}{4\pi} \iint_{E_{n-1}} \frac{(\operatorname{curl}_\Gamma \xi^i_h)(y) \cdot (\operatorname{curl}_\Gamma \xi^j_h)(x)|x-y|}{4\pi} ds_y ds_x$$

  end if
  Construct and store (W^{n-1}) by using the stored computation in the 2 timestep before and multiply with the corresponding time factors, i.e.

$$\begin{aligned} W^{n-1} = &-\frac{1}{(\Delta t)} w^{n-1}_1 + \frac{2}{(\Delta t)} w^{n-2}_1 - \frac{1}{(\Delta t)} w^{n-3}_1 + \frac{(\Delta t)}{2} n^2 w^{n-1}_{1,curl} - n w^{n-1}_{2,curl} \\ &+ \frac{1}{2(\Delta t)} w^{n-1}_{3,curl} - \frac{(\Delta t)}{2}((n-1)^2 + n^2 - 2) w^{n-2}_{1,curl} + (2(n-1)-1) w^{n-2}_{2,curl} \\ &- \frac{1}{(\Delta t)} w^{n-2}_{3,curl} + \frac{(\Delta t)}{2}(n-3)^2 w^{n-3}_{1,curl} - (n-3) w^{n-3}_{2,curl} + \frac{1}{2(\Delta t)} w^{n-3}_{3,curl} \end{aligned}$$

  Compute right hand side $F^n - \sum_{m=1}^{n-1} W^{n-m}\varphi^m$
  Solve system of linear equations (2.64)
  Store solution φ^n
end for

Algorithm 4: Marching-on-in-time algorithm for the retarded hypersingular integral operator with ansatz and test functions as in (2.63) and below.

Theorem 2.8. *Let $f \in H_\sigma^{\frac{3}{2}}(\mathbb{R}^+, H^{-\frac{1}{2}}(\Gamma))$. Then there exists a unique $u \in H_\sigma^{\frac{1}{2}}(\mathbb{R}^+, \widetilde{H}^{\frac{1}{2}}(\Gamma))$ such that for all $v \in H_\sigma^{-\frac{1}{2}}(\mathbb{R}^+, \widetilde{H}^{\frac{1}{2}}(\Gamma))$:*

$$\int_0^\infty \langle (W - (K' - \frac{1}{2}I)V^{-1}(K - \frac{1}{2}I))u, v\rangle_\Gamma e^{-2\sigma t} dt = \int_0^\infty \int_\Gamma f(x,t)v(x,t) ds_x e^{-2\sigma t} dt \tag{2.65}$$

Again we set $\sigma = 0$ and use (2.17), then the variational formulation reads: For given $f \in H_\sigma^{\frac{3}{2}}(\mathbb{R}^+, H^{-\frac{1}{2}}(\Gamma))$, find $\varphi \in H_\sigma^{\frac{1}{2}}(\mathbb{R}^+, \widetilde{H}^{\frac{1}{2}}(\Gamma)), p \in H_\sigma^{\frac{1}{2}}(\mathbb{R}^+, \widetilde{H}^{-\frac{1}{2}}(\Gamma))$ such that

$$\int_0^\infty \langle W\varphi - (K' - \tfrac{1}{2}I)p, \dot{w}\rangle_\Gamma \,\mathrm{d}t = \int_0^\infty \langle f, \dot{w}\rangle_\Gamma \,\mathrm{d}t \ , \tag{2.66}$$

$$\int_0^\infty [\langle Vp, \partial_t \omega\rangle_\Gamma - \langle (K - \tfrac{1}{2}I)\varphi, \partial_t \omega\rangle_\Gamma] \,\mathrm{d}t = 0, \tag{2.67}$$

holds for all $w \in H_\sigma^{\frac{1}{2}}(\mathbb{R}^+, \widetilde{H}^{\frac{1}{2}}(\Gamma))$, $\omega \in H_\sigma^{\frac{1}{2}}(\mathbb{R}^+, \widetilde{H}^{-\frac{1}{2}}(\Gamma))$. We want to discretize the retarded single layer potential, the double layer potential, the adjoint double layer potential and the hypersingular integral operator so that we get again a marching-on-in-time scheme. By choosing the ansatz and the test functions as below, the discrete system reads as follows: Find $\varphi_{h,\Delta t}$ and $p_{h,\Delta t}$ such that

$$\int_0^\infty \langle W\varphi_{h,\Delta t} - (K' - \frac{1}{2}I)p_{h,\Delta t}, \dot{w}_{h,\Delta t}\rangle_\Gamma \,\mathrm{d}t = \int_0^\infty \langle f, \dot{w}_{h,\Delta t}\rangle_\Gamma \,\mathrm{d}t \ , \tag{2.68}$$

$$\int_0^\infty [\langle Vp_{h,\Delta t}, \dot{\omega}_{h,\Delta t}\rangle_\Gamma - \langle (K - \frac{1}{2}I)\varphi_{\Delta t,h}, \dot{\omega}_{h,\Delta t}\rangle_\Gamma] \,\mathrm{d}t = 0, \tag{2.69}$$

holds for all $\dot{w}_{h,\Delta t}$ and $\dot{\omega}_{h,\Delta t}$ for $n = 1\ldots, N_t, j = 1, \ldots, N_s$. Let us begin with the hypersingular operator. Here we use the same ansatz and test functions in space and time as in Subsection 2.3.4:

$$\varphi_{h,\Delta t}(x,t) = \sum_{m=1}^{N_t}\sum_{i=1}^{N_s} \varphi_i^m \beta_{\Delta t}^m(t)\xi_h^i(x) \in V_{h,\Delta t}^{1,1}$$

and $\dot{w}_{h,\Delta t} = \gamma_{\Delta t}^n(t)\xi_h^j(x) \in V_{h,\Delta t}^{1,0}$ for $1 \le n \le N_t$ and $1 \le j \le N_s$. We get:

$$\begin{aligned}
&\int_0^\infty \int_\Gamma W\varphi_{h,\Delta t}(x,t)\cdot \dot{w}_{h,\Delta t}(x,t)\ ds_x dt \\
&= \sum_{m=1}^{N_t}\sum_{i=1}^{N_s} \varphi_i^m \Big[-\frac{1}{(\Delta t)} \iint_{E_{n-m}} \frac{(n_x\cdot n_y)\xi_h^i(y)\xi_h^j(x)}{|x-y|4\pi} ds_y ds_x \\
&+ \frac{2}{(\Delta t)} \iint_{E_{n-m-1}} \frac{(n_x\cdot n_y)\xi_h^i(y)\xi_h^j(x)}{|x-y|4\pi} ds_y ds_x - \frac{1}{(\Delta t)} \iint_{E_{n-m-2}} \frac{(n_x\cdot n_y)\xi_h^i(y)\xi_h^j(x)}{|x-y|4\pi} ds_y ds_x \Big] \\
&+ \sum_{m=1}^{N_t}\sum_{i=1}^{N_s} \varphi_i^m \frac{1}{4\pi} \iint_{\Gamma\times\Gamma} \frac{(\mathrm{curl}_\Gamma\, \xi_h^i)(y)\cdot(\mathrm{curl}_\Gamma\, \xi_h^j)(x)}{|x-y|} \mathcal{Y}^{n-m}(x,y) ds_y ds_x = \sum_{m=1}^{N_t} W^{n-m}\varphi^m.
\end{aligned}$$

We continue with the discretization of the retarded single layer potential. For the ansatz function we use piecewise linear functions in space and time.

$$p_{h,\Delta t}(x,t) = \sum_{m=1}^{N_t}\sum_{i=1}^{N_s} p_i^m \beta_{\Delta t}^m(t)\xi_h^i(x) \in V_{h,\Delta t}^{1,1} \ .$$

As test functions we use piecewise constant functions in time and piecewise linear functions in space, i.e. $\omega_{h,\Delta t} = \gamma_{\Delta t}^n(t)\xi_h^j(x) \in V_{h,\Delta t}^{1,0}$ for $1 \le n \le N_t$ and $1 \le j \le N_s$. This gives after some computation

$$\begin{aligned}
&\langle V p_{h,\Delta t}, \dot\omega_{h,\Delta t}\rangle_{\Gamma\times\mathbb{R}_+} = \int_0^\infty \int_\Gamma V p_{h,\Delta t}(x,t)\cdot\dot\omega_{h,\Delta t}(x,t) ds_x dt \\
&= \sum_{m=1}^{N_t}\sum_{i=1}^{N_s} p_i^m \Big[\iint\limits_{E_{n-m}} \left(-(n-m+1)\frac{\xi_h^i(y)\xi_h^j(x)}{4\pi|x-y|} + \frac{\xi_h^i(y)\xi_h^j(x)}{4\pi(\Delta t)}\right) ds_y ds_x \\
&+ \iint\limits_{E_{n-m-1}} \left((2(n-m)-1)\frac{\xi_h^i(y)\xi_h^j(x)}{4\pi|x-y|} - 2\frac{\xi_h^i(y)\xi_h^j(x)}{4\pi(\Delta t)}\right) ds_y ds_x \\
&+ \iint\limits_{E_{n-m-2}} \left(-(n-m-2)\frac{\xi_h^i(y)\xi_h^j(x)}{4\pi|x-y|} + \frac{\xi_h^i(y)\xi_h^j(x)}{4\pi(\Delta t)}\right) ds_y ds_x \Big] = \sum_{m=1}^{N_t}\sum_{i=1}^{N_s} V_{j,i}^{n-m} p_i^m = \sum_{m=1}^{N_t} V^{n-m} p^m .
\end{aligned}$$

Next with $\langle (\frac{1}{2}I - K^T) p_{h,\Delta t}, \dot w_{h,\Delta t}\rangle_{\Gamma\times\mathbb{R}_+} = \langle \frac{1}{2} I p_{h,\Delta t}, \dot w_{h,\Delta t}\rangle_{\Gamma\times\mathbb{R}_+} - \langle K^T p_{h,\Delta t}, \dot w_{h,\Delta t}\rangle_{\Gamma\times\mathbb{R}_+}$ we get for the retarded adjoint double layer potential after some computation :

$$\begin{aligned}
&\langle K^T p_{h,\Delta t}, \dot w_{h,\Delta t}\rangle_{\Gamma\times\mathbb{R}_+} = \int_0^\infty \int_\Gamma K^T p_{h,\Delta t} \dot w_{h,\Delta t} ds_x dt \\
&= \sum_{m=1}^{N_t}\sum_{i=1}^{N_s} p_i^m \iint\limits_{\Gamma\times\Gamma} \frac{n_x\cdot(x-y)}{4\pi|x-y|^3}\xi_h^i(y)\xi_h^j(x)\mathcal{Y}^{n-m}(x,y) ds_y ds_x \\
&+ \sum_{m=1}^{N_t}\sum_{i=1}^{N_s} p_i^m \Big[\iint\limits_{E_{n-m}} n_x\cdot(x-y)\left((n-m+1)\frac{\xi_h^i(y)\xi_h^j(x)}{4\pi|x-y|^2} - \frac{\xi_h^i(y)\xi_h^j(x)}{4\pi(\Delta t)|x-y|}\right) ds_y ds_x \\
&+ \iint\limits_{E_{n-m-1}} n_x\cdot(x-y)\left(-(2(n-m)-1)\frac{\xi_h^i(y)\xi_h^j(x)}{4\pi|x-y|^2} + 2\frac{\xi_h^i(y)\xi_h^j(x)}{4\pi(\Delta t)|x-y|}\right) ds_y ds_x \\
&+ \iint\limits_{E_{n-m-2}} n_x\cdot(x-y)\left((n-m-2)\frac{\xi_h^i(y)\xi_h^j(x)}{4\pi|x-y|^2} - \frac{\xi_h^i(y)\xi_h^j(x)}{4\pi(\Delta t)|x-y|}\right) ds_y ds_x \Big] \\
&=: \sum_{m=1}^{N_t}\sum_{i=1}^{N_s} (K^T)_{j,i}^{n-m} p_i^m = \sum_{m=1}^{N_t} (K^T)^{n-m} p^m
\end{aligned}$$

and for the identity part:

$$\begin{aligned}
&\langle \frac{1}{2} I p_{h,\Delta t}, \dot w_{h,\Delta t}\rangle_{\Gamma\times\mathbb{R}_+} = \frac{1}{2}\int_0^\infty \int_\Gamma \sum_{m=1}^{N_t}\sum_{i=1}^{N_s} p_i^m \beta_{\Delta t}^m(t)\xi_h^i(x)\gamma_{\Delta t}^n(t)\xi_h^j(x) ds_x dt \\
&= \frac{1}{2}\sum_{m=1}^{N_t}\sum_{i=1}^{N_s} p_i^m \Big(\int_\Gamma \xi_h^i(x)\xi_h^j(x) ds_x\Big)\Big(\int_0^\infty \beta_{\Delta t}^m(t)\gamma_{\Delta t}^n(t) dt\Big) \\
&= \frac{1}{2}\sum_{i=1}^{N_s} p_i^m \Big(\int_\Gamma \xi_h^i(x)\xi_h^j(x) ds_x\Big)\frac{(\Delta t)}{2}\begin{cases} p_i^1 & , n=1 \\ p_i^n + p_i^{n-1} & , n\ge 2\end{cases} = \frac{1}{2}\sum_{i=1}^{N_s} I_{j,i} p_I = \frac{1}{2} I p_I
\end{aligned}$$

with

$$p_I = \frac{(\Delta t)}{2}\begin{cases} p^1 & , n = 1 \\ p^n + p^{n-1} & , n \geq 2 \end{cases}.$$

In the same way we consider $\langle(-\frac{1}{2}I + K)\varphi_{h,\Delta t}, \dot{\omega}_{h,\Delta t}\rangle_{\Gamma\times\mathbb{R}_+} = \langle -\frac{1}{2}I\varphi_{h,\Delta t}, \dot{\omega}_{h,\Delta t}\rangle_{\Gamma\times\mathbb{R}_+} + \langle K\varphi_{h,\Delta t}, \dot{\omega}_{h,\Delta t}\rangle_{\Gamma\times\mathbb{R}_+}$:

$$\begin{aligned}
&\langle K\varphi_{h,\Delta t}, \dot{\omega}_{h,\Delta t}\rangle_{\Gamma\times\mathbb{R}_+} = \int_0^\infty \int_\Gamma K\varphi_{h,\Delta t}\dot{\omega}_{h,\Delta t} ds_x dt \\
&= \sum_{m=1}^{N_t}\sum_{i=1}^{N_s}\varphi_i^m\Big[\iint\limits_{E_{n-m}} n_y\cdot(x-y)\left(-(n-m+1)\frac{\xi_h^i(y)\xi_h^j(x)}{4\pi|x-y|^3} + \frac{\xi_h^i(y)\xi_h^j(x)}{4\pi(\Delta t)|x-y|^2}\right) ds_y ds_x \\
&+ \iint\limits_{E_{n-m-1}} n_y\cdot(x-y)\left((2(n-m)-1)\frac{\xi_h^i(y)\xi_h^j(x)}{4\pi|x-y|^3} - 2\frac{\xi_h^i(y)\xi_h^j(x)}{4\pi(\Delta t)|x-y|^2}\right) ds_y ds_x \\
&+ \iint\limits_{E_{n-m-2}} n_y\cdot(x-y)\left(-(n-m-2)\frac{\xi_h^i(y)\xi_h^j(x)}{4\pi|x-y|^3} + \frac{\xi_h^i(y)\xi_h^j(x)}{4\pi(\Delta t)|x-y|^2}\right) ds_y ds_x\Big] \\
&+ \sum_{m=1}^{N_t}\sum_{i=1}^{N_s}\varphi_i^m\Big[\iint\limits_{E_{n-m}} -\frac{n_y\cdot(x-y)}{4\pi(\Delta t)|x-y|^2}\xi_h^i(y)\xi_h^j(x) ds_y ds_x + \iint\limits_{E_{n-m-1}} \frac{2n_y\cdot(x-y)}{4\pi(\Delta t)|x-y|^2}\xi_h^i(y)\xi_h^j(x) ds_y ds_x \\
&+ \iint\limits_{E_{n-m-2}} -\frac{n_y\cdot(x-y)}{4\pi(\Delta t)|x-y|^2}\xi_h^i(y)\xi_h^j(x) ds_y ds_x\Big] = \sum_{m=1}^{N_t}\sum_{i=1}^{N_s} K_{j,i}^{n-m}\varphi_i^m = \sum_{m=1}^{N_t} K^{n-m}\varphi^m
\end{aligned}$$

and

$$\begin{aligned}
&\langle\frac{1}{2}I\varphi_{h,\Delta t}, \dot{\omega}_{h,\Delta t}\rangle_{\Gamma\times\mathbb{R}_+} = \frac{1}{2}\int_0^\infty\int_\Gamma \sum_{m=1}^{N_t}\sum_{i=1}^{N_s}\varphi_i^m\beta_{\Delta t}^m(t)\xi_h^i(x)\dot{\gamma}_{\Delta t}^n(t)\xi_h^j(x) ds_x dt \\
&= \frac{1}{2}\sum_{i=1}^{N_s}\varphi_i^m\Big(\int_\Gamma \xi_h^i(x)\xi_h^j(x) ds_x\Big)\Big(\int_0^\infty \beta_{\Delta t}^m(t)\dot{\gamma}_{\Delta t}^n dt\Big) \\
&= \frac{1}{2}\sum_{m=1}^{N_t}\sum_{i=1}^{N_s}\varphi_i^m\Big(\int_\Gamma \xi_h^i(x)\xi_h^j(x) ds_x\Big)\begin{cases} -\varphi_i^1 & , n = 1 \\ -(\varphi_i^n - \varphi_i^{n-1}) & , n \geq 2 \end{cases} \\
&= \frac{1}{2}\sum_{i=1}^{N_s} I_{j,i}\varphi_I = \frac{1}{2}I\varphi_I
\end{aligned}$$

with

$$\varphi_I = \begin{cases} -\varphi^1 & , n = 1 \\ -\varphi^n + \varphi^{n-1} & , n \geq 2 \end{cases}.$$

Finally we solve the following equation:

$$\sum_{m=1}^{N_t} W^{n-m}\varphi^m - \sum_{m=1}^{N_t}(K^T)^{n-m}p^m + \frac{1}{2}Ip_I + \frac{1}{2}I\varphi_I - \sum_{m=1}^{N_t} K^{n-m}\varphi^m + \sum_{m=1}^{N_t} V^{n-m}p^m = F^n \ . \tag{2.70}$$

We want to remark that W^k, K^k, K^{T^k}, V^k vanish if the index k is negative. Therefore we get for the first timestep ($n = 1$):

$$W^0\varphi^1 - K^{T^0}p^1 + \frac{1}{2}\frac{(\Delta t)}{2}Ip^1 - \frac{1}{2}I\varphi^1 - K^0\varphi^1 + V^0p^1 = F^1 \ .$$

We can write it as the following system of linear equations:

$$\mathcal{M}^0\begin{pmatrix}\varphi^1\\ p^1\end{pmatrix} := \begin{pmatrix} W^0 & -K^{T^0} + \frac{1}{2}\frac{(\Delta t)}{2}I \\ -K^0 - \frac{1}{2}I & V^0\end{pmatrix}\begin{pmatrix}\varphi^1\\ p^1\end{pmatrix} = \begin{pmatrix}F^1\\ 0\end{pmatrix} \ .$$

For an arbitrary timestep $n \geq 2$ we need to solve:

$$\sum_{m=1}^{n} W^{n-m}\varphi^m - \sum_{m=1}^{n}(K^T)^{n-m}p^m + \frac{1}{2}\frac{(\Delta t)}{2}I(p^n + p^{n-1}) + \frac{1}{2}I(-\varphi^n + \varphi^{n-1})$$
$$- \sum_{m=1}^{n} K^{n-m}\varphi^m + \sum_{m=1}^{n} V^{n-m}p^m = F^n \ .$$

We can define in addition to $\mathcal{M}^0$ and $\mathbb{N} \ni k \geq 2$:

$$\mathcal{M}^1 := \begin{pmatrix} W^1 & -(K^T)^1 + \frac{1}{2}\frac{\Delta t}{2}I \\ -K^1 + \frac{1}{2}I & V^1\end{pmatrix} \ , \quad \mathcal{M}^k := \begin{pmatrix} W^k & -(K^T)^k \\ -K^k & V^k\end{pmatrix}.$$

Since we already computed φ^k, p^k for all $k = 1, \ldots, n-1$ altogether we get:

$$\begin{pmatrix} W^0 & -K^{T^0} + \frac{1}{2}\frac{(\Delta t)}{2}I \\ -K^0 - \frac{1}{2}I & V^0\end{pmatrix}\begin{pmatrix}\varphi^n\\ p^n\end{pmatrix}$$
$$= \begin{pmatrix} F^n - \sum_{m=1}^{n-1} W^{n-m}\varphi^m + \sum_{m=1}^{n-1}(K^T)^{n-m}p^m - \frac{1}{2}\frac{(\Delta t)}{2}Ip^{n-1} \\ \sum_{m=1}^{n-1} K^{n-m}\varphi^m - \frac{1}{2}I\varphi^{n-1} - \sum_{m=1}^{n-1} V^{n-m}p^m\end{pmatrix} \ .$$

Or concisely written:

$$\mathcal{M}^0\begin{pmatrix}\varphi^n\\ p^n\end{pmatrix} = \begin{pmatrix}F^n\\ 0\end{pmatrix} - \sum_{m=1}^{n-1}\mathcal{M}^{n-m}\begin{pmatrix}\varphi^n\\ p^n\end{pmatrix} \ .$$

If we save the matrices from previous time steps, we only need to calculate one new matrix $\mathcal{M}^{n-1}$ in time step n to obtain the vector $[\varphi^n, p^n]^T$. We solve this system until the timestep N_t is reached.

Example 2.1. *We solve the Dirichlet-to-Neumann equation $\mathcal{S}v = f$ on the unit sphere, geometrically approximated by an icosahedron, with a right hand side obtained from the Neumann data of a known, radially symmetric solution to the wave equation:*

$$f = \partial_n v(t,x)\,|_{\{|x|=1\}} = (-\frac{3}{4} + \cos(\frac{\pi}{2}(4-t)) + \frac{\pi}{2}\sin(\frac{\pi}{2}(4-t))$$
$$- \frac{1}{4}(\cos(\pi(4-t)) + \pi\sin(\pi(4-t))))[H(4-t) - H(-t)] \ .$$

The solution v corresponds to the Dirichlet data of the solution to the wave equation. Therefore,

$$v(t,r)\,|_\Gamma = (\tfrac{3}{4} - \cos(\tfrac{\pi(4-t)}{2}) + \tfrac{1}{4}\cos(\pi(4-t)))[H(4-t) - H(-t)].$$

We hold the Courant-Friedrichs-Levy (CFL) ratio $\frac{\Delta t}{h} \approx 0.6$ and compute till $T = 5$.

Figure 2.2 shows the $L^2(\Gamma)$-norm of the exact solution together with the numerical solutions for various refinements of the unit sphere as a function of time. Figure 2.3 displays the error in this norm. We observe that the error remains uniformly bounded in time. In Figure 2.4 we consider the $L^2([0,T]\times\Gamma)$-norm of the error between the numerical solutions and the exact solution depending on the degrees of freedom (DOF). We obtain a convergence rate of $\alpha = 0.7$, which corresponds to 2.1 in terms of h, since the CFL $\frac{\Delta t}{h}$ is fixed and DOF is proportional to h^{-3}. We calculate the convergence rate α with

$$\alpha = \frac{\log Err(v_1) - \log Err(v_2)}{\log DOF_1 - \log DOF_2} \ ,$$

where $Err(v_j)$ denotes the $L^2([0,T]\times\Gamma)$-norm of the error between the numerical solution v_j and the exact solution u. We remark that we have an approximation error of the geometry.

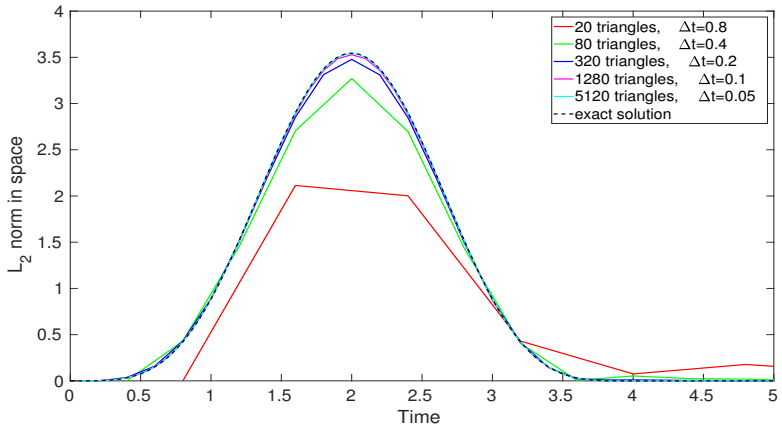

Figure 2.2: $L^2(\Gamma)$-norm of the solution to $\mathcal{S}v = f$ for fixed CFL ratio $\frac{\Delta t}{h} \approx 0.6$. Figure 1 in [47]

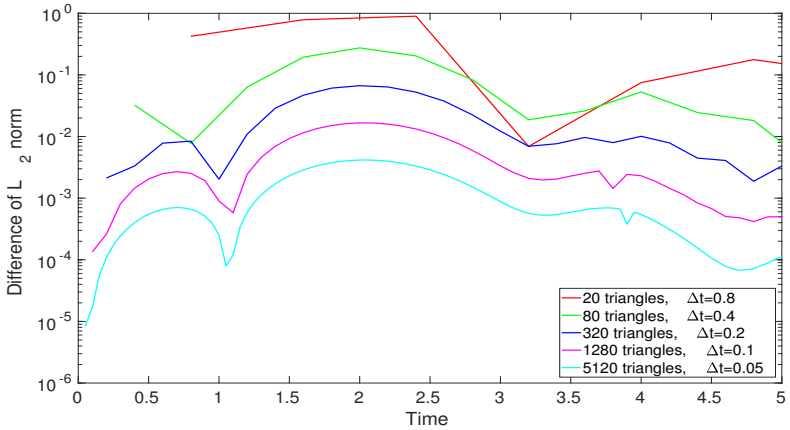

Figure 2.3: Absolute error of the exact solution and the numerical solution for the L^2 norm in space as a function of time for fixed $\frac{\Delta t}{h}$. Figure 2 in [47]

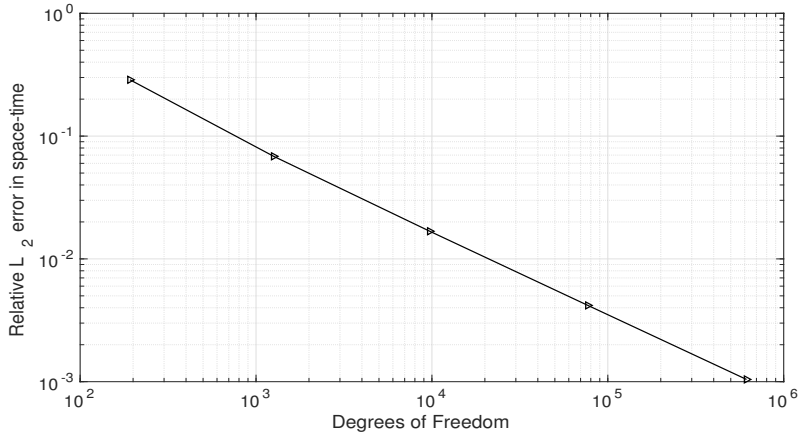

Figure 2.4: $L^2([0,T]\times\Gamma)$-error vs. degrees of freedom of the solution to $\mathcal{S}v = f$ for fixed $\frac{\Delta t}{h}$. Figure 3 in [47]

2.3.6 Retarded inverse Poincaré-Steklov operator

For the inverse retarded Poincaré-Steklov operator in (2.18), given $v^+ = f$ on Γ, we want to solve $\mathcal{S}^{-1}\partial_n^+ v = f$. With (2.19) the variational formulation reads:

For given $f \in H_\sigma^{\frac{3}{2}}(\mathbb{R}^+, H^{\frac{1}{2}}(\Gamma))$, find $\varphi \in H_\sigma^{\frac{1}{2}}(\mathbb{R}^+, \widetilde{H}^{\frac{1}{2}}(\Gamma)), p \in H_\sigma^{\frac{1}{2}}(\mathbb{R}^+, \widetilde{H}^{-\frac{1}{2}}(\Gamma))$ such that

$$\int_0^\infty \langle W\varphi - (K' + \tfrac{1}{2})p, \dot{w}\rangle_\Gamma \,\mathrm{d}t = 0, \tag{2.71}$$

$$\int_0^\infty [\langle -Vp, \partial_t\omega\rangle_\Gamma + \langle (K + \tfrac{1}{2})\varphi, \partial_t\omega\rangle_\Gamma] \,\mathrm{d}t = \int_0^\infty \langle f, \dot{\omega}\rangle_\Gamma \,\mathrm{d}t \ , \tag{2.72}$$

holds for all $w \in H_\sigma^{\frac{1}{2}}(\mathbb{R}^+, \widetilde{H}^{\frac{1}{2}}(\Gamma))$,$\omega \in H_\sigma^{\frac{1}{2}}(\mathbb{R}^+, \widetilde{H}^{-\frac{1}{2}}(\Gamma))$.

This leads to the following discretization: Find $\varphi_{h,\Delta t}$ and $p_{h,\Delta t}$ such that

$$\int_0^\infty \langle W\varphi_{h,\Delta t} - (K' + \frac{1}{2}I)p_{h,\Delta t}, w_{h,\Delta t}\rangle_\Gamma \,\mathrm{d}t = 0 \ , \tag{2.73}$$

$$\int_0^\infty [\langle -Vp_{h,\Delta t}, \dot{\omega}_{h,\Delta t}\rangle_\Gamma + \langle (K + \frac{1}{2}I)\varphi_{h,\Delta t}, \dot{\omega}_{h,\Delta t}\rangle_\Gamma] \,\mathrm{d}t = \int_0^\infty \langle f, w_{h,\Delta t}\rangle_\Gamma \,\mathrm{d}t, \tag{2.74}$$

holds for all $\dot{w}_{h,\Delta t}$ and $\dot{\omega}_{h,\Delta t}$ for $n = 1\ldots, N_t, j = 1, \ldots, N_s$. We use the same ansatz and test functions in space and time as in Subsection 2.3.5, i.e. $\varphi_{h,\Delta t} \in V_{h,\Delta t}^{1,1}, p_{h,\Delta t} \in V_{h,\Delta t}^{1,1}, \omega_{h,\Delta t} \in V_{h,\Delta t}^{1,0}, w_{h,\Delta t} \in V_{h,\Delta t}^{1,0}$. Now using the same computations as in Subsection 2.3.5, we get:

$$\sum_{m=1}^{N_t} W^{n-m}\varphi^m - \sum_{m=1}^{N_t} (K^T)^{n-m} p^m - \frac{1}{2}Ip_I + \sum_{m=1}^{N_t} K^{n-m}\varphi^m + \frac{1}{2}I\varphi_I + \sum_{m=1}^{N_t} V^{n-m}p^m = F^n \ .$$

For the first timestep ($n = 1$), we solve

$$\mathcal{N}^0 \begin{pmatrix} \varphi^1 \\ p^1 \end{pmatrix} := \begin{pmatrix} W^0 & -K^{T\,0} - \frac{1}{2}\frac{(\Delta t)}{2} I \\ K^0 - \frac{1}{2} I & -V^0 \end{pmatrix} \begin{pmatrix} \varphi^1 \\ p^1 \end{pmatrix} = \begin{pmatrix} 0 \\ F^1 \end{pmatrix} .$$

In addition to $\mathcal{N}^0$, we define for $\mathbb{N} \ni k \geq 2$:

$$\mathcal{N}^1 = \begin{pmatrix} W^1 & -(K^T)^1 - \frac{1}{2}\frac{\Delta t}{2} I \\ K^1 + \frac{1}{2} I & -V^1 \end{pmatrix} , \quad \mathcal{N}^k = \begin{pmatrix} W^k & -(K^T)^k \\ K^k & -V^k \end{pmatrix} .$$

For an arbitrary timestep n, we solve

$$\begin{pmatrix} W^0 & -K^{T\,0} - \frac{1}{2}\frac{(\Delta t)}{2} I \\ K^0 - \frac{1}{2} I & -V^0 \end{pmatrix} \begin{pmatrix} \varphi^n \\ p^n \end{pmatrix}$$
$$= \begin{pmatrix} -\sum_{m=1}^{n-1} W^{n-m} \varphi^m + \sum_{m=1}^{n-1} (K^T)^{n-m} p^m + \frac{1}{2}\frac{(\Delta t)}{2} I p^{n-1} \\ F^n - \sum_{m=1}^{n-1} K^{n-m} \varphi^m - \frac{1}{2} I \varphi^{n-1} + \sum_{m=1}^{n-1} V^{n-m} p^m \end{pmatrix} .$$

Written concisely

$$\mathcal{N}^0 \begin{pmatrix} \varphi^n \\ p^n \end{pmatrix} = \begin{pmatrix} 0 \\ F^n \end{pmatrix} - \sum_{m=1}^{n-1} \mathcal{N}^{n-m} \begin{pmatrix} \varphi^m \\ p^m \end{pmatrix} .$$

Saving the matrices for every timestep n again, we only need to calculate the new matrix $\mathcal{N}^{n-1}$ and obtain the vector $[\varphi^n, p^n]$. We solve this system until our desired timestep N_t is reached.

Example 2.2. *We solve the Neumann-to-Dirichlet equation $\mathcal{S}^{-1}\lambda = f$ on the unit sphere, geometrically approximated by an icosahedron, with a right hand side obtained from the Dirichlet data of a known, radially symmetric solution to the wave equation:*

$$f = v(t,r) \,|_\Gamma = (\tfrac{3}{4} - \cos(\tfrac{\pi(4-t)}{2}) + \tfrac{1}{4}\cos(\pi(4-t)))[H(4-t) - H(-t)].$$

The solution λ corresponds to the Neumann data of the solution to the wave equation. Therefore,

$$\lambda = \partial_n v(t,x) \,|_{\{|x|=1\}} = (-\frac{3}{4} + \cos(\frac{\pi}{2}(4-t)) + \frac{\pi}{2}\sin(\frac{\pi}{2}(4-t))$$
$$- \frac{1}{4}(\cos(\pi(4-t)) + \pi\sin(\pi(4-t))))[H(4-t) - H(-t)] .$$

We hold the CFL ratio $\frac{\Delta t}{h} \approx 0.6$ and compute till $T = 5$.

Figure 2.5 shows the $L^2(\Gamma)$-norm of the exact solution together with the numerical solutions for various refinements of the unit sphere as a function of time. Figure 2.6 displays the error in this norm. We observe that the error remains uniformly bounded in time. In Figure 2.4 we consider the $L^2([0,T] \times \Gamma)$-norm of the error between the numerical solutions and the exact solution depending on the degrees of freedom (DOF). We obtain a convergence rate of $\alpha = 0.5$, which corresponds to 1.5 in terms of h. We remark that we have an approximation error of the geometry.

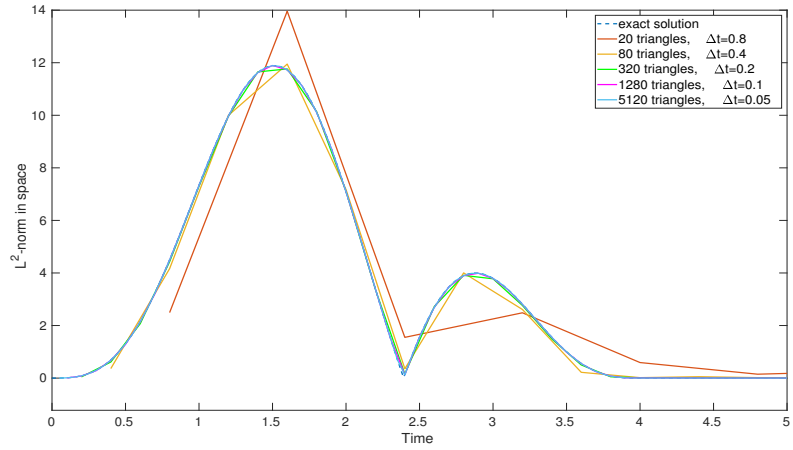

Figure 2.5: $L^2(\Gamma)$-norm of the solution to $\mathcal{S}^{-1}\lambda = f$ for fixed CFL ratio $\frac{\Delta t}{h} \approx 0.6$.

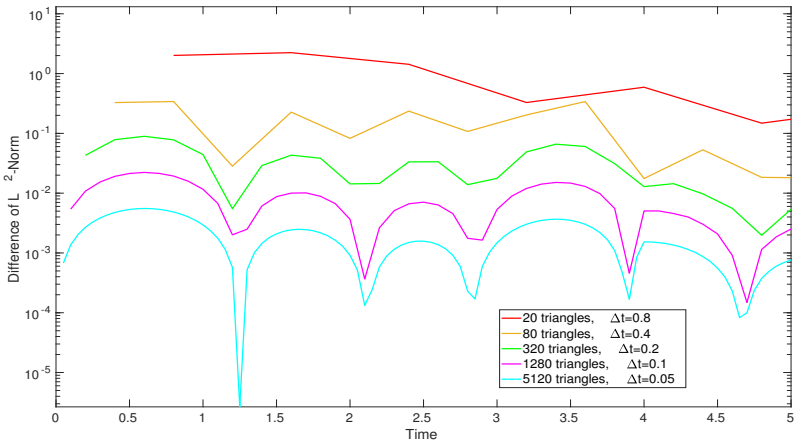

Figure 2.6: Absolute error of the exact solution and the numerical solution for the L^2 norm in space as a function of time for fixed $\frac{\Delta t}{h}$.

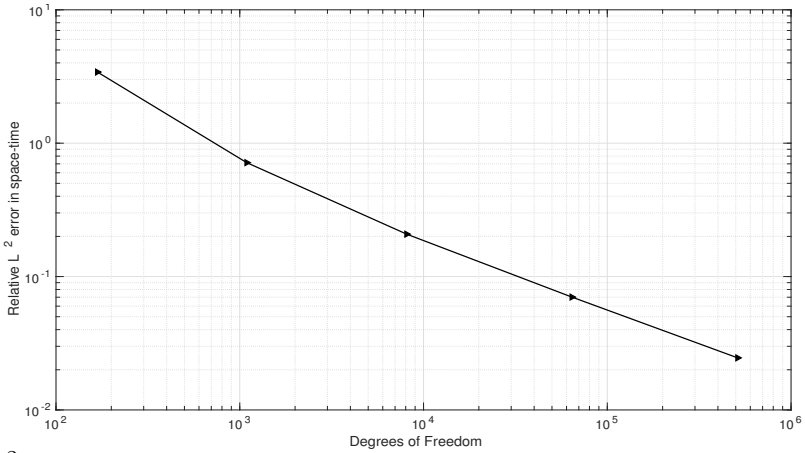

Figure 2.7: $L^2([0,T] \times \Gamma)$-error vs. degrees of freedom of the solution to $\mathcal{S}^{-1}\lambda = f$ for fixed $\frac{\Delta t}{h}$.

3 FEM-BEM coupling in time domain I : Fluid structure interaction with retarded single layer potential as test function

3.1 Introduction

Coupled adaptive finite and boundary element procedures provide an efficient and extensively investigated tool for the numerical solution of elliptic interface problems, especially in unbounded domains [92]. To describe the transient emission or scattering of waves from an elastic body, we use a coupling of time–domain finite and boundary elements as well.

In this chapter we address the coupling of finite and boundary element method in the context of fluid-structure interaction (FSI). Based on ideas from the time–independent coupling formulation and its a posteriori error analysis [25, 29, 35, 34], we give a priori and a posteriori error estimates, which demonstrate the convergence. A basic well–posedness theory for the time–dependent problem has been established in [44] by formulating the FSI problem as a Cauchy problem and proving the conditions of the theorem of Lumer-Phillips of semigroup theory. In this way Filipe proved in [44] Theorem 3.1 below.

We recall the equations which describe an elastic body submersed in a fluid. For a bounded, orientable Lipschitz domain $\Omega \subset \mathbb{R}^d$ with $d = 3$, let $\Omega^c = \mathbb{R}^d \setminus \overline{\Omega}$, we consider the wave equation in Ω^c with constant wave speed $c = 1$,

$$\partial_t^2 v - \Delta v = 0 \text{ in } \Omega^c \times \mathbb{R}_+ \ , \quad v = \partial_t v = 0 \ \text{ for } \ t = 0 \ , \tag{3.1}$$

coupled to a linearly elastic medium in Ω,

$$\varrho_1 \partial_t^2 \mathbf{u} - \Delta^* \mathbf{u} = 0 \text{ in } \Omega \times \mathbb{R}_+ \ , \quad \mathbf{u} = \partial_t \mathbf{u} = 0 \ \text{ for } \ t = 0. \tag{3.2}$$

On $\Gamma \times \mathbb{R}_+$ we impose transmission conditions

$$\tilde{\sigma}(\gamma^- \mathbf{u}) n + (\partial_t v_+ + \partial_t v_+^{inc}) n = 0 \qquad \text{and} \qquad \varrho_2 \partial_t \gamma^- \mathbf{u} n + \partial_n^+ v + \partial_n^+ v^{inc} = 0 \ , \tag{3.3}$$

where $n = n_x$ denotes the unit normal vector, always pointing towards Ω^c, ρ_1, ρ_2 are constants and $\Delta^* \mathbf{u} = \mu \Delta \mathbf{u} + (\lambda + \mu) \nabla(\mathrm{div} \mathbf{u}) = \mathrm{div}(\tilde{\sigma}(\mathbf{u}))$ with Lamé constants $\mu \geq 0$ and λ such that $3\lambda + 2\mu \geq 0$ and $\tilde{\sigma}(\mathbf{u}) = (\lambda \mathrm{div} \mathbf{u}) E + 2\mu \varepsilon(\mathbf{u}), \varepsilon(\mathbf{u}) = \frac{1}{2}((\nabla \mathbf{u}) + (\nabla \mathbf{u})^T)$

with E the unit matrix. For $x \in \Gamma$, we define $\gamma^- \mathbf{u}(x,t) := \mathbf{u}_-(x,t) := \lim_{x' \in \Omega \to x} \mathbf{u}(x',t)$, $\gamma^+ v(x,t) := v_+(x,t) := \lim_{x' \in \Omega^c \to x} v(x',t)$ and $\partial_n^+ v(x,t) = \frac{\partial v_+}{\partial n}(x,t) = \lim_{x' \in \Omega^c \to x} \frac{\partial v}{\partial n}(x',t) = \lim_{x' \in \Omega^c \to x} n_x \cdot \nabla v(x',t)$. We use retarded potentials for the exterior problem to recast the interface problem as a coupled domain / boundary integral equation. Using a retarded single layer ansatz for the pressure in Ω^c,

$$v(x,t) = Sq(x,t) = \int_{\mathbb{R}^+ \times \Gamma} \frac{q(y, t - |x-y|)}{4\pi |x-y|} dt ds_y \ ,$$

the equations for the fluid–structure interaction (3.1), (3.2) become

$$\begin{aligned} &\varrho_1 \partial_t^2 \mathbf{u} - \operatorname{div}(\tilde{\sigma}(\mathbf{u})) = 0 \text{ in } \Omega \times \mathbb{R}_+ \ , \\ &\tilde{\sigma}(\gamma^- \mathbf{u}) n + (\partial_t V q + \partial_t v_+^{inc}) n = 0 \ , \qquad \varrho_2 \partial_t \gamma^- \mathbf{u} n + (-\tfrac{1}{2} I + K') q + \partial_n^+ v^{inc} = 0 \text{ on } \mathbb{R}_+ \times \Gamma, \end{aligned} \tag{3.4}$$

with initial conditions $v = \partial_t v = 0$ and $\mathbf{u} = \partial_t \mathbf{u} = 0$ at $t = 0$.

We perform an a priori and a posteriori error analysis for space–time Galerkin discretisations of (3.4). The a posteriori error estimate is based on insights from the elliptic theory. The error indicators motivate a space–time adaptive mesh refinements as in [50, 53, 89] for time–dependent boundary integral equations. The theorems, lemmas and propositions in this chapter are also satisfied for $d = 2$, but we have to adapt the retarded integral operators.

3.2 Preliminaries and discretization spaces

From [44] we recall the well-posedness for the continuous problem (3.1), (3.2).

Theorem 3.1. *Let $s \geq 0$ and assume $v_+^{inc} \in H^{3+s}_\sigma(\mathbb{R}^+, H^{\frac{1}{2}}(\Gamma))$, $\partial_n^+ v^{inc} \in H^{3+s}_\sigma(\mathbb{R}^+, H^{-\frac{1}{2}}(\Gamma))$. Then the system (3.1), (3.2) and (3.3) admits a unique solution $(\mathbf{u}, v) \in H^{1+s}_\sigma(\mathbb{R}^+, H^1(\Omega)) \times H^s_\sigma(\mathbb{R}^+, H^1(\Omega^c))$, which depends continuously on the data.*

We consider a space–time discretization based on tensor products of piecewise polynomials, similar to Chapter 2:

If Ω is not polygonal, we approximate it by a polygonal domain and write Ω again for the approximation. For simplicity, we will use here a domain composed of N_s simplicies such that $\overline{\Omega} = \cup_{i=1}^{N_s} \Omega_i$, $\partial\Omega = \Gamma = \cup_{i=1}^{N_{s'}} \Gamma_i$. Each element Ω_i and Γ_i are closed with positive measure. For distinct Ω_i, $\Omega_j \subset \overline{\Omega}$ the intersection $int(\Omega_i) \cap int(\Omega_j) = \varnothing$. Γ_i satisfy an analogous property. For our numerical computations we divide $\overline{\Omega}$ into N_s tetrahedrals and Γ into the corresponding $N_{s'}$ triangles. Hence in particular, let $\mathcal{T}_{h,3}$ be a regular tetrahedralization of Ω into finite tetrahedrals Ω_j ($j \in \{1, \dots, N_s\}$) with the properties mentioned above. Let $T_{ref,3} := \{(z_1, z_2, z_3) : 0 \leq z_1, z_2, z_3; z_1 + z_2 + z_3 \leq 1\}$ be the reference element, then $\Omega_j \in \mathcal{T}_{h,3}$ is described as:

$$\Omega_j := \{x = x^j + a^{1,j} z_1 + a^{2,j} z_2 + a^{3,j} z_3 \text{ with } a^{1,j}, a^{2,j}, a^{3,j} \in \mathbb{R}^3, (z_1, z_2, z_3) \in T_{ref,3}\} \ .$$

Furthermore we define

$$S_h^{p_s}(T_{ref,3}) := \{\nu : T_{ref,3} \longrightarrow \mathbb{R} : \nu(z_1, z_2, z_3) = \sum_{i+j+k \le p_s} \alpha_{i,j,k} z_1^i z_2^j z_3^k \text{ with } \alpha_{i,j,k} \in \mathbb{R}\}$$

the space of polynomials on $T_{ref,3}$ with degree p_s. Therefore the space of splines on Ω_j for $p_s \ge 0$ is defined as follows:

$$S_h^{p_s}(\Omega_j) := \{\nu : \Omega_j \longrightarrow \mathbb{R} : \nu(x) = (\nu \circ F)(x) \text{ with } (\nu \circ F) \in S_h^{p_s}(T_{ref,3})\} \ ,$$

where $F : T_{ref,3} \longrightarrow \Omega_j$. Let W_h^p denote the space of piecewise polynomial functions of degree p in Ω. For $p \ge 1$ $W_h^p(\Omega)$ is continuous. For $p = 0$ and $p = 1$

$$W_h^0 = \{\nu \in L^2(\Omega) : \nu|_{\Omega_j} \in S_h^0(\Omega_j) \forall \Omega_j \in \mathcal{T}_{h,3}\} \ ,$$
$$W_h^1 = \{\nu \in C^0(\Omega) : \nu|_{\Omega_j} \in S_h^1(\Omega_j) \forall \Omega_j \in \mathcal{T}_{h,3}\} \ .$$

For interior functions going onto the boundary Γ we take the restrictions of functions in W_h^p to the boundary. For exterior functions on Γ we use the space $V_{h'}^{p'}$, which is already defined in Section 2.3. Also the time discretization remains the same as in Section 2.3. Therefore the space of piecewise polynomial functions of degree q in time is denoted by $V_{\Delta t}^q$. Altogether $\mathcal{T}_{h,3} = \{\Omega_1, \dots, \Omega_{N_s}\}$ is a regular tetrahedralization and $\mathcal{T}_{h,2} = \{\Gamma_1, \dots, \Gamma_{N_{s'}}\}$ is a regular triangulation. We divide $\mathbb{R}^+ = (0, \infty)$ into (Δt) equidistant subintervals $I_n = (t_{n-1}, t_n]$ $n \in \mathbb{N}$, with $t_n = n(\Delta t)$. As our temporal mesh $\mathcal{T}_t$ we take a discretization of a finite subinterval $[0, T]$ with $\mathcal{T}_t = \{I_1, I_2, \cdots, I_{N_t}\}$ whereas $T = N_t(\Delta t)$. For the numerical approximation of the solution, we consider the tensor product of the approximation spaces in space and time (as in (2.46))

$$W_{h,\Delta t}^{p,q} = W_h^p \otimes V_{\Delta t}^q \ , \ V_{h',\Delta t}^{p,q} = V_{h'}^p \otimes V_{\Delta t}^q \ .$$

For the a posteriori error estimate we will require an approximation result: Let $\Pi_{\Delta t}$ the orthogonal projection from $L^2(\mathbb{R}_+)$ to $V_{\Delta t}^q$, Π_h the orthogonal projection from $L^2(\Gamma)$ to V_h^p. Their approximation properties lead to corresponding properties of the composed operator $\Pi_h \circ \Pi_{\Delta t}$ in space–time, similar to [48]):

Lemma 3.1. *Let $f \in H_\sigma^s(\mathbb{R}^+, H^m(\Gamma) \cap \widetilde{H}^r(\Gamma))$, $0 < m \le q+1$, $0 < s \le p+1$, $r \le s$, $|l| \le \frac{1}{2}$ such that $l \cdot r \ge 0$. Then if $l, r \le 0$*

$$\|f - \Pi_h \circ \Pi_{\Delta t} f\|_{r,l,\Gamma} \le C(h^\alpha + (\Delta t)^\beta)\|f\|_{s,m,\Gamma} \ ,$$

where $\alpha = \min\{m - l, m - \frac{m(l+r)}{m+s}\}$, $\beta = \min\{m + s - (l + r), m + s - \frac{m+s}{m} l\}$. If $l, r > 0$, $\beta = m + s - (l + r)$.

We also recall the inverse estimate (see [11, Lemma 2 and the proof of the following corollary])

$$\|v_{h,\Delta t}\|_{1,1,\Omega} \lesssim \frac{1}{\Delta t} \|v_{h,\Delta t}\|_{0,1,\Omega} \tag{3.5}$$

for $v_{h,\Delta t}$ in the approximation spaces $W_{h,\Delta t}^{p,q}$.

3.3 An a priori error estimate

A variational formulation of (3.4) for $\sigma > 0$, derived in [44], is given in terms of the bilinear form

$$\begin{aligned}\widetilde{B}((\mathbf{u},q),(\mathbf{w},q')) = \int_{\mathbb{R}_+} e^{-2\sigma t}\Big\{ & \varrho_1\varrho_2 \int_\Omega (\partial_t^2\mathbf{u})(\partial_t\mathbf{w})\,dx + \varrho_2\int_\Omega \tilde\sigma(\mathbf{u}) : \varepsilon(\partial_t\mathbf{w})\,dx \\ & + \varrho_2\int_\Gamma (V\partial_t q)(\partial_t(\gamma^-\mathbf{w})n)\,ds_x - \varrho_2\int_\Gamma (\partial_t(\gamma^-\mathbf{u})n)(V\partial_t q')\,ds_x \\ & - \int_\Gamma ((-\tfrac12 + K')q)(V\partial_t q')\,ds_x\Big\}\,dt \end{aligned} \tag{3.6}$$

and the linear functional

$$F(\mathbf{w},q') = \int_{\mathbb{R}_+} e^{-2\sigma t}\Big\{ -\varrho_2\int_\Gamma (\partial_t v_+^{inc})(\partial_t(\gamma^-\mathbf{w})n)\,ds_x + \int_\Gamma \tfrac{\partial v_+^{inc}}{\partial n}(V\partial_t q')\,ds_x\Big\}\,dt\,. \tag{3.7}$$

Here, $\widetilde{B}$ is defined on $(H^1_\sigma(\mathbb{R}^+,H^1(\Omega))^d \times \mathcal{D}(V))^2$, where

$$\mathcal{D}(V) = \{q \in H^1_\sigma(\mathbb{R}^+,H^{-\frac12}(\Gamma)) : Vq \in H^1_\sigma(\mathbb{R}^+,H^{-\frac12}(\Gamma))\}\,. \tag{3.8}$$

The variational formulation for fluid-structure interaction then reads: Find $(\mathbf{u},q) \in H^1_\sigma(\mathbb{R}^+,H^1(\Omega))^d \times \mathcal{D}(V)$ such that

$$\widetilde{B}((\mathbf{u},q),(\mathbf{w},q')) = F((\mathbf{w},q')) \tag{3.9}$$

for all $(\mathbf{w},q') \in H^1_\sigma(\mathbb{R}^+,H^1(\Omega))^d \times \mathcal{D}(V)$. Its analysis relies on the following coercivity property, which follows from [44]:

Proposition 3.1. *Let $(\mathbf{u},q) \in H^1_\sigma(\mathbb{R}^+,H^1(\Omega))^d \times \mathcal{D}(V)$. Then*

$$\|\mathbf{u}\|^2_{0,1,\Omega} + \|q\|^2_{0,-\frac12,\Gamma} \lesssim \widetilde{B}((\mathbf{u},q),(\mathbf{u},q))\,. \tag{3.10}$$

Due to Proposition 3.1, the weak formulation (3.9) admits an unique solution $(\mathbf{u},q)$ with an ansatz $Sq = v_+$ and $(-\frac12 I + K')q = \partial_n^+ v$ provided that the solution of the original transmission problem satisfies $v_+ \in H^{3/2}_\sigma(\mathbb{R}^+,H^{1/2}(\Gamma))$.

We consider the Galerkin discretization of (3.9): Find $(\tilde{\mathbf{u}},\tilde q) \in (W^{p_1,q_1}_{h,\Delta t})^d \times V^{p_2,q_2}_{h',\Delta t}$ such that

$$\widetilde{B}((\tilde{\mathbf{u}},\tilde q),(\tilde{\mathbf{w}},\tilde q')) = F_{h',\Delta t}(\tilde{\mathbf{w}},\tilde q') \tag{3.11}$$

for all $(\tilde{\mathbf{w}},\tilde q') \in (W^{p_1,q_1}_{h,\Delta t})^d \times V^{p_2,q_2}_{h',\Delta t}$. Here

$$F_{h',\Delta t}(\mathbf{w},q) = \int_{\mathbb{R}_+} e^{-2\sigma t}\Big\{ -\varrho_2\int_\Gamma (\partial_t v_+^{inc})_{h',\Delta t}(\partial_t(\gamma^-\mathbf{w})n)ds_x + \int_\Gamma \Big(\tfrac{\partial^+ v^{inc}}{\partial n}\Big)_{h',\Delta t}(V\partial_t q)ds_x\Big\}dt$$

with $V^{p_3,q_3}_{h',\Delta t} \ni \partial_t v^I_{h',\Delta t} := (\partial_t v_+^{inc})_{h',\Delta t} \approx \partial_t v_+^{inc} =: \partial_t v^I \in H^3_\sigma(\mathbb{R}^+,H^{1/2}(\Gamma))$ and $(\frac{\partial v^I}{\partial n})_{h',\Delta t} := (\frac{\partial^+ v^{inc}}{\partial n})_{h',\Delta t} \approx (\frac{\partial^+ v^{inc}}{\partial n}) =: (\frac{\partial v^I}{\partial n}) \in H^3_\sigma(\mathbb{R}^+,H^{-1/2}(\Gamma))$. Our first main result is the following a priori error estimate for the time domain boundary element scheme:

Theorem 3.2. *Let* $(\mathbf{u},q) \in H^1_\sigma(\mathbb{R}^+,H^1(\Omega))^d \times \mathcal{D}(V)$ *be the solution of the continuous problem* (3.9) *and* $(\tilde{\mathbf{u}},\tilde{q}) \in (W^{p_1,q_1}_{h,\Delta t})^d \times V^{p_2,q_2}_{h',\Delta t}$ *the Galerkin solution of* (3.11)*. Then*

$$\begin{aligned}\|\tilde{\mathbf{u}}-\mathbf{u}\|^2_{0,1,\Omega} + \|\tilde{q}-q\|^2_{0,-\frac{1}{2},\Gamma} \lesssim_\sigma \|(v^{inc}_+)_{h',\Delta t} - v^{inc}_+\|^2_{2,\frac{1}{2},\Gamma} + \|\Big(\frac{\partial v^{inc}_+}{\partial n}\Big)_{h',\Delta t} - \frac{\partial v^{inc}_+}{\partial n}\|^2_{2,-\frac{1}{2},\Gamma} \\ + (1+(\Delta t)^{-2})\|\mathbf{u}-\tilde{\mathbf{w}}\|^2_{0,1,\Omega} + \|\gamma^-(\mathbf{u}-\tilde{\mathbf{w}})\|^2_{3,\frac{1}{2},\Gamma} + \|q-\tilde{r}\|^2_{3,-\frac{1}{2},\Gamma}\end{aligned}$$

hold for all $(\tilde{\mathbf{w}},\tilde{r}) \in (W^{p_1,q_1}_{h,\Delta t})^d \times V^{p_2,q_2}_{h',\Delta t}$.

Proof. Let $(\mathbf{u},q) \in H^1_\sigma(\mathbb{R}^+,H^1(\Omega))^d \times \mathcal{D}(V)$ resp. $(\tilde{\mathbf{u}},\tilde{q}) \in (W^{p_1,q_1}_{h,\Delta t})^d \times V^{p_2,q_2}_{h',\Delta t}$ be the solution of the continuous problem (3.9) resp. the Galerkin solution of (3.11). For $(\tilde{\mathbf{w}},\tilde{r}) \in (W^{p_1,q_1}_{h,\Delta t})^d \times V^{p_2,q_2}_{h',\Delta t}$, we obtain with the triangle inequality and Youngs inequality:

$$\begin{aligned}\|\tilde{\mathbf{u}}-\mathbf{u}\|^2_{0,1,\Omega} &= \|\tilde{\mathbf{u}}-\tilde{\mathbf{w}}+\tilde{\mathbf{w}}-\mathbf{u}\|_{0,1,\Omega}\|\tilde{\mathbf{u}}-\tilde{\mathbf{w}}+\tilde{\mathbf{w}}-\mathbf{u}\|_{0,1,\Omega} \\ &\le (\|\tilde{\mathbf{u}}-\tilde{\mathbf{w}}\|_{0,1,\Omega} + \|\tilde{\mathbf{w}}-\mathbf{u}\|_{0,1,\Omega})(\|\tilde{\mathbf{u}}-\tilde{\mathbf{w}}\|_{0,1,\Omega} + \|\tilde{\mathbf{w}}-\mathbf{u}\|_{0,1,\Omega}) \\ &= \|\tilde{\mathbf{u}}-\tilde{\mathbf{w}}\|^2_{0,1,\Omega} + \|\tilde{\mathbf{w}}-\mathbf{u}\|^2_{0,1,\Omega} + 2\|\tilde{\mathbf{u}}-\tilde{\mathbf{w}}\|_{0,1,\Omega}\|\tilde{\mathbf{w}}-\mathbf{u}\|_{0,1,\Omega} \\ &\le \|\tilde{\mathbf{u}}-\tilde{\mathbf{w}}\|^2_{0,1,\Omega} + \|\tilde{\mathbf{w}}-\mathbf{u}\|^2_{0,1,\Omega} + 2\Big(\frac{\|\tilde{\mathbf{u}}-\tilde{\mathbf{w}}\|^2_{0,1,\Omega}}{2} + \frac{\|\tilde{\mathbf{w}}-\mathbf{u}\|^2_{0,1,\Omega}}{2}\Big) \\ &= 2\|\tilde{\mathbf{u}}-\tilde{\mathbf{w}}\|^2_{0,1,\Omega} + 2\|\tilde{\mathbf{w}}-\mathbf{u}\|^2_{0,1,\Omega}\ .\end{aligned}$$

Analogously we can estimate:

$$\|\tilde{q}-q\|^2_{0,-1/2,\Gamma} \lesssim \|\tilde{q}-\tilde{r}\|^2_{0,-1/2,\Gamma} + \|\tilde{r}-q\|^2_{0,-1/2,\Gamma} \lesssim \|\tilde{q}-\tilde{r}\|^2_{0,-1/2,\Gamma} + \|\tilde{r}-q\|^2_{3,-1/2,\Gamma}\ ,$$

where the last inequality follows from estimating with a larger norm. We already see the terms $\|\tilde{\mathbf{w}}-\mathbf{u}\|^2_{0,1,\Omega}$ and $\|\tilde{r}-q\|^2_{3,-1/2,\Gamma}$ on the right hand side. Therefore we focus on the remaining parts. From the coercivity (3.10) we obtain

$$\begin{aligned}&\|\tilde{\mathbf{u}}-\tilde{\mathbf{w}}\|^2_{0,1,\Omega} + \|\tilde{q}-\tilde{r}\|^2_{0,-\frac{1}{2},\Gamma} \lesssim \widetilde{B}\Big(\begin{pmatrix}\tilde{\mathbf{u}}-\tilde{\mathbf{w}}\\ \tilde{q}-\tilde{r}\end{pmatrix}^{\mathrm{T}},\begin{pmatrix}\tilde{\mathbf{u}}-\tilde{\mathbf{w}}\\ \tilde{q}-\tilde{r}\end{pmatrix}^{\mathrm{T}}\Big) = \widetilde{B}\Big(\begin{pmatrix}\tilde{\mathbf{u}}-\mathbf{u}+\mathbf{u}-\tilde{\mathbf{w}}\\ \tilde{q}-q+q-\tilde{r}\end{pmatrix}^{\mathrm{T}},\begin{pmatrix}\tilde{\mathbf{u}}-\tilde{\mathbf{w}}\\ \tilde{q}-\tilde{r}\end{pmatrix}^{\mathrm{T}}\Big) \\ &= \widetilde{B}\Big(\begin{pmatrix}\tilde{\mathbf{u}}-\mathbf{u}\\ \tilde{q}-q\end{pmatrix}^{\mathrm{T}},\begin{pmatrix}\tilde{\mathbf{u}}-\mathbf{w}\\ \tilde{q}-\tilde{r}\end{pmatrix}^{\mathrm{T}}\Big) + \widetilde{B}\Big(\begin{pmatrix}\mathbf{u}-\tilde{\mathbf{w}}\\ q-\tilde{r}\end{pmatrix}^{\mathrm{T}},\begin{pmatrix}\tilde{\mathbf{u}}-\tilde{\mathbf{w}}\\ \tilde{q}-\tilde{r}\end{pmatrix}^{\mathrm{T}}\Big) \\ &= \widetilde{B}\Big(\begin{pmatrix}\tilde{\mathbf{u}}\\ \tilde{q}\end{pmatrix}^{\mathrm{T}},\begin{pmatrix}\tilde{\mathbf{u}}-\tilde{\mathbf{w}}\\ \tilde{q}-\tilde{r}\end{pmatrix}^{\mathrm{T}}\Big) - \widetilde{B}\Big(\begin{pmatrix}\mathbf{u}\\ q\end{pmatrix}^{\mathrm{T}},\begin{pmatrix}\tilde{\mathbf{u}}-\tilde{\mathbf{w}}\\ \tilde{q}-\tilde{r}\end{pmatrix}^{\mathrm{T}}\Big) + \widetilde{B}\Big(\begin{pmatrix}\mathbf{u}-\tilde{\mathbf{w}}\\ q-\tilde{r}\end{pmatrix}^{\mathrm{T}},\begin{pmatrix}\tilde{\mathbf{u}}-\tilde{\mathbf{w}}\\ \tilde{q}-\tilde{r}\end{pmatrix}^{\mathrm{T}}\Big) \\ &= F_{h',\Delta t}\Big(\begin{pmatrix}\tilde{\mathbf{u}}-\tilde{\mathbf{w}}\\ \tilde{q}-\tilde{r}\end{pmatrix}^{\mathrm{T}}\Big) - F\Big(\begin{pmatrix}\tilde{\mathbf{u}}-\tilde{\mathbf{w}}\\ \tilde{q}-\tilde{r}\end{pmatrix}^{\mathrm{T}}\Big) + \widetilde{B}\Big(\begin{pmatrix}\mathbf{u}-\tilde{\mathbf{w}}\\ q-\tilde{r}\end{pmatrix}^{\mathrm{T}},\begin{pmatrix}\tilde{\mathbf{u}}-\tilde{\mathbf{w}}\\ \tilde{q}-\tilde{r}\end{pmatrix}^{\mathrm{T}}\Big)\ .\end{aligned}$$

Now looking at the first two terms.

$$\begin{aligned}&F_{h',\Delta t}\Big(\begin{pmatrix}\tilde{\mathbf{u}}-\tilde{\mathbf{w}}\\ \tilde{q}-\tilde{r}\end{pmatrix}^{\mathrm{T}}\Big) - F\Big(\begin{pmatrix}\tilde{\mathbf{u}}-\tilde{\mathbf{w}}\\ \tilde{q}-\tilde{r}\end{pmatrix}^{\mathrm{T}}\Big) \\ &= \int_{\mathbb{R}_+} e^{-2\sigma t}\{-\rho_2\int_\Gamma (\partial_t v^I_{h',\Delta t} - \partial_t v^I)\partial_t(\tilde{\mathbf{u}}-\tilde{\mathbf{w}})\cdot n\,ds_x + \int_\Gamma ((\frac{\partial v^I}{\partial n})_{h',\Delta t} - (\frac{\partial v^I}{\partial n}))V(\partial_t(\tilde{q}-\tilde{r}))\,ds_x\}\,dt \\ &\lesssim_\sigma \|\partial_t v^I_{h',\Delta t} - \partial_t v^I\|_{1,-\frac{1}{2},\Gamma}\|\partial_t(\tilde{\mathbf{u}}-\tilde{\mathbf{w}})\cdot n\|_{-1,\frac{1}{2},\Gamma} + \|(\frac{\partial v^I}{\partial n})_{h',\Delta t} - (\frac{\partial v^I}{\partial n})\|_{2,-\frac{1}{2},\Gamma}\|V(\partial_t(\tilde{q}-\tilde{r}))\|_{-2,\frac{1}{2},\Gamma}\end{aligned}$$

$$\begin{aligned}
&\lesssim \|v^I_{h',\Delta t} - v^I\|_{2,-\frac{1}{2},\Gamma}\|\tilde{\mathbf{u}}-\tilde{\mathbf{w}}\|_{0,1,\Omega} + \|(\frac{\partial v^I}{\partial n})_{h',\Delta t} - (\frac{\partial v^I}{\partial n})\|_{2,-\frac{1}{2},\Gamma}\|(\partial_t(\tilde{q}-\tilde{r}))\|_{-1,-\frac{1}{2},\Gamma}\\
&\lesssim \|v^I_{h',\Delta t} - v^I\|_{2,-\frac{1}{2},\Gamma}\|\tilde{\mathbf{u}}-\tilde{\mathbf{w}}\|_{0,1,\Omega} + \|(\frac{\partial v^I}{\partial n})_{h',\Delta t} - (\frac{\partial v^I}{\partial n})\|_{2,-\frac{1}{2},\Gamma}\|\tilde{q}-\tilde{r}\|_{0,-\frac{1}{2},\Gamma} \ ,
\end{aligned}$$

where we have used the duality, the trace theorem and the mapping properties of V. Now using Young's inequality with small $\epsilon > 0$

$$\begin{aligned}
&F_{h',\Delta t}\Big(\begin{pmatrix}\tilde{\mathbf{u}}-\tilde{\mathbf{w}}\\ \tilde{q}-\tilde{r}\end{pmatrix}^{\mathrm{T}}\Big) - F\Big(\begin{pmatrix}\tilde{\mathbf{u}}-\tilde{\mathbf{w}}\\ \tilde{q}-\tilde{r}\end{pmatrix}^{\mathrm{T}}\Big)\\
&\lesssim \tfrac{1}{\epsilon}\|v^I_{h',\Delta t} - v^I\|^2_{2,-\frac{1}{2},\Gamma} + \epsilon\|\tilde{\mathbf{u}}-\tilde{\mathbf{w}}\|^2_{0,1,\Omega} + \tfrac{1}{\epsilon}\|(\frac{\partial v^I}{\partial n})_{h',\Delta t} - (\frac{\partial v^I}{\partial n})\|^2_{2,-\frac{1}{2},\Gamma} + \epsilon\|\tilde{q}-\tilde{r}\|^2_{0,-\frac{1}{2},\Gamma} \ .
\end{aligned}$$

Since $\|\tilde{\mathbf{u}}-\tilde{\mathbf{w}}\|^2_{0,1,\Omega}$ and $\|\tilde{q}-\tilde{r}\|^2_{0,-\frac{1}{2},\Gamma}$ occurs on the left hand side as well, we combine them together. Therefore

$$\|\tilde{\mathbf{u}}-\tilde{\mathbf{w}}\|^2_{0,1,\Omega}+\|\tilde{q}-\tilde{r}\|^2_{0,-\frac{1}{2},\Gamma}\lesssim \|v^I_{h',\Delta t}-v^I\|^2_{2,-\frac{1}{2},\Gamma}+\|(\partial_n v^I)_{h',\Delta t}-(\partial_n v^I)\|^2_{2,-\frac{1}{2},\Gamma}+\widetilde{B}\Big(\begin{pmatrix}\mathbf{u}-\tilde{\mathbf{w}}\\ q-\tilde{r}\end{pmatrix}^{\mathrm{T}},\begin{pmatrix}\tilde{\mathbf{u}}-\tilde{\mathbf{w}}\\ \tilde{q}-\tilde{r}\end{pmatrix}^{\mathrm{T}}\Big).$$

For

$$\begin{aligned}
&\widetilde{B}((\mathbf{u}-\tilde{\mathbf{w}},q-\tilde{r}),(\tilde{\mathbf{u}}-\tilde{\mathbf{w}},\tilde{q}-\tilde{r}))\\
&= \int_{\mathbb{R}_+} e^{-2\sigma t}\Big\{\varrho_1\varrho_2\int_\Omega(\partial_t^2(\mathbf{u}-\tilde{\mathbf{w}}))(\partial_t(\tilde{\mathbf{u}}-\tilde{\mathbf{w}}))\ dx + \varrho_2\int_\Omega\tilde{\sigma}(\mathbf{u}-\tilde{\mathbf{w}}):\varepsilon(\partial_t(\tilde{\mathbf{u}}-\tilde{\mathbf{w}}))\ dx\\
&\quad + \varrho_2\int_\Gamma(V\partial_t(q-\tilde{r}))(\partial_t(\gamma^-(\tilde{\mathbf{u}}-\tilde{\mathbf{w}}))n)\ ds_x - \varrho_2\int_\Gamma(\partial_t(\gamma^-(\mathbf{u}-\tilde{\mathbf{w}}))n)(V\partial_t(\tilde{q}-\tilde{r}))\ ds_x\\
&\quad - \int_\Gamma((-\tfrac{1}{2}+K')(q-\tilde{r}))(V\partial_t(\tilde{q}-\tilde{r}))\ ds_x\Big\}\ dt \ ,
\end{aligned}$$

we estimate every term separately. The first two terms of $\widetilde{B}$ are estimated using the duality and the inverse estimate (3.5) together with Young's inequality

$$\begin{aligned}
&\int_{\mathbb{R}_+} e^{-2\sigma t}\Big\{\int_\Omega(\partial_t^2(\mathbf{u}-\tilde{\mathbf{w}}))(\partial_t(\tilde{\mathbf{u}}-\tilde{\mathbf{w}}))\ dx + \varrho_2\int_\Omega\tilde{\sigma}(\mathbf{u}-\tilde{\mathbf{w}}):\varepsilon(\partial_t(\tilde{\mathbf{u}}-\tilde{\mathbf{w}}))\ dx\Big\}\ dt\\
&\lesssim_\sigma \|\partial_t^2(\mathbf{u}-\tilde{\mathbf{w}})\|_{0,-1,\Omega}\|\partial_t(\mathbf{u}-\tilde{\mathbf{w}})\|_{0,1,\Omega} + \|\tilde{\sigma}(\mathbf{u}-\tilde{\mathbf{w}})\|_{0,0,\Omega}\|\varepsilon(\partial_t(\mathbf{u}-\tilde{\mathbf{w}}))\|_{0,0,\Omega}\\
&\lesssim \|\mathbf{u}-\tilde{\mathbf{w}}\|_{0,1,\Omega}\|\tilde{\mathbf{u}}-\tilde{\mathbf{w}}\|_{1,1,\Omega} + \|\mathbf{u}-\tilde{\mathbf{w}}\|_{0,1,\Omega}\|\tilde{\mathbf{u}}-\tilde{\mathbf{w}}\|_{1,1,\Omega}\\
&\lesssim \|\mathbf{u}-\tilde{\mathbf{w}}\|_{0,1,\Omega}\|\tilde{\mathbf{u}}-\tilde{\mathbf{w}}\|_{1,1,\Omega}\\
&\lesssim (\Delta t)^{-1}\|\mathbf{u}-\tilde{\mathbf{w}}\|_{0,1,\Omega}\|\tilde{\mathbf{u}}-\tilde{\mathbf{w}}\|_{0,1,\Omega}\\
&\lesssim \tfrac{1}{\epsilon(\Delta t)^2}\|\mathbf{u}-\tilde{\mathbf{w}}\|^2_{0,1,\Omega} + \epsilon\|\tilde{\mathbf{u}}-\tilde{\mathbf{w}}\|^2_{0,1,\Omega} \quad .
\end{aligned}$$

Again we are able to combine the second term with the left hand side.

For the third term we similarly see with the help of the duality and the mapping properties of V (see Theorem 2.2)

$$\begin{aligned}
&\int_{\mathbb{R}_+} e^{-2\sigma t}\int_\Gamma(V\partial_t(q-\tilde{r}))(\partial_t(\gamma^-(\tilde{\mathbf{u}}-\tilde{\mathbf{w}}))n)\ ds_x\ dt\\
&\lesssim_\sigma \|V\partial_t(q-\tilde{r})\|_{0,\frac{1}{2},\Gamma}\|\partial_t\gamma^-((\tilde{\mathbf{u}}-\tilde{\mathbf{w}})n)\|_{0,-\frac{1}{2},\Gamma}\\
&\lesssim \|\partial_t(q-\tilde{r})\|_{1,-\frac{1}{2},\Gamma}\|\gamma^-((\tilde{\mathbf{u}}-\tilde{\mathbf{w}})n)\|_{1,-\frac{1}{2},\Gamma} \lesssim \|q-\tilde{r}\|_{2,-\frac{1}{2},\Gamma}\|\gamma^-(\tilde{\mathbf{u}}-\tilde{\mathbf{w}})n\|_{1,-\frac{1}{2},\Gamma} \quad . \qquad (3.12)
\end{aligned}$$

The continuous embedding of $H^0_\sigma(\mathbb{R}^+, H^{\frac{1}{2}}(\Gamma))$ into $H^1_\sigma(\mathbb{R}^+, H^{-\frac{1}{2}}(\Gamma))$ and the trace theorem then imply

$$\|\gamma^-(\tilde{\mathbf{u}}-\tilde{\mathbf{w}})n\|_{1,-\frac{1}{2},\Gamma} \lesssim \|\gamma^-(\tilde{\mathbf{u}}-\tilde{\mathbf{w}})\|_{0,\frac{1}{2},\Gamma} \lesssim \|\tilde{\mathbf{u}}-\tilde{\mathbf{w}}\|_{0,1,\Omega} \ .$$

Again using Young's inequality and taking advantage of $\|q-\tilde{r}\|^2_{2,-\frac{1}{2},\Gamma}$ dominated by $\|q-\tilde{r}\|^2_{3,-\frac{1}{2},\Gamma}$, we estimate (3.12) by

$$\lesssim \tfrac{1}{\epsilon}\|q-\tilde{r}\|^2_{2,-\frac{1}{2},\Gamma} + \epsilon\|\tilde{\mathbf{u}}-\tilde{\mathbf{w}}\|^2_{0,1,\Omega} \lesssim \tfrac{1}{\epsilon}\|q-\tilde{r}\|^2_{3,-\frac{1}{2},\Gamma} + \epsilon\|\tilde{\mathbf{u}}-\tilde{\mathbf{w}}\|^2_{0,1,\Omega} \ .$$

We combine $\epsilon\|\tilde{\mathbf{u}}-\tilde{\mathbf{w}}\|^2_{0,1,\Omega}$ with the left hand side.

The fourth term is similarly bounded as follows:

$$\begin{aligned}
&\int_{\mathbb{R}_+} e^{-2\sigma t}\int_\Gamma (\partial_t(\gamma^-(\mathbf{u}-\tilde{\mathbf{w}}))n)(V\partial_t(\tilde{q}-\tilde{r}))\ ds_x\ dt\\
&\lesssim_\sigma \|\partial_t(\gamma^-(\mathbf{u}-\tilde{\mathbf{w}})n)\|_{2,-\frac{1}{2},\Gamma}\|V\partial_t(\tilde{q}-\tilde{r})\|_{-2,\frac{1}{2},\Gamma}\\
&\lesssim \|\partial_t(\gamma^-(\mathbf{u}-\tilde{\mathbf{w}})n)\|_{2,-\frac{1}{2},\Gamma}\|\partial_t(\tilde{q}-\tilde{r})\|_{-1,-\frac{1}{2},\Gamma} \lesssim \|\gamma^-(\mathbf{u}-\tilde{\mathbf{w}})\|_{3,\frac{1}{2},\Gamma}\|\tilde{q}-\tilde{r}\|_{0,-\frac{1}{2},\Gamma} \ .
\end{aligned}$$

Using Young's inequality together with combining $\epsilon\|\tilde{q}-\tilde{r}\|^2_{0,-\frac{1}{2},\Gamma}$ with the left hand side, we get the additive term $\|\gamma^-(\mathbf{u}-\tilde{\mathbf{w}})\|^2_{3,\frac{1}{2},\Gamma}$.

For the last term, we use the duality and the mapping properties of K' and V. We observe

$$\begin{aligned}
&\int_{\mathbb{R}_+} e^{-2\sigma t}\int_\Gamma ((-\tfrac{1}{2}+K')(q-\tilde{r}))(V\partial_t(\tilde{q}-\tilde{r}))\ ds_x\ dt\\
&\lesssim \|(-\tfrac{1}{2}+K')(q-\tilde{r})\|_{2,-\frac{1}{2},\Gamma}\|V\partial_t(\tilde{q}-\tilde{r})\|_{-2,\frac{1}{2},\Gamma} \lesssim \|q-\tilde{r}\|_{3,-\frac{1}{2},\Gamma}\|\tilde{q}-\tilde{r}\|_{0,-\frac{1}{2},\Gamma} \ .
\end{aligned}$$

With Young's inequality and combining $\epsilon\|\tilde{q}-\tilde{r}\|^2_{0,-\frac{1}{2},\Gamma}$ with the left hand side we get the last additive term $\|q-\tilde{r}\|^2_{3,-\frac{1}{2},\Gamma}$ to the estimate. □

3.4 An a posteriori error estimate

For simplicity we assume $v^I_{h',\Delta t} = v^I$ and $(\frac{\partial v^I}{\partial n})_{h',\Delta t} = \frac{\partial v^I}{\partial n}$. Then we state the following a posteriori error estimate:

Theorem 3.3. *Let $(\mathbf{u},q) \in H^1_\sigma(\mathbb{R}^+, H^1(\Omega))^d \times \mathcal{D}(V)$ be the solution of the continuous problem (3.9) and $(\tilde{\mathbf{u}},\tilde{q}) \in (W^{p_1,q_1}_{h,\Delta t})^d \times V^{p_2,q_2}_{h,\Delta t}$ the Galerkin solution of (3.11). Let $\bigcup_{j=1}^{N_s}\partial\Omega_j = T = \bigcup_{i=1}^m T_i$, where each T_i is a face of one Ω_j. With $[v]$, a jump into a face T_i, the following a posteriori error estimate holds:*

$$\|\tilde{\mathbf{u}}-\mathbf{u}\|^2_{0,1,\Omega} + \|\tilde{q}-q\|^2_{0,-\frac{1}{2},\Gamma} \lesssim_\sigma \eta_1^2+\eta_2^2+\eta_3^2+\eta_4^2,$$

where

$$\begin{aligned}
\eta_1^2 &= \sum_{\Omega_i} \|\varrho_1 \partial_t^2 \tilde{\mathbf{u}} - \mathrm{div}\tilde{\sigma}(\tilde{\mathbf{u}})\|^2_{0,0,\Omega_i} \ , \\
\eta_2^2 &= \sum_{T_i \cap \Gamma = \varnothing} \max\{h, \Delta t\} \|[\tilde{\sigma}(\tilde{\mathbf{u}}) \cdot n]\|^2_{1,0,T_i} \ , \\
\eta_3^2 &= \max\{h, \Delta t\} \|\tilde{\sigma}(\gamma^- \tilde{\mathbf{u}}) \cdot n + V \partial_t \tilde{q} \cdot n + \partial_t v_+^{inc} \cdot n\|^2_{1,0,\Gamma} \ , \\
\eta_4^2 &= \|\varrho_2 \partial_t (\gamma^- \tilde{\mathbf{u}}) \cdot n + (-\tfrac{1}{2} + K') \tilde{q} + \tfrac{\partial^+ v^{inc}}{\partial n}\|^2_{2,-\frac{1}{2},\Gamma} \ .
\end{aligned}$$

Proof. Let $(\mathbf{u}, q) \in H^1_\sigma(\mathbb{R}^+, H^1(\Omega))^d \times \mathcal{D}(V)$ resp. $(\tilde{\mathbf{u}}, \tilde{q}) \in (W^{p_1,q_1}_{h,\Delta t})^d \times V^{p_2,q_2}_{h,\Delta t}$ be the solution of the continuous problem (3.9) resp. the Galerkin solution (3.11). From the coercivity estimate (3.10) and the variational formulations (3.9) resp. (3.11) we obtain for all $(\tilde{\mathbf{w}}, \tilde{r}) \in (W^{p_1,q_1}_{h,\Delta t})^d \times V^{p_2,q_2}_{h,\Delta t}$:

$$\begin{aligned}
&\|\tilde{\mathbf{u}} - \mathbf{u}\|^2_{0,1,\Omega} + \|\tilde{q} - q\|^2_{0,-\frac{1}{2},\Gamma} \\
&\lesssim \widetilde{B}((\tilde{\mathbf{u}} - \mathbf{u}, \tilde{q} - q), (\tilde{\mathbf{u}} - \mathbf{u}, \tilde{q} - q)) \\
&= \widetilde{B}((\tilde{\mathbf{u}}, \tilde{q}), (\tilde{\mathbf{u}} - \mathbf{u}, \tilde{q} - q)) - \widetilde{B}((\mathbf{u}, q), (\tilde{\mathbf{u}} - \mathbf{u}, \tilde{q} - q)) \\
&= \widetilde{B}((\tilde{\mathbf{u}}, \tilde{q}), (\tilde{\mathbf{u}} - \mathbf{u}, \tilde{q} - q)) - F(\tilde{\mathbf{u}} - \mathbf{u}, \tilde{q} - q) \\
&= \widetilde{B}((\tilde{\mathbf{u}}, \tilde{q}), (\tilde{\mathbf{u}} - \tilde{\mathbf{w}}, \tilde{q} - \tilde{r})) + \widetilde{B}((\tilde{\mathbf{u}}, \tilde{q}), (\tilde{\mathbf{w}} - \mathbf{u}, \tilde{r} - q)) - F(\tilde{\mathbf{u}} - \tilde{\mathbf{w}}, \tilde{q} - \tilde{r}) - F(\tilde{\mathbf{w}} - u, \tilde{r} - q) \\
&= \widetilde{B}((\tilde{\mathbf{u}}, \tilde{q}), (\tilde{\mathbf{w}} - \mathbf{u}, \tilde{r} - q)) - F(\tilde{\mathbf{w}} - \mathbf{u}, \tilde{r} - q) \\
&= \int_{\mathbb{R}_+} e^{-2\sigma t} \Big\{ \varrho_1 \varrho_2 \int_\Omega (\partial_t^2 \tilde{\mathbf{u}}) \cdot (\partial_t(\tilde{\mathbf{w}} - \mathbf{u}))\, dx + \varrho_2 \int_\Omega \tilde{\sigma}(\tilde{\mathbf{u}}) : \varepsilon(\partial_t(\tilde{\mathbf{w}} - \mathbf{u}))\, dx \\
&\quad + \varrho_2 \int_\Gamma (V \partial_t \tilde{q})(\partial_t(\gamma^-(\tilde{\mathbf{w}} - \mathbf{u})) \cdot n)\, ds_x - \varrho_2 \int_\Gamma (\partial_t(\gamma^- \tilde{\mathbf{u}}) \cdot n)(V \partial_t(\tilde{r} - q))\, ds_x \\
&\quad - \int_\Gamma ((-\tfrac{1}{2} + K')\tilde{q})(V \partial_t(\tilde{r} - q))\, ds_x + \varrho_2 \textstyle\int_\Gamma (\partial_t v_+^{inc})(\partial_t(\gamma^-(\tilde{\mathbf{w}} - \mathbf{u})) \cdot n)\, ds_x \\
&\quad - \int_\Gamma \tfrac{\partial^+ v^{inc}}{\partial n} (V \partial_t(\tilde{r} - q))\, ds_x \Big\}\, dt \ ,
\end{aligned}$$

where we used $\widetilde{B}((\tilde{\mathbf{u}}, \tilde{q}), (\tilde{\mathbf{u}} - \tilde{\mathbf{w}}, \tilde{q} - \tilde{r})) = F(\tilde{\mathbf{u}} - \tilde{\mathbf{w}}, \tilde{q} - \tilde{r})$ since we assumed $v^I_{h',\Delta t} = v^I$ and $(\frac{\partial v^I}{\partial n})_{h',\Delta t} = \frac{\partial v^I}{\partial n}$. Now using Betti's formula:

$$\langle \tilde{\sigma}(\gamma^- \mathbf{u}) \cdot n, \gamma^- \mathbf{w} \rangle_{\Gamma \times \mathbb{R}^+, \sigma} = (\tilde{\sigma}(\mathbf{u}), \varepsilon(\mathbf{w}))_{\Omega^- \times \mathbb{R}^+, \sigma} + (\Delta^* \mathbf{u}, \mathbf{w})_{\Omega^- \times \mathbb{R}^+, \sigma}$$

on each tetrahedron Ω_j, we get

$$\begin{aligned}
\|\tilde{\mathbf{u}} - \mathbf{u}\|^2_{0,1,\Omega} + \|\tilde{q} - q\|^2_{0,-\frac{1}{2},\Gamma} \lesssim \int_{\mathbb{R}_+} e^{-2\sigma t} \Big\{ &\varrho_2 \sum_{\Omega_i} \int_{\Omega_i} \big\{ \varrho_1 \partial_t^2 \tilde{\mathbf{u}} - \mathrm{div}\tilde{\sigma}(\tilde{\mathbf{u}}) \big\} \cdot (\partial_t(\tilde{\mathbf{w}} - \mathbf{u}))\, dx \\
&+ \varrho_2 \sum_{T_i \cap \Gamma = \varnothing} \int_{T_i} [\tilde{\sigma}(\tilde{\mathbf{u}}) \cdot n] \cdot (\partial_t(\tilde{\mathbf{w}} - \mathbf{u}))\, ds_x \\
&+ \varrho_2 \int_\Gamma \big\{ \tilde{\sigma}(\gamma^- \tilde{\mathbf{u}}) \cdot n + V \partial_t \tilde{q} \cdot n + \partial_t v_+^{inc} \cdot n \big\} \cdot (\partial_t(\gamma^-(\tilde{\mathbf{w}} - \mathbf{u})))\, ds_x \\
&- \int_\Gamma \Big\{ \varrho_2 \partial_t(\gamma^- \tilde{\mathbf{u}}) \cdot n + (-\tfrac{1}{2} + K')\tilde{q} + \tfrac{\partial^+ v^{inc}}{\partial n} \Big\} (V \partial_t(\tilde{r} - q))\, ds_x \Big\}\, dt \ .
\end{aligned}$$

Now estimating with the duality:

$$\begin{aligned}\|\tilde{\mathbf{u}}-\mathbf{u}\|^2_{0,1,\Omega}+\|\tilde{q}-q\|^2_{0,-\frac{1}{2},\Gamma} \lesssim_\sigma & \sum_{\Omega_i}\|\rho_1\partial_t^2\tilde{\mathbf{u}}-\mathrm{div}\tilde{\sigma}(\tilde{\mathbf{u}})\|_{0,0,\Omega_i}\|\partial_t(\tilde{\mathbf{w}}-\mathbf{u})\|_{0,0,\Omega_i}\\ &+\sum_{T_i\cap\Gamma=\varnothing}\|[\tilde{\sigma}(\tilde{\mathbf{u}})\cdot n]\|_{1,0,T_i}\|\partial_t(\tilde{\mathbf{w}}-\mathbf{u})\|_{-1,0,T_i}\\ &+\|\tilde{\sigma}(\gamma^-\tilde{\mathbf{u}})\cdot n+V\partial_t\tilde{q}\cdot n+\partial_t v^I\cdot n\|_{1,0,\Gamma}\|\partial_t(\tilde{\mathbf{w}}-\mathbf{u})\|_{-1,0,\Gamma}\\ &+\|\partial_t\gamma^-\tilde{\mathbf{u}}\cdot n+(-\frac{1}{2}I+K')\tilde{q}+\frac{\partial v^I}{\partial n}\|_{2,-1/2,\Gamma}\|V\partial_t(\tilde{r}-q)\|_{-2,1/2,\Gamma}\ .\end{aligned}$$

Now using the mapping properties of V, we further estimate

$$\begin{aligned}\|\tilde{\mathbf{u}}-\mathbf{u}\|^2_{0,1,\Omega}+\|\tilde{q}-q\|^2_{0,-\frac{1}{2},\Gamma} \lesssim & \sum_{\Omega_i}\|\rho_1\partial_t^2\tilde{\mathbf{u}}-\mathrm{div}\tilde{\sigma}(\tilde{\mathbf{u}})\|_{0,0,\Omega_i}\|\tilde{\mathbf{w}}-\mathbf{u}\|_{0,1,\Omega_i}\\ &+\sum_{T_i\cap\Gamma=\varnothing}\|[\tilde{\sigma}(\tilde{\mathbf{u}})\cdot n]\|_{1,0,T_i}\|\tilde{\mathbf{w}}-\mathbf{u}\|_{0,0,T_i}\\ &+\|\tilde{\sigma}(\gamma^-\tilde{\mathbf{u}})\cdot n+V\partial_t\tilde{q}\cdot n+\partial_t v^I\cdot n\|_{1,0,\Gamma}\|(\gamma^-(\tilde{\mathbf{w}}-\mathbf{u}))\|_{0,0,\Gamma}\\ &+\|\partial_t\gamma^-\tilde{\mathbf{u}}\cdot n+(-\frac{1}{2}I+K')\tilde{q}+\frac{\partial v^I}{\partial n}\|_{2,-1/2,\Gamma}\|\tilde{r}-q\|_{0,-1/2,\Gamma}\ .\end{aligned}$$

Next we choose $\tilde{\mathbf{w}}=\tilde{\mathbf{u}}+\Pi_h\circ\Pi_{\Delta t}(\mathbf{u}-\tilde{\mathbf{u}})$ for the second and the third term in order to use Lemma 3.1, $\tilde{\mathbf{w}}=\tilde{\mathbf{u}}$ for the first term and $\tilde{r}=\tilde{q}$ for the last term. We remember $\gamma^-\mathbf{u}\in H^1_\sigma(\mathbb{R}^+,H^{1/2}(\Gamma))$:

$$\begin{aligned}\|\tilde{\mathbf{u}}-\mathbf{u}\|^2_{0,1,\Omega}+\|\tilde{q}-q\|^2_{0,-\frac{1}{2},\Gamma} \lesssim & \sum_{\Omega_i}\|\rho_1\partial_t^2\tilde{\mathbf{u}}-\mathrm{div}\tilde{\sigma}(\tilde{\mathbf{u}})\|_{0,0,\Omega_i}\|\tilde{\mathbf{u}}-\mathbf{u}\|_{0,1,\Omega_i}\\ &+\sum_{T_i\cap\Gamma=\varnothing}\|[\tilde{\sigma}(\tilde{\mathbf{u}})\cdot n]\|_{1,0,T_i}\max\{\Delta t,h\}^{1/2}\|\tilde{\mathbf{u}}-\mathbf{u}\|_{0,1/2,T_i}\\ &+\|\tilde{\sigma}(\gamma^-\tilde{\mathbf{u}})\cdot n+V\partial_t\tilde{q}\cdot n+\partial_t v^I\cdot n\|_{1,0,\Gamma}\max\{\Delta t,h\}^{1/2}\|(\gamma^-(\tilde{\mathbf{u}}-\mathbf{u}))\|_{0,1/2,\Gamma}\\ &+\|\partial_t\gamma^-\tilde{\mathbf{u}}\cdot n+(-\frac{1}{2}I+K')\tilde{q}+\frac{\partial v^I}{\partial n}\|_{2,-1/2,\Gamma}\|\tilde{q}-q\|_{0,-1/2,\Gamma}\ .\end{aligned}$$

Now using Young's inequality and the trace theorem and combining $\|\tilde{\mathbf{u}}-\mathbf{u}\|^2_{0,1,\Omega}$ and $\|\tilde{q}-q\|^2_{0,-1/2,\Gamma}$ with the left hand side yields the estimate:

$$\begin{aligned}\|\tilde{\mathbf{u}}-\mathbf{u}\|^2_{0,1,\Omega}+\|\tilde{q}-q\|^2_{0,-\frac{1}{2},\Gamma} \lesssim & \sum_{\Omega_i}\|\rho_1\partial_t^2\tilde{\mathbf{u}}-\mathrm{div}\tilde{\sigma}(\tilde{\mathbf{u}})\|^2_{0,0,\Omega_i}\\ &+\sum_{T_i\cap\Gamma=\varnothing}\|[\tilde{\sigma}(\tilde{\mathbf{u}})\cdot n]\|^2_{1,0,T_i}\max\{\Delta t,h\}\\ &+\|\tilde{\sigma}(\gamma^-\tilde{\mathbf{u}})\cdot n+V\partial_t\tilde{q}\cdot n+\partial_t v^I\cdot n\|^2_{1,0,\Gamma}\max\{\Delta t,h\}\\ &+\|\partial_t\gamma^-\tilde{\mathbf{u}}\cdot n+(-\frac{1}{2}I+K')\tilde{q}+\frac{\partial v^I}{\partial n}\|^2_{2,-1/2,\Gamma}\ .\end{aligned}$$

□

For the upcoming sections, we set $\rho_1=\rho_2=1$ and $\sigma=0$ and continue with the discretizations of (3.6) and (3.7).

3.5 Discretization via generalized light cones

We begin with the discretization of (3.6). Since we want to focus on numerical experiments for 3D in time domain, we discretize Ω with N_s tetrahedrals and divide a finite temporal mesh into N_t equidistant intervals of length (Δt). The boundary Γ is being discretized with $N_{s'}$ triangles.

In this section we focus especially on the discretization of:

$$\int_0^\infty \int_\Gamma ((-\frac{1}{2}I + K')q)(V\dot{q}')ds_x dt \ .$$

As ansatz functions we first begin by choosing:

$$q_{h,\Delta t}(x,t) = \sum_{m=1}^{N_t}\sum_{i=1}^{N_{s'}} q_i^m \gamma_{\Delta t}^m(t)\xi_h^i(x) \ \in V_{h,\Delta t}^{1,0} \ . \tag{3.13}$$

Then as test functions we choose for $n = 1,\dots,N_t$ and $j = 1,\dots,N_{s'}$:

$$\dot{q}'_{h,\Delta t}(x,t) = \gamma_{\Delta t}^n(t)\xi_h^j(x) \ \in V_{h,\Delta t}^{1,0} \ . \tag{3.14}$$

We begin with the discretization of $\langle -\frac{1}{2}Iq, V\dot{q}'\rangle_{\Gamma\times\mathbb{R}_+}$. For $\langle Iq, V\dot{q}'\rangle_{\Gamma\times\mathbb{R}_+}$:

$$\begin{aligned}
\langle q_{h,\Delta t}, V\dot{q}'_{h,\Delta t}\rangle &= \sum_{m=1}^{N_t}\sum_{i=1}^{N_s} q_i^m \iint_{\Gamma\times\Gamma} \frac{\xi_h^i(x)\xi_h^j(y)}{4\pi|x-y|}\int_0^\infty \gamma_{\Delta t}^m(t)\gamma_{\Delta t}^n(t-|x-y|)dt ds_y ds_x \\
&= \sum_{m=1}^{N_t}\sum_{i=1}^{N_{s'}} q_i^m \iint_{\Gamma\times\Gamma} \frac{\xi_h^i(x)\xi_h^j(y)}{4\pi|x-y|}((t_{m-n+1}-|x-y|)\chi_{E_{m-n}}+(-t_{m-n-1}+|x-y|)\chi_{E_{m-n-1}})ds_y ds_x \\
&= \sum_{m=1}^{N_t}\sum_{i=1}^{N_{s'}} q_i^m \iint_{E_{m-n}} \frac{\xi_h^i(x)\xi_h^j(y)(t_{m-n+1}-|x-y|)}{4\pi|x-y|}ds_y ds_x - \iint_{E_{m-n-1}} \frac{\xi_h^i(x)\xi_h^j(y)(t_{m-n-1}-|x-y|)}{4\pi|x-y|}ds_y ds_x \\
&= \tilde{V}^T q \ ,
\end{aligned} \tag{3.15}$$

where for the time integral, we used (9.5) in Appendix with switched indices n and m. At last multiplying (3.15) with a prefactor $-\frac{1}{2}$ gives us the discretization of $\langle -\frac{1}{2}Iq, V\dot{q}'\rangle_{\Gamma\times\mathbb{R}_+}$. We notice that the indices of the lightcones are reversed compared to the lightcones for V in Subsection 2.3.1. In order to compute these matrices efficently we begin computing them at the furthest timestep and then going backwards until 0, see Section 3.7, (3.24) for the matrix structure of $\tilde{V}^T$. We continue with the discrete calculation of

$$\begin{aligned}
&\int_0^\infty \int_\Gamma (K' q_{h,\Delta t})(x,t)(V\dot{q}'_{h,\Delta t})ds_x dt \\
&= \int_0^\infty \int_\Gamma \Big(\int_\Gamma \frac{n_x\cdot(x-y)}{4\pi|x-y|}\Big(\frac{\sum_{m=1}^{N_t}\sum_{m=1}^{N_s} q_i^m \gamma_{\Delta t}^m(t-|x-y|)\xi_h^i(y)}{|x-y|^2} \\
&+ \frac{\sum_{m=1}^{N_t}\sum_{m=1}^{N_{s'}} q_i^m \dot{\gamma}_{\Delta t}^m(t-|x-y|)\xi_h^i(y)}{|x-y|}\Big)ds_y\Big)\left(\int_\Gamma \frac{\gamma_{\Delta t}^n(t-|x-z|)\xi_h^j(z)}{4\pi|x-z|}ds_z\right)ds_x dt \\
&= \sum_{m=1}^{N_t}\sum_{i=1}^{N_{s'}} q_i^m \iiint_{\Gamma\times\Gamma\times\Gamma} \frac{n_x(x-y)\xi_h^i(y)\xi_h^j(z)}{16\pi^2|x-y|^2|x-z|}\Big(\frac{1}{|x-y|}\int_0^\infty \gamma_{\Delta t}^m(t-|x-y|)\gamma_{\Delta t}^n(t-|x-z|)dt \\
&+ \int_0^\infty \dot{\gamma}_{\Delta t}^m(t-|x-y|)\gamma_{\Delta t}^n(t-|x-z|)\Big)dt\Big)ds_z ds_y ds_x \ .
\end{aligned}$$

For the time integral with the derivative in time:

$$\begin{aligned}
&\int_0^\infty \dot{\gamma}^m_{\Delta t}(t-|x-y|)\gamma^n_{\Delta t}(t-|x-z|)dt \\
&\quad = \int_0^\infty (\delta(t-|x-y|-t_{m-1})-\delta(t-|x-y|-t_m))\gamma^n_{\Delta t}(t-|x-z|)dt \\
&\quad = \gamma^n_{\Delta t}(|x-y|+t_{m-1}-|x-z|)-\gamma^n_{\Delta t}(|x-y|+t_m-|x-z|) \\
&\quad = (H(|x-y|+t_{m-1}-|x-z|-t_{n-1})-H(|x-y|+t_{m-1}-|x-z|-t_n)) \\
&\quad - (H(|x-y|+t_m-|x-z|-t_{n-1})-H(|x-y|+t_m-|x-z|-t_n)) \\
&\quad = (H(|x-y|-|x-z|+t_{m-n})-H(|x-y|-|x-z|+t_{m-1-n})) \\
&\quad - (H(|x-y|-|x-z|+t_{m+1-n})-H(|x-y|-|x-z|+t_{m-n})) \\
&\quad = \chi_{A_{m-n-1}}(x,y,z)-\chi_{A_{m-n}}(x,y,z)\ ,
\end{aligned}$$

with

$$\chi_{A_{m-n}}(x,y,z) = \begin{cases} 1 & ,\text{if } (x,y,z)\in A_{m-n} \\ 0 & ,\text{else} \end{cases},$$

where we denote A_{m-n} as generalized light cone:

$$A_{m-n} = \{x,y,z\in\Gamma : t_{m-n+1}+|x-y|\geq|x-z|\geq t_{m-n}+|x-y|\}.$$

For the other time integral with integration by parts:

$$\begin{aligned}
&\int_0^\infty \gamma^m_{\Delta t}(t-|x-y|)\gamma^n_{\Delta t}(t-|x-z|)dt \\
&=\int_0^\infty 1(H(t-|x-y|-t_{m-1})-H(t-|x-y|-t_m))(H(t-|x-z|-t_{n-1})-H(t-|x-z|-t_n))dt \\
&=-\int_0^\infty t[(\delta(t-|x-y|-t_{m-1})-\delta(t-|x-y|-t_m))(H(t-|x-z|-t_{n-1})-H(t-|x-z|-t_n)) \\
&+(H(t-|x-y|-t_{m-1})-H(t-|x-y|-t_m))(\delta(t-|x-z|-t_{n-1})-\delta(t-|x-z|-t_n))]dt \\
&= -[(H(|x-y|+t_{m-1}-|x-z|-t_{n-1})-H(|x-y|+t_{m-1}-|x-z|-t_n))(|x-y|+t_{m-1}) \\
&- (H(|x-y|+t_m-|x-z|-t_{n-1})-H(|x-y|+t_m-|x-z|-t_n))(|x-y|+t_m) \\
&+ (H(|x-z|+t_{n-1}-|x-y|-t_{m-1})-H(|x-z|+t_{n-1}-|x-y|-t_m))(|x-z|+t_{n-1}) \\
&- (H(|x-z|+t_n-|x-y|-t_{m-1})-H(|x-z|+t_n-|x-z|-t_m))(|x-z|+t_n)] \\
&= -[H(|x-y|-|x-z|+t_{m-n})-H(|x-y|-|x-z|+t_{m-n-1}))(|x-y|+t_{m-1}) \\
&- (H(|x-y|-|x-z|+t_{m-n+1})-H(|x-y|-|x-z|+t_{m-n}))(|x-y|+t_m) \\
&+ (H(|x-z|-|x-y|-t_{m-n})-H(|x-z|-|x-y|-t_{m+1-n}))(|x-z|+t_{n-1}) \\
&- (H(|x-z|-|x-y|-t_{m-n-1})-H(|x-z|-|x-y|-t_{m-n}))(|x-z|+t_n)] \\
&= -(|x-y|+t_{m-1})\chi_{A_{m-n-1}}(x,y,z)+(|x-y|+t_m)\chi_{A_{m-n}}(x,y,z) \\
&- (1-H(|x-y|-|x-z|+t_{m-n})-1+H(|x-y|-|x-z|+t_{m+1-n}))(|x-z|+t_{n-1}) \\
&+ (1-H(|x-y|-|x-z|+t_{m-n-1})-1+H(|x-y|-|x-z|+t_{m-n}))(|x-z|+t_n) \\
&= -(|x-y|+t_{m-1})\chi_{A_{m-n-1}}(x,y,z)+(|x-y|+t_m)\chi_{A_{m-n}}(x,y,z) \\
&- (|x-z|+t_{n-1})\chi_{A_{m-n}}(x,y,z)+(|x-z|+t_n)\chi_{A_{m-n-1}}(x,y,z) \\
&= (|x-z|-|x-y|-t_{m-n-1})\chi_{A_{m-n-1}}(x,y,z)+(|x-y|-|x-z|+t_{m-n+1})\chi_{A_{m-n}}(x,y,z).
\end{aligned}$$

Finally:

$$\sum_{m=1}^{N_t}\sum_{i=1}^{N_{s'}} q_i^m \iiint_{\Gamma\times\Gamma\times\Gamma} \frac{n_x(x-y)\xi_h^i(y)\xi_h^j(z)}{16\pi^2|x-y|^2|x-z|}\Big(\frac{1}{|x-y|}\big((|x-z|-|x-y|-t_{m-n-1})\chi_{A_{m-n-1}}$$
$$+ (|x-y|-|x-z|+t_{m-n+1})\chi_{A_{m-n}}\big) + (\chi_{A_{m-n-1}}-\chi_{A_{m-n}})\Big)ds_z ds_y ds_x$$
$$= \sum_{m=1}^{N_t}\sum_{i=1}^{N_{s'}} q_i^m \iiint_{\Gamma\times\Gamma\times\Gamma} \frac{n_x(x-y)\xi_h^i(y)\xi_h^j(z)}{16\pi^2|x-y|^2|x-z|}\Big(\frac{|x-z|}{|x-y|} - t_{m-n-1}\Big)\chi_{A_{m-n-1}}$$
$$+ \Big(-\frac{|x-z|}{|x-y|} + t_{m-n+1}\Big)\chi_{A_{m-n}}\Big)ds_z ds_y ds_x$$
$$= \sum_{m=1}^{N_t}\sum_{i=1}^{N_{s'}} q_i^m \iiint_{A_{m-n-1}} \frac{n_x(x-y)\xi_h^i(y)\xi_h^j(z)}{16\pi^2|x-y|^3} - \frac{n_x(x-y)\xi_h^i(y)\xi_h^j(z)t_{m-n-1}}{16\pi^2|x-y|^2|x-z|}ds_z ds_y ds_x$$
$$+ \iiint_{A_{m-n}} -\frac{n_x(x-y)\xi_h^i(y)\xi_h^j(z)}{16\pi^2|x-y|^3} + \frac{n_x(x-y)\xi_h^i(y)\xi_h^j(z)t_{m-n+1}}{16\pi^2|x-y|^2|x-z|}ds_z ds_y ds_x \ .$$

We get two generalized lightcones A_{m-n} and A_{m-n-1} and 2 kernels:

$$\frac{n_x(x-y)}{16\pi^2|x-y|^3} \quad , \quad \frac{n_x(x-y)}{16\pi^2|x-y|^2|x-z|} \ .$$

Next, changing ansatz functions from piecewise constant functions in time into piecewise linear functions in time, i.e.

$$q_{h,\Delta t} = \sum_{m=1}^{N_t}\sum_{i=1}^{N_{s'}} q_i^m \beta_\Delta^m(t)\xi_i^h(x) \ \in V_{h,\Delta t}^{1,1} \ ,$$

we calculate

$$\int_0^\infty \int_\Gamma (-\frac{1}{2}I + K')\Big(\sum_{m=1}^{N_t}\sum_{i=1}^{N_{s'}} q_i^m \xi_h^i(x)\beta_{\Delta t}^m(t)\Big)\Big(V(\xi_h^j(x)\gamma_{\Delta t}^n(t))\Big)ds_x dt$$
$$= \sum_{m=1}^{N_t}\sum_{i=1}^{N_{s'}} q_i^m \int_0^\infty \int_\Gamma (-\frac{1}{2}I + K')(\xi_h^i(x)\beta_{\Delta t}^m(t))\Big(V(\xi_h^j(x)\gamma_{\Delta t}^n(t))\Big)ds_x dt$$
$$= \sum_{m=1}^{N_t}\sum_{i=1}^{N_{s'}} q_i^m \int_0^\infty \int_\Gamma (-\frac{1}{2}I + K')(\xi_{\Delta t}^i(x)\beta_{\Delta t}^m(t))\Big(\int_\Gamma \frac{\gamma_{\Delta t}^n(t-|x-y|)\xi_{\Delta t}^j(y)}{4\pi|x-y|}ds_y\Big)ds_x dt$$
$$= \sum_{m=1}^{N_t}\sum_{i=1}^{N_{s'}} q_i^m \int_0^\infty \int_\Gamma (-\frac{1}{2}I)(\xi_{\Delta t}^i(x)\beta_{\Delta t}^m(t))\Big(\int_\Gamma \frac{\gamma_{\Delta t}^n(t-|x-y|)\xi_h^j(y)}{4\pi|x-y|}ds_y\Big)ds_x dt$$
$$+ \sum_{m=1}^{N_t}\sum_{i=1}^{N_{s'}} q_i^m \int_0^\infty \int_\Gamma (K')(\xi_h^i(x)\beta_{\Delta t}^m(t))\Big(\int_\Gamma \frac{\gamma_{\Delta t}^n(t-|x-y|)\xi_h^j(y)}{4\pi|x-y|}ds_y\Big)ds_x dt$$
$$= -\frac{1}{2}\sum_{m=1}^{N_t}\sum_{i=1}^{N_{s'}} q_i^m \int_0^\infty \int_\Gamma \xi_h^i(x)\beta_{\Delta t}^m(t)\Big(\int_\Gamma \frac{\gamma_{\Delta t}^n(t-|x-y|)\xi_h^j(y)}{4\pi|x-y|}ds_y\Big)ds_x dt$$
$$+ \sum_{m=1}^{N_t}\sum_{i=1}^{N_{s'}} q_i^m \int_0^\infty \int_\Gamma \Big(\int_\Gamma \frac{n_x\cdot(x-y)}{|x-y|}\Big(\frac{\xi_h^i(y)\beta_{\Delta t}^m(t-|x-y|)}{4\pi|x-y|^2} + \frac{\xi_h^i(y)\dot\beta_{\Delta t}^m(t-|x-y|)}{4\pi|x-y|}\Big)ds_y\Big)\times$$
$$\times \Big(\int_\Gamma \frac{\gamma_{\Delta t}^n(t-|x-y|)\xi_h^j(y)}{4\pi|x-y|}ds_y\Big)ds_x dt$$

$$
\begin{aligned}
&= -\frac{1}{2}\sum_{m=1}^{N_t}\sum_{i=1}^{N_{s'}} q_i^m \int_0^\infty \int_\Gamma \xi_h^i(x)\beta_{\Delta t}^m(t)\Big(\int_\Gamma \frac{\gamma_{\Delta t}^n(t-|x-y|)\xi_h^j(y)}{4\pi|x-y|}ds_y\Big)ds_x dt \\
&+\sum_{m=1}^{N_t}\sum_{i=1}^{N_{s'}} q_i^m \int_0^\infty \iiint_{\Gamma\times\Gamma\times\Gamma} \frac{n_x(x-y)\xi_h^i(y)\xi_h^j(z)}{|x-y||x-z|}\Big(\frac{\beta_{\Delta t}^m(t-|x-y|)}{|x-y|^2}+\frac{\dot\beta_{\Delta t}^m(t-|x-y|)}{|x-y|}\Big)\gamma_{\Delta t}^n(t-|x-z|)ds_z ds_y ds_x dt \\
&= -\frac{1}{2}\sum_{m=1}^{N_t}\sum_{i=1}^{N_{s'}} q_i^m \int_0^\infty \int_\Gamma \xi_h^i(x)\beta_{\Delta t}^m(t)\Big(\int_\Gamma \frac{\gamma_{\Delta t}^n(t-|x-y|)\xi_h^j(y)}{4\pi|x-y|}ds_y\Big)ds_x dt \\
&+\sum_{m=1}^{N_t}\sum_{i=1}^{N_{s'}} q_i^m \iiint_{\Gamma\times\Gamma\times\Gamma} \frac{n_x\cdot(x-y)\xi_h^i(y)\xi_h^j(z)}{|x-y|^2|x-z|}\Big(\frac{1}{|x-y|}\int_0^\infty \beta_{\Delta t}^m(t-|x-y|)\gamma_{\Delta t}^n(t-|x-z|)dt \\
&+\int_0^\infty \dot\beta_{\Delta t}^m(t-|x-y|)\gamma_{\Delta t}^n(t-|x-z|)dt\Big)ds_z ds_y ds_x \ .
\end{aligned}
$$

We get for the identity part:

$$
\begin{aligned}
&-\frac{1}{2}\sum_{m=1}^{N_t}\sum_{i=1}^{N_{s'}} q_i^m \int_0^\infty \int_\Gamma \xi_h^i(x)\beta_{\Delta t}^m(t)\Big(\int_\Gamma \frac{\gamma_{\Delta t}^n(t-|x-y|)\xi_h^j(y)}{4\pi|x-y|}ds_y\Big)ds_x dt \\
&= -\frac{1}{2}\sum_{m=1}^{N_t}\sum_{i=1}^{N_{s'}} q_i^k \iint_{\Gamma\times\Gamma} \frac{\xi_h^i(x)\xi_h^j(y)}{4\pi|x-y|}\Big(\int_0^\infty \beta_{\Delta t}^k(t)\gamma_{\Delta t}^n(t-|x-y|)dt\Big)ds_y ds_x \ .
\end{aligned}
$$

Using (9.11) gives:

$$
\begin{aligned}
&-\frac{1}{2}\sum_{m=1}^{N_t}\sum_{i=1}^{N_{s'}} q_i^m \iint_{\Gamma\times\Gamma} \frac{\xi_h^i(x)\xi_h^j(y)}{4\pi|x-y|}\Big(\big(-\frac{(\Delta t)}{2}+\frac{(|x-y|-t_{m-n})^2}{2(\Delta t)}\big)\chi_{E_{m-n-1}}(x,y) \\
&+\big(\frac{(\Delta t)}{2}-\frac{(|x-y|-t_{m-n+1})^2}{(\Delta t)}\big)\chi_{E_{m-n}}(x,y)+\frac{(|x-y|-t_{m-n+2})^2}{2(\Delta t)}\chi_{E_{m-n+1}}(x,y)\Big)ds_y ds_x \ .
\end{aligned}
$$

For the time integrals of the K' part, we compute first the following time integral:

$$
\begin{aligned}
&\int_0^\infty \beta_{\Delta t}^m(t-|x-y|)\gamma_{\Delta t}^n(t-|x-z|)dt \\
&= \int_0^\infty \frac{t-|x-y|-t_{m-1}}{(\Delta t)}\big(H(t-|x-y|-t_{m-1})-H(t-|x-y|-t_m)\big)\times \\
&\times\big(H(t-|x-z|-t_{n-1})-H(t-|x-z|-t_n)\big)dt \\
&-\int_0^\infty \frac{t-|x-y|-t_{m+1}}{(\Delta t)}\big(H(t-|x-y|-t_m)-H(t-|x-y|-t_{m+1})\big)\times \\
&\times\big(H(t-|x-z|-t_{n-1})-H(t-|x-z|-t_n)\big)dt \ .
\end{aligned}
$$

Using integration by parts twice where the difference of the heaviside function has a finite support, we get

$$
\int_0^\infty \beta_{\Delta t}^m(t-|x-y|)\gamma_{\Delta t}^n(t-|x-z|)dt
$$

$$
\begin{aligned}
&= -\int_0^\infty \frac{\frac{1}{2}t^2 - |x-y|t - tt_{m-1}}{\Delta t}(H(t-|x-y|-t_{m-1}) - H(t-|x-y|-t_m))\times \\
&\times (\delta(t-|x-z|-t_{n-1}) - \delta(t-|x-z|-t_n)) + (\delta(t-|x-y|-t_{m-1}) - \delta(t-|x-y|-t_m))\times \\
&\times (H(t-|x-z|-t_{n-1}) - H(t-|x-z|-t_n))dt \\
&+ \int_0^\infty \frac{\frac{1}{2}t^2 - |x-y|t - tt_{m+1}}{\Delta t}(H(t-|x-y|-t_m) - H(t-|x-y|-t_{m+1}))\times \\
&\times (\delta(t-|x-z|-t_{n-1}) - \delta(t-|x-z|-t_n)) + (\delta(t-|x-y|-t_m) - \delta(t-|x-y|-t_{m+1}))\times \\
&\times (H(t-|x-z|-t_{n-1}) - H(t-|x-z|-t_n))dt \\
&= -\frac{\frac{1}{2}(t_{n-1}+|x-z|)^2 - |x-y|(t_{n-1}+|x-z|) - (t_{n-1}+|x-z|)t_{m-1}}{\Delta t}\times \\
&\times (H(t_{n-1}+|x-z|-|x-y|-t_{m-1}) - H(t_{n-1}+|x-z|-|x-y|-t_m)) \\
&+\frac{\frac{1}{2}(t_n+|x-z|)^2 - |x-y|(t_n+|x-z|) - (t_n+|x-z|)t_{m-1}}{\Delta t}\times \\
&\times (H(t_n+|x-z|-|x-y|-t_{m-1}) - H(t_n+|x-z|-|x-y|-t_m)) \\
&-\frac{\frac{1}{2}(t_{m-1}+|x-y|)^2 - |x-y|(t_{m-1}+|x-y|) - (t_{m-1}+|x-y|)t_{m-1}}{\Delta t}\times \\
&\times (H(t_{m-1}+|x-y|-|x-z|-t_{n-1}) - H(t_{m-1}+|x-y|-|x-z|-t_n)) \\
&+\frac{\frac{1}{2}(t_m+|x-y|)^2 - |x-y|(t_m+|x-y|) - (t_m+|x-y|)t_{m-1}}{\Delta t}\times \\
&\times (H(t_m+|x-y|-|x-z|-t_{n-1}) - H(t_m+|x-y|-|x-z|-t_n)) \\
&+\frac{\frac{1}{2}(t_{n-1}+|x-z|)^2 - |x-y|(t_{n-1}+|x-z|) - (t_{n-1}+|x-z|)t_{m+1}}{\Delta t}\times \\
&\times (H(t_{n-1}+|x-z|-|x-y|-t_m) - H(t_{n-1}+|x-z|-|x-y|-t_{m+1})) \\
&-\frac{\frac{1}{2}(t_n+|x-z|)^2 - |x-y|(t_n+|x-z|) - (t_n+|x-z|)t_{m+1}}{\Delta t}\times \\
&\times (H(t_n+|x-z|-|x-y|-t_m) - H(t_n+|x-z|-|x-y|-t_{m+1})) \\
&+\frac{\frac{1}{2}(t_m+|x-y|)^2 - |x-y|(t_m+|x-y|) - (t_m+|x-y|)t_{m+1}}{\Delta t}\times \\
&\times (H(t_m+|x-y|-|x-z|-t_{n-1}) - H(t_m+|x-y|-|x-z|-t_n)) \\
&-\frac{\frac{1}{2}(t_{m+1}+|x-y|)^2 - |x-y|(t_{m+1}+|x-y|) - (t_{m+1}+|x-y|)t_{m+1}}{\Delta t}\times \\
&\times (H(t_{m+1}+|x-y|-|x-z|-t_{n-1}) - H(t_{m+1}+|x-y|-|x-z|-t_n)) \\
&=: -A(H(t_{n-m}+|x-z|-|x-y|) - H(t_{n-m-1}+|x-z|-|x-y|)) \\
&+ B(H(t_{n-m+1}+|x-z|-|x-y|) - H(t_{n-m}+|x-z|-|x-y|)) \\
&- C(H(t_{m-n}+|x-y|-|x-z|) - H(t_{m-1-n}+|x-y|-|x-z|)) \\
&+ D(H(t_{m-n+1}+|x-y|-|x-z|) - H(t_{m-n}+|x-y|-|x-z|)) \\
&+ E(H(t_{n-1-m}+|x-z|-|x-y|) - H(t_{n-m-2}+|x-z|-|x-y|)) \\
&- F(H(t_{m-n+1}+|x-y|-|x-z|) - H(t_{m-n}+|x-y|-|x-z|)) \\
&+ G(H(t_{m-n+1}+|x-y|-|x-z|) - H(t_{m-n}+|x-y|-|x-z|)) \\
&- Z(H(t_{m-n+2}+|x-y|-|x-z|) - H(t_{m+1-n}+|x-y|-|x-z|))
\end{aligned}
$$

$$
\begin{aligned}
&= -A(1 - H(t_{m-n} + |x-y| - |x-z|) - 1 + H(t_{m-n+1} + |x-y| - |x-z|)) \\
&+ B(1 - H(t_{m-n-1} + |x-y| - |x-z|) - 1 + H(t_{m-n} + |x-y| - |x-z|)) \\
&- C(H(t_{m-n} + |x-y| - |x-z|) - H(t_{m-1-n} + |x-y| - |x-z|)) \\
&+ D(H(t_{m-n+1} + |x-y| - |x-z|) - H(t_{m-n} + |x-y| - |x-z|)) \\
&+ E(1 - H(t_{m+1-n} + |x-y| - |x-z|) - 1 + H(t_{m+2-n} + |x-y| - |x-z|)) \\
&- F(H(t_{m-n+1} + |x-y| - |x-z|) - H(t_{m-n} + |x-y| - |x-z|)) \\
&+ G(H(t_{m-n+1} + |x-y| - |x-z|) - H(t_{m-n} + |x-y| - |x-z|)) \\
&- Z(H(t_{m-n+2} + |x-y| - |x-z|) - H(t_{m+1-n} + |x-y| - |x-z|)) \\
&= -A\chi_{A_{m-n}}(x,y,z) + B\chi_{A_{m-n-1}}(x,y,z) - C\chi_{A_{m-n-1}}(x,y,z) + D\chi_{A_{m-n}}(x,y,z) \\
&+ E\chi_{A_{m+1-n}}(x,y,z) - F\chi_{A_{m-n}}(x,y,z) + G\chi_{A_{m-n}}(x,y,z) - Z\chi_{A_{m+1-n}}(x,y,z) \ ,
\end{aligned}
$$

where A, B, C, D, E, F, G, Z are the prefactors of the corresponding heaviside functions with generalized lightcones A_{m-n}. For the other time integral, we calculate:

$$
\begin{aligned}
&\int_0^\infty \dot{\beta}^m_{\Delta t}(t - |x-y|)\gamma^n_{\Delta t}(t - |x-z|)dt \\
&= \int_0^\infty \frac{1}{\Delta t}(\gamma^m_{\Delta t}(t - |x-y|) - \gamma^{m+1}_{\Delta t}(t - |x-y|))\gamma^n_{\Delta t}(t - |x-z|)dt \\
&= \int_0^\infty 1 \cdot \frac{1}{\Delta t}(H(t-|x-y|-t_{m-1}) - H(t-|x-y|-t_m) - H(t-|x-y|-t_m) + H(t-|x-y|-t_{m+1})) \times \\
&\times (H(t - |x-z| - t_{n-1}) - H(t - |x-z| - t_n))dt \ .
\end{aligned}
$$

Again with integration by parts:

$$
\begin{aligned}
&\int_0^\infty \dot{\beta}^m_{\Delta t}(t - |x-y|)\gamma^n_{\Delta t}(t - |x-z|)dt \\
&= -\int_0^\infty t\frac{1}{\Delta t}(\delta(t - |x-y| - t_{m-1}) - 2\delta(t - |x-y| - t_m) + \delta(t - |x-y| - t_{m+1})) \times \\
&\times (H(t - |x-z| - t_{n-1}) - H(t - |x-z| - t_n)) + \big(H(t - |x-y| - t_{m-1}) \\
&-2H(t - |x-y| - t_m) + H(t - |x-y| - t_{m+1})\big)(\delta(t - |x-z| - t_{n-1}) - \delta(t - |x-z| - t_n))dt \\
&= -(t_{m-1} + |x-y|)\frac{1}{\Delta t}(H(t_{m-n} + |x-y| - |x-z|) - H(t_{m-n-1} + |x-y| - |x-z|)) \\
&+ 2(t_m + |x-y|)\frac{1}{\Delta t}(H(t_{m-n+1} + |x-y| - |x-z|) - H(t_{m-n} + |x-y| - |x-z|)) \\
&- (t_{m+1} + |x-y|)\frac{1}{\Delta t}(H(t_{m-n+2} + |x-y| - |x-z|) - H(t_{m-n+1} + |x-y| - |x-z|)) \\
&- (t_{n-1} + |x-z|)\frac{1}{\Delta t}\big(H(t_{n-m} + |x-z| - |x-y|) - 2H(t_{n-m-1} + |x-z| - |x-y|) \\
&+ H(t_{n-m-2} + |x-z| - |x-y|)\big) + (t_n + |x-z|)\frac{1}{\Delta t}\big(H(t_{n-m+1} + |x-z| - |x-y|) \\
&- 2H(t_{n-m} + |x-z| - |x-y|) + H(t_{n-m-1} + |x-z| - |x-y|)\big) \\
&= -\frac{(t_{m-1} + |x-y|)}{\Delta t}\chi_{A_{m-1-n}} + 2\frac{(t_m + |x-y|)}{\Delta t}\chi_{A_{m-n}} - \frac{(t_{m+1} + |x-y|)}{\Delta t}\chi_{A_{m-n+1}}
\end{aligned}
$$

$$
\begin{aligned}
&- \frac{(t_{n-1}+|x-z|)}{\Delta t}(1 - H(t_{m-n} - |x-z|+|x-y|) - 1 + H(t_{m+1-n} - |x-z|+|x-y|)\\
&- 1 + H(t_{m+1-n} - |x-z|+|x-y|) + 1 - H(t_{m+2-n} - |x-z|+|x-y|))\\
&+ \frac{(t_n+|x-z|)}{\Delta t}(1 - H(t_{m-n-1} - |x-z|+|x-y|) - 1 + H(t_{m-n} - |x-z|+|x-y|)\\
&- 1 + H(t_{m-n} - |x-z|+|x-y|) + 1 - H(t_{m+1-n} - |x-z|+|x-y|))\\
&= -\frac{(t_{m-1}+|x-y|)}{\Delta t}\chi_{A_{m-1-n}} + 2\frac{(t_m+|x-y|)}{\Delta t}\chi_{A_{m-n}} - \frac{(t_{m+1}+|x-y|)}{\Delta t}\chi_{A_{m-n+1}}\\
&- \frac{(t_{n-1}+|x-z|)}{\Delta t}\chi_{A_{m-n}} + \frac{(t_{n-1}+|x-z|)}{\Delta t}\chi_{A_{m-n+1}} + \frac{(t_n+|x-z|)}{\Delta t}\chi_{A_{m-1-n}}\\
&- \frac{(t_n+|x-z|)}{\Delta t}\chi_{A_{m-n}}\\
&= -\frac{t_{m-1-n}+|x-y|-|x-z|}{\Delta t}\chi_{A_{m-1-n}} + \frac{t_{2(m-n)+1}+2|x-y|-2|x-z|}{\Delta t}\chi_{A_{m-n}}\\
&- \frac{t_{m-n+2}+|x-y|-|x-z|}{\Delta t}\chi_{A_{m+1-n}} = -I\chi_{A_{m-1-n}} + J\chi_{A_{m-n}} - L\chi_{A_{k+1-n}}(x,y,z)\ ,
\end{aligned}
$$

where again A_{m-n} are the generalized light cones and I, J, L are the prefactors of the corresponding Heaviside functions. Now altogether we get:

$$
\begin{aligned}
&\sum_{m=1}^{N_t}\sum_{i=1}^{N_{s'}} q_i^m \iiint_{\Gamma\times\Gamma\times\Gamma} \frac{n_x\cdot(x-y)\xi_h^i(y)\xi_h^i(z)}{|x-y|^2|x-z|}\Big(\frac{1}{|x-y|}\int_0^\infty \beta_{\Delta t}^m(t-|x-y|)\gamma_{\Delta t}^n(t-|x-z|)dt\\
&+ \int_0^\infty \dot\beta_{\Delta t}^m(t-|x-y|)\gamma_{\Delta t}^n(t-|x-z|)dt\Big)ds_z ds_y ds_x\\
&= \sum_{m=1}^{N_t}\sum_{i=1}^{N_{s'}} q_i^m \iiint_{\Gamma\times\Gamma\times\Gamma} \frac{n_x\cdot(x-y)\xi_h^i(y)\xi_h^j(z)}{|x-y|^2|x-z|}\Big(-\frac{A}{|x-y|}\chi_{A_{m-n}} + \frac{B}{|x-y|}\chi_{A_{m-n-1}} - \frac{C}{|x-y|}\chi_{A_{m-n-1}}\\
&+ \frac{D}{|x-y|}\chi_{A_{m-n}} + \frac{E}{|x-y|}\chi_{A_{m+1-n}} - \frac{F}{|x-y|}\chi_{A_{m-n}} + \frac{G}{|x-y|}\chi_{A_{m-n}}\\
&- \frac{Z}{|x-y|}\chi_{A_{m+1-n}} - I\chi_{A_{m-n-1}} + J\chi_{A_{m-n}} - L\chi_{A_{m+1-n}}\Big)ds_z ds_y ds_x\\
&= \sum_{m=1}^{N_t}\sum_{i=1}^{N_{s'}} q_i^m \iiint_{\Gamma\times\Gamma\times\Gamma} \frac{n_x\cdot(x-y)\xi_h^i(y)\xi_h^j(z)}{|x-y|^2|x-z|}\Big(\frac{B}{|x-y|} - \frac{C}{|x-y|} - I\Big)\chi_{A_{m-n-1}}\\
&- \Big(\frac{A}{|x-y|} - \frac{D}{|x-y|} + \frac{F}{|x-y|} - \frac{G}{|x-y|} - J\Big)\chi_{A_{m-n}} + \Big(\frac{E}{|x-y|} - \frac{Z}{|x-y|} - L\Big)\chi_{A_{m+1-n}} ds_z ds_y ds_x\\
&= \sum_{m=1}^{N_t}\sum_{i=1}^{N_{s'}} q_i^m \iiint_{\Gamma\times\Gamma\times\Gamma} \frac{n_x\cdot(x-y)\xi_h^i(y)\xi_h^j(z)}{|x-y|^2|x-z|}\times\\
&\times\Big(\frac{\frac{1}{2}t_n^2 - t_n t_{m-1} + \frac{1}{2}t_{m-1}^2 + t_{n-m+1}|x-z| + \frac{1}{2}|x-z|^2 - \frac{1}{2}|x-y|^2}{(\Delta t)|x-y|}\chi_{A_{m-n-1}} -\\
&\frac{\frac{1}{2}t_{n-1}^2 - t_{n-1}t_{m-1} - t_m^2 + t_m t_{m-1} + \frac{1}{2}t_n^2 - t_n t_{m+1} + t_m t_{m+1} + t_{2(n-m)-1}|x-z| + |x-z|^2 - |x-y|^2}{(\Delta t)|x-y|}\chi_{A_{m-n}}\\
&+ \frac{\frac{1}{2}t_n^2 - t_n t_{m+1} + \frac{1}{2}t_{m+1}^2 + t_{n-m-1}|x-z| + \frac{1}{2}|x-z|^2 - \frac{1}{2}|x-y|^2}{(\Delta t)|x-y|}\chi_{A_{m+1-n}}\Big)ds_z ds_y ds_x\ .
\end{aligned}
$$

We get 3 generalized light cones $A_{m-n-1}, A_{m-n}, A_{m-n+1}$ and 4 kernels:

$$\frac{n_x(x-y)}{|x-y|^3|x-z|} \quad , \quad \frac{n_x(x-y)}{|x-y|^3} \quad , \quad \frac{n_x(x-y)|x-z|}{|x-y|^3|x-z|} \quad , \quad \frac{n_x(x-y)}{|x-y||x-z|} \; .$$

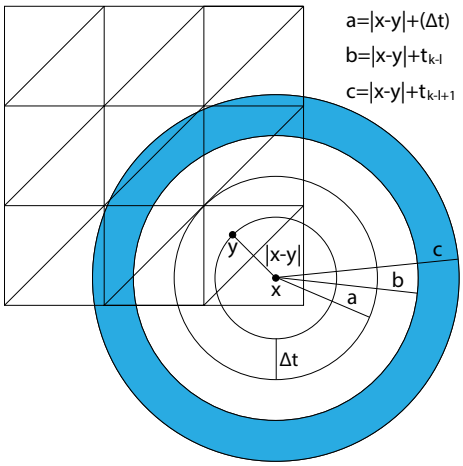

Figure 3.1: Generalized light cones after the use of a projection onto the same plane for $t_{k-l} = t_{n-m} = 2(\Delta t)$. For x, y as in this Figure the integral over z exists only on the intersection of the blue ring with the triangles.

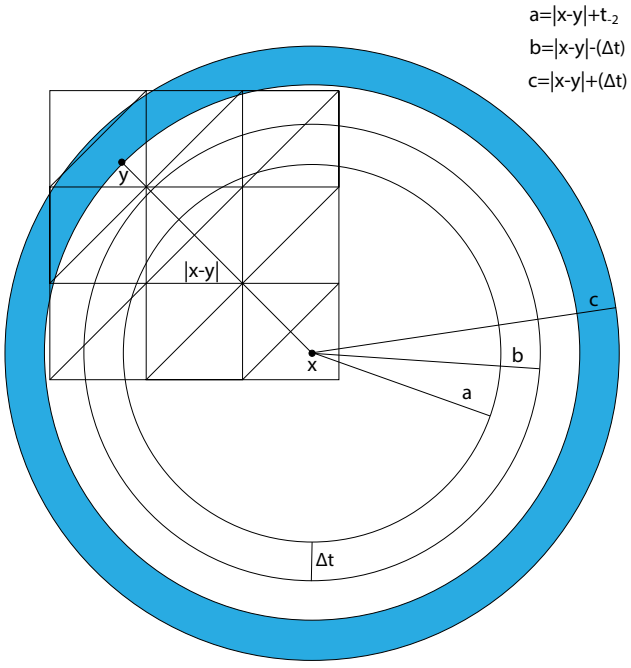

Figure 3.2: Generalized light cones after the use of a projection onto the same plane. The intersection of the blue ring with the triangles is, where a nonzero integral may exists for x, y as in this Figure. This is contained in A_0. The intersection of the first ring beneath the blue ring with the triangles for the same x, y is a subset of A_{-1} and the intersection of the second triangle beneath the first ring with the triangles for the same x, y ia a subset of A_{-2}.

A great difficulty of implementing A_{m-n} lies in the fact that the radii of the light-cones depend on the length of the quadrature points for the corresponding elements (see Figure 3.1). Therefore we may get entries even for negative t_{m-n+1} (see Figure 3.2). This leads to a space time matrix, which loses it's sparsity. Unfortunately the generalized lightcones aren't implemented yet, so first we focus on another way to deal with $\langle K^T q, V\dot{q}'\rangle_{\Gamma\times\mathbb{R}_+}$.

3.6 Discretization via an L^2-projection method in space and time

We consider again $\langle(-\frac{1}{2}I + K')q, V\dot{q}'\rangle_{\Gamma\times\mathbb{R}_+}$. We divide them into $\langle-\frac{1}{2}Iq, V\dot{q}'\rangle_{\Gamma\times\mathbb{R}_+}$ + $\langle K'q, V\dot{q}'\rangle_{\Gamma\times\mathbb{R}_+}$. Choosing ansatz functions $q_{h,\Delta t} \in V^{1,0}_{h,\Delta t}$ as in (3.13) and test functions $\dot{q}'_{h,\Delta t} \in V^{1,0}_{h,\Delta t}$ as in (3.14), we get for $\langle-\frac{1}{2}Iq_{h,\Delta t}, V\dot{q}'_{h,\Delta t}\rangle_{\Gamma\times\mathbb{R}_+}$ the same as in (3.15) below.

For $\langle K'q, V\dot{q}'\rangle_{\Gamma\times\mathbb{R}_+}$, the idea is to use an L^2-projection in space and time. We define for a discretized finite interval $[0,T]$ the projection $\Pi_H : H^r_\sigma([0,T], \widetilde{H}^{-\frac{1}{2}}(\Gamma)) \to H^r_\sigma([0,T], \widetilde{H}^0(\Gamma))$ applied to K' by

$$\Pi_H K'q = z = \sum_{m=1}^{N_t}\sum_{i=1}^{N_{s'}} z_i^m \xi_h^i(x)\gamma_{\Delta t}^m(t) \ .$$

We use it as an L^2-approximation in:

$$\begin{aligned}\int_0^\infty \int_\Gamma (K'q)(V\dot{q}')ds_x dt &\approx \int_0^\infty \int_\Gamma (\Pi_H K'q)(V\dot{q}')ds_x dt \\ &= \sum_{m=1}^{N_t}\sum_{i=1}^{N_{s'}} z_i^m \int_0^\infty \int_\Gamma \xi_h^i(x)\gamma_{\Delta t}^m(t)(V\dot{q}')ds_x dt \ . \end{aligned} \tag{3.16}$$

The integral (3.16) has the same discretization as (3.15) and therefore the same matrix entries. Further we make use of:

$$\int_0^\infty \int_\Gamma (z\nu - (K'q)\nu)ds_x dt = 0 \ .$$

Now choosing $\nu = \xi_h^j(x)\gamma_{\Delta t}^n(t) \in V^{1,0}_{h,\Delta t}$ for $j = 1,\dots,N_{s'}$ and $n = 1,\dots,N_t$. gives us the following discretization:

$$\begin{aligned}&\sum_{m=1}^{N_t}\sum_{i=1}^{N_{s'}} z_i^m \int_0^\infty \int_\Gamma \xi_h^i(x)\xi_h^j(x)\gamma_{\Delta t}^m(t)\gamma_{\Delta t}^n(t)ds_x dt \\ &- \sum_{m=1}^{N_t}\sum_{i=1}^{N_{s'}} q_i^m \int_0^\infty \int_\Gamma (K'(\xi_h^i(x)\gamma_{\Delta t}^m(t)))\xi_h^j(x)\gamma_{\Delta t}^n(t)ds_x dt = 0 \ .\end{aligned}$$

For the retarded adjoint double layer potential we get the same structured space-time matrix as in Subsection 2.3.2 only with piecewise linear functions in space. We denote the matrix also as K'. For the other integral we denote the corresponding matrix as P. Therefore we get:

$$Pz - K'q = 0 \Leftrightarrow z = P^{-1}K'q \ .$$

Now using it above, gives us a matrix which loses it's sparsity as in the Section before:

$$V^T P^{-1} K' q = \begin{pmatrix} * & * & * \\ 0 & * & * \\ 0 & 0 & * \end{pmatrix}\begin{pmatrix} * & 0 & 0 \\ 0 & * & 0 \\ 0 & 0 & * \end{pmatrix}\begin{pmatrix} * & 0 & 0 \\ * & * & 0 \\ * & * & * \end{pmatrix}\begin{pmatrix} q^1 \\ \vdots \\ q^{N_t} \end{pmatrix} = \begin{pmatrix} * & * & * \\ * & * & * \\ * & * & * \end{pmatrix}\begin{pmatrix} q^1 \\ \vdots \\ q^{N_t} \end{pmatrix}$$
$$= \begin{pmatrix} ZT_{1,1} & ZT_{1,2} & \dots & ZT_{1,N_t} \\ ZT_{2,1} & ZT_{2,2} & \dots & ZT_{2,N_t} \\ \vdots & \vdots & \ddots & \vdots \\ ZT_{N_t,1} & ZT_{N_t,2} & \dots & ZT_{N_t,N_t} \end{pmatrix}\begin{pmatrix} q^1 \\ q^2 \\ \vdots \\ q^{N_t} \end{pmatrix}, \tag{3.17}$$

where $ZT_{n,m}$ are block matrices with entries of $V^T P^{-1} K'$.

Next we want to consider a discretization of the integrals over the interior $\Omega = \Omega^-$. Let $\mathbf{u}_{h,\Delta t} \in (W^{1,1}_{h,\Delta t})^3$. We describe

$$\mathbf{u}_{h,\Delta t}(x,t) = \sum_{m=1}^{N_t}\sum_{\nu=1}^{3}\sum_{i=1}^{N_s} u^m_{\nu,i}\beta^m_{\Delta t}(t)\vec{e}_\nu \eta^i_h(x) \ ,$$

where $\beta^m_{\Delta t}(t)$ is a hat-function in time, $\eta^i_h(x)$ is a hat-function in the interior space Ω and $\vec{e}_\nu$ is the unit vector with the entry 1 on the ν-th place.

For the test function, we set $\dot{\mathbf{w}}_{h,\Delta t} = \eta^l_h(x)\gamma^n_{\Delta t}(t)\vec{e}_\mu \in (W^{1,0}_{h,\Delta t})^3$, for $l = 1,\dots,N_s$, $n = 1,\dots,N_t$ and $\mu = 1,2,3$. Then

$$\begin{aligned}
&(\tilde{\sigma}(\mathbf{u}_{h,\Delta t}), \varepsilon(\dot{\mathbf{w}}_{h,\Delta t})_{\Omega^-\times\mathbb{R}_+} = \int_0^\infty \int_{\Omega^-} \tilde{\sigma}(\mathbf{u}_{h,\Delta t}) : \varepsilon(\dot{\mathbf{w}}_{h,\Delta t}) dx dt \\
&= \int_0^\infty \int_{\Omega^-} \sum_{m=1}^{N_t}\sum_{\nu=1}^{3}\sum_{i=1}^{N_s} u^m_{\nu,i}\beta^m_{\Delta t}(t)\left(\tilde{\sigma}(\vec{e}_\nu\eta^i_h(x)) : \varepsilon(\vec{e}_\mu\eta^l_h(x))\right)\gamma^n_{\Delta t}(t) dx dt \\
&= \sum_{m=1}^{N_t}\sum_{\nu=1}^{3}\sum_{i=1}^{N_s} u^k_{\nu,i}\left(\int_{\Omega^-}\tilde{\sigma}(\vec{e}_\nu\eta^i_h(x)) : \varepsilon(\vec{e}_\mu\eta^l_h(x))dx\right)\left(\int_0^\infty \beta^m_{\Delta t}(t)\gamma^n_{\Delta t}(t)dt\right) \\
&= \sum_{\nu=1}^{3}\sum_{i=1}^{N_s}\left(\int_{\Omega^-}\tilde{\sigma}(\vec{e}_\nu\eta^i_h(x)) : \varepsilon(\vec{e}_\mu\eta^l_h(x))dx\right)(\Delta t)\cdot\begin{cases} \frac{1}{2}u^1_{\nu,i} & , n = 1 \\ \frac{u^n_{\nu,i}+u^{n-1}_{\nu,i}}{2} & , n \geq 2 \end{cases} \\
&=: \sum_{\nu=1}^{3}\sum_{i=1}^{N_s} A_{(i,\nu),(l,\eta)}(\Delta t)\cdot\begin{cases} \frac{1}{2}u^1_{\nu,i} & , n = 1 \\ \frac{u^n_{\nu,i}+u^{n-1}_{\nu,i}}{2} & , n \geq 2 \end{cases} \\
&= Au_A \ ,
\end{aligned} \tag{3.18}$$

where A is the discretized stiffness matrix with

$$u_A = (\Delta t)\cdot\begin{cases} \frac{1}{2}u^1 & , n = 1 \\ \frac{u^n+u^{n-1}}{2} & , n \geq 2 \end{cases}$$

and u^m containing all $u^m_{\nu,i}$.

For the other part:

$$
\begin{aligned}
&(\ddot{\mathbf{u}}_{h,\Delta t}, \dot{\mathbf{w}}_{h,\Delta t})_{\Omega^- \times \mathbb{R}_+} = \int_0^\infty \int_{\Omega^-} \ddot{\mathbf{u}}_{h,\Delta t} \cdot \dot{\mathbf{w}}_{h,\Delta t} dx dt \\
&= \int_0^\infty \int_{\Omega^-} \sum_{m=1}^{N_t} \sum_{\nu=1}^{3} \sum_{i=1}^{N_s} u^m_{\nu,i} \ddot{\beta}^m_{\Delta t}(t) \vec{e}_\nu \eta^i_h(x) \vec{e}_\mu \eta^j_h(x) \gamma^n_{\Delta t}(t) dx dt \\
&= \sum_{m=1}^{N_t} \sum_{\nu=1}^{3} \sum_{i=1}^{N_s} u^m_{\nu,i} \left(\int_{\Omega^-} \vec{e}_\nu \eta^i_h(x) \vec{e}_\mu \eta^j_h(x) dx \right) \left(\int_0^\infty \ddot{\beta}^m_{\Delta t}(t) \gamma^n_{\Delta t}(t) dt \right) \\
&= \sum_{\nu=1}^{3} \sum_{i=1}^{N_s} \left(\int_{\Omega^-} \vec{e}_\nu \eta^i_h(x) \vec{e}_\mu \eta^j_h(x) dx \right) \frac{1}{(\Delta t)} \cdot \begin{cases} u^1_{\nu,i} & , n = 1 \\ u^2_{\nu,i} - 2u^1_{\nu,i} & , n = 2 \\ u^n_{\nu,i} - 2u^{n-1}_{\nu,i} + u^{n-2}_{\nu,i} & , n \geq 3 \end{cases} \\
&=: \sum_{\nu=1}^{3} \sum_{i=1}^{N_s} M_{(i,\nu),(l,\eta)} \frac{1}{(\Delta t)} \cdot \begin{cases} u^1_{\nu,i} & , n = 1 \\ u^2_{\nu,i} - 2u^1_{\nu,i} & , n = 2 \\ u^n_{\nu,i} - 2u^{n-1}_{\nu,i} + u^{n-2}_{\nu,i} & , n \geq 3 \end{cases} \\
&= M u_M \ , \qquad (3.19)
\end{aligned}
$$

where M is the discretized mass matrix for the Lamé equation with

$$
u_M = \frac{1}{(\Delta t)} \cdot \begin{cases} u^1 & , n = 1 \\ u^2 - 2u^1 & , n = 2 \\ u^n - 2u^{n-1} + u^{n-2} & , n \geq 3 \ . \end{cases}
$$

Before beginning with the discretization of the coupling parts we need to divide u^n into

$$
\begin{pmatrix} (u^n_{\Omega \setminus \Gamma}) \\ (u^n_\Gamma) \end{pmatrix} ,
$$

where (u^n_Γ) has entries of u^n restricted to the boundary Γ and $(u^n_{\Omega\setminus\Gamma})$ has entries restricted to the interior of Ω. Now we begin with $\int_0^\infty \int_\Gamma (V \dot{q}) \gamma^- \dot{\mathbf{w}} \cdot n_x ds_x dt$ with $q_{h,\Delta t} \in V^{1,0}_{h,\Delta t}$ as in (3.13):

$$
\begin{aligned}
&\int_0^\infty \int_\Gamma (V \dot{q}_{h,\Delta t}) \gamma^- \dot{\mathbf{w}}_{h,\Delta t} \cdot n_x ds_x dt \\
&= \sum_{m=1}^{N_t} \sum_{i=1}^{N_{s'}} q^m_i \iint_{\Gamma \times \Gamma} \frac{\xi^i_h(y) \eta^l_h|_\Gamma(x) \vec{e}_\mu n_x}{4\pi |x-y|} \left(\int_0^\infty \dot{\gamma}^m_{\Delta t}(t - |x-y|) \right) \gamma^n_{\Delta t}(t) dt) ds_y ds_x \ .
\end{aligned}
$$

Using a formula from the Appendix (9.3), we get

$$
\sum_{m=1}^{N_t} \sum_{i=1}^{N_{s'}} q^m_i \iint\limits_{E_{n-m-1}} \frac{\xi^i_h(y) \eta^l_h|_\Gamma(x) \vec{e}_\mu n_x}{4\pi |x-y|} ds_y ds_x - \iint\limits_{E_{n-m}} \frac{\xi^i_h(y) \eta^l_h|_\Gamma(x) \vec{e}_\mu n_x}{4\pi |x-y|} ds_y ds_x =: \sum_{m=1}^{N_t} RV n_x^{n-m} q^m . \qquad (3.20)
$$

This leads to the same scheme as in Subsection 2.3.1:

$$
\begin{pmatrix} RV n_x^0 & 0 & \dots \\ RV n_x^1 & RV n_x^0 & 0 \\ \vdots & \ddots & \vdots \end{pmatrix} \begin{pmatrix} q^1 \\ q^2 \\ \vdots \end{pmatrix} .
$$

For the other coupling part with $\dot{q}'_{h,\Delta t} \in V^{1,0}_{h,\Delta t}$ as in (3.14) for $n = 1,\dots,N_t$ and $j = 1,\dots,N_{s'}$, we get for the discretization:

$$\int_0^\infty (\gamma^- \dot{\mathbf{u}}_{h,\Delta t} n_x)(V\dot{q}'_{h,\Delta t})ds_x dt = \sum_{m=1}^{N_t}\sum_{\nu=1}^{3}\sum_{i=1}^{N_s} u^m_{\nu,i} \int_0^\infty \Big(\int_\Gamma (\dot{\beta}^m_{\Delta t}\vec{e}_\nu \eta^i_h|_\Gamma n_x)\Big(\int_\Gamma \frac{\gamma^n_{\Delta t}(t-|x-y|)\xi^j_h(y)}{4\pi|x-y|}ds_y\Big)ds_x dt$$

$$= \sum_{m=1}^{N_t}\sum_{\nu=1}^{3}\sum_{i=1}^{N_s} u^m_{\nu,i} \iint_{\Gamma\times\Gamma} \frac{\vec{e}_\nu n_x \eta^i_h|_\Gamma(x)\xi^j_h(y)}{4\pi|x-y|}\Big(\int_0^\infty \dot{\beta}^m_{\Delta t}(t)\gamma^n_{\Delta t}(t-|x-y|)dt\Big)ds_y ds_x \ .$$

Computing the time integral:

$$\int_0^\infty \dot{\beta}^m_{\Delta t}(t)\gamma^n_{\Delta t}(t-|x-y|)dt = \int_0^\infty \frac{1}{(\Delta t)}(\gamma^m_{\Delta t}(t) - \gamma^{m+1}_{\Delta t}(t))\gamma^n_{\Delta t}(t-|x-y|)dt$$

$$= \int_0^\infty \frac{1}{(\Delta t)}\gamma^m_{\Delta t}(t)\gamma^n_{\Delta t}(t-|x-y|)dt - \int_0^\infty \frac{1}{(\Delta t)}\gamma^{m+1}_{\Delta t}(t)\gamma^n_{\Delta t}(t-|x-y|)dt \ .$$

Using (9.5) twice with switched indices, we get:

$$\int_0^\infty \dot{\beta}^m_{\Delta t}(t)\gamma^n_{\Delta t}(t-|x-y|)dt = \frac{1}{(\Delta t)}(t_{m-n+1} - |x-y|)\chi_{E_{m-n}}(x,y)$$
$$+ \frac{1}{(\Delta t)}(-t_{m-n-1} + |x-y|)\chi_{E_{m-n-1}}(x,y) - \frac{1}{(\Delta t)}(t_{m+1-n+1} - |x-y|)\chi_{E_{m+1-n}}(x,y)$$
$$- \frac{1}{(\Delta t)}(-t_{m+1-n-1} + |x-y|)\chi_{E_{m+1-n-1}}(x,y)$$
$$= \frac{1}{(\Delta t)}(t_{2(m-n)+1} - 2|x-y|)\chi_{E_{m-n}}(x,y) - \frac{1}{(\Delta t)}(t_{m-n-1} - |x-y|)\chi_{E_{m-n-1}}(x,y)$$
$$- \frac{1}{(\Delta t)}(t_{m+2-n} - |x-y|)\chi_{E_{m+1-n}}(x,y) \ .$$

Altogether we have 3 lightcones and 2 kernels. This leads to:

$$\sum_{m=1}^{N_t}\sum_{\nu=1}^{3}\sum_{i=1}^{N_s} u^m_{\nu,i} \iint_{\Gamma\times\Gamma} \frac{\vec{e}_\nu n_x \eta^i_h|_\Gamma(x)\xi^j_h(y)}{4\pi|x-y|}\Big(\frac{1}{(\Delta t)}(t_{2(m-n)+1} - 2|x-y|)\chi_{E_{m-n}}(x,y)$$
$$- \frac{1}{(\Delta t)}(t_{m-n-1} - |x-y|)\chi_{E_{m-n-1}}(x,y) - \frac{1}{(\Delta t)}(t_{m+2-n} - |x-y|)\chi_{E_{m+1-n}}(x,y)\Big)ds_y ds_x.$$

The integrals exist if the index of E_k is not negative. Therefore in order to understand the incoming scheme we consider the case $n = N_t$ (last timestep) first. We have:

$$\sum_{\nu=1}^{3}\sum_{i=1}^{N_s} u^{N_t-1}_{\nu,i} \iint_{\Gamma\times\Gamma} \frac{\vec{e}_\nu n_x \eta^i_h|_\Gamma(x)\xi^j_h(y)}{4\pi|x-y|}\Big(-\frac{1}{(\Delta t)}(t_1 - |x-y|)\chi_{E_0}\Big)ds_y ds_x =: n_x R V^{-1}(u^{N_t-1}_\Gamma)$$

and

$$\sum_{\nu=1}^{3}\sum_{i=1}^{N_s} u^{N_t}_{\nu,i} \iint_{\Gamma\times\Gamma} \frac{\vec{e}_\nu n_x \eta^i_h|_\Gamma(x)\xi^j_h(y)}{4\pi|x-y|}\Big(\frac{(t_1 - 2|x-y|)\chi_{E_0}}{\Delta t} - \frac{(t_2 - |x-y|)\chi_{E_1}}{(\Delta t)}\Big)ds_y ds_x =: n_x R V^0(u^{N_t}_\Gamma) \ .$$

For $n = N_t - 1$, we have $n_x R V^{-1}(u^{N_t-1}_\Gamma)_{h,\Delta t}$, $n_x R V^0(u^{N_t}_\Gamma)_{h,\Delta t}$ and

$$\sum_{\nu=1}^{3}\sum_{i=1}^{N_s} u^{N_t-2}_{\nu,i} \iint_{\Gamma\times\Gamma} \frac{\vec{e}_\nu n_x \eta^i_h|_\Gamma(x)\xi^j_h(y)}{4\pi|x-y|}\Big(\frac{1}{(\Delta t)}(t_3 - 2|x-y|)\chi_{E_1}(x,y)$$
$$- \frac{1}{(\Delta t)}(t_0 - |x-y|)\chi_{E_0}(x,y) - \frac{1}{(\Delta t)}(t_3 - |x-y|)\chi_{E_2}(x,y)\Big)ds_y ds_x =: n_x R V^1(u^{N_t}_\Gamma) \ .$$

Altogether we get the following space time matrix:

$$\begin{pmatrix} n_x RV^0 & n_x RV^1 & \dots & \dots & n_x RV^{N_t-1} \\ n_x RV^{-1} & n_x RV^0 & n_x RV^1 & \dots & n_x RV^{N_t-2} \\ 0 & \ddots & \ddots & & \vdots \\ \vdots & \ddots & \ddots & \ddots & \vdots \\ 0 & \dots & 0 & n_x RV^{-1} & n_x RV^0 \end{pmatrix} \begin{pmatrix} (u_\Gamma^1) \\ (u_\Gamma^2) \\ \vdots \\ \vdots \\ (u_\Gamma^{N_t}) \end{pmatrix} .$$

Next we discuss the discretization of the right hand side (3.7). We begin with the first term:

$$-\int_0^\infty \int_\Gamma (\partial_t v_+^{inc}) \gamma^-(\dot{\mathbf{w}}_{h,\Delta t} n) ds_x dt = -\int_0^\infty \int_\Gamma (\partial_t v_+^{inc} n) \gamma^-(\dot{\mathbf{w}}_{h,\Delta t}) ds_x dt \ .$$

We set $f := \partial_t v_+^{inc} n$. We approximate f in time via piecewise linear functions, i.e. $f = \sum_{m=1}^{N_t} f^m \beta_{\Delta t}^m(t)$, where $f^m = f(x, t_m)$. Then we get for $n = 1, \dots, N_t$ and $l = 1, \dots, N_{s'}$:

$$\begin{aligned} &-\sum_{m=1}^{N_t} \int_\Gamma f^m \eta_h^l|_\Gamma(x) ds_x \int_0^\infty \beta_{\Delta t}^m(t) \gamma_{\Delta t}^n(t) dt \\ &= -\int_\Gamma \frac{(\Delta t)}{2} (f^n + f^{n-1}) \eta_h^l|_\Gamma(x) ds_x =: F^n \ , \end{aligned}$$

where in space we use a Gauss quadrature. For the discretization of the other term

$$\int_0^\infty \int_\Gamma \frac{\partial v_+^{inc}}{\partial n} (V \dot{q}'_{h,\Delta t}) ds_x dt \ ,$$

we choose piecewise constant functions in time and piecewise linear functions in space:

$$(\frac{\partial v_+^{inc}}{\partial n})_{h,\Delta t} := g = \sum_{m=1}^{N_t} \sum_{i=1}^{N_{s'}} g_i^m \gamma_{\Delta t}^m(t) \xi_h^i(x)$$

to get the same right hand side as in (3.24) with g^n instead of f^n there. We denote it with

$$\begin{pmatrix} V^{N_t} & V^{N_t-1} & \dots & V^1 \\ 0 & \ddots & \ddots & \vdots \\ \vdots & \ddots & \ddots & \vdots \\ 0 & \dots & 0 & V^{N_t} \end{pmatrix} \begin{pmatrix} g^1 \\ \vdots \\ \vdots \\ g^{N_t} \end{pmatrix} := \begin{pmatrix} G^1 \\ \vdots \\ \vdots \\ G^{N_t} \end{pmatrix} ,$$

where the block matrices $V^1, \dots, V^{N_t}$ are explained in Section 3.7.

Now let us consider the space time system we want to solve. For $N_t = 1$:

$$\begin{pmatrix} (\frac{(\Delta t)}{2} A + \frac{1}{(\Delta t)} M)_{\Omega\setminus\Gamma,\Omega\setminus\Gamma} & (\frac{(\Delta t)}{2} A + \frac{1}{(\Delta t)} M)_{\Omega\setminus\Gamma,\Gamma} & 0 \\ (\frac{(\Delta t)}{2} A + \frac{1}{(\Delta t)} M)_{\Gamma,\Omega\setminus\Gamma} & (\frac{(\Delta t)}{2} A + \frac{1}{(\Delta t)} M)_{\Gamma,\Gamma} & RVn_x^0 \\ 0 & n_x RV^0 & ZT_{1,1} \end{pmatrix} \begin{pmatrix} (u_{\Omega\setminus\Gamma}^1) \\ (u_\Gamma^1) \\ q^1 \end{pmatrix} = \begin{pmatrix} 0 \\ F^1 \\ G^1 \end{pmatrix} .$$

We define the block matrices

$$K1_{i,i} = \begin{pmatrix} (\frac{(\Delta t)}{2} A + \frac{1}{(\Delta t)} M)_{\Omega\setminus\Gamma,\Omega\setminus\Gamma} & (\frac{(\Delta t)}{2} A + \frac{1}{(\Delta t)} M)_{\Omega\setminus\Gamma,\Gamma} & 0 \\ (\frac{(\Delta t)}{2} A + \frac{1}{(\Delta t)} M)_{\Gamma,\Omega\setminus\Gamma} & (\frac{(\Delta t)}{2} A + \frac{1}{(\Delta t)} M)_{\Gamma,\Gamma} & RVn_x^0 \\ 0 & n_x RV^0 & ZT_{i,i} \end{pmatrix} ,$$

$$K2_{i,j} = \begin{pmatrix} (\frac{(\Delta t)}{2}A - \frac{2}{(\Delta t)}M)_{\Omega\setminus\Gamma,\Omega\setminus\Gamma} & (\frac{(\Delta t)}{2}A - \frac{2}{(\Delta t)}M)_{\Omega\setminus\Gamma,\Gamma} & 0 \\ (\frac{(\Delta t)}{2}A - \frac{2}{(\Delta t)}M)_{\Gamma,\Omega\setminus\Gamma} & (\frac{(\Delta t)}{2}A - \frac{2}{(\Delta t)}M)_{\Gamma,\Gamma} & RVn_x^1 \\ 0 & n_x RV^{-1} & ZT_{i,j} \end{pmatrix},$$

$$K3_{i,j} = \begin{pmatrix} (\frac{1}{(\Delta t)}M)_{\Omega\setminus\Gamma,\Omega\setminus\Gamma} & (\frac{1}{(\Delta t)}M)_{\Omega\setminus\Gamma,\Gamma} & 0 \\ (\frac{1}{(\Delta t)}M)_{\Gamma,\Omega\setminus\Gamma} & (\frac{1}{(\Delta t)}M)_{\Gamma,\Gamma} & RVn_x^2 \\ 0 & 0 & ZT_{i,j} \end{pmatrix},$$

$$LB_{i,j,k} = \begin{pmatrix} 0 & 0 & 0 \\ 0 & 0 & RVn_x^k \\ 0 & 0 & ZT_{i,j} \end{pmatrix}, \quad UB_{i,j,k} = \begin{pmatrix} 0 & 0 & 0 \\ 0 & 0 & 0 \\ 0 & n_x RV^k & ZT_{i,j} \end{pmatrix}$$

and for some arbitrary $n = 1, \ldots, N_t$

$$uq^n := \begin{pmatrix} (u^n_{\Omega\setminus\Gamma}) \\ (u^n_\Gamma) \\ q^n \end{pmatrix}, \quad FG^n := \begin{pmatrix} 0 \\ F^n \\ G^n \end{pmatrix}.$$

For $N_t = 2$

$$\begin{pmatrix} K1_{1,1} & UB_{1,2,1} \\ K2_{2,1} & K1_{2,2} \end{pmatrix} \begin{pmatrix} uq^1 \\ uq^2 \end{pmatrix} = \begin{pmatrix} FG^1 \\ FG^2 \end{pmatrix}.$$

For $N_t \geq 3$, we have

$$\begin{pmatrix} K1_{1,1} & UB_{1,2,1} & UB_{1,3,2} & \ldots & \ldots & UB_{1,N_t,N_t-1} \\ K2_{2,1} & K1_{2,2} & UB_{2,3,1} & \ldots & \ldots & UB_{2,N_t,N_t-2} \\ K3_{3,1} & K2_{3,2} & K1_{3,3} & UB_{3,4,1} & \ldots & UB_{3,N_t,N_t-3} \\ LB_{4,1,3} & K3_{4,2} & K2_{4,3} & K1_{4,4} & \ddots & \vdots \\ \vdots & \ddots & \ddots & \ddots & \ddots & UB_{N_t-1,N_t,1} \\ LB_{N_t,1,N_t-1} & \ldots & LB_{N_t,N_t-3,3} & K3_{N_t,N_t-2} & K2_{N_t,N_t-1} & K1_{N_t,N_t} \end{pmatrix} \begin{pmatrix} uq^1 \\ uq^2 \\ \vdots \\ uq^{N_t} \end{pmatrix}$$
$$= \begin{pmatrix} FG^1 \\ FG^2 \\ \vdots \\ FG^{N_t} \end{pmatrix}.$$

An example for the fluid-structure interaction is derived in Section 3.8.

3.7 First numerical experiments with V as test function

In this section we execute first numerical experiments with V applied to the test function. For $p_{h,\Delta t} \in V_{h,\Delta t}^{1,0}$ and $q_{h,\Delta t} \in V_{h,\Delta t}^{1,0}$ and a given right hand side f, we solve

$$\langle p_{h,\Delta t}, V\dot{q}_{h,\Delta t}\rangle_{\Gamma\times\mathbb{R}_+} = \langle f, V\dot{q}_{h,\Delta t}\rangle_{\Gamma\times\mathbb{R}_+} \ . \tag{3.21}$$

We expect $p_{h,\Delta t}$ to approximate f. The reason for doing this numerical experiment is to understand the incoming scheme. We write

$$p_{h,\Delta t} = \sum_{m=1}^{N_t}\sum_{i=1}^{N_s} p_i^m \gamma_{\Delta t}^m(t)\xi_h^i(x) \ , \quad \dot{q}_{h,\Delta t} = \dot{\gamma}_{\Delta t}^n(t)\xi_h^j(x) \ . \tag{3.22}$$

Hence we get:

$$\begin{aligned}
\langle p_{h,\Delta t}, V\dot{q}_{h,\Delta t}\rangle_{\Gamma\times\mathbb{R}_+} &= \sum_{m=1}^{N_t}\sum_{i=1}^{N_s} p_i^m \iint\limits_{\Gamma\times\Gamma} \frac{\xi_h^i(x)\xi_h^j(y)}{4\pi|x-y|}\int_0^\infty \gamma_{\Delta t}^m(t)\dot{\gamma}_{\Delta t}^n(t-|x-y|)dtds_yds_x \\
&= \sum_{m=1}^{N_t}\sum_{i=1}^{N_s} \psi_i^m \iint\limits_{\Gamma\times\Gamma} \frac{\xi_h^i(x)\xi_h^j(y)}{4\pi|x-y|}(\chi_{E_{m-n}}(x,y) - \chi_{E_{m-n-1}}(x,y))ds_yds_xdt \\
&= \sum_{m=1}^{N_t}\sum_{i=1}^{N_s} p_i^m \iint\limits_{E_{m-n}} \frac{\xi_h^i(x)\xi_h^j(y)}{4\pi|x-y|}ds_yds_x - \iint\limits_{E_{m-n-1}} \frac{\xi_h^i(x)\xi_h^j(y)}{4\pi|x-y|}ds_yds_x \ ,
\end{aligned} \tag{3.23}$$

where the time integral part is in (9.3) in the Appendix with switched indices n and m.

Let us have a closer look at E_{m-n}. We begin with the case $n = N_t$ (last timestep). Then every index of E_{m-n} is negative, except when $m = N_t$. This is the only case where an integral exists. We obtain:

$$\sum_{i=1}^{N_s} p_i^{N_t} \iint\limits_{E_0} \frac{\xi_h^i(x)\xi_h^j(y)}{4\pi|x-y|}ds_yds_x =: V^{N_t}p^{N_t} \ .$$

For $n = N_t - 1$, there exists entries in cases of $m = N_t$ and $m = N_t - 1$:

$$\begin{aligned}
&\sum_{i=1}^{N_s} p_i^{N_t-1}\iint\limits_{E_0}\frac{\xi_h^i(x)\xi_h^j(y)}{4\pi|x-y|}ds_yds_x + \sum_{i=1}^{N_s} p_i^{N_t}\left(\iint\limits_{E_1} \frac{\xi_h^i(x)\xi_h^j(y)}{4\pi|x-y|}ds_yds_x - \iint\limits_{E_0} \frac{\xi_h^i(x)\xi_h^j(y)}{4\pi|x-y|}ds_yds_x\right) \\
&=: V^{N_t}p^{N_t-1} + V^{N_t-1}p^{N_t} \ .
\end{aligned}$$

Now for arbitrary n, every index beginning from $m = n$ till the last index $m = N_t$ gives us existing integrals. Altogether we have: $\sum_{k=n}^{N_t} V^k p^{n-k+N_t}$, where V^k has the entries

$$\iint\limits_{E_{N_t-k}} \frac{\xi_h^i(x)\xi_h^j(y)}{4\pi|x-y|}ds_yds_x - \iint\limits_{E_{N_t-k-1}} \frac{\xi_h^i(x)\xi_h^j(y)}{4\pi|x-y|}ds_yds_x$$

The same occurs for the right hand side as well, if we use the same ansatz for $f \approx \sum_{m=1}^{N_t}\sum_{i=1}^{N_s} f_i^m \gamma_{\Delta t}^m(t)\xi_h^i(x)$. Then the space-time linear equation system reads:

$$\begin{pmatrix} V^{N_t} & V^{N_t-1} & \dots & V^1 \\ 0 & \ddots & \ddots & \vdots \\ \vdots & \ddots & \ddots & \vdots \\ 0 & \dots & 0 & V^{N_t} \end{pmatrix} \begin{pmatrix} p_i^1 \\ \vdots \\ \vdots \\ p^{N_t} \end{pmatrix} = \begin{pmatrix} V^{N_t} & V^{N_t-1} & \dots & V^1 \\ 0 & \ddots & \ddots & \vdots \\ \vdots & \ddots & \ddots & \vdots \\ 0 & \dots & 0 & V^{N_t} \end{pmatrix} \begin{pmatrix} f^1 \\ \vdots \\ \vdots \\ f^{N_t} \end{pmatrix}, \tag{3.24}$$

where $f^m = (f_1^m, \dots, f_{N_s}^m)^T$ for $m = 1, \dots, N_t$. Since every V^k here is symmetric, in comparison to the V^{n-m} in Subsection 2.3.1 with using piecewise linear functions in space they differ from a sign. (3.24) contains in both sides the same matrix. In the FEM-BEM coupling case for the fluid-structure interaction we need it in order to setup the space time matrix. Now we can use a scheme similar to the MOT-scheme to solve this linear equation system. For an arbitrary n from N_t backwards to 1, we solve:

$$V^{N_t} p^n = \sum_{k=n}^{N_t} V^k f^{n-k+N_t} - \sum_{k=n}^{N_t-1} V^k p^{n-k+N_t}$$

Example 3.1. *We set the right hand side* $f = t^4 \exp(-2t)$ *and compute* (3.21) *on an icosahedron with 80 triangles. We set* $\Delta t = 0.01$ *and compute till time* 0.5.

In Figure 3.3, we plot the right hand side f and the solution p. Since the right hand side has no influences in space the solution also has no influences from the space. As expected the solution p and the right hand side coincide.

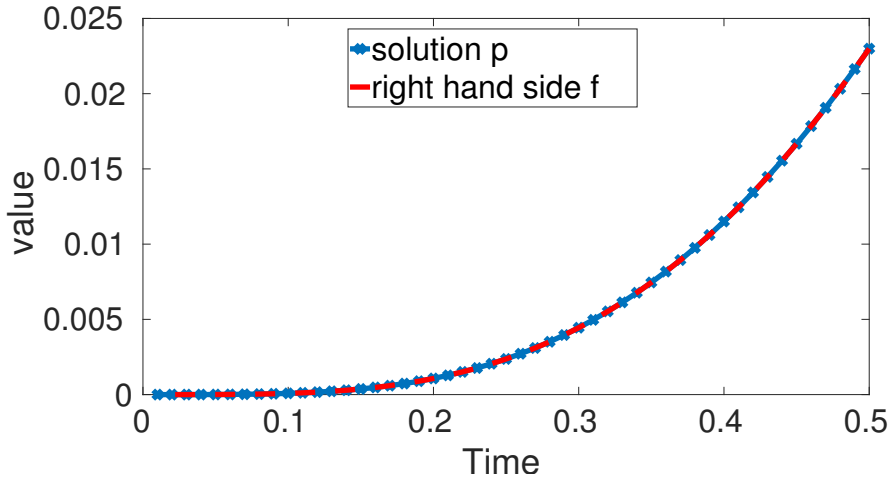

Figure 3.3: The solution and the right hand side for the computation of (3.21) for Example 3.1.

In the next experiment we compare the solution q of $\langle(-\frac{1}{2}I+K')q, V\dot{q}'\rangle_{\Gamma\times\mathbb{R}_+} = \langle f, V\dot{q}'\rangle_{\Gamma\times\mathbb{R}_+}$ with $\langle(-\frac{1}{2}I+K')q, \dot{q}'\rangle_{\Gamma\times\mathbb{R}_+} = \langle f, \dot{q}'\rangle_{\Gamma\times\mathbb{R}_+}$. We solve $\langle(-\frac{1}{2}I+K')q, V\dot{q}'\rangle_{\Gamma\times\mathbb{R}_+}$ in two ways. One way is by taking directly the matrices of $(-\frac{1}{2}I+K')$ in the ansatz and V in the test

function for piecewise constant ansatz and test functions in space and time, whereas for the matrix of $(-\frac{1}{2}I + K')$ see Subsection 2.3.2 (we denote the matrix with $(-\frac{1}{2}I + K')$ as well) and for the matrix of V in the test function see (3.15) with (3.24) as the structure. We solve the linear equation system

$$\tilde{V}^T(-\frac{1}{2}I + K')q = \tilde{V}^T f \ . \tag{3.25}$$

The other way is by using the L^2-Approximation. We use for $\dot{q}', q, z, \nu$ piecewise constant functions in space and time. This leads us to the linear equation system:

$$\tilde{V}^T(-\frac{1}{2}I + P^{-1}K')q = \tilde{V}^T f \ . \tag{3.26}$$

Example 3.2. *We set* $f(x,t) = t^4 \exp(-2t)$ *and solve* (3.25) *and* (3.26) *on an icosahedron with 80 triangles, approximating the unit sphere. We choose* $\Delta t = 0.01$ *and compute till* $T = 4$*. In case of an unit sphere the exact solution of* $(-\frac{1}{2}I + K')q = f$ *is known by Veit in his Phd thesis [99]:*

$$p(t) = -2\sum_{k=0}^{\lfloor t/2 \rfloor} f(t-2k) + 2\sum_{k=0}^{\lfloor t/2 \rfloor} \int_{2k}^{t} e^{-(\tau-2k)} f(t-\tau)d\tau \ .$$

We observe in Figure 3.4 that the systems (3.25) and (3.26) behaves similar. In Figures 3.5 resp. 3.6 we zoomed the Figure 3.4 at timestep 1.5 resp. 3.1. We notice only small differences between the solutions of (3.25) and (3.26). Due to geometric approximation errors, the curve for $(-\frac{1}{2}I + K')p = f$ has greater differences to the solution of (3.25) and (3.26). In Figure 3.7 we consider (3.25) and (3.26), but without $V^T = \tilde{V}^T$ at the right hand side. In this case as well, we observe only small differences (see Figure 3.8).

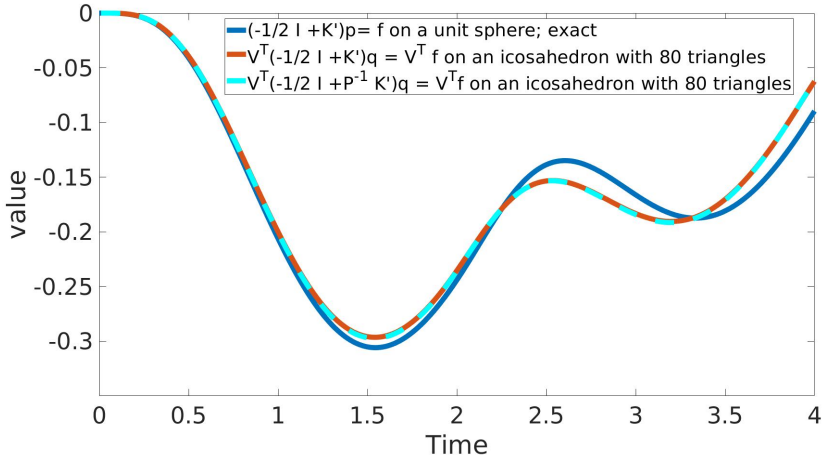

Figure 3.4: Results of the Example 3.2.

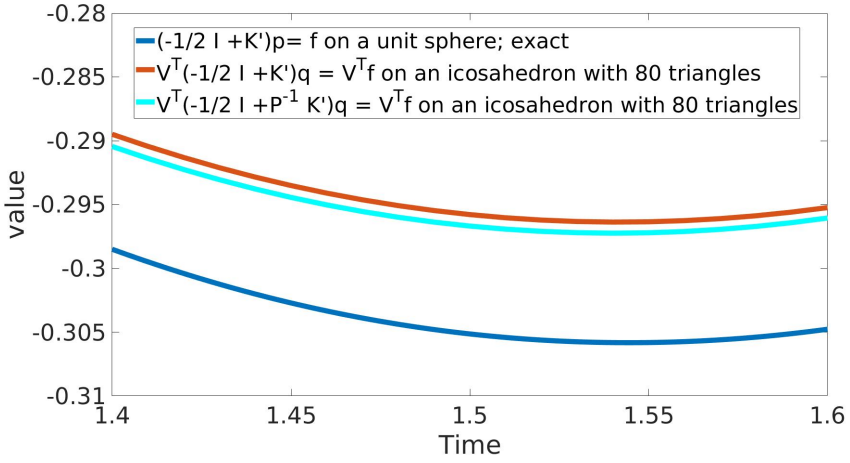

Figure 3.5: Results of the Example 3.2 zoomed at time 1.5.

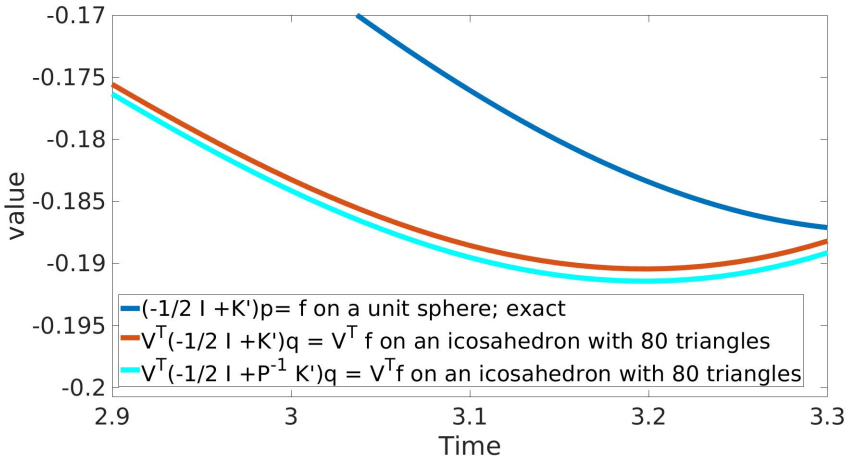

Figure 3.6: Results of the Example 3.2 zoomed at time 3.1.

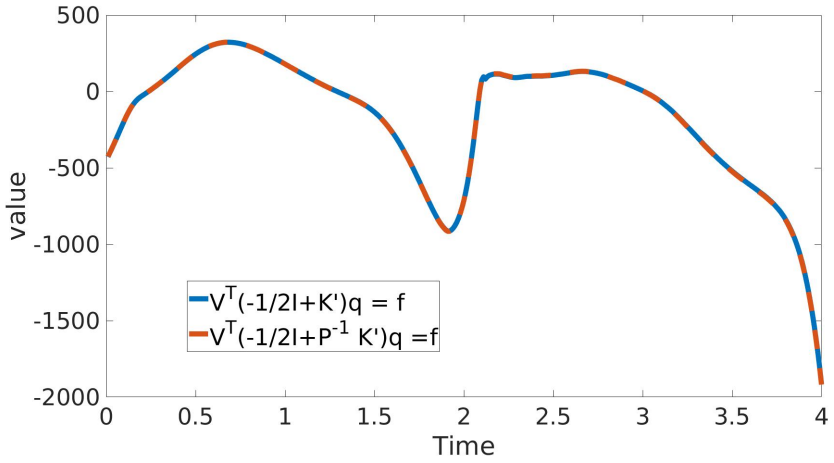

Figure 3.7: Results of the Example 3.2 without $V^T = \tilde{V}^T$ at the right hand side.

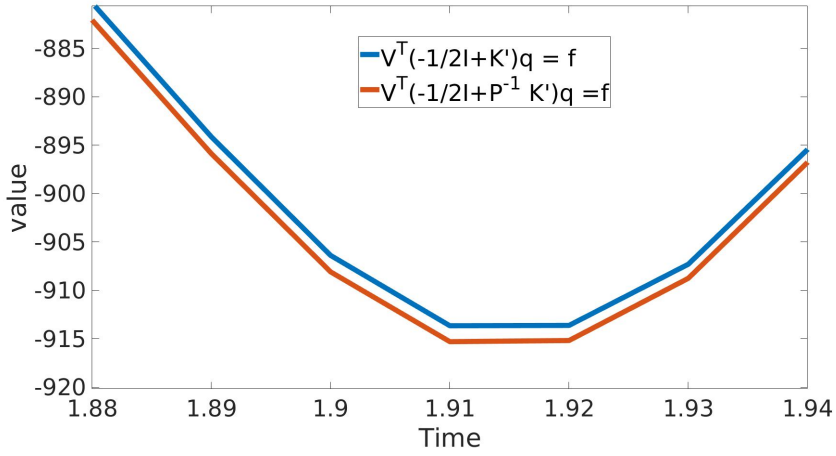

Figure 3.8: Results of the Example 3.2, without $V^T = \tilde{V}^T$ at the right hand side, zoomed at time 1.9.

3.8 Derivation of a numerical example for a fluid-strucuture interaction problem

Before showing our results of the fluid-structure interaction problem, we derive an exact solution. We know for the Cauchy-Problem:

$$\frac{\partial^2 v}{\partial t^2} - \Delta v = 0 \quad (x,t) \in \mathbb{R}^3 \times \mathbb{R}_+$$

$$v(x,0) = v_0(|x|) = 0 \quad \text{in } \mathbb{R}^3$$

$$\dot{v}(x,0) = v_1(|x|) = 0 \quad \text{in } \mathbb{R}^3$$

that the solution has the following form:

$$v(x,t) = |x|^{-1}(\phi(|x|+t) + \psi(|x|-t)) = \frac{1}{r}(\phi(r+t) - \psi(r-t))$$

with ϕ and ψ real functions on $\mathbb{R}$ and $r := |x|$. Taking the spherical Laplacian in $\mathbb{R}^3$ $\Delta v = (\frac{\partial^2}{\partial r^2} + \frac{2}{r}\frac{\partial}{\partial r})v$ one can proof easier that the homogenous wave equation is satisfied. Then with the initial conditons we get:

$$v(x,0) = |x|^{-1}(\phi(|x|) + \psi(|x|)) = v_0(|x|) = 0 \ ,$$
$$\dot{v}(x,0) = |x|^{-1}(\phi'(|x|) - \psi'(|x|)) = v_1(|x|) = 0.$$

Now we can write down:

$$\phi(|x|) + \psi(|x|) = |x|v_0(|x|) \Rightarrow \phi'(|x|) + \psi'(|x|) = (|x|v_0(|x|))' \ , \tag{3.28}$$
$$\phi(|x|)' - \psi'(|x|) = |x|v_1(|x|) \ . \tag{3.29}$$

Adding resp. subtracting (3.28) and (3.29) leads to:

$$\phi'(|x|) = \frac{1}{2}\left((|x|v_0(|x|))' + (|x|v_1(|x|))\right) ,$$
$$\psi'(|x|) = \frac{1}{2}\left((|x|v_0(|x|))' - (|x|v_1(|x|))\right) .$$

Now by integration, where C_1, C_2 are constants:

$$\phi(|x|) = \frac{1}{2}|x|v_0(|x|) + \frac{1}{2}\int_0^{|x|} rv_1(r)dr + C_1 ,$$
$$\psi(|x|) = \frac{1}{2}|x|v_0(|x|) - \frac{1}{2}\int_0^{|x|} rv_1(r)dr + C_2 ,$$

we get the following form for the solution v:

$$\begin{aligned} v(x,t) =& \frac{1}{2|x|}\Big((|x|+t)v_0(|x|+t) + \frac{1}{2}\int_0^{|x|+t} rv_1(r)dr + C_1 \\ &+ (|x|-t)v_0(|x|-t) - \frac{1}{2}\int_0^{|x|-t} rv_1(r)dr + C_2\Big) . \end{aligned}$$

For $t = 0$ the integral parts remove themselves and we get the following equation:

$$v(x,0) = \frac{1}{2|x|}(2|x|v_0(|x|) + C_1 + C_2) = v_0(|x|) + \frac{C_1}{2|x|} + \frac{C_2}{2|x|} = v_0(|x|) ,$$

where $C_1 = -C_2$ follows. We get:

$$\begin{aligned} v(x,t) =& \frac{1}{2|x|}\Big((|x|+t)v_0(|x|+t) + \frac{1}{2}\int_0^{|x|+t} rv_1(r)dr \\ &+ (|x|-t)v_0(|x|-t) - \frac{1}{2}\int_0^{|x|-t} rv_1(r)dr\Big) . \end{aligned}$$

For deriving an example of an exact solution of the fluid-structure interaction problem, we set $v_1(|x|) = 0$ and for some fixed $R > 0$ we set

$$v_0(|x|) = \begin{cases} 1 + \cos(\frac{\pi|x|}{R}) & , \text{ for } |x| < R \\ 0 & , \text{else , i.e } |x| \geq R . \end{cases}$$

Then we get as the exact solution:

$$v(x,t) = \frac{1}{2|x|}\Big((|x|+t)v_0(|x|+t) + (|x|-t)v_0(|x|-t)\Big) .$$

With the Heaviside-function we choose a down the solution of the Cauchy-Problem as:

$$\begin{aligned} v(x,t) &= \frac{1}{2|x|}\left((|x|-t)v_0(|x|-t)\right) \\ &= \frac{|x|-t}{2|x|}\left(1 + \cos\left(\frac{\pi(|x|-t)}{R}\right)\right)H(R - ||x|-t|) . \end{aligned}$$

We compute numerical experiments on an unit cube, i.e. $\Omega = [-1,1]^3$. For getting zero initial conditions for v, $x \in \Omega^c$ should satisfy $|x| \geq 1 > R$. Choosing $R = 0.9$ v is zero at time 0. Now taking the time-derivative of v:

$$\begin{aligned}\frac{\partial v}{\partial t}(x,t) = &\frac{-1}{2|x|}\left(1+\cos\left(\frac{\pi(|x|-t)}{R}\right)H(R-||x|-t|)\right)\\ &+\frac{|x|-t}{2|x|}\left(\frac{\pi}{R}\sin\left(\frac{\pi(|x|-t)}{R}\right)H(R-||x|-t|)\right)\\ &+\frac{|x|-t}{2|x|}\left(1+\cos\left(\frac{\pi(|x|-t)}{R}\right)\right)\delta(R-||x|-t|)\cdot(-1)\cdot sign(|x|-t)\ ,\end{aligned}$$

where δ is the δ–Distribution. Using again $t = 0$, we get:

$$\begin{aligned}\frac{\partial v}{\partial t}(x,0) = &\frac{-1}{2|x|}\left(1+\cos\left(\frac{\pi(|x|)}{R}\right)H(R-|x|)\right)\\ &+\frac{|x|}{2|x|}\left(\frac{\pi}{R}\sin\left(\frac{\pi(|x|)}{R}\right)H(R-|x|)\right)\\ &+\frac{|x|}{2|x|}\left(1+\cos\left(\frac{\pi(|x|)}{R}\right)\right)\delta(R-|x|)\cdot(-1)\cdot sign(|x|)\ .\end{aligned}$$

Remember that $|x| \geq 1 > R = 0.9$, means every part above disappears and we get a zero initial condition for the time-derivative of v. Altogether (3.1) is fulfilled. Next we want to get an example of the interior part of the fluid-structure interaction problem. The following plane wave with $\alpha = \sqrt{\lambda + 2\mu}$ satisfies the Lame equation with $\rho_1 = 1$:

$$\mathbf{u}(x,t) := \begin{pmatrix} f(t-\frac{x_1}{\alpha}) \\ 0 \\ 0 \end{pmatrix} \quad \text{with } x = \begin{pmatrix} x_1 \\ x_2 \\ x_3 \end{pmatrix}\ .$$

Since $\mathrm{div}\mathbf{u} = \frac{-1}{\alpha} f'(t-\frac{x_1}{\alpha})$ and $\nabla(\mathrm{div}\mathbf{u}) = \begin{pmatrix} \frac{1}{\alpha^2} f''(t-\frac{x_1}{\alpha}) \\ 0 \\ 0 \end{pmatrix}$, $\nabla\mathbf{u} = \begin{pmatrix} \frac{-1}{\alpha} f'(t-\frac{x_1}{\alpha}) & 0 & 0 \\ 0 & 0 & 0 \\ 0 & 0 & 0 \end{pmatrix}$,

$\Delta\mathbf{u} = \mathrm{div}(\nabla\mathbf{u}) = \begin{pmatrix} \frac{1}{\alpha^2} f''(t-\frac{x_1}{\alpha}) \\ 0 \\ 0 \end{pmatrix}$ and

$$\begin{aligned}\ddot{\mathbf{u}}(x,t) - \Delta^*(\mathbf{u}) &= \ddot{\mathbf{u}} - \mu\Delta\mathbf{u} - (\lambda+\mu)\nabla(\mathrm{div}\mathbf{u})\\ &= \begin{pmatrix} f''(t-\frac{x_1}{\alpha}) \\ 0 \\ 0 \end{pmatrix} - \mu\begin{pmatrix} \frac{1}{\alpha^2} f''(t-\frac{x_1}{\alpha}) \\ 0 \\ 0 \end{pmatrix} - (\lambda+\mu)\begin{pmatrix} \frac{1}{\alpha^2} f''(t-\frac{x_1}{\alpha}) \\ 0 \\ 0 \end{pmatrix}\\ &= \begin{pmatrix} f''(t-\frac{x_1}{\alpha}) \\ 0 \\ 0 \end{pmatrix} - \frac{\lambda+\mu}{\lambda+\mu}\begin{pmatrix} f''(t-\frac{x_1}{\alpha}) \\ 0 \\ 0 \end{pmatrix} = \begin{pmatrix} 0 \\ 0 \\ 0 \end{pmatrix}\ .\end{aligned}$$

Choosing $\mathbf{u}$ as:

$$\mathbf{u}(x,t) = \begin{pmatrix} \left(\sin\left(\pi\cdot(t-\frac{x_1}{2})\right)\right)^5 (H(R'+t-\frac{x_1}{2}) - H(R''+t-\frac{x_1}{2})) \\ 0 \\ 0 \end{pmatrix} =: \begin{pmatrix} u_1(x,t) \\ u_2(x,t) \\ u_3(x,t) \end{pmatrix},$$

where $\mu = 1, \lambda = 2$ ($\Rightarrow \alpha = 2$), $R' = -1$ and $R'' = -3$ the initial condition for u is satisfied, because

$$\mathbf{u}(x,0) = \begin{pmatrix} \left(\sin\left(-\pi \cdot (\frac{x_1}{2})\right)\right)^5 (H(-1-\frac{x_1}{2}) - H(-3-\frac{x_1}{2})) \\ 0 \\ 0 \end{pmatrix} = \begin{pmatrix} 0 \\ 0 \\ 0 \end{pmatrix},$$

since the argument of the Heaviside-function is negative for $x_1 \in [-1,1]$ (remember that $x \in \Omega = [-1,1]^3$). Taking the derivative in time of $\mathbf{u}$ and considering only the first entry gives

$$\begin{aligned} &5\pi\Big(\sin\left(\pi(t-\frac{x_1}{2})\right)\Big)^4 \cos\left(\pi(t-\frac{x_1}{2})\right)\Big(H(-1+t-\frac{x_1}{2}) - H(-3+t-\frac{x_1}{2})\Big) \\ &+\Big(\sin\left(\pi(t-\frac{x_1}{2})\right)\Big)^5 \Big(\delta(-1+t-\frac{x_1}{2}) - \delta(-3+t-\frac{x_1}{2})\Big). \end{aligned}$$

Setting again $t = 0$:

$$\begin{aligned} &5\pi\Big(\sin\left(\pi(-\frac{x_1}{2})\right)\Big)^4 \cos\left(\pi(-\frac{x_1}{2})\right)\Big(H(-1-\frac{x_1}{2}) - H(-3-\frac{x_1}{2})\Big) \\ &+\Big(\sin\left(\pi(-\frac{x_1}{2})\right)\Big)^5 \Big(\delta(-1-\frac{x_1}{2}) - \delta(-3-\frac{x_1}{2})\Big) \ . \end{aligned}$$

Since again for $x_1 \in [-1,1]$ the argument of the Heaviside-function and the delta-Distribution are negative. Therefore we get zero initial condition for $\frac{\partial \mathbf{u}}{\partial t}$. Hence (3.2) is satisfied. Now we have to set the tranmission conditions. We have to compute $\tilde{\sigma}(\mathbf{u}) = (\lambda(\mathrm{div}\mathbf{u}))E + 2\mu\varepsilon(\mathbf{u})$, with $\varepsilon(\mathbf{u}) = \frac{1}{2}((\nabla\mathbf{u}) + (\nabla\mathbf{u})^T)$ and E the 3×3 unit matrix. Since our given $\mathbf{u}$ uses only the first component x and maps only in it's first component we just need to compute $\frac{\partial u_1}{\partial x_1}(x,t)$:

$$\frac{\partial u_1}{\partial x_1}(x,t) = -\frac{5\pi}{2}\Big(\sin\left(\pi(t-\frac{x_1}{2})\right)\Big)^4 \cos\left(\pi(t-\frac{x_1}{2})\right)\Big(H(-1+t-\frac{x_1}{2}) - H(-3+t-\frac{x_1}{2})\Big).$$

We get:

$$\tilde{\sigma}(\mathbf{u}) \cdot n = \begin{pmatrix} 4\frac{\partial u_1}{\partial x_1}(x,t)n_1 \\ 2\frac{\partial u_1}{\partial x_1}(x,t)n_2 \\ 2\frac{\partial u_1}{\partial x_1}(x,t)n_3 \end{pmatrix}.$$

We also need:

$$\frac{\partial v}{\partial t}(x,t) = \left(-\frac{1}{2|x|}(1+\cos(\frac{\pi(|x|-t)}{0.9})) + \frac{|x|-t}{2|x|}\frac{\pi}{0.9}\sin(\frac{\pi(|x|-t)}{0.9})\right) H(0.9-||x|-t|).$$

As the first transmission condition we get:

$$\tilde{\sigma}(\mathbf{u}) \cdot n + \frac{\partial v}{\partial t}(x,t) \cdot n = \begin{pmatrix} 4\frac{\partial u_1}{\partial x_1}(x,t)n_1 + \frac{\partial v}{\partial t}(x,t)n_1 \\ 2\frac{\partial u_1}{\partial x_1}(x,t)n_2 + \frac{\partial v}{\partial t}(x,t)n_2 \\ 2\frac{\partial u_1}{\partial x_1}(x,t)n_3 + \frac{\partial v}{\partial t}(x,t)n_3 \end{pmatrix}. \tag{3.30}$$

Next we consider the second transmission condition. We need $\frac{\partial v}{\partial x_i}(x,t)$ for $i = 1,2,3$:

$$\frac{\partial v}{\partial x_i}(x,t) = \left(\frac{tx_i}{2|x|^3}\left(1+\cos\left(\frac{\pi(|x|-t)}{0.9}\right)\right) - \left(\frac{1}{2} - \frac{t}{2|x|}\right)\frac{\pi x_i}{0.9|x|}\sin\left(\frac{\pi(|x|-t)}{0.9}\right)\right) H(0.9-||x|-t|).$$

Next we need

$$\frac{\partial \mathbf{u}}{\partial t}(x,t) = \begin{pmatrix} 5\pi\Big(\sin\left(\pi(t-\frac{x_1}{2})\right)\Big)^4 \cos\left(\pi(t-\frac{x_1}{2})\right)\left(H(-1+t-\frac{x_1}{2}) - H(-3+t-\frac{x_1}{2})\right) \\ 0 \\ 0 \end{pmatrix}.$$

As our second tranmission condition we get:

$$\begin{aligned}
&\frac{\partial \mathbf{u}}{\partial t}(x,t)n + \frac{\partial v}{\partial n}(x,t) = 5\pi\left(\sin\left(\pi(t-\frac{x_1}{2})\right)\right)^4 \cos\left(\pi(t-\frac{x_1}{2})\right)\left(H(-1+t-\frac{x_1}{2}) - H(-3+t-\frac{x_1}{2})\right)n_1 \\
&+ \left(\frac{tx_1}{2|x|^3}(1+\cos(\frac{\pi(|x|-t)}{0.9})) - (\frac{1}{2} - \frac{t}{2|x|})\frac{\pi x_1}{0.9|x|}\sin(\frac{\pi(|x|-t)}{0.9})\right) H(0.9-||x|-t|)n_1 \\
&+ \left(\frac{tx_2}{2|x|^3}(1+\cos(\frac{\pi(|x|-t)}{0.9})) - (\frac{1}{2} - \frac{t}{2|x|})\frac{\pi x_2}{0.9|x|}\sin(\frac{\pi(|x|-t)}{0.9})\right) H(0.9-||x|-t|)n_2 \\
&+ \left(\frac{tx_3}{2|x|^3}(1+\cos(\frac{\pi(|x|-t)}{0.9})) - (\frac{1}{2} - \frac{t}{2|x|})\frac{\pi x_3}{0.9|x|}\sin(\frac{\pi(|x|-t)}{0.9})\right) H(0.9-||x|-t|)n_3 \,.
\end{aligned} \tag{3.31}$$

We will use these tranmission conditions as our right hand side in our Example 3.4 as well as in Example 4.3.

3.9 Numerical experiments

We begin with the a Dirichlet Lame-problem in the interior $\Omega = [-1,1]^3$, in order to check the implementation and the behaviour of the interior solution $\mathbf{u}$.

$$\frac{\partial^2 \mathbf{u}}{\partial t^2} - \Delta^* \mathbf{u} = 0 \quad (x,t) \in \Omega \times (0,\infty) \tag{3.32a}$$

$$\mathbf{u}(x,0) = \dot{\mathbf{u}}(x,0) = 0 \quad \text{in } \Omega \tag{3.32b}$$

$$\gamma^- \mathbf{u} = f \quad \text{on } \Gamma \times (0,\infty) \tag{3.32c}$$

For $\sigma = 0$ the variational formulation reads: Find $\mathbf{u} \in (H^1(\mathbb{R}_+, H^1(\Omega)))^3$ such that

$$\begin{aligned}
\int_0^\infty \int_\Omega \tilde{\sigma}(\mathbf{u}) : \varepsilon(\dot{\mathbf{w}}) dx dt + \int_0^\infty \int_\Omega \ddot{\mathbf{u}}\dot{\mathbf{w}} dx dt &= \int_0^\infty \int_\Gamma \tilde{\sigma}(\gamma^- \mathbf{u}) \cdot n(\gamma^- \dot{\mathbf{w}}) ds_x dt \\
&= \int_0^\infty \int_\Gamma \tilde{\sigma}(f) \cdot n(\gamma^- \dot{\mathbf{w}}) ds_x dt
\end{aligned}$$

for all $\mathbf{w} \in (H^1(\mathbb{R}_+, H^1(\Omega)))^3$. We discretize the left hand side as in Section 3.6 (3.18) and (3.19). For the right hand side we use an approximation $f(x,t) \approx \sum_{m=1}^{N_t} f^m \beta_{\Delta t}^m(t)$, where $f^m = f(x,t_m)$.

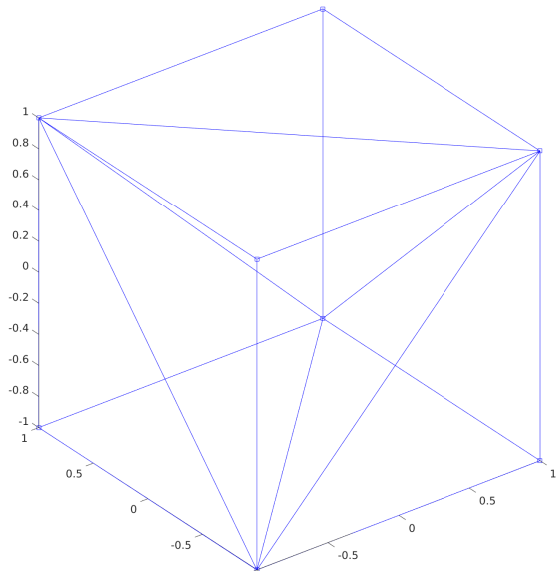

(a) Mesh with 8 nodes, 5 tetrahedrals, 12 triangles

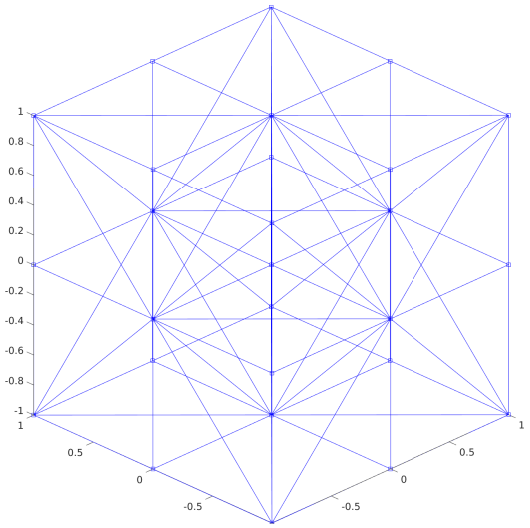

(b) Mesh with 27 nodes, 40 tetrahedrals, 48 triangles

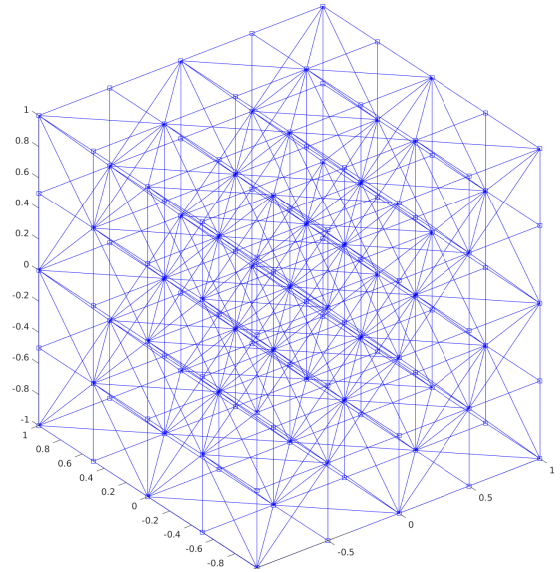

(c) Mesh with 125 nodes, 320 tetrahedrals, 192 triangles

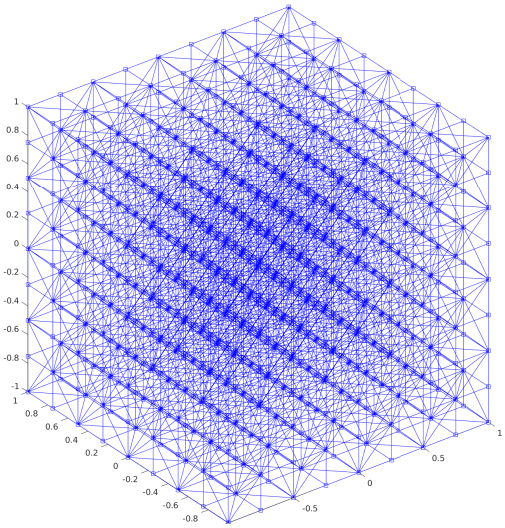

(d) Mesh with 729 nodes, 2560 tetrahedrals, 768 triangles

Figure 3.9: Mesh of the unit cube for (a) $N = 1$, (b) $N = 2$,(c) $N = 4$ and (d) $N = 8$

Example 3.3. *We set the right hand side into* $f(x,t) = \left(\sin(\pi(t - \frac{x_1}{2}))\right)^5 (H(-1 + t - \frac{x_1}{2}) - H(-3 + t - \frac{x_1}{2}))$ *the Problem as in* (3.18) *and* (3.19) *on an unit cube* $\Omega = [-1,1]^3$ *(see Figure 3.9) till time* $T = 4$. *We consider uniformly refined space time meshes, where the CFL is hold at* 0.1414. *The exact solution is as well* $\left(\sin(\pi(t - \frac{x_1}{2}))\right)^5 (H(-1 + t - \frac{x_1}{2}) - H(-3 + t - \frac{x_1}{2}))$.

In Figure 3.10 we compare different solvers at the point $(-1,-1,-1)$ for a mesh with 40

tetrahedrals, i.e. $N = 2$ and $\Delta t = 0.2$. We notice that solving a space time matrix with GMRES leads to unreasonable solutions, whereas using a MOT-scheme with GMRES as solver leads to almost the same solution as solving the space time matrix with Gauss. Therefore we use mainly Gauss or in cases of a MOT-scheme GMRES as solver.

In Figure 3.11, we plotted the L^2–Norm in space of the numerical solutions against the exact solution. Here we solved these systems with the MOT-scheme with GMRES as solver. While till time 1.3 the L^2–Norm in space of the numerical solution seems close to the L^2–Norm in space of the exact solution, we notice that after time 3.2 we get quite far away from it. We observe the same in Figure 3.12, where we plotted the L^2–error in time. In Figure 3.13 we computed the L^2-error in space and time. Hence we need a highly refined mesh. We get a convergence rate about 0.27. An alternative is trying Newmark's method out as a time stepping scheme instead of (3.18) and (3.19), which resembles central differential coefficients.

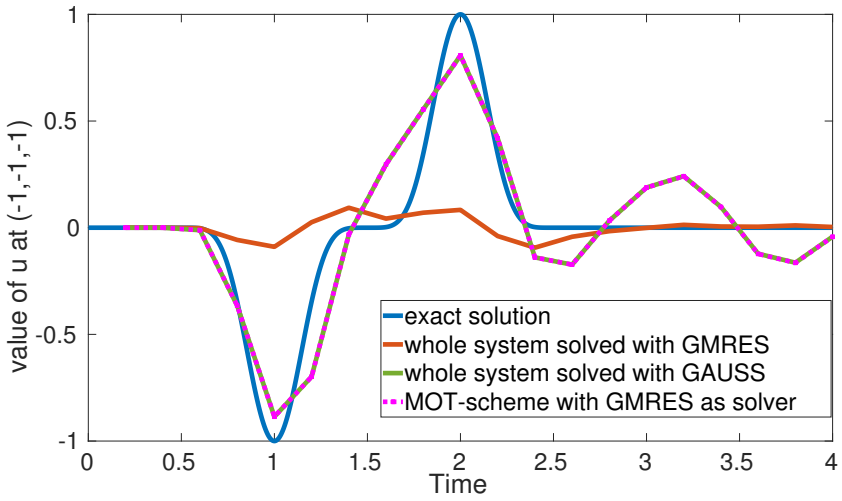

Figure 3.10: Value of $\mathbf{u}$ at $(-1,-1,-1)$ for $N = 2$, i.e. 40 tetrahedrals and $\Delta t = 0.2$ of the Example 3.3, where different solvers where used.

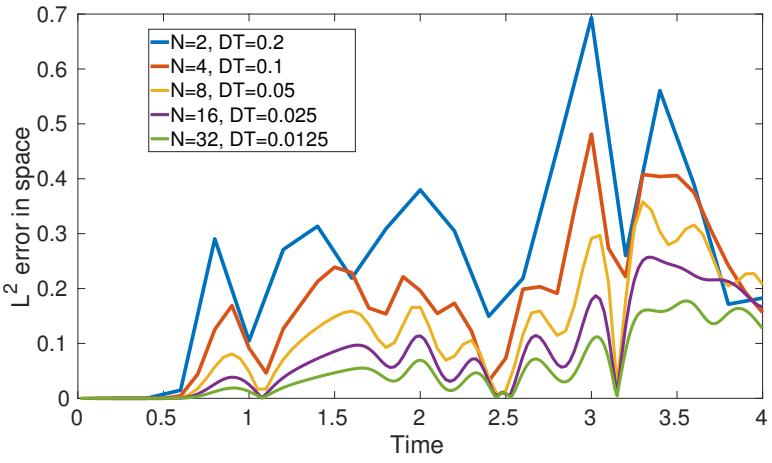

Figure 3.12: Error plot of the Example 3.3.

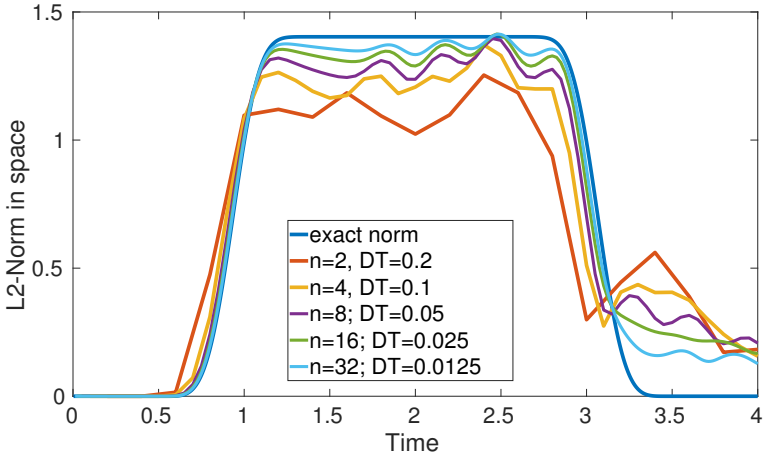

Figure 3.11: L^2-norm of the Example 3.3 for CFL 0.1414 .

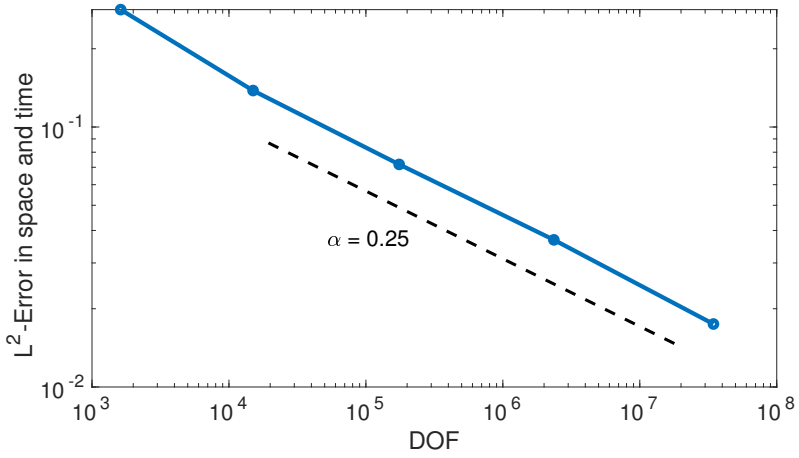

Figure 3.13: Convergence plot of the Example 3.3.

Next we consider an example for the fluid-structure interaction problem.

Example 3.4. *Now taking the right hand sides* (3.30) *and* (3.31)*, we finally compute the FSI problem on the unit cube. Since we are forced to use the whole the system, we solve it with Gauss. We compute for* $\Delta t = 0.2, 0.1$ *and* $N = 2, 4$*, i.e.* 40 *tetrahedrals resp.* 320 *tetrahedrals (see Figure 3.9).*

In Figure 3.14 we compare the solution in the interior $\mathbf{u}$ with the numerical solutions. We remark, that the solution behaves very different at all. Neither the exact solution is approximated nor similarities for $N = 2$ and $\Delta t = 0.2$ with $N = 4$ and $\Delta t = 0.1$ are seen. Besides possible errors in the implementation, the whole idea of using a L^2- approximation together with other approximations could lead to big errors. An alternative approach is done in Chapter 4 with the corresponding Example 4.3.

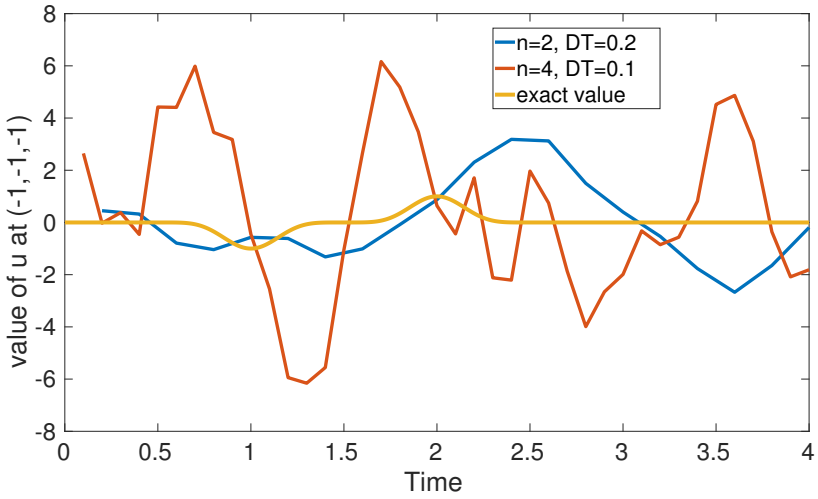

Figure 3.14: Result of $\mathbf{u}$ for the FSI problem in the corner $(-1,-1,-1)$ for Example 3.4.

4 FEM-BEM coupling in time domain II : Fluid structure interaction with symmetric coupling

4.1 Introduction

This chapter uses the ideas and the continuous bilinear form given in Hsiao, Sanchez-Vizuet, Sayas in [63] and Hsiao, Sayas, Weinacht in [64]. The well-posedness of the fluid structure interaction (FSI) problem (4.1) is proven in frequency domain in [63] and [64]. Therefore by applying an inverse Fourier transform we obtain the well-posedness of (4.1) in time domain (see [57, 90]). In the current chapter, like in the frequency domain in [63], we derive a coercivity estimate in time domain. We prove a priori and a posteriori error estimates in the space time domain and perform numerical experiments based on the bilinearform (4.6).

Let us consider again the following problem with $\Omega^- = \Omega$ and $\Omega^+ = \Omega^c = \mathbb{R}^3 \backslash \Gamma$:

$$\rho_1 \frac{\partial^2 \mathbf{u}}{\partial t^2} - \Delta^* \mathbf{u} = 0 \quad (x,t) \in \Omega \times (0,\infty) \ , \tag{4.1a}$$

$$\frac{\partial^2 v}{\partial t^2} - \Delta v = 0 \quad (x,t) \in \Omega^c \times (0,\infty) \ , \tag{4.1b}$$

$$\mathbf{u}(x,0) = \dot{\mathbf{u}}(x,0) = 0 \quad \text{in } \Omega \ , \tag{4.1c}$$

$$v(x,0) = \dot{v}(x,0) = 0 \quad \text{in } \Omega^c \ , \tag{4.1d}$$

$$\rho_2 \tilde{\sigma}(\gamma^- \mathbf{u}) \cdot n + \frac{\partial v_+}{\partial t} n = -\frac{\partial v_+^{inc}}{\partial t} n \quad \text{on } \Gamma \times (0,\infty) \ , \tag{4.1e}$$

$$\frac{\partial \gamma^- \mathbf{u}}{\partial t} n + \frac{\partial v_+}{\partial n} = -\frac{\partial v_+^{inc}}{\partial n} \quad \text{on } \Gamma \times (0,\infty) \ , \tag{4.1f}$$

where $n = n_x$ is the unit normal vector, pointing always towards Ω^c. On the one hand for $x \in \Gamma$ we define $\gamma^+ v(x,t) := v_+(x,t) = \lim_{x' \in \Omega^+ \to x} v(x',t)$ the limit of v to the boundary Γ from the exterior $\Omega^c = \Omega^+$ and on the other hand $\gamma^- v(x,t) := v_-(x,t) = \lim_{x' \in \Omega^- \to x} v(x',t)$ the limit of v to the boundary Γ from the bounded Lipschitz domain $\Omega = \Omega^-$. Further $\gamma^- \mathbf{u}(x,t) := \lim_{x' \in \Omega^- \to x} \mathbf{u}(x',t)$ the limit of the vector valued $\mathbf{u}$ to the boundary Γ from the bounded domain $\Omega = \Omega^-$. As in Chapter 2, $\partial_n^+ v(x,t) := \frac{\partial v_+}{\partial n}(x,t) := \lim_{x' \in \Omega^c \to x} n_x \cdot \nabla v(x',t)$ and $\partial_n^- v(x,t) := \frac{\partial v_-}{\partial n}(x,t) := \lim_{x' \in \Omega \to x} n_x \cdot \nabla v(x',t)$. ρ_1 and ρ_2 are constants. Here $\rho_1 = 1$

and $\rho_2 = 1$. $\Delta^* \mathbf{u} = \mu\Delta\mathbf{u} + (\lambda+\mu)\nabla(\mathrm{div}\mathbf{u}) = \mathrm{div}(\tilde{\sigma}(\mathbf{u}))$ with Lamé constants $\mu \geq 0$ and λ such that $3\lambda + 2\mu \geq 0$ and $\tilde{\sigma}(\mathbf{u}) = (\lambda\ \mathrm{div}\mathbf{u})E + 2\mu\varepsilon(\mathbf{u}), \varepsilon(\mathbf{u}) = \frac{1}{2}((\nabla\mathbf{u}) + (\nabla\mathbf{u})^T)$, with E the 3×3 unit matrix. We describe $\frac{\partial v_+}{\partial n}$ with the retarded Poincaré-Steklov operator $\mathcal{S}$ (see (2.16)), using it for (4.1f):

$$-\frac{\partial\gamma^-\mathbf{u}}{\partial t}n - \frac{\partial v_+}{\partial n} = \frac{\partial v_+^{inc}}{\partial n} \quad \Leftrightarrow \quad -\frac{\partial\gamma^-\mathbf{u}}{\partial t}n - \mathcal{S}v_+ = \frac{\partial v_+^{inc}}{\partial n}.$$

Next by setting $\phi = v_+ - v_-$, where v is extended into Ω^- by zero, we can write the retarded Poincaré-Steklov operator $\mathcal{S}$ as follows:

$$-\frac{\partial v_+}{\partial n} = -\mathcal{S}\phi = -W\phi - (K^T - \frac{1}{2}I)V^{-1}(K - \frac{1}{2}I)\phi \quad \Leftrightarrow \quad \begin{array}{c} -W\phi + (K^T - \frac{1}{2}I)\lambda = -\frac{\partial v_+}{\partial n} \\ (\frac{1}{2}I - K)\phi + V\lambda = 0 \end{array}$$

Altogether we get the following problem:

$$\rho_1\frac{\partial^2\mathbf{u}}{\partial t^2} - \Delta^*\mathbf{u} = 0 \quad (x,t) \in \Omega\times(0,\infty)\ , \tag{4.2a}$$

$$\mathbf{u}(x,0) = \dot{\mathbf{u}}(x,0) = 0 \quad \text{in } \Omega\ , \tag{4.2b}$$

$$\phi(x,t) = \dot{\phi}(x,t) = \lambda(x,t) = 0 \quad \text{on } \Gamma\times(-\infty,0]\ , \tag{4.2c}$$

$$\rho_2\tilde{\sigma}(\gamma^-\mathbf{u})\cdot n + \frac{\partial\phi}{\partial t}n = -\frac{\partial v_+^{inc}}{\partial t}n \quad \text{on } \Gamma\times(0,\infty)\ , \tag{4.2d}$$

$$\frac{1}{2}I\phi - K\phi + V\lambda = 0 \quad \text{on } \Gamma\times(0,\infty)\ , \tag{4.2e}$$

$$-\frac{\partial\gamma^-\mathbf{u}}{\partial t}n - W\phi + K^T\lambda - \frac{1}{2}\lambda = \frac{\partial v_+^{inc}}{\partial n} \quad \text{on } \Gamma\times(0,\infty)\ . \tag{4.2f}$$

Using Betti's formula with a test function $\mathbf{w}$ in $H^1_\sigma(\mathbb{R}^+, H^1(\Omega^\mp))^3$ for $\sigma > 0$:

$$\langle\tilde{\sigma}(\gamma^\mp\mathbf{u})\cdot n, \gamma^\mp\mathbf{w}\rangle_{\Gamma\times\mathbb{R}^+,\sigma} = \pm(\tilde{\sigma}(\mathbf{u}), \varepsilon(\mathbf{w}))_{\Omega^\mp\times\mathbb{R}^+,\sigma} \pm (\Delta^*\mathbf{u}, \mathbf{w})_{\Omega^\mp\times\mathbb{R}^+,\sigma}$$

yields for all $\dot{\mathbf{w}}$ in $H^1_\sigma(\mathbb{R}^+, H^1(\Omega^-))^3$

$$\begin{aligned}
&(\tilde{\sigma}(\mathbf{u}), \varepsilon(\dot{\mathbf{w}}))_{\Omega^-\times\mathbb{R}^+,\sigma} + (\ddot{\mathbf{u}}, \dot{\mathbf{w}})_{\Omega^-\times\mathbb{R}^+,\sigma} + \langle(\dot{\phi} + \dot{v}_+^{inc}), \gamma^-\dot{\mathbf{w}}\cdot n\rangle_{\Gamma\times\mathbb{R}^+,\sigma} \\
&= \langle\tilde{\sigma}(\gamma^-\mathbf{u})\cdot n, \gamma^-\dot{\mathbf{w}}\rangle_{\Gamma\times\mathbb{R}^+,\sigma} - (\Delta^*\mathbf{u}, \dot{\mathbf{w}})_{\Omega^-\times\mathbb{R}^+,\sigma} + (\ddot{\mathbf{u}}, \dot{\mathbf{w}})_{\Omega^-\times\mathbb{R}^+,\sigma} + \langle(\dot{\phi} + \dot{v}_+^{inc}), \gamma^-\dot{\mathbf{w}}\cdot n\rangle_{\Gamma\times\mathbb{R}^+,\sigma} \\
&= \langle\tilde{\sigma}(\gamma^-\mathbf{u})\cdot n, \gamma^-\dot{\mathbf{w}}\rangle_{\Gamma\times\mathbb{R}^+,\sigma} + \langle(\dot{\phi} + \dot{v}_+^{inc}), \gamma^-\dot{\mathbf{w}}\cdot n\rangle_{\Gamma\times\mathbb{R}^+,\sigma} \overset{(4.2d)}{=} 0.
\end{aligned}$$

We define:

$$a(\mathbf{u}, \dot{\mathbf{w}}) := (\tilde{\sigma}(\mathbf{u}), \varepsilon(\dot{\mathbf{w}}))_{\Omega^-\times\mathbb{R}^+,\sigma} + (\ddot{\mathbf{u}}, \dot{\mathbf{w}})_{\Omega^-\times\mathbb{R}^+,\sigma}\ .$$

Altogether we have:

$$a(\mathbf{u}, \dot{\mathbf{w}}) + \langle\dot{\phi}, \gamma^-\dot{\mathbf{w}}\cdot n\rangle_{\Gamma\times\mathbb{R}^+,\sigma} = -\langle\dot{v}_+^{inc}, \gamma^-\dot{\mathbf{w}}\cdot n\rangle_{\Gamma\times\mathbb{R}^+,\sigma}\ . \tag{4.3}$$

Now using another test function w in $H^1_\sigma(\mathbb{R}^+, H^{1/2}(\Gamma))$ we get with (4.2f):

$$-\langle\gamma^-\dot{\mathbf{u}}\cdot n, \dot{w}\rangle_{\Gamma\times\mathbb{R}^+,\sigma} - \langle W\phi, \dot{w}\rangle_{\Gamma\times\mathbb{R}^+,\sigma} + \langle(K^T - 1/2I)\lambda, \dot{w}\rangle_{\Gamma\times\mathbb{R}^+,\sigma} = \langle\partial_n^+ v^{inc}, \dot{w}\rangle_{\Gamma\times\mathbb{R}^+,\sigma}\ . \tag{4.4}$$

Using another test function m in $H^1_\sigma(\mathbb{R}^+, H^{-1/2}(\Gamma))$ we get with (4.2e)

$$\langle (1/2I - K)\phi, \dot{m}\rangle_{\Gamma\times\mathbb{R}^+,\sigma} + \langle V\lambda, \dot{m}\rangle_{\Gamma\times\mathbb{R}^+,\sigma} = 0 \ . \tag{4.5}$$

By adding (4.3), (4.4) and (4.5) we have the following variational formulation: Find $(\mathbf{u}, \phi, \lambda) \in X = H^1_\sigma(\mathbb{R}^+, H^1(\Omega))^3 \times H^1_\sigma(\mathbb{R}^+, H^{1/2}(\Gamma)) \times H^1_\sigma(\mathbb{R}^+, H^{-1/2}(\Gamma))$ such that

$$\begin{aligned} &a(\mathbf{u}, \dot{\mathbf{w}}) + \langle \dot{\phi}, \gamma^- \dot{\mathbf{w}} \cdot n\rangle_{\Gamma\times\mathbb{R}^+,\sigma} - \langle \gamma^- \dot{\mathbf{u}} \cdot n, \dot{w}\rangle_{\Gamma\times\mathbb{R}^+,\sigma} - \langle W\phi, \dot{w}\rangle_{\Gamma\times\mathbb{R}^+,\sigma} - \langle (\frac{1}{2}I - K^T)\lambda, \dot{w}\rangle_{\Gamma\times\mathbb{R}^+,\sigma} \\ &+ \langle (\frac{1}{2}I - K)\phi, \dot{m}\rangle_{\Gamma\times\mathbb{R}^+,\sigma} + \langle V\lambda, \dot{m}\rangle_{\Gamma\times\mathbb{R}^+,\sigma} = -\langle \dot{v}^{inc}_+ n, \gamma^- \dot{\mathbf{w}}\rangle_{\Gamma\times\mathbb{R}^+,\sigma} + \langle \partial^+_n v^{inc}, \dot{w}\rangle_{\Gamma\times\mathbb{R}^+,\sigma} \end{aligned} \tag{4.6}$$

hold for all $(\mathbf{w}, w, m)^T \in X$.

4.2 Preliminaries

Let $Z_{h,(\Delta t)} \subset H^1_\sigma(\mathbb{R}_+, H^1(\Omega))^3$, $Y_{h,(\Delta t)} \subset H^1_\sigma(\mathbb{R}_+, H^{1/2}(\Gamma))$, $X_{h,(\Delta t)} \subset H^1_\sigma(\mathbb{R}_+, H^{-1/2}(\Gamma))$ be the finite element spaces with the same properties as in Section 3.2. In order to state an a priori and a posteriori error estimate, we need a coercivity estimate first. The strategy is to derive an equivalent bilinearform, for which we prove the coercivity estimate with the help of an energy norm.

Proposition 4.1. *Let $(\mathbf{u}, \phi, \lambda) \in Z_{h,(\Delta t)} \times Y_{h,(\Delta t)} \times X_{h,(\Delta t)}$ satisfy*

$$a(\mathbf{u}, \mathbf{w}) + \langle \dot{\phi} + \dot{v}^{inc}_+, \gamma^- \mathbf{w} \cdot n\rangle_{\Gamma\times\mathbb{R}^+,\sigma} = 0 \quad \forall\ \mathbf{w} \in Z_{h,(\Delta t)} \ , \tag{4.7a}$$

$$-\langle \gamma^- \dot{\mathbf{u}} \cdot n, w\rangle_{\Gamma\times\mathbb{R}^+,\sigma} - \langle W\phi, w\rangle_{\Gamma\times\mathbb{R}^+,\sigma} + \langle (K^T - \frac{1}{2}I)\lambda, w\rangle_{\Gamma\times\mathbb{R}^+,\sigma} = \langle \partial^+_n v^{inc}, w\rangle_{\Gamma\times\mathbb{R}^+,\sigma} \ \forall w \in Y_{h,(\Delta t)}, \tag{4.7b}$$

$$\langle (\frac{1}{2}I - K)\phi, m\rangle_{\Gamma\times\mathbb{R}^+,\sigma} + \langle V\lambda, m\rangle_{\Gamma\times\mathbb{R}^+,\sigma} = 0 \quad \forall\ m \in X_{h,(\Delta t)} \ , \tag{4.7c}$$

with

$$v = D\phi - S\lambda \ , \tag{4.8}$$

where for $x \in \mathbb{R}^3\backslash\Gamma$ and $t \in \mathbb{R}_+$ (see also (2.4) and (2.5))

$$D\phi(x,t) := \frac{1}{4\pi} \int_\Gamma \frac{n_y \cdot (x-y)}{|x-y|} \left(\frac{\phi(y, t-|x-y|)}{|x-y|^2} + \frac{\dot{\phi}(y, t-|x-y|)}{|x-y|} \right) ds_y \ ,$$

and

$$S\lambda(x,t) := \frac{1}{4\pi} \int_\Gamma \frac{\lambda(y, t-|x-y|)}{|x-y|} ds_y \ .$$

Then $(\mathbf{u}, v) \in Z_{h,(\Delta t)} \times H^1_\sigma(\mathbb{R}_+, H^1(\mathbb{R}^3\backslash\Gamma))$ satisfies the following problem:

$$a(\mathbf{u}, \mathbf{w}) + \langle \frac{\partial [\![\gamma v]\!]}{\partial t} + \dot{v}^{inc}_+, \gamma^- \mathbf{w} \cdot n\rangle_{\Gamma\times\mathbb{R}^+,\sigma} = 0 \quad \forall \mathbf{w} \in Z_{h,(\Delta t)} \ , \tag{4.9a}$$

$$-\Delta v + \frac{\partial^2 v}{\partial t^2} = 0 \quad \text{in } \mathbb{R}^3\backslash\Gamma \ , \tag{4.9b}$$

$$[\![\gamma v]\!] \in Y_{h,(\Delta t)} \ , \tag{4.9c}$$

$$[\![\partial_n v]\!] \in X_{h,(\Delta t)} \ , \tag{4.9d}$$

$$-\langle \gamma^- \dot{\mathbf{u}} \cdot n, w\rangle_{\Gamma\times\mathbb{R}^+,\sigma} - \langle \partial_n^+ v, w\rangle_{\Gamma\times\mathbb{R}^+,\sigma} = \langle \frac{\partial v_+^{inc}}{\partial n}, w\rangle_{\Gamma\times\mathbb{R}^+,\sigma} \quad \forall w \in Y_{h,(\Delta t)} \ , \tag{4.9e}$$

$$\langle \gamma^- v, m\rangle_{\Gamma\times\mathbb{R}^+,\sigma} = 0 \quad \forall m \in X_{h,(\Delta t)} \ , \tag{4.9f}$$

where $[\![\gamma v]\!] = \gamma^+ v - \gamma^- v$ *and* $[\![\partial_n v]\!] = \partial_n^+ v - \partial_n^- v$.
Conversely, if $(\mathbf{u}, \phi, \lambda) = (\mathbf{u}, [\![\gamma v]\!], [\![\partial_n v]\!]) \in Z_{h,(\Delta t)} \times Y_{h,(\Delta t)} \times X_{h,(\Delta t)}$ *satisfies* (4.9) *then* (4.8) *and* (4.7) *hold.*

Proof. Let $(\mathbf{u}, \phi, \lambda) \in Z_{h,(\Delta t)} \times Y_{h,(\Delta t)} \times X_{h,(\Delta t)}$ fulfill (4.7) and (4.8). With $v = D\phi - S\lambda$ (4.9b) holds. Now going onto the boundary with the jump relations (Theorem 2.1):

$$\gamma^+ v = \gamma^+(D\phi) - \gamma^+(S\lambda) = (\frac{1}{2}I + K)\phi - V\lambda \ ,$$
$$\gamma^- v = \gamma^-(D\phi) - \gamma^-(S\lambda) = (-\frac{1}{2}I + K)\phi - V\lambda \ .$$

We get:

$$[\![\gamma v]\!] = \gamma^+ v - \gamma^- v = (K + \frac{1}{2}I)\phi - V\lambda - (K - \frac{1}{2}I)\phi + V\lambda = \phi \in Y_{h,(\Delta t)} \ . \tag{4.10}$$

So $[\![\gamma v]\!] \in Y_{h,(\Delta t)}$, i.e. (4.9c) hold. Now using it on (4.7a) yields (4.9a). Considering the normal derivative of v, we obtain with the jump relations:

$$\partial_n^+ v = \partial_n^+(D\phi) - \partial_n^+(S\lambda) = W\phi - K^T\lambda + \frac{1}{2}I\lambda \ ,$$
$$\partial_n^- v = \partial_n^-(D\phi) - \partial_n^-(S\lambda) = W\phi - K^T\lambda - \frac{1}{2}I\lambda \ .$$

We get:

$$[\![\partial_n v]\!] = \partial_n^+ v - \partial_n^- v = W\phi - K^T\lambda + \frac{1}{2}I\lambda - W\phi + K^T\lambda + \frac{1}{2}I\lambda = \lambda \in X_{h,(\Delta t)} \ . \tag{4.11}$$

So $[\![\partial_n v]\!] \in X_{h,(\Delta t)}$, i.e. (4.9d) holds. From (4.7b) with

$$-\partial_n^+ v = -W\phi + K^T\lambda - \frac{1}{2}I\lambda \ ,$$

(4.9e) holds. With (4.7c) and

$$-\gamma^- v = (\frac{1}{2}I - K)\phi + V\lambda \ ,$$

(4.9f) hold. Altogether (4.9) holds.

Now let us define $(\mathbf{u}, \phi, \lambda) := (\mathbf{u}, [\![\gamma v]\!], [\![\partial_n v]\!]) \in Z_{h,(\Delta t)} \times Y_{h,(\Delta t)} \times X_{h,(\Delta t)}$, where $\mathbf{u}$ and v fulfill (4.9). Since v satisfies the wave equation (4.9b), we get (4.8) by making use of the representation formula:

$$v = D[\![\gamma v]\!] - S[\![\partial_n v]\!] = D\phi - S\lambda \ .$$

Since (4.9e) holds, using the jump relation on $\partial_n^+ v$ yields (4.7b). Analogously since (4.9f) holds, using the jump relation on $\gamma^- v$ yields (4.7c). We get (4.7a) by using ϕ in the equation (4.9a). □

Proposition 4.2. *Let* $\widetilde{Z}_{h,(\Delta t)} = \{v \in H^1_\sigma(\mathbb{R}_+, H^1(\mathbb{R}^3 \backslash \Gamma)) : [\![\gamma v]\!] \in Y_{h,(\Delta t)}, \langle \gamma^- v, m \rangle_{\Gamma \times \mathbb{R}^+,\sigma} = 0 \ \forall m \in X_{h,(\Delta t)}\}$. *Problem* (4.9) *is equivalent to:*
Find $(\mathbf{u}, v) \in Z_{h,(\Delta t)} \times \widetilde{Z}_{h,(\Delta t)}$ *such that*

$$\mathcal{A}((\mathbf{u}, v), (\mathbf{w}, w)) = f((\mathbf{w}, w)) \quad \forall (\mathbf{w}, w) \in Z_{h,(\Delta t)} \times \widetilde{Z}_{h,(\Delta t)} \ . \tag{4.12}$$

Here

$$\begin{aligned}\mathcal{A}((\mathbf{u}, v), (\mathbf{w}, w)) &:= (\tilde{\sigma}(\mathbf{u}), \varepsilon(\mathbf{w}))_{\Omega^- \times \mathbb{R}^+,\sigma} + (\ddot{\mathbf{u}}, \mathbf{w})_{\Omega^- \times \mathbb{R}^+,\sigma} + (\nabla v, \nabla w)_{\mathbb{R}^3 \backslash \Gamma \times \mathbb{R}^+,\sigma} \\ &+ (\ddot{v}, w)_{\mathbb{R}^3 \backslash \Gamma \times \mathbb{R}^+,\sigma} - \langle \gamma^- \dot{\mathbf{u}} \cdot n, [\![\gamma w]\!] \rangle_{\Gamma \times \mathbb{R}^+,\sigma} + \langle \frac{\partial [\![\gamma v]\!]}{\partial t}, \gamma^- \mathbf{w} \cdot n \rangle_{\Gamma \times \mathbb{R}^+,\sigma}\end{aligned}$$

and

$$f((\mathbf{w}, w)) := -\langle \dot{v}_+^{inc}, \gamma^- \mathbf{w} \cdot n \rangle_{\Gamma \times \mathbb{R}^+,\sigma} + \langle \frac{\partial v_+^{inc}}{\partial n}, [\![\gamma w]\!] \rangle_{\Gamma \times \mathbb{R}^+,\sigma} \ .$$

Proof. First, (4.9) holds with $(\mathbf{u}, \phi, \lambda) \in Z_{h,(\Delta t)} \times Y_{h,(\Delta t)} \times X_{h,(\Delta t)}$. Since (4.9c) and (4.9f) hold, we know that $(\mathbf{u}, v) \in Z_{h,(\Delta t)} \times \widetilde{Z}_{h,(\Delta t)}$. Now for all $w \in \widetilde{Z}_{h,(\Delta t)}$ using (4.9d) with $\langle [\![\partial_n v]\!], \gamma^- w \rangle_{\Gamma \times \mathbb{R}^+} = 0$, Green's formula and (4.9b) lead to

$$\begin{aligned}-\langle \partial_n^+ v, [\![\gamma w]\!] \rangle_{\Gamma \times \mathbb{R}^+,\sigma} &= -\langle \partial_n^+ v, \gamma^+ w - \gamma^- w \rangle_{\Gamma \times \mathbb{R}^+,\sigma} = \langle \partial_n^+ v, \gamma^- w \rangle_{\Gamma \times \mathbb{R}^+,\sigma} - \langle \partial_n^+ v, \gamma^+ w \rangle_{\Gamma \times \mathbb{R}^+,\sigma} \\ &= \langle \partial_n^+ v + \partial_n^- v - \partial_n^- v, \gamma^- w \rangle_{\Gamma \times \mathbb{R}^+,\sigma} - \langle \partial_n^+ v, \gamma^+ w \rangle_{\Gamma \times \mathbb{R}^+,\sigma} \\ &= \langle \partial_n^- v, \gamma^- w \rangle_{\Gamma \times \mathbb{R}^+,\sigma} - \langle \partial_n^+ v, \gamma^+ w \rangle_{\Gamma \times \mathbb{R}^+,\sigma} + \langle [\![\partial_n v]\!], \gamma^- w \rangle_{\Gamma \times \mathbb{R}^+,\sigma} \\ &= \langle \partial_n^- v, \gamma^- w \rangle_{\Gamma \times \mathbb{R}^+,\sigma} - \langle \partial_n^+ v, \gamma^+ w \rangle_{\Gamma \times \mathbb{R}^+,\sigma} \\ &= (\nabla v, \nabla w)_{\Omega^- \times \mathbb{R}^+} + (\Delta v, w)_{\Omega^- \times \mathbb{R}^+} + (\nabla v, \nabla w)_{\Omega^+ \times \mathbb{R}^+,\sigma} + (\Delta v, w)_{\Omega^+ \times \mathbb{R}^+,\sigma} \\ &= (\nabla v, \nabla w)_{\mathbb{R}^3 \backslash \Gamma \times \mathbb{R}^+,\sigma} + (\frac{\partial^2 v}{\partial t^2}, w)_{\mathbb{R}^3 \times \mathbb{R}^+,\sigma} \ .\end{aligned}$$

Therefore testing (4.9e) with $[\![\gamma w]\!]$ for $w \in \widetilde{Z}_{h,(\Delta t)}$,

$$-\langle \gamma^- \frac{\partial \mathbf{u}}{\partial t} \cdot n + \partial_n^+ v + \frac{\partial v_+^{inc}}{\partial n}, [\![\gamma w]\!] \rangle_{\Gamma \times \mathbb{R}^+,\sigma} = 0 \ ,$$

we get for all $w \in \widetilde{Z}_{h,(\Delta t)}$

$$-\langle \gamma^- \frac{\partial \mathbf{u}}{\partial t} \cdot n, [\![\gamma w]\!] \rangle_{\Gamma \times \mathbb{R}^+,\sigma} + (\nabla v, \nabla w)_{\mathbb{R}^3 \backslash \Gamma \times \mathbb{R}^+,\sigma} + (\frac{\partial^2 v}{\partial t^2}, w)_{\mathbb{R}^3 \times \mathbb{R}^+,\sigma} = \langle \partial_n^+ v^{inc}, [\![\gamma w]\!] \rangle_{\Gamma \times \mathbb{R}^+,\sigma}. \tag{4.13}$$

With (4.9a) we have

$$a(\mathbf{u}, \mathbf{w}) + \langle (\frac{\partial [\![\gamma v]\!]}{\partial t}), \gamma^- \mathbf{w} \cdot n \rangle_{\Gamma \times \mathbb{R}^+,\sigma} = -\langle \dot{v}_+^{inc}, \gamma^- \mathbf{w} \cdot n \rangle_{\Gamma \times \mathbb{R}^+,\sigma}. \tag{4.14}$$

Now adding together (4.13) and (4.14) yields $\mathcal{A}((\mathbf{u}, v), (\mathbf{w}, w)) = f((\mathbf{w}, w))$.

Conversely, let $\mathcal{A}((\mathbf{u},v),(\mathbf{w},w)) = f((\mathbf{w},w))$ hold. (4.13) still holds. Testing with a function $w \in \widetilde{Z}_{h,(\Delta t)}$, with compact support in $\mathbb{R}^3\backslash\Gamma$, yields

$$(\frac{\partial^2 v}{\partial t^2}, w)_{\mathbb{R}^3\times\mathbb{R}^+,\sigma} + (\nabla v, \nabla w)_{\mathbb{R}^3\backslash\Gamma\times\mathbb{R}^+,\sigma} - \langle\gamma\dot{\mathbf{u}}\cdot n, [\![\gamma w]\!]\rangle_{\Gamma\times\mathbb{R}^+,\sigma} = \langle\partial_n^+ v^{inc}, [\![\gamma w]\!]\rangle_{\Gamma\times\mathbb{R}^+,\sigma}.$$

With Green's formula:

$$\begin{aligned}(\frac{\partial^2 v}{\partial t^2}, w)_{\mathbb{R}^3\times\mathbb{R}^+,\sigma} + (\partial_n^- v, \gamma^- w)_{\Gamma\times\mathbb{R}^+,\sigma} - (\Delta v, w)_{\Omega^-\times\mathbb{R}^+,\sigma} - (\Delta v, w)_{\Omega^+\times\mathbb{R}^+,\sigma} \\ - \langle\partial_n^+ v, \gamma^+ w\rangle_{\Gamma\times\mathbb{R}^+,\sigma} - \langle\gamma^-\dot{\mathbf{u}}\cdot n, [\![\gamma w]\!]\rangle_{\Gamma\times\mathbb{R}^+,\sigma} = \langle\partial_n^+ v^{inc}, [\![\gamma w]\!]\rangle_{\Gamma\times\mathbb{R}^+,\sigma}.\end{aligned}$$

Since w has a compact support in $\mathbb{R}^3\backslash\Gamma$, we see that

$$(\frac{\partial^2 v}{\partial t^2}, w)_{\mathbb{R}^3\backslash\Gamma\times\mathbb{R}^+,\sigma} - (\Delta v, w)_{\mathbb{R}^3\backslash\Gamma\times\mathbb{R}^+,\sigma} = 0\ .$$

Therefore

$$(-\Delta v + \frac{\partial^2 v}{\partial t^2}, w)_{\mathbb{R}^3\backslash\Gamma\times\mathbb{R}^+,\sigma} = 0\ .$$

and hence

$$-\Delta v + \frac{\partial^2 v}{\partial t^2} = 0 \quad \text{in } \mathbb{R}^3\backslash\Gamma.$$

So we get (4.9b). Next

$$\langle\partial_n^- v, \gamma^- w\rangle_{\Gamma\times\mathbb{R}^+,\sigma} - \langle\partial_n^+ v, \gamma^+ w\rangle_{\Gamma\times\mathbb{R}^+,\sigma} - \langle\gamma^-\dot{\mathbf{u}}\cdot n, [\![\gamma w]\!]\rangle_{\Gamma\times\mathbb{R}^+,\sigma} = \langle\partial_n^+ v^{inc}, [\![\gamma w]\!]\rangle_{\Gamma\times\mathbb{R}^+,\sigma}\ .$$

Adding zero:

$$\begin{aligned}&\langle\partial_n^- v,\gamma^- w\rangle_{\Gamma\times\mathbb{R}^+,\sigma} - \langle\partial_n^+ v,\gamma^- w\rangle_{\Gamma\times\mathbb{R}^+,\sigma} + \langle\partial_n^+ v,\gamma^- w\rangle_{\Gamma\times\mathbb{R}^+,\sigma} - \langle\partial_n^+ v,\gamma^+ w\rangle_{\Gamma\times\mathbb{R}^+,\sigma} - \langle\gamma^-\dot{\mathbf{u}}\cdot n,[\![\gamma w]\!]\rangle_{\Gamma\times\mathbb{R}^+,\sigma} \\ &= \langle\partial_n^+ v^{inc}, [\![\gamma w]\!]\rangle_{\Gamma\times\mathbb{R}^+,\sigma}\end{aligned}$$

with

$$\langle\partial_n^- v - \partial_n^+ v, \gamma^- w\rangle_{\Gamma\times\mathbb{R}^+,\sigma} = -\langle[\![\partial_n v]\!], \gamma^- w\rangle_{\Gamma\times\mathbb{R}^+,\sigma}, \langle\partial_n^+ v, \gamma^- w - \gamma^+ w\rangle_{\Gamma\times\mathbb{R}^+,\sigma} = -\langle\partial_n^+ v, [\![\gamma w]\!]\rangle_{\Gamma\times\mathbb{R}^+,\sigma}$$

there holds

$$-\langle\partial_n^+ v, [\![\gamma w]\!]\rangle_{\Gamma\times\mathbb{R}^+,\sigma} - \langle[\![\partial_n v]\!], \gamma^- w\rangle_{\Gamma\times\mathbb{R}^+,\sigma} - \langle\gamma^-\dot{\mathbf{u}}\cdot n, [\![\gamma w]\!]\rangle_{\Gamma\times\mathbb{R}^+,\sigma} = \langle\partial_n^+ v^{inc}, [\![\gamma w]\!]\rangle_{\Gamma\times\mathbb{R}^+,\sigma}\ .$$

We get

$$-\langle\partial_n^+ v + \gamma^-\dot{\mathbf{u}}\cdot n + \frac{\partial v_+^{inc}}{\partial n}, [\![\gamma w]\!]\rangle_{\Gamma\times\mathbb{R}^+,\sigma} - \langle[\![\partial_n v]\!], \gamma^- w\rangle_{\Gamma\times\mathbb{R}^+,\sigma} = 0\ . \tag{4.15}$$

The equation (4.15) holds for all $w \in \widetilde{Z}_{h,(\Delta t)}$. We first choose $[\![\gamma w]\!] = 0$. In this case we get

$$\langle[\![\partial_n v]\!], \gamma^- w\rangle_{\Gamma\times\mathbb{R}^+,\sigma} = 0.$$

Therefore since $\gamma^- w$ lies in the orthogonal space of $X_{h,(\Delta t)}$, we get $[\![\partial_n v]\!] \in X_{h,(\Delta t)}$, i.e. (4.9d). Second, choose $w \in \widetilde{Z}_{h,(\Delta t)}$ such that $\gamma^- w = 0$. Yielding from $[\![\gamma w]\!] \in Y_{h,(\Delta t)}$ and (4.15):

$$-\langle\partial_n^+ v + \gamma^-\dot{\mathbf{u}}\cdot n + \frac{\partial v_+^{inc}}{\partial n}, [\![\gamma w]\!]\rangle_{\Gamma\times\mathbb{R}^+,\sigma} = 0\ .$$

Hence we conclude (4.9e). From the definition of $\widetilde{Z}_{h,(\Delta t)}$ we already get (4.9f) and (4.9c). By (4.14)

$$a(\mathbf{u},\mathbf{w}) + \langle \frac{\partial [\![\gamma v]\!]}{\partial t}, \gamma^- \mathbf{w}\cdot n\rangle_{\Gamma\times\mathbb{R}^+,\sigma} = -\langle \dot{v}_+^{inc}, \gamma^- \mathbf{w}\cdot n\rangle_{\Gamma\times\mathbb{R}^+,\sigma} \ ,$$

which contains the remaining 3 terms of (4.12), we deduce (4.9a). □

Propositions 4.1 and 4.2 hold analogously as well, if we take instead of the finite element spaces the whole space X.

Now we define the energy norm:

$$|\!|\!|(\mathbf{u},v)|\!|\!|^2 = (\tilde{\sigma}(\mathbf{u}),\varepsilon(\mathbf{u}))_{\Omega_-\times\mathbb{R}^+,\sigma} + (\dot{\mathbf{u}},\dot{\mathbf{u}})_{\Omega_-\times\mathbb{R}^+,\sigma} + (\nabla v,\nabla v)_{\mathbb{R}^3\setminus\Gamma\times\mathbb{R}^+,\sigma} + (\dot{v},\dot{v})_{\mathbb{R}^3\setminus\Gamma\times\mathbb{R}^+,\sigma} \ .$$

Therefore we get:

$$\begin{aligned}
&\mathcal{A}((\mathbf{u},v),(\dot{\mathbf{u}},\dot{v})) = (\tilde{\sigma}(\mathbf{u}),\varepsilon(\dot{\mathbf{u}}))_{\Omega^-\times\mathbb{R}^+,\sigma} + (\ddot{\mathbf{u}},\dot{\mathbf{u}})_{\Omega^-\times\mathbb{R}^+,\sigma} + (\nabla v,\nabla\dot{v})_{\mathbb{R}^3\setminus\Gamma\times\mathbb{R}^+,\sigma}\\
&+ (\ddot{v},\dot{v})_{\mathbb{R}^3\setminus\Gamma\times\mathbb{R}^+,\sigma} - \langle\gamma^-\dot{\mathbf{u}}\cdot n, [\![\gamma\dot{v}]\!]\rangle_{\Gamma\times\mathbb{R}^+,\sigma} + \langle\frac{\partial[\![\gamma v]\!]}{\partial t},\gamma^-\dot{\mathbf{u}}\cdot n\rangle_{\Gamma\times\mathbb{R}^+,\sigma}\\
&= (\tilde{\sigma}(\mathbf{u}),\varepsilon(\dot{\mathbf{u}}))_{\Omega^-\times\mathbb{R}^+,\sigma} + (\ddot{\mathbf{u}},\dot{\mathbf{u}})_{\Omega^-\times\mathbb{R}^+,\sigma} + (\nabla v,\nabla\dot{v})_{\mathbb{R}^3\setminus\Gamma\times\mathbb{R}^+,\sigma} + (\ddot{v},\dot{v})_{\mathbb{R}^3\setminus\Gamma\times\mathbb{R}^+,\sigma}\\
&= \int_0^\infty\int_{\Omega^-}\tilde{\sigma}(\mathbf{u}):\varepsilon(\dot{\mathbf{u}})dx e^{-2\sigma t}dt + \int_0^\infty\int_{\Omega^-}\ddot{\mathbf{u}}\dot{\mathbf{u}}dx e^{-2\sigma t}dt\\
&+ \int_0^\infty\int_{\mathbb{R}^3\setminus\Gamma}\nabla v\nabla\dot{v}dx e^{-2\sigma t}dt + \int_0^\infty\int_{\mathbb{R}^3\setminus\Gamma}\ddot{v}\dot{v}dx e^{-2\sigma t}dt\\
&= \int_0^\infty\frac{1}{2}\partial_t\Big(\int_{\Omega^-}\tilde{\sigma}(\mathbf{u}):\varepsilon(\mathbf{u})dx\Big)e^{-2\sigma t}dt + \int_0^\infty\frac{1}{2}\partial_t\Big(\int_{\Omega^-}\dot{\mathbf{u}}\dot{\mathbf{u}}dx\Big)e^{-2\sigma t}dt\\
&+ \int_0^\infty\frac{1}{2}\partial_t\Big(\int_{\mathbb{R}^3\setminus\Gamma}\nabla v\nabla v dx\Big)e^{-2\sigma t}dt + \int_0^\infty\frac{1}{2}\partial_t\Big(\int_{\mathbb{R}^3\setminus\Gamma}\dot{v}\dot{v}dx\Big)e^{-2\sigma t}dt \ .
\end{aligned}$$

With integration by parts in time and using the conditions that $\mathbf{u}$ and v at time 0 are zero and that with $t\to\infty$, $e^{-2\sigma t}$ tends to zero, we get:

$$\begin{aligned}
&\mathcal{A}((\mathbf{u},v),(\dot{\mathbf{u}},\dot{v})) = \frac{-1}{2}\int_0^\infty\Big(\int_{\Omega^-}\tilde{\sigma}(\mathbf{u}):\varepsilon(\mathbf{u})dx\Big)\partial_t(e^{-2\sigma t})dt - \frac{1}{2}\int_0^\infty\Big(\int_{\Omega^-}\dot{\mathbf{u}}\dot{\mathbf{u}}dx\Big)\partial_t(e^{-2\sigma t})dt\\
&- \frac{1}{2}\int_0^\infty\Big(\int_{\mathbb{R}^3\setminus\Gamma}\nabla v\nabla v dx\Big)\partial_t(e^{-2\sigma t})dt - \frac{1}{2}\int_0^\infty\Big(\int_{\mathbb{R}^3\setminus\Gamma}\dot{v}\dot{v}dx\Big)\partial_t(e^{-2\sigma t})dt\\
&= \sigma\Big(\int_0^\infty\Big(\int_{\Omega^-}\tilde{\sigma}(\mathbf{u}):\varepsilon(\mathbf{u})dx\Big)e^{-2\sigma t}dt + \int_0^\infty\Big(\int_{\Omega^-}\dot{\mathbf{u}}\dot{\mathbf{u}}dx\Big)e^{-2\sigma t}dt\\
&+ \int_0^\infty\Big(\int_{\mathbb{R}^3\setminus\Gamma}\nabla v\nabla v dx\Big)e^{-2\sigma t}dt + \int_0^\infty\Big(\int_{\mathbb{R}^3\setminus\Gamma}\dot{v}\dot{v}dx\Big)e^{-2\sigma t}dt\Big)\\
&= \sigma|\!|\!|(\mathbf{u},v)|\!|\!|^2 \gtrsim \|\mathbf{u}\|^2_{0,1,\Omega^-} + \|v\|^2_{0,1,\Omega^+} \ .
\end{aligned}$$

Hence we derived a coercivity estimate.

4.3 A priori error estimate

We state an a priori error estimate:

Theorem 4.1. *Let* $(\mathbf{u},\phi,\lambda)\in X$ *satisfy* (4.6) *and* $(\mathbf{u}_h,\phi_h,\lambda_h)\in Z_{h,\Delta t}\times Y_{h,\Delta t}\times X_{h,\Delta t}$ *satisfy* (4.7) *and* (4.8). *Then*

$$\|\mathbf{u}-\mathbf{u}_h\|^2_{0,1,\Omega}+\|\phi-\phi_h\|^2_{0,1/2,\Gamma,*}+\|\lambda-\lambda_h\|^2_{0,-1/2,\Gamma,*}\lesssim_\sigma \inf_{\substack{(\mathbf{w}_h,\psi_h,\mu_h)\in\\ Z_{h,\Delta t}\times Y_{h,\Delta t}\times X_{h,\Delta t}}} (1+\frac{1}{(\Delta t)^2})\|\mathbf{u}-\mathbf{w}_h\|^2_{1,1,\Omega}+(1+\frac{1}{(\Delta t)^2})\|\phi-\psi_h\|^2_{1,1/2,\Gamma,*}+(1+\frac{1}{(\Delta t)^2})\|\lambda-\mu_h\|^2_{1,-1/2,\Gamma,*}.$$

Proof. Let $(\mathbf{u},\phi,\lambda)\in X$ satisfy (4.6) and $(\mathbf{u}_h,\phi_h,\lambda_h)\in Z_{h,\Delta t}\times Y_{h,\Delta t}\times X_{h,\Delta t}$ satisfy (4.7) and (4.8), then with $(\tilde{\mathbf{w}},\tilde\phi,\tilde\lambda)\in Z_{h,\Delta t}\times Y_{h,\Delta t}\times X_{h,\Delta t}$:

$$\begin{aligned}
&\|\mathbf{u}-\mathbf{u}_h\|^2_{0,1,\Omega}+\|\phi-\phi_h\|^2_{0,1/2,\Gamma,*}+\|\lambda-\lambda_h\|^2_{0,-1/2,\Gamma,*}\\
&\lesssim \|\mathbf{u}-\tilde{\mathbf{w}}\|^2_{0,1,\Omega}+\|\tilde{\mathbf{w}}-\mathbf{u}_h\|^2_{0,1,\Omega}+\|\phi-\tilde\phi\|^2_{0,1/2,\Gamma,*}+\|\tilde\phi-\phi_h\|^2_{0,1/2,\Gamma,*}\\
&+\|\lambda-\tilde\lambda\|^2_{0,-1/2,\Gamma,*}+\|\tilde\lambda-\lambda_h\|^2_{0,-1/2,\Gamma,*}\ .
\end{aligned}$$

So we focus on estimates for $\|\tilde{\mathbf{w}}-\mathbf{u}_h\|^2_{0,1,\Omega}+\|\tilde\phi-\phi_h\|^2_{0,1/2,\Gamma,*}+\|\tilde\lambda-\lambda_h\|^2_{0,-1/2,\Gamma,*}$. We know the following properties from the Proposition 4.1: v, v_h satisfy the wave equation with $v=D\phi-S\lambda$, $v_h=D\phi_h-S\lambda_h$. $\tilde r:=D\tilde\phi-S\tilde\lambda$ satisfies also the wave equation. Further $[\![\gamma v_h]\!]$, $[\![\gamma\tilde r]\!]\in Y_{h,\Delta t}$, $[\![\partial_n v_h]\!]$, $[\![\partial_n\tilde r]\!]\in X_{h,\Delta t}$ and $\langle\gamma^- v_h,m\rangle_{\Gamma\times\mathbb{R}^+,\sigma}=0$, $\langle\gamma^-\tilde r,m\rangle_{\Gamma\times\mathbb{R}^+,\sigma}=0$. Now using the trace theorem and estimating with the energy norm, we get with the Galerkin orthogonality and Green's formula:

$$\begin{aligned}
&\|\tilde{\mathbf{w}}-\mathbf{u}_h\|^2_{0,1,\Omega}+\|\tilde\phi-\phi_h\|^2_{0,1/2,\Gamma,*}+\|\tilde\lambda-\lambda_h\|^2_{0,-1/2,\Gamma,*}\lesssim\|\tilde{\mathbf{w}}-\mathbf{u}_h\|^2_{0,1,\Omega}+\|\tilde r-v_h\|^2_{0,1,\mathbb{R}^3\setminus\Gamma}\\
&\lesssim\sigma|\!|\!|(\tilde{\mathbf{w}}-\mathbf{u}_h,\tilde r-v_h)|\!|\!|^2=\mathcal{A}\Big(\begin{pmatrix}\tilde{\mathbf{w}}-\mathbf{u}_h\\ \tilde r-v_h\end{pmatrix}^{\mathrm T},\begin{pmatrix}\partial_t(\tilde{\mathbf{w}}-\mathbf{u}_h)\\ \partial_t(\tilde r-v_h)\end{pmatrix}^{\mathrm T}\Big)\\
&=\mathcal{A}\Big(\begin{pmatrix}\tilde{\mathbf{w}}-\mathbf{u}\\ \tilde r-v\end{pmatrix}^{\mathrm T},\begin{pmatrix}\partial_t(\tilde{\mathbf{w}}-\mathbf{u}_h)\\ \partial_t(\tilde r-v_h)\end{pmatrix}^{\mathrm T}\Big)+\mathcal{A}\Big(\begin{pmatrix}\mathbf{u}-\mathbf{u}_h\\ v-v_h\end{pmatrix}^{\mathrm T},\begin{pmatrix}\partial_t(\tilde{\mathbf{w}}-\mathbf{u}_h)\\ \partial_t(\tilde r-v_h)\end{pmatrix}^{\mathrm T}\Big)\\
&=\mathcal{A}\Big(\begin{pmatrix}\tilde{\mathbf{w}}-\mathbf{u}\\ \tilde r-v\end{pmatrix}^{\mathrm T},\begin{pmatrix}\partial_t(\tilde{\mathbf{w}}-\mathbf{u}_h)\\ \partial_t(\tilde r-v_h)\end{pmatrix}^{\mathrm T}\Big)\\
&=\int_0^\infty e^{-2\sigma t}\Big\{\int_\Omega\tilde\sigma(\tilde{\mathbf{w}}-\mathbf{u}):\varepsilon(\partial_t(\tilde{\mathbf{w}}-\mathbf{u}_h))dx+\int_\Omega\partial_t^2(\tilde{\mathbf{w}}-\mathbf{u})\partial_t(\tilde{\mathbf{w}}-\mathbf{u}_h)dx\\
&+\int_{\mathbb{R}^3\setminus\Gamma}\nabla(\tilde r-v)\nabla(\partial_t(\tilde r-v_h))dx+\int_{\mathbb{R}^3\setminus\Gamma}\partial_t^2(\tilde r-v)\partial_t(\tilde r-v_h)dx\\
&-\int_\Gamma\gamma^-(\partial_t(\tilde{\mathbf{w}}-\mathbf{u}))\cdot n[\![\gamma(\partial_t(\tilde r-v_h))]\!]ds_x+\int_\Gamma[\![\gamma(\partial_t(\tilde r-v))]\!]\gamma^-(\partial_t(\tilde{\mathbf{w}}-\mathbf{u}_h))\cdot nds_x\Big\}dt\\
&=\int_0^\infty e^{-2\sigma t}\Big\{\int_\Omega\tilde\sigma(\tilde{\mathbf{w}}-\mathbf{u}):\varepsilon(\partial_t(\tilde{\mathbf{w}}-\mathbf{u}_h))dx+\int_\Omega\partial_t^2(\tilde{\mathbf{w}}-\mathbf{u})\partial_t(\tilde{\mathbf{w}}-\mathbf{u}_h)dx\\
&+\int_\Gamma\partial_n^+(\tilde r-v)[\![\gamma(\partial_t(\tilde r-v_h))]\!]ds_x-\int_\Gamma\gamma^-(\partial_t(\tilde{\mathbf{w}}-\mathbf{u}))\cdot n[\![\gamma(\partial_t(\tilde r-v_h))]\!]ds_x\\
&+\int_\Gamma[\![\gamma(\partial_t(\tilde r-v))]\!]\gamma^-(\partial_t(\tilde{\mathbf{w}}-\mathbf{u}_h))\cdot nds_x\Big\}dt\ .
\end{aligned}$$

Now using the jump relation on $\partial_n^+(\tilde{r}-v) = W(\tilde{\phi}-\phi) - (K^T - \frac{1}{2}I)(\tilde{\lambda}-\lambda)$, (4.10) and (4.7c), we obtain

$$
\begin{aligned}
&= \int_0^\infty e^{-2\sigma t}\Big\{ \int_\Omega \tilde{\sigma}(\tilde{\mathbf{w}}-\mathbf{u}) : \varepsilon(\partial_t(\tilde{\mathbf{w}}-\mathbf{u}_h))dx + \int_\Omega \partial_t^2(\tilde{\mathbf{w}}-\mathbf{u})\partial_t(\tilde{\mathbf{w}}-\mathbf{u}_h)dx \\
&+ \int_\Gamma (W(\tilde{\phi}-\phi) - (K^T - \frac{1}{2}I)(\tilde{\lambda}-\lambda))(\partial_t(\tilde{\phi}-\phi_h))ds_x \\
&+ \int_\Gamma ((\frac{1}{2}I - K)(\tilde{\phi}-\phi) + V(\tilde{\lambda}-\lambda))(\partial_t(\tilde{\lambda}-\lambda_h))ds_x \\
&- \int_\Gamma \gamma^-(\partial_t(\tilde{\mathbf{w}}-\mathbf{u}))\cdot n(\partial_t(\tilde{\phi}-\phi_h))ds_x + \int_\Gamma (\partial_t(\tilde{\phi}-\phi))\gamma^-(\partial_t(\tilde{\mathbf{w}}-\mathbf{u}_h))\cdot n ds_x \Big\} dt \ .
\end{aligned}
$$

We estimate every term separately. The first two terms can be estimated as in the proof of the a priori error estimator in Section 3.3. We obtain with a small $\epsilon > 0$

$$
\begin{aligned}
&\int_0^\infty e^{-2\sigma t}\Big\{ \int_\Omega \tilde{\sigma}(\tilde{\mathbf{w}}-\mathbf{u}) : \varepsilon(\partial_t(\tilde{\mathbf{w}}-\mathbf{u}_h))dx + \int_\Omega \partial_t^2(\tilde{\mathbf{w}}-\mathbf{u})\partial_t(\tilde{\mathbf{w}}-\mathbf{u}_h)dx\Big\}dt \\
&\lesssim_\sigma \tfrac{1}{\epsilon(\Delta t)^2}\|\tilde{\mathbf{w}}-\mathbf{u}\|_{0,1,\Omega}^2 + \epsilon\|\tilde{\mathbf{w}}-\mathbf{u}\|_{0,1,\Omega}^2 \ .
\end{aligned}
$$

We are able to combine $\epsilon\|\tilde{\mathbf{w}}-\mathbf{u}\|_{0,1,\Omega}^2$ with the left hand side. Next we estimate

$$
\begin{aligned}
&\int_0^\infty e^{-2\sigma t}\int_\Gamma (W(\tilde{\phi}-\phi) - (K^T - \frac{1}{2}I)(\tilde{\lambda}-\lambda))(\partial_t(\tilde{\phi}-\phi_h))ds_x dt \\
&\lesssim_\sigma \|(W(\tilde{\phi}-\phi) - (K^T - \frac{1}{2}I)(\tilde{\lambda}-\lambda))\|_{0,-1/2,\Gamma}\|(\partial_t(\tilde{\phi}-\phi_h))\|_{0,1/2,\Gamma,*} \\
&\lesssim (\|W(\tilde{\phi}-\phi)\|_{0,-1/2,\Gamma} + \|(K^T - \frac{1}{2}I)(\tilde{\lambda}-\lambda)\|_{0,-1/2,\Gamma})\|\tilde{\phi}-\phi_h\|_{1,1/2,\Gamma,*} \ .
\end{aligned}
$$

Using the following inverse estimate as in (3.182) in [53] for $\tilde{\phi}$ in the finite element spaces:

$$
\|\tilde{\phi}\|_{1,1/2,\Gamma,*} \lesssim \frac{1}{\Delta t}\|\tilde{\phi}\|_{0,1/2,\Gamma,*} \ .
$$

yields

$$
\begin{aligned}
&\int_0^\infty e^{-2\sigma t}\int_\Gamma (W(\tilde{\phi}-\phi) - (K^T - \frac{1}{2}I)(\tilde{\lambda}-\lambda))(\partial_t(\tilde{\phi}-\phi_h))ds_x dt \\
&\lesssim_\sigma (\|W(\tilde{\phi}-\phi)\|_{0,-1/2,\Gamma} + \|(K^T - \frac{1}{2}I)(\tilde{\lambda}-\lambda)\|_{0,-1/2,\Gamma})\frac{1}{\Delta t}\|\tilde{\phi}-\phi_h\|_{0,1/2,\Gamma,*} \ .
\end{aligned}
$$

Now using mapping properties (see Theorem 2.2) with Young's inequality, we see

$$
\begin{aligned}
&\int_0^\infty e^{-2\sigma t}\int_\Gamma (W(\tilde{\phi}-\phi) - (K^T - \frac{1}{2}I)(\tilde{\lambda}-\lambda))(\partial_t(\tilde{\phi}-\phi_h))ds_x dt \\
&\lesssim_\sigma \frac{1}{\Delta t}\|\tilde{\phi}-\phi\|_{1,1/2,\Gamma,*}\|\tilde{\phi}-\phi_h\|_{0,1/2,\Gamma,*} + \frac{1}{\Delta t}\|\tilde{\lambda}-\lambda\|_{1,-1/2,\Gamma,*}\|\tilde{\phi}-\phi_h\|_{0,1/2,\Gamma,*} \\
&\lesssim \tfrac{1}{\epsilon(\Delta t)^2}\|\tilde{\phi}-\phi\|_{0,1/2,\Gamma,*}^2 + \tfrac{1}{\epsilon(\Delta t)^2}\|\tilde{\lambda}-\lambda\|_{1,-1/2,\Gamma,*}^2 + \epsilon\|\tilde{\phi}-\phi_h\|_{0,1/2,\Gamma,*}^2 \ .
\end{aligned}
$$

Again we are able to combine $\|\tilde{\phi}-\phi_h\|^2_{0,1/2,\Gamma,*}$ with the left hand side. For the fourth term:

$$\int_0^\infty e^{-2\sigma t}\int_\Gamma ((\frac{1}{2}I-K)(\tilde{\phi}-\phi)+V(\tilde{\lambda}-\lambda))(\partial_t(\tilde{\lambda}-\lambda_h))ds_x dt$$
$$\lesssim_\sigma \|(\frac{1}{2}I-K)(\tilde{\phi}-\phi)+V(\tilde{\lambda}-\lambda)\|_{0,1/2,\Gamma}\|\partial_t(\tilde{\lambda}-\lambda_h)\|_{0,-1/2,\Gamma}$$
$$\lesssim (\|(\frac{1}{2}I-K)(\tilde{\phi}-\phi)\|_{0,1/2,\Gamma}+\|V(\tilde{\lambda}-\lambda)\|_{0,1/2,\Gamma})\|\tilde{\lambda}-\lambda_h\|_{1,-1/2,\Gamma,*}\ .$$

Now using the mapping properties, we further estimate:

$$(\|(\tfrac{1}{2}I-K)(\tilde{\phi}-\phi)\|_{0,\frac{1}{2},\Gamma}+\|V(\tilde{\lambda}-\lambda)\|_{0,\frac{1}{2},\Gamma})\|\tilde{\lambda}-\lambda_h\|_{1,-\frac{1}{2},\Gamma,*}\lesssim(\|\tilde{\phi}-\phi\|_{1,\frac{1}{2},\Gamma,*}+\|\tilde{\lambda}-\lambda\|_{1,-\frac{1}{2},\Gamma,*})\|\tilde{\lambda}-\lambda_h\|_{1,-\frac{1}{2},\Gamma,*}.$$

With the inverse estimate, (in (3.182) [53]):

$$\|\tilde{\lambda}-\lambda_h\|_{1,-1/2,\Gamma,*}\lesssim\frac{1}{\Delta t}\|\tilde{\lambda}-\lambda_h\|_{0,-1/2,\Gamma,*}\ ,$$

we obtain together with Young's inequality:

$$(\|\tilde{\phi}-\phi\|_{1,\frac{1}{2},\Gamma,*}+\|\tilde{\lambda}-\lambda\|_{1,-\frac{1}{2},\Gamma,*})\|\tilde{\lambda}-\lambda_h\|_{1,-\frac{1}{2},\Gamma,*}\lesssim\tfrac{1}{\epsilon(\Delta t)^2}\|\tilde{\phi}-\phi\|^2_{1,\frac{1}{2},\Gamma,*}+\tfrac{1}{\epsilon(\Delta t)^2}\|\tilde{\lambda}-\lambda\|^2_{1,-\frac{1}{2},\Gamma,*}+\epsilon\|\tilde{\lambda}-\lambda_h\|^2_{0,-\frac{1}{2},\Gamma,*}.$$

Now we can combine it again with the left hand side. For the fifth term:

$$\int_0^\infty e^{-2\sigma t}\int_\Gamma \gamma^-(\partial_t(\tilde{\mathbf{w}}-\mathbf{u}))\cdot n\partial_t(\tilde{\phi}-\phi_h)ds_x dt$$
$$\lesssim_\sigma \|\gamma^-(\partial_t(\tilde{\mathbf{w}}-\mathbf{u}))\cdot n\|_{0,-1/2,\Gamma}\|\partial_t(\tilde{\phi}-\phi_h)\|_{0,1/2,\Gamma}$$
$$\lesssim \|\gamma^-(\tilde{\mathbf{w}}-\mathbf{u})\|_{1,1/2,\Gamma}\|\tilde{\phi}-\phi_h\|_{1,1/2,\Gamma}\ .$$

With the inverse estimate, the trace theorem and Young's inequality, we get

$$\|\gamma^-(\tilde{\mathbf{w}}-\mathbf{u})\|_{1,1/2,\Gamma}\|\tilde{\phi}-\phi_h\|_{1,1/2,\Gamma}\lesssim\tfrac{1}{\epsilon(\Delta t)^2}\|\tilde{\mathbf{w}}-\mathbf{u}\|^2_{1,1,\Omega}+\epsilon\|\tilde{\phi}-\phi_h\|^2_{0,1/2,\Gamma,*}\ ,$$

where we combine $\epsilon\|\tilde{\phi}-\phi_h\|^2_{0,1/2,\Gamma,*}$ with the left hand side. For the last term, analogously with the trace theorem, the inverse estimate and Young's inequality:

$$\int_0^\infty e^{-2\sigma t}\int_\Gamma \partial_t(\tilde{\phi}-\phi)\gamma^-(\partial_t(\tilde{\mathbf{w}}-\mathbf{u}_h))\cdot n ds_x dt$$
$$\lesssim_\sigma \|\partial_t(\tilde{\phi}-\phi)\|_{0,1/2,\Gamma}\|\gamma^-(\partial_t(\tilde{\mathbf{w}}-\mathbf{u}_h))\cdot n\|_{0,-1/2,\Gamma}$$
$$\lesssim \|\tilde{\phi}-\phi\|_{1,1/2,\Gamma}\|(\tilde{\mathbf{w}}-\mathbf{u}_h)\|_{1,1,\Omega}$$
$$\lesssim \frac{1}{\Delta t}\|\tilde{\phi}-\phi\|_{1,1/2,\Gamma}\|(\tilde{\mathbf{w}}-\mathbf{u}_h)\|_{0,1,\Omega}$$
$$\lesssim \tfrac{1}{\epsilon(\Delta t)^2}\|\tilde{\phi}-\phi\|^2_{1,1/2,\Gamma,*}+\epsilon\|(\tilde{\mathbf{w}}-\mathbf{u}_h)\|^2_{0,1,\Omega}\ .$$

We combine $\epsilon\|(\tilde{\mathbf{w}}-\mathbf{u}_h)\|^2_{0,1,\Omega}$ again with the left hand side. Altogether

$$\|\tilde{\mathbf{w}}-\mathbf{u}_h\|^2_{0,1,\Omega}+\|\tilde{\phi}-\phi_h\|^2_{0,1/2,\Gamma,*}+\|\tilde{\lambda}-\lambda_h\|^2_{0,-1/2,\Gamma,*}$$
$$\lesssim_\sigma \frac{1}{(\Delta t)^2}\|\tilde{\mathbf{w}}-\mathbf{u}\|^2_{0,1,\Omega}+\frac{1}{(\Delta t)^2}\|\tilde{\phi}-\phi\|^2_{1,1/2,\Gamma,*}+\frac{1}{(\Delta t)^2}\|\tilde{\lambda}-\lambda\|^2_{1,-1/2,\Gamma,*}$$
$$+\frac{1}{(\Delta t)^2}\|\tilde{\phi}-\phi\|^2_{1,1/2,\Gamma,*}+\frac{1}{(\Delta t)^2}\|\tilde{\lambda}-\lambda\|^2_{1,-1/2,\Gamma,*}$$
$$+\frac{1}{(\Delta t)^2}\|\tilde{\mathbf{w}}-\mathbf{u}\|^2_{1,1,\Omega}+\frac{1}{(\Delta t)^2}\|\tilde{\phi}-\phi\|^2_{1,1/2,\Gamma,*}\ .$$

Therefore

$$\begin{aligned}&\|\mathbf{u}-\mathbf{u}_h\|^2_{0,1,\Omega}+\|\phi-\phi_h\|^2_{0,1/2,\Gamma,*}+\|\lambda-\lambda_h\|^2_{0,-1/2,\Gamma,*}\\&\lesssim_\sigma (1+\frac{1}{(\Delta t)^2})\Big(\|\tilde{\mathbf{w}}-\mathbf{u}\|^2_{1,1,\Omega}+\|\tilde{\phi}-\phi\|^2_{1,1/2,\Gamma,*}+\|\tilde{\lambda}-\lambda\|^2_{1,-1/2,\Gamma,*}\Big)\ .\end{aligned}$$

Now taking the infimum gives the assertion. □

4.4 A posteriori error estimate

From Section 4.2 we concluded

$$\mathcal{A}((\mathbf{u},v),(\dot{\mathbf{u}},\dot{v}))=\sigma|\!|\!|(\mathbf{u},v)|\!|\!|^2\ . \tag{4.16}$$

Due to Proposition 4.2, (4.9) is equivalent to: Find $(\mathbf{u}_h,v_h)\in Z_{,\Delta t}\times\widetilde{Z}_{h,\Delta t}$ such that

$$\mathcal{A}((\mathbf{u}_h,v_h),(\dot{\mathbf{w}}_h,\dot{w}_h))=f((\dot{\mathbf{w}}_h,\dot{w}_h))\quad\forall\ (\mathbf{w}_h,w_h)\ \in Z_{h,(\Delta t)}\times\widetilde{Z}_{h,(\Delta t)},$$

and analogously the continuous equation is equivalent to: Find $\mathbf{u}\in H^1_\sigma(\mathbb{R}^+,H^1(\Omega))^3$ and $w\in\{w\in H^1_\sigma(\mathbb{R}^+,H^1(\mathbb{R}^3\backslash\Gamma))^3:[\![\gamma w]\!]\in H^1_\sigma(\mathbb{R}^+\ ,H^{1/2}(\Gamma)),\langle\gamma^- w,m\rangle_{\Gamma\times\mathbb{R}^+,\sigma}=0\ \ \forall m\in H^1_\sigma(\mathbb{R}^+,H^{-1/2}(\Gamma))\}$ such that

$$\mathcal{A}((\mathbf{u},v),(\dot{\mathbf{w}},\dot{w}))=f((\dot{\mathbf{w}},\dot{w}))$$

for all $w\in\{w\in H^1_\sigma(\mathbb{R}^+,H^1(\mathbb{R}^3\backslash\Gamma))^3:[\![\gamma w]\!]\in H^1_\sigma(\mathbb{R}^+\ ,H^{1/2}(\Gamma)),\langle\gamma^- w,m\rangle_{\Gamma\times\mathbb{R}^+,\sigma}=0\ \ \forall m\in H^1_\sigma(\mathbb{R}^+,H^{-1/2}(\Gamma))\}$ and $\mathbf{w}\in H^1_\sigma(\mathbb{R}^+,H^1(\Omega))^3$.

With the representation formula

$$v=D\phi-S\lambda\quad,\quad v_h=D\phi_h-S\lambda_h\ .$$

We conclude with (4.10) and (4.11)

$$\phi-\phi_h=[\![\gamma(v-v_h)]\!]=\gamma^+(v-v_h)-\gamma^-(v-v_h)=\gamma^+(v-v_h), \tag{4.17a}$$

$$\lambda-\lambda_h=[\![\frac{\partial v}{\partial n}-\frac{\partial v_h}{\partial n}]\!]=(\frac{\partial^+ v}{\partial n}-\frac{\partial^+ v_h}{\partial n})-(\frac{\partial^- v}{\partial n}-\frac{\partial^- v_h}{\partial n})=\frac{\partial^+ v}{\partial n}-\frac{\partial^+ v_h}{\partial n}, \tag{4.17b}$$

where we remember with this ansatz, we extended v and v_h to the interior by zero, see Section 2.2 after (2.5). With (4.16) we have

$$\sigma|\!|\!|(\mathbf{u}-\mathbf{u}_h,v-v_h)|\!|\!|^2=\mathcal{A}((\mathbf{u}-\mathbf{u}_h,v-v_h),(\dot{\mathbf{u}}-\dot{\mathbf{u}}_h,\dot{v}-\dot{v}_h))\ , \tag{4.18}$$

and using

$$|\!|\!|(\mathbf{u}-\mathbf{u}_h,v-v_h)|\!|\!|^2\gtrsim\|\mathbf{u}-\mathbf{u}_h\|^2_{0,1,\Omega^-}+\|v-v_h\|^2_{0,1,\mathbb{R}^3\backslash\Gamma}\ , \tag{4.19}$$

with (4.17) and the trace theorem, we obtain

$$\|v-v_h\|^2_{0,1,\mathbb{R}^3\backslash\Gamma}\gtrsim_{\sigma_0}\|\phi-\phi_h\|^2_{0,1/2,\Gamma}+\|\lambda-\lambda_h\|^2_{0,-\frac{1}{2},\Gamma}\ . \tag{4.20}$$

Let $\tilde{\mathbf{w}} \in Z_{h,\Delta t}$ and $\tilde{r} \in \widetilde{Z}_{h,\Delta t}$ with $\tilde{r}$ satisfying the wave equation. Therefore with $\tilde{\phi} \in Y_{h,\Delta t}$ and $\tilde{\lambda} \in X_{h,\Delta t}$ we write $\tilde{r} = D\tilde{\phi} - S\tilde{\lambda}$. With (4.18) and the Galerkin orthogonality, we deduce

$$
\begin{aligned}
&\sigma |\!|\!| (\mathbf{u}-\mathbf{u}_h, v-v_h) |\!|\!|^2 = \mathcal{A}((\mathbf{u},v),(\dot{\mathbf{u}}-\dot{\mathbf{u}}_h,\dot{v}-\dot{v}_h)) - \mathcal{A}((\mathbf{u}_h,v_h),(\dot{\mathbf{u}}-\dot{\mathbf{u}}_h,\dot{v}-\dot{v}_h)) \\
&= f(\dot{\mathbf{u}}-\dot{\mathbf{u}}_h,\dot{v}-\dot{v}_h) - \mathcal{A}((\mathbf{u}_h,v_h),(\dot{\mathbf{u}}-\dot{\mathbf{u}}_h,\dot{v}-\dot{v}_h)) \\
&= f(\partial_t(\mathbf{u}-\tilde{\mathbf{w}}),\partial_t(v-\tilde{r})) + f(\partial_t(\tilde{\mathbf{w}}-\mathbf{u}_h),\partial_t(\tilde{r}-v_h)) \\
&- \mathcal{A}((\mathbf{u}_h,v_h),(\partial_t(\mathbf{u}-\tilde{\mathbf{w}}),\partial_t(v-\tilde{r}))) - \mathcal{A}((\mathbf{u}_h,v_h),(\partial_t(\tilde{\mathbf{w}}-\mathbf{u}_h),\partial_t(\tilde{r}-v_h))) \\
&= f(\partial_t(\mathbf{u}-\tilde{\mathbf{w}}),\partial_t(v-\tilde{r})) - \mathcal{A}((\mathbf{u}_h,v_h),(\partial_t(\mathbf{u}-\tilde{\mathbf{w}}),\partial_t(v-\tilde{r}))) \\
&= -\langle \dot{v}_+^{inc}, \gamma^-(\partial_t(\mathbf{u}-\tilde{\mathbf{w}}))\cdot n\rangle_{\Gamma\times\mathbb{R}^+,\sigma} + \langle \partial_n^+ v^{inc}, \gamma^+(\partial_t(v-\tilde{r}))\rangle_{\Gamma\times\mathbb{R}^+,\sigma} - (\sigma(\mathbf{u}_h), \epsilon(\partial_t(\mathbf{u}-\tilde{\mathbf{w}})))_{\Omega\times\mathbb{R}^+,\sigma} \\
&- (\partial_t^2\mathbf{u}_h, \partial_t(\mathbf{u}-\tilde{\mathbf{w}}))_{\Omega\times\mathbb{R}^+,\sigma} - (\nabla v_h, \nabla\partial_t v - \nabla\partial_t\tilde{r})_{\mathbb{R}^3\setminus\Gamma\times\mathbb{R}^+,\sigma} - (\partial_t^2 v_h, \partial_t(v-\tilde{r}))_{\mathbb{R}^3\setminus\Gamma\times\mathbb{R}^+,\sigma} \\
&+ \langle \gamma^-\partial_t\mathbf{u}_h\cdot n, [\![\gamma(\partial_t(v-\tilde{r}))]\!]\rangle_{\Gamma\times\mathbb{R}^+,\sigma} - \langle [\![\gamma\partial_t v_h]\!], \gamma^-(\partial_t(\mathbf{u}-\tilde{\mathbf{w}}))\cdot n\rangle_{\Gamma\times\mathbb{R}^+,\sigma} \ .
\end{aligned}
$$

With v, v_h satisfying the wave equation, $v = v_h = 0$ in $\Omega^-\times\mathbb{R}^+$ and Green's formula, we get

$$
\begin{aligned}
&-(\nabla v_h, \nabla\dot{v} - \nabla\dot{\tilde{r}})_{\mathbb{R}^3\setminus\Gamma\times\mathbb{R}^+,\sigma} - (\ddot{v}_h, \dot{v}-\dot{\tilde{r}})_{\mathbb{R}^3\setminus\Gamma\times\mathbb{R}^+,\sigma} = -(\nabla v_h, \nabla\dot{v} - \nabla\dot{\tilde{r}})_{\Omega^+\times\mathbb{R}^+,\sigma} - (\ddot{v}_h, \dot{v}-\dot{\tilde{r}})_{\Omega^+\times\mathbb{R}^+,\sigma} \\
&= -(\nabla v_h, \nabla\dot{v} - \nabla\dot{\tilde{r}})_{\Omega^+\times\mathbb{R}^+,\sigma} - (\Delta v_h, \dot{v}-\dot{\tilde{r}})_{\Omega^+\times\mathbb{R}^+,\sigma} = \langle \partial_n^+ v_h, \gamma^+(\dot{v}-\dot{\tilde{r}})\rangle_{\Gamma\times\mathbb{R}^+,\sigma} \ . \qquad (4.21)
\end{aligned}
$$

Now using $\gamma^+(\dot{v}-\dot{\tilde{r}}) = \gamma^+(\dot{v}) - \gamma^+(\dot{\tilde{r}}) = \dot{\phi} - \dot{\tilde{\phi}}$ and $[\![\gamma\dot{v}_h]\!] = \dot{\phi}_h$, we get with (4.21)

$$
\begin{aligned}
&\sigma |\!|\!| (\mathbf{u}-\mathbf{u}_h, v-v_h) |\!|\!|^2 = -\langle \dot{v}_+^{inc}, \gamma^-(\partial_t(\mathbf{u}-\tilde{\mathbf{w}}))\cdot n\rangle_{\Gamma\times\mathbb{R}^+,\sigma} + \langle \partial_n^+ v^{inc}, \partial_t(\phi-\tilde{\phi})\rangle_{\Gamma\times\mathbb{R}^+,\sigma} \\
&- (\tilde{\sigma}(\mathbf{u}_h), \varepsilon(\partial_t(\mathbf{u}-\tilde{\mathbf{w}})))_{\Omega\times\mathbb{R}^+,\sigma} - (\partial_t^2\mathbf{u}_h, \partial_t(\mathbf{u}-\tilde{\mathbf{w}}))_{\Omega\times\mathbb{R}^+,\sigma} + \langle \partial_n^+ v_h, \partial_t(\phi-\tilde{\phi})\rangle_{\Gamma\times\mathbb{R}^+,\sigma} \\
&+ \langle \gamma^-\dot{\mathbf{u}}_h\cdot n, \partial_t(\phi-\tilde{\phi})\rangle_{\Gamma\times\mathbb{R}^+,\sigma} - \langle \dot{\phi}_h, \gamma^-(\partial_t(\mathbf{u}-\tilde{\mathbf{w}}))\cdot n\rangle_{\Gamma\times\mathbb{R}^+,\sigma} \ .
\end{aligned}
$$

Further with the jump relation $\partial_n^+ v_h = W\phi_h - (K^T - \frac{1}{2}I)\lambda_h$ and $0 = \gamma^- v_h = (-\frac{1}{2}I + K)\phi_h - V\lambda_h$:

$$
\begin{aligned}
&\sigma |\!|\!| (\mathbf{u}-\mathbf{u}_h, v-v_h) |\!|\!|^2 = -\langle \dot{v}_+^{inc}, \gamma^-(\partial_t(\mathbf{u}+\tilde{\mathbf{w}}))\cdot n\rangle_{\Gamma\times\mathbb{R}^+,\sigma} - \langle \partial_n^+ v^{inc}, \partial_t(\phi-\tilde{\phi})\rangle_{\Gamma\times\mathbb{R}^+,\sigma} \\
&- (\tilde{\sigma}(\mathbf{u}_h), \varepsilon(\partial_t(\mathbf{u}-\tilde{\mathbf{w}})))_{\Omega\times\mathbb{R}^+,\sigma} - (\partial_t^2\mathbf{u}_h, \partial_t(\mathbf{u}-\tilde{\mathbf{w}}))_{\Omega\times\mathbb{R}^+,\sigma} + \langle W\phi_h - (K^T - \tfrac{1}{2}I)\lambda_h, \partial_t(\phi-\tilde{\phi})\rangle_{\Gamma\times\mathbb{R}^+,\sigma} \\
&+ \langle \gamma^-\dot{\mathbf{u}}_h\cdot n, \partial_t(\phi-\tilde{\phi})\rangle_{\Gamma\times\mathbb{R}^+,\sigma} - \langle \dot{\phi}_h, \gamma^-(\partial_t(\mathbf{u}-\tilde{\mathbf{w}}))\cdot n\rangle_{\Gamma\times\mathbb{R}^+,\sigma} + \langle (K-\tfrac{1}{2}I)\phi_h - V\lambda_h, \partial_t(\lambda-\tilde{\lambda})\rangle_{\Gamma\times\mathbb{R}^+,\sigma} \\
&= \int_0^\infty e^{-2\sigma t}\Bigg\{ -\int_\Omega \sigma(\mathbf{u}_h) : \epsilon(\partial_t(\mathbf{u}-\tilde{\mathbf{w}}))dx - \int_\Omega \partial_t^2\mathbf{u}_h\partial_t(\mathbf{u}-\tilde{\mathbf{w}})dx \\
&+ \int_\Gamma (\partial_n^+ v^{inc} + W\phi_h - (K^T - \tfrac{1}{2}I)\lambda_h + \gamma^-\partial_t\mathbf{u}_h\cdot n)\partial_t(\phi-\tilde{\phi})ds_x \\
&+ \int_\Gamma (-\partial_t v_+^{inc} - \partial_t\phi_h)\cdot n(\gamma^-(\partial_t(\mathbf{u}-\tilde{\mathbf{w}}))) + \int_\Gamma ((K-\tfrac{1}{2}I)\phi_h - V\lambda_h)\partial_t(\lambda-\tilde{\lambda})ds_x \Bigg\} dt \ .
\end{aligned}
$$

Analogously as in Section 3.4 in the proof of Theorem 3.3 we use Betti's formula:

$$
\langle \tilde{\sigma}(\gamma^-\mathbf{u})\cdot n, \gamma^-\mathbf{w}\rangle_{\Gamma\times\mathbb{R}^+,\sigma} = (\tilde{\sigma}(\mathbf{u}), \varepsilon(\mathbf{w}))_{\Omega^-\times\mathbb{R}^+,\sigma} + (\Delta^*\mathbf{u}, \mathbf{w})_{\Omega^-\times\mathbf{R}^+,\sigma}
$$

on each tetrahedron Ω_j, where we define T_i as the face of one Ω_j and $[v]$ denoting the

jump into the face T_i.

$$
\begin{aligned}
&\sigma |\!|\!| (\mathbf{u}-\mathbf{u}_h, v-v_h) |\!|\!|^2 \\
&= \int_0^\infty e^{-2\sigma t} \Bigg\{ \sum_{\Omega_i} \int_{\Omega_i} (-\partial_t^2 \mathbf{u}_h + \Delta^* \mathbf{u}_h)(\partial_t(\mathbf{u}-\tilde{\mathbf{w}}))dx + \sum_{T_i \cap \Gamma = \varnothing} \int_{T_i} [-\tilde{\sigma}(\mathbf{u}_h)\cdot n](\partial_t(\mathbf{u}-\tilde{\mathbf{w}}))ds_x \\
&+ \int_\Gamma (-\tilde{\sigma}(\mathbf{u}_h)\cdot n - \partial_t v_+^{inc}\cdot n - \partial_t \phi_h \cdot n)(\gamma^-(\partial_t(\mathbf{u}-\tilde{\mathbf{w}})))ds_x \\
&+ \int_\Gamma (\partial_n^+ v^{inc} + W\phi_h - (K^T - \tfrac{1}{2}I)\lambda_h + \gamma^- \partial_t \mathbf{u}_h \cdot n)(\partial_t(\phi - \tilde{\phi}))ds_x \\
&+ \int_\Gamma ((K-\tfrac{1}{2}I)\phi_h - V\lambda_h)(\partial_t(\lambda - \tilde{\lambda}))ds_x \Bigg\} dt \ .
\end{aligned}
$$

Now estimating with the duality:

$$
\begin{aligned}
&\sigma |\!|\!| (\mathbf{u}-\mathbf{u}_h, v-v_h) |\!|\!|^2 \\
&\lesssim_\sigma \sum_{\Omega_i} \|-\partial_t^2 \mathbf{u}_h + \Delta^* \mathbf{u}_h\|_{0,0,\Omega_i} \|(\partial_t(\mathbf{u}-\tilde{\mathbf{w}}))\|_{0,0,\Omega_i} + \sum_{T_i \cap \Gamma = \varnothing} \|[\tilde{\sigma}(\mathbf{u}_h)\cdot n]\|_{1,0,T_i} \|(\partial_t(\mathbf{u}-\tilde{\mathbf{w}}))\|_{-1,0,T_i} \\
&+ \|(-\tilde{\sigma}(\mathbf{u}_h)\cdot n - \partial_t v_+^{inc}\cdot n - \partial_t \phi_h \cdot n)\|_{1,0,\Gamma} \|\gamma^-(\partial_t(\mathbf{u}-\tilde{\mathbf{w}}))\|_{-1,0,\Gamma} \\
&+ \|\partial_n^+ v^{inc} + W\phi_h - (K^T - \tfrac{1}{2}I)\lambda_h + \gamma^- \partial_t \mathbf{u}_h \cdot n\|_{1,-1/2,\Gamma} \|\partial_t(\phi - \tilde{\phi})\|_{-1,1/2,\Gamma} \\
&+ \|(K-\tfrac{1}{2}I)\phi_h - V\lambda_h\|_{1,1/2,\Gamma} \|(\partial_t(\lambda - \tilde{\lambda}))\|_{-1,-1/2,\Gamma} \\
&\lesssim \sum_{\Omega_i} \|-\partial_t^2 \mathbf{u}_h + \Delta^* \mathbf{u}_h\|_{0,0,\Omega_i} \|\mathbf{u}-\tilde{\mathbf{w}}\|_{0,1,\Omega_i} + \sum_{T_i \cap \Gamma = \varnothing} \|[\tilde{\sigma}(\mathbf{u}_h)\cdot n]\|_{1,0,T_i} \|\mathbf{u}-\tilde{\mathbf{w}}\|_{0,0,T_i} \\
&+ \|(-\tilde{\sigma}(\mathbf{u}_h)\cdot n - \partial_t v_+^{inc}\cdot n - \partial_t \phi_h \cdot n)\|_{1,0,\Gamma} \|\gamma^-(\mathbf{u}-\tilde{\mathbf{w}})\|_{0,0,\Gamma} \\
&+ \|\partial_n^+ v^{inc} + W\phi_h - (K^T - \tfrac{1}{2}I)\lambda_h + \gamma^- \partial_t \mathbf{u}_h \cdot n\|_{1,-1/2,\Gamma} \|\phi - \tilde{\phi}\|_{0,1/2,\Gamma} \\
&+ \|(K-\tfrac{1}{2}I)\phi_h - V\lambda_h\|_{1,1/2,\Gamma} \|\lambda - \tilde{\lambda}\|_{0,-1/2,\Gamma} \ .
\end{aligned}
$$

In order to use Lemma 3.1, we choose $\tilde{\mathbf{w}} = \mathbf{u}_h + \Pi_h \circ \Pi_{\Delta t}(\mathbf{u}-\mathbf{u}_h)$ for the second and the third term. Further we choose $\tilde{\mathbf{w}} = \mathbf{u}_h$ for the first term and $\tilde{\phi} = \phi_h$, $\tilde{\lambda} = \lambda_h$. We obtain:

$$
\begin{aligned}
&\sigma |\!|\!| (\mathbf{u}-\mathbf{u}_h, v-v_h) |\!|\!|^2 \\
&\lesssim \sum_{\Omega_i} \|-\partial_t^2 \mathbf{u}_h + \Delta^* \mathbf{u}_h\|_{0,0,\Omega_i} \|\mathbf{u}-\mathbf{u}_h\|_{0,1,\Omega_i} + \sum_{T_i \cap \Gamma = \varnothing} \|[\tilde{\sigma}(\mathbf{u}_h)\cdot n]\|_{1,0,T_i} \max\{\Delta t, h\}^{1/2} \|\mathbf{u}-\mathbf{u}_h\|_{0,1/2,T_i} \\
&+ \|(-\tilde{\sigma}(\mathbf{u}_h)\cdot n - \partial_t v_+^{inc}\cdot n - \partial_t \phi_h \cdot n)\|_{1,0,\Gamma} \max\{\Delta t, h\}^{1/2} \|\gamma^-(\mathbf{u}-\mathbf{u}_h)\|_{0,1/2,\Gamma} \\
&+ \|\partial_n^+ v^{inc} + W\phi_h - (K^T - \tfrac{1}{2}I)\lambda_h + \gamma^- \partial_t \mathbf{u}_h \cdot n\|_{1,-1/2,\Gamma} \|\phi - \phi_h\|_{0,1/2,\Gamma} \\
&+ \|(K-\tfrac{1}{2}I)\phi_h - V\lambda_h\|_{1,1/2,\Gamma} \|\lambda - \lambda_h\|_{0,-1/2,\Gamma} \ .
\end{aligned}
$$

Now using the trace theorem and Young's inequality gives

$$
\begin{aligned}
\sigma |\!|\!| (\mathbf{u}-\mathbf{u}_h, v-v_h) |\!|\!|^2 &\lesssim \sum_{\Omega_i} \|-\partial_t^2 \mathbf{u}_h + \Delta^* \mathbf{u}_h\|_{0,0,\Omega_i}^2 + \sum_{T_i \cap \Gamma = \varnothing} \|[\tilde{\sigma}(\mathbf{u}_h)\cdot n]\|_{1,0,T_i}^2 \max\{\Delta t, h\} \\
&+ \|(-\tilde{\sigma}(\mathbf{u}_h)\cdot n - \partial_t v_+^{inc}\cdot n - \partial_t \phi_h \cdot n)\|_{1,0,\Gamma}^2 \max\{\Delta t, h\} \\
&+ \|\partial_n^+ v^{inc} + W\phi_h - (K^T - \tfrac{1}{2}I)\lambda_h + \gamma^- \partial_t \mathbf{u}_h \cdot n\|_{1,-1/2,\Gamma}^2 + \|(K-\tfrac{1}{2}I)\phi_h - V\lambda_h\|_{1,1/2,\Gamma}^2 \\
&+ \|(\mathbf{u}-\mathbf{u}_h)\|_{0,1,\Omega}^2 + \|\phi - \phi_h\|_{0,1/2,\Gamma}^2 + \|\lambda - \lambda_h\|_{0,-1/2,\Gamma}^2 \ .
\end{aligned}
$$

Estimating $\sigma|\!|\!|(\mathbf{u}-\mathbf{u}_h, v-v_h)|\!|\!|^2$ from below by (4.19) and (4.20) and combining them with $\|(\mathbf{u}-\mathbf{u}_h)\|^2_{0,1,\Omega} + \|\phi-\phi_h\|^2_{0,1/2,\Gamma} + \|\lambda-\lambda_h\|^2_{0,-1/2,\Gamma}$ we have proved the following a posteriori error estimate:

Theorem 4.2. *Let $(\mathbf{u},\phi,\lambda) \in X$ satisfy (4.6) and $(\mathbf{u}_h,\phi_h,\lambda_h) \in Z_{h,\Delta t} \times Y_{h,\Delta t} \times X_{h,\Delta t}$ satisfy (4.7) and (4.8). Let $\cup_{j=1}^{N_s}(\partial\Omega_j) = T = \cup_{i=1}^{m} T_i$, where each T_i is a face of one Ω_j with Ω being discretized as in Section 3.2. With $[v]$ denoting the jump into a face T_i, it holds*

$$\|(\mathbf{u}-\mathbf{u}_h)\|^2_{0,1,\Omega} + \|\phi-\phi_h\|^2_{0,1/2,\Gamma} + \|\lambda-\lambda_h\|^2_{0,-1/2,\Gamma} \lesssim_\sigma \eta_1^2+\eta_2^2+\eta_3^2+\eta_4^2+\eta_5^2 \ ,$$

where

$$\begin{aligned}
\eta_1^2 &= \sum_{\Omega_i} \|-\partial_t^2\mathbf{u}_h + \Delta^*\mathbf{u}_h\|^2_{0,0,\Omega_i} \ , \\
\eta_2^2 &= \sum_{T_i\cap\Gamma=\varnothing} \|[\tilde\sigma(\mathbf{u}_h)\cdot n]\|^2_{1,0,T_i} \max\{\Delta t, h\} \ , \\
\eta_3^2 &= \|(-\tilde\sigma(\mathbf{u}_h)\cdot n - \partial_t v_+^{inc}\cdot n - \partial_t\phi_h\cdot n)\|^2_{1,0,\Gamma} \max\{\Delta t, h\} \ , \\
\eta_4^2 &= \|\partial_n^+ v^{inc} + W\phi_h - (K^T - \tfrac{1}{2}I)\lambda_h + \gamma^-\partial_t\mathbf{u}_h\cdot n\|^2_{1,-1/2,\Gamma} \ , \\
\eta_5^2 &= \|(K-\tfrac{1}{2}I)\phi_h - V\lambda_h\|^2_{1,1/2,\Gamma} \ .
\end{aligned}$$

4.5 Discretization and MOT-Algorithm

In the following we want to discretize the equations (4.3), (4.4) and (4.5). We use the same discretization spaces as in Chapter 3. We set $\sigma = 0$. Then the discretization of the interior part results in (3.18) and (3.19) by choosing the ansatz function as

$$\mathbf{u}_{h,\Delta t}(x,t) = \sum_{k=1}^{N_t}\sum_{\nu=1}^{3}\sum_{i=1}^{N_s} u^k_{\nu,i}\beta^k_{\Delta t}(t)\vec{e}_\nu\eta^i_h(x) \ \in (W^{1,1}_{h,\Delta t})^3$$

and the test function as $\dot{\mathbf{w}}_{h,\Delta t} = \eta^l_h(x)\gamma^n_{\Delta t}(t)\vec{e}_\mu \in (W^{1,0}_{h,\Delta t})^3$, for $l = 1,\dots,N_s$, $n = 1,\dots,N_t$ and $\mu = 1,2,3$. We divide for a timestep n the solution vector u^n, with entries $u^n_{\nu,i}$, into $\begin{pmatrix} u^n_{\Omega\setminus\Gamma} \\ u^n_\Gamma \end{pmatrix}$, where $u^n_{\Omega\setminus\Gamma}$ contains the entries of the interior elements whereas u^n_Γ contains the entries on the boundary.

For the discretization of the boundary integral operators, we begin with the retarded hypersingular operator. We choose the ansatz function

$$\phi_{h,\Delta t}(x,t) = \sum_{m=1}^{N_t}\sum_{i=1}^{N_{s'}} \varphi^m_i\beta^m_{\Delta t}(t)\xi^i_h(x) \ \in V^{1,1}_{h,\Delta t}$$

and the test function $\dot w_{h,\Delta t} = \gamma^n_{\Delta t}(t)\xi^j_h(x) \in V^{1,0}_{h,\Delta t}$ for $1 \le n \le N_t$ and $1 \le j \le N_{s'}$. Then

the discretization is already calculated in Subsection 2.3.4. We get:

$$\begin{aligned}
\langle W\phi_{h,\Delta t}, \dot{w}_{h,\Delta t}\rangle_{\Gamma\times\mathbb{R}_+} &= \sum_{m=1}^{N_t}\sum_{i=1}^{N_{s'}} \varphi_i^m \Big[-\iint\limits_{E_{n-m}} \frac{(n_x\cdot n_y)\xi_h^i(y)\xi_h^j(x)}{(\Delta t)|x-y|4\pi} ds_y ds_x \\
&+ 2\iint\limits_{E_{n-m-1}} \frac{(n_x\cdot n_y)\xi_h^i(y)\xi_h^j(x)}{(\Delta t)|x-y|4\pi} ds_y ds_x - \iint\limits_{E_{n-m-2}} \frac{(n_x\cdot n_y)\xi_h^i(y)\xi_h^j(x)}{(\Delta t)|x-y|4\pi} ds_y ds_x \Big] \\
&+ \sum_{m=1}^{N_t}\sum_{i=1}^{N_{\tilde{s}}} \varphi_i^m \iint_{\Gamma\times\Gamma} \frac{(curl_\Gamma\,\xi_h^i)(y)\cdot(curl_\Gamma\,\xi_h^j)(x))}{4\pi|x-y|} \mathcal{Y}^{n-m} ds_y ds_x =: \sum_{m=1}^{N_t}\sum_{i=1}^{N_{s'}} W_{j,i}^{n-m}\varphi_i^m \\
&=: \sum_{m=1}^{N_t} W^{n-m}\varphi^m \ ,
\end{aligned}$$

where

$$\begin{aligned}
\mathcal{Y}^{n-m}(x,y) &= (2(\Delta t))^{-1}(|x-y|^2 - 2|x-y|(n-m+1)(\Delta t) + ((n-m+1)(\Delta t))^2)\chi_{E_{n-m}} \\
&+ (2(\Delta t))^{-1}(|x-y|^2 - 2|x-y|(n-m-2)(\Delta t) + ((n-m-2)(\Delta t))^2)\chi_{E_{n-m-2}} \\
&+ (2(\Delta t))^{-1}(-2|x-y|^2 + 2|x-y|((n-m-1)(\Delta t) + (n-m)(\Delta t)) \\
&- (((n-m-1)(\Delta t))^2 + ((n-m)(\Delta t))^2) + 2(\Delta t)^2)\chi_{E_{n-m-1}} \ .
\end{aligned}$$

We continue with the discretization of the retarded single layer potential. For the ansatz function we use piecewise linear functions in space and time.

$$\lambda_{h,\Delta t}(x,t) = \sum_{m=1}^{N_t}\sum_{i=1}^{N_{s'}} \lambda_i^m \beta_{\Delta t}^m(t)\xi_h^i(x) \ .$$

As test function we use piecewise constant functions in time and piecewise linear functions in space, i.e. $m_{h,\Delta t} = \gamma_{\Delta t}^n(t)\xi_h^j(x) \in V_{h,\Delta t}^{1,0}$ for $1 \le n \le N_t$ and $1 \le j \le N_{s'}$. This gives after some computation

$$\begin{aligned}
\langle V\lambda_{h,\Delta t}, \dot{m}_{h,\Delta t}\rangle_{\Gamma\times\mathbb{R}_+} &= \int_0^\infty \int_\Gamma V\lambda_{h,\Delta t}(x,t)\cdot\dot{m}_{h,\Delta t}(x,t) ds_x dt \\
&= \sum_{m=1}^{N_t}\sum_{i=1}^{N_{s'}} \lambda_i^m \Big[\iint\limits_{E_{n-m}} \left(-(n-m+1)\frac{\xi_h^i(y)\xi_h^j(x)}{4\pi|x-y|} + \frac{\xi_h^i(y)\xi_h^j(x)}{4\pi(\Delta t)} \right) ds_y ds_x \\
&+ \iint\limits_{E_{n-m-1}} \left((2(n-m)-1)\frac{\xi_h^i(y)\xi_h^j(x)}{4\pi|x-y|} - 2\frac{\xi_h^i(y)\xi_h^j(x)}{4\pi(\Delta t)} \right) ds_y ds_x \\
&+ \iint\limits_{E_{n-m-2}} \left(-(n-m-2)\frac{\xi_h^i(y)\xi_h^j(x)}{4\pi|x-y|} + \frac{\xi_h^i(y)\xi_h^j(x)}{4\pi(\Delta t)} \right) ds_y ds_x \Big] =: \sum_{m=1}^{N_t}\sum_{i=1}^{N_{s'}} V_{j,i}^{n-m}\lambda_i^m =: \sum_{m=1}^{N_t} V^{n-m}\lambda^m .
\end{aligned}$$

Next with $\langle(-\frac{1}{2}I+K^T)\lambda_{h,\Delta t}, \dot{w}_{h,\Delta t}\rangle_{\Gamma\times\mathbb{R}_+} = \langle -\frac{1}{2}I\lambda_{h,\Delta t}, \dot{w}_{h,\Delta t}\rangle_{\Gamma\times\mathbb{R}_+} + \langle K^T\lambda_{h,\Delta t}, \dot{w}_{h,\Delta t}\rangle_{\Gamma\times\mathbb{R}_+}$ we get for the retarded adjoint double layer potential after some computation:

$$\langle K^T\lambda_{h,\Delta t}, \dot{w}_{h,\Delta t}\rangle_{\Gamma\times\mathbb{R}_+} = \int_0^\infty \int_\Gamma K^T\lambda_{h,\Delta t}\dot{w}_{h,\Delta t} ds_x dt$$

$$= \sum_{m=1}^{N_t}\sum_{i=1}^{N_{s'}} \lambda_i^m \iint\limits_{\Gamma\times\Gamma} \frac{n_x\cdot(x-y)}{4\pi|x-y|^3}\xi_h^i(y)\xi_h^j(x)\mathcal{Y}^{n-m}(x,y)ds_y ds_x$$

$$+ \sum_{m=1}^{N_t}\sum_{i=1}^{N_{s'}} \lambda_i^m \Big[\iint\limits_{E_{n-m}} n_x\cdot(x-y)\left((n-m+1)\frac{\xi_h^i(y)\xi_h^j(x)}{4\pi|x-y|^2} - \frac{\xi_h^i(y)\xi_h^j(x)}{4\pi(\Delta t)|x-y|}\right)ds_y ds_x$$

$$+ \iint\limits_{E_{n-m-1}} n_x\cdot(x-y)\left(-(2(n-m)-1)\frac{\xi_h^i(y)\xi_h^j(x)}{4\pi|x-y|^2} + 2\frac{\xi_h^i(y)\xi_h^j(x)}{4\pi(\Delta t)|x-y|}\right)ds_y ds_x$$

$$+ \iint\limits_{E_{n-m-2}} n_x\cdot(x-y)\left((n-m-2)\frac{\xi_h^i(y)\xi_h^j(x)}{4\pi|x-y|^2} - \frac{\xi_h^i(y)\xi_h^j(x)}{4\pi(\Delta t)|x-y|}\right)ds_y ds_x\Big]$$

$$=: \sum_{m=1}^{N_t}\sum_{i=1}^{N_{s'}} (K^T)_{j,i}^{n-m}\lambda_i^m =: \sum_{m=1}^{N_t} K^{T^{n-m}}\lambda^m$$

and

$$\langle \frac{1}{2}I\lambda_{h,\Delta t}, \dot{w}_{h,\Delta t}\rangle_{\Gamma\times\mathbb{R}_+} = \frac{1}{2}\int_0^\infty \int_\Gamma \sum_{m=1}^{N_t}\sum_{i=1}^{N_{s'}} \lambda_i^m \beta_{\Delta t}^m(t)\xi_h^i(x)\gamma_{\Delta t}^n(t)\xi_h^j(x)ds_x dt$$

$$= \frac{1}{2}\sum_{m=1}^{N_t}\sum_{i=1}^{N_{s'}} \lambda_i^m \Big(\int_\Gamma \xi_h^i(x)\xi_h^j(x)ds_x\Big)\Big(\int_0^\infty \beta_{\Delta t}^m(t)\gamma_{\Delta t}^n dt\Big)$$

$$= \frac{1}{2}\sum_{i=1}^{N_{s'}} \lambda_i^m \Big(\int_\Gamma \xi_h^i(x)\xi_h^j(x)ds_x\Big)\frac{(\Delta t)}{2}\begin{cases}\lambda_i^1 & ,n=1\\ \lambda_i^n+\lambda_i^{n-1} & ,n\geq 2\end{cases}$$

$$=: \frac{1}{2}\sum_{i=1}^{N_{s'}} I_{j,i}\lambda_I =: \frac{1}{2}I\lambda_I$$

with

$$\lambda_I = \frac{(\Delta t)}{2}\begin{cases}\lambda^1 & ,n=1\\ \lambda^n+\lambda^{n-1} & ,n\geq 2\end{cases}.$$

Further $\langle(\frac{1}{2}I-K)\phi_{h,\Delta t}, \dot{m}_{h,\Delta t}\rangle_{\Gamma\times\mathbb{R}_+} = \langle\frac{1}{2}I\phi_{h,\Delta t}, \dot{m}_{h,\Delta t}\rangle_{\Gamma\times\mathbb{R}_+} - \langle K\phi_{h,\Delta t}, \dot{m}_{h,\Delta t}\rangle_{\Gamma\times\mathbb{R}_+}$:

$$\langle K\phi_{h,\Delta t}, \dot{m}\rangle_{\Gamma\times\mathbb{R}_+} = \int_0^\infty \int_\Gamma K\phi_{h,\Delta t}\dot{m}_{h,\Delta t}ds_x dt$$

$$= \sum_{m=1}^{N_t}\sum_{i=1}^{N_{s'}} \varphi_i^m \Big[\iint\limits_{E_{n-m}} n_y\cdot(x-y)\left(-(n-m+1)\frac{\xi_h^i(y)\xi_h^j(x)}{4\pi|x-y|^3} + \frac{\xi_h^i(y)\xi_h^j(x)}{4\pi(\Delta t)|x-y|^2}\right)ds_y ds_x$$

$$+ \iint\limits_{E_{n-m-1}} n_y\cdot(x-y)\left((2(n-m)-1)\frac{\xi_h^i(y)\xi_h^j(x)}{4\pi|x-y|^3} - 2\frac{\xi_h^i(y)\xi_h^j(x)}{4\pi(\Delta t)|x-y|^2}\right)ds_y ds_x$$

$$+ \iint\limits_{E_{n-m-2}} n_y\cdot(x-y)\left(-(n-m-2)\frac{\xi_h^i(y)\xi_h^j(x)}{4\pi|x-y|^3} + \frac{\xi_h^i(y)\xi_h^j(x)}{4\pi(\Delta t)|x-y|^2}\right)ds_y ds_x\Big]$$

$$+ \sum_{m=1}^{N_t}\sum_{i=1}^{N_{s'}} \varphi_i^m \Big[\iint\limits_{E_{n-m}} \frac{-n_y\cdot(x-y)}{4\pi(\Delta t)|x-y|^2}\xi_h^i(y)\xi_h^j(x)ds_y ds_x + \iint\limits_{E_{n-m-1}} \frac{2n_y\cdot(x-y)}{4\pi(\Delta t)|x-y|^2}\xi_h^i(y)\xi_h^j(x)ds_y ds_x$$

$$+ \iint\limits_{E_{n-m-2}} -\frac{n_y\cdot(x-y)}{4\pi(\Delta t)|x-y|^2}\xi_h^i(y)\xi_h^j(x)ds_y ds_x\Big] =: \sum_{m=1}^{N_t}\sum_{i=1}^{N_{s'}} K_{j,i}^{n-m}\varphi_i^m =: \sum_{m=1}^{N_t} K^{n-m}\varphi^m$$

and

$$\langle \frac{1}{2} I\phi_{h,\Delta t}, \dot{m}_{h,\Delta t}\rangle_{\Gamma\times\mathbb{R}_+} = \frac{1}{2}\int_0^\infty \int_\Gamma \sum_{m=1}^{N_t}\sum_{i=1}^{N_{s'}} \varphi_i^m \beta_{\Delta t}^m(t)\xi_h^i(x)\dot{\gamma}_{\Delta t}^n(t)\xi_h^j(x) ds_x dt$$

$$= \frac{1}{2}\sum_{i=1}^{N_{s'}} \varphi_i^m \Big(\int_\Gamma \xi_h^i(x)\xi_h^j(x) ds_x\Big)\Big(\int_0^\infty \beta_{\Delta t}^m(t)\dot{\gamma}_{\Delta t}^n dt\Big)$$

$$= \frac{1}{2}\sum_{m=1}^{N_t}\sum_{i=1}^{N_{s'}} \varphi_i^m \Big(\int_\Gamma \xi_h^i(x)\xi_h^j(x) ds_x\Big) \begin{cases} -\varphi_i^1 & , n=1 \\ -(\varphi_i^n - \varphi_i^{n-1}) & , n\geq 2 \end{cases}$$

$$= \frac{1}{2}\sum_{i=1}^{N_{s'}} I_{j,i}\varphi_I = \frac{1}{2} I\varphi_I$$

with

$$\varphi_I = \begin{cases} -\varphi^1 & , n=1 \\ -\varphi^n + \varphi^{n-1} & , n\geq 2 \end{cases} .$$

Now let us look at the coupling contributions. For $j = 1,\dots,N_{s'}$

$$\langle \dot{\mathbf{u}}_{h,\Delta t}\cdot n, \dot{w}_{h,\Delta t}\rangle_{\Gamma\times\mathbb{R}_+} = \int_0^\infty \int_\Gamma \dot{\mathbf{u}}_{h,\Delta t}\cdot n \dot{w}_{h,\Delta t} ds_x dt$$

$$= \sum_{\nu=1}^{3}\sum_{i=1}^{N_s} \Big(\int_\Gamma \eta_h^i|_\Gamma(x)\vec{e}_\nu \cdot n\ \xi_h^j(x) ds_x\Big) \begin{cases} u_{\nu,i}^1 & , n=1 \\ u_{\nu,i}^n - u_{\nu,i}^{n-1} & , n\geq 2 \end{cases}$$

$$=: \sum_{\nu=1}^{3}\sum_{i=1}^{N_s} (RIn_x)_{(i,\nu),j} u_T =: RIn_x u_T$$

with

$$u_T = \begin{cases} u_\Gamma^1 & , n=1 \\ u_\Gamma^n - u_\Gamma^{n-1} & , n\geq 2 \end{cases} .$$

For the other coupling part:

$$\begin{aligned} \langle \dot{\phi}_{h,\Delta t}\cdot n, \gamma^-\dot{\mathbf{w}}_{h,\Delta t}\rangle_{\Gamma\times\mathbb{R}_+} &= \int_0^\infty \int_\Gamma \dot{\phi}_{h,\Delta t}\cdot n\gamma^-\dot{\mathbf{w}}_{h,\Delta t} ds_x dt \\ &= \sum_{i=1}^{N_{s'}} \Big(\int_\Gamma \xi_h^i(x) n\cdot \eta_h^j|_\Gamma(x)\vec{e}_\mu ds_x\Big) \begin{cases} \varphi_i^1 & , n=1 \\ \varphi_i^n - \varphi_i^{n-1} & , n\geq 2 \end{cases} \\ &=: \sum_{i=1}^{N_{s'}} (n_x RI)_{i,(j,\eta)}\varphi_T = n_x RI\varphi_T \end{aligned}$$

with

$$\varphi_T = \begin{cases} \varphi^1 & , n=1 \\ \varphi^n - \varphi^{n-1} & , n\geq 2 \end{cases} .$$

Now we look at the right hand side briefly. We set $h = \dot{v}_+^{inc} n$ and $g = \frac{\partial v_+^{inc}}{\partial n}$. We approximate the time integral with the trapezoidal rule, i.e. we get:

$$-\langle \dot{v}_+^{inc} n, \gamma^-\dot{\mathbf{w}}\rangle_{\Gamma\times\mathbb{R}_+} = -\langle h, \gamma^-\dot{\mathbf{w}}\rangle_{\Gamma\times\mathbb{R}_+} = -\frac{(\Delta t)}{2}\int_\Gamma (h^n + h^{n-1})\eta_h^j|_\Gamma(x) e_\mu ds_x =: H^n + H^{n-1}$$

$$\langle \frac{\partial v_+^{inc}}{\partial n}, \dot{w}\rangle_\Gamma = \langle g, \dot{w}\rangle_\Gamma = \frac{(\Delta t)}{2}\int_\Gamma (g^n + g^{n-1})\xi_h^j(x) ds_x =: G^n + G^{n-1} ,$$

where $h^n = h(x,t_n)$ and $g^n = g(x,t_n)$. Finally we solve the following equation:

$$Au_A + Mu_M - RIn_x u_T + n_x RI\varphi_T - \sum_{m=1}^{N_t} W^{n-m}\varphi^m + \sum_{m=1}^{N_t} K^{T^{n-m}}\lambda^m - \frac{1}{2}I\lambda_I$$
$$+ \frac{1}{2}I\varphi_I - \sum_{m=1}^{N_t} K^{n-m}\varphi^m + \sum_{m=1}^{N_t} V^{n-m}\lambda^m = H^n + H^{n-1} + G^n + G^{n-1} \ . \tag{4.22}$$

We remark that W^k, K^k, K^{T^k}, V^k vanishes if the index k is negative. Therefore we get for (4.22) in the first timestep ($n = 1$):

$$A\frac{(\Delta t)}{2}u^1 + M\frac{1}{(\Delta t)}u^1 - RIn_x u_\Gamma^1 + n_x RI\varphi^1 - W^0\varphi^1 + K^{T^0}\lambda^1$$
$$- \frac{1}{2}\frac{(\Delta t)}{2}I\lambda^1 - \frac{1}{2}I\varphi^1 - K^0\varphi^1 + V^0\lambda^1 = G^1 + G^0 + H^1 + H^0 \ .$$

We can write it down as a system of linear equations:

$$\begin{pmatrix} \frac{(\Delta t)}{2}A + \frac{1}{(\Delta t)}M & [0, n_x RI]^T & 0 \\ [0, -RIn_x] & -W^0 & K^{T^0} - \frac{1}{2}\frac{(\Delta t)}{2}I \\ 0 & -K^0 - \frac{1}{2}I & V^0 \end{pmatrix} \begin{pmatrix} u^1 \\ \varphi^1 \\ \lambda^1 \end{pmatrix} = \begin{pmatrix} H^1 + H^0 \\ G^1 + G^0 \\ 0 \end{pmatrix} \ ,$$

which we need to solve first. Next for the second timestep ($n = 2$) we obtain:

$$A\frac{(\Delta t)}{2}(u^2 + u^1) + M\frac{1}{(\Delta t)}(u^2 - 2u^1) - RIn_x(u^2 - u^1) + n_x RI(\varphi^2 - \varphi^1) - \sum_{m=1}^{2} W^{2-m}\varphi^m$$
$$+ \sum_{m=1}^{2} K^{T^{2-m}}\lambda^m - \frac{1}{2}\frac{(\Delta t)}{2}I(\lambda^2 + \lambda^1) + \frac{1}{2}I(-\varphi^2 + \varphi^1) - \sum_{m=1}^{2} K^{2-m}\varphi^m + \sum_{m=1}^{2} V^{2-m}\lambda^m$$
$$= G^2 + G^1 + H^2 + H^1 \ .$$

Since we already computed the first time step, we have the values for u^1, φ^1 and λ^1. So again we get the same matrix-vector system with a changed right hand side, which has to be solved:

$$\begin{pmatrix} \frac{(\Delta t)}{2}A + \frac{1}{(\Delta t)}M & [0, n_x RI]^T & 0 \\ [0, -RIn_x] & -W^0 & K^{T^0} - \frac{(\Delta t)}{4}I \\ 0 & -K^0 - \frac{1}{2}I & V^0 \end{pmatrix} \begin{pmatrix} u^2 \\ \varphi^2 \\ \lambda^2 \end{pmatrix} = \begin{pmatrix} H^2 + H^1 - A\frac{(\Delta t)}{2}u^1 + M\frac{2}{(\Delta t)}u^1 + n_x RI\varphi^1 \\ G^2 + G^1 + RIn_x u_\Gamma^1 + W\varphi^1 + K^{T^1}\lambda^1 + \frac{(\Delta t)}{4}I\lambda^1 \\ K^1\varphi^1 - \frac{1}{2}I\varphi^1 - V^1\lambda^1 \end{pmatrix}.$$

For an arbitrary timestep $n \geq 3$ we need to solve:

$$A\tfrac{(\Delta t)}{2}(u^n + u^{n-1}) + M\tfrac{1}{(\Delta t)}(u^n - 2u^{n-1} + u^{n-2}) - RIn_x(u_\Gamma^n - u_\Gamma^{n-1}) + n_x RI(\varphi^n - \varphi^{n-1}) - \sum_{m=1}^{n} W^{n-m}\varphi^m$$
$$+ \sum_{m=1}^{n} K^{T^{n-m}}\lambda^m - \frac{1}{2}\frac{(\Delta t)}{2}I(\lambda^n + \lambda^{n-1}) + \frac{1}{2}I(-\varphi^n + \varphi^{n-1}) - \sum_{m=1}^{n} K^{n-m}\varphi^m + \sum_{m=1}^{n} V^{n-m}\lambda^m$$
$$= G^n + G^{n-1} + H^n + H^{n-1}.$$

Since we already computed $u^m, \varphi^m, \lambda^m$ for all $m = 1, \dots, n-1$ altogether we get:

$$\begin{pmatrix} \frac{(\Delta t)}{2}A + \frac{1}{(\Delta t)}M & [0, n_x RI]^T & 0 \\ [0, -RIn_x] & -W^0 & K^{T^0} - \frac{1}{2}\frac{(\Delta t)}{2}I \\ 0 & -K^0 - \frac{1}{2}I & V^0 \end{pmatrix} \begin{pmatrix} u^n \\ \varphi^n \\ \lambda^n \end{pmatrix}$$
$$= \begin{pmatrix} H^n + H^{n-1} - A\frac{(\Delta t)}{2}u^{n-1} + M\frac{2}{(\Delta t)}u^{n-1} - M\frac{1}{(\Delta t)}u^{n-2} + n_x RI\varphi^{n-1} \\ G^n + G^{n-1} + RIn_x u_\Gamma^{n-1} + \sum_{m=1}^{n-1} W^{n-m}\varphi^m - \sum_{m=1}^{n-1} K^{T^{n-m}}\lambda^m + \frac{1}{2}\frac{(\Delta t)}{2}I\lambda^{n-1} \\ \sum_{m=1}^{n-1} K^{n-m}\varphi^m - \frac{1}{2}I\varphi^{n-1} - \sum_{m=1}^{n-1} V^{n-m}\lambda^m \end{pmatrix}.$$

We solve this system repeatedly until our desired timestep $N_t \geq 3$ is reached.

4.6 Numerical results

Example 4.1. *We solve a fluid-structure interaction problem on an unit cube* $\Omega = [-1,1]^3$ *(see Figure 3.9) with vanishing interior* $\mathbf{u}$ *and the exterior* v *given as*

$$v(x,t) = (\frac{1}{2} - \frac{t}{2|x|})(1 + \cos(\frac{\pi(|x| - t)}{0.9}))H(0.9 - ||x| - t|).$$

Hence, the transmission conditions are $\frac{\partial v_+}{\partial t} \cdot n$ *in* (3.30) *and* $\frac{\partial v_+}{\partial n}$ *in* (3.31)*. We hold the CFL at 0.1414. We refine the mesh uniformly and compute numerical solutions till time* 4*.*

In Figure 4.1 we plot the L^2-norm of the exact solution of the exterior v and the vanishing interior $\mathbf{u}$ against the numerical solutions. The numerical solutions give quite good approximations of the exact solutions v and $\mathbf{u}$, as we refine in space and time. We also observe that the difference of the L^2-norms stays below a threshhold value. For example at $N = 16$ (20480 tetrahedrals and 3048 triangles) and $(\Delta t) = DT = 0.025$, the difference for v stays in all times below 10^{-3}, see Figure 4.2. The same behaviour is seen for $\mathbf{u}$.

In Figure 4.3 we present a convergence plot in L^2 space time in terms of degree of freedom. The convergence rate for higher degrees of freedom are approximately 0.5. We notice that the error for the exterior part is significantly higher than the error for the interior part. This could be due to edge and corner singularities of the cube. The same behaviour occurs if we compare instead of the degree of freedom, the refinement in space in h as the diameter of a triangle, see Figure 4.4. The convergence rate for smaller h is 1.76.

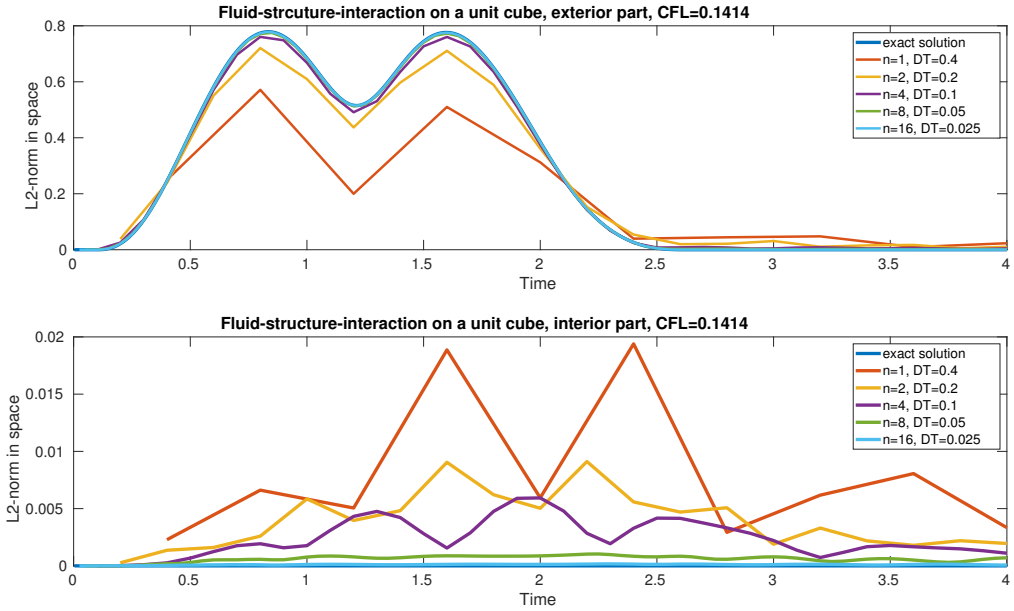

Figure 4.1: L2-Norm of the numerical solution of Example 4.1

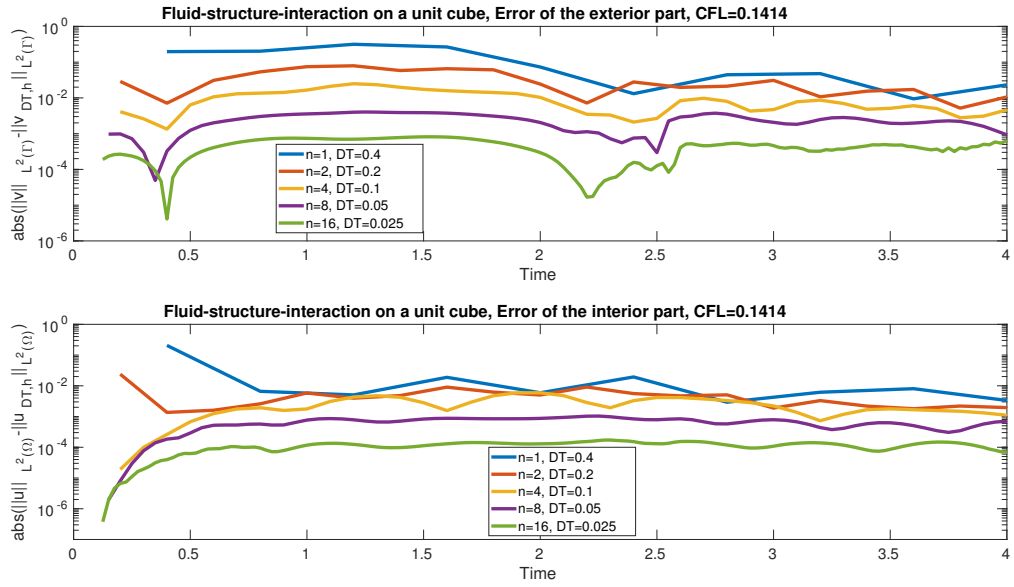

Figure 4.2: Error of the L2-Norm of the numerical solution of Example 4.1

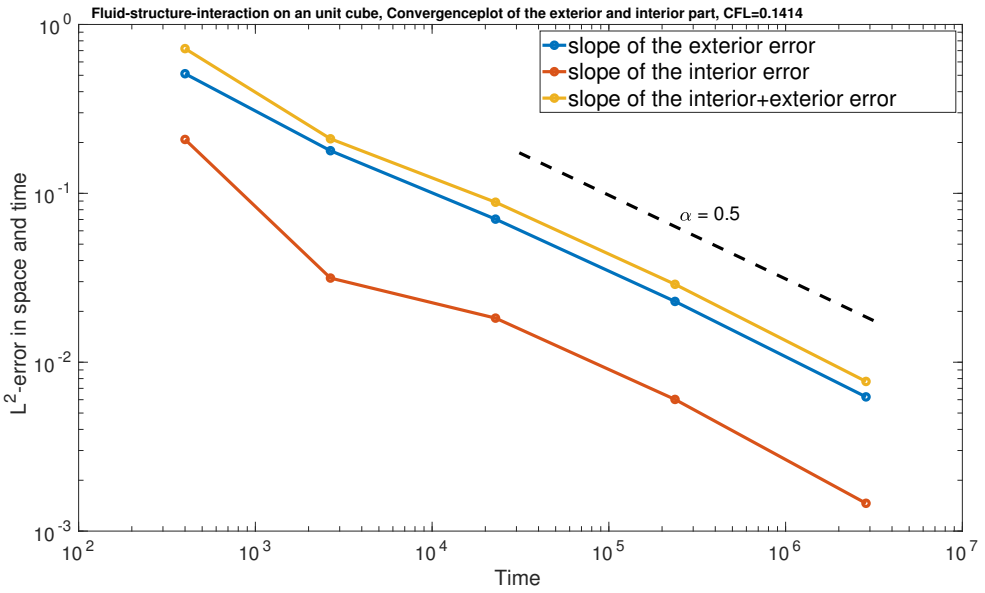

Figure 4.3: The complete error of the fluid-structure interaction problem as function of DOF, Example 4.1

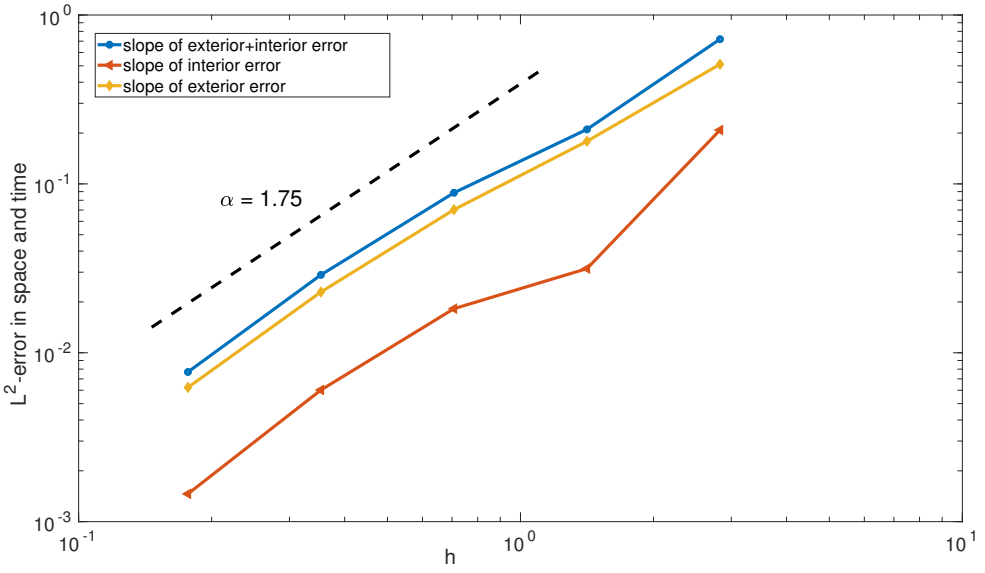

Figure 4.4: The complete error of the fluid-structure interaction problem as function of h, Example 4.1

Example 4.2. *We solve a fluid-structure interaction problem on an unit cube* $\Omega = [-1,1]^3$ *(see Figure 3.9)with a vanishing exterior* v *and an interior* $\mathbf{u}$ *given by*

$$\mathbf{u} = \begin{pmatrix} \left(\sin(\pi(t-\frac{x_1}{2}))\right)^5 (H(-1+t-\frac{x_1}{2}) - H(-3+t-\frac{x_1}{2})) \\ 0 \\ 0 \end{pmatrix}.$$

The transmission conditions are $\tilde{\sigma}(\mathbf{u}) \cdot n$ *in* (3.30) *and* $\frac{\partial \mathbf{u}}{\partial t} \cdot n$ *in* (3.31). *We hold the CFL at 0.1414. We refine the mesh uniformly and compute numerical solutions till time* 4.

In Figure 4.5 we plot the L^2–norm of the exact solution of the vanishing exterior v and the interior $\mathbf{u}$ against the numerical solutions. In contrary to Figure 4.1 the numerical solutions differ significantly from the L^2-norm of the exact solution, in particular the exterior part v. The interior part suffers from the same problems as in Example 3.3, see Figure 4.6 and Figure 4.7 for a zoom. We still observe that the difference in the L^2-norms decreases, as we refine in space and time, but we can't expect a high convergence rate as in Example 4.1. In Figures 4.8 resp. 4.9 we see a convergence rate in terms of degree of freedom at approximately 0.32 resp. in terms of h at approximately 1.1 for higher degree of freedom resp. for smaller diameters h. As in Figures 4.3 and 4.4 the error for the exterior part is higher than the error in the interior part. At least in the numerical example of 4.1 in comparison to the numerical example of 4.2, the influence, coming only from the exterior, don't affect the interior as much as an influence, coming from the interior, affecting the exterior.

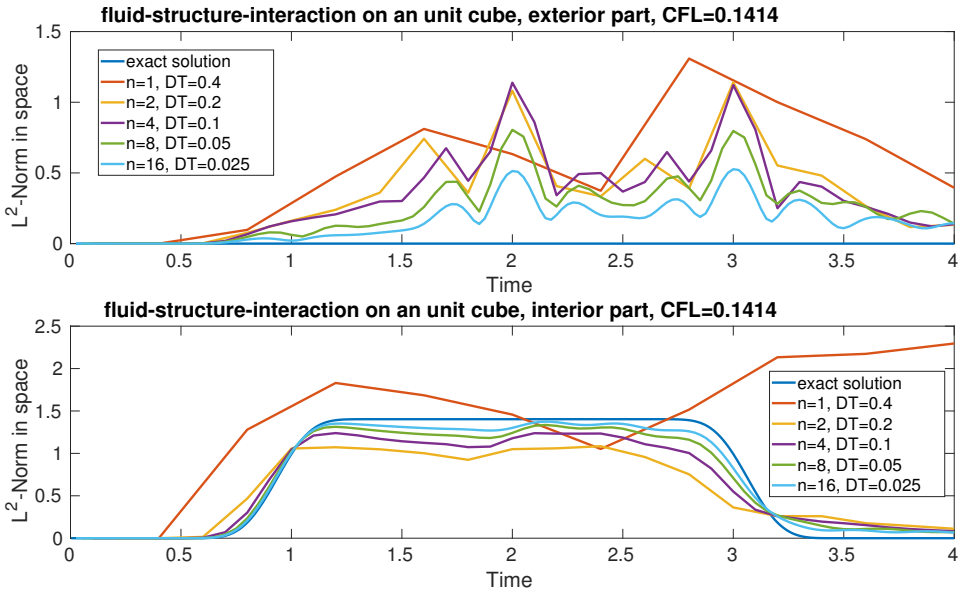

Figure 4.5: L2-Norm of the numerical solution of Example 4.2

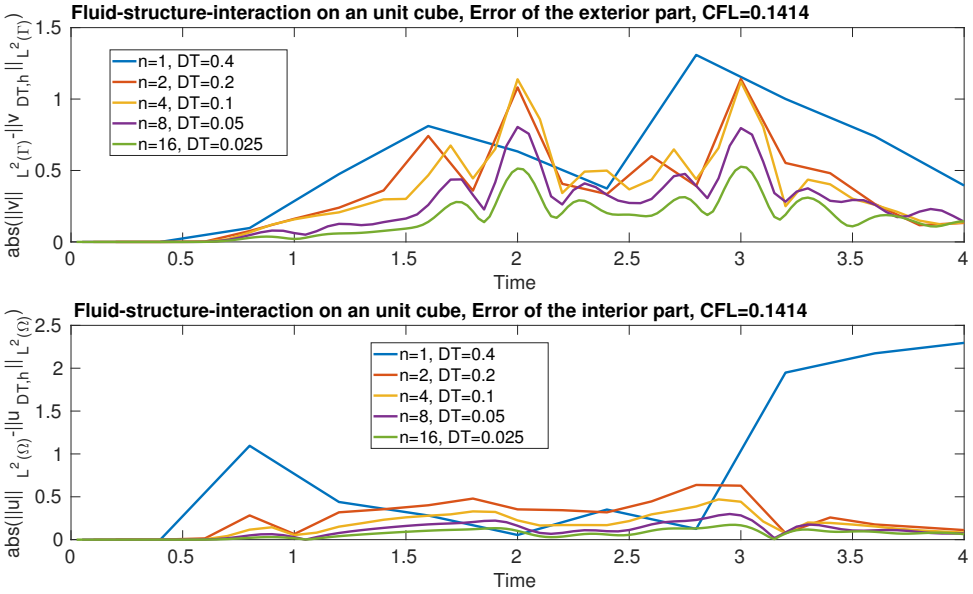

Figure 4.6: Error of the numerical solution of Example 4.2

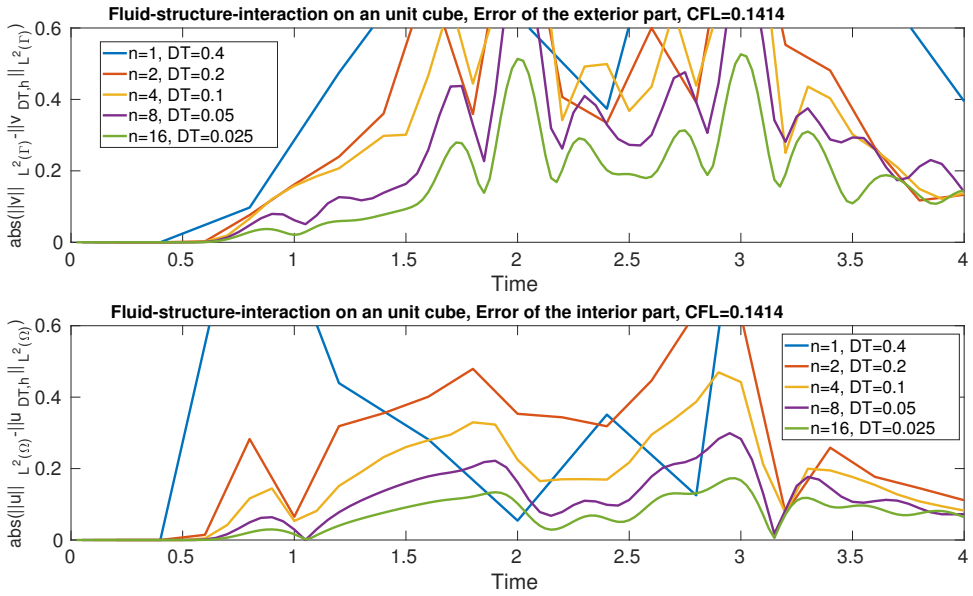

Figure 4.7: Figure 4.6 zoomed, error of the numerical solution of Example 4.2

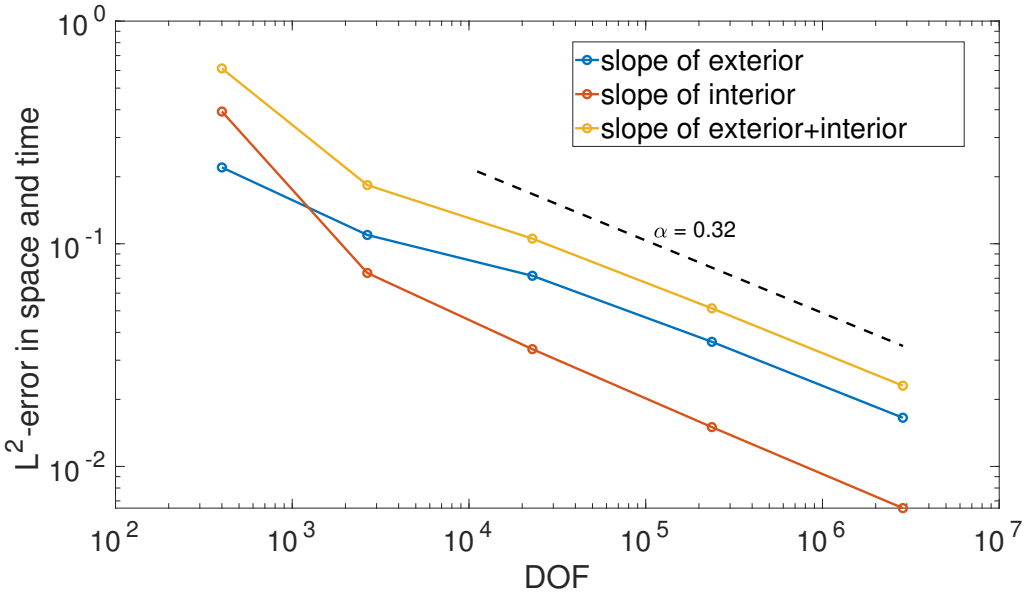

Figure 4.8: The complete error of the fluid-structure interaction problem as function of DOF, Example 4.2

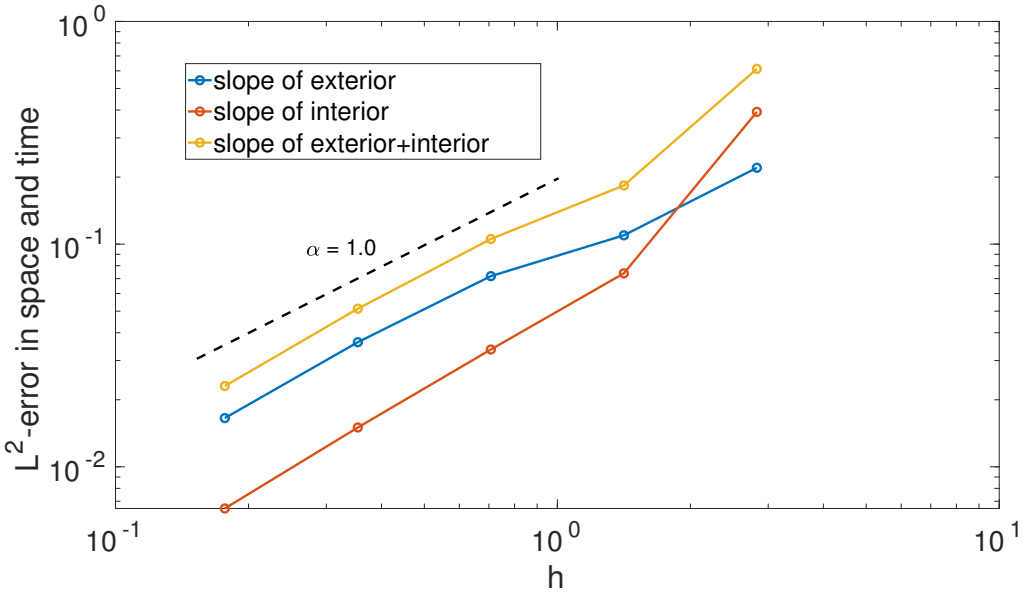

Figure 4.9: The complete error of the fluid-structure interaction problem as function of h, Example 4.2

Example 4.3. *We combine both the exterior part from Example 4.1 and the interior part from Example 4.2 to get a fluid-structure interaction problem on the unit cube (see Figure 3.9), where the interior as well as the exterior influences each other. Hence we use* (3.30) *and* (3.31) *as transmission conditions. We compute a numerical solutions till time* 4 *for a refinement of space and time, where a CFL of* 0.1414 *is hold. The finest mesh consists* 69120 *tetrahedrals with* 6912 *triangles* ($N = 24$) *and* $\Delta t = DT = 0.0166667$.

Figure 4.10 shows the exact solution of the interior $\mathbf{u}$ at the corner $(-1,-1,-1)$ against numerical solutions. $N = 2$ and $dt = 0.05$ (40 tetrahedrals with 48 triangles) with a CFL around 0.03536 clearly differs from the corresponding mesh with CFL of 0.1414. In this case we have a large discretization error. For $N = 1$ (5 tetrahedrals with 12 triangles) and $dt = 0.4$ the refinement is too coarse, to get a good approximation. The numerical solutions for CFL 0.1414 approximate the exact solution at $(-1,-1,-1)$ more accurate as we refine in space time. For larger times, the approximation differs more, as in Example 3.3. We see this behaviour in Figure 4.11 as well, where we look at the L^2-norms of the solutions. For small times, we achieve an excellent approximation of the exact L^2-norms. After time 1 we get a small gap between the exact interior L^2-norm and the numerical results, which also affects the exterior in a later time about 1.7. The difference of the L^2-norms in space, which is plotted in Figure 4.12 aren't as high as in Example 4.2 Figure 4.6 for the exterior, see e.g. in time 2. The behaviour of the interior numerical solutions resemble the behaviour of the numerical solutions for Example 4.2 as well. It seems like the exterior solution of this FSI problem doesn't influences the interior solution as much as vice versa.

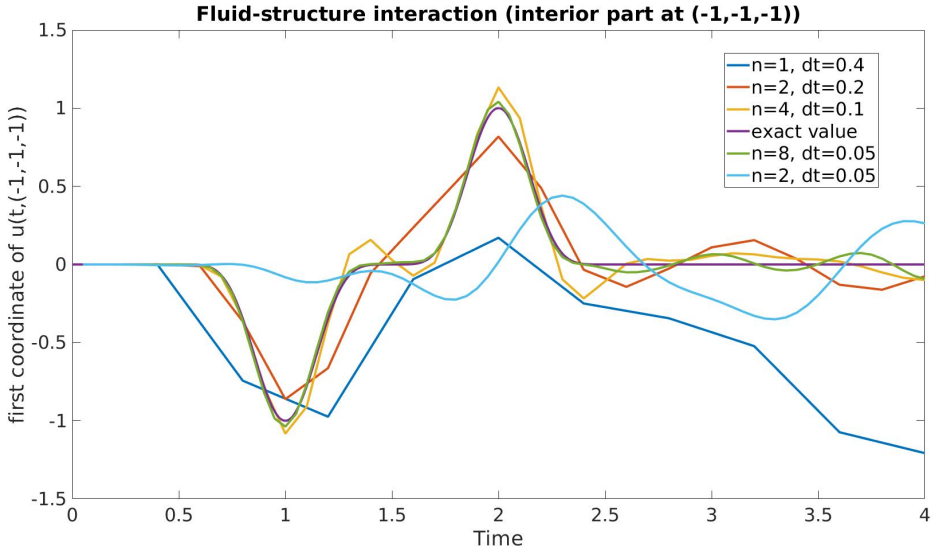

Figure 4.10: Numerical solutions of the interior against the exact solution of the interior at $(-1,-1,-1)$, Example 4.3

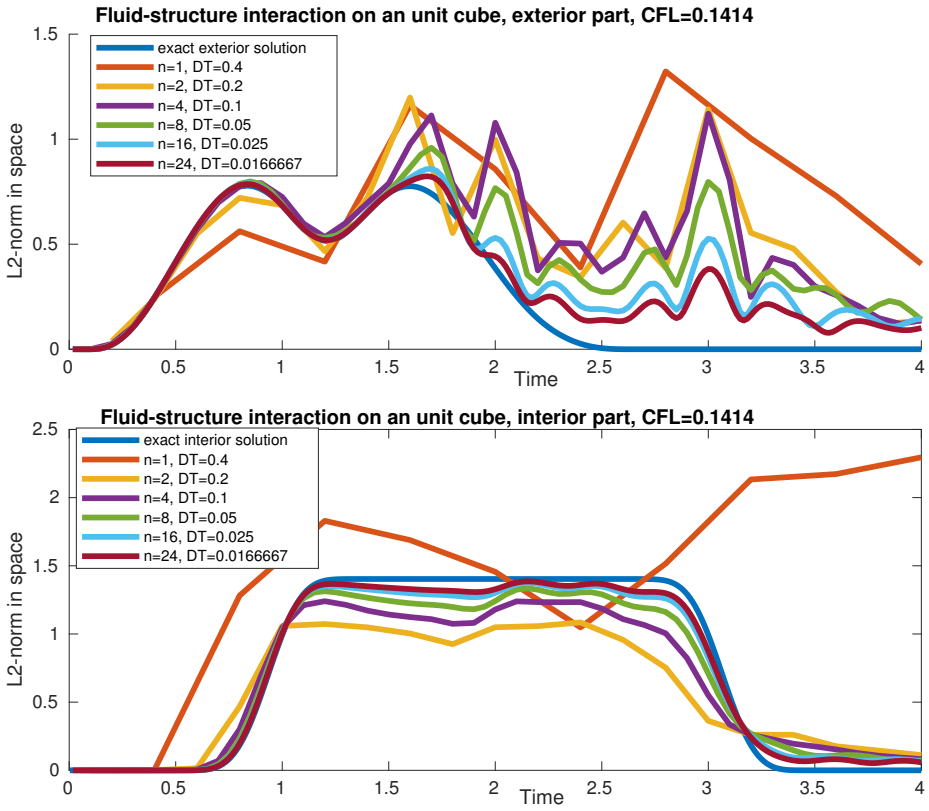

Figure 4.11: L2-Norm of the numerical solution of Example 4.3

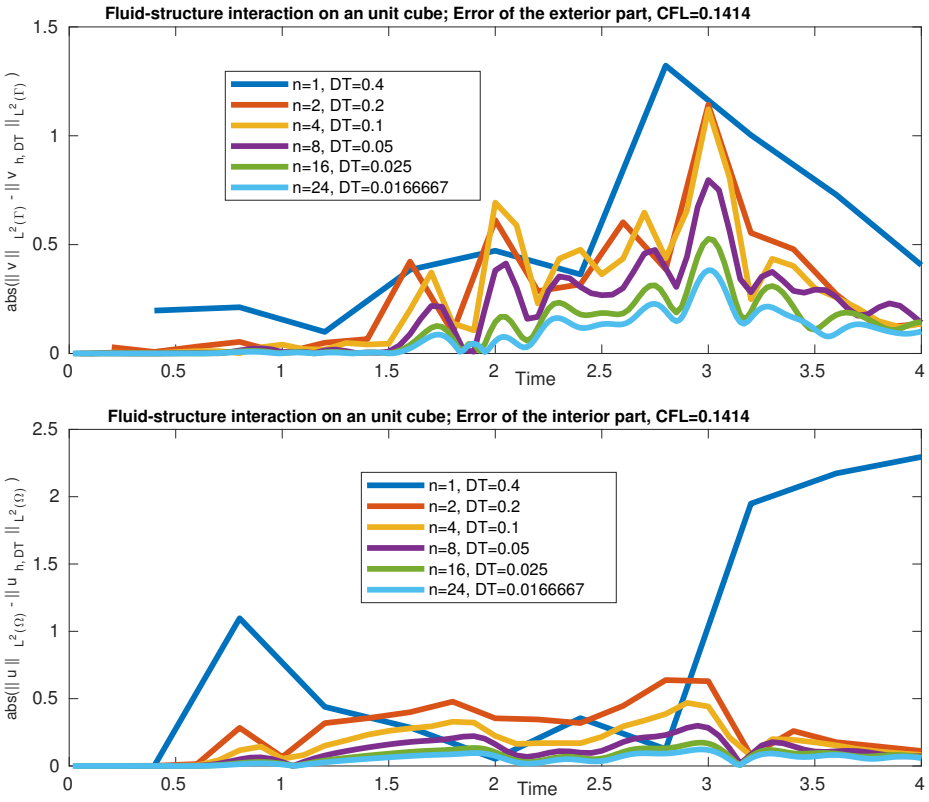

Figure 4.12: Error of the numerical solution of Example 4.3

In Figure 4.13, 4.14 we plot various convergence plots for the L^2–error in space time in terms of degrees of freedom resp. in terms of the diameter h with respect to the time. The curve till the time 2.0 (marker $\triangledown$) has a higher interior space time error than the exterior. The exterior curve has a higher convergence rate as well. After time 2.8 (marker $\triangleleft$) the exterior space time error becomes higher than the interior. For time 3.6 and 4 (marker $\triangleright$, Δ) the convergence plots are almost identical. We receive a convergence rate of 0.17 in terms of degrees of freedom resp. 0.58 of the diameter h.

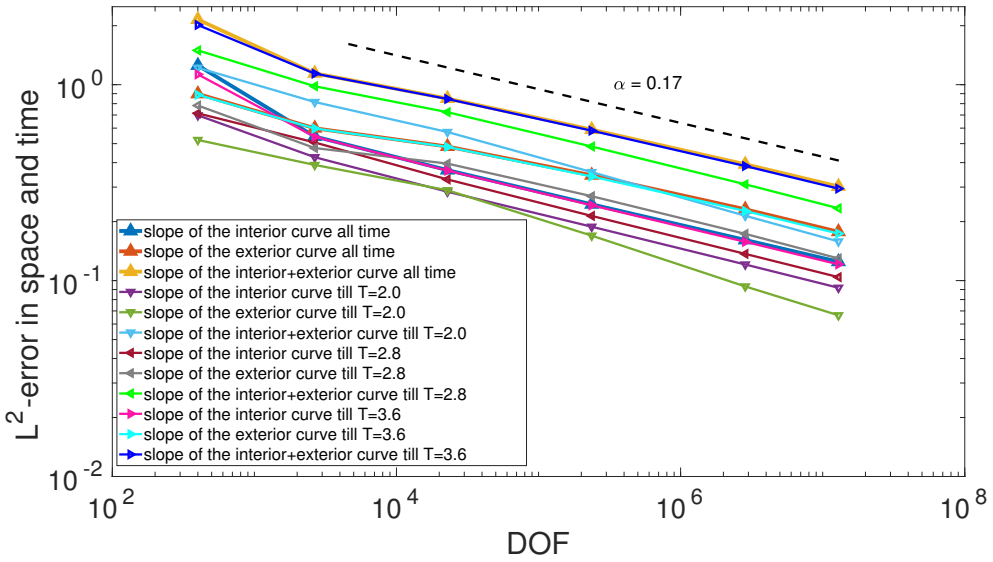

Figure 4.13: The L^2-error in space and time of the fluid-structure interaction problem as function of DOF, Example 4.3

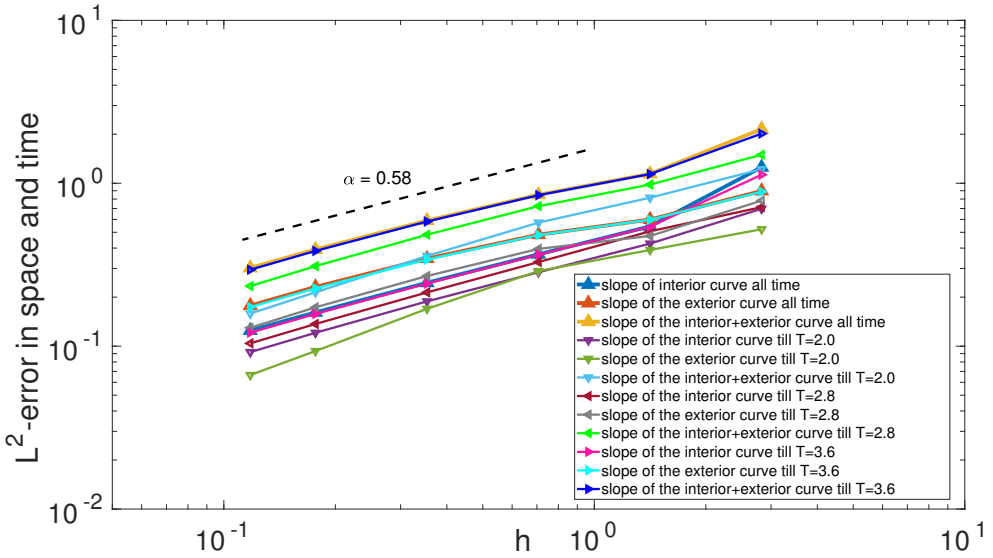

Figure 4.14: The L^2-error in space and time of fluid-structure interaction problem as function of h, Example 4.3

5 FEM-BEM coupling in time domain III : The treatment of a wave propagation interface problem

5.1 Introduction

This chapter deals with a finite element – boundary element coupling of a wave propagation interface problem. We couple the wave equation in the interior $\Omega =: \Omega^-$ together with the wave equation in the exterior $\Omega^+ := \Omega^c := \mathbb{R}^3 \backslash \overline{\Omega}$, where Ω is a bounded, orientable Lipschitz domain. Further we impose homogenous initial conditions in both domains. Then on the boundary $\Gamma \times \mathbb{R}_+$, we impose transmission conditons. Altogether we get the wave interface problem

$$\frac{1}{c_1^2}\frac{\partial^2 u}{\partial t^2} - \Delta u = 0 \quad (x,t) \in \Omega^- \times (0,\infty) \ , \tag{5.1a}$$

$$\frac{1}{c_2^2}\frac{\partial^2 v}{\partial t^2} - \Delta v = 0 \quad (x,t) \in \Omega^+ \times (0,\infty) \ , \tag{5.1b}$$

$$u(x,0) = \dot{u}(x,0) = 0 \quad \text{in } \Omega \ , \tag{5.1c}$$

$$v(x,0) = \dot{v}(x,0) = 0 \quad \text{in } \Omega^c \ , \tag{5.1d}$$

$$\gamma^- u - \gamma^+ v = f \quad \text{on } \Gamma \times (0,\infty) \ , \tag{5.1e}$$

$$\partial_n^- u - \partial_n^+ v = g \quad \text{on } \Gamma \times (0,\infty) \ , \tag{5.1f}$$

where $n = n_x$ is the unit normal vector, always pointing towards $\Omega^+ = \Omega^c$. For $x \in \Gamma$ on the one hand, we define $\gamma^+ v(x,t) := v_+(x,t) := \lim\limits_{x' \in \Omega^+ \to x} v(x',t)$ the limit of v to the boundary $\Gamma := \partial\Omega$ from the exterior $\Omega^c = \Omega^+$ and on the other hand, we define $\gamma^- u(x,t) = u_-(x,t) = \lim\limits_{x' \in \Omega^- \to x} u(x',t)$ the limit of u to the boundary Γ from the interior $\Omega^- = \Omega$. Further $\partial_n^+ v(x,t) := \frac{\partial v_+}{\partial n}(x,t) := \lim\limits_{x' \in \Omega^+ \to x} n_x \cdot \nabla v(x',t)$ and $\partial_n^- v(x,t) := \frac{\partial v_-}{\partial n}(x,t) := \lim\limits_{x' \in \Omega^- \to x} n_x \cdot \nabla v(x',t)$. The well-posedness of (5.1) in the frequency domain is done in [70]. Appyling an inverse Fourier transform, we obtain the well posedness of (5.1) in the time domain, see [57, 90]. In the following the wave velocities are set to $c_1 = c_2 = 1$. We use retarded potentials to formulate the interface problem (5.1) as a coupled domain / boundary integral equation. We address the interface problem (5.1) with a symmetric coupling.

Other approaches in order to deal with the interface problem have been considered:

coupling discontinuous Galerkin methods with retarded potentials in [1], an energetic FEM-BEM coupling in [5], a symmetric FEM-BEM coupling in [59] and a Costabel-Stephan system of boundary integral equations in [87].

5.2 Symmetric wave-wave coupling

We consider the problem (5.1). The goal is to derive a bilinearform satisfying the coercivity, in order to state an a priori and an a posteriori error estimate.

We take the approach of [2] and extend it from 2D to 3D. We begin with the definition of the energy for the wave equation in Ω^c for $t \in \mathbb{R}^+$:

$$E_{\Omega^c}(t) = \frac{1}{2}\int_{\Omega^c} |\dot{v}|^2 + |\nabla v|^2 dx \ .$$

We remember Green's formula for a test function $w \in H^1(\mathbb{R}_+, H^1(\Omega^\mp))$

$$\langle \partial_n^\mp v, \gamma^\mp w\rangle_{\Gamma\times\mathbb{R}_+} = \pm(\nabla v, \nabla w)_{\Omega^\mp\times\mathbb{R}_+} \pm (\Delta u, w)_{\Omega^\mp\times\mathbb{R}_+} \ .$$

Considering the derivative of the energy, with Green's formula and the solution v to the the wave equation in Ω^+:

$$\begin{aligned}\frac{\partial E_{\Omega^c}(t)}{\partial t} &= \frac{1}{2}\int_{\Omega^c} \partial_t(\nabla v\cdot\nabla v) + \partial_t(\dot{v}\cdot\dot{v})dx = \int_{\Omega^c} \nabla v\cdot\nabla\dot{v} + \dot{v}\cdot\ddot{v}dx \\ &= \int_{\Omega^c} \dot{v}\cdot\ddot{v} - \Delta v\cdot\dot{v}dx - \int_\Gamma \partial_n^+ v\gamma^+\dot{v}ds_x = -\int_\Gamma \partial_n^+ v\gamma^+\dot{v}ds_x = -\langle\partial_n^+ v, \gamma^+\dot{v}\rangle_\Gamma \ .\end{aligned}$$

Therefore we get for a time T

$$E_{\Omega^c}(T) = -\langle\partial_n^+ v, \gamma^+\dot{v}\rangle_{\Gamma\times[0,T]} \ . \tag{5.2}$$

Next we need some observations from Chapter 2.

$$\frac{1}{2}(\gamma^+ v) = K(\gamma^+ v) - V(\partial_n^+ v) \ , \quad \frac{1}{2}(\partial_n^+ v) = W(\gamma^+ v) - K'(\partial_n^+ v) \ . \tag{5.3}$$

Taking the derivative in time of the first equation and testing with $\partial_n^+ v$ and testing the second equation of (5.3) with $\gamma^+\dot{v}$, we get:

$$\frac{1}{2}\langle\partial_n^+ v, \gamma^+\dot{v}\rangle_{\Gamma\times[0,T]} = \langle\partial_t(K(\gamma^+ v)), \partial_n^+ v\rangle_{\Gamma\times[0,T]} - \langle\partial_t(V(\partial_n^+ v)), \partial_n^+ v\rangle_{\Gamma\times[0,T]} \ , \tag{5.4}$$

$$\frac{1}{2}\langle\partial_n^+ v, \gamma^+\dot{v}\rangle_{\Gamma\times[0,T]} = \langle W(\gamma^+ v), \gamma^+\dot{v}\rangle_{\Gamma\times[0,T]} - \langle(K'(\partial_n^+ v)), \gamma^+\dot{v}\rangle_{\Gamma\times[0,T]} \ . \tag{5.5}$$

We get the equations

$$0 = \langle\partial_t(K(\gamma^+ v)), \partial_n^+ v\rangle_{\Gamma\times[0,T]} - \langle\partial_t(V(\partial_n^+ v)), \partial_n^+ v\rangle_{\Gamma\times[0,T]} - \frac{1}{2}\langle\partial_n^+ v, \gamma^+\dot{v}\rangle_{\Gamma\times[0,T]} \ , \tag{5.6}$$

$$0 = \langle W(\gamma^+ v), \gamma^+\dot{v}\rangle_{\Gamma\times[0,T]} - \langle(K'(\partial_n^+ v)), \gamma^+\dot{v}\rangle_{\Gamma\times[0,T]} - \frac{1}{2}\langle\partial_n^+ v, \gamma^+\dot{v}\rangle_{\Gamma\times[0,T]} \ . \tag{5.7}$$

Now we test (5.6) and (5.7) with test functions $m \in H^1([0,T], H^{-1/2}(\Gamma))$ and $\omega \in H^1([0,T], H^{1/2}(\Gamma))$ to obtain

$$0 = \langle \partial_t(K(\gamma^+ v)), m\rangle_{\Gamma\times[0,T]} - \langle \partial_t(V(\partial_n^+ v)), m\rangle_{\Gamma\times[0,T]} - \frac{1}{2}\langle \gamma^+ \dot{v}, m\rangle_{\Gamma\times[0,T]} \ , \tag{5.8}$$

$$0 = \langle W(\gamma^+ v), \dot{\omega}\rangle_{\Gamma\times[0,T]} - \langle (K'(\partial_n^+ v)), \dot{\omega}\rangle_{\Gamma\times[0,T]} - \frac{1}{2}\langle \partial_n^+ v, \dot{\omega}\rangle_{\Gamma\times[0,T]} \ . \tag{5.9}$$

We continue by testing (5.1a) with a test function $w \in H^1([0,T], H^1(\Omega))$, where we use $\dot{w}$. We observe with Green's formula:

$$\int_0^T \int_\Omega \ddot{u}\dot{w}dxdt - \int_0^T \int_\Omega \Delta u \dot{w}dxdt = \int_0^T \int_\Omega \ddot{u}\dot{w}dxdt + \int_0^T \int_\Omega \nabla u \nabla \dot{w}dxdt - \int_0^T \int_\Gamma \partial_n^- u \gamma^- \dot{w} ds_x dt. \tag{5.10}$$

We define

$$a(u,w) := \int_0^T \int_\Omega \ddot{u}\dot{w}dxdt + \int_0^T \int_\Omega \nabla u \nabla \dot{w}dxdt \ .$$

For $w = u$ as the test function, we get the relationship to the energy in the interior Ω

$$E_\Omega(T) = a(u,u) \ . \tag{5.11}$$

Therefore we get the equation

$$a(u,w) - \langle \partial_n^- u, \gamma^- \dot{w}\rangle_{\Gamma\times[0,T]} = 0 \ . \tag{5.12}$$

Subtracting (5.8) and (5.9), from (5.12), we get:

$$\begin{aligned} &a(u,w) - \langle \partial_n^- u, \gamma^- \dot{w}\rangle_{\Gamma\times[0,T]} \\ &- \langle \partial_t(K(\gamma^+ v)), m\rangle_{\Gamma\times[0,T]} + \langle \partial_t(V(\partial_n^+ v)), m\rangle_{\Gamma\times[0,T]} + \frac{1}{2}\langle \gamma^+ \dot{v}, m\rangle_{\Gamma\times[0,T]} \\ &- \langle W(\gamma^+ v), \dot{\omega}\rangle_{\Gamma\times[0,T]} + \langle (K'(\partial_n^+ v)), \dot{\omega}\rangle_{\Gamma\times[0,T]} + \frac{1}{2}\langle \partial_n^+ v, \dot{\omega}\rangle_{\Gamma\times[0,T]} = 0 \ . \end{aligned} \tag{5.13}$$

First by integration by parts in time:

$$\begin{aligned} &a(u,w) - \langle \partial_n^- u, \gamma^- \dot{w}\rangle_{\Gamma\times[0,T]} \\ &+ \langle K(\gamma^+ v), \dot{m}\rangle_{\Gamma\times[0,T]} - \langle V(\partial_n^+ v), \dot{m}\rangle_{\Gamma\times[0,T]} - \frac{1}{2}\langle \gamma^+ v, \dot{m}\rangle_{\Gamma\times[0,T]} \\ &- \langle W(\gamma^+ v), \dot{\omega}\rangle_{\Gamma\times[0,T]} + \langle (K'(\partial_n^+ v)), \dot{\omega}\rangle_{\Gamma\times[0,T]} + \frac{1}{2}\langle \partial_n^+ v, \dot{\omega}\rangle_{\Gamma\times[0,T]} = 0 \ . \end{aligned}$$

Next by using (5.1f)

$$\begin{aligned} &a(u,w) - \langle g, \gamma^- \dot{w}\rangle_{\Gamma\times[0,T]} - \langle \partial_n^+ v, \gamma^- \dot{w}\rangle_{\Gamma\times[0,T]} \\ &+ \langle K(\gamma^+ v), \dot{m}\rangle_{\Gamma\times[0,T]} - \langle V(\partial_n^+ v), \dot{m}\rangle_{\Gamma\times[0,T]} - \frac{1}{2}\langle \gamma^+ v, \dot{m}\rangle_{\Gamma\times[0,T]} \\ &- \langle W(\gamma^+ v), \dot{\omega}\rangle_{\Gamma\times[0,T]} + \langle (K'(\partial_n^+ v)), \dot{\omega}\rangle_{\Gamma\times[0,T]} + \frac{1}{2}\langle \partial_n^+ v, \dot{\omega}\rangle_{\Gamma\times[0,T]} = 0 \ . \end{aligned}$$

Now adding $0 = -\frac{1}{2}\langle\gamma^+ v, \dot{m}\rangle_{\Gamma\times[0,T]} + \frac{1}{2}\langle\gamma^+ v, \dot{m}\rangle_{\Gamma\times[0,T]}$, we get

$$
\begin{aligned}
&a(u,w) - \langle g, \gamma^- \dot{w}\rangle_{\Gamma\times[0,T]} - \langle \partial_n^+ v, \gamma^- \dot{w}\rangle_{\Gamma\times[0,T]} \\
&+ \langle K(\gamma^+ v), \dot{m}\rangle_{\Gamma\times[0,T]} - \langle V(\partial_n^+ v), \dot{m}\rangle_{\Gamma\times[0,T]} - \langle \gamma^+ v, \dot{m}\rangle_{\Gamma\times[0,T]} + \frac{1}{2}\langle \gamma^+ v, \dot{m}\rangle_{\Gamma\times[0,T]} \\
&- \langle W(\gamma^+ v), \dot{\omega}\rangle_{\Gamma\times[0,T]} + \langle (K'(\partial_n^+ v)), \dot{\omega}\rangle_{\Gamma\times[0,T]} + \frac{1}{2}\langle \partial_n^+ v, \dot{\omega}\rangle_{\Gamma\times[0,T]} = 0 \ .
\end{aligned}
$$

Using (5.1e) gives

$$
\begin{aligned}
&a(u,w) - \langle g, \gamma^- \dot{w}\rangle_{\Gamma\times[0,T]} - \langle \partial_n^+ v, \gamma^- \dot{w}\rangle_{\Gamma\times[0,T]} + \langle K(\gamma^+ v), \dot{m}\rangle_{\Gamma\times[0,T]} \\
&- \langle V(\partial_n^+ v), \dot{m}\rangle_{\Gamma\times[0,T]} - \langle \gamma^- u, \dot{m}\rangle_{\Gamma\times[0,T]} + \langle f, \dot{m}\rangle_{\Gamma\times[0,T]} + \frac{1}{2}\langle \gamma^+ v, \dot{m}\rangle_{\Gamma\times[0,T]} \\
&- \langle W(\gamma^+ v), \dot{\omega}\rangle_{\Gamma\times[0,T]} + \langle (K'(\partial_n^+ v)), \dot{\omega}\rangle_{\Gamma\times[0,T]} + \frac{1}{2}\langle \partial_n^+ v, \dot{\omega}\rangle_{\Gamma\times[0,T]} = 0 \ .
\end{aligned}
$$

Finally the weak formulation with $\phi = \gamma^+ v$ and $\partial_n^+ v = \lambda$ reads: For $g \in H^2([0,T], H^{-\frac{1}{2}}(\Gamma))$ and $f \in H^2([0,T], H^{\frac{1}{2}}(\Gamma))$ find $u \in H^1([0,T], H^1(\Omega))$, $\phi \in H^1([0,T], H^{\frac{1}{2}}(\Gamma))$ and $\lambda \in H^1([0,T], H^{-\frac{1}{2}}(\Gamma))$ such that

$$
\begin{aligned}
&\mathcal{A}((u,\phi,\lambda),(w,\omega,m)) := a(u,w) - \langle \lambda, \gamma^- \dot{w}\rangle_{\Gamma\times[0,T]} \\
&+ \langle K\phi, \dot{m}\rangle_{\Gamma\times[0,T]} - \langle V\lambda, \dot{m}\rangle_{\Gamma\times[0,T]} - \langle \gamma^- u, \dot{m}\rangle_{\Gamma\times[0,T]} + \frac{1}{2}\langle \phi, \dot{m}\rangle_{\Gamma\times[0,T]} \\
&- \langle W\phi, \dot{\omega}\rangle_{\Gamma\times[0,T]} + \langle K'\lambda, \dot{\omega}\rangle_{\Gamma\times[0,T]} + \frac{1}{2}\langle \lambda, \dot{\omega}\rangle_{\Gamma\times[0,T]} \\
&= \langle g, \gamma^- \dot{w}\rangle_{\Gamma\times[0,T]} - \langle f, \dot{m}\rangle_{\Gamma\times[0,T]} \ .
\end{aligned} \tag{5.14}
$$

holds for all $w \in H^1([0,T], H^1(\Omega))$, $\omega \in H^1([0,T], H^{\frac{1}{2}}(\Gamma))$ and $m \in H^1([0,T], H^{-\frac{1}{2}}(\Gamma))$. Considering $\mathcal{A}((u,\gamma^+ v, \partial_n^+ v),(u,\gamma^+ v,\partial_n^+ v))$, doing the same steps back to (5.13), we get

$$
\begin{aligned}
&a(u,u) - \langle \partial_n^- u, \gamma^- \dot{u}\rangle_{\Gamma\times[0,T]} \\
&- \langle \partial_t(K(\gamma^+ v)), \partial_n^+ v\rangle_{\Gamma\times[0,T]} + \langle \partial_t(V(\partial_n^+ v)), \partial_n^+ v\rangle_{\Gamma\times[0,T]} + \frac{1}{2}\langle \gamma^+ \dot{v}, \partial_n^+ v\rangle_{\Gamma\times[0,T]} \\
&- \langle W(\gamma^+ v), \gamma^+ \dot{v}\rangle_{\Gamma\times[0,T]} + \langle (K'(\partial_n^+ v)), \gamma^+ \dot{v}\rangle_{\Gamma\times[0,T]} + \frac{1}{2}\langle \partial_n^+ v, \gamma^+ \dot{v}\rangle_{\Gamma\times[0,T]} = 0 \ .
\end{aligned} \tag{5.15}
$$

By using (5.1e) and (5.1f) we obtain

$$
\begin{aligned}
&a(u,u) - \langle g, \gamma^- \dot{u}\rangle_{\Gamma\times[0,T]} - \langle \partial_n^+ v, \gamma^- \dot{u}\rangle_{\Gamma\times[0,T]} - \langle \partial_t(K(\gamma^+ v)), \partial_n^+ v\rangle_{\Gamma\times[0,T]} \\
&+ \langle \partial_t(V(\partial_n^+ v)), \partial_n^+ v\rangle_{\Gamma\times[0,T]} + \langle \gamma^- \dot{u}, \partial_n^+ v\rangle_{\Gamma\times[0,T]} - \langle \dot{f}, \partial_n^+ v\rangle_{\Gamma\times[0,T]} \\
&- \langle W(\gamma^+ v), \gamma^+ \dot{v}\rangle_{\Gamma\times[0,T]} + \langle (K'(\partial_n^+ v)), \gamma^+ \dot{v}\rangle_{\Gamma\times[0,T]} = 0 \ .
\end{aligned} \tag{5.16}
$$

Therefore with integration by parts in time for the right hand side f:

$$
\begin{aligned}
&a(u,u) \\
&- \langle \partial_t(K(\gamma^+ v)), \partial_n^+ v\rangle_{\Gamma\times[0,T]} + \langle \partial_t(V(\partial_n^+ v)), \partial_n^+ v\rangle_{\Gamma\times[0,T]} \\
&- \langle W(\gamma^+ v), \gamma^+ \dot{v}\rangle_{\Gamma\times[0,T]} + \langle (K'(\partial_n^+ v)), \gamma^+ \dot{v}\rangle_{\Gamma\times[0,T]} = \langle g, \gamma^- \dot{u}\rangle_{\Gamma\times[0,T]} - \langle f, \partial_n^+ \dot{v}\rangle_{\Gamma\times[0,T]} \ .
\end{aligned} \tag{5.17}
$$

Now using (5.4), (5.5) and (5.11) we obtain a connection to the energy

$$E_\Omega(T) + E_{\Omega^c}(T) = \langle g, \gamma^- \dot{u} \rangle_{\Gamma\times([0,T]} - \langle f, \partial_n^+ \dot{v} \rangle_{\Gamma\times[0,T]} \ . \tag{5.18}$$

Defining the energy norm with $|\!|\!| (u,v) |\!|\!|^2 := E_\Omega(T) + E_{\Omega^c}(T)$, we get with $v = D\phi - S\lambda$, $\phi = \gamma^+ v$, $\lambda = \partial_n^+ v$, (5.14) and (5.18):

$$\begin{aligned} |\!|\!| (u,v) |\!|\!|^2 = E_\Omega(T) + E_{\Omega^c}(T) &= \frac{1}{2} \int_0^T \int_\Omega |\dot{u}|^2 + |\nabla u|^2 dx dt + \frac{1}{2} \int_0^T \int_{\Omega^c} |\dot{v}|^2 + |\nabla v|^2 dx dt \\ &= \langle g, \gamma^- \dot{u} \rangle_{\Gamma\times[0,T]} - \langle f, \partial_n^+ \dot{v} \rangle_{\Gamma\times[0,T]} = \mathcal{A}((u,\phi,\lambda),(u,\phi,\lambda)) \ . \end{aligned} \tag{5.19}$$

Hence we have a coercivity for $\mathcal{A}$.

We consider the same discretization as in Section 3.2. Therefore the Galerkin discretization of (5.14) reads: Find $u_h \in W_{h,\Delta t}^{p_1,q_1}$, $\phi_h \in V_{h',\Delta t}^{p_2,q_2}$, and $\lambda_h \in V_{h',\Delta t}^{p_3,q_3}$ such that

$$\mathcal{A}((u_h,\phi_h,\lambda_h),(w_h,\omega_h,m_h)) = \langle g, \gamma^- \dot{w}_h \rangle_{\Gamma\times[0,T]} - \langle f, \dot{m}_h \rangle_{\Gamma\times[0,T]} \tag{5.20}$$

for all $w_h \in W_{h,\Delta t}^{p_1,q_1}$, $\omega_h \in V_{h',\Delta t}^{p_2,q_2}$ and $m_h \in V_{h',\Delta t}^{p_3,q_3}$.

5.2.1 A priori error estimate

We state an a priori error estimate

Theorem 5.1. *Let* $(u,\phi,\lambda) \in H^1([0,T],H^1(\Omega)) \times H^1([0,T],H^{\frac{1}{2}}(\Gamma)) \times H^1([0,T],H^{-\frac{1}{2}}(\Gamma))$ *solve* (5.14) *and* $(u_h,\phi_h,\lambda_h) \in W_{h,\Delta t}^{p_1,q_1} \times V_{h',\Delta t}^{p_2,q_2} \times V_{h',\Delta t}^{p_3,q_3}$ *satisfy the corresponding Galerkin equation* (5.20)*. Then there hold*

$$\begin{aligned} &\|u-u_h\|_{0,1,\Omega\times[0,T]}^2 + \|\phi-\phi_h\|_{0,1/2,\Gamma\times[0,T]}^2 + \|\lambda-\lambda_h\|_{0,-1/2,\Gamma\times[0,T]}^2 \lesssim \\ &\inf_{\substack{w_h,\psi_h,\mu_h \\ \in W_{h,\Delta t}^{p_1,q_1}\times V_{h',\Delta t}^{p_2,q_2}\times V_{h',\Delta t}^{p_3,q_3}}} (1+\tfrac{1}{(\Delta t)^2}) \left\{ \|u-w_h\|_{0,1,\Omega\times[0,T]}^2 + \|\phi-\psi_h\|_{1,1/2,\Gamma\times[0,T]}^2 + \|\lambda-\mu_h\|_{1,-1/2,\Gamma\times[0,T]}^2 \right\}. \end{aligned}$$

Proof. Let $(u,\phi,\lambda) \in H^1([0,T],H^1(\Omega)) \times H^1([0,T],H^{1/2}(\Gamma)) \times H^1([0,T],H^{-1/2}(\Gamma))$ solve (5.14) and $(u_h,\phi_h,\lambda_h) \in W_{h,\Delta t}^{p_1,q_1} \times V_{h',\Delta t}^{p_2,q_2} \times V_{h',\Delta t}^{p_3,q_3}$ satisfy the corresponding Galerkin equation (5.20). Then with $(\tilde{u},\tilde{\phi},\tilde{\lambda}) \in W_{h,\Delta t}^{p_1,q_1} \times V_{h',\Delta t}^{p_2,q_2} \times V_{h',\Delta t}^{p_3,q_3}$ we get with the triangle inequality

$$\begin{aligned} &\|u-u_h\|_{0,1,\Omega\times[0,T]}^2 + \|\phi-\phi_h\|_{0,\frac{1}{2},\Gamma\times[0,T],*}^2 + \|\lambda-\lambda_h\|_{0,-\frac{1}{2},\Gamma\times[0,T],*}^2 \lesssim \|u-\tilde{u}\|_{0,1,\Omega\times[0,T]}^2 + \|\tilde{u}-u_h\|_{0,1,\Omega\times[0,T]}^2 \\ &+ \|\phi-\tilde{\phi}\|_{0,\frac{1}{2},\Gamma\times[0,T],*}^2 + \|\tilde{\phi}-\phi_h\|_{0,\frac{1}{2},\Gamma\times[0,T],*}^2 + \|\lambda-\tilde{\lambda}\|_{0,-\frac{1}{2},\Gamma\times[0,T],*}^2 + \|\tilde{\lambda}-\lambda_h\|_{0,-\frac{1}{2},\Gamma\times[0,T],*}^2 \ . \end{aligned}$$

With $\tilde{r} := D\tilde{\phi} - S\tilde{\lambda}$ and $v_h := D\phi_h - S\lambda_h$ with $\gamma^+(\tilde{r}-v_h) = \tilde{\phi}-\phi_h$ and $\partial_n^+(\tilde{r}-v_h) = \tilde{\lambda}-\lambda_h$, we

consider with the trace theorem (Lemma 9.4, 9.5), (5.19) and the Galerkin orthogonality

$$\begin{aligned}
&\|\tilde{u}-u_h\|^2_{0,1,\Omega\times[0,T]}+\|\tilde{\phi}-\phi_h\|^2_{0,\frac{1}{2},\Gamma\times[0,T],*}+\|\tilde{\lambda}-\lambda_h\|^2_{0,-\frac{1}{2},\Gamma\times[0,T],*}\lesssim\|\tilde{u}-u_h\|^2_{0,1,\Omega\times[0,T]}+\|\tilde{r}-v_h\|^2_{0,1,\Omega^c\times[0,T]}\\
&\lesssim |\!|\!|(\tilde{u}-u_h),(\tilde{r}-v_h)|\!|\!|^2\\
&=\mathcal{A}(\begin{pmatrix}\tilde{u}-u_h\\ \tilde{\phi}-\phi_h\\ \tilde{\lambda}-\lambda_h\end{pmatrix}^T,\begin{pmatrix}\tilde{u}-u_h\\ \tilde{\phi}-\phi_h\\ \tilde{\lambda}-\lambda_h\end{pmatrix}^T)=\mathcal{A}(\begin{pmatrix}\tilde{u}-u\\ \tilde{\phi}-\phi\\ \tilde{\lambda}-\lambda\end{pmatrix}^T,\begin{pmatrix}\tilde{u}-u_h\\ \tilde{\phi}-\phi_h\\ \tilde{\lambda}-\lambda_h\end{pmatrix}^T)+\mathcal{A}(\begin{pmatrix}u-u_h\\ \phi-\phi_h\\ \lambda-\lambda_h\end{pmatrix}^T,\begin{pmatrix}\tilde{u}-u_h\\ \tilde{\phi}-\phi_h\\ \tilde{\lambda}-\lambda_h\end{pmatrix}^T)\\
&=\mathcal{A}(\begin{pmatrix}\tilde{u}-u\\ \tilde{\phi}-\phi\\ \tilde{\lambda}-\lambda\end{pmatrix}^T,\begin{pmatrix}\tilde{u}-u_h\\ \tilde{\phi}-\phi_h\\ \tilde{\lambda}-\lambda_h\end{pmatrix}^T)\ .
\end{aligned}$$

Now consider every term separately

$$\begin{aligned}
&\int_0^T\int_\Omega\partial_t^2(\tilde{u}-u)\partial_t(\tilde{u}-u_h)dxdt+\int_0^T\int_\Omega\nabla(\tilde{u}-u)\nabla(\partial_t(\tilde{u}-u_h))dxdt\\
&\lesssim\|\partial_t^2(\tilde{u}-u)\|_{0,-1,\Omega\times[0,T]}\|\partial_t(\tilde{u}-u_h)\|_{0,1,\Omega\times[0,T]}+\|\nabla(\tilde{u}-u)\|_{0,0,\Omega\times[0,T]}\|\nabla(\partial_t(\tilde{u}-u_h))\|_{0,0,\Omega\times[0,T]}\\
&\lesssim\|\tilde{u}-u\|_{0,1,\Omega\times[0,T]}\|(\tilde{u}-u_h)\|_{1,1,\Omega\times[0,T]}+\|\tilde{u}-u\|_{0,1,\Omega\times[0,T]}\|(\tilde{u}-u_h)\|_{1,1,\Omega\times[0,T]}\\
&\lesssim\|\tilde{u}-u\|_{0,1,\Omega\times[0,T]}\|(\tilde{u}-u_h)\|_{1,1,\Omega\times[0,T]}\ .
\end{aligned}$$

With the inverse estimate and Young's inequality we get for small $\epsilon>0$:

$$\|\tilde{u}-u\|_{0,1,\Omega\times[0,T]}\|(\tilde{u}-u_h)\|_{1,1,\Omega\times[0,T]}\lesssim\tfrac{1}{\epsilon(\Delta t)^2}\|\tilde{u}-u\|^2_{0,1,\Omega\times[0,T]}+\epsilon\|(\tilde{u}-u_h)\|^2_{0,1,\Omega\times[0,T]}\ .$$

Next for the first coupling contribution, with the inverse estimate and Young's inequality

$$\begin{aligned}
&-\langle\tilde{\lambda}-\lambda,\gamma^-(\partial_t(\tilde{u}-u_h))\rangle_{\Gamma\times[0,T]}\lesssim\|\tilde{\lambda}-\lambda\|_{0,-1/2,\Gamma\times[0,T]}\|\gamma^-(\partial_t(\tilde{u}-u_h)\|_{0,1/2,\Gamma\times[0,T]}\\
&\lesssim\|\tilde{\lambda}-\lambda\|_{0,-1/2,\Gamma\times[0,T]}\|\gamma^-(\tilde{u}-u_h)\|_{1,1/2,\Gamma\times[0,T]}\lesssim\|\tilde{\lambda}-\lambda\|_{0,-1/2,\Gamma\times[0,T]}\|\tilde{u}-u_h\|_{1,1,\Omega\times[0,T]}\\
&\lesssim\|\tilde{\lambda}-\lambda\|_{0,-1/2,\Gamma\times[0,T]}(\Delta t)^{-1}\|(\tilde{u}-u_h)\|_{0,1,\Omega\times[0,T]}\\
&\lesssim\tfrac{1}{\epsilon(\Delta t)^2}\|\tilde{\lambda}-\lambda\|^2_{0,-1/2,\Gamma\times[0,T],*}+\epsilon\|(\tilde{u}-u_h)\|^2_{0,1,\Omega\times[0,T]}\ .
\end{aligned}$$

Now estimating the retarded single and double layer potential:

$$\begin{aligned}
&\langle(K+\frac{1}{2}I)(\tilde{\phi}-\phi)-V(\tilde{\lambda}-\lambda),\partial_t(\tilde{\lambda}-\lambda_h)\rangle_{\Gamma\times[0,T]}\\
&\lesssim\|(K+\frac{1}{2}I)(\tilde{\phi}-\phi)-V(\tilde{\lambda}-\lambda)\|_{0,1/2,\Gamma\times[0,T]}\|\partial_t(\tilde{\lambda}-\lambda_h)\|_{0,-1/2,\Gamma\times[0,T]}\\
&(\|(K+\frac{1}{2}I)(\tilde{\phi}-\phi)\|_{0,1/2,\Gamma\times[0,T]}+\|V(\tilde{\lambda}-\lambda)\|_{0,1/2,\Gamma\times[0,T]})\|\tilde{\lambda}-\lambda_h\|_{1,-1/2,\Gamma\times[0,T],*}\\
&\lesssim(\|\tilde{\phi}-\phi\|_{1,1/2,\Gamma\times[0,T],*}+\|\tilde{\lambda}-\lambda\|_{1,-1/2,\Gamma\times[0,T],*})\|\tilde{\lambda}-\lambda_h\|_{1,-1/2,\Gamma\times[0,T],*})\\
&\lesssim\tfrac{1}{\epsilon(\Delta t)^2}\|\tilde{\phi}-\phi\|^2_{1,1/2,\Gamma\times[0,T],*}+\tfrac{1}{\epsilon(\Delta t)^2}\|\tilde{\lambda}-\lambda\|^2_{1,-1/2,\Gamma\times[0,T],*}+\epsilon\|\tilde{\lambda}-\lambda_h\|^2_{1,-1/2,\Gamma\times[0,T],*}\ ,
\end{aligned}$$

where we used the mapping properties of V and K, the inverse estimate and Young's inequality. We continue with the other coupling contribution:

$$\begin{aligned}
&-\langle\gamma^-(\tilde{u}-u),\partial_t(\tilde{\lambda}-\lambda_h)\rangle_{\Gamma\times[0,T]}\lesssim\|\gamma^-(\tilde{u}-u)\|_{0,1/2,\Gamma\times[0,T]}\|\partial_t(\tilde{\lambda}-\lambda_h)\|_{0,-1/2,\Gamma\times[0,T]}\\
&\lesssim\|\tilde{u}-u\|_{0,1,\Gamma\times[0,T]}\|\tilde{\lambda}-\lambda_h\|_{1,-1/2,\Gamma\times[0,T],*}\lesssim\tfrac{1}{\epsilon(\Delta t)^2}\|\tilde{u}-u\|^2_{0,1,\Gamma\times[0,T]}+\epsilon\|\tilde{\lambda}-\lambda_h\|^2_{0,-1/2,\Gamma\times[0,T],*},
\end{aligned}$$

where we used the trace theorem, the inverse estimate and Young's inequality. Next

$$\begin{aligned}
&\langle -W(\tilde{\phi}-\phi)+(K'+\frac{1}{2}I)(\tilde{\lambda}-\lambda), \partial_t(\tilde{\phi}-\phi_h)\rangle_{\Gamma\times[0,T]} \\
&\lesssim \|-W(\tilde{\phi}-\phi)+(K'+\frac{1}{2}I)(\tilde{\lambda}-\lambda)\|_{0,-\frac{1}{2},\Gamma\times[0,T]} \|\partial_t(\tilde{\phi}-\phi_h)\|_{0,\frac{1}{2},\Gamma\times[0,T]} \|\partial_t(\tilde{\phi}-\phi_h)\|_{0,\frac{1}{2},\Gamma\times[0,T]} \\
&\lesssim (\|W(\tilde{\phi}-\phi)\|_{0,-1/2,\Gamma\times[0,T]} + \|(K'+\frac{1}{2}I)(\tilde{\lambda}-\lambda)\|_{0,-1/2,\Gamma\times[0,T]}) \|\tilde{\phi}-\phi_h\|_{1,1/2,\Gamma\times[0,T]} \\
&\lesssim \tfrac{1}{\epsilon(\Delta t)^2}\|\tilde{\phi}-\phi\|^2_{1,1/2,\Gamma\times[0,T],*} + \tfrac{1}{\epsilon(\Delta t)^2}\|\tilde{\lambda}-\lambda\|^2_{1,-1/2,\Gamma\times[0,T],*} + \epsilon\|\tilde{\phi}-\phi_h\|^2_{0,1/2,\Gamma\times[0,T],*},
\end{aligned}$$

where we used the mapping properties of W and K', the inverse estimate and Young's inequality. At last combining all $\epsilon\|\tilde{u}-u_h\|^2_{0,1,\Omega\times[0,T]}, \epsilon\|\tilde{\phi}-\phi_h\|^2_{0,\frac{1}{2},\Gamma\times[0,T],*}, \epsilon\|\tilde{\lambda}-\lambda_h\|^2_{0,-\frac{1}{2},\Gamma\times[0,T],*}$ with the left hand side, gives

$$\begin{aligned}
&\|\tilde{u}-u_h\|^2_{0,1,\Omega\times[0,T]} + \|\tilde{\phi}-\phi_h\|^2_{0,1/2,\Gamma\times[0,T],*} + \|\tilde{\lambda}-\lambda_h\|^2_{0,-1/2,\Gamma\times[0,T],*} \lesssim \\
&\frac{1}{(\Delta t)^2}\|\tilde{u}-u\|^2_{0,1,\Omega\times[0,T]} + \frac{1}{(\Delta t)^2}\|\tilde{\phi}-\phi\|^2_{1,1/2,\Gamma\times[0,T],*} + \frac{1}{(\Delta t)^2}\|\tilde{\lambda}-\lambda\|^2_{1,-1/2,\Gamma\times[0,T],*} .
\end{aligned}$$

Therefore

$$\begin{aligned}
&\|u-u_h\|^2_{0,1,\Omega\times[0,T]} + \|\phi-\phi_h\|^2_{0,1/2,\Gamma\times[0,T],*} + \|\lambda-\lambda_h\|^2_{0,-1/2,\Gamma\times[0,T],*} \\
&\lesssim (1+\frac{1}{(\Delta t)^2})(\|\tilde{u}-u\|^2_{0,1,\Omega\times[0,T]} + \|\tilde{\phi}-\phi\|^2_{1,1/2,\Gamma\times[0,T],*} + \|\tilde{\lambda}-\lambda\|^2_{1,-1/2,\Gamma\times[0,T],*}) .
\end{aligned}$$

Taking the infimum yields the assertion. □

5.2.2 A posteriori error estimate

We state the following a posteriori error estimate

Theorem 5.2. *Let* $(u,\phi,\lambda) \in H^1([0,T],H^1(\Omega)) \times H^1([0,T],H^{\frac{1}{2}}(\Gamma)) \times H^1([0,T],H^{-\frac{1}{2}}(\Gamma))$ *and* $(u_h,\phi_h,\lambda_h) \in W^{p_1,q_1}_{h,\Delta t} \times V^{p_2,q_2}_{h',\Delta t}, V^{p_3,q_3}_{h',\Delta t}$ *satisfy the wave wave coupling problem* (5.14) *resp. the corresponding Galerkin equation* (5.20). *Let* $\cup_{j=1}^{N_s}\partial\Omega_j = \tilde{T} = \cup_{i=1}^{m} T_i$, *where each* T_i *is a face of one* Ω_j. *With* $[v]$, *a jump into a face* T_i *the following a posteriori error estimate holds:*

$$\|u_h-u\|^2_{0,1,\Omega\times[0,T]} + \|\phi_h-\phi\|^2_{0,1/2,\Gamma\times[0,T]} + \|\lambda_h-\lambda\|^2_{0,-1/2,\Gamma\times[0,T]} \lesssim \eta_1^2+\eta_2^2+\eta_3^2+\eta_4^2+\eta_5^2$$

where

$$\begin{aligned}
\eta_1^2 &= \sum_{\Omega_i} \|\ddot{u}_h - \Delta u_h\|^2_{0,0,\Omega_i\times[0,T]}, \\
\eta_2^2 &= \sum_{T_i\cap\Gamma=\varnothing} \|[\tfrac{\partial u_h}{\partial n}]\|^2_{1,0,T_i\times[0,T]} \max\{\Delta t,h\}, \\
\eta_3^2 &= \|-\lambda_h - g + \partial_n^- u_h\|^2_{1,0,\Gamma\times[0,T]} \max\{\Delta t,h\} , \\
\eta_4^2 &= \|(K+\frac{1}{2}I)\phi_h - V\lambda_h - \gamma^-(u_h) + f\|^2_{1,1/2,\Gamma\times[0,T]} , \\
\eta_5^2 &= \|(K'+\frac{1}{2}I)\lambda_h - W\phi_h\|^2_{1,-1/2,\Gamma\times[0,T]} .
\end{aligned}$$

Proof. Let $(u,\phi,\lambda) \in H^1([0,T],H^1(\Omega)) \times H^1([0,T],H^{1/2}(\Gamma)) \times H^1([0,T],H^{-1/2}(\Gamma))$ and $(u_h,\phi_h,\lambda_h) \in W^{p_1,q_1}_{h,\Delta t} \times V^{p_2,q_2}_{h',\Delta t}, V^{p_3,q_3}_{h',\Delta t}$ satisfy (5.14) resp. the corresponding Galerkin discretization (5.20). We define $v := D\phi - S\lambda$ and $v_h := D\phi_h - S\lambda_h$ with $\gamma^+(v-v_h) = \phi - \phi_h$ and $\partial_n^+(v-v_h) = \lambda - \lambda_h$. Then by using the trace theorem together with (5.19)

$$\|u_h-u\|^2_{0,1,\Omega\times[0,T]} + \|\phi_h-\phi\|^2_{0,\frac{1}{2},\Gamma\times[0,T]} + \|\lambda_h-\lambda\|^2_{0,-\frac{1}{2},\Gamma\times[0,T]} \lesssim \|u_h-u\|^2_{0,1,\Omega\times[0,T]} + \|v_h-v\|^2_{0,1,\Omega^c\times[0,T]}$$

$$\lesssim |\!|\!|((u_h-u),(v_h-v))|\!|\!|^2 = \mathcal{A}\left(\begin{pmatrix} u_h-u \\ \phi_h-\phi \\ \lambda_h-\lambda \end{pmatrix}^T, \begin{pmatrix} u_h-u \\ \phi_h-\phi \\ \lambda_h-\lambda \end{pmatrix}^T\right)$$

$$= \mathcal{A}\left(\begin{pmatrix} u_h \\ \phi_h \\ \lambda_h \end{pmatrix}^T, \begin{pmatrix} u_h-u \\ \phi_h-\phi \\ \lambda_h-\lambda \end{pmatrix}^T\right) - \mathcal{A}\left(\begin{pmatrix} u \\ \phi \\ \lambda \end{pmatrix}^T, \begin{pmatrix} u_h-u \\ \phi_h-\phi \\ \lambda_h-\lambda \end{pmatrix}^T\right) = \mathcal{A}\left(\begin{pmatrix} u_h \\ \phi_h \\ \lambda_h \end{pmatrix}^T, \begin{pmatrix} u_h-u \\ \phi_h-\phi \\ \lambda_h-\lambda \end{pmatrix}^T\right) - F\left(\begin{pmatrix} u_h-u \\ \phi_h-\phi \\ \lambda_h-\lambda \end{pmatrix}^T\right)$$

$$= \mathcal{A}\left(\begin{pmatrix} u_h \\ \phi_h \\ \lambda_h \end{pmatrix}^T, \begin{pmatrix} u_h-\tilde{u} \\ \phi_h-\tilde{\phi} \\ \lambda_h-\tilde{\lambda} \end{pmatrix}^T\right) + \mathcal{A}\left(\begin{pmatrix} u_h \\ \phi_h \\ \lambda_h \end{pmatrix}^T, \begin{pmatrix} \tilde{u}-u \\ \tilde{\phi}-\phi \\ \tilde{\lambda}-\lambda \end{pmatrix}^T\right) - F\left(\begin{pmatrix} u_h-\tilde{u} \\ \phi_h-\tilde{\phi} \\ \lambda_h-\tilde{\lambda} \end{pmatrix}^T\right) - F\left(\begin{pmatrix} \tilde{u}-u \\ \tilde{\phi}-\phi \\ \tilde{\lambda}-\lambda \end{pmatrix}^T\right).$$

By using the Galerkin orthogonality above, we get

$$|\!|\!|((u_h-u),(v_h-v))|\!|\!|^2$$

$$= \mathcal{A}\left(\begin{pmatrix} u_h \\ \phi_h \\ \lambda_h \end{pmatrix}^T, \begin{pmatrix} \tilde{u}-u \\ \tilde{\phi}-\phi \\ \tilde{\lambda}-\lambda \end{pmatrix}^T\right) - F\left(\begin{pmatrix} \tilde{u}-u \\ \tilde{\phi}-\phi \\ \tilde{\lambda}-\lambda \end{pmatrix}^T\right) = \int_0^T \{ \int_\Omega \ddot{u}_h \partial_t(\tilde{u}-u)dx + \int_\Omega \nabla u_h \nabla(\partial_t(\tilde{u}-u))dx$$

$$- \int_\Gamma \lambda_h \gamma^-(\partial_t(\tilde{u}-u))ds_x + \int_\Gamma (K+\frac{1}{2}I)\phi_h \partial_t(\tilde{\lambda}-\lambda)ds_x - \int_\Gamma V\lambda_h \partial_t(\tilde{\lambda}-\lambda)ds_x$$

$$- \int_\Gamma \gamma^-(u_h)\partial_t(\tilde{\lambda}-\lambda)ds_x - \int_\Gamma W\phi_h \partial_t(\tilde{\phi}-\phi)ds_x + \int_\Gamma (K'+\frac{1}{2}I)\lambda_h \partial_t(\tilde{\phi}-\phi)ds_x$$

$$- \int_\Gamma g\ \gamma^-(\partial_t(\tilde{u}-u))ds_x + \int_\Gamma f\ \partial_t(\tilde{\lambda}-\lambda)ds_x\}dt$$

$$= \int_0^T \{ \sum_{\Omega_i} \int_{\Omega_i} \ddot{u}_h \partial_t(\tilde{u}-u)dx + \int_{\Omega_i} \nabla u_h \nabla(\partial_t(\tilde{u}-u))dx - \int_\Gamma (\lambda_h+g)\partial_t(\tilde{u}-u)ds_x$$

$$+ \int_\Gamma ((K+\frac{1}{2}I)\phi_h - V\lambda_h - \gamma^-(u_h)+f)\partial_t(\tilde{\lambda}-\lambda)ds_x + \int_\Gamma ((K'+\frac{1}{2}I)\lambda_h - W\phi_h)\partial_t(\tilde{\phi}-\phi)ds_x\}dt\ .$$

Next using integration by parts on each Ω_i, and estimating

$$|\!|\!|((u_h-u),(v_h-v))|\!|\!|^2$$

$$= \int_0^T \Big\{ \sum_{\Omega_i} \int_{\Omega_i} (\ddot{u}_h - \Delta u_h)\partial_t(\tilde{u}-u)dx + \sum_{T_i \cap \Gamma = \varnothing} \int_{T_i} [\frac{\partial^- u_h}{\partial n}](\partial_t(\tilde{u}-u))ds_x$$

$$+ \int_\Gamma (-\lambda_h - g + \frac{\partial^- u_h}{\partial n})\gamma^-(\partial_t(\tilde{u}-u))ds_x + \int_\Gamma ((K+\frac{1}{2}I)\phi_h - V\lambda_h - \gamma^-(u_h)+f)\partial_t(\tilde{\lambda}-\lambda)ds_x$$

$$+ \int_\Gamma ((K'+\frac{1}{2}I)\lambda_h - W\phi_h)\partial_t(\tilde{\phi}-\phi)ds_x\Big\}dt$$

$$
\begin{aligned}
&\lesssim \sum_{\Omega_i} \|\ddot{u}_h - \Delta u_h\|_{0,0,\Omega_i\times[0,T]} \|\partial_t(\tilde{u}-u)\|_{0,0,\Omega_i\times[0,T]} + \sum_{T_i\cap\Gamma=\varnothing} \|[\frac{\partial u_h}{\partial n}]\|_{1,0,T_i\times[0,T]} \|\partial_t(\tilde{u}-u)\|_{-1,0,T_i\times[0,T]} \\
&+ \|-\lambda_h - g + \partial_n^- u_h\|_{1,0,\Gamma\times[0,T]} \|\gamma^-(\partial_t(\tilde{u}-u))\|_{-1,0,\Gamma\times[0,T]} \\
&+ \|(K+\frac{1}{2}I)\phi_h - V\lambda_h - \gamma^-(u_h) + f\|_{1,\frac{1}{2},\Gamma\times[0,T]} \|\partial_t(\tilde{\lambda}-\lambda)\|_{-1,-\frac{1}{2},\Gamma\times[0,T]} \\
&+ \|(K'+\frac{1}{2}I)\lambda_h - W\phi_h\|_{1,-1/2,\Gamma\times[0,T]} \|\partial_t(\tilde{\phi}-\phi)\|_{-1,1/2,\Gamma\times[0,T]} \\
&\lesssim \sum_{\Omega_i} \|\ddot{u}_h - \Delta u_h\|_{0,0,\Omega_i\times[0,T]} \|\tilde{u}-u\|_{0,1,\Omega_i} + \sum_{T_i\cap\Gamma=\varnothing} \|[\frac{\partial u_h}{\partial n}]\|_{1,0,T_i\times[0,T]} \|\tilde{u}-u\|_{0,0,T_i\times[0,T]} \\
&+ \|-\lambda_h - g + \partial_n^- u_h\|_{1,0,\Gamma\times[0,T]} \|\gamma^-(\tilde{u}-u)\|_{0,0,\Gamma\times[0,T]} \\
&+ \|(K+\frac{1}{2}I)\phi_h - V\lambda_h - \gamma^-(u_h) + f\|_{1,1/2,\Gamma\times[0,T]} \|\tilde{\lambda}-\lambda\|_{0,-1/2,\Gamma\times[0,T]} \\
&+ \|(K'+\frac{1}{2}I)\lambda_h - W\phi_h\|_{1,-1/2,\Gamma\times[0,T]} \|\tilde{\phi}-\phi\|_{0,1/2,\Gamma\times[0,T]} \ .
\end{aligned}
$$

Next choose $\tilde{u} = u_h + \Pi_h \circ \Pi_{\Delta t}(u - u_h)$ for the second and third term in order to do Lemma 3.1. Further choose $\tilde{u} = u_h$ for the first term and $\tilde{\phi} = \phi_h$ and $\tilde{\lambda} = \lambda_h$.

$$
\begin{aligned}
&|||((u_h-u),(v_h-v))|||^2 \lesssim \sum_{\Omega_i} \|\ddot{u}_h - \Delta u_h\|_{0,0,\Omega_i\times[0,T]} \|u_h-u\|_{0,1,\Omega_i\times[0,T]} \\
&+ \sum_{T_i\cap\Gamma=\varnothing} \|[\frac{\partial u_h}{\partial n}]\|_{1,0,T_i\times[0,T]} \|u_h-u\|_{0,1/2,T_i} \max\{\Delta t, h\}^{1/2} \\
&+ \|-\lambda_h - g + \partial_n^- u_h\|_{1,0,\Gamma\times[0,T]} \|\gamma^-(u_h-u)\|_{0,1/2,\Gamma\times[0,T]} \max\{\Delta t, h\}^{1/2} \\
&+ \|(K+\frac{1}{2}I)\phi_h - V\lambda_h - \gamma^-(u_h) + f\|_{1,1/2,\Gamma\times[0,T]} \|\lambda_h-\lambda\|_{0,-1/2,\Gamma} \\
&+ \|(K'+\frac{1}{2}I)\lambda_h - W\phi_h\|_{1,-1/2,\Gamma\times[0,T]} \|\phi_h-\phi\|_{0,1/2,\Gamma\times[0,T]} \ .
\end{aligned}
$$

Using Young's inequality and the trace theorem

$$
\begin{aligned}
&|||((u_h-u),(v_h-v))|||^2 \lesssim \sum_{\Omega_i} \|\ddot{u}_h - \Delta u_h\|^2_{0,0,\Omega_i\times[0,T]} + \sum_{T_i\cap\Gamma=\varnothing} \|[\frac{\partial u_h}{\partial n}]\|^2_{1,0,T_i\times[0,T]} \max\{\Delta t, h\} \\
&+ \|-\lambda_h - g + \partial_n^- u_h\|^2_{1,0,\Gamma\times[0,T]} \max\{\Delta t, h\} + \|(K+\frac{1}{2}I)\phi_h - V\lambda_h - \gamma^-(u_h) + f\|^2_{1,1/2,\Gamma\times[0,T]} \\
&+ \|(K'+\frac{1}{2}I)\lambda_h - W\phi_h\|^2_{1,-1/2,\Gamma\times[0,T]} \\
&+ \|\phi_h-\phi\|^2_{0,1/2,\Gamma\times[0,T]} + \|\lambda_h-\lambda\|^2_{0,-1/2,\Gamma\times[0,T]} + \|u_h-u\|^2_{0,1,\Omega\times[0,T]} \ .
\end{aligned}
$$

Combining the last three terms with the left hand side yields the estimate. □

5.2.3 Discretization of the symmetric wave-wave coupling

We choose as ansatz and test functions in space and time:

- $u_{h,\Delta t} = \sum_{m=1}^{N_t} \sum_{i=1}^{N_s} u_i^m \beta_{\Delta t}^m(t) \eta_h^i(x) \in W_{h,\Delta t}^{1,1}$ piecewise linear in time and piecewise linear in the interior space $\overline{\Omega}$

- $\dot{w}_{h,\Delta t} = \eta_h^l(x)\gamma_{\Delta t}^n(t) \in W_{h,\Delta t}^{1,0}$ piecewise constant in time and in piecewise linear in the interior space $\overline{\Omega}$ with $l = 1, \ldots, N_s$ and $n = 1, \ldots, N_t$
- $\lambda_{h,\Delta t} = \sum_{m=1}^{N_t} \sum_{i=1}^{N_{s'}} \lambda_i^m \beta_{\Delta t}^m(t)\xi_h^i(x) \in V_{h,\Delta t}^{1,1}$ piecewise linear in time and pieceweise linear in space Γ
- $\omega_{h,\Delta t} = \gamma_{\Delta t}^n(t)\xi_h^j(x) \in V_{h,\Delta t}^{1,0}$ piecewiese constant in time and piecewise linear in space in Γ for $n = 1, \ldots N_t$ and $j = 1, \ldots, N_{s'}$
- $\phi_{h,\Delta t} = \sum_{m=1}^{N_t} \sum_{i=1}^{N_s} \phi_i^m \beta_{\Delta t}^m(t)\xi_h^i(x) \in V_{h,\Delta t}^{1,1}$ piecewise linear in time and piecewise linear in space Γ
- $\dot{m}_{h,\Delta t} = \gamma_{\Delta t}^n(t)\xi_h^i(x) \in V_{h,\Delta t}^{1,0}$ piecewise constant in time and piecewise linear in space Γ for $n = 1, \ldots N_t$ and $i = 1, \ldots, N_{s'}$

We begin with the discretization of $a(u, w)$:

$$a(u_{h,\Delta t}, w_{h,\Delta t}) = \int_{\mathbb{R}^+} \int_\Omega \ddot{u}_{h,\Delta t}\dot{w}_{h,\Delta t} + \nabla(u_{h,\Delta t})\nabla(\dot{w}_{h,\Delta t})dxdt$$

we perform the calculation in the same way as in Section 3.6. The second term gives for $l = 1, \ldots N_s$ and $n = 1, \ldots, N_t$:

$$\begin{aligned}
&\int_0^\infty \int_{\Omega^-} \nabla(u_{h,\Delta t})\nabla(\dot{w}_{h,\Delta t})dxdt \\
&= \int_0^\infty \int_{\Omega^-} \sum_{k=1}^{N_t} \sum_{i=1}^{N_s} u_i^k \beta_{\Delta t}^k(t) \left(\nabla(\eta_h^i(x))\nabla(\eta_h^l(x))\right) \gamma_{\Delta t}^n(t)dxdt \\
&= \sum_{k=1}^{N_t} \sum_{i=1}^{N_s} u_i^k \left(\int_{\Omega^-} \nabla(\eta_h^i(x))\nabla(\eta_h^l(x))dx\right)\left(\int_0^\infty \beta_{\Delta t}^k(t)\gamma_{\Delta t}^n(t)dt\right) \\
&= \sum_{i=1}^{N_s} \left(\int_{\Omega^-} \nabla(\eta_h^i(x))\nabla(\eta_h^l(x))dx\right)(\Delta t) \cdot \begin{cases} \frac{1}{2}u_i^1 & , n = 1 \\ \frac{u_i^n + u_i^{n-1}}{2} & , n \geq 2 \end{cases} \\
&=: \sum_{i=1}^{N_s} A_{(i,l)}(\Delta t) \cdot \begin{cases} \frac{1}{2}u_i^1 & , n = 1 \\ \frac{u_i^n + u_i^{n-1}}{2} & , n \geq 2 \end{cases} \\
&= Au_A \ ,
\end{aligned} \tag{5.21}$$

where A is the stiffness matrix for the Laplacian with

$$u_A = (\Delta t) \cdot \begin{cases} \frac{1}{2}u^1 & , n = 1 \\ \frac{u^n + u^{n-1}}{2} & , n \geq 2 \end{cases}$$

and u^k containing all u_i^k.

Considering the first term

$$
\begin{aligned}
&= \int_0^\infty \int_{\Omega^-} \ddot{u}_{h,\Delta t} \cdot \dot{w}_{h,\Delta t} dx dt = \int_0^\infty \int_{\Omega^-} \sum_{k=1}^{N_t} \sum_{i=1}^{N_s} u_i^k \ddot{\beta}_{\Delta t}^k(t) \eta_h^i(x) \eta_h^l(x) \gamma_{\Delta t}^n(t) dx dt \\
&= \sum_{k=1}^{N_t} \sum_{\nu=1}^{3} \sum_{i=1}^{N_s} u_{\nu,i}^k \left(\int_{\Omega^-} \eta_h^i(x) \eta_h^l(x) dx \right) \left(\int_0^\infty \ddot{\beta}_k(t) \gamma^n(t) dt \right) \\
&= \sum_{i=1}^{N_s} \left(\int_{\Omega^-} \eta_h^i(x) \eta_h^l(x) dx \right) \frac{1}{(\Delta t)} \cdot \begin{cases} u_i^1 & , n = 1 \\ u_i^2 - 2u_i^1 & , n = 2 \\ u_i^n - 2u_i^{n-1} + u_i^{n-2} & , n \geq 3 \end{cases} \\
&=: \sum_{i=1}^{N_s} M_{(i,l)} \frac{1}{(\Delta t)} \cdot \begin{cases} u_i^1 & , n = 1 \\ u_i^2 - 2u_i^1 & , n = 2 \\ u_i^n - 2u_i^{n-1} + u_i^{n-2} & , n \geq 3 \end{cases} \\
&= M u_M \ , \qquad (5.22)
\end{aligned}
$$

where M is the mass matrix with

$$
u_M = \frac{1}{(\Delta t)} \cdot \begin{cases} u^1 & , n = 1 \\ u^2 - 2u^1 & , n = 2 \\ u^n - 2u^{n-1} + u^{n-2} & , n \geq 3 \ . \end{cases}
$$

We divide u^n into $\begin{pmatrix} (u_{\Omega \setminus \Gamma}^n) \\ (u_\Gamma^n) \end{pmatrix}$. The coupling part will need (u_Γ^n). The boundary element part is discretized in the same way as in Subsection 2.3.6. The discretization of the coupling part is as follows: For $n = 1, \dots N_t$, $j = 1, \dots N_{s'}$ and $l = 1, \dots, N_s$, we obtain

$$
\begin{aligned}
&\sum_{m=1}^{N_t} \sum_{i=1}^{N_s} u_i^m \int_\Gamma \eta_h^i|_\Gamma(x) \xi_h^j(x) ds_x \left(\int_0^\infty \beta_{\Delta t}^m(t) \gamma_{\Delta t}^n(t) dt \right) \\
&= \sum_{i=1}^{N_s} \int_\Gamma (u_i^n + u_i^{n-1}) \frac{\Delta t}{2} \eta_h^i|_\Gamma(x) \xi_h^j(x) ds_x =: RI \frac{\Delta t}{2} (u_\Gamma^n + u_\Gamma^{n-1}) \ ,
\end{aligned}
$$

$$
\begin{aligned}
&\sum_{m=1}^{N_t} \sum_{i=1}^{N_{s'}} \lambda_i^m \int_\Gamma \xi_h^i(x) \eta_h^l|_\Gamma(x) ds_x \left(\int_0^\infty \beta_{\Delta t}^m(t) \gamma_{\Delta t}^n(t) dt \right) \\
&= \sum_{i=1}^{N_s} \int_\Gamma (\lambda_i^n + \lambda_i^{n-1}) \frac{\Delta t}{2} \xi_h^i(x) \eta_h^l|_\Gamma(x) ds_x =: RI \frac{\Delta t}{2} (\lambda^n + \lambda^{n-1}) \ .
\end{aligned}
$$

For the right hand side:

$$
\int_{\mathbb{R}_+} \int_\Gamma g \dot{w}_{h,\Delta t} ds_x dt = \frac{(\Delta t)}{2} \int_\Gamma (g^n + g^{n-1}) \eta_h^l|_\Gamma(x) ds_x =: G^n + G^{n-1} \ , \qquad (5.23)
$$

$$
\int_{\mathbb{R}_+} \int_\Gamma f \dot{m}_{h,\Delta t} ds_x dt = \int_\Gamma (f^{n-1} - f^n) \xi_h^j(x) ds_x =: -F^n + F^{n-1} \ , \qquad (5.24)
$$

where $g^n = g(x,t_n), g \approx \sum_{m=1}^{N_t} g^m \beta_{\Delta t}^m(t)$ and $f^n = f(x,t_n), f \approx \sum_{m=1}^{N_t} f^m \gamma_{\Delta t}^m(t)$.

Altogether we obtain a marching-on-in time scheme: For $n = 1$:

$$\begin{pmatrix} \frac{\Delta t}{2}A + \frac{1}{\Delta t}M & [0, -\frac{\Delta t}{2}RI]^T & 0 \\ -[0, \frac{\Delta t}{2}RI] & -V^0 & K^0 - \frac{1}{2}I \\ 0 & (K')^0 + \frac{1}{2}\frac{\Delta t}{2}I & -W^0 \end{pmatrix} \begin{pmatrix} u^1 \\ \lambda^1 \\ \phi^1 \end{pmatrix} = \begin{pmatrix} G^1 + G^0 \\ F^1 - F^0 \\ 0 \end{pmatrix} .$$

For $n = 2$:

$$\begin{pmatrix} \frac{\Delta t}{2}A + \frac{1}{\Delta t}M & [0, -\frac{\Delta t}{2}RI]^T & 0 \\ -[0, \frac{\Delta t}{2}RI] & -V^0 & K^0 - \frac{1}{2}I \\ 0 & (K')^0 + \frac{1}{2}\frac{\Delta t}{2}I & -W^0 \end{pmatrix} \begin{pmatrix} u^2 \\ \lambda^2 \\ \phi^2 \end{pmatrix}$$
$$= \begin{pmatrix} G^2 + G^1 - \frac{\Delta t}{2}Au^1 + \frac{2}{\Delta t}Mu^1 + [0; \frac{\Delta t}{2}RI\lambda^1]^T \\ F^2 - F^1 + \frac{\Delta t}{2}RIu_\Gamma^1 + V^1\lambda^1 - K^1\phi^1 - \frac{1}{2}I\phi^1 \\ W^1\phi^1 - (K')^1\lambda^1 - \frac{1}{2}\frac{\Delta t}{2}I\lambda^1 \end{pmatrix} .$$

For $n \geq 3$:

$$\begin{pmatrix} \frac{\Delta t}{2}A + \frac{1}{\Delta t}M & [0, -\frac{\Delta t}{2}RI]^T & 0 \\ -[0, \frac{\Delta t}{2}RI] & -V^0 & K^0 - \frac{1}{2}I \\ 0 & (K')^0 + \frac{1}{2}\frac{\Delta t}{2}I & -W^0 \end{pmatrix} \begin{pmatrix} u^n \\ \lambda^n \\ \phi^n \end{pmatrix}$$
$$= \begin{pmatrix} G^n + G^{n-1} - \frac{\Delta t}{2}Au^{n-1} + \frac{2}{\Delta t}Mu^{n-1} - \frac{1}{\Delta t}Mu^{n-2} + [0, \frac{\Delta t}{2}RI\lambda^{n-1}]^T \\ F^n - F^{n-1} + \frac{\Delta t}{2}RIu_\Gamma^{n-1} + \sum_{m=1}^{n-1} V^{n-m}\lambda^m - \sum_{m=1}^{n-1} K^{n-m}\phi^m - \frac{1}{2}I\phi^{n-1} \\ \sum_{m=1}^{n-1} W^{n-m}\phi^m - \sum_{m=1}^{n-1}(K')^{n-m}\lambda^m - \frac{1}{2}\frac{\Delta t}{2}I\lambda^{n-1} \end{pmatrix} .$$

5.2.4 Derivation of a numerical example for the wave wave coupling

We derive a numerical example for the unit cube $\Omega = [-1,1]^3$. For the exterior solution we use the same as in Section 3.8:

$$v(x,t) = \frac{|x| - t}{2|x|}\left(1 + \cos\left(\frac{\pi(|x| - t)}{0.9}\right)\right) H(0.9 - ||x| - t|) .$$

As the interior solution, we choose for $x = (x_1, x_2, x_3)$:

$$u(x,t) = f(t - x_1) = \Big(\sin((t - x_1)\pi)\Big)^5 (H(-1 + t - x_1) - H(-3 + t - x_1)) . \tag{5.25}$$

By choosing $u(x,t) = f(t - x_1)$ the homogenous wave equation is satisfied. For (5.25) on an unit cube one observes $u(x,0) = 0$ and $\dot{u}(x,0) = 0$. Next for the first transmission condition, we get:

$$u^- - v^+ = \Big(\sin((t - x_1)\pi)\Big)^5 (H(-1 + t - x_1) - H(-3 + t - x_1))$$
$$- \frac{|x| - t}{2|x|}\left(1 + \cos\left(\frac{\pi(|x| - t)}{0.9}\right)\right) H(0.9 - ||x| - t|) =: f ,$$

whereas the second transmission condition is:

$$\begin{aligned}
&\frac{\partial u^-}{\partial n} - \frac{\partial v^+}{\partial n} = \nabla u^- \cdot n - \nabla v^+ \cdot n \\
&= -5\pi\Big(\sin((t-x_1)\pi)\Big)^4 \cos((t-x_1)\pi)(H(-1+t-x_1) - H(-3+t-x_1)) \cdot n_1 \\
&-\left(\frac{tx_1}{2|x|^3}(1+\cos(\frac{\pi(|x|-t)}{0.9})) - (\frac{1}{2} - \frac{t}{2|x|})\frac{\pi x_1}{0.9|x|}\sin(\frac{\pi(|x|-t)}{0.9})\right) H(0.9 - ||x| - t|)n_1 \\
&-\left(\frac{tx_2}{2|x|^3}(1+\cos(\frac{\pi(|x|-t)}{0.9})) - (\frac{1}{2} - \frac{t}{2|x|})\frac{\pi x_2}{0.9|x|}\sin(\frac{\pi(|x|-t)}{0.9})\right) H(0.9 - ||x| - t|)n_2 \\
&-\left(\frac{tx_3}{2|x|^3}(1+\cos(\frac{\pi(|x|-t)}{0.9})) - (\frac{1}{2} - \frac{t}{2|x|})\frac{\pi x_3}{0.9|x|}\sin(\frac{\pi(|x|-t)}{0.9})\right) H(0.9 - ||x| - t|)n_3 =: g \ .
\end{aligned}$$

In Section 5.3 we perform numerical experiments, coming from these transmission conditions.

5.3 Numerical results

Analogously to Section 3.9 we begin with a Dirichlet problem for the wave equation given on an unit cube in order to check the implementation and the behaviour of the interior solution u. We set $\Omega = [-1,1]^3$.

$$\frac{\partial^2 u}{\partial t^2} - \Delta u = 0 \quad (x,t) \in \Omega \times [0,T] \ , \tag{5.26a}$$

$$u(x,0) = \dot{u}(x,0) = 0 \quad \text{in } \Omega \ , \tag{5.26b}$$

$$u = f \quad \text{on } \Gamma \times [0,T] \ . \tag{5.26c}$$

The variational formulation reads: For $f \in H^2([0,T], H^1(\Omega))$ find $u \in H^1([0,T], H^1(\Omega))$ such that

$$\int_0^T \int_\Omega \nabla(u)\nabla(\dot{w})dxdt + \int_0^T \int_\Omega \ddot{u}\dot{w}dxdt = \int_0^T \int_\Gamma \frac{\partial f}{\partial n}(\gamma^-\dot{w})ds_x dt$$

for all $w \in H^1([0,T], H^1(\Omega))$. We discretize the left hand side as in Subsection (5.21) and (5.22). For the right hand side we use an approximation $f(x,t) \approx \sum_{m=1}^{N_t} f^m \beta^m_{\Delta t}(t)$, where $f^m = f(x,t_m)$, where we use a Gauss quadrature for the integral over Γ.

Example 5.1. *We set* $f(x,t) = \Big(\sin(\pi(t-x_1))\Big)^5 (H(-1+t-x_1) - H(-3+t-x_1))$ *and solve the wave equation in* $\Omega = [-1,1]^3$ *(see Figure 3.9) till time* $T = 4$*. We refine the space time mesh uniformly, where we hold the CFL at* 0.2828*.*

In Figure 5.1 and Figure 5.2 we plotted the L^2-norm in space of the exact solution against the L^2-norms of the numerical solutions. Here we obtain similar difficulties as in Example 3.3. In Figure 5.3 we consider the difference of the L^2-norm in space between

the exact solution and the numerical results. The curves show a similar progress. In Figure 5.4 we make a convergence plot for the L^2-error in space and time,which show a rate of 0.27. Here we left out the first data $N = 2, (\Delta t) = dt = 0.4$ (40 tetrahedrals with 48 triangles), since the mesh seems not to be fine enough. Due to the expeience, achieved in Example 3.3, we didn't expect a high convergence rate at all. Other time iteration methods like Newmark's method could lead to better solutions.

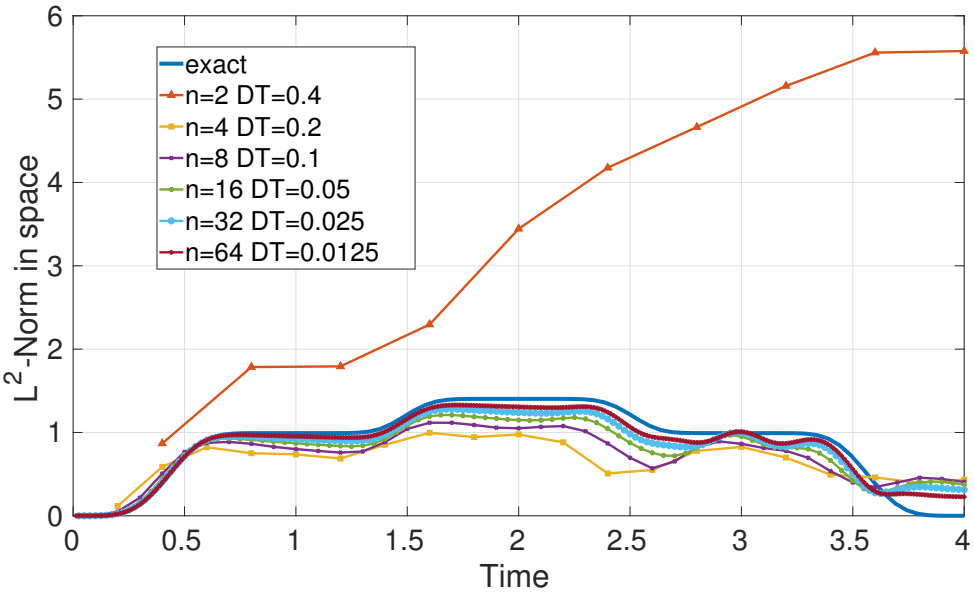

Figure 5.1: L^2-norm of the numerical solutions for Example 5.1.

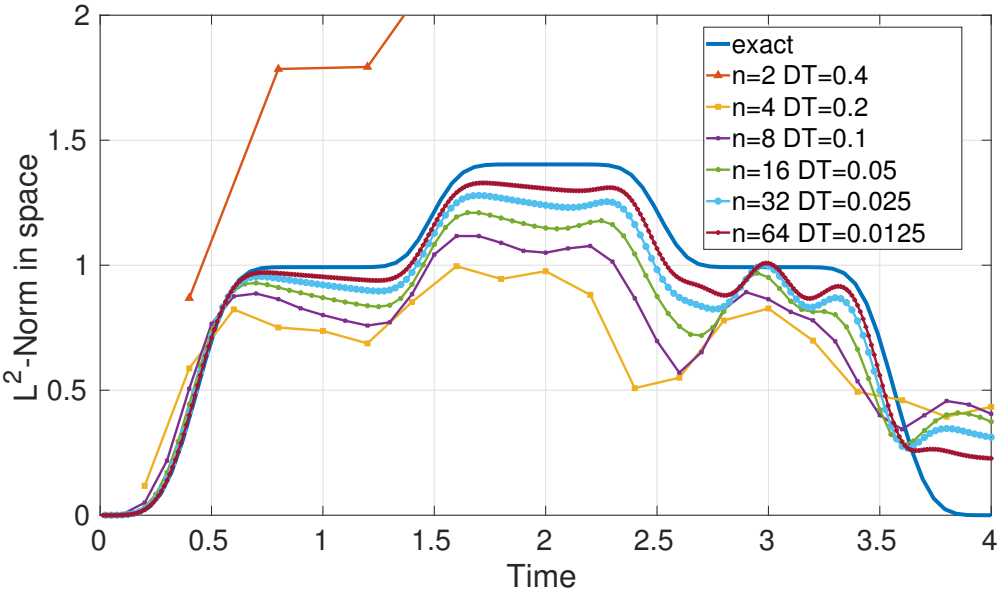

Figure 5.2: L^2-norm of the numerical solutions for Example 5.1 (zoomed).

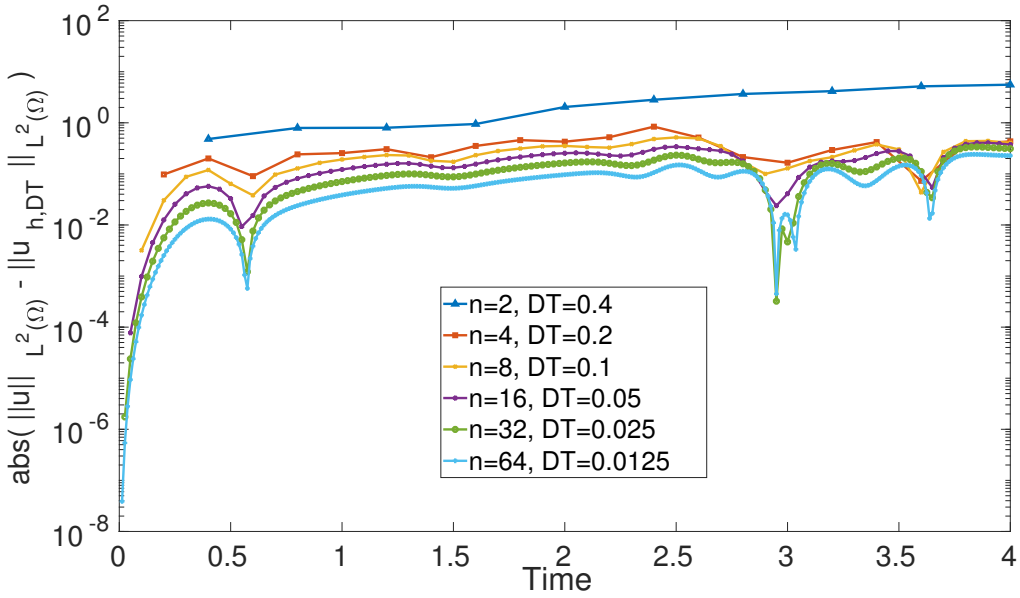

Figure 5.3: L^2-error of the numerical solutions for Example 5.1.

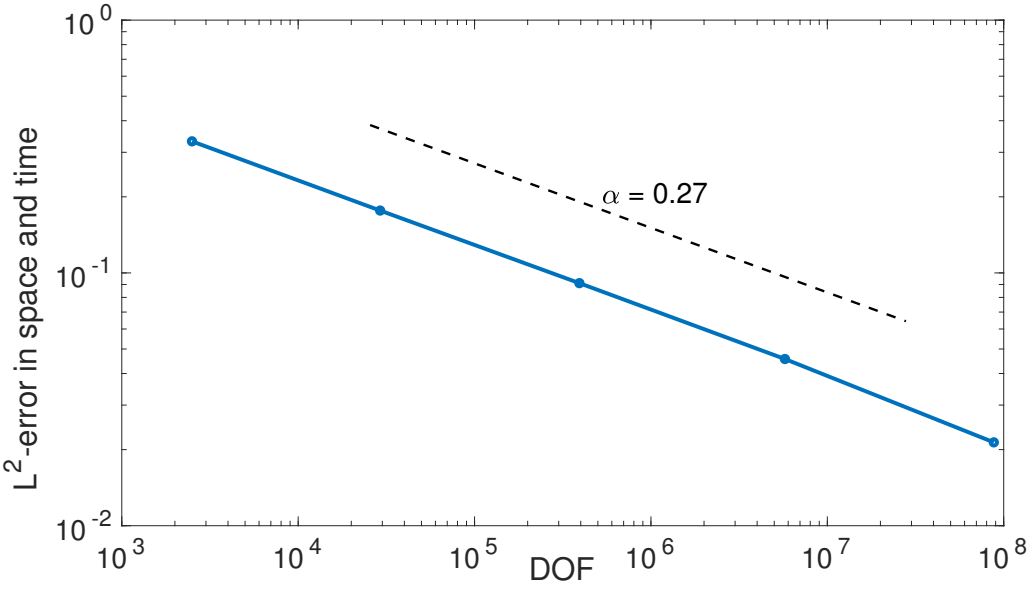

Figure 5.4: Convergence plot of the Example 5.1 for $N = 4, 8, 16, 32, 64$.

Next we continue with the whole wave-wave coupling system

Example 5.2. *We compute a wave-wave coupling system with the discretization as in Subsection 5.2.3 on the unit cube (see Figure 3.9). We set the first transmission data as*

$$u^- - v^+ = f(x,t) = -\frac{|x|-t}{2|x|}(1+\cos(\frac{\pi(|x|-t)}{0.9}))(H(0.9-||x|-t|)$$

and the second the tranmission data as $\frac{\partial u^-}{\partial n} - \frac{\partial v^+}{\partial n} = g(x,t)$

$$= -\left(\frac{tx_1}{2|x|^3}(1+\cos(\frac{\pi(|x|-t)}{0.9})) - (\frac{1}{2}-\frac{t}{2|x|})\frac{\pi x_1}{0.9|x|}\sin(\frac{\pi(|x|-t)}{0.9})\right)H(0.9-||x|-t|)n_1$$
$$-\left(\frac{tx_2}{2|x|^3}(1+\cos(\frac{\pi(|x|-t)}{0.9})) - (\frac{1}{2}-\frac{t}{2|x|})\frac{\pi x_2}{0.9|x|}\sin(\frac{\pi(|x|-t)}{0.9})\right)H(0.9-||x|-t|)n_2$$
$$-\left(\frac{tx_3}{2|x|^3}(1+\cos(\frac{\pi(|x|-t)}{0.9})) - (\frac{1}{2}-\frac{t}{2|x|})\frac{\pi x_3}{0.9|x|}\sin(\frac{\pi(|x|-t)}{0.9})\right)H(0.9-||x|-t|)n_3 \quad .$$

The exact solution is known with $u = 0$ *and*

$$v = \frac{|x|-t}{2|x|}(1+\cos(\frac{\pi(|x|-t)}{0.9}))(H(0.9-||x|-t|) \quad .$$

The mesh is again the unit cube $\Omega = [-1,1]^3$*. We refine the space time mesh uniformly, where we hold the CFL at* 0.2828*. We compute till time* $T = 5$ *is reached.*

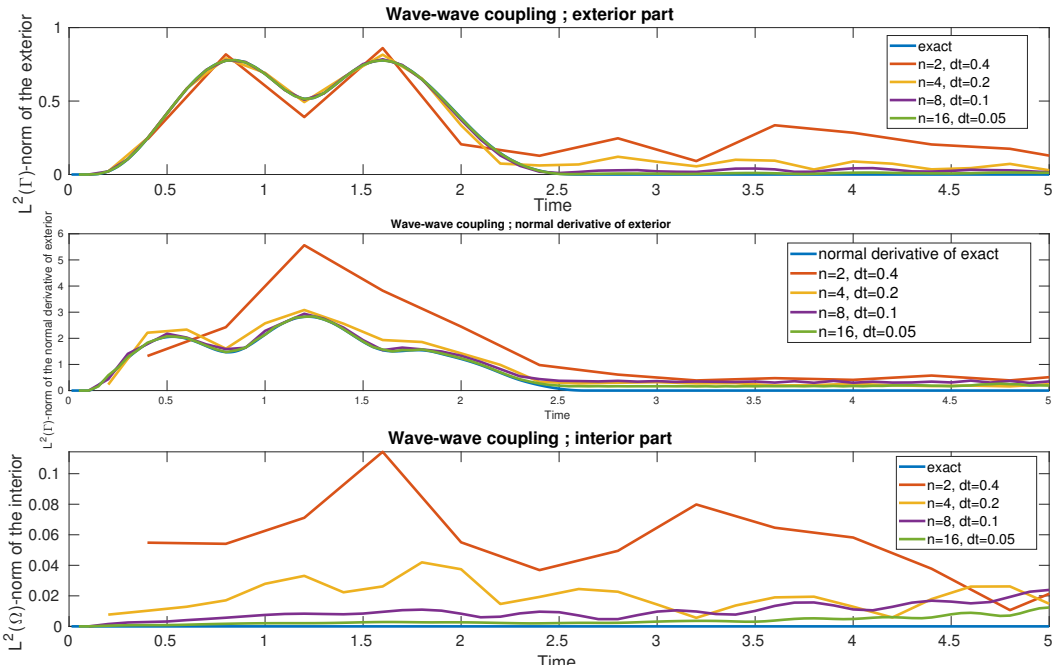

Figure 5.5: L^2-norm in space of the numerical solutions for the exterior, the normal derivative of the exterior, and the interior, Example 5.2.

In Figure 5.5 we plot the L^2-norms in space for the solutions of the wave-wave coupling problem treated as in Subsection 5.2.3. The numerical solutions seems to approximate the exact solution in a reliable way. As expected for larger times the error becomes higher, see Figure 5.6. We remark that for the normal derivative after time 2.5, we are doing almost constant errors of about 0.2 for $n = 16$ and $dt = 0.05$. In Figure 5.7 we made a convergence plot. We observe that the L^2-error in space and time for the interior is higher than the exterior part in contrary to the examples of the fluid-structure interaction problem in Chapter 4. But the L^2-error in space and time for the exterior

normal derivative is higher than the error for the interior, as we expected from Figure 5.6. The convergence rate for the exterior normal derivative though is around 0.38 higher than the convergence rate of 0.22 for the interior. The convergence rate for the exterior part is around 0.75.

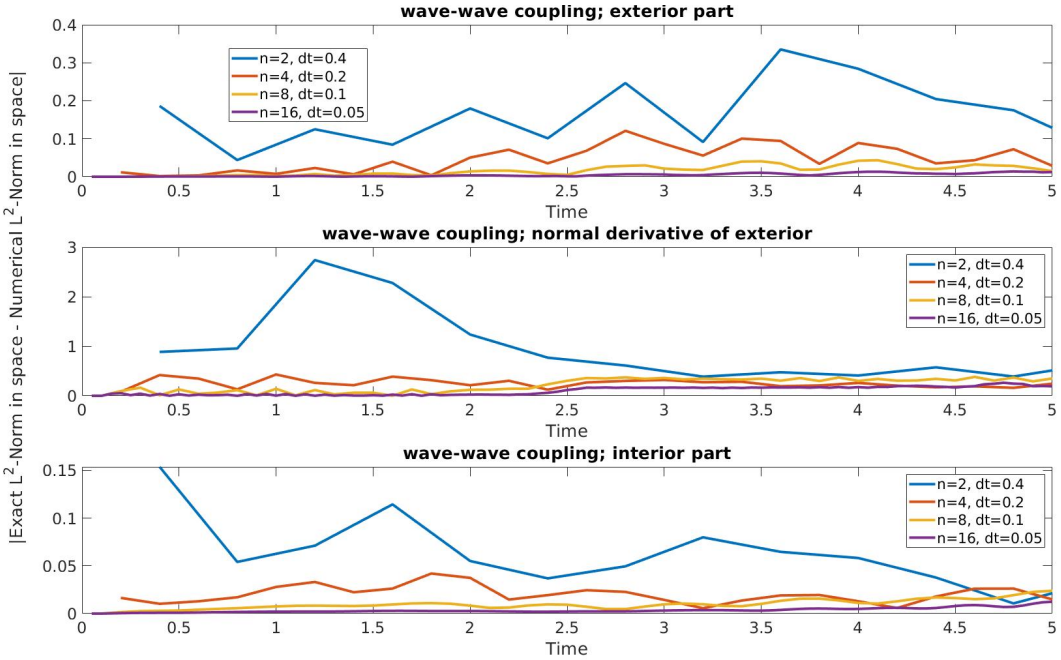

Figure 5.6: Absolute difference of the L^2-norm in space of the numerical solutions against the L^2-norm in space of the exact solutions for the exterior, the normal derivative of the exterior, and the interior, Example 5.2.

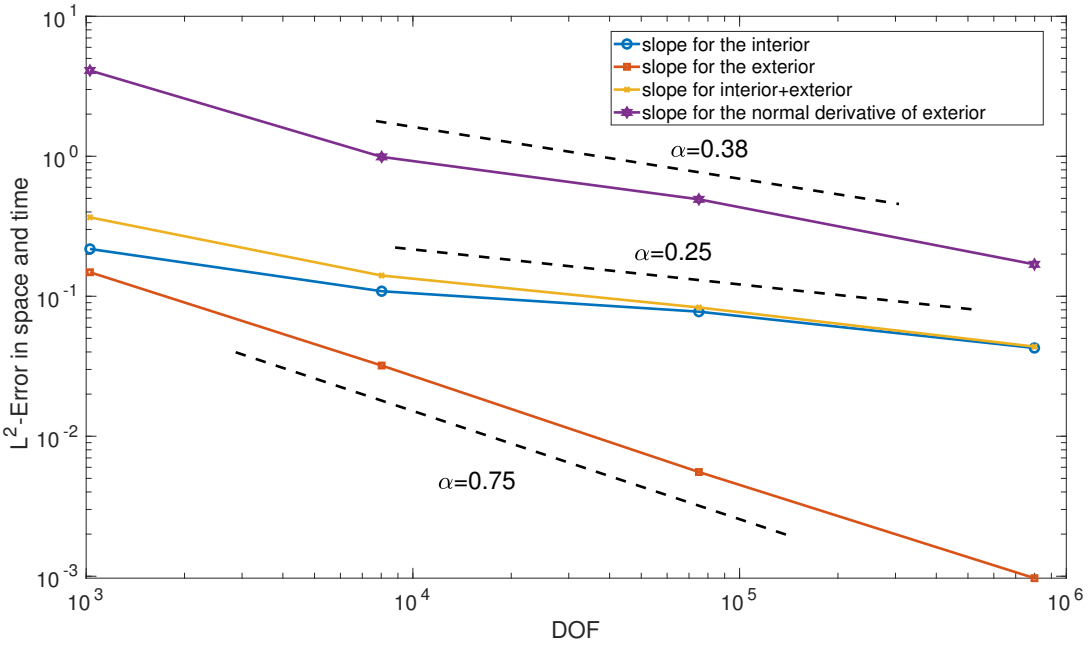

Figure 5.7: Convergence plot of Example 5.2.

6 Time domain BEM: graded meshes and hp-version on quasi-uniform meshes

6.1 Introduction

The asymptotic behaviour of solutions for elliptic and parabolic equations near the edges and corners of a polyhedral domain has been studied, see e.g. in [41, 90]. The explicit singular expansions allow to recover optimal convergence rates for finite [7, 8] and boundary element methods [56, 101, 102]. We consider the homogeneous wave equation on a screen $\Gamma \subset \mathbb{R}^3$ with connected complement $\Omega = \mathbb{R}^3 \backslash \overline{\Gamma}$, i.e. the problem

$$\begin{aligned} \partial_t^2 u(x,t) - \Delta u(x,t) &= 0 \quad \text{in } \Omega \times \mathbb{R}^+ , \\ u(x,0) = \dot{u}(x,0) &= 0 \quad \text{in } \Omega , \\ Bu &= g \quad \text{on } \Gamma . \end{aligned}$$

We consider Dirichlet boundary conditions ($Bu = u_+$ on Γ) as well as Neumann boundary conditions ($Bu = \partial_n^+ u$ on Γ), where $\partial_n^+ u$ and u_+ are defined in Section 2.1 with n the unit normal vector pointing towards Ω. Since the mesh is a screen we denote with $\partial_n^+ u := \partial_n u := \partial_n u|_\Gamma$ and $u_+ := u|_\Gamma$. Solutions to the wave equation in the exterior of a polyhedral domain or a screen in $\mathbb{R}^3$ also exhibit singular behaviour from the edges and corners. Plamenevskii and coauthors obtained in [68, 69, 79, 86] a similar asymptotic behaviour for the wave equation in domains with conical or wedge singularities. The wave equation is transformed into the Helmholtz equation, where they considered the eigenvalues and eigenfunctions. Then they prove an asymptotic expansion of u_+ for a Neumann problem resp. $\partial_n^+ u$ for a Dirichlet problem. Using an inverse Fourier transform we achieve the asymptotic expansions in time domain. We deduce from [46], that the asymptotic expansion of the solution to the wave equation holds the same exponent as for the elliptic equations for fixed times.

Furthermore p and hp–versions of the boundary element method for the wave equation are considered in [49]. For p and hp–versions of the finite element method fast approximations of geometric singularities and smooth solutions for elliptic problems are gained by incresing the polynomial degree p of the elements together with an increasing of the refinement of the given quasi-uniform mesh [9, 10, 36, 37]. For the boundary element method they are introduced in [93, 94]. For screens and polyhedral surfaces in 3D optimal convergence rates have been achieved, see e.g. in [20, 24, 23, 21, 22].

This chapter presents the main results and numerical experiments based on the paper

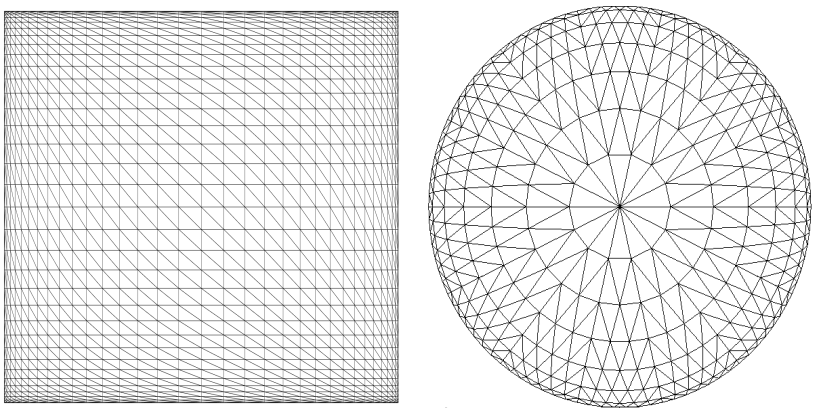

(a) (b)

Figure 6.1: β-graded meshes for (a) square and (b) circular screens, with $\beta = 2$. Figure 1 in [46]

jointly with H. Gimperlein, F. Meyer, D. Stark and E. P. Stephan [46] and the submitted paper jointly with H. Gimperlein, D. Stark and E. P. Stephan [49].

6.2 β-graded meshes

We begin with the construction of a $\beta-$graded mesh on a square. Since the mesh is symmetric , it is enough to consider the mesh with a graduation parameter $\beta \geq 0$ for $[-1, 0]$. We define the nodes of the β-graded mesh on the square in one direction as

$$y_k = x_k = -1 + (\frac{k}{N_l})^\beta \quad \text{for } k = 1, \ldots, N_l \ . \tag{6.1}$$

Therefore $(x_k, y_l),\ k, l = 1, \ldots, N_l$ is the set of all nodes of this mesh. In case of $\beta = 1$, we have a uniform square. The 2$-$graded mesh on a square is depicted in the left of Figure 6.1.

A $\beta-$graded L-shape is build by taking 3 $\beta-$graded squares and combining them into an L-shape.

For a circular screen with radius 1, the nodes are given on concentric circles. We get for a β-graded mesh on concentric circles the following $\beta-$graduated radii:

$$r_k = 1 - (\frac{k}{N_l})^\beta \quad \text{for } k = 0, \ldots, N_l - 1. \tag{6.2}$$

In case of $\beta = 1$, we get a uniform mesh with nodes on $1 - (\frac{k}{N_l})$, with $k = 0, \ldots, N_l - 1$. The 2-graded mesh on a circular screen is depicted in the right of Figure 6.1.

6.3 Asymptotic expansions and numerical approximation

6.3.1 Singularities for circular screens and approximation for graded meshes

We consider the circular screen $\{(x_1, x_2, 0) \in \mathbb{R}^3 : x_1^2 + x_2^2 \leq 1\}$. From [46] and [95] we get the following asymptotic expansions near the edge $\{(x_1, x_2, 0) \in \mathbb{R}^3 : x_1^2 + x_2^2 = 1\}$ with the polar coordinates (r, θ) in the $x_1 - x_2$-plane, $y = r - 1$ and $z = \theta$ for a, b smooth for smooth boundary conditions and $\tilde{v}, \check{v}$ regular terms :

$$u_+ := u(y,t,z)|_\Gamma = a(t,z)|y|^{1/2} + \check{v}(y,t,z) \ , \tag{6.3}$$

$$\partial_n^+ u := \partial_n u(y,t,z)|_\Gamma = b(t,z)|y|^{-\frac{1}{2}} + \tilde{v}(y,z,t) \ . \tag{6.4}$$

The analysis from T. von Petersdorff in [101] in the elliptic case is expanded to the hyperbolic case in [46] in order to reach optimal convergence approximation properties for graded meshes. The theorem below gives the convergence for circular screens for Dirichlet and Neumann conditions.

Theorem 6.1 ([46], Theorem 15)**.** *Let $\varepsilon > 0$. a) Let u be a strong solution to the homogeneous wave equation with inhomogeneous Neumann boundary conditions $\partial_n u|_\Gamma = g$, with g smooth. Further, let $\phi^\beta_{h,\Delta t}$ be the best approximation in the norm of $H^r_\sigma(\mathbb{R}^+, \widetilde{H}^{\frac{1}{2}-s}(\Gamma))$ to the Dirichlet trace $u|_\Gamma$ in $\tilde{V}^{1,p}_{h,\Delta t}$ on a β-graded spatial mesh with $\Delta t \lesssim h^\beta$. Then $\|u - \phi^\beta_{h,\Delta t}\|_{r,\frac{1}{2}-s,\Gamma,*} \leq C_{\beta,\varepsilon} h^{\min\{\beta(\frac{1}{2}+s), \frac{3}{2}+s\}-\varepsilon}$, where $s \in [0, \frac{1}{2}]$ and $r \in [0, p)$.*

b) Let u be a strong solution to the homogeneous wave equation with inhomogeneous Dirichlet boundary conditions $u|_\Gamma = g$, with g smooth. Further, let $\psi^\beta_{h,\Delta t}$ be the best approximation in the norm of $H^r_\sigma(\mathbb{R}^+, \widetilde{H}^{-\frac{1}{2}}(\Gamma))$ to the Neumann trace $\partial_n u|_\Gamma$ in $V^{0,p}_{h,\Delta t}$ on a β-graded spatial mesh with $\Delta t \lesssim h^\beta$. Then $\|\partial_n u - \psi^\beta_{h,\Delta t}\|_{r,-\frac{1}{2},\Gamma,*} \leq C_{\beta,\varepsilon} h^{\min\{\frac{\beta}{2}, \frac{3}{2}\}-\varepsilon}$, where $r \in [0, p+1)$.

Due to Theorem 6.1 we also achieve results for the retarded single layer integral equation and the retarded hypersingular integral equation on the circular screen.

Corollary 6.2 ([46], Corollary 16)**.** *Let $\varepsilon > 0$. a) Let ϕ be the solution to the retarded hypersingular integral equation (2.42) and $\phi^\beta_{h,\Delta t}$ the best approximation in the norm of $H^r_\sigma(\mathbb{R}^+, \widetilde{H}^{\frac{1}{2}-s}(\Gamma))$ to ϕ in $\tilde{V}^{1,p}_{h,\Delta t}$ on a β-graded spatial mesh with $\Delta t \lesssim h^\beta$. Then $\|\phi - \phi^\beta_{h,\Delta t}\|_{r,\frac{1}{2}-s,\Gamma,*} \leq C_{\beta,\varepsilon} h^{\min\{\beta(\frac{1}{2}+s), \frac{3}{2}+s\}-\varepsilon}$, where $s \in [0, \frac{1}{2}]$ and $r \in [0, p)$.*

b) Let ψ be the solution to the retarded single layer integral equation (2.27) and $\psi^\beta_{h,\Delta t}$ the best approximation in the norm of $H^r_\sigma(\mathbb{R}^+, \widetilde{H}^{-\frac{1}{2}}(\Gamma))$ to ψ in $V^{0,p}_{h,\Delta t}$ on a β-graded spatial mesh with $\Delta t \lesssim h^\beta$. Then $\|\psi - \psi^\beta_{h,\Delta t}\|_{r,-\frac{1}{2},\Gamma,*} \leq C_{\beta,\varepsilon} h^{\min\{\frac{\beta}{2}, \frac{3}{2}\}-\varepsilon}$, where $r \in [0, p+1)$.

On a screen the retarded double layer potential and the retarded adjoint double layer potential vanish. The solutions to the integral equations with Neumann condition is

$\phi = [u]$, whereas the solutions to the integral equations with Dirichlet condition is $\psi = [\partial_n u]$, where $[\cdot]$ is defined in (2.6).

6.3.2 Singularities for circular screens and approximation for hp-version

Due to the decomposition (6.3) and (6.4), the following theorem states a quasi-optimal convergence of the *hp*−version for an arbitrary small $\varepsilon > 0$ on circular screens.

Theorem 6.3 ([49], Theorem 15)**.** *Let $\varepsilon > 0$. a) Let u be a solution to the homogeneous wave equation with inhomogeneous Neumann boundary conditions $\partial_n u|_\Gamma = g$, with $g \in H^\alpha_\sigma(\mathbb{R}^+, \widetilde{H}^\beta(\Gamma))$ for some α, β, so that the regular part $\check{v} \in H^\mu_\sigma(\mathbb{R}^+, \widetilde{H}^\eta(\Gamma))$ in the singular expansion of $u|_\Gamma$, with η, μ sufficiently large. Further, let $\phi_{h,\Delta t}$ be the best approximation in the norm of $H^r_\sigma(\mathbb{R}^+, \widetilde{H}^{\frac{1}{2}-s}(\Gamma))$ to the Dirichlet trace $u|_\Gamma$ in $\tilde{V}^{p,p}_{h,\Delta t}$ on a quasi-uniform spatial mesh with $\Delta t \lesssim h$. Then*

$$\|u - \phi_{h,\Delta t}\|_{r,\frac{1}{2}-s,\Gamma,*} \lesssim \left(\frac{h}{p^2}\right)^{\frac{1}{2}+s-\varepsilon} + \left(\frac{h}{p}\right)^{-\frac{1}{2}+s+\eta} + \left(\frac{\Delta t}{p}\right)^{\mu+s-r-\frac{1}{2}},$$

where $r \in [0, p)$.

b) Let u be a solution to the homogeneous wave equation with inhomogeneous Dirichlet boundary conditions $u|_\Gamma = g$, with $g \in H^\alpha_\sigma(\mathbb{R}^+, \widetilde{H}^\beta(\Gamma))$ for some α, β, so that the regular part $\tilde{v} \in H^\mu_\sigma(\mathbb{R}^+, \widetilde{H}^\eta(\Gamma))$ in the singular expansion of $\partial_n u|_\Gamma$, with η, μ sufficiently large. Further, let $\psi_{h,\Delta t}$ be the best approximation in the norm of $H^r_\sigma(\mathbb{R}^+, \widetilde{H}^{-\frac{1}{2}}(\Gamma))$ to the Neumann trace $\partial_n u|_\Gamma$ in $V^{p,p}_{h,\Delta t}$ on a quasi-uniform spatial mesh with $\Delta t \lesssim h$. Then

$$\|\partial_n u - \psi_{h,\Delta t}\|_{r,-\frac{1}{2},\Gamma,*} \lesssim \left(\frac{h}{(p+1)^2}\right)^{\frac{1}{2}-\varepsilon} + \left(\frac{h}{p+1}\right)^{\frac{1}{2}+\eta} + \left(\frac{\Delta t}{p+1}\right)^{\mu+1-r},$$

where $r \in [0, p+1)$.

Due to Theorem 6.3, we gain analogous results for the *hp*−version of the retarded single layer integral equations and the retarded hypersingular integral equations on circular screens.

Corollary 6.4 ([49], Corollary 16)**.** *Let $\varepsilon > 0$. a) Let ϕ be the solution to the retarded hypersingular integral equation (2.42) and $\phi_{h,\Delta t}$ the best approximation in the norm of $H^r_\sigma(\mathbb{R}^+, \widetilde{H}^{\frac{1}{2}-s}(\Gamma))$ to ϕ in $\tilde{V}^{p,p}_{h,\Delta t}$ on a quasi-uniform spatial mesh with $\Delta t \lesssim h$. Assume that the right hand side $g \in H^\alpha_\sigma(\mathbb{R}^+, \widetilde{H}^\beta(\Gamma))$ for some α, β, so that the regular part $\check{v} \in H^\mu_\sigma(\mathbb{R}^+, \widetilde{H}^\eta(\Gamma))$ in the singular expansion of $u|_\Gamma$, with η, μ sufficiently large. Then*

$$\|\phi - \phi_{h,\Delta t}\|_{r,\frac{1}{2}-s,\Gamma,*} \lesssim \left(\frac{h}{p^2}\right)^{\frac{1}{2}+s-\varepsilon} + \left(\frac{h}{p}\right)^{-\frac{1}{2}+s+\eta} + \left(\frac{\Delta t}{p}\right)^{\mu+s-r-\frac{1}{2}},$$

where $r \in [0, p)$, $s \in [0, \frac{1}{2}]$.

b) Let ψ be the solution to the retarded single layer integral equation (2.27) and $\psi_{h,\Delta t}$ the best approximation in the norm of $H^r_\sigma(\mathbb{R}^+, \widetilde{H}^{-\frac{1}{2}}(\Gamma))$ to ψ in $V^{p,p}_{h,\Delta t}$ on a quasi-uniform spatial mesh with $\Delta t \lesssim h$. Assume that the right hand side $f \in H^\alpha_\sigma(\mathbb{R}^+, \widetilde{H}^\beta(\Gamma))$ for some α, β, so that the regular part $\tilde{v} \in H^\mu_\sigma(\mathbb{R}^+, \widetilde{H}^\eta(\Gamma))$ in the singular expansion of $\partial_n u|_\Gamma$, with η, μ sufficiently large. Then for $r \in [0, p+1)$

$$\|\psi - \psi_{h,\Delta t}\|_{r,-\frac{1}{2},\Gamma,*} \lesssim \left(\frac{h}{(p+1)^2}\right)^{\frac{1}{2}-\varepsilon} + \left(\frac{h}{p+1}\right)^{\frac{1}{2}+\eta} + \left(\frac{\Delta t}{p+1}\right)^{\mu+1-r} .$$

6.3.3 Singularities for polygonal screens and approximation for graded meshes

We consider a polygonal screen. From [46] we get the following asymptotic expansions in terms of the polar coordinates (r, θ) near the vertex $(0,0)$ with a, b_1, b_2 smooth for smooth boundary conditions, $\chi, \tilde{\chi} \in C^\infty_c$ are cut-off functions with $\chi, \tilde{\chi} = 1$ in a neighborhood of 0 and v_0, ψ_0 are regular terms:

$$\begin{aligned} u(t,x)|_\Gamma &= v_0(t,r,\theta) + \chi(r) r^\gamma \alpha(t,\theta) + \tilde{\chi}(\theta) b_1(t,r) (\sin(\theta))^{\frac{1}{2}} \\ &\quad + \tilde{\chi}(\tfrac{\pi}{2} - \theta) b_2(t,r) (\cos(\theta))^{\frac{1}{2}} , \qquad (6.5) \\ \partial_n u(t,x)|_\Gamma &= \psi_0(t,r,\theta) + \chi(r) r^{\gamma-1} \alpha(t,\theta) + \tilde{\chi}(\theta) b_1(t,r) r^{-1} (\sin(\theta))^{-\frac{1}{2}} \\ &\quad + \tilde{\chi}(\tfrac{\pi}{2} - \theta) b_2(t,r) r^{-1} (\cos(\theta))^{-\frac{1}{2}} . \qquad (6.6) \end{aligned}$$

Here γ denotes the singular exponent. The square screen $\Gamma = (0,1) \times (0,1) \times \{0\}$ gives at the corner $(0,0)$ an exponent $\gamma \approx 0.2966$, whereas an L-shaped screen $\Gamma = [-1,1]^2 \times \{0\} \backslash [0,1]^2 \times \{0\}$ gives at the corner $(0,0)$ an exponent $\gamma \approx 0.8146$, see [80]. In [79], the authors handled the remainder terms with an elliptic a priori weighted estimates near the singularities.

These decompositions are crucial in order to obtain optimal convergence on graded meshes for polygonal screens. The following theorem states the convergence for polygonal screens for β large enough, depending on γ.

Theorem 6.5 ([46], Theorem 20)**.** *Let $\varepsilon > 0$. a) Let u be a strong solution to the homogeneous wave equation with inhomogeneous Neumann boundary conditions $\partial_n u|_\Gamma = g$, with g smooth. Further, let $\phi^\beta_{h,\Delta t}$ be the best approximation in the norm of $H^r_\sigma(\mathbb{R}^+, \widetilde{H}^{\frac{1}{2}-s}(\Gamma))$ to the Dirichlet trace $u|_\Gamma$ in $\tilde{V}^{1,p}_{h,\Delta t}$ on a β-graded spatial mesh with $\Delta t \lesssim h^\beta$ and $\beta \geq \frac{3}{2(\gamma+\frac{1}{2})}$. Then $\|u - \phi^\beta_{h,\Delta t}\|_{r,\frac{1}{2}-s,\Gamma,*} \leq C_{\beta,\varepsilon} h^{\min\{\frac{\beta}{2},\frac{3}{2}\}+s-\varepsilon}$, where $s \in [0, \frac{1}{2}]$ and $r \in [0,p)$.*

b) Let u be a strong solution to the homogeneous wave equation with inhomogeneous Dirichlet boundary conditions $u|_\Gamma = g$, with g smooth. Further, let $\psi^\beta_{h,\Delta t}$ be the best approximation in the norm of $H^r_\sigma(\mathbb{R}^+, \widetilde{H}^{-\frac{1}{2}}(\Gamma))$ to the Neumann trace $\partial_n u|_\Gamma$ in $V^{0,p}_{h,\Delta t}$ on a β-graded spatial mesh with $\Delta t \lesssim h^\beta$ and $\beta \geq \frac{3}{2(\gamma+\frac{1}{2})}$. Then $\|\partial_n u - \psi^\beta_{h,\Delta t}\|_{r,-\frac{1}{2},\Gamma,*} \leq C_{\beta,\varepsilon} h^{\min\{\frac{\beta}{2},\frac{3}{2}\}-\varepsilon}$, where $r \in [0,p+1)$.

We achieve an analogous result for the retarded single layer integral equations and the retarded hypersingular integral equations from Theorem 6.5.

Corollary 6.6 ([46], Corollary 21)**.** *Let $\varepsilon > 0$. a) Let ϕ be the solution to the retarded hypersingular integral equation (2.42) and $\phi^{\beta}_{h,\Delta t}$ the best approximation in the norm of $H^r_\sigma(\mathbb{R}^+, \widetilde{H}^{\frac{1}{2}-s}(\Gamma))$ to ϕ in $\tilde{V}^{1,p}_{h,\Delta t}$ on a β-graded spatial mesh with $\Delta t \lesssim h^\beta$ and $\beta \geq \frac{3}{2(\gamma+\frac{1}{2})}$. Then $\|\phi - \phi^{\beta}_{h,\Delta t}\|_{r,\frac{1}{2}-s,\Gamma,*} \leq C_{\beta,\varepsilon} h^{\min\{\beta(\frac{1}{2}+s),\frac{3}{2}+s\}-\varepsilon}$, where $s \in [0, \frac{1}{2}]$ and $r \in [0, p)$.*

b) Let ψ be the solution to the retarded single layer integral equation (2.27) and $\psi^{\beta}_{h,\Delta t}$ the best approximation in the norm of $H^r_\sigma(\mathbb{R}^+, \widetilde{H}^{-\frac{1}{2}}(\Gamma))$ to ψ in $V^{0,p}_{h,\Delta t}$ on a β-graded spatial mesh with $\Delta t \lesssim h^\beta$ and $\beta \geq \frac{3}{2(\gamma+\frac{1}{2})}$. Then $\|\psi - \psi^{\beta}_{h,\Delta t}\|_{r,-\frac{1}{2},\Gamma,*} \leq C_{\beta,\varepsilon} h^{\min\{\frac{\beta}{2},\frac{3}{2}\}-\varepsilon}$, where $r \in [0, p+1)$.

6.3.4 Singularities for polygonal screens and approximation for hp-version

Due to the decomposition given in (6.5) and (6.6), the following theorem states the convergence of the *hp*−version for an arbitrary small $\varepsilon > 0$ on polygonal screens.

Theorem 6.7 ([49], Theorem 19)**.** *Let $\varepsilon > 0$. a) Let u be a solution to the homogeneous wave equation with inhomogeneous Neumann boundary conditions $\partial_n u|_\Gamma = g$, with $g \in H^\alpha_\sigma(\mathbb{R}^+, \widetilde{H}^\beta(\Gamma))$ for some α, β, so that the regular part $v_0 \in H^\mu_\sigma(\mathbb{R}^+, \widetilde{H}^\eta(\Gamma))$ in the singular expansion of $u|_\Gamma$, with η, μ sufficiently large. Further, let $\phi_{h,\Delta t}$ be the best approximation in the norm of $H^r_\sigma(\mathbb{R}^+, \widetilde{H}^{\frac{1}{2}-s}(\Gamma))$ to the Dirichlet trace $u|_\Gamma$ in $\tilde{V}^{p,p}_{h,\Delta t}$ on a quasi-uniform spatial mesh with $\Delta t \lesssim h$. Then*

$$\|u - \phi_{h,\Delta t}\|_{r,\frac{1}{2}-s,\Gamma,*} \lesssim \left(\frac{h}{p^2}\right)^{\frac{1}{2}+\min\{\gamma,0\}+s-\varepsilon} + \left(\frac{h}{p}\right)^{-\frac{1}{2}+s+\eta} + \left(\frac{\Delta t}{p}\right)^{\mu+s-r-\frac{1}{2}},$$

where $r \in [0, p)$.

b) Let u be a solution to the homogeneous wave equation with inhomogeneous Dirichlet boundary conditions $u|_\Gamma = g$, with $g \in H^\alpha_\sigma(\mathbb{R}^+, \widetilde{H}^\beta(\Gamma))$ for some α, β, so that the regular part $\psi_0 \in H^\mu_\sigma(\mathbb{R}^+, \widetilde{H}^\eta(\Gamma))$ in the singular expansion of $\partial_n u|_\Gamma$, with η, μ sufficiently large. Further, let $\psi_{h,\Delta t}$ be the best approximation in the norm of $H^r_\sigma(\mathbb{R}^+, \widetilde{H}^{-\frac{1}{2}}(\Gamma))$ to the Neumann trace $\partial_n u|_\Gamma$ in $V^{p,p}_{h,\Delta t}$ on a quasi-uniform spatial mesh with $\Delta t \lesssim h$. Then

$$\|\partial_n u - \psi_{h,\Delta t}\|_{r,-\frac{1}{2},\Gamma,*} \lesssim \left(\frac{h}{(p+1)^2}\right)^{\frac{1}{2}+\min\{\gamma,0\}-\varepsilon} + \left(\frac{h}{p+1}\right)^{\frac{1}{2}+\eta} + \left(\frac{\Delta t}{p+1}\right)^{\mu+1-r},$$

where $r \in [0, p+1)$.

From Theorem 6.7 analogous results follow for the *hp*−version of the retarded single layer equations and the retarded hypersingular integral equations on polygonal screens.

Corollary 6.8 ([49], Corollary 20)**.** *Let $\varepsilon > 0$. a) Let ϕ be the solution to the retarded hypersingular integral equation (2.42) and $\phi_{h,\Delta t}$ the best approximation in the norm of $H^r_\sigma(\mathbb{R}^+, \widetilde{H}^{\frac{1}{2}-s}(\Gamma))$ to ϕ in $\tilde{V}^{p,p}_{h,\Delta t}$ on a quasi-uniform spatial mesh with $\Delta t \lesssim h$. Assume that the right hand side $g \in H^\alpha_\sigma(\mathbb{R}^+, \widetilde{H}^\beta(\Gamma))$ for some α, β, so that the regular part $v_0 \in H^\mu_\sigma(\mathbb{R}^+, \widetilde{H}^\eta(\Gamma))$ in the singular expansion of $u|_\Gamma$, with η, μ sufficiently large. Then*

$$\|\phi - \phi_{h,\Delta t}\|_{r,\frac{1}{2}-s,\Gamma,*} \lesssim \left(\frac{h}{p^2}\right)^{\frac{1}{2}+\min\{\gamma,0\}+s-\varepsilon} + \left(\frac{h}{p}\right)^{-\frac{1}{2}+s+\eta} + \left(\frac{\Delta t}{p}\right)^{\mu+s-r-\frac{1}{2}},$$

where $r \in [0, p)$, $s \in [0, \frac{1}{2}]$.

b) Let ψ be the solution to the retarded single layer integral equation (2.27) and $\psi_{h,\Delta t}$ the best approximation in the norm of $H^r_\sigma(\mathbb{R}^+, \widetilde{H}^{-\frac{1}{2}}(\Gamma))$ to ψ in $V^{p,p}_{h,\Delta t}$ on a quasi-uniform spatial mesh with $\Delta t \lesssim h$. Assume that the right hand side $f \in H^\alpha_\sigma(\mathbb{R}^+, \widetilde{H}^\beta(\Gamma))$ for some α, β, so that the regular part $\psi_0 \in H^\mu_\sigma(\mathbb{R}^+, \widetilde{H}^\eta(\Gamma))$ in the singular expansion of $\partial_n u|_\Gamma$, with η, μ sufficiently large. Then

$$\|\psi - \psi_{h,\Delta t}\|_{r,-\frac{1}{2},\Gamma,*} \lesssim \left(\frac{h}{(p+1)^2}\right)^{\frac{1}{2}+\min\{\gamma,0\}-\varepsilon} + \left(\frac{h}{p+1}\right)^{\frac{1}{2}+\eta} + \left(\frac{\Delta t}{p+1}\right)^{\mu+1-r},$$

where $r \in [0, p+1)$ and the regular part $\psi_0 \in H^{\mu+1}_\sigma(\mathbb{R}^+, \widetilde{H}^\eta(\Gamma))$ of the singular expansion of $\psi = \partial_n u|_\Gamma$, with η, μ sufficiently large.

6.4 Numerical experiments

6.4.1 Single layer potential for graded meshes

Example 6.1. *We compute the solution to the retarded single layer integral equation $V\psi = f$ on $\Gamma \times \mathbb{R}^+$ for the circular screen $\Gamma = \{(x, y, 0) : 0 \le \sqrt{x^2 + y^2} \le 1\}$ with the discretization from Subsection 2.3.1. The weak form (2.49) with constant ansatz and test functions in space and time are used. The right hand side is specified with $f(x,t) = \cos(|k|t - k \cdot x)\exp(-1/(10t^2))$, where $k = (0.2, 0.2, 0.2)$. We choose $\Delta t = 0.005$ and compute the solution till $T = 1$. The finest graded mesh in our computation contains 2662 triangles with $\Delta t = 0.005$ and $\beta = 2$, where it serves as a reference solution.*

Figure 6.2 shows the density along a cross-section of the reference solution at time 0.5. The figure displays the expected edge singularities known by the decomposition (6.4).

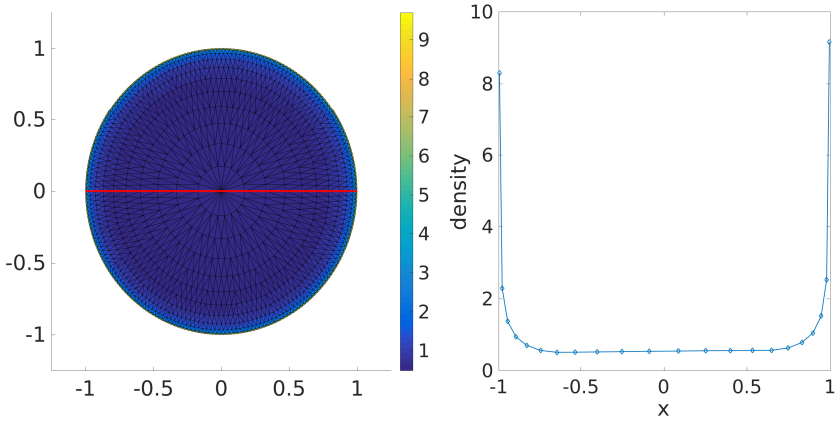

Figure 6.2: Solution of the single layer equation at $T = 0.5$ along $y = 0$ on the circular screen, Example 6.1. Figure 3 in [46]

In Figure 6.3 the numerical density of the reference solution at times $0.5, 0.75, 1.0$ are plotted against the distance to the edge at $(1, 0)$ along the x-axis. The numerical solutions are in close agreement with the theoretical value of $-\frac{1}{2}$ of (6.4) for the edge singularities. We remark that we can't deduce from the convergence of the boundary element method in the energy norm a corresponding convergence of the numerically computed singular exponents.

We finally consider the relative energy error compared to the reference solution. We can't expect a convergence in $L^2([0,T] \times \Gamma)$ since the solution exhibits a low spatial regularity. Therefore we consider the energy norm, as in (2.56), $\tilde{E}(T) = \vec{\psi}\tilde{V}\vec{\psi} - 2\vec{\psi}\vec{f}$ for $T = 1$ with the solution vector $\vec{\psi}$ after solving the MOT-scheme (2.54) till $T = 1$. $H^0_\sigma(\mathbb{R}^+, \widetilde{H}^{-\frac{1}{2}}(\Gamma))$ is comparable or stronger than the energy norm. Figure 6.4 describes the relative energy error against the degrees of freedom. We computed the relative energy error with

$$\frac{|\tilde{E}_{num}(T) - \tilde{E}_{ref}(T)|}{|E_{ref}(T)|} \ ,$$

where $\tilde{E}_{num}$ is the discretized energy of the numerical solutions, whereas $\tilde{E}_{ref}$ is the discretized energy of the reference solution. We see for the 2-graded mesh a rate of -0.52, whereas the uniform mesh shows a rate -0.26. The error behaves in agreement to the expected approximation properties proportional to h (equivalently $\sim DOF^{-1/2}$) on the 2-graded mesh resp. $\sim h^{1/2}$ ($\sim DOF^{-1/4}$) on the uniform mesh.

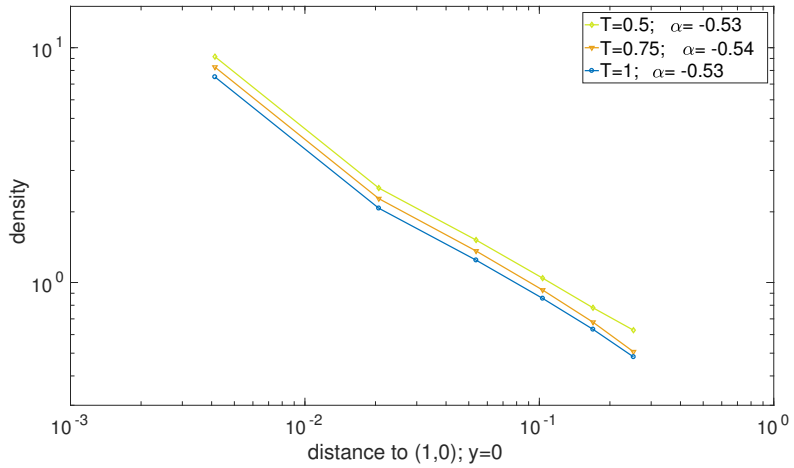

Figure 6.3: Asymptotic behavior of the solution to the single layer equation near edge along $y = 0$, Example 6.1, Figure 4 in [46]

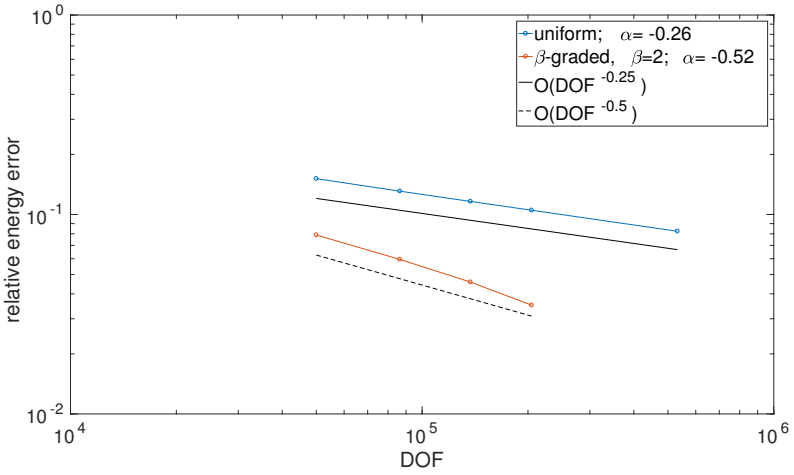

Figure 6.4: Energy error for single layer equation on circular screen, Example 6.1, Figure 5 [46]

Example 6.2. *We compute the solution to the retarded single layer integral equation* $V\psi = f$ *on* $\Gamma\times\mathbb{R}^+$ *for the square screen* $\Gamma = [-1,1]^2\times\{0\}$ *with the discretization from Subsection 2.3.1. The weak form* (2.49) *with constant ansatz and test functions in space and time are used. The right hand side is specified with* $f(x,t) = \cos(|k|t - k\cdot x)\exp(-1/(10t^2))$, *where* $k = (0.2, 0.2, 0.2)$. *We choose* $\Delta t = 0.005$ *and compute the solution till* $T = 1$. *The finest graded mesh in our computation contains* 2312 *triangles with* $\Delta t = 0.005$ *and* $\beta = 2$, *where it serves as a reference solution.*

Figures 6.5 and 6.6 show the density along the diagonal $x = y$ and along the x-axis of

the reference solution at time $T = 0.5$. The figures display the expected corner and edge singularities known by the decomposition (6.6). In Figure 6.7 the density along $y = x$ of the reference solution is compared to 2 uniform meshes with 8000 and 20000 triangles each with $\Delta t = 0.005$. The 2-graded mesh exhibits a higher resolution of the corner singularities than the uniform meshes.

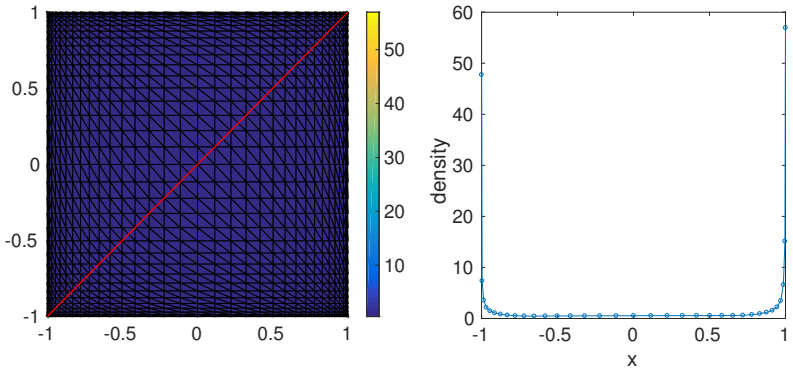

Figure 6.5: Solution of the single layer equation at $T = 0.5$ along $y = x$ on the square screen, Example 6.2, Figure 6 in [46]

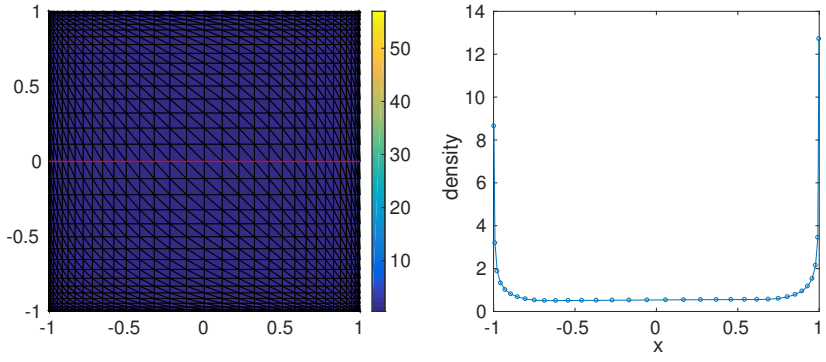

Figure 6.6: Solution of the single layer equation at $T = 0.5$ along $y = 0$ on the square screen, Example 6.2, Figure 7 in [46]

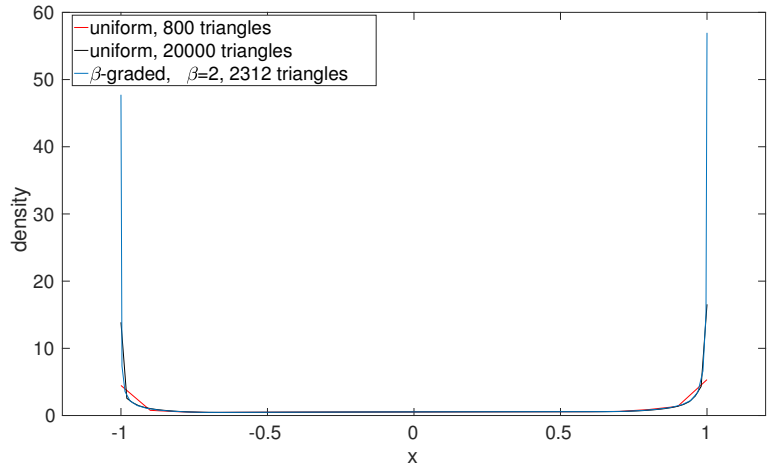

Figure 6.7: Numerical computation of the corner singularity along diagonal from $(-1,-1)$ to $(1,1)$ at time $T = 0.5$, Example 6.2, Figure 8 in [46]

In Figure 6.8 the numerical density of the reference solution at times $0.5, 0.75, 1.0$ are plotted against the distance to the corner at $(1,1)$ along $x = y$. The singular exponents are around -0.78, where the theoretical exponent gives $\gamma - 1 = 0.2966 - 1 = 0.7034$. In Figure 6.9 the numerical density of the reference solution at times $0.5, 0.75, 1.0$ are plotted against the distance to the edge at $(1,0)$ along the x-axis. The singular exponents are in close agreement with the theoretical value of $-\frac{1}{2}$. We remember that we can't deduce from the convergence of the boundary element method in the energy a convergence of the numerically computed singular exponents.

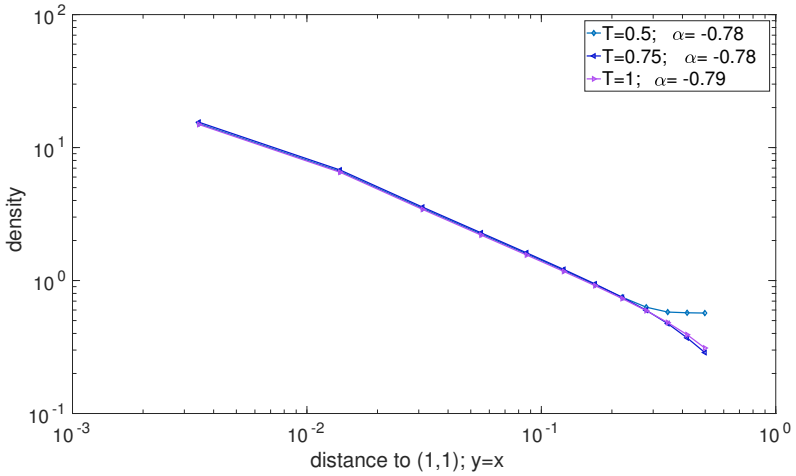

Figure 6.8: Asymptotic behavior of the solution to the single layer equation near corner along $y = x$, Example 6.2, Figure 9 in [46]

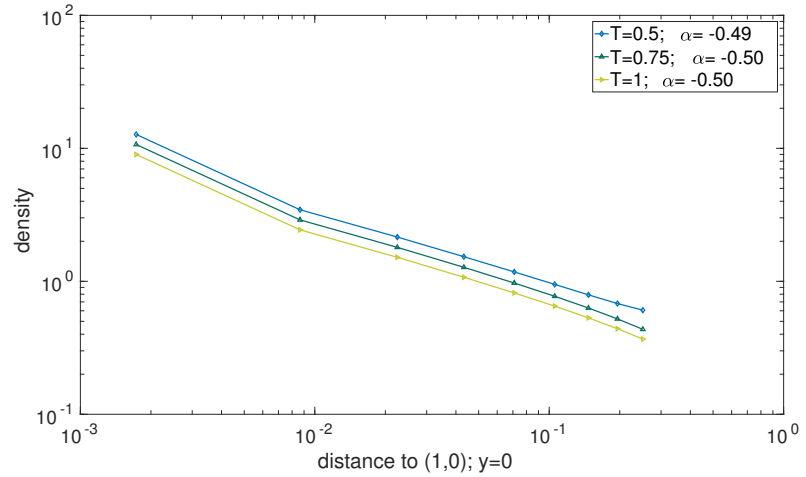

Figure 6.9: Asymptotic behavior of the solution to the single layer equation near edge along $y = 0$, Example 6.2, Figure 10 in [46]

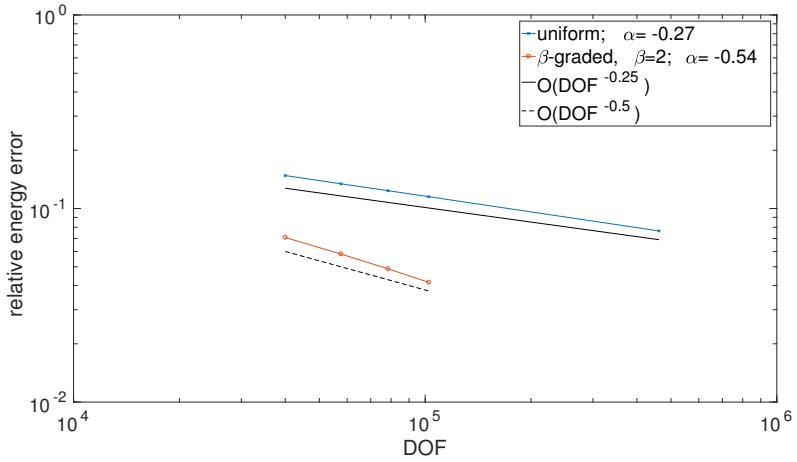

Figure 6.10: Relative energy error for the single layer equation on square screen, Example 6.2, Figure 11 in [46]

We finally consider the relative energy error compared to the reference solution. We can't expect a convergence in $L^2([0,T]\times\Gamma)$, since the solution exhibits a low spatial regularity. Therefore we consider the energy norm, as in (2.56), $\tilde{E}(T) = \vec{\psi}\tilde{V}\vec{\psi} - 2\vec{\psi}\vec{f}$ for $T = 1$ with the solution vector $\vec{\psi}$ after solving the MOT-scheme (2.54) till $T = 1$. $H^0_\sigma(\mathbb{R}^+, \widetilde{H}^{-\frac{1}{2}}(\Gamma))$ is comparable or stronger than the energy norm. Figure 6.10 describes the relative energy error against the degrees of freedom. We see for the 2-graded mesh a rate of -0.54, whereas the uniform mesh shows a rate of -0.27. The error behaves in agreement to the expected approximation properties proportional to h (equivalently

$\sim DOF^{-1/2}$) on the 2-graded mesh resp. $\sim h^{1/2}$ ($\sim DOF^{-1/4}$) on the uniform mesh.

Next we consider the L_2–norm in time of the sound pressure evaluated in a point by computing $S\psi_{h,\Delta t}$. Figure 6.11 presents the L_2–error in time of the sound pressure evaluated at $(1,1,0.004), (0.75,0.75,1)$ and $(1,1.25,0.25)$. Each of the points exhibit a convergence rate proportional to h^2 resp. h as for the energy norm. However the error in $(1,1,0.004)$ with distance 0.004 to the corner of the screen is higher than the other points.

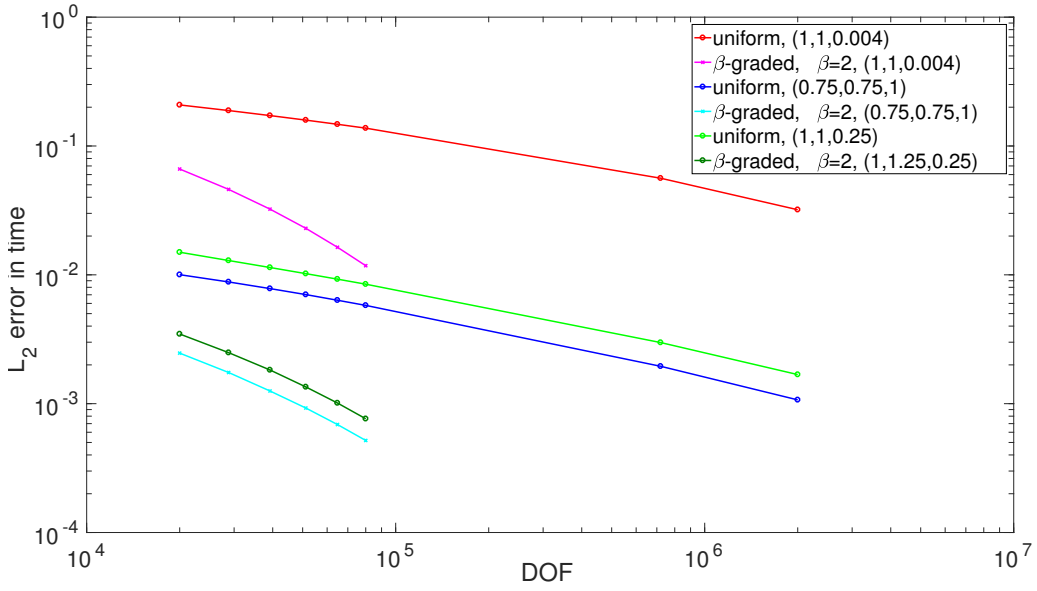

Figure 6.11: $L_2([0,T])$-error for the sound pressure in three points outside square screen, computed from single layer equation, Example 6.2, Figure 12 in [46]

Example 6.3. *We compute the solution to the retarded single layer integral equation* $V\psi = f$ *on* $\Gamma \times \mathbb{R}^+$ *for the L-shaped screen* $\Gamma = [-1,1]^2 \times \{0\} \backslash [0,1]^2 \times \{0\}$ *with the discretization from Subsection 2.3.1. The weak form* (2.49) *with constant ansatz and test functions in space and time are used. The right hand side is specified with* $f(x,t) = \cos(|k|t - k \cdot x) \exp(-1/(10t^2))$, *where* $k = (0.2, 0.2, 0.2)$. *We choose* $\Delta t = 0.005$ *and compute the solution till* $T = 1$. *The finest graded mesh in our computation contains* 6936 *triangles with* $\Delta t = 0.005$ *and* $\beta = 2$, *where it serves as a reference solution.*

Figure 6.12 shows the density along the diagonal $(-1,-1)$ to $(0,0)$ of the reference solution at time 0.5. The Figure exhibits a stronger corner singularity at $(0,0)$ than at $(-1,-1)$.

In Figure 6.13 the numerical density of the reference solution at times $0.5, 0.75, 1.0$ are plotted against the distance to the corner at $(0,0)$ along the diagonal. The singular exponents are around -0.22, which is expected to be $\gamma - 1 = 0.8146 - 1 = -0.1854$.

In Figure 6.14 the numerical density of the reference solution at times $0.5, 0.75, 1.0$ are plotted against the distance to the corner at $(-1,-1)$ along the diagonal. The singular exponents are around -0.71, which is very close to the theoretical value of $\gamma - 1 = 0.2966 - 1 = 0.7034$. We achieve here a better approximation of the singular exponents than in Example 6.2, since we use a more refined mesh. We remember that we can't deduce from the convergence of the boundary element method in the energy norm a convergence of the numerically computed singular exponents.

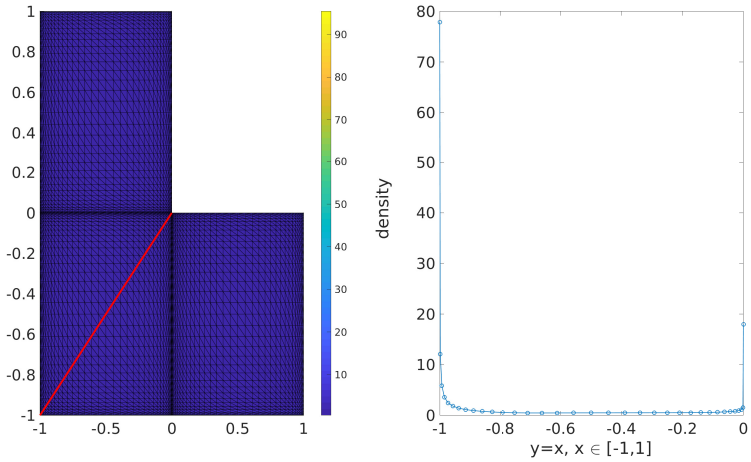

Figure 6.12: Solution of the single layer equation at $T = 0.5$ along $y = x$ on the L-shaped screen, Example 6.3

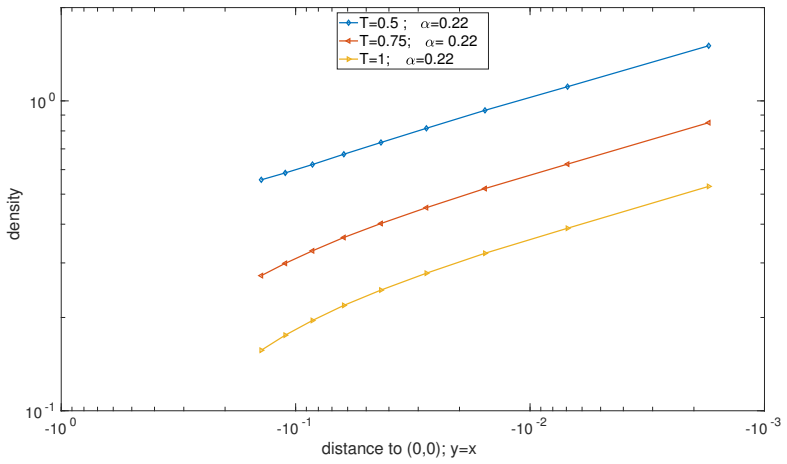

Figure 6.13: Asymptotic behavior of the solution to the single layer equation near the corner (0,0) along $y = x$, Example 6.3

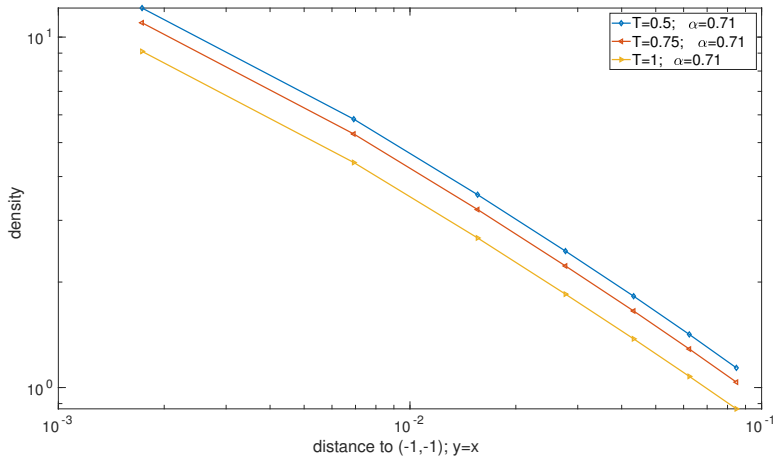

Figure 6.14: Asymptotic behavior of the solution to the single layer equation near the corner (-1,-1) along $y = x$, Example 6.3

We finally consider the relative energy error compared to the reference solution. We can't expect a convergence in $L^2([0,T]\times\Gamma)$ since the solution exhibits a low spatial regularity. Therefore we consider the energy norm as in (2.56), $\tilde{E}(T) = \vec{\psi}\tilde{V}\vec{\psi} - 2\vec{\psi}\vec{f}$ for $T = 1$ with the solution vector $\vec{\psi}$ after solving the MOT-scheme (2.54) till $T = 1$. $H^0_\sigma(\mathbb{R}^+, \widetilde{H}^{-\frac{1}{2}}(\Gamma))$ is comparable or stronger than the energy norm. Figure 6.15 describes the relative energy error against the degrees of freedom. We see for the 2-graded mesh a rate of -0.5, whereas the uniform mesh shows a rate of -0.26. The error behaves in agreement to the expected approximation properties proportional to h (equivalently $\sim DOF^{-1/2}$) on the 2-graded mesh resp. $\sim h^{1/2}$ ($\sim DOF^{-1/4}$) on the uniform mesh.

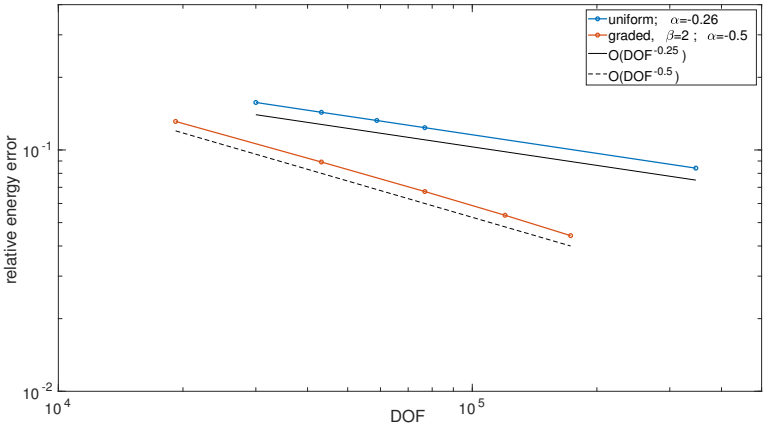

Figure 6.15: Energy error norm for single layer equation on L-shaped screen, Example 6.3

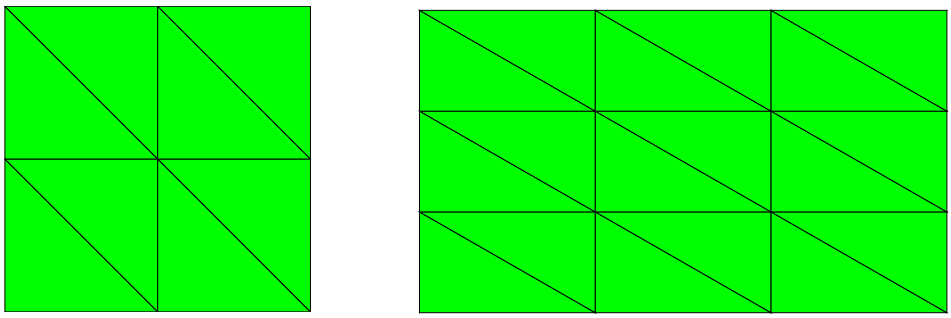

(a) Mesh with 8 triangular elements and 9 nodes, (b) Mesh with 18 triangular elements and 16 nodes. Figure 2 in [49]

Figure 6.16: Mesh of a square screen

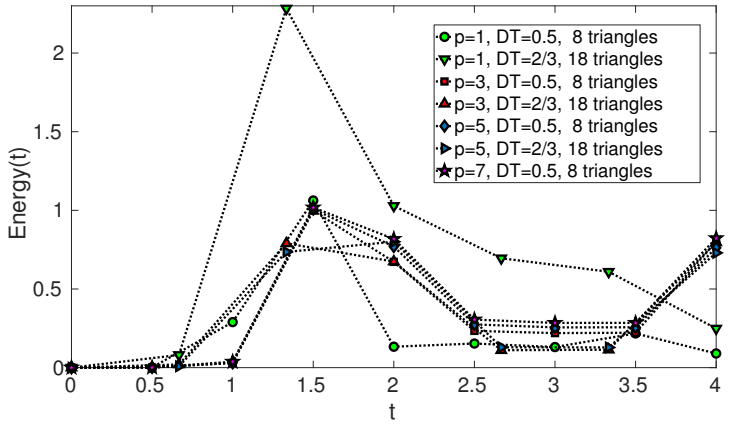

Figure 6.17: Energy as a function of time for time-singular f_4, Example 6.4. Figure 5 in [49]

6.4.2 Single layer potential for p-version

Example 6.4. *We compute the solution to the retarded single layer integral equation* $V\psi = f$ *on* $\Gamma \times \mathbb{R}^+$ *for the square screen* $\Gamma = [-\frac{1}{2}, \frac{1}{2}]^2 \times \{0\}$, *discretized with piecewise polynomials of degree* p *as in [91, 96]. We study the convergence of the numerical solution* ψ_p *for* $\Delta t = 0.5$ *with* 8 *triangles and* $\Delta t = \frac{2}{3}$ *with* 18 *triangles (see Figure 6.16), till* $T = 4$ *in terms of an increasing polynomial degree* p. *We compare various right hand sides in the square-root of the discretized energy* $\tilde{E}_p(T) = \sqrt{-\psi_p \tilde{V}_p \psi_p}$, *where* $\tilde{V}_p$ *is the corresponding space time matrix for the polynomial degree* p.

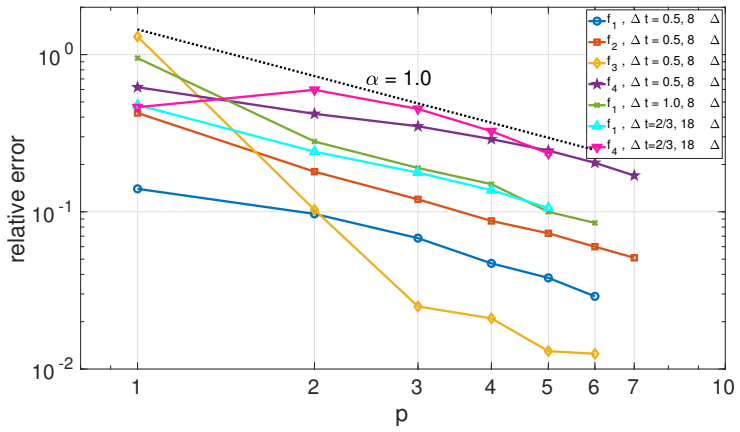

Figure 6.18: Relative error in energy norm for the single-layer equation on a square screen, Example 6.4. Figure 4 in [49]

We define the right hand sides:

$$
\begin{aligned}
&f_1(t,(x,y,z)) = \sin^5(t)x^2 \ , \\
&f_2(t,(x,y,z)) = \exp(-2/t^2)cos(\omega t - k\cdot(x,y,z)) \ , \text{ with } k = (2,0.5,0.1) \text{ and } \omega = |k| \ , \\
&f_3(t,(x,y,z)) = \exp(-2/t^2)cos(\omega t - k\cdot(x,y,z)) \ , \text{ with } k = (6,0.5,0.1) \text{ and } \omega = |k| \ , \\
&f_4(t,(x,y,z)) = \sin^5(t)|1-t|^{\alpha}\cos(k\cdot(x,y,z)) \ , \text{ with } \alpha = \tfrac{1}{2} \text{ and } k = (6,0.5,0.1) \ .
\end{aligned}
$$

Figure 6.17 displays the discretized energy $\tilde{E}_p(t)$ for $t \in [0,4]$ of f_4 at multiples of times $\Delta t = 0.5$ with 8 triangles for $p = 1,3,5,7$ and $\Delta t = \frac{2}{3}$ with 18 triangles for $p = 1,3,5$. While $p = 1$ for $\Delta t = \frac{2}{3}$ differs greatly from the other curves $p = 1$ for $\Delta t = 0.5$ is close to the other curves at times 0.5 and 1. After the kink of the right hand side at $t = 1$ only higher polynomials within the same Δt are close to each other. For the time $2,4$, where all the curves meet, the curves for $p = 5$ $\Delta t = 0.5$, $p = 5$ $\Delta t = \frac{2}{3}$ and $p = 7$ $\Delta t = 0.5$ are close to each other. The different Δt in the computations are noticed in particular for the time interval $[2.5,3.5]$, where there is almost no change in the energy.

Figure 6.18 depicts the convergence in the squar-root of the discretized energy as a function depending on the polynomial degree for $f_1,\ldots,f_4$ $\Delta t = 0.5$ 8 triangles, f_1 $\Delta t = 1.0$ 8 triangles and f_1, f_4 $\Delta t = \frac{2}{3}$, 18 triangles. The convergence rate for the p-version is expected to be twice as the convergence rate of the h-version. We used an Aitken extrapolation as the reference for the relative energy error. While for f_1 $\Delta t = 0.5$ resp. $\Delta t = 1.0$, we have a convergence rate approximately at 1.02 resp. 1.12. We get for $\Delta t = \frac{2}{3}$ a convergence rate of 1.01. For f_2, $\Delta t = 0.5$ we have a convergence rate of 1.02. For f_3, $\Delta t = 0.5$ we have a convergence rate for higher p around 1.01. For f_4, $\Delta t = 0.5$, we have a convergence rate for higher p around -0.95, whereas for $\Delta t = \frac{2}{3}$, we have a convergence rate of approximately 1.02.

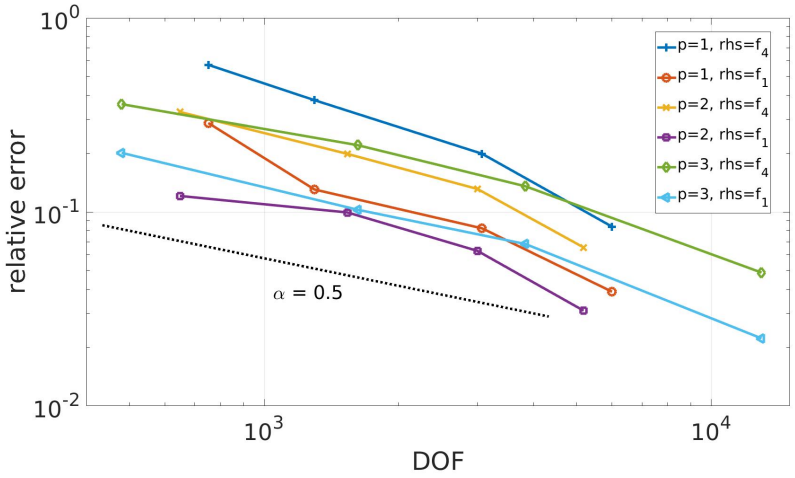

Figure 6.19: Relative error in the square of the energy norm for the single-layer equation on a square screen, h-version for $p = 1, 2, 3$, Example 6.5. Figure 6 in [49]

The next example studies the h-version for different polynomial degrees p.

Example 6.5. *We compute the solution to the retarded single layer integral equation* $V\psi = f$ *on* $\Gamma \times \mathbb{R}^+$ *on the square screen* $\Gamma = [-\frac{1}{2}, \frac{1}{2}]$ *discretized with piecewise polynomials of degree* p *as in [91, 96]. We study the convergence of the numerical solution* ψ_p *in a discretized energynorm till time* 2. *We use solutions for* $\Delta t = \frac{1}{6}$ *and* 288 *triangles for* $p = 1$, $\Delta t = 0.25$ *and* 128 *triangles for* $p = 2, 3$ *as benchmarks for each* p.

In Figure 6.19 we plotted the relative error of the square of the discretized energy for f_1, f_4 depending on the degrees of freedom. We expect from the approximation properties a rate proportional to h (equivalently $\sim DOF^{-1/2}$). The points in the curves for $p = 1$ corresponds to the mesh $\Delta t = 0.4$ 50 triangles, $\Delta t = \frac{1}{3}$ 72 triangles, $\Delta t = 0.25$ 128 triangles and $\Delta t = 0.2$ 200 triangles. The curves for $p = 2$ corresponds to $\Delta t = \frac{2}{3}$ 18 triangles, $\Delta t = 0.5$ 32 triangles, $\Delta t = 0.4$ 50 triangles and $\Delta t = \frac{1}{3}$ 72 triangles. Finally for $p = 3$, we use $\Delta t = 1.0$ 8 triangles, $\Delta t = \frac{2}{3}$ 18 triangles, $\Delta t = \frac{1}{3}$ 72 triangles. For $p = 3$ and f_1, we get a convergence rate of 0.52, whereas for f_4 we get 0.468. For $p = 2$ and f_1 resp. f_4 we get a convergence rate of 0.48 resp. 0.425. The mesh $\Delta t = \frac{1}{3}$ with 72 triangles is close to the benchmark mesh, which explains the kink at the last point. The same occurs for $\Delta t = 0.2$ and 200 triangle for $p = 1$. For $p = 1$ we suffer from very coarse meshes, whereas the polynomial degree isn't high enough to compensate it. Altogether, the numerical results confirm the theoretical conclusion that the p-version converges twice as fast as the $h-$version.

6.4.3 Hypersingular operator for graded meshes

Example 6.6. *We compute the solution to the retarded hypersingular integral equation* $W\phi = g$ *on* $\Gamma \times \mathbb{R}^+$ *on the circular screen* $\Gamma = \{(x, y, 0) : 0 \leq \sqrt{x^2 + y^2} \leq 1\}$ *with the discretization from Subsection 2.3.4. The weak form* (2.62) *with linear ansatz and test functions in space and linear ansatz and constant test functions in time are used. The right hand side is specified*

$$g(x,t) = (-\tfrac{3}{4} + \cos(\tfrac{\pi}{2}(4-t)) + \tfrac{\pi}{2}\sin(\tfrac{\pi}{2}(4-t)) - \tfrac{1}{4}(\cos(\pi(4-t)) + \pi\sin(\pi(4-t))))\times \\ \times [H(4-t) - H(-t)],$$

where H *is the Heaviside function. We choose* $\Delta t = 0.01$ *and compute till* $T = 4$*. The finest graded mesh in our computation contains* 2662 *triangles with* $\Delta t = 0.01$ *and* $\beta = 2$*, where it serves as a reference solution.*

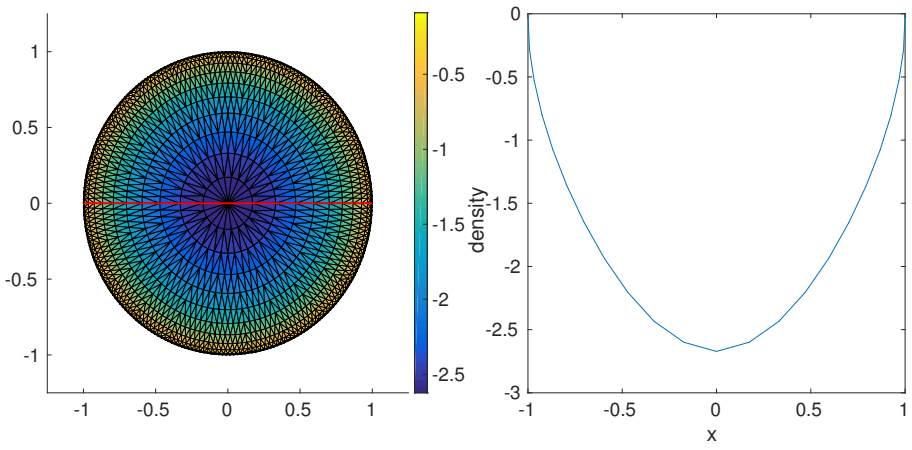

Figure 6.20: Solution of the hypersingular equation at $T = 2$ along $y = 0$ on the circular screen, Example 6.6, Figure 13 in [46]

Figure 6.20 shows the density along a cross-section of the reference solution at time 2. The figure shows the expected edge singularities known by the decomposition (6.3).

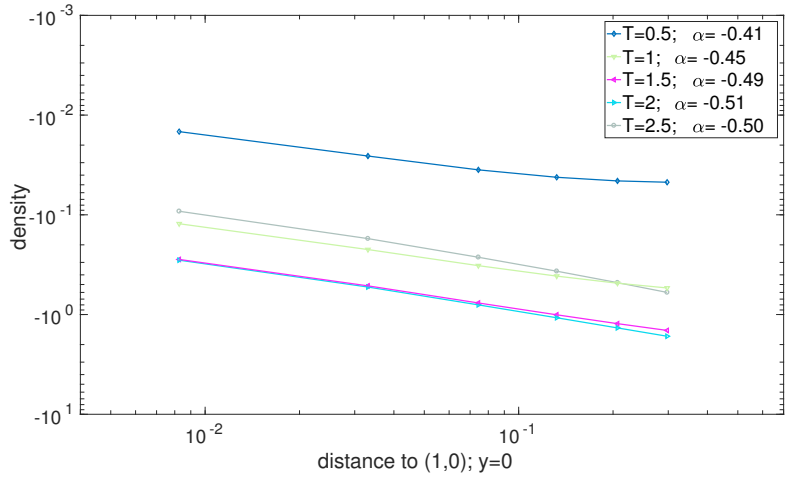

Figure 6.21: Asymptotic behavior of the solution to the hypersingular equation near edge along $y = 0$, Example 6.6, Figure 14 in [46]

In Figure 6.21 the numerical density of the reference solution at times $0.5, 1, 1.5, 2, 2.5$ are plotted against the distance to the edge at $(1, 0)$, along the x-axis. The numerical solution are in close agreement with the theoretical value of $\frac{1}{2}$, where for earlier times the difference is greater.

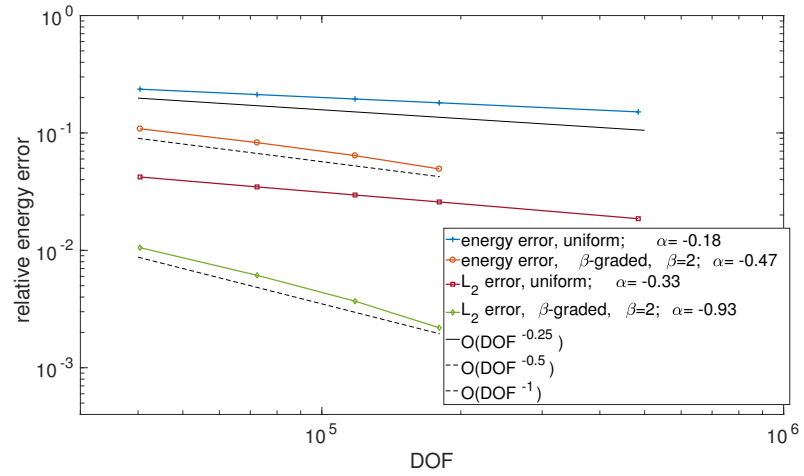

Figure 6.22: $L_2([0,T], L_2(\Gamma))$ and energy error for hypersingular equation on circular screen, Example 6.6, Figure 15 in [46]

Figure 6.22 describes the relative energy error and the L_2-error compared to the reference solution in terms of degrees of freedom. We see for the 2-graded mesh a convergence rate of -0.47 in energy and -0.93 in $L_2([0,T], L_2(\Gamma))$. The error behaves

in agreement with the expected approximation properties in the energy norm proportional to h (equivalently $\sim DOF^{-1/2}$) in the energy and $\sim h^2$ (equivalently $\sim DOF^{-1}$) in $L_2([0,T], L_2(\Gamma))$. For the uniform mesh, we get a rate of -0.18 in energy and -0.33 in L_2, where we expect a rate proportional to $h^{1/2}$ (equivalently $\sim DOF^{-1/4}$) in energy and $\sim h$ (equivalently $\sim DOF^{-1/2}$) in L_2.

Example 6.7. *We compute the solution to the retarded hypersingular integral equation $W\phi = g$ on $\Gamma \times \mathbb{R}^+$ for the square screen $\Gamma = [-1,1]^2 \times \{0\}$ with the discretization from Subsection 2.3.4. The weak form (2.62) with linear ansatz and test functions in space and linear ansatz and constant test functions in time are used. The right hand side is specified*

$$g(x,t) = (-\tfrac{3}{4} + \cos(\tfrac{\pi}{2}(4-t)) + \tfrac{\pi}{2}\sin(\tfrac{\pi}{2}(4-t)) - \tfrac{1}{4}(\cos(\pi(4-t)) + \pi\sin(\pi(4-t))))\times \\ \times [H(4-t) - H(-t)],$$

where H is the Heaviside function. We choose $\Delta t = 0.01$ and compute till $T = 4$. The finest graded mesh in our computation contains 2312 triangles with $\Delta t = 0.01$ and $\beta = 2$, where it serves as a reference solution.

Figure 6.23 and 6.24 show the density along the diagonal $x = y$ and along the x-axis of the reference solution at time 2. The figures display the expected corner and edge singularities known by the decomposition. Since the solution of the hypersingular integral equation lies in $H^{1/2}_\sigma(\mathbb{R}^+, \widetilde{H}^{1/2}(\Gamma))$, the conforming numerical approximation tends to zero at both edges and corners.

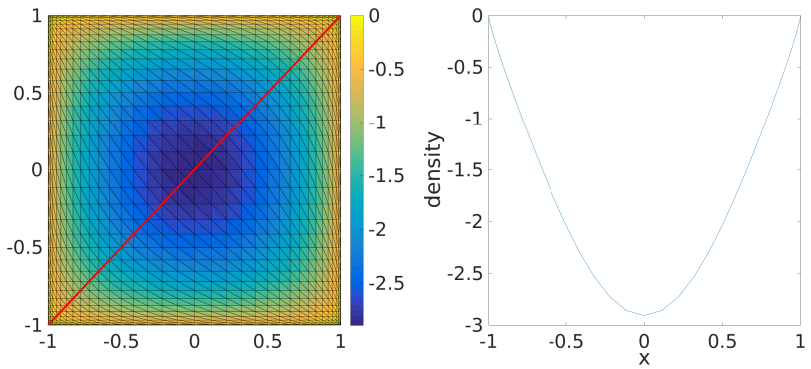

Figure 6.23: Solution of the hypersingular equation at $T = 2$ along $y = x$ on the square screen, Example 6.7, Figure 16 in [46]

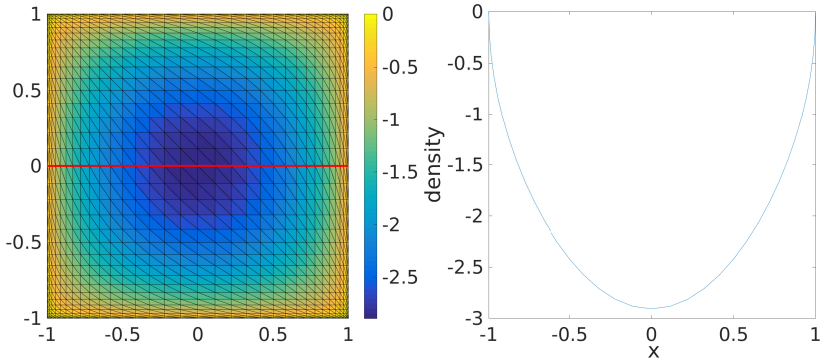

Figure 6.24: Solution of the hypersingular equation at $T = 2$ along $y = 0$ on the square screen, Example 6.7, Figure 17 in [46]

In Figure 6.25 the numerical density of the reference solution at times $0.5, 1, 1.5, 2, 2.5$ are plotted against the distance to the corner at $(1, 1)$ along $x = y$. The singular exponents are between 0.65 and 0.71, which do not show a good agreement with the exact corner exponent $\gamma = 0.2966$.

In Figure 6.26 the numerical densities of the reference solution are plotted at the same times against the distance to the edge at $(1, 0)$ along the x-axis. The singular exponents are between 0.46 and 0.49, which do show a good agreement with the theoretical value of $\frac{1}{2}$.

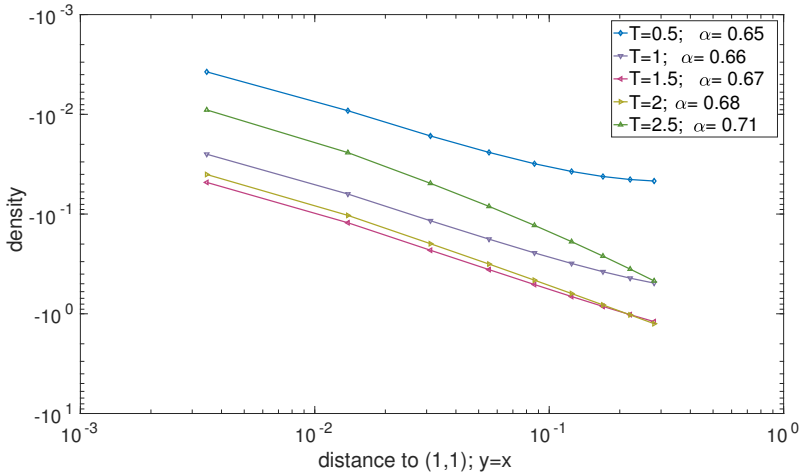

Figure 6.25: Asymptotic behavior of the solution to the hypersingular equation near corner along $y = x$, Example 6.6, Figure 18 in [46]

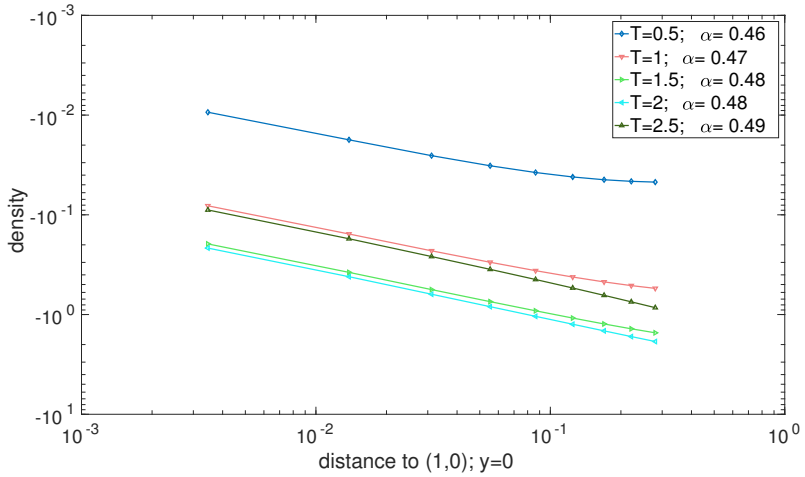

Figure 6.26: Asymptotic behavior of the solution to the hypersingular equation near edge along $y = 0$, Example 6.6, Figure 19 in [46]

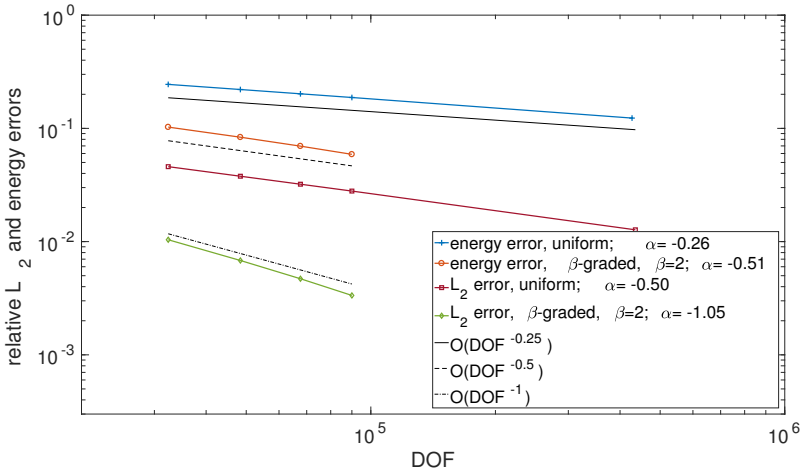

Figure 6.27: $L_2([0,T], L_2(\Gamma))$ and energy error for hypersingular equation on square screen, Example 6.7, Figure 20 in [46]

Finally, Figure 6.27 shows the error in both the energy and $L_2([0,T], L_2(\Gamma))$-norms with respect to the benchmark solution. The convergence rate in terms of the degrees of freedom on the 2-graded mesh is -0.51 in energy and -1.05 in L_2. On the uniform mesh the rate is -0.26 in energy and -0.50 in L_2. The rates on the 2-graded meshes are in close agreement with a convergence proportional to $\sim h$ (equivalently, $\sim DOF^{-1/2}$) predicted by the approximation properties in the energy norm, and $\sim h^{1/2}$ ($\sim DOF^{-1/4}$) on uniform meshes. Also in the L_2-norm, the convergence corresponds to the expected rates: Approximately $\sim h^2$ (equivalently, $\sim DOF^{-1}$) on 2-graded meshes, $\sim h$ (equiva-

lently, $\sim DOF^{-1/2}$) on uniform meshes. In all cases the convergence is twice as fast on the 2-graded meshes compared to the uniform meshes.

Figure 6.27 describes the relative energy error and the L_2−error compared to the reference solution in terms of degrees of freedom. We see for the 2-graded mesh a convergence rate of −0.51 in energy and −1.05 in L_2. The error behaves in close agreement with the expected approximation properties in the energy norm proportional to $\sim h$ (equivalently $\sim DOF^{-1/2}$) and in L_2 $\sim h^2$ (equivalently $\sim DOF^{-1}$). For the uniform mesh we get a rate of −0.26 in energy and −0.5 in L_2 which is in good agreement with the expected rate proportional to $h^{1/2}$ (equivalently $\sim DOF^{-1/4}$) in energy and $\sim h$ (equivalently $\sim DOF^{-1/2}$) in L_2.

Example 6.8. *We compute the solution to the retarded hypersingular integral equation* $W\phi = g$ *on* $\Gamma \times \mathbb{R}^+$ *for the L-shaped screen* $\Gamma = [-1,1]^2 \times \{0\} \backslash [0,1]^2 \times \{0\}$ *with the discretization from Subsection 2.3.4. The weak form* (2.62) *with linear ansatz and test functions in space and linear ansatz and constant test functions in time are used. The right hand side is specified*

$$g(x,t) = (-\tfrac{3}{4} + \cos(\tfrac{\pi}{2}(4-t)) + \tfrac{\pi}{2}\sin(\tfrac{\pi}{2}(4-t)) - \tfrac{1}{4}(\cos(\pi(4-t)) + \pi\sin(\pi(4-t))))\times \\ \times [H(4-t) - H(-t)],$$

where H *is the Heaviside function. We choose* $\Delta t = 0.01$ *and compute till* $T = 4$. *The finest graded mesh in our computation contains* 6936 *triangles with* $\Delta t = 0.01$ *and* $\beta = 2$, *where it serves as a reference solution.*

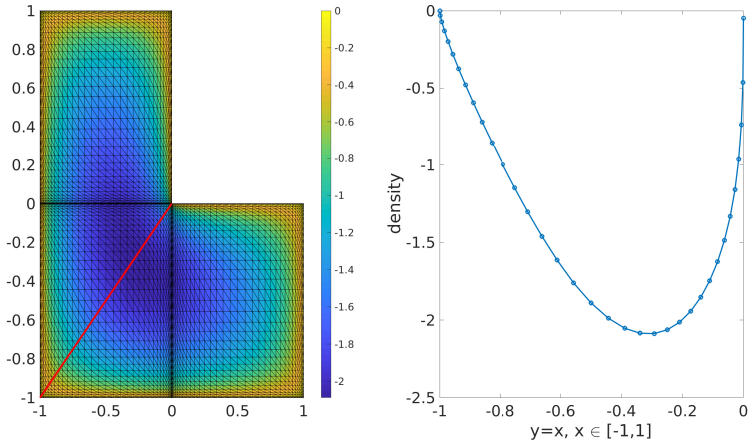

Figure 6.28: Solution of the hypersingular equation at $T = 2$ along $y = x$ on the L-shaped screen, Example 6.8

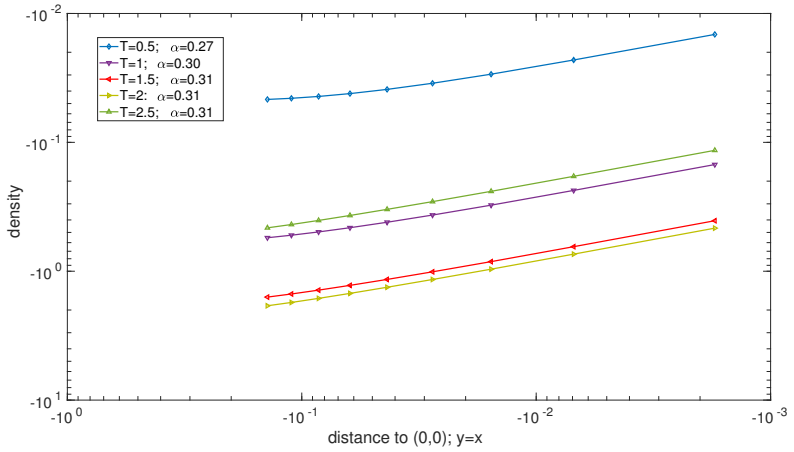

Figure 6.29: Asymptotic behavior of the solution to the hypersingular equation near the corner (0,0) along $y = x$, Example 6.8

Figure 6.28 shows the density along the diagonal $(-1,-1)$ to $(0,0)$ of the reference solution at time 2. The figure exhibits a stronger corner singularity at $(0,0)$ than at $(-1,-1)$. Since the solution of the retarded hypersingular integral equation lies in $H_\sigma^{1/2}(\mathbb{R}^+, \widetilde{H}^{1/2}(\Gamma))$, the conforming numerical approximation tends to zero at both corners.

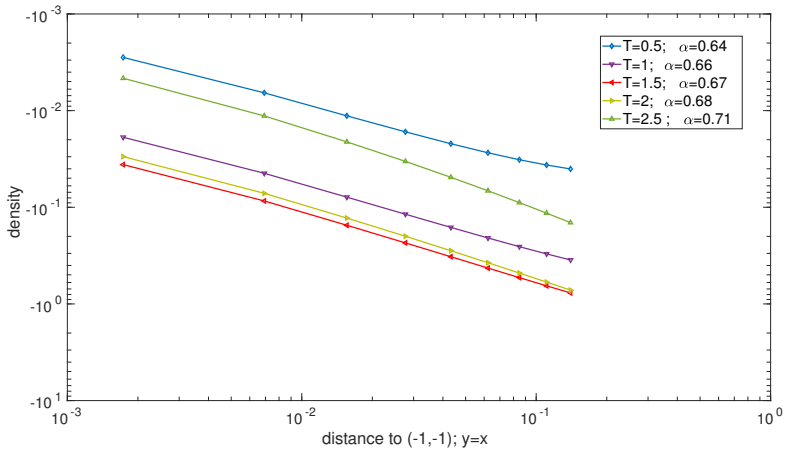

Figure 6.30: Asymptotic behavior of the solution to the hypersingular equation near the corner (-1,-1) along $y = x$, Example 6.8

In Figure 6.29 the numerical density of the reference solution at times $0.5, 1, 1.5, 2, 2.5$ are plotted against the distance to the corner at $(0,0)$ along the diagonal. The singular exponents lie between 0.27 and 0.31, which do not show a good agreement with the

exact corner exponent $\gamma \approx 0.8146$.

In Figure 6.30 the numerical density of the reference solution at times $0.5, 1, 1.5, 2, 2.5$ are plotted against the distance to the corner $(-1,-1)$ along the diagonal. The singular exponents are similar to Figure 6.25, where both do not show a good agreement with the exact corner exponent $\gamma \approx 0.2966$.

Figure 6.31 describes the relative energy error compared to the reference solution in terms of degrees of freedom. We see for the 2-graded mesh a convergence rate of -0.5, where the uniform mesh admits a convergence rate -0.26. Both are in good agreement with the expected rates proportional to h (equivalently $\sim DOF^{-1/2}$) for the 2-graded mesh and $\sim h^{1/2}$ (equivalently $\sim DOF^{-1/4}$) for the uniform mesh.

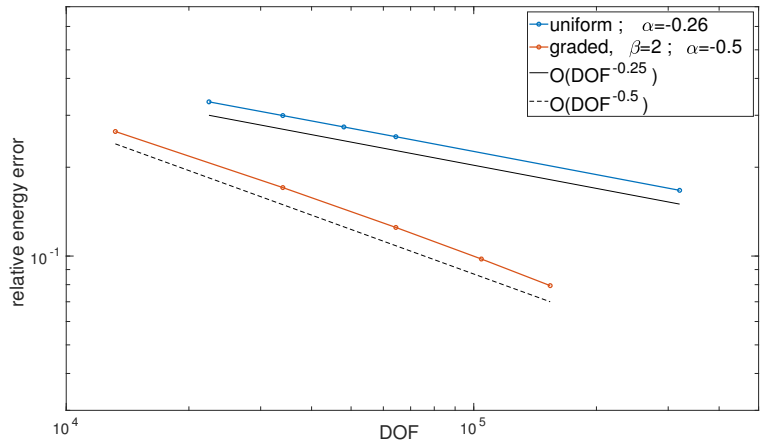

Figure 6.31: Energy error for the hypersingular equation on the L-shaped screen, Example 6.8

6.4.4 Dirichlet-to-Neumann operator for graded meshes

At last we consider the Poincaré-Steklov operator on screens. We will use the form given in Subsection 2.3.5 to compute this operator.

Example 6.9. *We compute the solution to the integral equation $\mathcal{S}u = h$ on $\Gamma \times \mathbb{R}^+$ for the square screen $\Gamma = [-1,1]^2 \times \{0\}$ with the discretization from Subsection 2.3.5. The right hand side is specified*

$$h(x,t) = (-\tfrac{3}{4} + \cos(\tfrac{\pi}{2}(4-t)) + \tfrac{\pi}{2}\sin(\tfrac{\pi}{2}(4-t)) - \tfrac{1}{4}(\cos(\pi(4-t)) + \pi\sin(\pi(4-t))))\times \\ \times [H(4-t) - H(-t)],$$

where H is the Heaviside function. We choose $\Delta t = 0.01$ and compute till $T = 0.65$. The finest mesh in our computation contains 2312 triangles with $\Delta t = 0.01$ and $\beta = 2$, where it serves as a reference solution.

Figure 6.32 and 6.33 show the density along the diagonal $x = y$ and along the longitudinal y at $x = -0.8754$ of the reference solution at time 0.65. The figures display the expected corner and edge singularities known by the decomposition (6.5). Since the solution of the Poincaré-Steklov operator lies in $H_\sigma^{1/2}(\mathbb{R}^+, \widetilde{H}^{1/2}(\Gamma))$, the conforming numerical approximation is zero at the edges and corners.

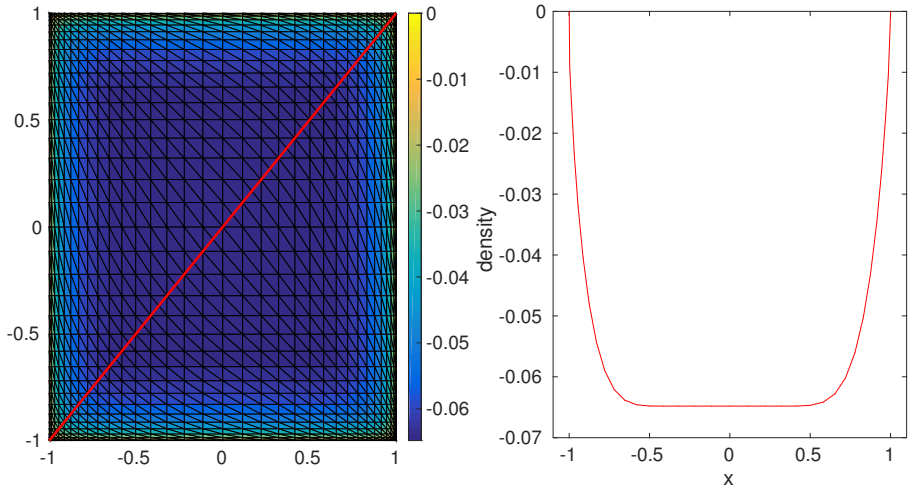

Figure 6.32: Solution of the Dirichlet-to-Neumann equation at $T = 0.65$ along $y = x$ on the square screen, Example 6.9, Figure 21 in [46]

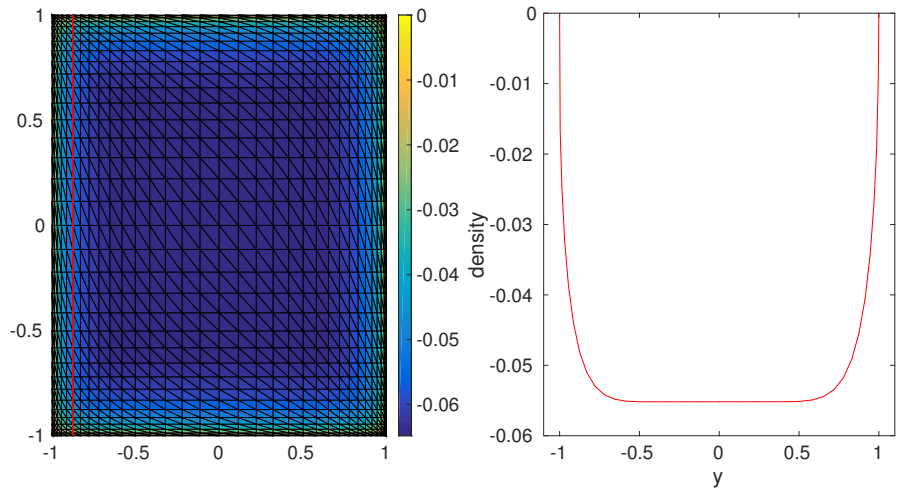

Figure 6.33: Solution of the Dirichlet-to-Neumann equation at $T = 0.65$ along $x = -0.8754$ on the square screen, Example 6.9, Figure 22 in [46]

In Figure 6.34 the numerical density of the reference solution at times $0.25, 0.5, 0.6, 0.65$ are plotted against the distance to the corner at $(1, 1)$ along the $x = y$. The singular

exponents rise from 0.54 for $T = 0.25$ up to $0.65, 0.66, 0.67$ for times $0.5, 0.6, 0.65$, similar in Figure 6.25, which significantly differs from the exact value $\gamma \approx 0.2966$.

In Figure 6.35 the numerical density of the reference solution at times $0.25, 0.5, 0.6, 0.65$ are plotted against the distance to the edge at $(-0.8754, 1)$, along the longitudinal y for a fixed $x = -0.8754$. The singular exponents rise from 0.35 for $T = 0.25$ up to $0.40, 0.41, 0.41$ for times $0.5, 0.6, 0.65$, which is in qualitative agreement with the exact value $\frac{1}{2}$.

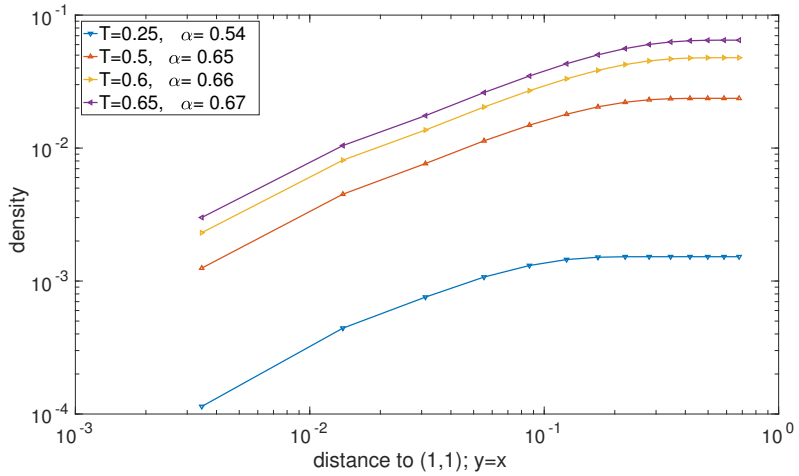

Figure 6.34: Asymptotic behavior of the solution to the Dirichlet-to-Neumann equation near corner along $y = x$, Example 6.9, Figure 23 in [46]

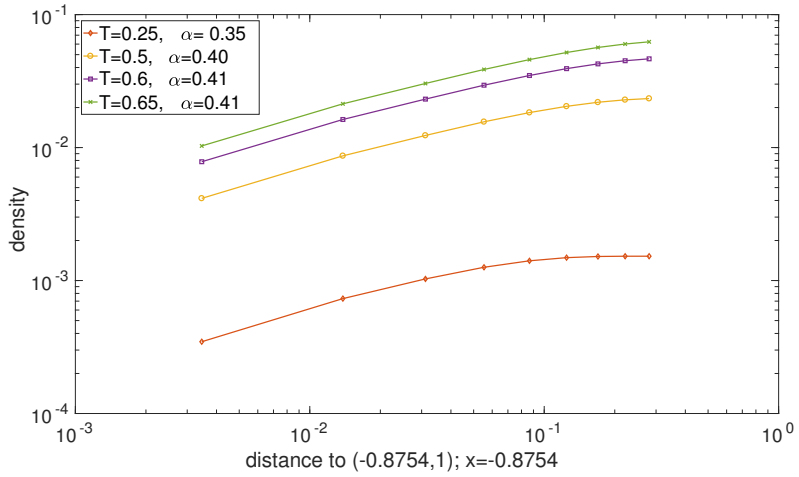

Figure 6.35: Asymptotic behavior of the solution to the Dirichlet-to-Neumann equation near edge along $x = -0.8754$, Example 6.9, Figure 24 in [46]

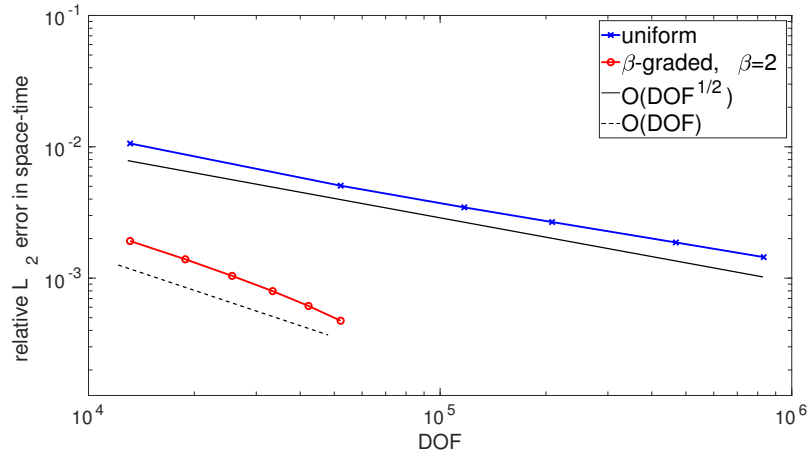

Figure 6.36: Error in $L_2([0,T],L_2(\Gamma))$ norm for Dirichlet-to-Neumann equation on square screen, Example 6.9, Figure 25 in [46]

Figure 6.36 describes the relative error in $L_2([0,T],L_2(\Gamma))$ compared to the reference solution in terms of degrees of freedom. We see for the 2-graded mesh a convergence rate around -1.01, where the uniform mesh admits a convergence rate -0.48. Both rates are in good agreement with the expected rates proportional to h^2 (equivalently $\sim DOF^{-1}$) for the 2-graded mesh and proportional to h (equivalently $\sim DOF^{-1/2}$) for the uniform mesh. These results are also similar to the retarded hypersingular integral equation on the square screen (see Example 6.7).

7 Unilateral contact problems: Punch problems / Crack problems

7.1 Introduction

Contact between objects is ubiquitous in mechanics, yet the analysis and the computations pose severe challenges. Contact problems have a wide range of applications like in fracture dynamics, crash analysis, biomechanics and thermo-electro-mechanical contact [103]. We consider a unilateral contact at the interface of two materials. We assume that if contact takes place, there is no penetration of the elasic material. In [67] unilateral contact has been studied for various types, like static, quasi-static and dynamic contact problems. For time-dependent contact problems one can find computations in [38, 39, 60, 61, 66, 58]. But a study of time-dependent contact problems is difficult [40], and existence of weak solutions is shown in few cases, such as viscoelasticity or modified contact conditions [31]. The existence of solutions in time-dependent cases is at least known for flat contact areas [33, 71]. To our knowledge for curved surfaces there is no proof for existence of solutions for time-dependent contact problems, without dissipation in the equation.

In this chapter we follow the steps based on the paper jointly with H. Gimperlein, F. Meyer and E. P. Stephan [47]. The analysis and the a priori error estimates for punch and crack problems are done for the half-space case in 3 dimensions. Numerical experiments for flat contact and non-flat contact surfaces on the unit cube are done for 3 dimensions as well, where we solve it with a space-time Uzawa algorithm.

Let $x = (x', x_3) := (x_1, x_2, x_3) \in \mathbb{R}^3$ the coordinates, where we consider the half-space $\Omega = \mathbb{R}^3_+$, with the third coordinate x_3 is positive, or $\Omega = \mathbb{R}^3_-$, with the third coordinate x_3 is negative. Then the flat contact area G is a Lipshitz subdomain of $\Gamma = \partial\Omega = \mathbb{R}^2 \times 0$, modeling a crack in G between the material in Ω and the other material in $\mathbb{R}^3 \backslash \overline{\Omega}$. Since we won't allow penetration, we describe the condition with $w^+ - w^- \geq 0$, where w^+ resp. w^- is a displacement of the upper face resp. the lower face in G. For areas without contact, i.e. $w^+ - w^- > 0$, the tractions $\sigma^+_{x_n} := -\mu \frac{\partial^+ w}{\partial n} = -\mu \frac{\partial^+ w}{\partial x_3}$, $\sigma^-_{x_n} := -\mu \frac{\partial^- w}{\partial n} = -\mu \frac{\partial^- w}{\partial x_3}$ vanish, where μ is a constant, n is the unit normal vector pointing in the same direction as x_3 and $\frac{\partial^+ w}{\partial x_3}(x,t) = \lim_{\tilde{x} \in \mathbb{R}^3_+ \to x \in \Gamma} \frac{\partial w}{\partial x_3}(\tilde{x}, t)$ and $\frac{\partial^- w}{\partial x_3}(x,t) = \lim_{\tilde{x} \in \mathbb{R}^3_- \to x \in \Gamma} \frac{\partial w}{\partial x_3}(\tilde{x}, t)$. Now we prescribe the opening crack to be symmetric with respect to G. Therefore $w^+ = -w^-$ and $\sigma^+_{x_n} = -\sigma^-_{x_n}$. Hence it is enough to consider the positive half-space $\Omega = \mathbb{R}^3_+$ with

$w := w^+$ and $\sigma^+_{x_n} = -\mu\frac{\partial^+ w}{\partial n} = -\mu\frac{\partial w}{\partial n}$. For given forces g the contact conditions are:

$$\begin{array}{lll} w(x,t) & \geq 0 & \text{for } (x,t) \in G \times \mathbb{R}^+ \ , \\ -\mu\frac{\partial w}{\partial n}(x,t) & \geq g(x,t) & \text{for } (x,t) \in G \times \mathbb{R}^+ \ , \\ w(x,t) & > 0 & \text{for } (x,t) \in G \times \mathbb{R}^+ \Longrightarrow -\mu\frac{\partial w}{\partial n}(x,t) = g(x,t) \ , \\ w(x,t) & = 0 & \text{for } (x,t) \in (\Gamma \backslash G) \times \mathbb{R}^+ \ . \end{array}$$

Therefore we get the crack problem

$$\begin{array}{lll} \frac{\partial^2 w}{\partial t^2} - \Delta w & = 0 & \text{for } (x,t) \in \Omega \times \mathbb{R}^+ \ , \\ w(x,0) = \dot{w}(x,0) & = 0 & \text{for } x \in \Omega \ , \\ w(x,t) & = 0 & \text{for } (x,t) \in (\Gamma \backslash G) \times \mathbb{R}^+ \ , \\ w(x,t) & \geq 0 & \text{for } (x,t) \in G \times \mathbb{R}^+ \ , \\ -\mu\frac{\partial w}{\partial n}(x,t) & \geq g(x,t) & \text{for } (x,t) \in G \times \mathbb{R}^+ \ , \\ (-\mu\frac{\partial w}{\partial n}(x,t) - g(x,t))w(x,t) & = 0 & \text{for } (x,t) \in G \times \mathbb{R}^+ \ . \end{array}$$

Now we extend w to negative terms by zero as well and using the continuity of w, we consider the following crack problem:

$$\begin{array}{lll} \frac{\partial^2 w}{\partial t^2} - \Delta w & = 0 & \text{for } (x,t) \in \Omega \times \mathbb{R}^+ \ , \\ w(x,t) & = 0 & \text{for } x \in \Omega, t \in (-\infty, 0] \ , \\ w(x,t) & = 0 & \text{for } (x,t) \in (\Gamma \backslash G) \times \mathbb{R}^+ \ , \\ w(x,t) & \geq 0 & \text{for } (x,t) \in G \times \mathbb{R}^+ \ , \\ -\mu\frac{\partial w}{\partial n}(x,t) & \geq g(x,t) & \text{for } (x,t) \in G \times \mathbb{R}^+ \ , \\ (-\mu\frac{\partial w}{\partial n}(x,t) - g(x,t))w(x,t) & = 0 & \text{for } (x,t) \in G \times \mathbb{R}^+ \ . \end{array} \tag{7.1}$$

The physical crack problem involves instead of the scalar wave equation used here, the time-dependent Lame equation, with analogous contact conditions for the normal component of the displacement and the stress. But we still refer to (7.1) as the crack problem, even though it is simplified.

Punch (stamp) problems, considered in [26, 42, 73], model a punch hitting an elastic material, where the punch doesn't penetrate the elastic material. In this case we don't have the information on where contact between the punch and the elastic material appears. We study the punch problem for a half-space $\Omega = \mathbb{R}^3_+$ and $\Gamma = \partial\Omega = \mathbb{R}^2 \times \{0\}$ with the scalar wave equation instead of the time-dependent Lame equation. The boundary conditions also involve the displacement w and the traction $\sigma_{x_n} := -\mu\frac{\partial w}{\partial n} = -\mu\frac{\partial w}{\partial x_3}$, instead of the corresponding normal component of the displacement and the stress in the time-dependent Lame case. We still refer to this simplified problem as punch problem. We describe the surface of the punch with $x_3 = \phi((x_1, x_2), t) \leq 0$. Further we state the assumption $\phi((0,0),t) = 0$, $\phi((x_1,x_2),t) \to -\infty$ for $\sqrt{x_1^2 + x_2^2} \to \infty$, which means that we consider the punch on a bounded domain with the tip at $(0,0)$. Let G denote the flat unknown contact area and η denote the displacement of the punch in x_3–direction. Then in the contact area with $g(x,t) = \phi(x',t) + \eta(x,t)$ with $x' = (x_1, x_2)$,

we get the contact conditions:

$$\begin{aligned}
&\sigma_{x_n}(x,t) \quad \geq 0 && \text{for } (x,t) \in G \times \mathbb{R}^+ \ , \\
&w(x,t) \quad \geq g(x,t) && \text{for } (x,t) \in G \times \mathbb{R}^+ \ , \\
&\sigma_{x_n}(x,t) \quad > 0 && \text{for } (x,t) \in G \times \mathbb{R}^+ \Longrightarrow w(x,t) = g(x,t) \ , \\
&\sigma_{x_n}(x,t) \quad = 0 && \text{for } (x,t) \in (\Gamma \backslash G) \times \mathbb{R}^+ \ .
\end{aligned}$$

Therefore we get the punch problem:

$$\begin{aligned}
&\tfrac{\partial^2 w}{\partial t^2} - \Delta w && = 0 && \text{for } (x,t) \in \Omega \times \mathbb{R}^+ \ , \\
&w(x,0) = \dot{w}(x,0) && = 0 && \text{for } x \in \Omega \ , \\
&\sigma_{x_n}(x,t) && = 0 && \text{for } (x,t) \in \Gamma \backslash G \times \mathbb{R}^+ \ , \\
&\sigma_{x_n}(x,t) && \geq 0 && \text{for } (x,t) \in G \times \mathbb{R}^+ \ , \\
&w(x,t) && g(x,t) && \text{for } (x,t) \in G \times \mathbb{R}^+ \ , \\
&(w-g)\sigma_{x_n} && = 0 && \text{for } (x,t) \in G \times \mathbb{R}^+ \ .
\end{aligned}$$

Again extending w to negative times by zero as well and using the continuity of w, we get

$$\begin{aligned}
&\tfrac{\partial^2 w}{\partial t^2} - \Delta w && = 0 && \text{for } (x,t) \in \Omega \times \mathbb{R}^+ \ , \\
&w(x,t) && = 0 && \text{for } x \in \Omega, t \in (-\infty, 0] \ , \\
&\sigma_{x_n}(x,t) && = 0 && \text{for } (x,t) \in \Gamma \backslash G \times \mathbb{R}^+ \ , \\
&\sigma_{x_n}(x,t) && \geq 0 && \text{for } (x,t) \in G \times \mathbb{R}^+ \ , \\
&w(x,t) && g(x,t) && \text{for } (x,t) \in G \times \mathbb{R}^+ \ , \\
&(w-g)\sigma_{x_n} && = 0 && \text{for } (x,t) \in G \times \mathbb{R}^+ \ .
\end{aligned} \tag{7.2}$$

In order to analyze these problems we remember the set of nonnegative distributions for $r \in \mathbb{R}$ $H^r_\sigma(\mathbb{R}^+, \widetilde{H}^{-1/2}(G))^+$ and the restriction p_Q to $Q = G \times \mathbb{R}$. We will need them in the following.

7.2 Boundary integral formulation and well-posedness for the crack problem

We proceed as in Cooper [33] by considering a regularized contact problem with parameter $\sigma > 0$, where the analysis allow with $\sigma \to 0^+$ at the end an existence of weak solutions for the Crack problem (7.1). We define $w_\sigma := e^{-\sigma t} w$ and the right hand side $g_\sigma = e^{-\sigma t} g$. Then we obtain the following problem:

$$\begin{cases}
\left(\frac{\partial}{\partial t} + \sigma\right)^2 w_\sigma = \Delta w_\sigma & \text{for } (x,t) \in \Omega \times \mathbb{R} \ , \\
w_\sigma = 0 & \text{on } \Gamma \backslash G \times \mathbb{R} \ , \\
w_\sigma \geq 0 \ , -\mu \frac{\partial w_\sigma}{\partial n} \geq g_\sigma & \text{on } G \times \mathbb{R} \ , \\
\left(-\mu \frac{\partial w_\sigma}{\partial n} - g_\sigma\right) w_\sigma = 0 & \text{on } G \times \mathbb{R} \ , \\
w_\sigma = 0 & \text{for } (x,t) \in \Omega \times (-\infty, 0) \ .
\end{cases} \tag{7.3}$$

Through the application of the Fourier transform in (x',t) with $x' = (x_1, x_2)$ (for details see [47, 88]), we define the Dirichlet-to-Neumann operator S_σ by:

$$\mathcal{S}_\sigma\, w_\sigma|_{\Gamma\times\mathbb{R}} := -\mu\frac{\partial w_\sigma}{\partial n} \tag{7.4}$$

with $\mathcal{S}_\sigma$ a generalized pseudodifferential operator with symbol $-i\mu\Gamma(\cdot,\cdot)$

$$\mathcal{S}_\sigma\, u_\sigma = (2\pi)^{-3}\int_{\mathbb{R}^3} e^{it\xi_0+ix'\xi'}(-i\mu\Gamma(\xi_0+i\sigma,\xi'))\hat{u}_\sigma(\xi_0,\xi')\,\mathrm{d}\xi_0\mathrm{d}\xi'\,, \tag{7.5}$$

where $\Gamma(\xi_0+i\sigma,\xi') = \sqrt{c_s^{-2}(\xi_0+i\sigma)^2-|\xi'|^2}$, $\xi' = (\xi_1,\xi_2)$. For the half-space $\Omega = \mathbb{R}^3_+$, we get mapping properties and a coercivity estimate to the Dirichlet-to-Neumann operator. Further we use the restriction to p_Q to $Q = G\times\mathbb{R}$

Theorem 7.1 ([47], Theorem 5)**.** *$p_Q\,\mathcal{S}_\sigma : H^s_\sigma(\mathbb{R}^+,\widetilde{H}^{\frac12}(G)) \to H^s_\sigma(\mathbb{R}^+,H^{-\frac12}(G))$ continuously and $\|\phi\|^2_{-\frac12,\frac12,\sigma,*} \lesssim_\sigma \langle p_Q\,\mathcal{S}_\sigma\,\phi,\phi\rangle_\sigma \lesssim \|\phi\|^2_{0,\frac12,\sigma,*}$.*

An application of (7.4) to the boundary conditions on $G\times\mathbb{R}$, we obtain an equivalent inequality with the trace $u_\sigma = w_\sigma|_\Gamma$: Find u_σ with $\operatorname{supp} u_\sigma \subset Q_0 = G\times\mathbb{R}^+$ satisfying

$$u_\sigma \geq 0\ ,\ \mathcal{S}_\sigma\, u_\sigma \geq g_\sigma \text{ and } (\mathcal{S}_\sigma\, u_\sigma - g_\sigma)\ u_\sigma = 0 \text{ on } Q = G\times\mathbb{R}\ . \tag{7.6}$$

Using the restriction p_Q and testing with $v \in H^{1/2}_\sigma(\mathbb{R}^+,\widetilde{H}^{1/2}(G))^+$, we get for smooth g_σ a variational inequality:
Find $u_\sigma \in H^{\frac12}_\sigma(\mathbb{R}^+,\widetilde{H}^{\frac12}(G))^+$ satisfying $\forall v \in H^{\frac12}_\sigma(\mathbb{R}^+,\widetilde{H}^{\frac12}(G))^+$:

$$\langle p_Q\,\mathcal{S}_\sigma\, u_\sigma, v-u_\sigma\rangle_{G\times\mathbb{R}^+,\sigma} \geq \langle g_\sigma, v-u_\sigma\rangle_{G\times\mathbb{R}^+,\sigma}\ . \tag{7.7}$$

Theorem 7.2 ([47], Theorem 6)**.** *The contact problem* (7.3) *is equivalent to the variational inequality* (7.7)*.*

Proof. It is enough to prove the equivalence of (7.6) and (7.7). In order to derive (7.7) from (7.6), we test the second inequality of (7.6) by $v \geq 0$:

$$\langle p_Q\,\mathcal{S}_\sigma\, u_\sigma - g_\sigma, v\rangle_{G\times\mathbb{R}^+,\sigma} \geq 0.$$

By the third equality in (7.6) and choosing $v = u_\sigma$ we see $\langle p_Q\,\mathcal{S}_\sigma\, u_\sigma - g_\sigma, u_\sigma\rangle_{G\times\mathbb{R}^+,\sigma} = 0$. Therefore we obtain the variational inequality (7.7).
Conversely assume that (7.7) holds. Since $u_\sigma \in H^{1/2}_\sigma(\mathbb{R}^+,\widetilde{H}^{1/2}(G))^+$, we need to prove the second and third (in-)equalities of (7.6). We choose $v \in H^{1/2}_\sigma(\mathbb{R}^+,\widetilde{H}^{1/2}(G))^+$ in (7.7) such that $v - u_\sigma := v' \geq 0$ to obtain $\langle p_Q\,\mathcal{S}_\sigma\, u_\sigma - g_\sigma, v'\rangle_{G\times\mathbb{R}^+,\sigma} \geq 0$. Therefore $\mathcal{S}_\sigma\, u_\sigma - g_\sigma \geq 0$ follows. Now setting on the one hand $v = 2u_\sigma \geq 0$ in (7.7) to get $\langle p_Q\,\mathcal{S}_\sigma\, u_\sigma, u_\sigma\rangle_{G\times\mathbb{R}^+,\sigma} \geq \langle g_\sigma, u_\sigma\rangle_{G\times\mathbb{R}^+,\sigma}$ and on the other hand $v = 0$ in (7.7) to get $\langle p_Q\,\mathcal{S}_\sigma\, u_\sigma, u_\sigma\rangle_{G\times\mathbb{R}^+,\sigma} \leq \langle g_\sigma, u_\sigma\rangle_{G\times\mathbb{R}^+,\sigma}$, we deduce $\langle p_Q\,\mathcal{S}_\sigma\, u_\sigma - g_\sigma, u_\sigma\rangle_{G\times\mathbb{R}^+,\sigma} = 0$. Since the first and the second inequalities already hold, we get the remaining equality $(\mathcal{S}_\sigma\, u_\sigma - g_\sigma)u_\sigma = 0$. □

Theorem 7.3 ([47], Theorem 7, [33], p. 450)**.** *Let $g \in H_\sigma^{\frac{3}{2}}(\mathbb{R}^+, H^{-\frac{1}{2}}(G))$. Then there exists a unique solution $u_\sigma \in H_\sigma^{\frac{1}{2}}(\mathbb{R}^+, \tilde{H}^{\frac{1}{2}}(G))^+$ of (7.7).*

Theorem 7.4 ([47], Theorem 8, [33], p. 451)**.** *Let $g \in H_\sigma^{\frac{3}{2}}(\mathbb{R}^+, H^{-\frac{1}{2}}(G))$. Then there exists a unique $w(\cdot, x_3) \in C(\overline{\mathbb{R}}^+_{x_3}; H_\sigma^{\frac{1}{2}}(\mathbb{R}^+, H^{\frac{1}{2}}(\mathbb{R}^2)) \cap H_\sigma^0(\mathbb{R}^+, H^1(\mathbb{R}^3))$ satisfying (7.3).*

7.3 Discretization and a priori error estimates for the crack problem

For the discretization spaces, we refer to Section 2.3 and assume that the triangulation to be compatible with the contact area G, such that for $\Gamma_i \cap G \neq \varnothing$ for all $i = 1, \dots, N_s$, then $\operatorname{int} \Gamma_i \subset G$. Therefore we have $\tilde{V}_h^p(G) \subset V_h^p(G) \subset V_h^p(\Gamma)$. For $u_{h,\Delta t} \in V_{h,\Delta t}^{p,q}$ we will use the same functions in space and time as in Subsection 2.3.5.

We recapitulate the continuous variational inequality:
Find $u_\sigma \in H_\sigma^{\frac{1}{2}}(\mathbb{R}^+, \widetilde{H}^{\frac{1}{2}}(G))^+$ such that for all $v \in H_\sigma^{\frac{1}{2}}(\mathbb{R}^+, \widetilde{H}^{\frac{1}{2}}(G))^+$, there holds

$$\langle p_Q \, \mathcal{S}_\sigma \, u_\sigma, v - u_\sigma \rangle_{G \times \mathbb{R}^+, \sigma} \geq \langle g, v - u_\sigma \rangle_{G \times \mathbb{R}^+, \sigma} \ . \tag{7.8}$$

Let $\tilde{K}_{h,\Delta t}^+ \subset V_{h,\Delta t}^{p,q}$ be the subspace of nonnegative piecewise polynomials. The discretized variational inequality reads: Find $u_{h,\Delta t} \in \tilde{K}_{h,\Delta t}^+$ such that for all $v_{h,\Delta t} \in \tilde{K}_{h,\Delta t}^+$, there holds

$$\langle p_Q \mathcal{S}_\sigma u_{h,\Delta t}, v_{h,\Delta t} - u_{h,\Delta t} \rangle_{G \times \mathbb{R}^+, \sigma} \geq \langle g, v_{h,\Delta t} - u_{h,\Delta t} \rangle_{G \times \mathbb{R}^+, \sigma} \ . \tag{7.9}$$

For the theoretical analysis, $\mathcal{S}_\sigma$ can be computed from the retarded integral operators V,K,K',W, like in Subsection 2.3.5, where $\sigma > 0$ is required. As in Falk [43] in the elliptic case, we state an a priori error estimate for the variational inequality for a conforming ansatz space.

Theorem 7.5 ([47], Theorem 10)**.** *Let $g \in H_\sigma^{\frac{3}{2}}(\mathbb{R}^+, H^{-\frac{1}{2}}(G))$ and let $u \in H_\sigma^{\frac{1}{2}}(\mathbb{R}^+, \widetilde{H}^{\frac{1}{2}}(G))^+$, respectively $u_{h,\Delta t} \in \tilde{K}_{h,\Delta t}^+ \subset H_\sigma^{\frac{1}{2}}(\mathbb{R}^+, \widetilde{H}^{\frac{1}{2}}(G))^+$ be the solutions of (7.8), respectively (7.9). Then the following estimate holds:*

$$\|u - u_{h,\Delta t}\|^2_{-\frac{1}{2},\frac{1}{2},\sigma,\star} \lesssim_\sigma \inf_{\phi_{h,\Delta t} \in \tilde{K}_{h,\Delta t}^+} (\|g - p_Q \, \mathcal{S}_\sigma \, u\|_{\frac{1}{2},-\frac{1}{2},\sigma} \|u - \phi_{h,\Delta t}\|_{-\frac{1}{2},\frac{1}{2},\sigma,\star} + \|u - \phi_{h,\Delta t}\|^2_{\frac{1}{2},\frac{1}{2},\sigma,\star}). \tag{7.10}$$

Proof. Let $g \in H_\sigma^{\frac{3}{2}}(\mathbb{R}^+, H^{-\frac{1}{2}}(G))$ and $u \in H_\sigma^{\frac{1}{2}}(\mathbb{R}^+, \widetilde{H}^{1/2}(G))^+$ be the solution of (7.8). Testing (7.8) with $\phi \in H_\sigma^{\frac{1}{2}}(\mathbb{R}^+, \widetilde{H}^{\frac{1}{2}}(G))^+$ we divide

$$\langle p_Q \, \mathcal{S}_\sigma \, u, \phi - u \rangle_{G \times \mathbb{R}^+, \sigma} = \langle p_Q \, \mathcal{S}_\sigma \, u, \phi \rangle_{G \times \mathbb{R}^+, \sigma} - \langle p_Q \, \mathcal{S}_\sigma \, u, u \rangle_{G \times \mathbb{R}^+, \sigma} \ .$$

Now shifting $\langle p_Q \mathcal{S}_\sigma u, \phi\rangle_{G\times\mathbb{R}^+,\sigma}$ to the right hand side of the inequality (7.8), we get

$$-\langle p_Q \mathcal{S}_\sigma u, u\rangle_{G\times\mathbb{R}^+,\sigma} \geq \langle g, \phi - u\rangle_{G\times\mathbb{R}^+,\sigma} - \langle p_Q \mathcal{S}_\sigma u, \phi\rangle_{G\times\mathbb{R}^+,\sigma} \ .$$

Therefore

$$\langle p_Q \mathcal{S}_\sigma u, u\rangle_{G\times\mathbb{R}^+,\sigma} \leq \langle g, u - \phi\rangle_{G\times\mathbb{R}^+,\sigma} + \langle p_Q \mathcal{S}_\sigma u, \phi\rangle_{G\times\mathbb{R}^+,\sigma} \ . \tag{7.11}$$

Analogously for (7.9) testing with $\phi_{h,\Delta t} \in \tilde{K}^+_{h,\Delta t}$, we note that

$$\langle p_Q \mathcal{S}_\sigma u_{h,\Delta t}, u_{h,\Delta t}\rangle_{G\times\mathbb{R}^+,\sigma} \leq \langle g, u_{h,\Delta t} - \phi_{h,\Delta t}\rangle_{G\times\mathbb{R}^+,\sigma} + \langle p_Q \mathcal{S}_\sigma u_{h,\Delta t}, \phi_{h,\Delta t}\rangle_{G\times\mathbb{R}^+,\sigma}. \tag{7.12}$$

Using the coercivity in Theorem 7.1, we obtain with (7.11) and (7.12)

$$\begin{aligned}
&\|u - u_{h,\Delta t}\|^2_{-\frac{1}{2},\frac{1}{2},\sigma,\star} \lesssim_\sigma \langle p_Q \mathcal{S}_\sigma(u - u_{h,\Delta t}), u - u_{h,\Delta t}\rangle_{G\times\mathbb{R}^+,\sigma} \\
&= \langle p_Q \mathcal{S}_\sigma(u - u_{h,\Delta t}), u\rangle_{G\times\mathbb{R}^+,\sigma} - \langle p_Q \mathcal{S}_\sigma(u - u_{h,\Delta t}), u_{h,\Delta t}\rangle_{G\times\mathbb{R}^+,\sigma} \\
&= \langle p_Q\mathcal{S}_\sigma u,u\rangle_{G\times\mathbb{R}^+,\sigma} - \langle p_Q\mathcal{S}_\sigma u_{h,\Delta t},u\rangle_{G\times\mathbb{R}^+,\sigma} - \langle p_Q\mathcal{S}_\sigma u,u_{h,\Delta t}\rangle_{G\times\mathbb{R}^+,\sigma} + \langle p_Q\mathcal{S}_\sigma u_{h,\Delta t},u_{h,\Delta t}\rangle_{G\times\mathbb{R}^+,\sigma} \\
&\leq \langle g, u - \phi\rangle_{G\times\mathbb{R}^+,\sigma} + \langle g, u_{h,\Delta t} - \phi_{h,\Delta t}\rangle_{G\times\mathbb{R}^+,\sigma} + \langle p_Q \mathcal{S}_\sigma u_{h,\Delta t}, \phi_{h,\Delta t}\rangle_{G\times\mathbb{R}^+,\sigma} \\
&\quad + \langle p_Q \mathcal{S}_\sigma u, \phi\rangle_{G\times\mathbb{R}^+,\sigma} - \langle p_Q \mathcal{S}_\sigma u, u_{h,\Delta t}\rangle_{G\times\mathbb{R}^+,\sigma} - \langle p_Q \mathcal{S}_\sigma u_{h,\Delta t}, u\rangle_{G\times\mathbb{R}^+,\sigma} \\
&= \langle g, u - \phi\rangle_{G\times\mathbb{R}^+,\sigma} + \langle g, u_{h,\Delta t} - \phi_{h,\Delta t}\rangle_{G\times\mathbb{R}^+,\sigma} + \langle p_Q \mathcal{S}_\sigma u, \phi - u_{h,\Delta t}\rangle_{G\times\mathbb{R}^+,\sigma} \\
&\quad + \langle p_Q \mathcal{S}_\sigma u_{h,\Delta t}, \phi_{h,\Delta t} - u\rangle_{G\times\mathbb{R}^+,\sigma}.
\end{aligned}$$

We add $0 = \langle p_Q \mathcal{S}_\sigma u, u - \phi_{h,\Delta t}\rangle_{G\times\mathbb{R}^+,\sigma} - \langle p_Q \mathcal{S}_\sigma u, u - \phi_{h,\Delta t}\rangle_{G\times\mathbb{R}^+,\sigma}$ into:

$$\langle p_Q\mathcal{S}_\sigma u_{h,\Delta t},\phi_{h,\Delta t} - u\rangle_{G\times\mathbb{R}^+,\sigma} = \langle p_Q\mathcal{S}_\sigma(u-u_{h,\Delta t}),u - \phi_{h,\Delta t}\rangle_{G\times\mathbb{R}^+,\sigma} - \langle p_Q\mathcal{S}_\sigma u,u-\phi_{h,\Delta t}\rangle_{G\times\mathbb{R}^+,\sigma} \ .$$

Hence, we get

$$\begin{aligned}
&\|u - u_{h,\Delta t}\|^2_{-\frac{1}{2},\frac{1}{2},\sigma,\star} \lesssim_\sigma \langle g, u - \phi\rangle_{G\times\mathbb{R}^+,\sigma} + \langle g, u_{h,\Delta t} - \phi_{h,\Delta t}\rangle_{G\times\mathbb{R}^+,\sigma} + \langle p_Q \mathcal{S}_\sigma u, \phi - u_{h,\Delta t}\rangle_{G\times\mathbb{R}^+,\sigma} \\
&\qquad + \langle p_Q \mathcal{S}_\sigma(u - u_{h,\Delta t}), u - \phi_{h,\Delta t}\rangle_{G\times\mathbb{R}^+,\sigma} - \langle p_Q \mathcal{S}_\sigma u, u - \phi_{h,\Delta t}\rangle_{G\times\mathbb{R}^+,\sigma} \\
&= \langle g,u\rangle_{G\times\mathbb{R}^+,\sigma} - \langle g,\phi\rangle_{G\times\mathbb{R}^+,\sigma} + \langle g,u_{h,\Delta t}\rangle_{G\times\mathbb{R}^+,\sigma} - \langle g,\phi_{h,\Delta t}\rangle_{G\times\mathbb{R}^+,\sigma} + \langle p_Q\mathcal{S}_\sigma u,\phi\rangle_{G\times\mathbb{R}^+,\sigma} \\
&- \langle p_Q\mathcal{S}_\sigma u,u_{h,\Delta t}\rangle_{G\times\mathbb{R}^+,\sigma} + \langle p_Q\mathcal{S}_\sigma(u-u_{h,\Delta t}),u-\phi_{h,\Delta t}\rangle_{G\times\mathbb{R}^+,\sigma} \\
&- \langle p_Q\mathcal{S}_\sigma u,u\rangle_{G\times\mathbb{R}^+,\sigma} + \langle p_Q\mathcal{S}_\sigma u,\phi_{h,\Delta t}\rangle_{G\times\mathbb{R}^+,\sigma} \\
&= \langle g, u_{h,\Delta t} - \phi\rangle_{G\times\mathbb{R}^+,\sigma} - \langle p_Q \mathcal{S}_\sigma u, \phi_{h,\Delta t} - \phi\rangle_{G\times\mathbb{R}^+,\sigma} + \langle g, u - \phi_{h,\Delta t}\rangle_{G\times\mathbb{R}^+,\sigma} \\
&- \langle p_Q \mathcal{S}_\sigma u, u - \phi_{h,\Delta t}\rangle_{G\times\mathbb{R}^+,\sigma} + \langle p_Q \mathcal{S}_\sigma(u - u_{h,\Delta t}), u - \phi_{h,\Delta t}\rangle_{G\times\mathbb{R}^+,\sigma} \\
&= \langle g - p_Q \mathcal{S}_\sigma u, u - \phi_{h,\Delta t}\rangle_{G\times\mathbb{R}^+,\sigma} + \langle g - p_Q \mathcal{S}_\sigma u_{h,\Delta t}, u_{h,\Delta t} - \phi\rangle_{G\times\mathbb{R}^+,\sigma} \\
&+ \langle p_Q \mathcal{S}_\sigma(u - u_{h,\Delta t}), u - \phi_{h,\Delta t}\rangle_{G\times\mathbb{R}^+,\sigma}.
\end{aligned}$$

Because of the conforming discretization, we may choose $\phi = u_{h,\Delta t}$ and conclude

$$\|u - u_{h,\Delta t}\|^2_{-\frac{1}{2},\frac{1}{2},\sigma,\star} \lesssim_\sigma \langle g - p_Q\mathcal{S}_\sigma u, u - \phi_{h,\Delta t}\rangle_{G\times\mathbb{R}^+,\sigma} + \langle p_Q\mathcal{S}_\sigma(u - u_{h,\Delta t}), u - \phi_{h,\Delta t}\rangle_{G\times\mathbb{R}^+,\sigma}. \tag{7.13}$$

We estimate both terms by duality:

$$\|u - u_{h,\Delta t}\|^2_{-\frac{1}{2},\frac{1}{2},\sigma,\star} \lesssim_\sigma \|g - p_Q\mathcal{S}_\sigma u\|_{\frac{1}{2},-\frac{1}{2},\sigma}\|u - \phi_{h,\Delta t}\|_{-\frac{1}{2},\frac{1}{2},\sigma,\star} + \|p_Q\mathcal{S}_\sigma(u - u_{h,\Delta t})\|_{-\frac{1}{2},-\frac{1}{2},\sigma}\|u - \phi_{h,\Delta t}\|_{\frac{1}{2},\frac{1}{2},\sigma,\star}.$$

With the continuity of $p_Q \mathcal{S}_\sigma : H_\sigma^{-\frac{1}{2}}(\mathbb{R}^+, \widetilde{H}^{\frac{1}{2}}(G)) \to H_\sigma^{-\frac{1}{2}}(\mathbb{R}^+, H^{-\frac{1}{2}}(G))$, in Theorem 7.1 with $s = -\frac{1}{2}$, we obtain

$$\|u-u_{h,\Delta t}\|^2_{-\frac{1}{2},\frac{1}{2},\sigma,\star} \lesssim_\sigma \|g-p_Q\mathcal{S}_\sigma u\|_{\frac{1}{2},-\frac{1}{2},\sigma}\|u-\phi_{h,\Delta t}\|_{-\frac{1}{2},\frac{1}{2},\sigma,\star}+\|u-u_{h,\Delta t}\|_{-\frac{1}{2},\frac{1}{2},\sigma,\star}\|u-\phi_{h,\Delta t}\|_{\frac{1}{2},\frac{1}{2},\sigma,\star}.$$

We conclude with the help of Young's inequality for small $\epsilon > 0$ and combining $\epsilon\|u - u_{h,\Delta t}\|^2_{-\frac{1}{2},\frac{1}{2},\sigma,\star}$ with the left hand side

$$\|u - u_{h,\Delta t}\|^2_{-\frac{1}{2},\frac{1}{2},\sigma,\star} \lesssim_\sigma \|g - p_Q\,\mathcal{S}_\sigma\,u\|_{\frac{1}{2},-\frac{1}{2},\sigma}\|u - \phi_{h,\Delta t}\|_{-\frac{1}{2},\frac{1}{2},\sigma,\star} + \|u - \phi_{h,\Delta t}\|^2_{\frac{1}{2},\frac{1}{2},\sigma,\star}.$$

It follows the statement by taking the infimum over all $\phi_{h,\Delta t}$. □

7.4 Mixed formulation of the crack problem

We define the Lagrange multiplier $\lambda := \mathcal{S}_\sigma\,u - g$. Then λ describes the difference of the traction $\mathcal{S}_\sigma = -\mu\frac{\partial w_\sigma}{\partial n}$ and the given forces g in G. It determines the additional forces occuring during actual contact, and therefore we are interested in a formulation, where λ as well as u appears.

Theorem 7.6 (Mixed formulation, [47], Theorem 14)**.** *Let $g \in H_\sigma^{\frac{3}{2}}(\mathbb{R}^+, H^{-\frac{1}{2}}(G))$. The variational inequality formulation (7.8) is equivalent to the following formulation: Find $(u,\lambda) \in H_\sigma^{\frac{1}{2}}(\mathbb{R}^+, \widetilde{H}^{\frac{1}{2}}(G)) \times H_\sigma^{\frac{1}{2}}(\mathbb{R}^+, H^{-\frac{1}{2}}(G))^+$ such that*

$$\begin{cases}(a)\ \langle \mathcal{S}_\sigma\,u, v\rangle_{G\times\mathbb{R}^+,\sigma} - \langle\lambda, v\rangle_{G\times\mathbb{R}^+,\sigma} = \langle g, v\rangle_{G\times\mathbb{R}^+,\sigma}\ ,\\ (b)\ \langle u, \mu-\lambda\rangle_{G\times\mathbb{R}^+,\sigma} \geq 0,\end{cases} \tag{7.14}$$

for all $(v,\mu) \in H_\sigma^{\frac{1}{2}}(\mathbb{R}^+, \widetilde{H}^{\frac{1}{2}}(G)) \times H_\sigma^{\frac{1}{2}}(\mathbb{R}^+, H^{-\frac{1}{2}}(G))^+$.

Proof. First, we observe an equivalence of (7.8) to the following problem: Find $u \in H_\sigma^{\frac{1}{2}}(\mathbb{R}^+, \widetilde{H}^{\frac{1}{2}}(G))^+$ such that for all $v \in H_\sigma^{\frac{1}{2}}(\mathbb{R}^+, \widetilde{H}^{\frac{1}{2}}(G))^+$, u solves

$$\begin{cases}(a)\ \langle \mathcal{S}_\sigma\,u, u\rangle_{G\times\mathbb{R}^+,\sigma} = \langle g, u\rangle_{G\times\mathbb{R}^+,\sigma}\ ,\\ (b)\ \langle \mathcal{S}_\sigma\,u, v\rangle_{G\times\mathbb{R}^+,\sigma} \geq \langle g, v\rangle_{G\times\mathbb{R}^+,\sigma}.\end{cases} \tag{7.15}$$

This is due to setting $v = 2u$ on the one hand and $v = 0$ on the hand in the variational inequality (7.8). We get

$$\langle \mathcal{S}_\sigma\,u, u\rangle_{G\times\mathbb{R}^+,\sigma} \geq \langle g, u\rangle_{G\times\mathbb{R}^+,\sigma}\ ,\ \text{and}\ \langle \mathcal{S}_\sigma\,u, u\rangle_{G\times\mathbb{R}^+,\sigma} \leq \langle g, u\rangle_{G\times\mathbb{R}^+,\sigma}\ ,$$

Therefore (7.15a) holds. Using (7.15a) on (7.8) we obtain:

$$\langle \mathcal{S}_\sigma\,u, v\rangle_{G\times\mathbb{R}^+,\sigma} - \langle \mathcal{S}_\sigma\,u, u\rangle_{G\times\mathbb{R}^+,\sigma} \geq \langle g, v\rangle_{G\times\mathbb{R}^+,\sigma} - \langle g, u\rangle_{G\times\mathbb{R}^+,\sigma}\ ,$$

where (7.15b) follows. Conversely, we subtract (7.15a) from (7.15b) in order to get (7.8) from (7.15).

For getting (7.15) from (7.8), we prove (7.15) $\Rightarrow$ (7.14). With (7.15b) for $\lambda = \mathcal{S}_\sigma u - g$, we get for all $v \in H_\sigma^{\frac{1}{2}}(\mathbb{R}^+, \widetilde{H}^{\frac{1}{2}}(G))^+$, $0 \le \langle \mathcal{S}_\sigma u - g, v\rangle_{G\times\mathbb{R}^+,\sigma} = \langle \lambda, v\rangle_{G\times\mathbb{R}^+,\sigma}$. Since $v \ge 0$, we deduce $\lambda \ge 0$ and therefore $\lambda \in H_\sigma^{\frac{1}{2}}(\mathbb{R}^+, H^{-\frac{1}{2}}(G))^+$. (7.14a) holds by substracting $\langle \lambda, v\rangle_{G\times\mathbb{R}^+,\sigma}$ of the left hand side of (7.15b) and using the definition of λ.
Via (7.15a) we see $\langle \lambda, u\rangle_{G\times\mathbb{R}^+,\sigma} = 0$, and hence, $\langle u, \mu-\lambda\rangle_{G\times\mathbb{R}^+,\sigma} = \langle u, \mu\rangle_{G\times\mathbb{R}^+,\sigma} \ge 0$, because $u \in H_\sigma^{\frac{1}{2}}(\mathbb{R}^+, \widetilde{H}^{\frac{1}{2}}(G))^+$ and $\mu \in H_\sigma^{\frac{1}{2}}(\mathbb{R}^+, \widetilde{H}^{-\frac{1}{2}}(G))^+$.

Conversely we prove (7.14) $\Rightarrow$ (7.8). Let $(u, \lambda) \in H_\sigma^{\frac{1}{2}}(\mathbb{R}^+, \widetilde{H}^{\frac{1}{2}}(G)) \times H_\sigma^{\frac{1}{2}}(\mathbb{R}^+, H^{-\frac{1}{2}}(G))^+$ be the solution to (7.14). Again setting on the one hand $\mu = 2\lambda$ and on the other hand $\mu = 0$, we get $\langle u, \lambda\rangle_{G\times\mathbb{R}^+,\sigma} \ge 0$, $\langle u, \lambda\rangle_{G\times\mathbb{R}^+,\sigma} \le 0$. Therefore $\langle u, \lambda\rangle_{G\times\mathbb{R}^+,\sigma} = 0$.

If we assume that u is not ≥ 0, then there exists $\mu \in H_\sigma^{\frac{1}{2}}(\mathbb{R}^+, H^{-\frac{1}{2}}(G))^+$ such that $\langle u, \mu\rangle_{G\times\mathbb{R}^+,\sigma} < 0$, and we observe from (7.14b) the contradiction

$$0 \le \langle u, \mu - \lambda\rangle_{G\times\mathbb{R}^+,\sigma} = \langle u, \mu\rangle_{G\times\mathbb{R}^+,\sigma} - \langle u, \lambda\rangle_{G\times\mathbb{R}^+,\sigma} = \langle u, \mu\rangle_{G\times\mathbb{R}^+,\sigma} < 0 \ .$$

Therefore $u \in H_\sigma^{\frac{1}{2}}(\mathbb{R}^+, \widetilde{H}^{\frac{1}{2}}(G))^+$. Applying $v-u$ as u in (7.14b) for $v \in H_\sigma^{\frac{1}{2}}(\mathbb{R}^+, \widetilde{H}^{\frac{1}{2}}(G))^+$, we get $\langle v-u, \lambda\rangle_{G\times\mathbb{R}^+,\sigma} = \langle v, \lambda\rangle_{G\times\mathbb{R}^+,\sigma} - \langle u, \lambda\rangle_{G\times\mathbb{R}^+,\sigma} = \langle v, \lambda\rangle_{G\times\mathbb{R}^+,\sigma} \ge 0$. Testing (7.14a) with $v - u$, we obtain

$$\langle \mathcal{S}_\sigma u, v - u\rangle_{G\times\mathbb{R}^+,\sigma} - \langle \lambda, v - u\rangle_{G\times\mathbb{R}^+,\sigma} = \langle g, v - u\rangle_{G\times\mathbb{R}^+,\sigma} \ ,$$

or equivalently

$$\langle \mathcal{S}_\sigma u - g, v - u\rangle_{G\times\mathbb{R}^+,\sigma} = \langle \lambda, v - u\rangle_{G\times\mathbb{R}^+,\sigma} \ge 0.$$

So we get (7.8) and therefore (7.15), too. □

The discrete formulation reads as follows: Find $(u_{h_1,\Delta t_1}, \lambda_{h_2,\Delta t_2}) \in \tilde{V}_{h_1,\Delta t_1}^{1,1} \times (V_{h_2,\Delta t_2}^{0,0})^+$ satisfying for all $(v_{h_1,\Delta t_1}, \mu_{h_2,\Delta t_2}) \in \tilde{V}_{h_1,\Delta t_1}^{1,1} \times (V_{h_2,\Delta t_2}^{0,0})^+$

$$\begin{cases} (a)\ \langle \mathcal{S}_\sigma u_{h_1,\Delta t_1}, v_{h_1,\Delta t_1}\rangle_{G\times\mathbb{R}^+,\sigma} - \langle \lambda_{h_2,\Delta t_2}, v_{h_1,\Delta t_1}\rangle_{G\times\mathbb{R}^+,\sigma} = \langle g, v_{h_1,\Delta t_1}\rangle_{G\times\mathbb{R}^+,\sigma} \ , \\ (b)\ \langle u_{h_1,\Delta t_1}, \mu_{h_2,\Delta t_2} - \lambda_{h_2,\Delta t_2}\rangle_{G\times\mathbb{R}^+,\sigma} \ge 0 \ . \end{cases} \tag{7.16}$$

Next in [47] for sufficiently different meshes to the Lagrange multiplier $\lambda_{h_2,\Delta t_2}$ and the solution $u_{h_1,\Delta t_1}$ a discrete inf-sup condition is obtained:

Theorem 7.7 ([47], Theorem 15)**.** *Let $C > 0$ sufficiently small, and $\frac{\max\{h_1,\Delta t_1\}}{\min\{h_2,\Delta t_2\}} < C$. Then there exists $\alpha > 0$ such that for all $\lambda_{h_2,\Delta t_2}$:*

$$\sup_{\mu_{h_1,\Delta t_1}} \frac{\langle \mu_{h_1,\Delta t_1}, \lambda_{h_2,\Delta t_2}\rangle_{G\times\mathbb{R}^+,\sigma}}{\|\mu_{h_1,\Delta t_1}\|_{0,\frac{1}{2},\sigma,*}} \ge \alpha \|\lambda_{h_2,\Delta t_2}\|_{0,-\frac{1}{2},\sigma} \ . \tag{7.17}$$

The existence of an unique solution of (7.16) is done in [47]. Now we state an a priori error estimate for the mixed formulation (7.16).

Theorem 7.8 ([47], Theorem 16). *Let* $(u,\lambda) \in H_\sigma^{\frac{1}{2}}(\mathbb{R}^+,\widetilde{H}^{\frac{1}{2}}(G)) \times H_\sigma^{\frac{1}{2}}(\mathbb{R}^+,H^{-\frac{1}{2}}(G))^+$ *solve* (7.14) *and* $(u_{h_1,\Delta t_1},\lambda_{h_2,\Delta t_2}) \in \tilde{V}_{h_1,\Delta t_1}^{1,1} \times (V_{h_2,\Delta t_2}^{0,0})^+$ *solve* (7.16). *Then the following a priori error estimates hold:*

$$\|\lambda-\lambda_{h_2,\Delta t_2}\|_{0,-\frac{1}{2},\sigma} \lesssim \inf_{\tilde{\lambda}_{h_2,\Delta t_2}} \|\lambda-\tilde{\lambda}_{h_2,\Delta t_2}\|_{0,-\frac{1}{2},\sigma} + (\Delta t_1)^{-\frac{1}{2}}\|u-u_{h_1,\Delta t_1}\|_{-\frac{1}{2},\frac{1}{2},\sigma,*} \ , \quad (7.18)$$

$$\begin{aligned}\|u-u_{h_1,\Delta t_1}\|_{-\frac{1}{2},\frac{1}{2},\sigma,*} \lesssim_\sigma & \inf_{v_{h_1,\Delta t_1}} \|u-v_{h_1,\Delta t_1}\|_{\frac{1}{2},\frac{1}{2},\sigma,*} \\ & + \inf_{\tilde{\lambda}_{h_2,\Delta t_2}} \left\{\|\tilde{\lambda}_{h_2,\Delta t_2}-\lambda\|_{\frac{1}{2},-\frac{1}{2},\sigma} + \|\tilde{\lambda}_{h_2,\Delta t_2}-\lambda_{h_2,\Delta t_2}\|_{\frac{1}{2},-\frac{1}{2},\sigma}\right\} \ . \quad (7.19)\end{aligned}$$

Proof. In order to prove the a priori error estimate for the Lagrange multiplier (7.18), we take advantage of (7.14) and (7.16) to observe

$$\begin{aligned}&\langle\lambda_{h_2,\Delta t_2}-\tilde{\lambda}_{h_2,\Delta t_2}, v_{h_1,\Delta t_1}\rangle_{G\times\mathbb{R}^+,\sigma} \\ &= \langle\mathcal{S}_\sigma u_{h_1,\Delta t_1}, v_{h_1,\Delta t_1}\rangle_{G\times\mathbb{R}^+,\sigma} - \langle g, v_{h_1,\Delta t_1}\rangle_\sigma - \langle\tilde{\lambda}_{h_2,\Delta t_2}, v_{h_1,\Delta t_1}\rangle_{G\times\mathbb{R}^+,\sigma} \\ &= \langle\mathcal{S}_\sigma u_{h_1,\Delta t_1}, v_{h_1,\Delta t_1}\rangle_{G\times\mathbb{R}^+,\sigma} - \langle\mathcal{S}_\sigma u, v_{h_1,\Delta t_1}\rangle_{G\times\mathbb{R}^+,\sigma} + \langle\lambda, v_{h_1,\Delta t_1}\rangle_{G\times\mathbb{R}^+,\sigma} - \langle\tilde{\lambda}_{h_2,\Delta t_2}, v_{h_1,\Delta t_1}\rangle_{G\times\mathbb{R}^+,\sigma} \\ &= \langle\mathcal{S}_\sigma(u_{h_1,\Delta t_1}-u), v_{h_1,\Delta t_1}\rangle_{G\times\mathbb{R}^+,\sigma} + \langle\lambda-\tilde{\lambda}_{h_2,\Delta t_2}, v_{h_1,\Delta t_1}\rangle_{G\times\mathbb{R}^+,\sigma} \ . \quad (7.20)\end{aligned}$$

Then using (7.17) in Theorem 7.7 and (7.20), we obtain:

$$\begin{aligned}\alpha\|\lambda_{h_2,\Delta t_2}-\tilde{\lambda}_{h_2,\Delta t_2}\|_{0,-\frac{1}{2},\sigma} &\le \sup_{v_{h_1,\Delta t_1}} \frac{\langle\lambda_{h_2,\Delta t_2}-\tilde{\lambda}_{h_2,\Delta t_2}, v_{h_1,\Delta t_1}\rangle_{G\times\mathbb{R}^+,\sigma}}{\|v_{h_1,\Delta t_1}\|_{0,\frac{1}{2},\sigma,*}} \\ = \sup_{v_{h_1,\Delta t_1}} &\frac{\langle\mathcal{S}_\sigma(u_{h_1,\Delta t_1}-u), v_{h_1,\Delta t_1}\rangle_{G\times\mathbb{R}^+,\sigma} + \langle\lambda-\tilde{\lambda}_{h_2,\Delta t_2}, v_{h_1,\Delta t_1}\rangle_{G\times\mathbb{R}^+,\sigma}}{\|v_{h_1,\Delta t_1}\|_{0,\frac{1}{2},\sigma,*}} \ .\end{aligned}$$

From duality, the mapping properties in Theorem 7.1 and an inverse estimate in time for $v_{h_1,\Delta t_1} \in \tilde{V}_{h_1,\Delta t_1}^{1,1}$,, see [53] (3.177):

$$\|v_{h_1,\Delta t_1}\|_{\frac{1}{2},\frac{1}{2},\sigma,*} \lesssim \frac{1}{(\Delta t_1)^{1/2}}\|v_{h_1,\Delta t_1}\|_{0,\frac{1}{2},\sigma,*} \ ,$$

we have for the first term

$$\begin{aligned}|\langle\mathcal{S}_\sigma(u_{h_1,\Delta t_1}-u), v_{h_1,\Delta t_1}\rangle_{G\times\mathbb{R}^+,\sigma}| &\lesssim \|\mathcal{S}_\sigma(u_{h_1,\Delta t_1}-u)\|_{-\frac{1}{2},-\frac{1}{2},\sigma}\|v_{h_1,\Delta t_1}\|_{\frac{1}{2},\frac{1}{2},\sigma,*} \\ &\lesssim \|u_{h_1,\Delta t_1}-u\|_{-\frac{1}{2},\frac{1}{2},\sigma,*}(\Delta t_1)^{-\frac{1}{2}}\|v_{h_1,\Delta t_1}\|_{0,\frac{1}{2},\sigma,*} \ .\end{aligned}$$

Estimating the second term with the duality:

$$|\langle\lambda-\tilde{\lambda}_{h_2,\Delta t_2}, v_{h_1,\Delta t_1}\rangle_{G\times\mathbb{R}^+,\sigma}| \lesssim \|\lambda-\tilde{\lambda}_{h_2,\Delta t_2}\|_{0,-\frac{1}{2},\sigma}\|v_{h_1,\Delta t_1}\|_{0,\frac{1}{2},\sigma,*} \ .$$

With the triangle inequality, we get

$$\begin{aligned}&\|\lambda-\lambda_{h_2,\Delta t_2}\|_{0,-\frac{1}{2},\sigma} \le \|\lambda-\tilde{\lambda}_{h_2,\Delta t_2}\|_{0,-\frac{1}{2},\sigma} + \|\tilde{\lambda}_{h_2,\Delta t_2}-\lambda_{h_2,\Delta t_2}\|_{0,-\frac{1}{2},\sigma} \\ &\lesssim \|\lambda-\tilde{\lambda}_{h_2,\Delta t_2}\|_{0,-\frac{1}{2},\sigma} + (\Delta t_1)^{-\frac{1}{2}}\|u_{h_1,\Delta t_1}-u\|_{-\frac{1}{2},\frac{1}{2},\sigma,*} \ .\end{aligned}$$

Therefore taking the infimum over $\tilde{\lambda}_{h_2,\Delta t_2}$ yields the a priori error estimate (7.18).

$$\|\lambda - \lambda_{h_2,\Delta t_2}\|_{0,-\frac{1}{2},\sigma} \lesssim \inf_{\tilde{\lambda}_{h_2,\Delta t_2}} \|\lambda - \tilde{\lambda}_{h_2,\Delta t_2}\|_{0,-\frac{1}{2},\sigma} + (\Delta t_1)^{-\frac{1}{2}} \|u_{h_1,\Delta t_1} - u\|_{-\frac{1}{2},\frac{1}{2},\sigma,*} \ . \quad (7.21)$$

In order to prove (7.19) we note the Galerkin orthogonality

$$\langle \mathcal{S}_\sigma(u - u_{h_1,\Delta t_1}), v_{h_1,\Delta t_1} \rangle_{G\times\mathbb{R}^+,\sigma} = \langle \lambda - \lambda_{h_2,\Delta t_2}, v_{h_1,\Delta t_1} \rangle_{G\times\mathbb{R}^+,\sigma} \ .$$

Using the coercivity of the Dirichlet-to-Neumann operator in Theorem 7.1, we get for all $v_{h_1,\Delta t_1}$ and $\tilde{\lambda}_{h_2,\Delta t_2}$

$$\begin{aligned}
&\|u_{h_1,\Delta t_1} - v_{h_1,\Delta t_1}\|^2_{-\frac{1}{2},\frac{1}{2},\sigma,*} \lesssim_\sigma \langle \mathcal{S}_\sigma(u_{h_1,\Delta t_1} - v_{h_1,\Delta t_1}), u_{h_1,\Delta t_1} - v_{h_1,\Delta t_1} \rangle_{G\times\mathbb{R}^+,\sigma} \\
&= \langle \mathcal{S}_\sigma(u - v_{h_1,\Delta t_1}), u_{h_1,\Delta t_1} - v_{h_1,\Delta t_1} \rangle_{G\times\mathbb{R}^+,\sigma} + \langle \mathcal{S}_\sigma(u_{h_1,\Delta t_1} - u), u_{h_1,\Delta t_1} - v_{h_1,\Delta t_1} \rangle_{G\times\mathbb{R}^+,\sigma} \\
&= \langle \mathcal{S}_\sigma(u - v_{h_1,\Delta t_1}), u_{h_1,\Delta t_1} - v_{h_1,\Delta t_1} \rangle_{G\times\mathbb{R}^+,\sigma} + \langle \tilde{\lambda}_{h_2,\Delta t_2} - \lambda + \lambda_{h_2,\Delta t_2} - \tilde{\lambda}_{h_2,\Delta t_2}, u_{h_1,\Delta t_1} - v_{h_1,\Delta t_1} \rangle_{G\times\mathbb{R}^+,\sigma}.
\end{aligned}$$

The mapping properties in Theorem 7.1 and the duality, yield

$$\begin{aligned}
&\|u_{h_1,\Delta t_1} - v_{h_1,\Delta t_1}\|^2_{-\frac{1}{2},\frac{1}{2},\sigma,*} \lesssim_\sigma \|u - v_{h_1,\Delta t_1}\|_{\frac{1}{2},\frac{1}{2},\sigma,*} \|u_{h_1,\Delta t_1} - v_{h_1,\Delta t_1}\|_{-\frac{1}{2},\frac{1}{2},\sigma,*} \\
&+ \|\tilde{\lambda}_{h_2,\Delta t_2} - \lambda\|_{\frac{1}{2},-\frac{1}{2},\sigma} \|u_{h_1,\Delta t_1} - v_{h_1,\Delta t_1}\|_{-\frac{1}{2},\frac{1}{2},\sigma,*} + \|\tilde{\lambda}_{h_2,\Delta t_2} - \lambda_{h_2,\Delta t_2}\|_{\frac{1}{2},-\frac{1}{2},\sigma} \|u_{h_1,\Delta t_1} - v_{h_1,\Delta t_1}\|_{-\frac{1}{2},\frac{1}{2},\sigma,*}.
\end{aligned}$$

Dividing by $\|u_{h_1,\Delta t_1} - v_{h_1,\Delta t_1}\|_{-\frac{1}{2},\frac{1}{2},\sigma,*}$ leads to

$$\|u_{h_1,\Delta t_1} - v_{h_1,\Delta t_1}\|_{-\frac{1}{2},\frac{1}{2},\sigma,*} \lesssim_\sigma \|u - v_{h_1,\Delta t_1}\|_{\frac{1}{2},\frac{1}{2},\sigma,*} + \|\tilde{\lambda}_{h_2,\Delta t_2} - \lambda\|_{\frac{1}{2},-\frac{1}{2},\sigma} + \|\tilde{\lambda}_{h_2,\Delta t_2} - \lambda_{h_2,\Delta t_2}\|_{\frac{1}{2},-\frac{1}{2},\sigma}.$$

With the triangle inequality and estimating with the stronger norm, we get

$$\begin{aligned}
&\|u - u_{h_1,\Delta t_1}\|_{-\frac{1}{2},\frac{1}{2},\sigma,*} \le \|u - v_{h_1,\Delta t_1}\|_{-\frac{1}{2},\frac{1}{2},\sigma,*} + \|v_{h_1,\Delta t_1} - u_{h_1,\Delta t_1}\|_{-\frac{1}{2},\frac{1}{2},\sigma,*} \\
&\lesssim_\sigma \|u - v_{h_1,\Delta t_1}\|_{\frac{1}{2},\frac{1}{2},\sigma,*} + \|\tilde{\lambda}_{h_2,\Delta t_2} - \lambda\|_{\frac{1}{2},-\frac{1}{2},\sigma} + \|\tilde{\lambda}_{h_2,\Delta t_2} - \lambda_{h_2,\Delta t_2}\|_{\frac{1}{2},-\frac{1}{2},\sigma} \ .
\end{aligned}$$

Taking the infimum yields (7.19). □

7.5 A variational inequality for the punch problem

We consider the punch problem, described in (7.2) with a retarded single layer potential ansatz $w = S\sigma_{x_n} =: Su$ with $u := \sigma_{x_n}$ and the shearing strains vanish in the half-space. With the jump relation of S, we write the punch conditions

$$\begin{array}{lll}
u(x,t) & \ge 0 & \text{for } (x,t) \in G \times \mathbb{R} \ , \\
(Vu)(x,t) & \ge g(x,t) & \text{for } (x,t) \in G \times \mathbb{R} \ , \\
u(x,t) & > 0 & \text{for } (x,t) \in G \times \mathbb{R} \Longrightarrow (Vu)(x,t) = g \ , \\
u(x,t) & = 0 & \text{for } (x,t) \in \Gamma \backslash G \times \mathbb{R} \ .
\end{array}$$

We can write (7.2) as:
Find $u \in H^{\frac{1}{2}}_\sigma(\mathbb{R}^+, H^{-\frac{1}{2}}(G))$ with supp $u \subset Q_0 = G \times \mathbb{R}^+$ such that

$$u \ge 0 \ , \ w = Vu \ge g \ , \ (w - (\phi + \eta))u = (Vu - g)u = 0 \text{ on } G \times \mathbb{R} \ . \quad (7.22)$$

Using the restriction p_Q to Q and testing with $v \in H^{\frac{1}{2}}_{\sigma}(\mathbb{R}^+, H^{-\frac{1}{2}}(G))^+$, we get for smooth g the variational formulation:
Find $u \in H^{\frac{1}{2}}_{\sigma}(\mathbb{R}^+, \widetilde{H}^{-\frac{1}{2}}(G))^+$ such that for all $v \in H^{\frac{1}{2}}_{\sigma}(\mathbb{R}^+, \widetilde{H}^{-\frac{1}{2}}(G))^+$:

$$\langle p_Q V u, v-u\rangle_{G\times\mathbb{R}^+,\sigma} \geq \langle g, v-u\rangle_{G\times\mathbb{R}^+,\sigma} \ . \tag{7.23}$$

For flat contact area, $\Omega = \mathbb{R}^3_+$, we use the following estimates known from [33, 56], which doesn't include a time derivative:

$$\|\phi\|^2_{-\frac{1}{2},-\frac{1}{2},\sigma,*} \lesssim_{\sigma} \langle p_Q V\phi, \phi\rangle_{\sigma} \lesssim \|\phi\|^2_{\frac{1}{2},-\frac{1}{2},\sigma,*} \tag{7.24}$$

The following theorem is only stated in [47], but proven here.

Theorem 7.9 ([47], Theorem 17)**.** *The punch problem* (7.2) *is equivalent to the variational inequality* (7.23)*.*

Proof. The proof goes analogous to Theorem 7.2. It is enough to prove the equivalence of (7.22) and (7.23). In order to derive (7.23) from (7.22), we test the second inequality of (7.22) by $v \geq 0$:

$$\langle p_Q V u - g, v\rangle_{G\times\mathbb{R}^+,\sigma} \geq 0.$$

By the third equality in (7.22) and choosing $v = u_\sigma$ we see $\langle p_Q V u - g, u\rangle_{G\times\mathbb{R}^+,\sigma} = 0$. Therefore we obtain the variational inequality (7.23).
Conversely (7.23) holds. Since $u \in H^{1/2}_{\sigma}(\mathbb{R}^+, \widetilde{H}^{-1/2}(G))^+$, we need to prove the second and third (in-)equalities of (7.22). We choose $v \in H^{1/2}_{\sigma}(\mathbb{R}^+, \widetilde{H}^{-1/2}(G))^+$ in (7.23) such that $v - u := v' \geq 0$ to obtain $\langle p_Q V u - g, v'\rangle_{G\times\mathbb{R}^+,\sigma} \geq 0$. Therefore $Vu - g \geq 0$ follows. Now setting on the one hand $v = 2u \geq 0$ in (7.23) to get $\langle p_Q V u, u\rangle_{G\times\mathbb{R}^+,\sigma} \geq \langle g, u\rangle_{G\times\mathbb{R}^+,\sigma}$ and on the other hand $v = 0$ in (7.23) to get $\langle p_Q V u, u\rangle_{G\times\mathbb{R}^+,\sigma} \leq \langle g, u\rangle_{G\times\mathbb{R}^+,\sigma}$, we deduce $\langle p_Q V u - g, u\rangle_{G\times\mathbb{R}^+,\sigma} = 0$. Since the first and the second inequalities already hold, we get the remaining equality $(Vu - g)u = 0$. □

As for the variational inequality for the Dirichlet-to-Neumann operator, a coercivity estimate for V in the half space is known. Therefore a unique solution exists:

Theorem 7.10 ([47], Theorem 18, [33], p. 456)**.** *Let $\sigma > 0$ and $h \in H^{\frac{3}{2}}_{\sigma}(\mathbb{R}^+, H^{\frac{1}{2}}(G))$. Then there exists a unique classical solution $u \in H^{\frac{1}{2}}_{\sigma}(\mathbb{R}^+, \widetilde{H}^{-\frac{1}{2}}(G))^+$ of* (7.23)*.*

The corresponding discretized variational inequality reads:
Find $u_{h,\Delta t} \in \tilde{K}^+_{h,\Delta t}$ such that for all $v_{h,\Delta t} \in \tilde{K}^+_{h,\Delta t}$.:

$$\langle p_Q V u_{h,\Delta t}, v_{h,\Delta t} - u_{h,\Delta t}\rangle_{G\times\mathbb{R}^+,\sigma} \geq \langle h, v_{h,\Delta t} - u_{h,\Delta t}\rangle_{G\times\mathbb{R}^+,\sigma} \ . \tag{7.25}$$

We get the following a priori error estimate.

Theorem 7.11 ([47], Theorem 19). *Let $g \in H^{\frac{3}{2}}_{\sigma}(\mathbb{R}^+, H^{\frac{1}{2}}(G))$, and let $u \in H^{\frac{1}{2}}_{\sigma}(\mathbb{R}^+, \widetilde{H}^{-\frac{1}{2}}(G))^+$, $u_{h,\Delta t} \in \tilde{K}^+_{h,\Delta t}$ be the solutions of (7.23), respectively (7.25). Then the following estimate holds:*

$$\|u - u_{h,\Delta t}\|^2_{-\frac{1}{2},-\frac{1}{2},\sigma,\star} \lesssim_{\sigma} \inf_{\phi_{h,\Delta t} \in \tilde{K}^+_{h,\Delta t}} \left(\|g - p_Q V u\|_{\frac{1}{2},\frac{1}{2},\sigma} \|u - \phi_{h,\Delta t}\|_{-\frac{1}{2},-\frac{1}{2},\sigma,\star} + \|u - \phi_{h,\Delta t}\|^2_{\frac{1}{2},-\frac{1}{2},\sigma,\star} \right) . \tag{7.26}$$

By using the mapping properties of V in the half space, as in Theorem 2.3, and (7.24) the steps of the proof are analogous to the proof of Theorem 7.5. The proof is missing in [47], so we complete it here.

Proof. Let $g \in H^{\frac{3}{2}}_{\sigma}(\mathbb{R}^+, H^{\frac{1}{2}}(G))$ and $u \in H^{\frac{1}{2}}_{\sigma}(\mathbb{R}^+, \widetilde{H}^{-1/2}(G))^+$ be the solution of (7.23). Testing (7.23) with $\phi \in H^{\frac{1}{2}}_{\sigma}(\mathbb{R}^+, \widetilde{H}^{-\frac{1}{2}}(G))^+$ we divide

$$\langle p_Q V u, \phi - u \rangle_{G \times \mathbb{R}^+,\sigma} = \langle p_Q V u, \phi \rangle_{G \times \mathbb{R}^+,\sigma} - \langle p_Q V u, u \rangle_{G \times \mathbb{R}^+,\sigma} .$$

Now shifting $\langle p_Q V u, \phi \rangle_{G \times \mathbb{R}^+,\sigma}$ to the right hand side of the inequality (7.23), we get

$$-\langle p_Q V u, u \rangle_{G \times \mathbb{R}^+,\sigma} \geq \langle g, \phi - u \rangle_{G \times \mathbb{R}^+,\sigma} - \langle p_Q V u, \phi \rangle_{G \times \mathbb{R}^+,\sigma}$$

Therefore

$$\langle p_Q V u, u \rangle_{G \times \mathbb{R}^+,\sigma} \leq \langle g, u - \phi \rangle_{G \times \mathbb{R}^+,\sigma} + \langle p_Q V u, \phi \rangle_{G \times \mathbb{R}^+,\sigma} . \tag{7.27}$$

Analogously for (7.25) testing with $\phi_{h,\Delta t} \in \tilde{K}^+_{h,\Delta t}$, we note that

$$\langle p_Q V u_{h,\Delta t}, u_{h,\Delta t} \rangle_{G \times \mathbb{R}^+,\sigma} \leq \langle g, u_{h,\Delta t} - \phi_{h,\Delta t} \rangle_{G \times \mathbb{R}^+,\sigma} + \langle p_Q V u_{h,\Delta t}, \phi_{h,\Delta t} \rangle_{G \times \mathbb{R}^+,\sigma}. \tag{7.28}$$

Using the coercivity in (7.24), we obtain with (7.27) and (7.28)

$$\begin{aligned}
&\|u - u_{h,\Delta t}\|^2_{-\frac{1}{2},-\frac{1}{2},\sigma,\star} \lesssim_{\sigma} \langle p_Q V(u - u_{h,\Delta t}), u - u_{h,\Delta t} \rangle_{G \times \mathbb{R}^+,\sigma} \\
&= \langle p_Q V(u - u_{h,\Delta t}), u \rangle_{G \times \mathbb{R}^+,\sigma} - \langle p_Q V(u - u_{h,\Delta t}), u_{h,\Delta t} \rangle_{G \times \mathbb{R}^+,\sigma} \\
&= \langle p_Q V u, u \rangle_{G \times \mathbb{R}^+,\sigma} - \langle p_Q V u_{h,\Delta t}, u \rangle_{G \times \mathbb{R}^+,\sigma} - \langle p_Q V u, u_{h,\Delta t} \rangle_{G \times \mathbb{R}^+,\sigma} + \langle p_Q V u_{h,\Delta t}, u_{h,\Delta t} \rangle_{G \times \mathbb{R}^+,\sigma} \\
&\leq \langle g, u - \phi \rangle_{G \times \mathbb{R}^+,\sigma} + \langle g, u_{h,\Delta t} - \phi_{h,\Delta t} \rangle_{G \times \mathbb{R}^+,\sigma} + \langle p_Q V u_{h,\Delta t}, \phi_{h,\Delta t} \rangle_{G \times \mathbb{R}^+,\sigma} \\
&\quad + \langle p_Q V u, \phi \rangle_{G \times \mathbb{R}^+,\sigma} - \langle p_Q V u, u_{h,\Delta t} \rangle_{G \times \mathbb{R}^+,\sigma} - \langle p_Q V u_{h,\Delta t}, u \rangle_{G \times \mathbb{R}^+,\sigma} \\
&= \langle g, u - \phi \rangle_{G \times \mathbb{R}^+,\sigma} + \langle g, u_{h,\Delta t} - \phi_{h,\Delta t} \rangle_{G \times \mathbb{R}^+,\sigma} + \langle p_Q V u, \phi - u_{h,\Delta t} \rangle_{G \times \mathbb{R}^+,\sigma} \\
&\quad + \langle p_Q V u_{h,\Delta t}, \phi_{h,\Delta t} - u \rangle_{G \times \mathbb{R}^+,\sigma}.
\end{aligned}$$

We add $0 = \langle p_Q V u, u - \phi_{h,\Delta t} \rangle_{G \times \mathbb{R}^+,\sigma} - \langle p_Q V u, u - \phi_{h,\Delta t} \rangle_{G \times \mathbb{R}^+,\sigma}$ into:

$$\langle p_Q V u_{h,\Delta t}, \phi_{h,\Delta t} - u \rangle_{G \times \mathbb{R}^+,\sigma} = \langle p_Q V(u - u_{h,\Delta t}), u - \phi_{h,\Delta t} \rangle_{G \times \mathbb{R}^+,\sigma} - \langle p_Q V u, u - \phi_{h,\Delta t} \rangle_{G \times \mathbb{R}^+,\sigma} .$$

Hence, we get

$$\begin{aligned}
\|u-u_{h,\Delta t}\|^2_{-\frac12,-\frac12,\sigma,\star} &\lesssim_\sigma \langle g,u-\phi\rangle_{G\times\mathbb{R}^+,\sigma}+\langle g,u_{h,\Delta t}-\phi_{h,\Delta t}\rangle_{G\times\mathbb{R}^+,\sigma}+\langle p_QVu,\phi-u_{h,\Delta t}\rangle_{G\times\mathbb{R}^+,\sigma}\\
&\quad+\langle p_QV(u-u_{h,\Delta t}),u-\phi_{h,\Delta t}\rangle_{G\times\mathbb{R}^+,\sigma}-\langle p_QVu,u-\phi_{h,\Delta t}\rangle_{G\times\mathbb{R}^+,\sigma}\\
&=\langle g,u\rangle_{G\times\mathbb{R}^+,\sigma}-\langle g,\phi\rangle_{G\times\mathbb{R}^+,\sigma}+\langle g,u_{h,\Delta t}\rangle_{G\times\mathbb{R}^+,\sigma}-\langle g,\phi_{h,\Delta t}\rangle_{G\times\mathbb{R}^+,\sigma}+\langle p_QVu,\phi\rangle_{G\times\mathbb{R}^+,\sigma}\\
&\quad-\langle p_QVu,u_{h,\Delta t}\rangle_{G\times\mathbb{R}^+,\sigma}+\langle p_QV(u-u_{h,\Delta t}),u-\phi_{h,\Delta t}\rangle_{G\times\mathbb{R}^+,\sigma}\\
&\quad-\langle p_QVu,u\rangle_{G\times\mathbb{R}^+,\sigma}+\langle p_QVu,\phi_{h,\Delta t}\rangle_{G\times\mathbb{R}^+,\sigma}\\
&=\langle g,u_{h,\Delta t}-\phi\rangle_{G\times\mathbb{R}^+,\sigma}-\langle p_QVu,\phi_{h,\Delta t}-\phi\rangle_{G\times\mathbb{R}^+,\sigma}+\langle g,u-\phi_{h,\Delta t}\rangle_{G\times\mathbb{R}^+,\sigma}\\
&\quad-\langle p_QVu,u-\phi_{h,\Delta t}\rangle_{G\times\mathbb{R}^+,\sigma}+\langle p_QV(u-u_{h,\Delta t}),u-\phi_{h,\Delta t}\rangle_{G\times\mathbb{R}^+,\sigma}\\
&=\langle g-p_QVu,u-\phi_{h,\Delta t}\rangle_{G\times\mathbb{R}^+,\sigma}+\langle g-p_QVu_{h,\Delta t},u_{h,\Delta t}-\phi\rangle_{G\times\mathbb{R}^+,\sigma}\\
&\quad+\langle p_QV(u-u_{h,\Delta t}),u-\phi_{h,\Delta t}\rangle_{G\times\mathbb{R}^+,\sigma}.
\end{aligned}$$

Because of the conforming discretization, we may choose $\phi = u_{h,\Delta t}$ and conclude

$$\|u-u_{h,\Delta t}\|^2_{-\frac12,-\frac12,\sigma,\star} \lesssim_\sigma \langle g-p_QVu,u-\phi_{h,\Delta t}\rangle_{G\times\mathbb{R}^+,\sigma}+\langle p_QV(u-u_{h,\Delta t}),u-\phi_{h,\Delta t}\rangle_{G\times\mathbb{R}^+,\sigma}. \quad (7.29)$$

We estimate both terms by duality:

$$\|u-u_{h,\Delta t}\|^2_{-\frac12,\frac12,\sigma,\star}\lesssim_\sigma\|g-p_QVu\|_{\frac12,-\frac12,\sigma}\|u-\phi_{h,\Delta t}\|_{-\frac12,\frac12,\sigma,\star}+\|p_QV(u-u_{h,\Delta t})\|_{-\frac12,-\frac12,\sigma}\|u-\phi_{h,\Delta t}\|_{\frac12,\frac12,\sigma,\star}.$$

With the mapping properties of V, we obtain

$$\|u-u_{h,\Delta t}\|^2_{-\frac12,-\frac12,\sigma,\star}\lesssim_\sigma\|g-p_QVu\|_{\frac12,\frac12,\sigma}\|u-\phi_{h,\Delta t}\|_{-\frac12,-\frac12,\sigma,\star}+\|u-u_{h,\Delta t}\|_{\frac12,-\frac12,\sigma,\star}\|u-\phi_{h,\Delta t}\|_{\frac12,-\frac12,\sigma,\star}.$$

We conclude with Young's inequality for small $\epsilon>0$ and combine $\epsilon\|u-u_{h,\Delta t}\|^2_{\frac12,-\frac12,\sigma,\star}$ with the left hand side

$$\|u-u_{h,\Delta t}\|^2_{-\frac12,-\frac12,\sigma,\star}\lesssim_\sigma \|g-p_QVu\|_{\frac12,\frac12,\sigma}\|u-\phi_{h,\Delta t}\|_{-\frac12,-\frac12,\sigma,\star}+\|u-\phi_{h,\Delta t}\|^2_{\frac12,-\frac12,\sigma,\star}.$$

It follows the statement by taking the infimum over all $\phi_{h,\Delta t}$. □

Analogously to the contact problem we consider a mixed formulation, where the equivalence is proven here:

Theorem 7.12 (Mixed formulation, [47], Theorem 20)**.** *Let $g\in H^{\frac32}_\sigma(\mathbb{R}^+,H^{\frac12}(G))$. The variational inequality formulation (7.23) is equivalent to the following formulation: Find $(u,\lambda)\in H^{\frac12}_\sigma(\mathbb{R}^+,\widetilde{H}^{-\frac12}(G))\times H^{\frac12}_\sigma(\mathbb{R}^+,H^{\frac12}(G))^+$ such that*

$$\begin{cases}(a)\ \langle Vu,v\rangle_{G\times\mathbb{R}^+,\sigma}-\langle\lambda,v\rangle_{G\times\mathbb{R}^+,\sigma}=\langle h,v\rangle_{G\times\mathbb{R}^+,\sigma}\\ (b)\ \langle u,\mu-\lambda\rangle_{G\times\mathbb{R}^+,\sigma}\geq 0,\end{cases} \quad (7.30)$$

for all $(v,\mu)\in H^{\frac12}_\sigma(\mathbb{R}^+,\widetilde{H}^{-\frac12}(G))\times H^{\frac12}_\sigma(\mathbb{R}^+,H^{\frac12}(G))^+$.

Proof. First, we observe an equivalence of (7.23) to the following problem: Find $u \in H^{\frac{1}{2}}_{\sigma}(\mathbb{R}^+, \widetilde{H}^{-\frac{1}{2}}(G))^+$ such that for all $v \in H^{\frac{1}{2}}_{\sigma}(\mathbb{R}^+, \widetilde{H}^{-\frac{1}{2}}(G))^+$, u solves

$$\begin{cases} (a)\ \langle Vu, u\rangle_{G\times\mathbb{R}^+,\sigma} = \langle g, u\rangle_{G\times\mathbb{R}^+,\sigma} \\ (b)\ \langle Vu, v\rangle_{G\times\mathbb{R}^+,\sigma} \geq \langle g, v\rangle_{G\times\mathbb{R}^+,\sigma}. \end{cases} \tag{7.31}$$

This is due to setting $v = 2u$ on the one hand and $v = 0$ on the hand in the variational inequality (7.23). We get

$$\langle Vu, u\rangle_{G\times\mathbb{R}^+,\sigma} \geq \langle g, u\rangle_{G\times\mathbb{R}^+,\sigma}\ ,\ \text{and}\ \langle Vu, u\rangle_{G\times\mathbb{R}^+,\sigma} \leq \langle g, u\rangle_{G\times\mathbb{R}^+,\sigma}\ ,$$

Therefore (7.31a) holds. Using (7.31a) on (7.23) we obtain:

$$\langle Vu, v\rangle_{G\times\mathbb{R}^+,\sigma} - \langle Vu, u\rangle_{G\times\mathbb{R}^+,\sigma} \geq \langle g, v\rangle_{G\times\mathbb{R}^+,\sigma} - \langle g, u\rangle_{G\times\mathbb{R}^+,\sigma}\ ,$$

where (7.31b) follows. Conversely, we subtract (7.31a) from (7.31b) in order to get (7.23) from (7.31).

For getting (7.31) from (7.23), we prove (7.31) $\Rightarrow$ (7.30). With (7.31b) for $\lambda = Vu - g$, we get for all $v \in H^{\frac{1}{2}}_{\sigma}(\mathbb{R}^+, \widetilde{H}^{-\frac{1}{2}}(G))^+$, $0 \leq \langle Vu - g, v\rangle_{G\times\mathbb{R}^+,\sigma} = \langle \lambda, v\rangle_{G\times\mathbb{R}^+,\sigma}$. Since $v \geq 0$, we deduce $\lambda \geq 0$ and therefore $\lambda \in H^{\frac{1}{2}}_{\sigma}(\mathbb{R}^+, H^{\frac{1}{2}}(G))^+$. (7.30a) holds by substracting $\langle \lambda, v\rangle_{G\times\mathbb{R}^+,\sigma}$ of the left hand side of (7.31b) and using the definition of λ.
Via (7.31a) we see $\langle \lambda, u\rangle_{G\times\mathbb{R}^+,\sigma} = 0$, and hence, $\langle u, \mu - \lambda\rangle_{G\times\mathbb{R}^+,\sigma} = \langle u, \mu\rangle_{G\times\mathbb{R}^+,\sigma} \geq 0$, because $u \in H^{\frac{1}{2}}_{\sigma}(\mathbb{R}^+, \widetilde{H}^{\frac{1}{2}}(G))^+$ and $\mu \in H^{\frac{1}{2}}_{\sigma}(\mathbb{R}^+, \widetilde{H}^{-\frac{1}{2}}(G))^+$.

Conversely we prove (7.30) $\Rightarrow$ (7.23). Let $(u, \lambda) \in H^{\frac{1}{2}}_{\sigma}(\mathbb{R}^+, \widetilde{H}^{\frac{1}{2}}(G)) \times H^{\frac{1}{2}}_{\sigma}(\mathbb{R}^+, H^{-\frac{1}{2}}(G))^+$ be the solution to (7.30). Again setting on the one hand $\mu = 2\lambda$ and on the other hand $\mu = 0$, we get $\langle u, \lambda\rangle_{G\times\mathbb{R}^+,\sigma} \geq 0$, $\langle u, \lambda\rangle_{G\times\mathbb{R}^+,\sigma} \leq 0$. Therefore $\langle u, \lambda\rangle_{G\times\mathbb{R}^+,\sigma} = 0$.

If we assume that u is not ≥ 0, then there exists $\mu \in H^{\frac{1}{2}}_{\sigma}(\mathbb{R}^+, H^{-\frac{1}{2}}(G))^+$ such that $\langle u, \mu\rangle_{G\times\mathbb{R}^+,\sigma} < 0$, and we observe from (7.30b) the contradiction

$$0 \leq \langle u, \mu - \lambda\rangle_{G\times\mathbb{R}^+,\sigma} = \langle u, \mu\rangle_{G\times\mathbb{R}^+,\sigma} - \langle u, \lambda\rangle_{G\times\mathbb{R}^+,\sigma} = \langle u, \mu\rangle_{G\times\mathbb{R}^+,\sigma} < 0\ .$$

Therefore $u \in H^{\frac{1}{2}}_{\sigma}(\mathbb{R}^+, \widetilde{H}^{-\frac{1}{2}}(G))^+$. Applying $v-u$ as u in (7.30b) for $v \in H^{\frac{1}{2}}_{\sigma}(\mathbb{R}^+, \widetilde{H}^{-\frac{1}{2}}(G))^+$, we get $\langle v - u, \lambda\rangle_{G\times\mathbb{R}^+,\sigma} = \langle v, \lambda\rangle_{G\times\mathbb{R}^+,\sigma} - \langle u, \lambda\rangle_{G\times\mathbb{R}^+,\sigma} = \langle v, \lambda\rangle_{G\times\mathbb{R}^+,\sigma} \geq 0$. Testing (7.30a) with $v - u$, we obtain

$$\langle Vu, v - u\rangle_{G\times\mathbb{R}^+,\sigma} - \langle \lambda, v - u\rangle_{G\times\mathbb{R}^+,\sigma} = \langle g, v - u\rangle_{G\times\mathbb{R}^+,\sigma}\ ,$$

or equivalently

$$\langle Vu - g, v - u\rangle_{G\times\mathbb{R}^+,\sigma} = \langle \lambda, v - u\rangle_{G\times\mathbb{R}^+,\sigma} \geq 0.$$

So we get (7.23) and therefore (7.31), too. □

The discrete formulation reads as follows:
Find $(u_{h_1,\Delta t_1}, \lambda_{h_2,\Delta t_2}) \in V^{1,1}_{h_1,\Delta t_1} \times (V^{1,1}_{h_2,\Delta t_2})^+$ satisfying for all $(v_{h_1,\Delta t_1}, \mu_{h_2,\Delta t_2}) \in V^{1,1}_{h_1,\Delta t_1} \times (V^{1,1}_{h_2,\Delta t_2})^+$

$$\begin{cases} (a)\ \langle V u_{h_1,\Delta t_1}, v_{h_1,\Delta t_1}\rangle_{G\times\mathbb{R}^+,\sigma} - \langle \lambda_{h_2,\Delta t_2}, v_{h_1,\Delta t_1}\rangle_{G\times\mathbb{R}^+,\sigma} = \langle g, v_{h_1,\Delta t_1}\rangle_{G\times\mathbb{R}^+,\sigma} \\ (b)\ \langle u_{h_1,\Delta t_1}, \mu_{h_2,\Delta t_2} - \lambda_{h_2,\Delta t_2}\rangle_{G\times\mathbb{R}^+,\sigma} \geq 0. \end{cases} \tag{7.32}$$

Next for sufficiently different meshes to the Lagrange multiplier $\lambda_{h_2,\Delta t_2}$ and the solution $u_{h_1,\Delta t_1}$ we obtain another discrete inf-sup condition, which we will need to prove the a priori error estimate:

Theorem 7.13. *Let $C > 0$ sufficiently small, and $\frac{\max\{h_1,\Delta t_1\}}{\min\{h_2,\Delta t_2\}} < C$. Then there exists $\alpha > 0$ such that for all $\lambda_{h_2,\Delta t_2}$:*

$$\sup_{\mu_{h_1,\Delta t_1}} \frac{\langle \mu_{h_1,\Delta t_1}, \lambda_{h_2,\Delta t_2}\rangle_{G\times\mathbb{R}^+,\sigma}}{\|\mu_{h_1,\Delta t_1}\|_{-\frac{1}{2},-\frac{1}{2},\sigma,*}} \geq \alpha \|\lambda_{h_2,\Delta t_2}\|_{\frac{1}{2},-\frac{1}{2},\sigma} \ . \tag{7.33}$$

Proof. We proceed similarly to [47]. Let z be a solution of

$$z - \partial_t^2 z - \Delta z = 0 \ \text{ in } \Omega\times\mathbb{R}^+ \ , \quad z(x,0) = \dot z(x,0) = 0 \ \text{ in } \Omega \ ,$$
$$z|_G = \lambda_{h_2,\Delta t_2} \ \text{ on } G\times\mathbb{R}^+ \ , \qquad z|_{\Gamma\setminus G} = 0 \ \text{ on } \Gamma\setminus G\times\mathbb{R}^+ \ , \quad z \longrightarrow 0 \ \text{ for } t\to\infty \ \text{ in } \Omega \ .$$

The coercivity of the Dirichlet-to-Neumann operator yields:

$$\|z\|^2_{-1/2,1/2,\sigma} \lesssim_\sigma \langle S_\sigma z, z\rangle_{G\times\mathbb{R}^+,\sigma} = \langle \partial_n z, z\rangle_{G\times\mathbb{R}^+,\sigma} = \langle \partial_n z, \lambda_{h_2,\Delta t_2}\rangle_{G\times\mathbb{R}^+,\sigma} \ . \tag{7.34}$$

Now we choose δ such that $\|\partial_n z\|_{-1/2,-1/2+\delta,\sigma} < \infty$. Due to the approximation properties in [53, Proposition 3.56], we get $\tilde\mu_{h_2,\Delta t_2}$ such that

$$\|\partial_n z - \tilde\mu_{h_1,\Delta t_1}\|_{-1/2,-1/2,\sigma} \lesssim (\max\{h_1,\Delta t_1\})^\delta \|\partial_n z\|_{-1/2,-1/2+\delta,\sigma} \ .$$

From [47, Proof of Theorem 5] ($\|S_\sigma z\|_{-1/2,-1/2,\sigma} \lesssim \|z\|_{-1/2,1/2,\sigma}$) together with the inverse estimate in [53] (i.e. $\|\lambda_{h_2,\Delta t_2}\|_{-1/2,1/2+\delta,\sigma} \lesssim \frac{1}{(\min\{h_2,\Delta t_2\})^\delta}\|\lambda_{h_2,\Delta t_2}\|_{-1/2,1/2,\sigma}$), we get

$$\|\partial_n z - \tilde\mu_{h_1,\Delta t_1}\|_{-1/2,-1/2,\sigma} \lesssim \frac{(\max\{h_1,\Delta t_1\})^\delta}{(\min\{h_2,\Delta t_2\})^\delta}\|\lambda_{h_2,\Delta t_2}\|_{-1/2,1/2,\sigma} \ . \tag{7.35}$$

Altogether, we conclude:

$$\begin{aligned} \|\tilde\mu_{h_1,\Delta t_1}\|_{-1/2,-1/2,\sigma} &\leq \|\partial_n z - \tilde\mu_{h_1,\Delta t_1}\|_{-1/2,-1/2,\sigma} + \|\partial_n z\|_{-1/2,-1/2,\sigma} \\ &\lesssim \frac{(\max\{h_1,\Delta t_1\})^\delta}{(\min\{h_2,\Delta t_2\})^\delta}\|\lambda_{h_2,\Delta t_2}\|_{-1/2,1/2,\sigma} + \|\lambda_{h_2,\Delta t_2}\|_{-1/2,1/2,\sigma} \end{aligned}$$

Taking advantage of $\tilde\mu_{h_1,\Delta t_1}$ as above and defining $K := \frac{(\max\{h_1,\Delta t_1\})^\delta}{(\min\{h_2,\Delta t_2\})^\delta}$, we obtain

$$\begin{aligned} &\sup_{\tilde\mu_{h_1,\Delta t_1}} \frac{\langle \mu_{h_1,\Delta t_1}, \lambda_{h_2,\Delta t_2}\rangle_{G\times\mathbb{R}^+,\sigma}}{\|\mu_{h_1,\Delta t_1}\|_{-1/2,-1/2,\sigma}} \geq \frac{\langle \tilde\mu_{h_1,\Delta t_1}, \lambda_{h_2,\Delta t_2}\rangle_{G\times\mathbb{R}^+,\sigma}}{\|\tilde\mu_{h_1,\Delta t_1}\|_{-1/2,-1/2,\sigma}} \\ &\gtrsim \frac{\langle \tilde\mu_{h_1,\Delta t_1}, \lambda_{h_2,\Delta t_2}\rangle_{G\times\mathbb{R}^+}}{K\|\lambda_{h_2,\Delta t_2}\|_{-1/2,1/2,\sigma} + \|\lambda_{h_2,\Delta t_2}\|_{-1/2,1/2,\sigma}} \\ &\gtrsim \frac{1}{(1+K)\|\lambda_{h_2,\Delta t_2}\|_{-1/2,1/2,\sigma}} \left(\langle \partial_n z, \lambda_{h_2,\Delta t_2}\rangle_{G\times\mathbb{R}^+,\sigma} - \langle \partial_n z - \tilde\mu_{h_1,\Delta t_1}, \lambda_{h_2,\Delta t_2}\rangle_{G\times\mathbb{R}^+,\sigma}\right) \ . \end{aligned}$$

Estimating $\langle \partial_n z, \lambda_{h_2,\Delta t_2}\rangle_{G\times\mathbb{R}^+,\sigma}$ with (7.34) and the other term with (7.35)

$$\begin{aligned}\langle \partial_n z - \tilde{\mu}_{h_1,\Delta t_1}, \lambda_{h_2,\Delta t_2}\rangle_{G\times\mathbb{R}^+,\sigma} &\lesssim \|\partial_n z - \tilde{\mu}_{h_1,\Delta t_1}\|_{-1/2,-1/2,\sigma}\|\lambda_{h_2,\Delta t_2}\|_{1/2,1/2,\sigma}\\ &\lesssim K\|\lambda_{h_2,\Delta t_2}\|_{-1/2,1/2,\sigma}\|\lambda_{h_2,\Delta t_2}\|_{1/2,1/2,\sigma}\ ,\end{aligned}$$

we further estimate

$$\begin{aligned}&\sup_{\tilde{\mu}_{h_1,\Delta t_1}} \frac{\langle \mu_{h_1,\Delta t_1}, \lambda_{h_2,\Delta t_2}\rangle_{G\times\mathbb{R}^+,\sigma}}{\|\mu_{h_1,\Delta t_1}\|_{-1/2,-1/2,\sigma}}\\ &\gtrsim \frac{(\|\lambda_{h_2,\Delta t_2}\|^2_{-1/2,1/2,\sigma} + K\|\lambda_{h_2,\Delta t_2}\|_{-1/2,1/2,\sigma}\|\lambda_{h_2,\Delta t_2}\|_{1/2,1/2,\sigma})}{(1+K)\|\lambda_{h_2,\Delta t_2}\|_{-1/2,1/2,\sigma}}\\ &\geq \frac{\|\lambda_{h_2,\Delta t_2}\|_{-1/2,1/2,\sigma} + K\|\lambda_{h_2,\Delta t_2}\|_{1/2,1/2,\sigma}}{(1+K)} \geq \alpha\|\lambda_{h_2,\Delta t_2}\|_{1/2,1/2,\sigma}\ .\end{aligned}$$

□

Next we prove an a priori error estimate:

Theorem 7.14. *Let (u,λ) solve the mixed formulation (7.30) and $(u_{h_1,\Delta t_1}, \lambda_{h_2,\Delta t_2})$ solve the discrete mixed formulation (7.32). Then the following a priori error estimate hold:*

$$\|\lambda - \lambda_{h_2,\Delta t_2}\|_{\frac{1}{2},\frac{1}{2},\sigma} \lesssim \inf_{\tilde{\lambda}_{h_2,\Delta t_2}} \|\lambda - \tilde{\lambda}_{h_2,\Delta t_2}\|_{\frac{1}{2},\frac{1}{2},\sigma} + (\Delta t_1)^{-1}\|u - u_{h_1,\Delta t_1}\|_{\frac{1}{2},-\frac{1}{2},\sigma,*}\ , \tag{7.36}$$

$$\|u - u_{h_1,\Delta t_1}\|_{-\frac{1}{2},-\frac{1}{2},\sigma,*} \lesssim_\sigma (1+\tfrac{1}{\Delta t_1}) \inf_{v_{h_1,\Delta t_1}} \|u - v_{h_1,\Delta t_1}\|_{\frac{1}{2},-\frac{1}{2},\sigma,*} + \inf_{\tilde{\lambda}_{h_2,\Delta t_2}} \|\lambda - \tilde{\lambda}_{h_2,\Delta t_2}\|_{\frac{1}{2},\frac{1}{2},\sigma}. \tag{7.37}$$

Proof. In order to prove the a priori error estimate for the Lagrange multiplier (7.36), we take advantage of (7.30) and (7.32) to observe

$$\begin{aligned}&\langle \lambda_{h_2,\Delta t_2} - \tilde{\lambda}_{h_2,\Delta t_2}, v_{h_1,\Delta t_1}\rangle_{G\times\mathbb{R}^+,\sigma}\\ &= \langle V u_{h_1,\Delta t_1}, v_{h_1,\Delta t_1}\rangle_{G\times\mathbb{R}^+,\sigma} - \langle g, v_{h_1,\Delta t_1}\rangle_\sigma - \langle \tilde{\lambda}_{h_2,\Delta t_2}, v_{h_1,\Delta t_1}\rangle_{G\times\mathbb{R}^+,\sigma}\\ &= \langle V u_{h_1,\Delta t_1}, v_{h_1,\Delta t_1}\rangle_{G\times\mathbb{R}^+,\sigma} - \langle V u, v_{h_1,\Delta t_1}\rangle_{G\times\mathbb{R}^+,\sigma} + \langle \lambda, v_{h_1,\Delta t_1}\rangle_{G\times\mathbb{R}^+,\sigma} - \langle \tilde{\lambda}_{h_2,\Delta t_2}, v_{h_1,\Delta t_1}\rangle_{G\times\mathbb{R}^+,\sigma}\\ &= \langle V(u_{h_1,\Delta t_1} - u), v_{h_1,\Delta t_1}\rangle_{G\times\mathbb{R}^+,\sigma} + \langle \lambda - \tilde{\lambda}_{h_2,\Delta t_2}, v_{h_1,\Delta t_1}\rangle_{G\times\mathbb{R}^+,\sigma},\end{aligned} \tag{7.38}$$

Then using (7.33) in Theorem 7.13 and (7.38), we obtain:

$$\begin{aligned}\alpha\|\lambda_{h_2,\Delta t_2} - \tilde{\lambda}_{h_2,\Delta t_2}\|_{\frac{1}{2},\frac{1}{2},\sigma} &\leq \sup_{v_{h_1,\Delta t_1}} \frac{\langle \lambda_{h_2,\Delta t_2} - \tilde{\lambda}_{h_2,\Delta t_2}, v_{h_1,\Delta t_1}\rangle_{G\times\mathbb{R}^+,\sigma}}{\|v_{h_1,\Delta t_1}\|_{-\frac{1}{2},-\frac{1}{2},\sigma,*}}\\ &= \sup_{v_{h_1,\Delta t_1}} \frac{\langle V(u_{h_1,\Delta t_1} - u), v_{h_1,\Delta t_1}\rangle_{G\times\mathbb{R}^+,\sigma} + \langle \lambda - \tilde{\lambda}_{h_2,\Delta t_2}, v_{h_1,\Delta t_1}\rangle_{G\times\mathbb{R}^+,\sigma}}{\|v_{h_1,\Delta t_1}\|_{-\frac{1}{2},-\frac{1}{2},\sigma,*}}\ .\end{aligned}$$

From duality, the mapping properties of V and an inverse estimate in time for $v_{h_1,\Delta t_1} \in V^{1,1}_{h_1,\Delta t_1}$, see [11, Lemma 2 and the proof of the following corollary]

$$\|v_{h_1,\Delta t_1}\|_{\frac{1}{2},-\frac{1}{2},\sigma,*} \lesssim \frac{1}{(\Delta t_1)}\|v_{h_1,\Delta t_1}\|_{-\frac{1}{2},-\frac{1}{2},\sigma,*}\ ,$$

we have for the first term

$$|\langle V(u_{h_1,\Delta t_1}-u), v_{h_1,\Delta t_1}\rangle_{G\times\mathbb{R}^+,\sigma}| \lesssim \|V(u_{h_1,\Delta t_1}-u)\|_{-\frac{1}{2},\frac{1}{2},\sigma}\|v_{h_1,\Delta t_1}\|_{\frac{1}{2},-\frac{1}{2},\sigma,*} \\ \lesssim \|u_{h_1,\Delta t_1}-u\|_{\frac{1}{2},-\frac{1}{2},\sigma,*}(\Delta t_1)^{-1}\|v_{h_1,\Delta t_1}\|_{-\frac{1}{2},-\frac{1}{2},\sigma,*} \ .$$

Estimating the second term with the duality:

$$|\langle \lambda-\tilde\lambda_{h_2,\Delta t_2}, v_{h_1,\Delta t_1}\rangle_{G\times\mathbb{R}^+,\sigma}| \le \|\lambda-\tilde\lambda_{h_2,\Delta t_2}\|_{\frac{1}{2},\frac{1}{2},\sigma}\|v_{h_1,\Delta t_1}\|_{-\frac{1}{2},-\frac{1}{2},\sigma,*} \ .$$

With the triangle inequality, we get

$$\|\lambda-\lambda_{h_2,\Delta t_2}\|_{\frac{1}{2},\frac{1}{2},\sigma} \le \|\lambda-\tilde\lambda_{h_2,\Delta t_2}\|_{\frac{1}{2},\frac{1}{2},\sigma} + \|\tilde\lambda_{h_2,\Delta t_2}-\lambda_{h_2,\Delta t_2}\|_{\frac{1}{2},\frac{1}{2},\sigma} \\ \lesssim \|\lambda-\tilde\lambda_{h_2,\Delta t_2}\|_{\frac{1}{2},\frac{1}{2},\sigma} + (\Delta t_1)^{-1}\|u_{h_1,\Delta t_1}-u\|_{\frac{1}{2},-\frac{1}{2},\sigma,*} \ .$$

Therefore taking the infimum over $\tilde\lambda_{h_2,\Delta t_2}$ yields the a priori error estimate (7.36).

$$\|\lambda-\lambda_{h_2,\Delta t_2}\|_{0,-\frac{1}{2},\sigma} \lesssim \inf_{\tilde\lambda_{h_2,\Delta t_2}} \|\lambda-\tilde\lambda_{h_2,\Delta t_2}\|_{0,-\frac{1}{2},\sigma} + (\Delta t_1)^{-\frac{1}{2}}\|u_{h_1,\Delta t_1}-u\|_{-\frac{1}{2},\frac{1}{2},\sigma,*} \ . \quad (7.39)$$

In order to prove (7.37) we note the Galerkin orthogonality

$$\langle V(u-u_{h_1,\Delta t_1}), v_{h_1,\Delta t_1}\rangle_{G\times\mathbb{R}^+,\sigma} = \langle \lambda-\lambda_{h_2,\Delta t_2}, v_{h_1,\Delta t_1}\rangle_{G\times\mathbb{R}^+,\sigma} \ .$$

Using the coercivity of V, we get for all $v_{h_1,\Delta t_1}$ and $\tilde\lambda_{h_2,\Delta t_2}$

$$\|u_{h_1,\Delta t_1}-v_{h_1,\Delta t_1}\|^2_{-\frac{1}{2},\frac{1}{2},\sigma,*} \lesssim_\sigma V(u_{h_1,\Delta t_1}-v_{h_1,\Delta t_1}), u_{h_1,\Delta t_1}-v_{h_1,\Delta t_1}\rangle_{G\times\mathbb{R}^+,\sigma} \\ = \langle V(u-v_{h_1,\Delta t_1}), u_{h_1,\Delta t_1}-v_{h_1,\Delta t_1}\rangle_{G\times\mathbb{R}^+,\sigma} + \langle V(u_{h_1,\Delta t_1}-u), u_{h_1,\Delta t_1}-v_{h_1,\Delta t_1}\rangle_{G\times\mathbb{R}^+,\sigma} \\ = \langle V(u-v_{h_1,\Delta t_1}), u_{h_1,\Delta t_1}-v_{h_1,\Delta t_1}\rangle_{G\times\mathbb{R}^+,\sigma} + \langle \lambda_{h_2,\Delta t_2}-\lambda, u_{h_1,\Delta t_1}-v_{h_1,\Delta t_1}\rangle_{G\times\mathbb{R}^+,\sigma}.$$

The mapping properties of V and the duality, yield

$$\|u_{h_1,\Delta t_1}-v_{h_1,\Delta t_1}\|^2_{-\frac{1}{2},-\frac{1}{2},\sigma,*} \lesssim \|u-v_{h_1,\Delta t_1}\|_{-\frac{1}{2},-\frac{1}{2},\sigma,*}\|u_{h_1,\Delta t_1}-v_{h_1,\Delta t_1}\|_{-\frac{1}{2},-\frac{1}{2},\sigma,*} \\ + \|\lambda-\lambda_{h_2,\Delta_2}\|_{\frac{1}{2},\frac{1}{2},\sigma}\|u_{h_1,\Delta t_1}-v_{h_1,\Delta t_1}\|_{-\frac{1}{2},-\frac{1}{2},\sigma,*}.$$

Dividing by $\|u_{h_1,\Delta t_1}-v_{h_1,\Delta t_1}\|_{-\frac{1}{2},-\frac{1}{2},\sigma,*}$ leads to

$$\|u_{h_1,\Delta t_1}-v_{h_1,\Delta t_1}\|_{-\frac{1}{2},-\frac{1}{2},\sigma,*} \lesssim_\sigma \|u-v_{h_1,\Delta t_1}\|_{-\frac{1}{2},-\frac{1}{2},\sigma,*} + \|\lambda-\lambda_{h_2,\Delta_2}\|_{\frac{1}{2},\frac{1}{2},\sigma}$$

With the triangle inequality, estimating with the stronger norm and (7.36), we get

$$\|u-u_{h_1,\Delta t_1}\|_{-\frac{1}{2},-\frac{1}{2},\sigma,*} \le \|u-v_{h_1,\Delta t_1}\|_{-\frac{1}{2},-\frac{1}{2},\sigma,*} + \|v_{h_1,\Delta t_1}-u_{h_1,\Delta t_1}\|_{-\frac{1}{2},-\frac{1}{2},\sigma,*} \\ \lesssim_\sigma \|u-v_{h_1,\Delta t_1}\|_{-\frac{1}{2},-\frac{1}{2},\sigma,*} + \|\lambda-\lambda_{h_2,\Delta_2}\|_{\frac{1}{2},\frac{1}{2},\sigma} \\ \lesssim \|u-v_{h_1,\Delta t_1}\|_{-\frac{1}{2},-\frac{1}{2},\sigma,*} + \|\lambda-\lambda_{h_2,\Delta t_2}\|_{\frac{1}{2},\frac{1}{2},\sigma,*} + \frac{1}{(\Delta t)}\|u-v_{h_1,\Delta t_1}\|_{\frac{1}{2},-\frac{1}{2},\sigma,*} \\ \lesssim (1+\frac{1}{(\Delta t)})\|u-v_{h_1,\Delta t_1}\|_{\frac{1}{2},-\frac{1}{2},\sigma,*} + \|\lambda-\lambda_{h_2,\Delta t_2}\|_{\frac{1}{2},\frac{1}{2},\sigma,*}.$$

Taking the infimum yields (7.37). □

7.6 Algorithmic considerations and space time Uzawa algorithm

The crack problem requires a consideration of the Poincaré-Steklov operator on the contact region G. We repeat the variational formulation: For given $g \in H_\sigma^{\frac{3}{2}}(\mathbb{R}^+, H^{-\frac{1}{2}}(\Gamma))$, find $\varphi \in H_\sigma^{\frac{1}{2}}(\mathbb{R}^+, \widetilde{H}^{\frac{1}{2}}(\Gamma)), p \in H_\sigma^{\frac{1}{2}}(\mathbb{R}^+, \widetilde{H}^{-\frac{1}{2}}(\Gamma))$ such that

$$\int_0^\infty \langle W\varphi - (K' - \tfrac{1}{2}I)p, \dot{w}\rangle_G \,\mathrm{dt} = \int_0^\infty \langle g, \dot{w}\rangle_G \,\mathrm{dt}\ ,$$

$$\int_0^\infty [\langle Vp, \partial_t\omega\rangle_G - \langle (K - \tfrac{1}{2}I)\varphi, \partial_t\omega\rangle_G] \,\mathrm{dt} = 0,$$

holds for all $w \in H_\sigma^{\frac{1}{2}}(\mathbb{R}^+, \widetilde{H}^{\frac{1}{2}}(\Gamma))$, $\omega \in H_\sigma^{\frac{1}{2}}(\mathbb{R}^+, \widetilde{H}^{-\frac{1}{2}}(\Gamma))$.

We use the Poincaré-Steklov operator discretized in the same way as in Subsection 2.3.5 for $\sigma = 0$. We remember using for the ansatz functions $\varphi_{h,\Delta t}(x,t) = \sum_{m=1}^{N_t}\sum_{i=1}^{N_s}\varphi_i^m\beta_{\Delta t}^m(t)\xi_h^i(x) \in V_{h,\Delta t}^{1,1}$ and $p_{h,\Delta t}(x,t) = \sum_{m=1}^{N_t}\sum_{i=1}^{N_s}p_i^m\beta_{\Delta t}^m(t)\xi_h^i(x) \in V_{h,\Delta t}^{1,1}$ and for the test functions $\dot{w}_{h,\Delta t} = \gamma_{\Delta t}^{n_t}(t)\xi_h^j(x) \in V_{h,\Delta t}^{1,0}$ and $\omega_{h,\Delta t} = \gamma_{\Delta t}^{n_t}(t)\xi_h^j(x) \in V_{h,\Delta t}^{1,0}$ each for $1 \le n_t \le N_t$ and $1 \le j \le N_s$. This discretization leads to the marching-on in time scheme, where we solve for each $n_t = 1, \ldots, N_t$ the system:

$$\mathcal{M}^0\begin{pmatrix}\varphi^{n_t}\\ p^{n_t}\end{pmatrix} = \begin{pmatrix}G^{n_t}\\ 0\end{pmatrix} - \sum_{m=1}^{n_t-1}\mathcal{M}^{n_t-m}\begin{pmatrix}\varphi^m\\ p^m\end{pmatrix}\ , \tag{7.40}$$

where $g_{h,\Delta t} = \sum_m g^m\beta_{\Delta t}^m \approx g$ with $g^m = g(x,t_m)$, $\frac{(\Delta t)}{2}\int_\Gamma (g^{n_t} + g^{n_t-1})\xi_h^j(x)ds_x =: G^{n_t}$,

$$\mathcal{M}^0 = \begin{pmatrix}W^0 & -K^{T0} + \frac{1}{2}\frac{(\Delta t)}{2}I\\ -K^0 - \frac{1}{2}I & V^0\end{pmatrix}, \mathcal{M}^1 = \begin{pmatrix}W^1 & -(K^T)^1 + \frac{1}{2}\frac{\Delta t}{2}I\\ -K^1 + \frac{1}{2}I & V^1\end{pmatrix}$$

$$\text{and } \mathcal{M}^{n_t-m} = \begin{pmatrix}W^{n_t-m} & -(K^T)^{n_t-m}\\ -K^{n_t-m} & V^{n_t-m}\end{pmatrix}.$$

We solve the discrete mixed formulation (7.16) with a space-time Uzawa algorithm.

choose $\rho > 0$:
$k = 0 : y^{(0)} = \vec{0}$
while stopping criterion not satisfied **do**
  solve: $\mathcal{S}z^{(k)} = g + y^{(k)}$
  compute: $y^{(k+1)} = \mathrm{Pr}_K(y^{(k)} - \rho z^{(k)})$, where $(\mathrm{Pr}_K y)_i = \max\{y_i, 0\}$
  $k \leftarrow k + 1$
end while

Algorithm 5: Space-time Uzawa algorithm

Lemma 7.1 ([47], Lemma 22)**.** *The space-time Uzawa algorithm converges, provided that $0 < \rho < 2C_\sigma$. Here C_σ is the coercivity constant in Theorem 7.1.*

For the computation of the mixed variational formulation (7.16) an Uzawa algorithm in space-time is used with the ansatz functions $z^{(k)}(x,t) = \sum_{m=1}^{N_t}\sum_{i=1}^{N_s}(z_i^m)^k\beta_{\Delta t}^m(t)\xi_h^i(x) \in V_{h,\Delta t}^{1,1}$ and $d^{(k)}(x,t) = \sum_{m=1}^{N_t}\sum_{i=1}^{N_s} d_i^m\beta_{\Delta t}^m(t)\xi_h^i(x) \in V_{h,\Delta t}^{1,1}$ in order to obtain a marching-on-in time scheme as in (7.40). With a given stopping criterion and choosing the Lagrange multiplier as piecewise linear functions in space and time, i.e. $\lambda_{h,\Delta t}^{(k)} := y^{(k)} = \sum_{m=1}^{N_t}\sum_{i=1}^{N_s}(y_i^m)^k\beta_{\Delta t}^m(t)\xi_h^i(x)$, we get to solve with the corresponding test function $\gamma_{\Delta t}^{n_t}(t)\xi_h^j(x) \in V_{h,\Delta t}^{1,0}$ for $1 \le n_t \le N_t$ and $1 \le j \le N_s$:

$$\langle \mathcal{S}z^{(k)}, \gamma_{\Delta t}^{n_t}\xi_h^j\rangle_{\Gamma\times(0,\infty)} = \langle \sum_{m,i}(y_i^m)^{k-1}\beta_{\Delta t}^m\xi_h^i, \gamma_{\Delta t}^n\xi_h^j\rangle_{\Gamma\times(0,\infty)} + \langle \sum_m g^m\beta_{\Delta t}^m, \gamma_{\Delta t}^n\xi_h^j\rangle_{\Gamma\times(0,\infty)}. \tag{7.41}$$

Therefore we solve for every $n_t = 1,\dots,N_t$ with $(z^m)^k = ((z_1^m)^k,\dots,(z_{N_s}^m)^k)^T$, $(y^m)^k = ((y_1^m)^k,\dots,(y_{N_s}^m)^k)^T$ and $(d^m)^k = ((d_1^m)^k,\dots,(d_{N_s}^m)^k)^T$:

$$\sum_{m=1}^{n_t}\mathcal{M}^{n_t-m}\begin{pmatrix}(z^m)^k\\(d^m)^k\end{pmatrix} = \begin{pmatrix}\frac{\Delta t}{2}I((y^{n_t-1})^{k-1} + (y^{n_t})^{k-1})\\0\end{pmatrix} + \begin{pmatrix}G^n\\0\end{pmatrix}. \tag{7.42}$$

The mixed formulation for the punch problem (7.30) is discretized with piecewise constant ansatz functions in space and time $z^{(k)} = \sum_{m=1}^{N_t}\sum_{i=1}^{N_s}(z_i^m)^k\gamma_{\Delta t}^m(t)\psi_h^i(x)$, for the Lagrange multiplier $\lambda_{h,\Delta t} = y^{(k)} = \sum_{m=1}^{N_t}\sum_{i=1}^{N_s}(y_i^m)^k\beta_{\Delta t}^m\psi_h^i$ and for $1 \le n_t \le N_t$ and $1 \le j \le N_s$, we solve

$$\langle Vz^{(k)}, \gamma_{\Delta t}^{n_t}\psi_h^j\rangle_{\Gamma\times(0,\infty)} = \langle \sum_{m,i}(y_i^m)^{k-1}\beta_{\Delta t}^m\xi_h^i, \gamma_{\Delta t}^{n_t}\xi_h^j\rangle_{\Gamma\times(0,\infty)} + \langle \sum_m g^m\beta_{\Delta t}^m, \gamma_{\Delta t}^{n_t}\xi_h^j\rangle_{\Gamma\times(0,\infty)}. \tag{7.43}$$

Therefore analogously as above we solve for $n_t = 1,\dots,N_t$

$$\sum_{m=1}^{n_t}V^{n_t-m}(z^m)^k = \frac{(\Delta t)}{2}I((y^{n_t-1})^{k-1} + (y^{n_t})^k) + G^n\ . \tag{7.44}$$

For the Lagrange multiplier, $\lambda_{h,\Delta t} = y^{(k)} = \sum_{m,i}(y_i^m)^k\gamma_{\Delta t}^m(t)\psi_h^i(x)$, piecewise constant in space and time, the first term on the right hand side of (7.42) becomes $\Delta t\begin{pmatrix}I(y^{n_t})^{k-1}\\0\end{pmatrix}$.

The computation of the space time matrices $\mathcal{M}^k$, resp. V^k is the most time consuming contribution of this algorithm. In terms of memory allocation we also need every nonzero matrix $\mathcal{M}^k$, resp. V^k. Here since we use a MOT-scheme, experience tells us that it is fine to solve the system with GMRES, see also Example 3.3.

7.7 Numerical experiments

We begin with the numerical experiments for the contact problem (7.7) discretized as in Section 7.6.

7.7.1 Numerical experiments for the crack problem

Example 7.1. *We solve the nonlinear contact problem* (7.7) *by solving* (7.42) *on a uniform square* $\Gamma = [-2,2] \times \{0\}$ *with contact area* $G = [-1,1]^2 \times \{0\}$ *for times up to* $T = 6$ *with the CFL ratio* $\frac{\Delta t}{h} \approx 1.06$. *The right hand side is prescribed by:*

$$g(x,t) = e^{-2t} t \cos(2\pi x_1) \cos(2\pi x_2) \chi_{[-0.25,0.25]}(x_1) \chi_{[-0.25,0.25]}(x_2) \ .$$

The reference solution is given by 12800 triangles, where we use $\Delta t = 0.075$. *For the Uzawa algorithm we set* $\rho = 20$. *We stop the Uzawa iterations if the relative difference is less than* 10^{-11}.

Figure 7.1 illustrates the solution $u_{h,\Delta t}$ (left column) and the corresponding Lagrange multiplier $\lambda_{h,\Delta t}$ (right column) for the reference solution at times $0.075, 2.55, 4.275, 5.025$. The solution exhibits a bump in the center of the contact area, where the Lagrange multiplier vanishes (see $t = 2.55$). As time passes the solution in the center becomes smaller, but the Lagrange multiplier gets greater than zero on the whole contact area. It shows the contact forces here for times 4.275 and 5.025.

In Figure 7.2 the relative error in $L^2((0,T) \times G)$ of the solutions for coarser meshes compared to the reference solution is displayed. We get a convergence rate of approximately $\alpha \approx 0.8$ in terms of degrees of freedom.

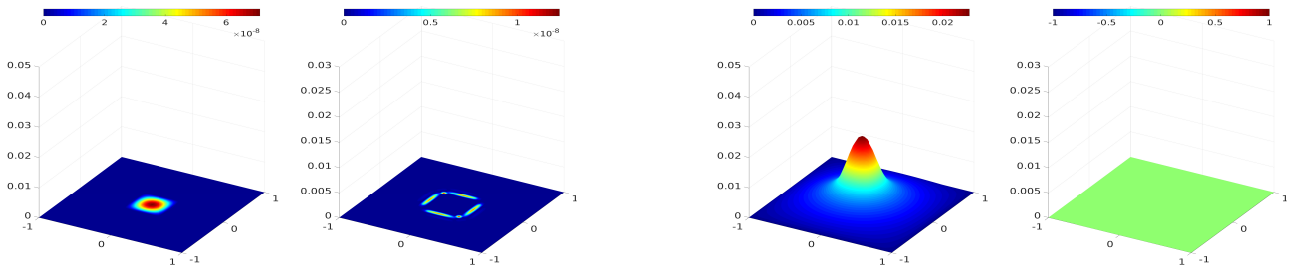

(a) t=0.075

(b) t=2.55

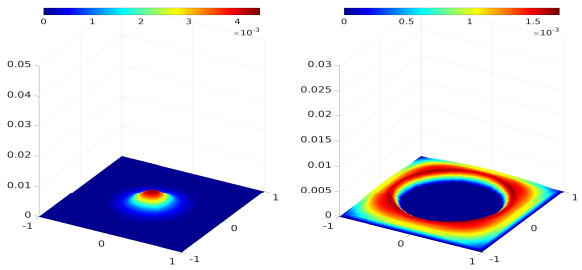

(c) t=4.275

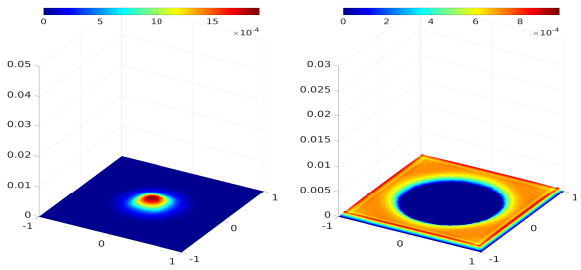

(d) t=5.025

Figure 7.1: Evolution of u and λ in $G = [-1,1]^2 \times \{0\}$ for the contact problem, Example 7.1. Figure 4 in [47]

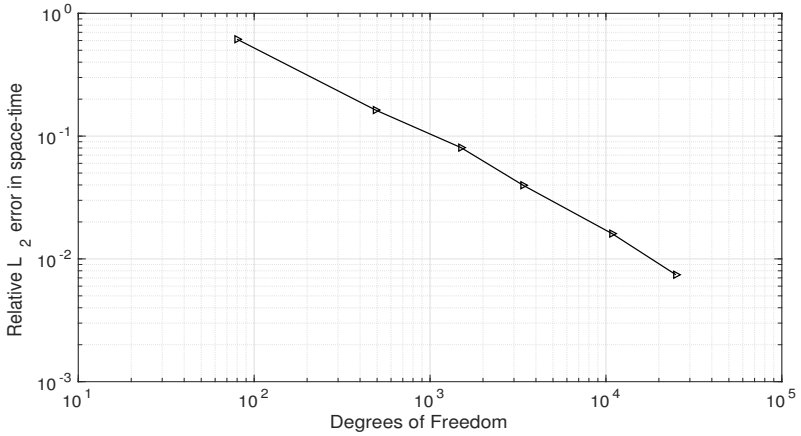

Figure 7.2: Relative $L^2([0,T]\times G)$-error vs. degrees of freedom of the solutions to the contact problem for fixed $\frac{\Delta t}{h}$, Example 7.1. Figure 5 in [47]

Next we consider a cube, where we have contact on three faces. We imagine a rigid cube, where the 3 other faces are fixed.

Example 7.2. *We solve the nonlinear contact problem* (7.7) *by solving* (7.42) *on the surface a uniform cube* $[-2,2]^3$ *with contact area* G *as the top, front and right faces for times up to* $T = 6$*, with the CFL ratio* $\frac{\Delta t}{h} \approx 0.53$*. The right hand side on each contact face is prescribed as:*

$$g(x,t) = \begin{cases} e^{-2t}t^4\cos(2\pi x_1)\cos(2\pi x_2)\chi_{[-0.25,0.25]}(x_1)\chi_{[-0.25,0.25]}(x_2) & \text{on the top face,} \\ e^{-2t}t^4\cos(2\pi x_2)\cos(2\pi x_3)\chi_{[-0.25,0.25]}(x_2)\chi_{[-0.25,0.25]}(x_3) & \text{on the front face,} \\ e^{-2t}t^4\cos(2\pi x_1)\cos(2\pi x_3)\chi_{[-0.25,0.25]}(x_1)\chi_{[-0.25,0.25]}(x_3) & \text{on the right face.} \end{cases}$$

We use a benchmark obtained by extrapolation. For the Uzawa algorithm the same ρ *and the same stopping criterion as in Example 7.1 are used.*

Figure 7.3 illustrates the solution $u_{h,\Delta t}$ (left column) and the corresponding Lagrange multiplier $\lambda_{h,\Delta t}$ (right column) at the top face of the cube consisting 10800 triangles on the boundary at times $0.1, 3, 5, 6$. We see the solution $u_{h,\Delta t}$ spreading to the corner $(2,-2)$ at time $t = 5$. As time passes the Lagrange multiplier gets nonzero entries near the corner $(-2,2)$ at time $t = 6$. It indicates to a strong contact near that corner.

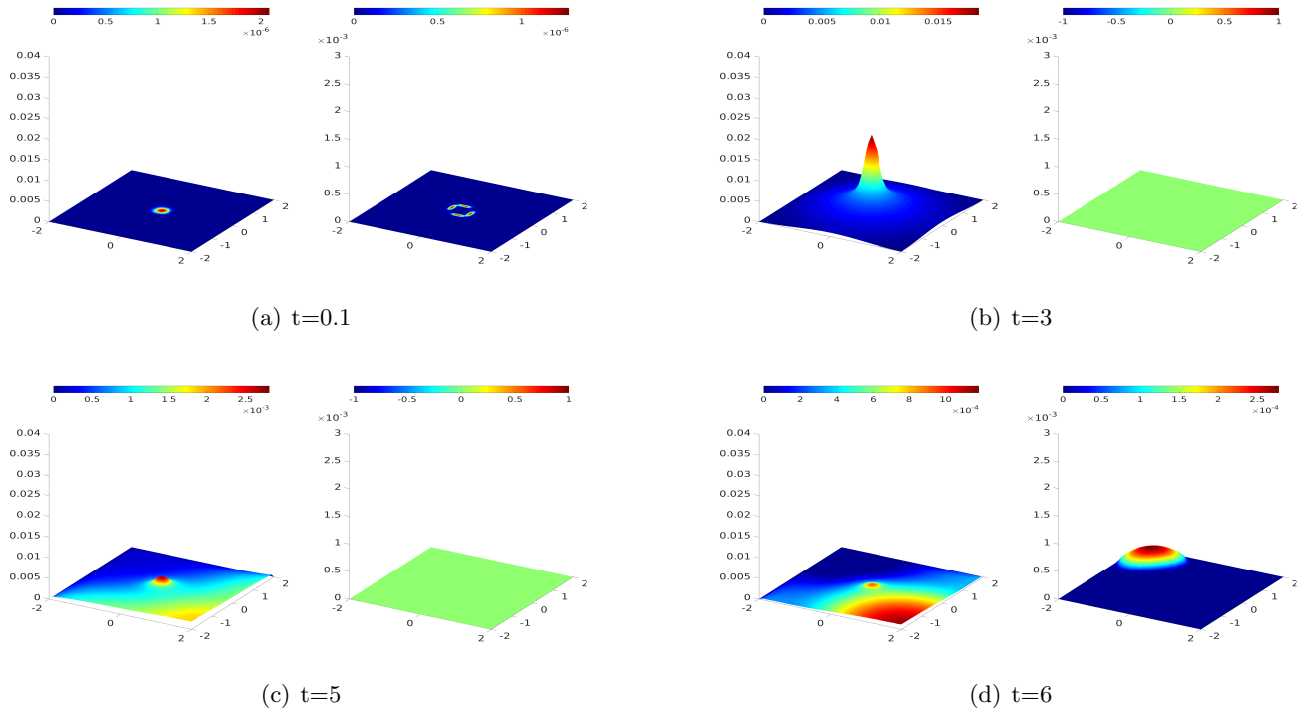

(a) t=0.1 (b) t=3

(c) t=5 (d) t=6

Figure 7.3: Evolution of u and λ in $[-2,2]^2 \times \{2\}$ for the contact problem on $[-2,2]^3$, Example 7.2. Figure 7 in [47]

In Figure 7.4 the relative error in $L^2((0,T)\times G)$ of the solution compared to the benchmark is displayed. We get a convergence rate of $\alpha \approx 0.6$. The considered meshes here are not necessarily refinements of each other, which could explain the kink at the third point.

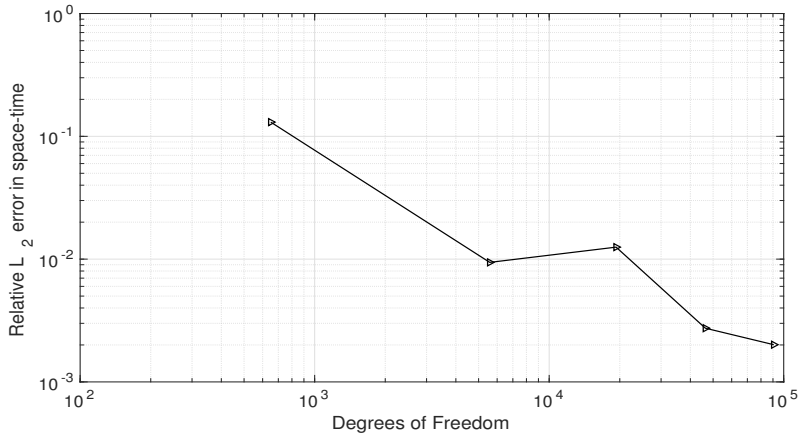

Figure 7.4: Relative $L^2([0,T]\times G)$-error vs. degrees of freedom for the contact problem for fixed $\frac{\Delta t}{h} \approx 0.53$, Example 7.2. Figure 8 in [47]

Next we continue with the punch problem (7.23) discretized as in Section 7.6.

7.7.2 Numerical experiments for the punch problem

Example 7.3. *We solve the punch problem* (7.23) *by solving* (7.44) *on a uniform square screen* $\Gamma = [-2,2]^2 \times \{0\}$ *with the contact area* $G = [-1,2,1.2]^2 \times \{0\}$ *for times up to* $T = 6$ *with the CFL ratio* $\frac{\Delta t}{h} \approx 1.06$. *The right hand side is prescribed by*

$$g(x,t) = e^{-2t} t \cos(2\pi x_1)\cos(2\pi x_2)\chi_{[-0.25,0.25]}(x_1)\chi_{[-0.25,0.25]}(x_2) \ .$$

The reference solution is given by 12800 *triangles, where we use* $\Delta t = 0.075$. *For the Uzawa algorithm, we set* $\rho = 0.01$. *we stop the Uzawa iterations if the relative difference is less than* 10^{-12}, *or if the* L^∞*-norm is less than* 10^{-10}.

Figure 7.5 illustrates the solution $u_{h,\Delta t}$ (left column) and the corresponding Lagrange multiplier $\lambda_{h,\Delta t}$ (right column) for the reference solution at times $0.075, 1.05, 3, 6$. For the solution, we observe a bump in the center of the contact area. Since the Lagrange multiplier is not zero at these times, we have contact for the displayed times.

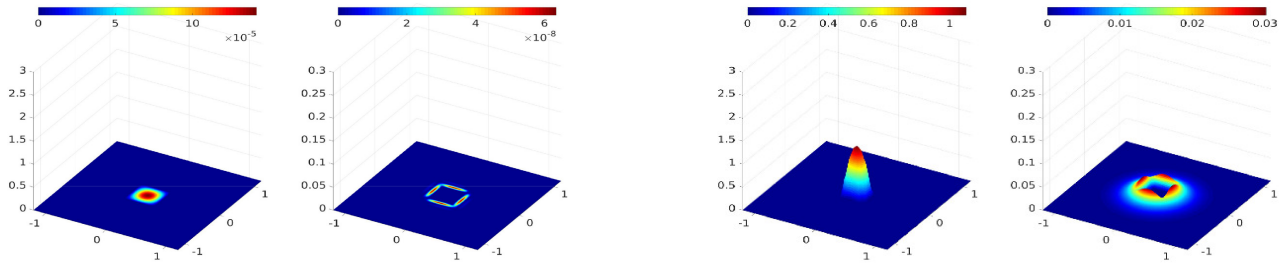

(a) t=0.075 (b) t=1.05

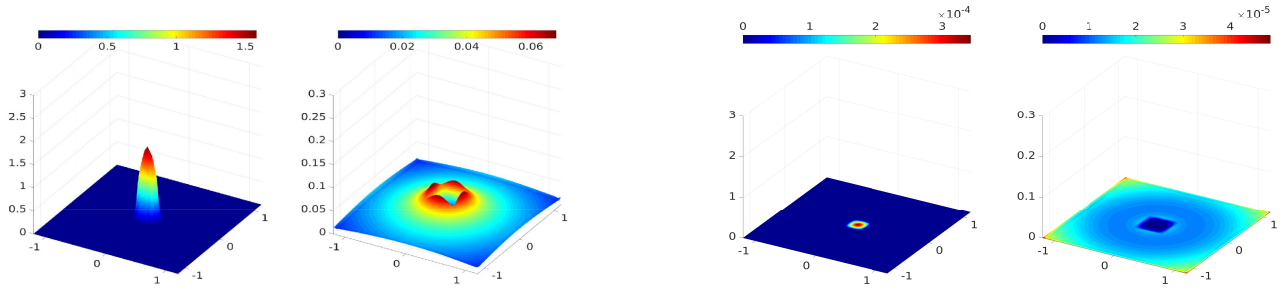

(c) t=3 (d) t=6

Figure 7.5: Evolution of u and λ for the punch problem on $G = [-1.2,1.2]^2 \times \{0\}$, Example (7.3). Figure 9 in [47]

Due to the low spatial regularity of the solution, we consider the error in the discretized energy as in (2.56). In Figure 7.6 the relative error in energy (2.56) of the solution for coarser meshes compared to the reference solution is displayed. We get a convergence rate of approximately 0.76 in terms of degrees of freedom.

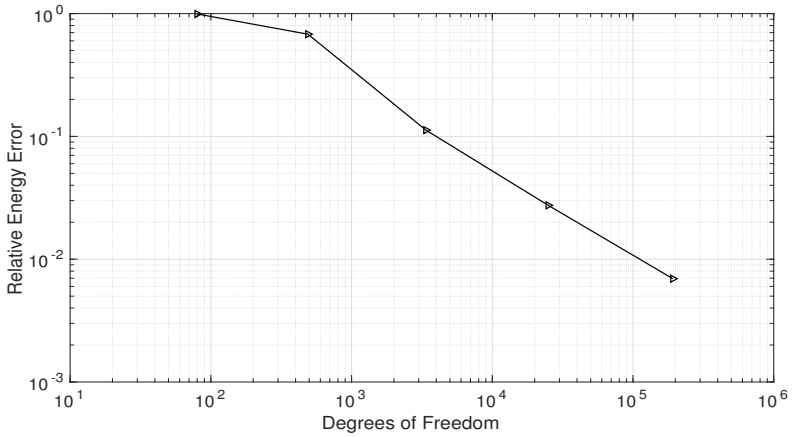

Figure 7.6: Relative energy error for the punch problem for fixed $\frac{\Delta t}{h}$, Example 7.3. Figure 10 in [47]

Next we consider a cube, where we have contact on the entire surface of the cube.

Example 7.4. *We solve the punch problem* (7.23) *by solving* (7.44) *on the surface of an uniform cube* $[-2,2]^3$*, where also contact takes place for times up to* $T = 3.6$*. The right hand side is prescribed as in Example 7.2. We compare the numerical results with a benchmark of the energy obtained by extrapolation. For the Uzawa algorithm, we use the same* ρ *and the same stopping criterion as in Example 7.3 is used.*

Figure 7.7 illustrates the solution $u_{h,\Delta t}$ (left column) and the corresponding Lagrange multiplier $\lambda_{h,\Delta t}$ (right column) on the top of the cube with 19200 triangles and $\Delta t = 0.01$ at times $0.1, 2, 3, 3.6$. The CFL ratio is $\frac{\Delta t}{h} \approx 0.7$. We observe contact at all these times, where from $t = 2$ we see the contact forces focusing on the center, where in later times it scatters. The solution behaves similar to Figure 7.5.

In Figure 7.8 the relative error in the discretized energy of the solution compared to the benchmark is displayed. The considered meshes correspond to $\frac{\Delta t}{\Delta x} \approx 0.53$. The convergence rate is roughly approximated with 0.9 from the last 4 points in terms of degrees of freedom.They are not necessarily refinements of each other. That could explain the kink at the third point.

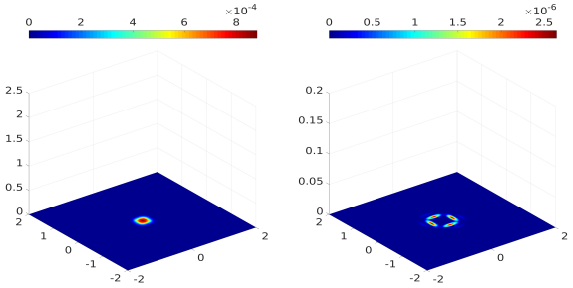

(a) t=0.1

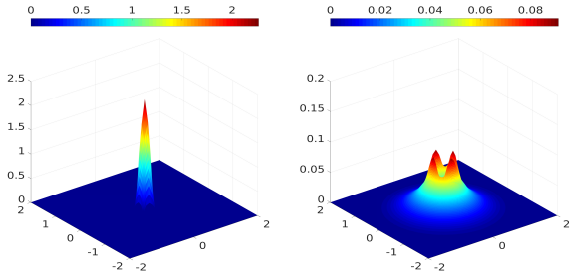

(b) t=2

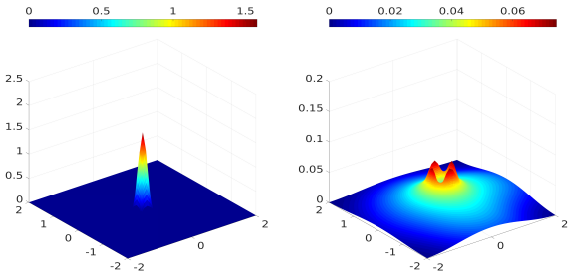

(c) t=3

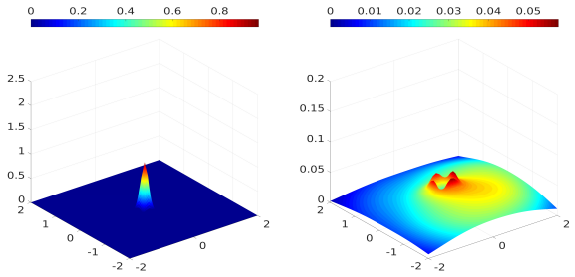

(d) t=3.6

Figure 7.7: Evolution of u and λ in $[-2,2]^2 \times \{2\}$ for the punch problem on $[-2,2]^3$, Example 7.4. Figure 11 in [47]

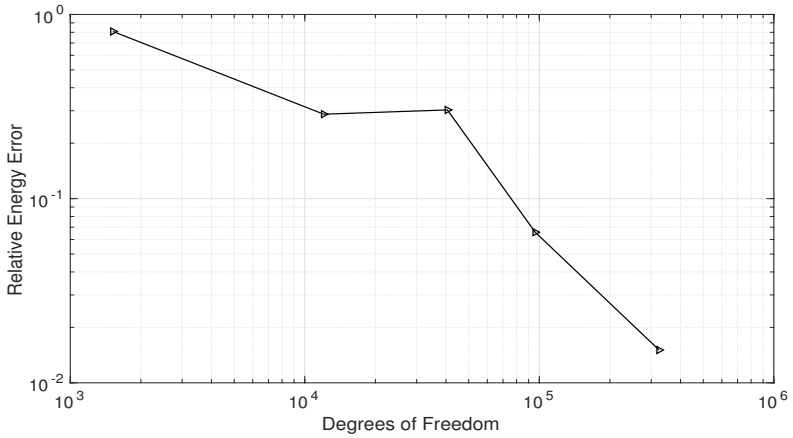

Figure 7.8: Relative error of the energy for the punch problem for fixed $\frac{\Delta t}{h}$, Example 7.4. Figure 12 in [47]

8 Applications to sound emission of tyres

8.1 Introduction

Traffic noise is an omnipresent problem causing harm to people and environment. The dominant factor, where highway traffic noise emerges, comes from the interaction of tyres and the pavement (street) [19]. Hence there is research interest on how to reduce the traffic noise emitting from tyres, see [100]. In our case we are interested in the treatment of sound radiation of tyres. In detail we consider a model problem based on the wave equation on an exterior domain, and solve it with the boundary element method for given incident waves.

Let $\Omega \subset \mathbb{R}^3_+$ be a bounded, orientable Lipschitz domain on the positive half-space with a connected Lipschitz exterior $\Omega^c = \mathbb{R}^3_+ \backslash \overline{\Omega}$. We denote $\Gamma = \partial\Omega$ and $\Gamma_\infty = \mathbb{R}^2 \times \{0\}$. Hence we consider the following problem for a given g:

$$\begin{array}{lll} \frac{\partial^2 u}{\partial t^2}(x,t) - \Delta u(x,t) & = 0 & \text{in } \Omega^c \times \mathbb{R}^+ \ , \\ u(x,0) = \dot{u}(x,0) & = 0 & \text{in } \Omega^c \ , \\ \frac{\partial u}{\partial n}|_\Gamma(x,t) - \alpha(x)\frac{\partial u}{\partial t}|_\Gamma(x,t) & = g(x,t) & \text{on } \Gamma \times \mathbb{R}^+ \ , \\ \frac{\partial u}{\partial n}|_{\Gamma_\infty}(x,t) - \alpha_\infty \frac{\partial u}{\partial t}|_{\Gamma_\infty}(x,t) & = 0 & \text{on } \Gamma_\infty \times \mathbb{R}^+ \ , \end{array} \tag{8.1}$$

where $n = n_x$ denotes the unit normal vector always pointing towards Ω^c with $\frac{\partial u}{\partial n}|_\Gamma(x,t) = \lim\limits_{x' \in \Omega^c \to x \in \Gamma} \nabla u(x',t) \cdot n_x$, $u|_\Gamma(x,t) = \lim\limits_{x' \in \Omega^c \to x \in \Gamma} u(x',t)$ and $\frac{\partial u}{\partial n}|_{\Gamma_\infty}(x,t) = \lim\limits_{x' \in \Omega^c \to x \in \Gamma_\infty} \nabla u(x',t) \cdot n_x$, $u|_{\Gamma_\infty}(x,t) = \lim\limits_{x' \in \Omega^c \to x \in \Gamma_\infty} u(x',t)$, $\alpha \in L^\infty(\Gamma)$ and , $\alpha_\infty \in \mathbb{C}$. Since we have conditions on the half-space, we get a slightly modified fundamental solution taking the reflections into account, see [83]. An a priori error analysis of (8.1) is done in [48]. Numerical experiments are done in [15] on passenger car tyres as well as truck tyres for $\alpha = 0$ and $\alpha_\infty = 0$, which leads to Neumann boundary conditions on Γ and on the street Γ_∞.

In this chapter we consider Neumann boundary conditions on Γ (i.e. set $\alpha = 0$) as well, but with $\alpha_\infty \geq 0$, which resembles an absorbing street. We derive a variational formulation and present numerical results based on the joint works with H. Gimperlein and E. P. Stephan in [51] and H. Gimperlein, F. Meyer, D. Stark and E. P. Stephan in [46] on a graded tyre.

8.2 Boundary integral formulation

In order to use the boundary element method on problem (8.1), we require a fundamental solution . While for $\mathbb{R}^3$, G is known as:

$$G(x,y,t) = \frac{\delta(t-r(y_3)}{4\pi r(y_3)} \ ,$$

in the half-space case $\mathbb{R}^3_+$, it is given in [83]:

$$G(x,y,t) = \frac{\delta(t-r(y_3)}{4\pi r(y_3)} + \frac{\delta(t-r(-y_3)}{4\pi r(-y_3)} + \Sigma$$

with

$$\Sigma = \frac{\alpha_\infty}{2\pi}\frac{\partial}{\partial t}\frac{H(t-r(-y_3))}{\sqrt{(t+\alpha_\infty(x_3+y_3))^2+(\alpha_\infty^2-1)R^2}}$$

for H denoting the Heaviside function, $r(\pm y_3)^2 = R^2 + (x_3 \mp y_3)^2$ and $R^2 = (x_1-y_1)^2 + (x_2-y_2^2)^2$ with $x = (x_1,x_2,x_3)$ and $y = (y_1,y_2,y_3)$. The additional two terms describe the reflection of the plane $\mathbb{R}^2 \times \{0\}$.

With a retarded single layer potential ansatz, we write the solution u as:

$$u(x,t) = \int_{\Gamma\times\mathbb{R}^+} G(x,y,t-\tau)\varphi(y,\tau)d\tau ds_y =: S\varphi(x,t) \ .$$

We consider Neumann boundary conditions on Γ, using the jump relation, we get the retarded integral equation

$$(-\frac{1}{2}I + K')\varphi = g \ ,$$

with the retarded adjoint double layer potential:

$$\begin{aligned} K'\varphi &= \int_{\Gamma\times\mathbb{R}^+} \frac{\partial G}{\partial n_x}(x,y,t-\tau)\varphi(y,\tau)d\tau ds_y \\ &= \int_{\Gamma\times\mathbb{R}^+} \frac{\partial}{\partial n_x}(\frac{\delta(t-|x-y|)}{4\pi|x-y|})\varphi(y,\tau)ds_y + \int_{\Gamma\times\mathbb{R}^+} \frac{\partial}{\partial n_x}(\frac{\delta(t-|x-y'|)}{4\pi|x-y'|})\varphi(y,\tau)ds_y \\ &+ \int_{\Gamma\times\mathbb{R}^+} \frac{\partial\Sigma}{\partial n_x}(x,y,t-\tau)\varphi(y,\tau)d\tau ds_y =: K_1\varphi(x,t) + K_2\varphi(x,t) + K_3\varphi(x,t) \end{aligned}$$

with $y' = (y_1,y_2,-y_3)$. While K_1 and K_2 are similar to the case in $\mathbb{R}^3$:

$$\begin{aligned} K_1\varphi(x,t) &= \frac{1}{4\pi}\int_\Gamma \frac{n_x^T\cdot(y-x)}{|x-y|}(\frac{\varphi(t-|x-y|,y)}{|x-y|^2} + \frac{\dot\varphi(y,t-|x-y|)}{|x-y|})ds_y \ , \\ K_2\varphi(x,t) &= \frac{1}{4\pi}\int_\Gamma \frac{n_x^T\cdot(y'-x)}{|x-y|}(\frac{\varphi(y,t-|x-y'|)}{|x-y'|^2} + \frac{\dot\varphi(y,t-|x-y'|)}{|x-y'|})ds_y \ , \end{aligned}$$

we get for K_3 with integration by parts in time:

$$K_3\varphi(x,t) = -\frac{\alpha_\infty}{2\pi}\int_{\Gamma\times\mathbb{R}^+}\frac{\partial}{\partial n_x}[\frac{H(t-\tau-|x-y'|)}{A(t,\tau)}]\dot\varphi(y,\tau)ds_y d\tau \ ,$$

where $A(t,\tau) := \sqrt{(t-\tau+\alpha_\infty\nu_3)^2 + (\alpha_\infty^2-1)R^2}$ with $\nu_3 = x_3 + y_3$. In a first approximation, we neglect the derivative in space of A, as the corresponding delayed reflection waves are much smaller than the main term coming from the derivative of the Heaviside function. This approximation simplifies the implementation significantly, as it neglects contributions away from the lightcone.

$$\frac{\partial}{\partial n_x}\Big[\frac{H(t-\tau-|x-y'|)}{A(t,\tau)}\Big] = -\frac{n_x^T\cdot(x-y')\delta(t-\tau-|x-y'|)}{|x-y'|A(t,\tau)} + \dots$$

Altogether, we use:

$$K_3\varphi(x,t) = \frac{\alpha_\infty}{2\pi}\int_\Gamma \frac{n_x^T\cdot(x-y')}{|x-y'|A(t,t-|x-y'|)}\dot\varphi(t-|x-y'|,y)ds_y \ .$$

Now the variational formulation reads ([51]): Find $\varphi \in H_\sigma^{1/2}(\mathbb{R}^+, \widetilde{H}^{-1/2}(\Gamma))$ such that for all $\psi \in H_\sigma^{1/2}(\mathbb{R}^+, \widetilde{H}^{1/2}(\Gamma))$ there holds, with $g \in H_\sigma^{5/2}(\mathbb{R}^+, H^{-1/2}(\Gamma))$:

$$\langle(-\frac{1}{2}I + K')\varphi,\psi\rangle_{\Gamma\times\mathbb{R}^+,\sigma} = \langle g,\psi\rangle_{\Gamma\times\mathbb{R}^+,\sigma} \ .$$

Next we use the same discretization spaces as in Section 2.3 and choose piecewise constant ansatz and test functions in space and time, i.e. $\gamma_{\Delta t}^n(t)\psi_h^i(x) \in V_{h,\Delta t}^{0,0}$ for $n = 1,\dots,N_t$ and $i = 1,\dots,N_s$. For a detailed discussion of the discretization of K_2, where reflected lightcones E'_{n-m}, E'_{n-m-1} for y' appear, we refer to [15]. The discretization of K_1 is the same as in Subsection 2.3.2. The discretization of K_3 leads to the lightcones E'_{n-m} and E'_{n-m-1} as well, but with a different kernel, containing α_∞. Similar to Subsection 2.3.2 the corresponding system is solved with a MOT-scheme. For $n = 1,\dots,N_t$, solve:

$$((\tilde K')^0 - \frac{1}{2}(\Delta t)I)\varphi^n = G^n - \sum_{m=1}^{n-1}(\tilde K')^{n-m}\varphi^m \tag{8.2}$$

with $(\tilde K')^k$ the corresponding matrix for lightcones E_k, E_{k-1} and E'_k, E'_{k-1} and G^k the right hand side for time k and I the mass matrix in space on the boundary Γ.

8.3 Numerical experiments

8.3.1 Numerical experiments on a sphere

In our first experiment we consider the unit sphere with the center at $(0,0,1.63)$ with 1280 triangle and $\Delta t = 0.1$, where the whole sphere lies in $\mathbb{R}^3_+$. For $\alpha_\infty = 0$ we have Neumann boundary conditions on $\mathbb{R}^3_+$, which physically refers to a hard scatterer, whereas for $\alpha_\infty > 0$, we have an absorbing scatterer. Here for a bounded $\frac{\partial u}{\partial n}$, we can write the boundary condition $\frac{\partial u}{\partial n}|_{\Gamma_\infty} - \alpha_\infty\frac{\partial u}{\partial t}|_{\Gamma_\infty} = 0$ as:

$$-\frac{1}{\alpha_\infty}\frac{\partial u}{\partial n}|_{\Gamma_\infty} + \frac{\partial u}{\partial t}|_{\Gamma_\infty} = 0 \tag{8.3}$$

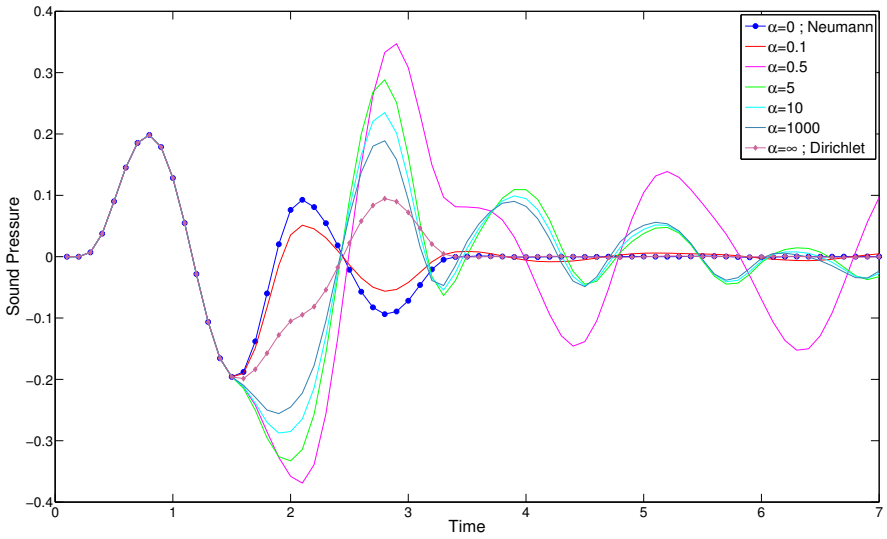

Figure 8.1: Sound pressure at $(\frac{1}{\sqrt{2}}, 0, \frac{1}{\sqrt{2}})$ in $\mathbb{R}^3_+$ as a function of the reflectivity α. Figure 5.7 in [51]

For $\alpha_\infty \to \infty$, we get the condition $\frac{\partial u}{\partial t}|_{\Gamma_\infty} = 0$. Using the homogeneous initial condition, we get a Dirichlet problem $u|_\Gamma = 0$ after all. Therefore we refer $\alpha_\infty = \infty$ as a Dirichlet problem, which is physically a soft scattering problem. On Γ, we use Neumann boundary conditions $\frac{\partial u}{\partial n}|_\Gamma = g$. In case of $\alpha_\infty = 0$, we use the exact solution from [82]:

$$u(x,t) = \frac{r_+ - t}{2r_+}[1+\cos(\frac{\pi(r_+-t)}{R})]H(R-|r_+-t|) + \frac{r_- - t}{2r_-}[1+\cos(\frac{\pi(r_--t)}{R})]H(R-|r_--t|)$$

with $r_+ = \|(x_1, x_2, x_3 - 1.63)\|$ and $r_- = \|(x_1, x_2, x_3 + 1.63)\|$ and $R = 0.9$. Then we get the Neumann boundary condition on Γ with

$$g(x,t) = \left[\frac{t}{2r_+^2}\left(1+\cos\left(\frac{\pi(r_+-t)}{R}\right)\right) - \frac{\pi}{R}\frac{r_+-t}{2r_+}\sin\left(\frac{\pi(r_+-t)}{R}\right)\right]H(R-|r_+-t|)$$
$$+ \frac{x^2+y^2+z^2-1.63^2}{r_+r_-}\left(\left[\frac{t}{2r_-^2}\left(1+\cos\left(\frac{\pi(r_--t)}{R}\right)\right) - \frac{\pi}{R}\frac{r_--t}{2r_-}\sin\left(\frac{\pi(r_--t)}{R}\right)\right]H(R-|r_--t|)\right).$$

The exact solutions for the absorbing scatterer and the soft scatterer are not known.

In Figure 8.1, we plot the evaluated sound pressure $u_{h,\Delta t}(x,t)$ at the point $x = (\frac{1}{\sqrt{2}}, 0, \frac{1}{\sqrt{2}})$ as a function of t for various α_∞. Till time 1.5, all numerical solutions for different α_∞ behave identical. The reflected waves don't reach the point $(\frac{1}{\sqrt{2}}, 0, \frac{1}{\sqrt{2}})$ until 1.5. After 1.5 as α is increasing, the sound pressure $u_{h,\Delta t}$ at $(\frac{1}{\sqrt{2}}, 0, \frac{1}{\sqrt{2}})$ tends from the solution for the Neumann boundary condition on Γ_∞ to a Dirichlet boundary condition on Γ_∞. We also notice a strong interference between direct and reflected waves. For the sound emission of tyres, with a horn geometry due to the tyre thread, similar effects have been observed in [15].

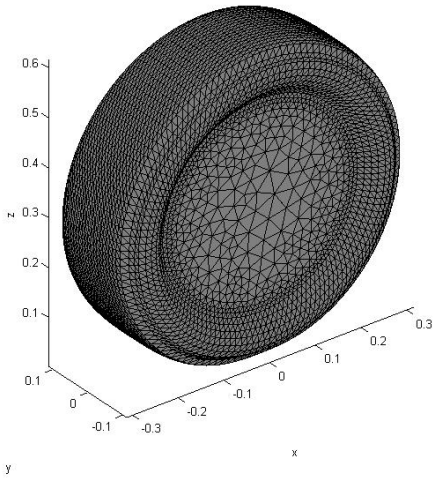

Figure 8.2: Mesh of the passenger car tire, Figure 5.9 in [51]

8.3.2 Numerical experiments on a tyre

In our next numerical experiment, we consider a sound emission by a Dirac point source located at $y_{src} = (0.08, 0, 0)$:

$$p^I = \frac{\delta(t - |x - y_{src}|)}{4\pi|x - y_{src}|} + \frac{\delta(t - |x - y'_{src}|)}{4\pi|x - y'_{src}|} \ . \tag{8.4}$$

The street Γ_∞ amplifies the sound source. Hence we are interested in a computation of the amplification for broad band frequencies [15, 16]. Since we use piecewise constant test functions, we get with $g(x,t) = \frac{\partial p^I}{\partial n}|_\Gamma(x,t)$

$$\begin{aligned} &\int_0^\infty \int_\Gamma g(x,t)\psi_h^i(x)\gamma_{\Delta t}^n(t)\, ds_x\, dt \\ &= -\int_{\Gamma_i \cap E(y_{src})} \frac{n_x^\top(y_{src} - x)}{\pi|x - y_{src}|^3}\, ds_x + n_x^\top(y_{src} - x)\left\{\frac{\zeta(t_{n-1})}{\pi t_{n-1}^2} - \frac{\zeta(t_n)}{\pi t_n^2}\right\} \ , \end{aligned} \tag{8.5}$$

where $E(y_{src}) = \{x \in \Gamma : t_{n-1} \le |x - y_{src}| \le t_n\}$ the domain of influence of y_{src}, $\Gamma_i = \text{supp}\ \psi_h^i$ the corresponding triangle, $\zeta(t)$ the length of the curve $\Gamma_i \cap \{|x - y_{src}| = t\}$ inside the triangle Γ_i. Furthermore after solving (8.2) we evaluate the sound pressure at $(2.8, 0, 1.0)$. For details on the computation of (8.5), see [15]. We consider in this experiment Dirichlet and Neumann boundary conditions on the street Γ_∞ with ISO10844 surface. The grown slick 205/55R16 passenger car tyre of diameter 60cm at 2 bar pressure contains 6027 nodes and is subject to at 3415N axle load a 50 km/h (see Figure 8.2). The tyre is lifted 2.1cm above the street with $\Delta t = 0.01$. Therefore we get $\frac{\Delta t}{h} \approx 0.2$.

In Figure 8.3 we illustrate the density at time steps $100, 200, 300$ for the Dirichlet problem. In [15] we find a similar density for the Neumann problem.

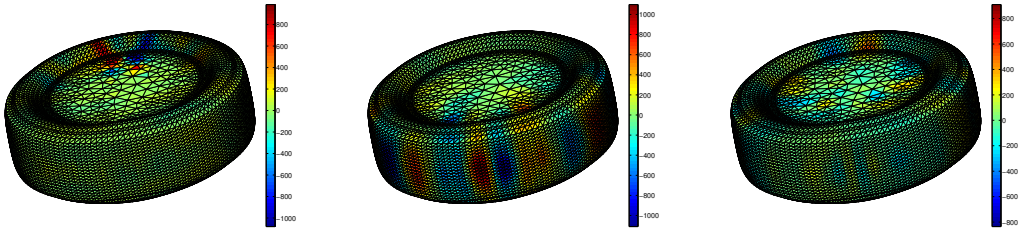

(a) (b) (c)

Figure 8.3: Visualization of the density for $\Delta t = 0.01$, time step: 100 (a), 200 (b), 300 (c). Figure 5.10 in [51]

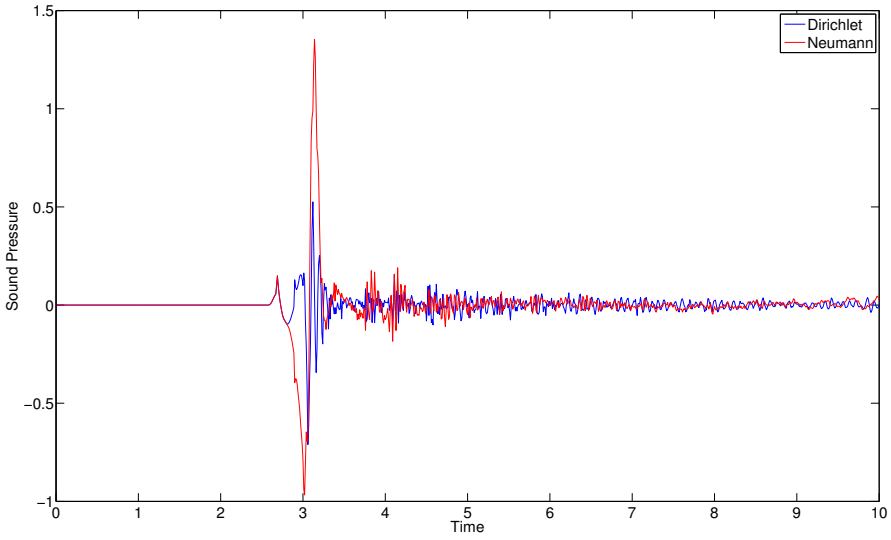

Figure 8.4: Sound pressure at $(2.8m, 0, 1.0m)$ as emitted by a car tire, Dirichlet or Neumann boundary conditions on the street. Figure 5.8 in [51]

In Figure 8.4 the sound pressure $u_{h,\Delta t}$ at $(2.8, 0, 1.0)$ is plotted. For short times the Dirichlet and Neumann boundary conditions are the same. Once the reflected wave reaches the point $(2.8, 0, 1.0)$, we observe the influence of the different boundary conditions. For long times both sound pressures go to zero.

In Figure 8.5 we present the absolute value of a fast Fourier transform of the sound pressure for times ≥ 5.145. For approximately 4800Hz we observe a broad peak for the Dirichlet problem, whereas for the Neumann problem broad peaks are observed in 100Hz and 1000Hz. These results are in agreement with direct computations for passenger car tyres and a truck tyre lifted 1mm above the street with a Neumann boundary condition on the street (see [15]). Further the human perception of the tyre noise are considered. We use an A-weighted sound pressure (see [62, 19]) in order to simulate the human perception, which has been plotted in Figure 8.6 up to 2000Hz

averaged over 321 points on the positive half-sphere $\{x \in \mathbb{R}^3_+ : \|x\|_2 = 2\}$. From 300Hz to 800Hz Dirichlet and Neumann conditions show similar average noise emission. Above 800Hz the Neumann boundary condition exhibits a higher noise level than the Dirichlet boundary condition.

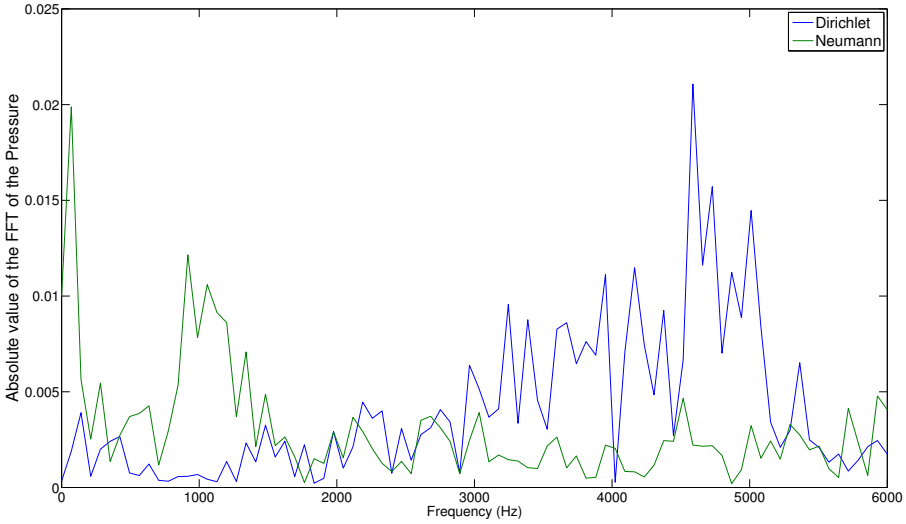

Figure 8.5: Sound pressure at $(2.8m, 0, 1.0m)$ in frequency domain, as emitted by a car tire. Figure 5.11 in [51]

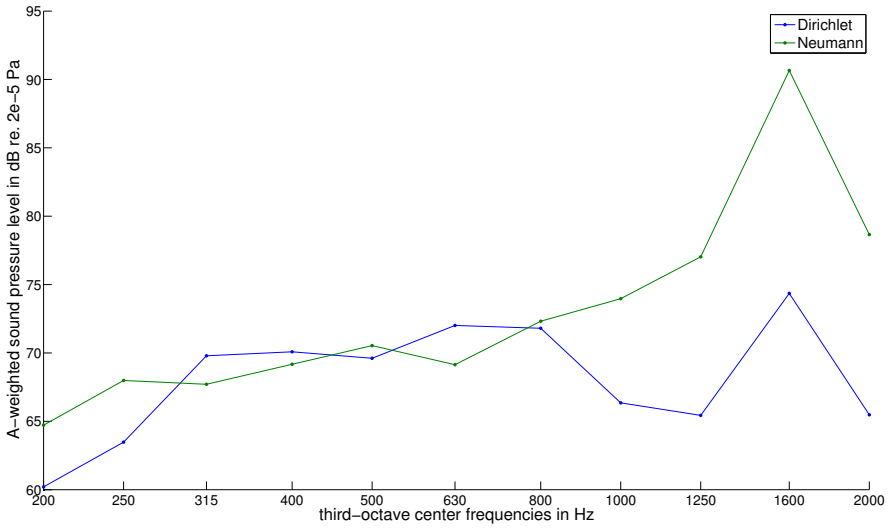

Figure 8.6: A-weighted sound pressure for Dirichlet and Neumann conditions, averaged over 321 points., Figure 5.12 in [51]

8.3.3 Numerical experiments on a graded tyre

Using the same right hand side as in Subsection 8.3.2, we consider a tyre, depicted in Figure 8.7(b), where the refinement is focused at the part, where in genereal the tyre meets the street Γ_∞. We denote this tyre as the graded tyre. We compare the graded tyre (see Figure 8.7(b)) with the other (uniform) tyre (see Figure 8.7(a)) in the Example before. The time step size is given with $\Delta t = 0.005, 0.01, 0.04$ for the graded tyre and $\Delta t = 0.005$ for the uniform tyre. We state the Neumann boundary condition on Γ_∞ and evaluate the sound pressure at $x_{fp} = (1, 0, 0)$. The amplification factor in [16, Eq. 7] is given via

$$\Delta L_H(\omega) = 20 \log_{10} \left(\frac{|\hat{u}(\omega, x_{fp}) + \hat{p}^I(\omega, x_{fp})|}{|\hat{p}^I(\omega, x_{fp})|} \right) ,$$

where $\hat{u}$ and $\hat{p}^I$ are the Fourier transform of the sound pressure and the incident field and are computed using a discrete fast Fourier transform with the same time step size as for the discretization.

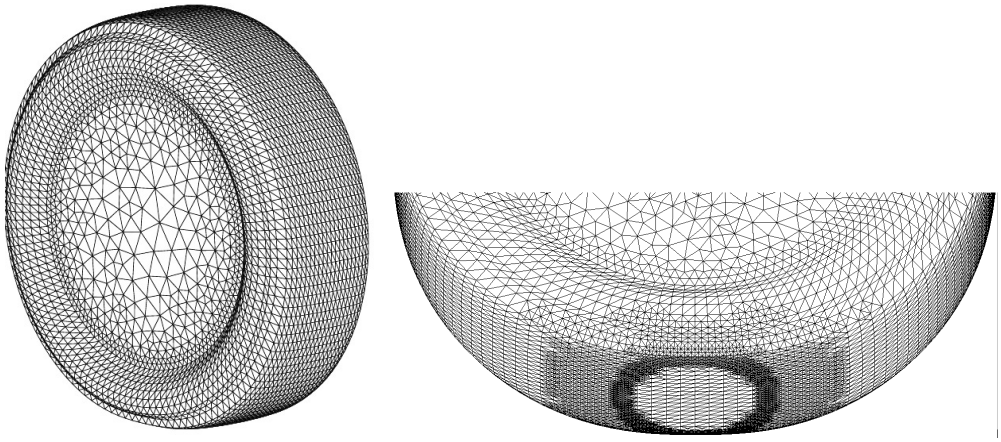

(a) (b)

Figure 8.7: Mesh of (a) slick 205/55R16 tire and (b) graded refinement. Figure 27 in [46]

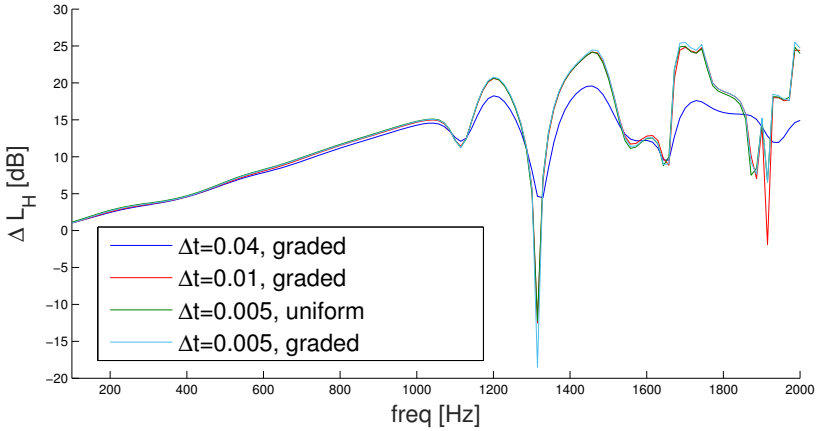

Figure 8.8: Amplification due to horn effect: Graded mesh approximations for different Δt, compared to a uniform mesh approximation. Figure 28 in [46]

In Figure 8.8 we plot the amplification factors ΔL_H. Up to 100Hz we notice a similar behaviour of all the curves. Above 1000Hz we observe several resonances for different approximations. Therefore we consider the difference of the approximations in Figures 8.9 and 8.10. Figure 8.9 displays the difference between the graded meshes and the uniform mesh. Especially in 1300Hz we see a strong resonance, where a greater difference for small Δt with the graded mesh is observed as the reflections are resolved more accurately. Figure 8.10 compares the difference of the amplification ΔL_H within the graded mesh. In 1300Hz the difference of Δt = 0.005 with Δt = 0.01 are around 6dB and in 1900Hz around 8dB. These differences are significant for the human perception of the noise and show the value of a graded mesh for the sound emission.

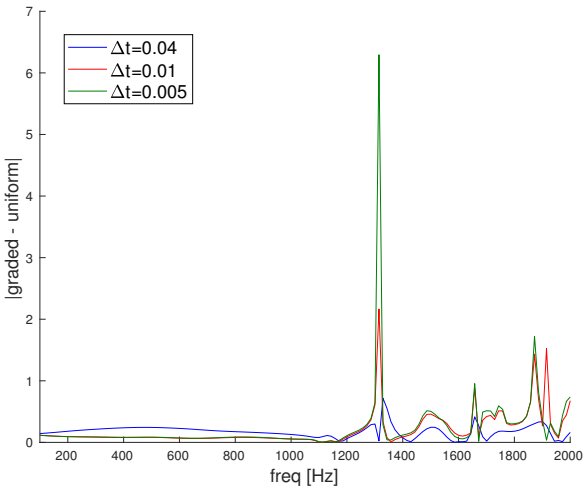

Figure 8.9: Differences of amplification factors in dB between graded and uniform meshes for fixed Δt. Figure 29 in [46]

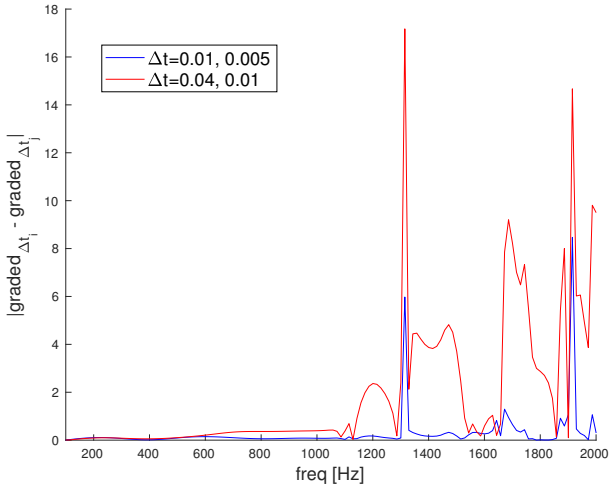

Figure 8.10: Differences of amplification factors in dB within graded meshes for different Δt. Figure 29 in [46]

9 Appendix

9.1 The computation of the retarded time integrals

In this section we focus on the computation of the retarded time integrals, which we used throughout this thesis. The time interval is divided into equidistant intervals of length (Δt). We denote $t_n = n(\Delta t)$. Let $\tau = t - |x-y|$. Then we begin with the derivative of piecewise constant functions with piecewise constant functions:

$$\int_0^\infty \gamma^m_{\Delta t}(\tau)\dot{\gamma}^n_{\Delta t}(t)dt = \int_0^\infty \gamma^m_{\Delta t}(\tau)\left(\delta(t-t_{n-1}) - \delta(t-t_n)\right)dt = \gamma^m_{\Delta t}(t_{n-1}-|x-y|) - \gamma^m_{\Delta t}(t_n-|x-y|)$$
$$= H(t_{n-1}-|x-y|-t_{m-1}) - H(t_{n-1}-|x-y|-t_m) - H(t_n-|x-y|-t_{m-1}) + H(t_n-|x-y|-t_m)\ . \tag{9.1}$$

We have

$$\begin{aligned} t_{n-1} - t_{m-1} &= (n-1)(\triangle t) - (m-1)(\triangle t) = (n-1-(m-1))(\triangle t) = (n-m)(\triangle t) = t_{n-m}, \\ t_n - t_{m-1} &= (n)(\triangle t) - (m-1)(\triangle t) = (n-(m-1))(\triangle t) = (n-m+1)(\triangle t) = t_{n-m+1}, \\ t_{n-1} - t_m &= (n-1)(\triangle t) - (m)(\triangle t) = (n-1-(m))(\triangle t) = (n-m-1)(\triangle t) = t_{n-m-1}, \\ t_n - t_m &= (n)(\triangle t) - (m)(\triangle t) = (n-(m))(\triangle t) = (n-m)(\triangle t) = t_{n-m}\ . \end{aligned}$$

This yields for (9.1):

$$\int_0^\infty \gamma^m_{\Delta t}(\tau)\dot{\gamma}^n_{\Delta t}(t)dt = H(t_{n-m}-|x-y|) - H(t_{n-m-1}-|x-y|) - H(t_{n-m+1}-|x-y|) + H(t_{n-m}-|x-y|).$$

Since $H(t_l - |x-y|) = \begin{cases} 1 & , |x-y| \le t_l \\ 0 & , \text{else} \end{cases}$, we can define the acoustic lightcone:

$$E_l := \{(x,y) \in \Gamma \times \Gamma : t_l \le |x-y| \le t_{l+1}\} \subset \Gamma \times \Gamma\ .$$

Let χ be an indicator function $\chi_A = \begin{cases} 1 & , x \in A \\ 0 & , x \notin A \end{cases}$, then we get at last for the time integral:

$$\int_0^\infty \gamma^m_{\Delta t}(\tau)\dot{\gamma}^n_{\Delta t}(t)dt = \chi_{E_{n-m-1}}(x,y) - \chi_{E_{n-m}}(x,y)\ . \tag{9.2}$$

Via integration by parts we get as well:

$$\int_0^\infty \dot{\gamma}^m_{\Delta t}(\tau)\gamma^n_{\Delta t}(t)dt = -\chi_{E_{n-m-1}}(x,y) + \chi_{E_{n-m}}(x,y)\ . \tag{9.3}$$

Next considering the derivative of piecewise linear functions with the derivative of piecewise constant functions:

$$\int_0^\infty \dot{\beta}^m_{\Delta t}(\tau)\dot{\gamma}^n_{\Delta t}(t)dt = \int_0^\infty (\Delta t)^{-1}(\gamma^m_{\Delta t}(\tau) - \gamma^{m+1}_{\Delta t}(\tau))\dot{\gamma}^n_{\Delta t}(t)dt$$
$$= \int_0^\infty (\Delta t)^{-1}\gamma^m_{\Delta t}(\tau)\dot{\gamma}^n_{\Delta t}(t)dt - \int_0^\infty (\Delta t)^{-1}\gamma^{m+1}_{\Delta t}(\tau)\dot{\gamma}^n_{\Delta t}(t)dt \ .$$

Now we can use (9.1)

$$\int_0^\infty \dot{\beta}^m_{\Delta t}(\tau)\dot{\gamma}^n_{\Delta t}(t)dt = \tfrac{1}{(\Delta t)}\Big(H(t_{n-m}-|x-y|)-H(t_{n-m-1}-|x-y|)-H(t_{n-m+1}-|x-y|)+H(t_{n-m}-|x-y|)\Big)$$
$$-\tfrac{1}{(\Delta t)}\Big(H(t_{n-m-1}-|x-y|)-H(t_{n-m-2}-|x-y|)-H(t_{n-m}-|x-y|)+H(t_{n-m-1}-|x-y|)\Big)$$
$$= \tfrac{1}{(\Delta t)}(-\chi_{E_{n-m-2}}(x,y) + 2\chi_{E_{n-m-1}}(x,y) - \chi_{E_{n-m}}(x,y)) \ . \tag{9.4}$$

Next we have a look at the time integral with piecewise constant functions:

$$\int_0^\infty \gamma^m_{\Delta t}(\tau)\gamma^n_{\Delta t}(t)dt = \int_{t_{n-1}}^{t_n} \gamma^m_{\Delta t}(\tau)dt = \int_{t_{n-1}}^{t_n} H(t-|x-y|-t_{m-1}) - H(t-|x-y|-t_m)dt$$
$$= \int_0^{\Delta t} H(s+t_{n-m}-|x-y|)-H(s+t_{n-m-1}-|x-y|)ds = \int_0^{\Delta t} 1\cdot H(s+t_{n-m}-|x-y|)-H(s+t_{n-m-1}-|x-y|)ds$$
$$= [s\Big(H(s+t_{n-m}-|x-y|)-H(s+t_{n-m-1}-|x-y|)\Big)]_{s=0}^{(\Delta t)} - \int_0^{\Delta t} s\Big(\delta(s+t_{n-m}-|x-y|)-\delta(s+t_{n-m-1}-|x-y|)\Big)ds$$
$$= (\Delta t)\Big(H((\Delta t)+t_{n-m}-|x-y|) - H((\Delta t)+t_{n-m-1}-|x-y|)\Big)$$
$$- \int_0^\infty s\cdot\Big(\delta(s+t_{n-m}-|x-y|) - \delta(s+t_{n-m-1}-|x-y|)\Big)\Big(H(s)-H(s-(\Delta t))\Big)ds$$
$$= (\Delta t)\Big(H(t_{n-m+1}-|x-y|)-H((t_{n-m}-|x-y|)\Big) - \int_0^\infty s\delta(s+t_{n-m}-|x-y|)\Big(H(s)-H(s-(\Delta t))\Big)ds$$
$$+ \int_0^\infty s\delta(s+t_{n-m-1}-|x-y|)\Big(H(s)-H(s-(\Delta t))\Big)ds$$
$$= (\Delta t)\chi_{E_{n-m}}(x,y) - (|x-y|-t_{n-m})\Big(H(|x-y|-t_{n-m})-H(|x-y|-t_{n-m+1})\Big)$$
$$+ (|x-y|-t_{n-m-1})\Big(H(|x-y|-t_{n-m-1})-H(|x-y|-t_{n-m})\Big) \ .$$

Here we used the substitution $s = t - t_{n-1}$ and integration by parts. Now writing $1 = H(t) + H(-t)$ for every t except 0, we have

$$\int_0^\infty \gamma^m_{\Delta t}(\tau)\gamma^n_{\Delta t}(t)dt = (\Delta t)\chi_{E_{n-m}}(x,y) + (t_{n-m}-|x-y|)\chi_{E_{n-m}}(x,y) + (|x-y|-t_{n-m-1})\chi_{E_{n-m-1}}(x,y)$$
$$= (t_{n-m+1} - |x-y|)\chi_{E_{n-m}}(x,y) + (-t_{n-m-1} + |x-y|)\chi_{E_{n-m-1}}(x,y) \ .$$

So we get:

$$\int_0^\infty \gamma^m_{\Delta t}(\tau)\gamma^n_{\Delta t}(t)dt = (t_{n-m+1} - |x-y|)\chi_{E_{n-m}}(x,y) + (-t_{n-m-1} + |x-y|)\chi_{E_{n-m-1}}(x,y) \ . \tag{9.5}$$

For the time integral of the derivative of piecewise linear functions with piecewise constant functions:

$$\int_0^\infty \dot{\beta}^m_{\Delta t}(\tau)\gamma^n_{\Delta t}(t)dt = \int_0^\infty (\Delta t)^{-1}(\gamma^m_{\Delta t}(\tau) - \gamma^{m+1}_{\Delta t}(\tau))\gamma^n_{\Delta t}(t)dt$$
$$= \int_0^\infty (\Delta t)^{-1}\gamma^m_{\Delta t}(\tau)\gamma^n_{\Delta t}(t)dt - \int_0^\infty (\Delta t)^{-1}\gamma^{m+1}_{\Delta t}(\tau)\gamma^n_{\Delta t}(t)dt \ .$$

Now using the same steps as in (9.5)

$$\begin{aligned}\int_0^\infty \dot{\beta}^m_{\Delta t}(\tau)\gamma^n_{\Delta t}(t)dt &= \tfrac{1}{(\Delta t)}(t_{n-m+1} - |x-y|)\chi_{E_{n-m}}(x,y) + \tfrac{1}{(\Delta t)}(-t_{n-m+1} + |x-y|)\chi_{E_{n-m-1}}(x,y)\\ &- \tfrac{1}{(\Delta t)}(t_{n-m} - |x-y|)\chi_{E_{n-m-1}}(x,y) - \tfrac{1}{(\Delta t)}(-t_{n-m-2} + |x-y|)\chi_{E_{n-m-2}}(x,y)\\ &= \tfrac{1}{(\Delta t)}(t_{n-m+1} - |x-y|)\chi_{E_{n-m}}(x,y) + \tfrac{1}{(\Delta t)}(t_{n-m-2} - |x-y|)\chi_{E_{n-m-2}}(x,y)\\ &+ \tfrac{1}{(\Delta t)}(-t_{2(n-m)-1} + 2|x-y|)\chi_{E_{n-m-1}}(x,y) \ . \end{aligned} \tag{9.6}$$

Since we have functions with compact support, we can use integration by parts, which gives the same lightcones, except for another sign.

$$\begin{aligned}\int_0^\infty \beta^m_{\Delta t}(\tau)\dot{\gamma}^n_{\Delta t}(t)dt &= -(\Delta t)^{-1}(t_{n-m+1} - |x-y|)\chi_{E_{n-m}}(x,y)\\ &- (\Delta t)^{-1}(t_{n-m-2} - |x-y|)\chi_{E_{n-m-2}}(x,y) - (\Delta t)^{-1}(-t_{2(n-m)-1} + 2|x-y|)\chi_{E_{n-m-1}}(x,y) \ . \end{aligned} \tag{9.7}$$

Next, the time integral of piecewise linear functions with piecewise constant functions:

$$\int_0^\infty \beta^m_{\Delta t}(\tau)\gamma^n_{\Delta t}(t)dt = \int_0^\infty \tfrac{1}{(\Delta t)}\Big((t-|x-y|-t_{m-1})\gamma^m_{\Delta t}(t-|x-y|) - (t-|x-y|-t_{m+1})\gamma^{m+1}_{\Delta t}(t-|x-y|)\Big)\gamma^n_{\Delta t}(t)dt$$
$$= \tfrac{1}{(\Delta t)}\int_0^\infty (t-|x-y|-t_{m-1})\gamma^m_{\Delta t}(t-|x-y|)\gamma^n_{\Delta t}(t)dt - \tfrac{1}{(\Delta t)}\int_0^\infty (t-|x-y|-t_{m+1})\gamma^{m+1}_{\Delta t}(t-|x-y|)\gamma^n_{\Delta t}(t)dt \ .$$

For the computation of these both integrals, let us introduce a $\nu \in \mathbb{Z}$ and consider the following integral:

$$\int_0^\infty (t-|x-y|-t_{m+\nu})\gamma^m_{\Delta t}(t-|x-y|)\gamma^n_{\Delta t}(t)dt = \int_{t_{n-1}}^{t_n} (t-|x-y|-t_{m+\nu})\gamma^m_{\Delta t}(t-|x-y|)dt$$
$$= \int_{t_{n-1}}^{t_n} (t-|x-y|-t_{m+\nu})[H(t-|x-y|-t_{m-1}) - H(t-|x-y|-t_m)]dt \ . \tag{9.8}$$

With the substitution $s(t) = t - t_{n-1}$ and integration by parts together with $-t_k = t_{-k}$:

$$\begin{aligned}(9.8) &= \int_0^{(\Delta t)} (s-|x-y|-t_{m+\nu-n+1})[H(s-|x-y|-t_{m-n}) - H(s-|x-y|-t_{m-n+1})]ds\\ &= \int_0^{(\Delta t)} (s-|x-y|+t_{n-m-\nu-1})[H(s-|x-y|+t_{n-m-\nu-1}) - H(s-|x-y|+t_{n-m-1})]ds\\ &= \int_0^{(\Delta t)} (s-|x-y|+t_{n-m-\nu-1})[H(s-|x-y|+t_{n-m}) - H(s-|x-y|+t_{n-m-1})]ds\\ &= \left[\frac{(s-|x-y|+t_{n-m-\nu-1})^2}{2}(H(s-|x-y|+t_{n-m}) - H(s-|x-y|+t_{n-m-1}))\right]_{s=0}^{(\Delta t)}\\ &- \int_0^{(\Delta t)} \frac{(s-|x-y|+t_{n-m-\nu-1})^2}{2}(\delta(s-|x-y|+t_{n-m}) - \delta(s-|x-y|+t_{n-m-1}))ds \ . \end{aligned}$$

We first consider the part without an integral.

$$
\begin{aligned}
&\left[\frac{(s-|x-y|+t_{n-m-\nu-1})^2}{2}(H(s-|x-y|+t_{n-m})-H(s-|x-y|+t_{n-m-1}))\right]_{s=0}^{(\Delta t)}\\
&=\left[\frac{((\Delta t)-|x-y|+t_{n-m-\nu-1})^2}{2}(H((\Delta t)-|x-y|+t_{n-m})-H((\Delta t)-|x-y|+t_{n-m-1}))\right]\\
&-\left[\frac{(0-|x-y|+t_{n-m-\nu-1})^2}{2}(H(0-|x-y|+t_{n-m})-H(0-|x-y|+t_{n-m-1}))\right]\\
&=\left[\frac{(t_1-|x-y|+t_{n-m-\nu-1})^2}{2}(H(t_1-|x-y|+t_{n-m})-H(t_1-|x-y|+t_{n-m-1}))\right]\\
&-\left[\frac{(t_{n-m-\nu-1}-|x-y|)^2}{2}\underbrace{(H(t_{n-m}-|x-y|)-H(t_{n-m-1}-|x-y|))}_{=\chi_{E_{n-m-1}}(x,y)}\right]\\
&=\left[\frac{(t_{n-m-\nu}-|x-y|)^2}{2}\underbrace{(H(t_{n+1-m}-|x-y|)-H(t_{n-m}-|x-y|))}_{=\chi_{E_{n-m}}(x,y)}\right]-\frac{(t_{n-m-\nu-1}-|x-y|)^2}{2}\chi_{E_{n-m-1}}(x,y)\\
&=\frac{(t_{n-m-\nu}-|x-y|)^2}{2}\chi_{E_{n-m}}(x,y)-\frac{(t_{n-m-\nu-1}-|x-y|)^2}{2}\chi_{E_{n-m-1}}(x,y)\ .
\end{aligned}
$$

Next we consider the integral part. Here we again use $1 = H(t) + H(-t)$ for every t except zero.

$$
\begin{aligned}
&\int_0^{(\Delta t)}\frac{(s-|x-y|+t_{n-m-\nu-1})^2}{2}(\delta(s-|x-y|+t_{n-m})-\delta(s-|x-y|+t_{n-m-1}))ds\\
&=\int_0^{\infty}\frac{(s-|x-y|+t_{n-m-\nu-1})^2}{2}(H(s)-H(s-(\Delta t)))\,(\delta(s-|x-y|+t_{n-m})-\delta(s-|x-y|+t_{n-m-1}))\,ds\\
&=\int_0^{\infty}\frac{(s-|x-y|+t_{n-m-\nu-1})^2}{2}(H(s)-H(s-(\Delta t)))\,\delta(s-|x-y|+t_{n-m})ds\\
&-\int_0^{\infty}\frac{(s-|x-y|+t_{n-m-\nu-1})^2}{2}(H(s)-H(s-(\Delta t)))\,\delta(s-|x-y|+t_{n-m-1})ds\\
&\underset{|x-y|-t_{n-m-1}}{\overset{|x-y|-t_{n-m}}{=}}\frac{(|x-y|-t_{n-m}-|x-y|+t_{n-m-\nu-1})^2}{2}(H(|x-y|-t_{n-m})-H(|x-y|-t_{n-m}-t_1))\\
&-\frac{(|x-y|-t_{n-m-1}-|x-y|+t_{n-m-\nu-1})^2}{2}(H(|x-y|-t_{n-m-1})-H(|x-y|-t_{n-m-1}-t_1))\\
&=\frac{(-t_{\nu+1})^2}{2}[H(|x-y|-t_{n-m})-H(|x-y|-t_{n-m+1})]-\frac{(-t_\nu)^2}{2}[H(|x-y|-t_{n-m-1})-H(|x-y|-t_{n-m})]\\
&\overset{H(-t)=1-H(t)}{=}\frac{(t_{\nu+1})^2}{2}[1-H(t_{n-m}-|x-y|)-1+H(t_{n-m+1}-|x-y|)]\\
&-\frac{(t_\nu)^2}{2}[1-H(t_{n-m-1}-|x-y|)-1+H(t_{n-m}-|x-y|)]\\
&=\frac{(t_{\nu+1})^2}{2}[H(t_{n-m+1}-|x-y|)-H(t_{n-m}-|x-y|)]-\frac{(t_\nu)^2}{2}[H(t_{n-m}-|x-y|)-H(t_{n-m-1}-|x-y|)]\\
&=\frac{(t_{\nu+1})^2}{2}\chi_{E_{n-m}}(x,y)-\frac{(t_\nu)^2}{2}\chi_{E_{n-m-1}}(x,y)\ .
\end{aligned}
$$

Now we get with both parts:

$$\int_0^\infty (t-|x-y|-t_{m+\nu})\gamma_{\Delta t}^m(t-|x-y|)\gamma_{\Delta t}^n(t)dt = \frac{(t_{n-m-\nu}-|x-y|)^2}{2}\chi_{E_{n-m}}(x,y)$$
$$-\frac{(t_{n-m-\nu-1}-|x-y|)^2}{2}\chi_{E_{n-m-1}}(x,y)-\frac{(t_{\nu+1})^2}{2}\chi_{E_{n-m}}(x,y)+\frac{(t_\nu)^2}{2}\chi_{E_{n-m-1}}(x,y)$$
$$=\tfrac{1}{2}\big(t_{n-m-\nu}^2-2|x-y|t_{n-m-\nu}+|x-y|^2-t_{\nu+1}^2\big)\chi_{E_{n-m}}(x,y)$$
$$-\tfrac{1}{2}\big(t_{n-m-\nu-1}^2-2|x-y|t_{n-m-\nu-1}+|x-y|^2-t_\nu^2\big)\chi_{E_{n-m-1}}(x,y)$$
$$=\tfrac{1}{2}\big(|x-y|^2-2|x-y|t_{n-m-\nu}+(t_{n-m-\nu}^2-t_{\nu+1}^2)\big)\chi_{E_{n-m}}(x,y)$$
$$-\tfrac{1}{2}\big(|x-y|^2-2|x-y|t_{n-m-\nu-1}+(t_{n-m-\nu-1}^2-t_\nu^2)\big)\chi_{E_{n-m-1}}(x,y)\ .$$

Using it with $\nu = 0$ and $\nu = -1$

$$\int_0^\infty \beta_{\Delta t}^m(\tau)\gamma_{\Delta t}^n(t)dt = (\Delta t)^{-1}\Bigg(\frac{1}{2}(|x-y|^2-2|x-y|t_{n-m+1}+t_{n-m+1}^2)\chi_{E_{n-m}}(x,y)$$
$$-\frac{1}{2}(|x-y|^2-2|x-y|t_{n-m}+(t_{n-m}^2-t_{-1}^2))\chi_{E_{n-m-1}}(x,y)$$
$$-\frac{1}{2}(|x-y|^2-2|x-y|t_{n-(m+1)}+(t_{n-(m+1)}^2-t_1^2))\chi_{E_{n-(m+1)}}(x,y)$$
$$+\frac{1}{2}(|x-y|^2-2|x-y|t_{n-(m+1)-1}+t_{n-(m+1)-1}^2)\chi_{E_{n-(m+1)-1}}(x,y)\Bigg)$$
$$\overset{t_{-1}^2=t_1^2}{=}(2(\Delta t))^{-1}(|x-y|^2-2|x-y|t_{n-m+1}+t_{n-m+1}^2)\chi_{E_{n-m}}(x,y)$$
$$+(2(\Delta t))^{-1}(|x-y|^2-2|x-y|t_{n-m-2}+t_{n-m-2}^2)\chi_{E_{n-m-2}}(x,y)$$
$$+(2(\Delta t))^{-1}(-2|x-y|^2+2|x-y|(t_{n-m}+t_{n-m-1})-(t_{n-m}^2+t_{n-m-1}^2)+2(\Delta t)^2)\chi_{E_{n-m-1}}(x,y)\ . \tag{9.9}$$

On the other hand considering the retarded contribution in the piecewise constant function:

$$\int_0^\infty \beta_{\Delta t}^m(t)\gamma_{\Delta t}^n(\tau)dt = \int_0^\infty \frac{1}{(\Delta t)}\Big((t-t_k)\gamma_{\Delta t}^m(t)-(t-t_{k+1})\gamma^{m+1}(t)\Big)\gamma_{\Delta t}^n(t-|x-y|)dt$$
$$=\int_{t_{m-1}}^{t_m}\frac{1}{(\Delta t)}(t-t_m)\gamma_{\Delta t}^n(t-|x-y|)dt-\int_{t_m}^{t_{m+1}}\frac{1}{(\Delta t)}(t-t_{m+1})\gamma_{\Delta t}^n(t-|x-y|)dt\ .$$

Let's have a look at the first term of the time integral. Substituting $s = t - t_{m-1}$ and with integration by parts:

$$\int_{t_{m-1}}^{t_m}\frac{1}{(\Delta t)}(t-t_m)\left(H(t-|x-y|-t_{n-1})-H(t-|x-y|-t_n)\right)dt$$
$$=\Big[\frac{1}{2(\Delta t)}(s-(\Delta t))^2\left(H(s-|x-y|-t_{m-n})-H(s-|x-y|-t_{m-n-1})\right)\Big]_0^{\Delta t}$$
$$-\int_0^{(\Delta t)}\frac{1}{2(\Delta t)}(s-(\Delta t))^2\left(\delta(s-|x-y|-t_{m-n})-\delta(s-|x-y|-t_{m-n-1})\right)ds\ .$$

The summand without the integral gives:

$$\Big[\frac{1}{2(\Delta t)}(s-(\Delta t))^2\,(H(s-|x-y|-t_{m-n})-H(s-|x-y|-t_{m-n-1}))\Big]_0^{\Delta t}$$
$$=-\frac{(\Delta t)}{2}(H(t_{m-n}-|x-y|)-H(t_{m-n-1}-|x-y|))=-\frac{(\Delta t)}{2}\chi_{E_{n-m-1}}(x,y)\ .$$

The summand with the integral

$$-\int_0^{\Delta t}\frac{1}{2(\Delta t)}(s-(\Delta t))^2\delta(s-|x-y|-t_{m-n})ds+\int_0^{\Delta t}\frac{1}{2(\Delta t)}(s-(\Delta t))^2\delta(s-|x-y|-t_{m-n-1})ds$$
$$=-\int_0^{\infty}\frac{1}{2(\Delta t)}(s-(\Delta t))^2(H(s)-H(s-(\Delta t)))\delta(s-|x-y|-t_{m-n})ds$$
$$+\int_0^{\infty}\frac{1}{2(\Delta t)}(s-(\Delta t))^2(H(s)-H(s-(\Delta t)))\delta(s-|x-y|-t_{m-n-1})ds$$
$$=-\tfrac{1}{2(\Delta t)}(|x-y|-t_{m-n}-t_1)^2(H(|x-y|-t_{m-n})-H(|x-y|-t_{m-n}-t_1))$$
$$+\tfrac{1}{2(\Delta t)}(|x-y|-t_{m-n-1}-t_1)^2(H(|x-y|-t_{m-n-1})-H(|x-y|-t_{m-n-1}-t_1))$$
$$=-\tfrac{(|x-y|-t_{m-n+1})^2}{2(\Delta t)}(H(t_{m-n+1}-|x-y|)-H(t_{m-n}-|x-y|))+\tfrac{(|x-y|-t_{m-n})^2}{2(\Delta t)}(H(t_{m-n}-|x-y|)-H(t_{m-n-1}-|x-y|))$$
$$=-\tfrac{(|x-y|-t_{m-n+1})^2}{2(\Delta t)}\chi_{E_{m-n}}(x,y)+\tfrac{(|x-y|-t_{m-n})^2}{2(\Delta t)}\chi_{E_{m-n-1}}(x,y)\ .$$

Altogether we get:

$$\int_{t_{m-1}}^{t_m}\tfrac{1}{(\Delta t)}(t-t_m)\gamma_{\Delta t}^n(t-|x-y|)dt$$
$$=-\tfrac{(\Delta t)}{2}\chi_{E_{m-n-1}}(x,y)-\tfrac{(|x-y|-t_{m-n+1})^2}{2(\Delta t)}\chi_{E_{m-n}}(x,y)+\tfrac{(|x-y|-t_{m-n})^2}{2(\Delta t)}\chi_{E_{m-n-1}}(x,y)\ . \tag{9.10}$$

Now let us consider (9.10) with $m=m+1$, we get immediately:

$$\int_{t_m}^{t_{m+1}}\frac{1}{(\Delta t)}(t-t_{m+1})\gamma_{\Delta t}^n(t-|x-y|)dt=$$
$$-\tfrac{\Delta t}{2}\chi_{E_{m-n}}(x,y)+\tfrac{(|x-y|-t_{m-n+2})^2}{2(\Delta t)}\chi_{E_{m-n+1}}(x,y)-\tfrac{(|x-y|-t_{m-n+1})^2}{2(\Delta t)}\chi_{E_{m-n}}(x,y)\ .$$

Substracting gives:

$$\int_0^{\infty}\beta_{\Delta t}^m(t)\gamma_{\Delta t}^n(t-|x-y|)dt=-\tfrac{(\Delta t)}{2}\chi_{E_{m-n-1}}(x,y)-\tfrac{(|x-y|-t_{m-n+1})^2}{2(\Delta t)}\chi_{E_{m-n}}(x,y)+\tfrac{(|x-y|-t_{m-n})^2}{2(\Delta t)}\chi_{E_{m-n-1}}(x,y)$$
$$+\tfrac{(\Delta t)}{2}\chi_{E_{m-n}}(x,y)+\tfrac{(|x-y|-t_{m-n+2})^2}{2(\Delta t)}\chi_{E_{m-n+1}}(x,y)-\tfrac{(|x-y|-t_{m-n+1})^2}{2(\Delta t)}\chi_{E_{m-n}}(x,y)$$
$$=(-\tfrac{(\Delta t)}{2}+\tfrac{(|x-y|-t_{m-n})^2}{2(\Delta t)})\chi_{E_{m-n-1}}(x,y)+(\tfrac{(\Delta t)}{2}-\tfrac{(|x-y|-t_{m-n+1})^2}{(\Delta t)})\chi_{E_{m-n}}(x,y)+\tfrac{(|x-y|-t_{m-n+2})^2}{2(\Delta t)}\chi_{E_{m-n+1}}(x,y). \tag{9.11}$$

Next we consider using piecewise linear functions in time against pw. linear functions.

$$\int_0^{\infty}\beta_{\Delta t}^m(\tau)\dot\beta_{\Delta t}^n(t)dt=\int_0^{\infty}\beta_{\Delta t}^m(\tau)\frac{1}{(\Delta t)}(\gamma_{\Delta t}^n(t)-\gamma_{\Delta t}^{n+1}(t))dt$$
$$=\frac{1}{(\Delta t)}\int_0^{\infty}\beta_{\Delta t}^m(\tau)\gamma_{\Delta t}^n(t)dt-\frac{1}{(\Delta t)}\int_0^{\infty}\beta_{\Delta t}^m(\tau)\gamma_{\Delta t}^{n+1}(t)dt\ .$$

Now using (9.9) twice:

$$
\begin{aligned}
&\int_0^\infty \beta^m_{\Delta t}(\tau)\dot\beta^n_{\Delta t}(t)dt\\
&= \frac{1}{2(\Delta t)^2}(|x-y|^2 - 2|x-y|t_{n-m+1} + t^2_{n-m+1})\chi_{E_{n-m}}(x,y)\\
&+ \frac{1}{2(\Delta t)^2}(|x-y|^2 - 2|x-y|t_{n-m-2} + t^2_{n-m-2})\chi_{E_{n-m-2}}(x,y)\\
&+ \frac{1}{2(\Delta t)^2}(-2|x-y|^2 + 2|x-y|(t_{n-m} + t_{n-m-1}) - (t^2_{n-m} + t^2_{n-m-1}) + 2(\Delta t)^2)\chi_{E_{n-m-1}}(x,y)\\
&- \frac{1}{2(\Delta t)^2}(|x-y|^2 - 2|x-y|t_{n-m+2} + t^2_{n-m+2})\chi_{E_{n+1-m}}(x,y)\\
&- \frac{1}{2(\Delta t)^2}(|x-y|^2 - 2|x-y|t_{n-m-1} + t^2_{n-m-1})\chi_{E_{n-m-1}}(x,y)\\
&- \frac{1}{2(\Delta t)^2}(-2|x-y|^2 + 2|x-y|(t_{n+1-m} + t_{n-m}) - (t^2_{n+1-m} + t^2_{n-m}) + 2(\Delta t)^2)\chi_{E_{n-m}}(x,y)\\
&= \frac{1}{2(\Delta t)^2}(|x-y|^2 - 2|x-y|t_{n-m-2} + t^2_{n-m-2})\chi_{E_{n-m-2}}(x,y)\\
&- \frac{1}{2(\Delta t)^2}(|x-y|^2 - 2|x-y|t_{n-m+2} + t^2_{n-m+2})\chi_{E_{n+1-m}}(x,y)\\
&+ \frac{1}{2(\Delta t)^2}(|x-y|^2 - 2|x-y|t_{n-m+1} + t^2_{n-m+1}\\
&+ 2|x-y|^2 - 2|x-y|(t_{n+1-m} + t_{n-m}) + (t^2_{n+1-m} + t^2_{n-m}) - 2(\Delta t)^2)\chi_{E_{n-m}}(x,y)\\
&+ \frac{1}{2(\Delta t)^2}(-2|x-y|^2 + 2|x-y|(t_{n-m} + t_{n-m-1}) - (t^2_{n-m} + t^2_{n-m-1}) + 2(\Delta t)^2\\
&- |x-y|^2 + 2|x-y|t_{n-m-1} - t^2_{n-m-1})\chi_{E_{n-m-1}}(x,y)\\
&= \frac{1}{2(\Delta t)^2}(t_{n-m-2} - |x-y|)^2\chi_{E_{n-m-2}}(x,y) - \frac{1}{2(\Delta t)^2}(t_{n-m+2} - |x-y|)^2\chi_{E_{n-m+1}}(x,y)\\
&+ \frac{1}{2(\Delta t)^2}(2(t_{n-m+1} - |x-y|)^2 - 2(\Delta t)^2 + (t_{n-m} - |x-y|)^2)\chi_{E_{n-m}}(x,y)\\
&- \frac{1}{2(\Delta t)^2}((t_{n-m} - |x-y|)^2 + 2(t_{n-m-1} - |x-y|)^2 - 2(\Delta t)^2)\chi_{E_{n-m-1}}(x,y)\ .
\end{aligned}
$$

9.2 Important theorems

In this section we mention important theorems, used throughout this thesis. Let $\Omega \subset \mathbb{R}^3$ be a bounded, orientable Lipschitz domain. We begin with the trace theorems.

Lemma 9.1 ([57]). *For all $u \in H^1(\Omega)$ and $\omega \in \{w \in \mathbb{C}; \mathrm{Im} w \geq \sigma_0 > 0\}$, there exists a positive contant C depending on Ω and σ_0 such that:*

$$\|\gamma u\|_{1/2,\omega,\Gamma} \leq C\|u\|_{1,\omega,\Omega}\ ,$$

where γ denotes the trace operator in $H^1(\Omega)$.

Lemma 9.2 ([57]). *For all $\varphi \in H^{1/2}(\Omega)$ and $\omega \in \{w \in \mathbb{C}; \mathrm{Im} w \geq \sigma_0 > 0\}$, there exists $u \in H^1(\Omega)$ and a positive contant C depending on Ω and σ_0 such that:*

$$\|u\|_{1,\omega,\Omega} \leq C \|\varphi\|_{1/2,\omega,\Gamma} \ .$$

Lemma 9.3 ([57]). *For all $u \in H^1(\Omega)$ fulfilling the homogeneous Helmholtz equation in Ω and $\omega \in \{w \in \mathbb{C}; \mathrm{Im} w \geq \sigma_0 > 0\}$, there exists a positive contant C depending on Ω and σ_0 such that:*

$$\|\frac{\partial u}{\partial n}\|_{-1/2,\omega,\Gamma} \leq C \|u\|_{1,\omega,\Omega} \ ,$$

where $\|\cdot\|_{-1/2,\omega,\Gamma}$ is the dual norm of $\|\cdot\|_{1/2,\omega,\Gamma}$.

Next in order to state the Paley-Wiener theorem and Parseval theorem, we need to proceed as in [57] and define for a Hilbert space E

$$LT(\sigma, E) := \{f \in D'_+(E), e^{-\sigma t} f \in S'_+(E)\} \ ,$$

where $D'_+(E)$ resp. $S'_+(E)$ denote the sets of distributions resp. tempered distributions on $\mathbb{R}$ with values in E and support in $[0, \infty)$. For $\sigma < \sigma'$, $LT(\sigma, E) \subset LT(\sigma', E)$, there exists $\sigma(f) = \inf\{\sigma : f \in LT(\sigma, E)\}$. The set of Laplace transformable distributions with values in E is denoted by

$$LT(E) = \cup_{\sigma \in \mathbb{R}} LT(\sigma, E) \ .$$

For $\sigma > \sigma(f)$ and $\omega = \eta + i\sigma$ the Fourier-Laplace transform of $f \in LT(E)$ in the half plane $\{\omega \in \mathbb{C} : \mathrm{Im}\omega \geq \sigma(f)\}$ with $\mathrm{Im}\omega$ denotes the imaginary part of ω is given by

$$\widehat{f}(\omega) = \mathcal{F}(e^{-\sigma t} f)(\eta) = \int_{-\infty}^{\infty} e^{i\omega t} f(t) dt \ .$$

Theorem 9.1 (Paley-Wiener theorem, [57], [17]). *The following statements are equivalent:*

(i) $h(\omega) = \hat{f}(\omega)$ with values in E is the Fourier-Laplace transfom of $f \in LT(E)$

(ii) (a) h is holomorphic in some half plane $\{\omega \in \mathbb{C}; \mathrm{Im}\omega > \omega_I^0\}$ with values in E and

(b) $\exists \omega_1 > \omega_I^0, C > 0$ and $k \geq 0$ such that $\|h(\omega)\|_E \leq C(1+|\omega|)^k \forall \omega$ with $\mathrm{Im}(\omega) \geq \omega_1$.

Theorem 9.2 ([57]). *The following statements are equivalent:*

(i) (i) of the Paley-Wiener theorem hold and additionally with $\mathrm{supp}\, f \subset [T, \infty[$

(ii) (ii) and (a) of the Paley-Wiener theorem hold and $\exists\ \omega_1 > \omega_I^0, C > 0$ and $k \geq 0$ such that $\|h(\omega)\|_E \leq C(1+|\omega|)^k e^{(-\mathrm{Im}(\omega))T} \quad \forall \omega$ with $\mathrm{Im}(\omega) \geq \omega_1$.

Theorem 9.3 (Parseval theorem, [57]). *If $f, g \in L^1_{loc}(\mathbb{R}_+, E) \cap LT(E)$, it yields:*

$$\frac{1}{2\pi} \int_{-\infty+i\omega_I}^{\infty+i\omega_I} \langle \hat{f}(\omega), \hat{g}(\omega) \rangle_E \ d\omega = \int_{-\infty}^{\infty} e^{-2\omega_I t} \langle f(t), g(t) \rangle_E dt \ ,$$

where $\langle \cdot, \cdot \rangle_E$ is the hermitian product of E and $\omega_I \geq \max(\omega(f), \omega(g))$.

9.3 Road map with spaces and norms

In this section, we write a brief translation of the norms and spaces used in this thesis with the one used by Ha-Duong in the lecture notes [57]. Ha-Duong defines the Hilbert space

$$H^{1,1}_{\sigma,\Omega} = \{u \in LT(\sigma, H^1(\Omega)) : \int_{\mathbb{R}+i\sigma} \|\hat{u}\|_{1,\omega,\Omega} d\omega < \infty\}$$

with

$$\|u\|^2_{1,1,\sigma} = \int_{\mathbb{R}+i\sigma} \|\hat{u}\|^2_{1,\omega,\Omega} d\omega \ ,$$

whereas it corresponds to Definition 2.4 except for the infimum of σ:

$$H^0_\sigma(\mathbb{R}, H^1(\Omega)) = \{u \in LT(H^1(\Omega)) : \|u\|_{0,1,\sigma,\Omega} < \infty\}$$

with

$$\|u\|_{0,1,\sigma,\Omega} = (\int_{\mathbb{R}+i\sigma} \|\hat{u}\|^2_{1,\omega,\Omega} d\omega)^{1/2}$$

and $\|\hat{u}\|_{1,\omega,\Omega}$ as in (2.21). Furthermore using Parseval's equality Ha-Duong derives:

$$u \in H^{1,1}_{\sigma,\Omega} \Leftrightarrow u \in LT(\sigma, H^1(\Omega)) \ \text{ and } \int_{-\infty}^{\infty} e^{-2\sigma t} \int_\Omega |\nabla u(x,t)|^2 + |\dot{u}(x,t)|^2 dx dt < \infty \ .$$

Therefore $e^{-\sigma t} u \in L^2(\mathbb{R}, H^1(\Omega)) \cap H^1(\mathbb{R}, L^2(\Omega))$. Hence it is used to define for finite times:

$${}_0H^{1,1}(\Omega \times [0,T]) = \{u \in L^2([0,T], H^1(\Omega)) \cap H^1([0,T], L^2(\Omega)) \text{ with } u(\cdot,0) = 0\}$$

with the norm as in Lions, Magenes [72, Chapter 4.2]

$$(\|u\|^2_{L^2([0,T],H^1(\Omega))} + \|u\|_{H^1([0,T],L^2(\Omega))})^{1/2} = \Big(\int_0^T \|u\|_{H^1(\Omega)} dt + \|u\|^2_{H^1([0,T],L^2(\Omega))} \Big)^{1/2}, \tag{9.12}$$

where $H^s([0,T], L^2(\Omega))$ is defined as $H^s([0,T])$ for $s \geq 0$. Here we say u needs to be "$H^1(\Omega)$ in space" and "$H^1([0,T])$ in time". Due to Cauchy-Schwarz inequality

$$|u(x,t)|^2 = \Big| \int_0^t \dot{u}(x,r) dr \Big|^2 = \Big| \int_0^t 1 \cdot \dot{u}(x,r) dr \Big|^2 \leq \Big(\int_0^t 1 dr \Big) \Big(\int_0^t |\dot{u}(x,r)|^2 dr \Big) \leq t \Big(\int_0^t |\dot{u}(x,r)|^2 dr \Big)$$

the energy norm

$$\int_0^T E(u)(t) dt = \int_0^T \frac{1}{2} (\int_\Omega |\nabla u|^2 + |\dot{u}|^2 dx) dt$$

is equivalent to the norm (9.12) in this space.

In this thesis however for a finite time interval, we have

$$H^0([0,T], H^1(\Omega)) = \{\nabla u \text{ and } \dot{u} \text{ are square integrable in } \Omega \text{ and } [0,T] \text{ with } u(\cdot,0) = 0\},$$

where the norm is defined as well in Lions, Magenes [72, Chapter 4.2]

$$\|u\|_{0,1,\Omega\times[0,T]} := \Big(\int_0^T \|u\|^2_{H^1(\Omega)} dt + \int_\Omega \|u\|^2_{H^1([0,T])} dx \Big)^{1/2} \ .$$

For the trace spaces, Ha-Duong defines

$$H^{1/2,1/2}_{\sigma,\Gamma} = \{u \in LT(\sigma, H^{1/2}(\Gamma)) : \int_{\mathbb{R}+i\sigma} |\hat{u}|^2_{1/2,\omega,\Gamma} d\omega < \infty\} \ ,$$

whereas in Definition 2.4 except for the infimum of σ:

$$H^0_\sigma(\mathbb{R}, H^{1/2}(\Gamma)) = \{u \in LT(H^{1/2}(\Gamma)) : \|u\|_{0,1/2,\sigma,\Gamma} < \infty\}$$

with the norm

$$\|u\|_{0,1/2,\sigma,\Gamma} = \Big(\int_{\mathbb{R}+i\sigma} \|\hat{u}\|^2_{1/2,\omega,\Gamma} \Big)^{1/2} \ .$$

Here the definition of $|\hat{u}|_{1/2,\omega,\Gamma} = \|\hat{u}\|_{1/2,\omega,\Gamma}$ coincide.

For a finite time interval $[0,T]$, Ha-Duong passes the definition of ${}_0H^{1,1}(\Omega \times [0,T])$ on the trace space of ${}_0H^{1,1}(\Omega \times [0,T])$:

$${}_0H^{1/2,1/2}(\Gamma \times [0,T]) = L^2([0,T], H^{1/2}(\Gamma)) \cap {}_0H^{1/2}([0,T], L^2(\Gamma)) \ ,$$

where the subscript 0 indicates for u regular enough in time $u(\cdot, 0) = 0$.

Therefore we say in this case u needs to be "$H^{1/2}(\Gamma)$ in space" and "$H^{1/2}([0,T])$ in time". In this thesis we write

$$H^0([0,T], H^{1/2}(\Gamma)) := \{u : u(\cdot,0) = 0, \ \Big(\int_0^T \|u\|^2_{H^{1/2}(\Gamma)} dt + \int_\Omega \|u\|^2_{H^{1/2}([0,T])} dx\Big)^{1/2} < \infty\}$$

with the norm

$$\|u\|_{0,1/2,\Gamma\times[0,T]} = \Big(\int_0^T \|u\|^2_{H^{1/2}(\Gamma)} dt + \int_\Omega \|u\|^2_{H^{1/2}([0,T])} dx\Big)^{1/2} \ .$$

The space $H^0([0,T], H^{-1/2}(\Gamma))$ is defined as the dual space of $H^0([0,T], H^{1/2}(\Gamma))$ similarly with $\|u\|_{0,-1/2,\Gamma\times[0,T]}$ the dual norm of $\|u\|_{0,1/2,\Gamma\times[0,T]}$.

Further Ha-Duong considers the Hilbert space for $k \in \mathbb{N}_0$

$$H^{k,1/2,1/2}_{\sigma,\Gamma} = \{u \in LT(H^{1/2}(\Gamma)) : \|u\|_{H^{k,1/2,1/2}_{\sigma,\Gamma}} < \infty\}$$

with the norm

$$\|u\|_{H^{k,1/2,1/2}_{\sigma,\Gamma}} = \int_{\mathbb{R}+i\sigma} |\omega|^k |\hat{u}|_{1/2,\omega,\Gamma} d\omega \ .$$

With $\mathrm{Im}\omega \geq \sigma_0 > 0$ and

$$(|\omega|^2 + |\xi|^2)^{1/2} \leq (1 + |\omega|^2)^{1/2} + (1 + |\xi|^2)^{1/2} \leq 2(\frac{1+\sigma_0^2}{\sigma_0^2})^{1/2} (|\omega|^2 + |\xi|^2)^{1/2} \ ,$$

we get that $e^{-\sigma t} u \in H^k(\mathbb{R}, H^{1/2}(\Gamma)) \cap H^{k+1/2}(\mathbb{R}, L^2(\Gamma))$. For example $k = 1$

$$\begin{aligned} H^{1,1/2,1/2}_{\sigma,\Gamma} = \{u \in LT(H^{1/2}(\Gamma)) : \dot{u} \in H^{1/2,1/2}_{\sigma.\Gamma}\} &= \{u \in LT(H^{1/2}(\Gamma)) : \|u\|_{H^{1,1/2,1/2}_{\sigma,\Gamma}} < \infty\} \\ &= H^1(\mathbb{R}, H^{1/2}(\Gamma)) \cap H^{3/2}(\mathbb{R}, L^2(\Gamma)) \end{aligned}$$

possesses the norm

$$\|u\|_{H^{1,1/2,1/2}_{\sigma,\Gamma}} = \int_{\mathbb{R}+i\sigma} |\omega| |\hat{u}|_{1/2,\omega,\Gamma} d\omega \ ,$$

since a Fourier transform leads a time derivative to $|\omega|$. Therefore we say u has to be "$H^{1/2}(\Gamma)$ in space" and "$H^{3/2}(\mathbb{R})$ in time". $H^{0,1/2,1/2}_{\sigma,\Gamma}$ corresponds to $H^{1/2,1/2}_{\sigma,\Gamma}$.

We define the spaces in this thesis as in Definition 2.4

$$H^k_\sigma(\mathbb{R}, H^{1/2}(\Gamma)) = \{u \in LT(H^{1/2}(\Gamma)) : \|u\|_{k,1/2,\sigma,\Gamma} < \infty\}$$

with the norm

$$\|u\|_{k,1/2,\sigma,\Gamma} = \Big(\int_{\mathbb{R}+i\sigma} |\omega|^{2k} \|\hat{u}\|^2_{1/2,\omega,\Gamma} d\omega \Big)^{1/2} \ .$$

Analogously for a finite time interval, Ha-Duong defines for $k \in \mathbb{N}$

$$\begin{aligned} &H^k([0,T], H^{1/2}(\Gamma)) \cap {}_0H^{k+1/2}([0,T], L^2(\Gamma)) \\ &= \{u : u(\cdot,0) = 0, u^{(k)} \in H^0([0,T], H^{1/2}(\Gamma)) \cap H^{1/2}([0,T], L^2(\Gamma))\} \ , \end{aligned}$$

where $f^{(k)}(x,t) = \partial_t^k f(x,t)$ denotes the $k-$th derivative in time, and with the norm

$$\Big(\|u\|^2_{L^2([0,T],H^{1/2}(\Gamma))} + \|u\|^2_{H^{k+1/2}([0,T],L^2(\Gamma))} \Big)^{1/2} \ .$$

Therefore for $k \in \mathbb{N}_0, r \geq 0$ we consider the space

$$H^k([0,T], H^r(\Gamma)) \cap {}_0H^{k+r}([0,T], L^2(\Gamma))$$

with the following norm:

$$\Big(\|u\|^2_{L^2([0,T],H^r(\Gamma))} + \|u\|^2_{H^{k+r}([0,T],L^2(\Gamma))} \Big)^{1/2} \ .$$

This corresponds in this thesis the space

$$H^k([0,T], H^r(\Gamma)) = \{u : u(\cdot,0) = 0 \ , \Big(\int_0^T \|u\|^2_{H^r(\Gamma)} dt + \int_\Gamma \|u\|^2_{H^{k+r}([0,T])} ds_x \Big)^{1/2} < \infty\}$$

with the norm

$$\|u\|_{k,r,\Gamma\times[0,T]} = \Big(\int_0^T \|u\|^2_{H^r(\Gamma)} dt + \int_\Gamma \|u\|^2_{H^{k+r}([0,T])} ds_x \Big)^{1/2} \ .$$

For negative indices k, r we use the dual space together with the dual norm of $\|u\|_{-k,-r,\Gamma\times[0,T]}$.

Altogether we write a brief translation of the norms

In this thesis	In the lecture notes of Ha-Duong in [57]
$\|u\|_{0,1,\sigma,\Omega}$	$\|u\|_{1,1,\sigma}$
$\|u\|_{0,1/2,\sigma,\Gamma}$	$\|u\|_{H^{1/2,1/2}_{\sigma,\Gamma}}$
$\|u\|_{s,r,\sigma,\Gamma}$	$\|u\|_{H^{s,r,r}_{\sigma,\Gamma}}$
$\|u\|_{0,1,\Omega\times[0,T]}$	$\|u\|^2_{L^2([0,T],H^1(\Omega))}+\|u\|^2_{H^1([0,T],L^2(\Omega))}=\int_0^T\|u\|^2_{H^1(\Omega)}dt+\|u\|^2_{H^1([0,T],L^2(\Omega))}$
$\|u\|_{0,\frac{1}{2},\Gamma\times[0,T]}$	$\|u\|^2_{L^2([0,T],H^{\frac{1}{2}}(\Gamma))}+\|u\|^2_{H^{\frac{1}{2}}([0,T],L^2(\Gamma))}=\int_0^T\|u\|^2_{H^{\frac{1}{2}}(\Gamma)}dt+\|u\|^2_{H^{\frac{1}{2}}([0,T],L^2(\Gamma))}$
$\|u\|_{s,r,\Gamma\times[0,T]}$	$\|u\|^2_{L^2([0,T],H^r(\Gamma))}+\|u\|^2_{H^{s+r}([0,T],L^2(\Gamma))}=\int_0^T\|u\|^2_{H^r(\Gamma)}dt+\|u\|^2_{H^{s+r}([0,T],L^2(\Gamma))}$

With this setting, we get the trace theorem for a finite time interval $[0,T]$.

Lemma 9.4 (Chapter 4, Lemma 5 in [55]). *For $u \in H^0([0,T],H^1(\Omega))$, the trace of u, $u|_{\Gamma\times[0,T]}$ is well-defined, which fulfills for a constant C depending on the space Ω and T*

$$\|u|_{\Gamma\times[0,T]}\|_{0,1/2,\Gamma\times[0,T]} \leq C\|u\|_{0,1,\Omega\times[0,T]}$$

Lemma 9.5 (Chapter 4, Lemma 7 in [55]). *For $u \in H^0([0,T],H^1(\Omega))$ with u satisfying the homogeneous wave equation in $\Omega\times[0,T]$, the normal derivative of the trace $\frac{\partial u}{\partial n}$ is well defined in $H^0([0,T],H^{-1/2}(\Gamma))$, fulfilling with a constant C depending on Ω*

$$\|\frac{\partial u}{\partial n}\|_{0,-1/2,\Gamma\times[0,T]} \leq C\|u\|_{0,1,\Omega\times[0,T]}$$

Remark 9.1. *In the proof of this lemma in [55], we require test functions to be zero at the boundaries 0 and T. Therefore we need the dual space of functions in $H^0([0,T],H^{1/2}(\Gamma))$ with $v(\cdot,0)=v(\cdot,T)=0$. This space is a subspace of $H^0([0,T],H^{1/2}(\Gamma))$ and hence we may estimate further by taking the dual space of $H^0([0,T],H^{1/2}(\Gamma))$.*

9.4 Computation of the retarded single layer potential with $\sigma > 0$

In this section, together with the discretization spaces as in Section 2.3, we consider the retarded single layer potential as in Subsection 2.3.1 with $\sigma > 0$. We use piecewise constant ansatz function in space and in time, i.e.

$$p_{h,\triangle t}(x,t) = \sum_{m=1}^{N_t}\sum_{i=1}^{N_s} p_i^m \gamma^m_{\Delta t}(t)\psi^i_h(x) \quad \in V^{0,0}_{h,\Delta t}$$

and piecewise constant test functions in space and time, i.e $q_{h,\triangle t}(x,t) = \gamma^n_{\Delta t}(t)\psi^j_h(x) \in V^{0,0}_{h,\Delta t}$ for $1 \le n \le N_t$ and $1 \le j \le N_s$. We obtain for the left hand side:

$$\sum_{m=1}^{N_t}\sum_{i=1}^{N_s} p_i^m \int_0^\infty e^{-2\sigma t} \int_\Gamma \int_\Gamma \frac{1}{4\pi} \frac{\gamma^m_{\Delta t}(t-|x-y|)\psi^i_h(y)}{|x-y|} \dot\gamma^n_{\Delta t}(t)\psi^j_h(x)\, ds_y ds_x dt$$
$$= \sum_{m=1}^{N_t}\sum_{i=1}^{N_s} p_i^m \int_\Gamma \int_\Gamma \Big[\int_0^\infty e^{-2\sigma t}\gamma^m_{\Delta t}(t-|x-y|)\dot\gamma^n_{\Delta t}(t)dt \Big] \frac{\psi^i_h(y)\psi^j_h(x)}{4\pi|x-y|}\, ds_y ds_x \ . \qquad (9.13)$$

For the time integral, we receive:

$$\int_0^\infty e^{-2\sigma t}\gamma^m_{\Delta t}(t-|x-y|)\dot\gamma^n_{\Delta t}(t)dt = \int_0^\infty e^{-2\sigma t}\gamma^m_{\Delta t}(t-|x-y|)(\delta(t-t_{n-1}) - \delta(t-t_n))dt$$
$$= e^{-2\sigma t_{n-1}}\gamma^m_{\Delta t}(t_{n-1}-|x-y|) - e^{-2\sigma t_n}\gamma^m_{\Delta t}(t_n-|x-y|) = e^{-2\sigma t_{n-1}}\chi_{E_{n-m-1}} - e^{-2\sigma t_n}\chi_{E_{n-m}} \ .$$

Altogether we get for (9.13):

$$\sum_{m=1}^{N_t}\sum_{i=1}^{N_s} p_i^m \Big(\int_\Gamma \int_\Gamma \big[e^{-2\sigma t_{n-1}}\chi_{E_{n-m-1}} - e^{-2\sigma t_n}\chi_{E_{n-m}} \big] \frac{\psi^i_h(y)\psi^j_h(x)}{4\pi|x-y|}\, ds_y ds_x \Big)$$
$$= \sum_{m=1}^{N_t}\sum_{i=1}^{N_s} p_i^m \Big(\iint\limits_{E_{n-m-1}} \frac{\psi^i_h(y)\psi^j_h(x)}{4\pi|x-y|} e^{-2\sigma t_{n-1}} ds_y ds_x - \iint\limits_{E_{n-m}} \frac{\psi^i_h(y)\psi^j_h(x)}{4\pi|x-y|}\, ds_y ds_x e^{-2\sigma t_n} \Big) \ .$$

We approximate the right hand side f as $\sum_{m=1}^{N_t} f^m \gamma^m_{\Delta t}(t)$ with $f^m = f(x,t_m)$. We get

$$\int_0^\infty \int_\Gamma e^{-2\sigma t} \Big(\sum_{m=1}^{N_t} f^m \gamma^m_{\Delta t}(t)\Big) \dot\gamma^m_{\Delta t}(t)\psi^j_h(x) ds_x dt$$
$$= \sum_{m=1}^{N_t} \int_\Gamma \Big(\int_0^\infty e^{-2\sigma t}\gamma^m_{\Delta t}(t)\dot\gamma^n_{\Delta t}(t)dt \Big) f^m \psi^j_h(x) ds_x$$
$$= \sum_{m=1}^{N_t} \int_\Gamma \Big(\int_0^\infty e^{-2\sigma t}\gamma^m_{\Delta t}(t)\delta(t-t_{n-1}) - \delta(t-t_n)dt \Big) f^m \psi^j_h(x) ds_x$$
$$= \sum_{m=1}^{N_t} \int_\Gamma (e^{-2\sigma t_{n-1}}\gamma^m_{\Delta t}(t_{n-1}) - e^{-2\sigma t_n}\gamma^m_{\Delta t}(t_n)) f^m \psi^j_h(x) ds_x \ .$$

We remember

$$\gamma^m_{\Delta t}(t_n) = \begin{cases} 1 & \text{if } n = m \\ 0 & \text{else} \end{cases} \ .$$

Therefore we obtain

$$\int_\Gamma (f^{n-1}e^{-2\sigma t_{n-1}} - f^n e^{-2\sigma t_n})\psi^j_h(x) ds_x \ . \qquad (9.14)$$

We compute (9.14) with the standard Gauss-quadrature. Now for $n = 1$ (first timestep), remember that the integral over E_k disappears if k is a negative integer. We get for the left hand side:

$$\sum_{m=1}^{N_t}\sum_{i=1}^{N_s} p_i^m \Big(\iint\limits_{E_{1-m-1}} \frac{\psi^i_h(y)\psi^j_h(x)}{4\pi|x-y|} e^{-2\sigma t_0} ds_y ds_x - \iint\limits_{E_{1-m}} \frac{\psi^i_h(y)\psi^j_h(x)}{4\pi|x-y|}\, ds_y ds_x e^{-2\sigma t_1} \Big)$$
$$= -\sum_{i=1}^{N_s} p_i^1 \Big(\iint_{E_0} \frac{\psi^i_h(y)\psi^j_h(x)}{4\pi|x-y|} e^{-2\sigma t_1} ds_y ds_x \Big) \ .$$

So we need to solve:

$$-\sum_{i=1}^{N_s} p_i^1 \Big(\iint_{E_0} \frac{\psi_h^i(y)\psi_h^j(x)}{4\pi|x-y|} e^{-2\sigma t_1} ds_y ds_x \Big) = \int_\Gamma (f^0 - f^1 e^{-2\sigma t_1}) \psi_h^j(x) ds_x \ .$$

For an arbitrary timestep n, we need to solve:

$$\begin{aligned} &= \sum_{m=1}^{N_t} \sum_{i=1}^{N_s} p_i^m \Big(\iint_{E_{n-m-1}} \frac{\psi_h^i(y)\psi_h^j(x)}{4\pi|x-y|} e^{-2\sigma t_{n-1}} ds_y ds_x - \iint_{E_{n-m}} \frac{\psi_h^i(y)\psi_h^j(x)}{4\pi|x-y|} e^{-2\sigma t_n \ ds_y ds_x} \Big) \\ &= \int_\Gamma (f^{n-1} e^{-2\sigma t_{n-1}} - f^n e^{-2\sigma t_n}) \psi_h^j(x) ds_x \ . \end{aligned}$$

Now dividing through $e^{-2\sigma t_n}$:

$$\begin{aligned} \sum_{m=1}^{N_t} \sum_{i=1}^{N_s} V^{n-m} p_i^m &:= \sum_{m=1}^{N_t} \sum_{i=1}^{N_s} p_i^m \Big(\iint_{E_{n-m-1}} \frac{\psi_h^i(y)\psi_h^j(x)}{4\pi|x-y|} e^{2\sigma(\Delta t)} ds_y ds_x - \iint_{E_{n-m}} \frac{\psi_h^i(y)\psi_h^j(x)}{4\pi|x-y|} ds_y ds_x \Big) \\ &= \int_\Gamma (f^{n-1} e^{2\sigma(\Delta t)} - f^n) \psi_h^j(x) ds_x =: F^n, \end{aligned}$$

where V^{n-m} is a matrix with entries containing the two integrals over lightcones E_{n-m-1} and E_{n-m}. Now we can solve this system with a MOT (marching-on-in-time) scheme. Therefore for each timestep $n = 1, 2, \ldots, N_t$, we solve:

$$\sum_{m=1}^{n} V^{n-m} p^m = F^n \ \Leftrightarrow \ V^0 p^n = F^n - \sum_{m=1}^{n-1} V^{n-m} p^m \ .$$

The implementation is almost the same as in Algorithm 1 with the difference that the integral over E_{n-2} and the term f^{n-1} are multiplied with $e^{2\sigma(\Delta t)}$.

We continue with a numerical example.

Example 9.1. *We set the right hand side $f(x,t) = f(t) = t^4 e^{-2t}$. The exact solution is in case of an unit sphere given in the Phd thesis of Veit [99] with $p(x,t) = p(t) = 2\sum_{k=0}^{\lfloor t/2 \rfloor} \dot{f}(t-2k)$. The numerical solutions are computed for $\Delta t = 0.01$ till time 16, with an icosahedron with 320 triangles approximating the unit sphere.*

Figure 9.1 presents the L^2-norm of the exact solution together with the numerical solutions for $\sigma = 0, 0.01, 0.5$. We observe that the solution for $\sigma = 0$ is almost identical as the solution for $\sigma > 0$. Therefore it seems reasonable to use $\sigma = 0$ for all retarded potential boundary integral equations, since the implementation gets easier. For this computation the L^2–norm of the numerical solution differs from the L^2–norm of the exact solution more for larger times. This could be due to the fact that the geometric errors are accumulating more as more time passes.

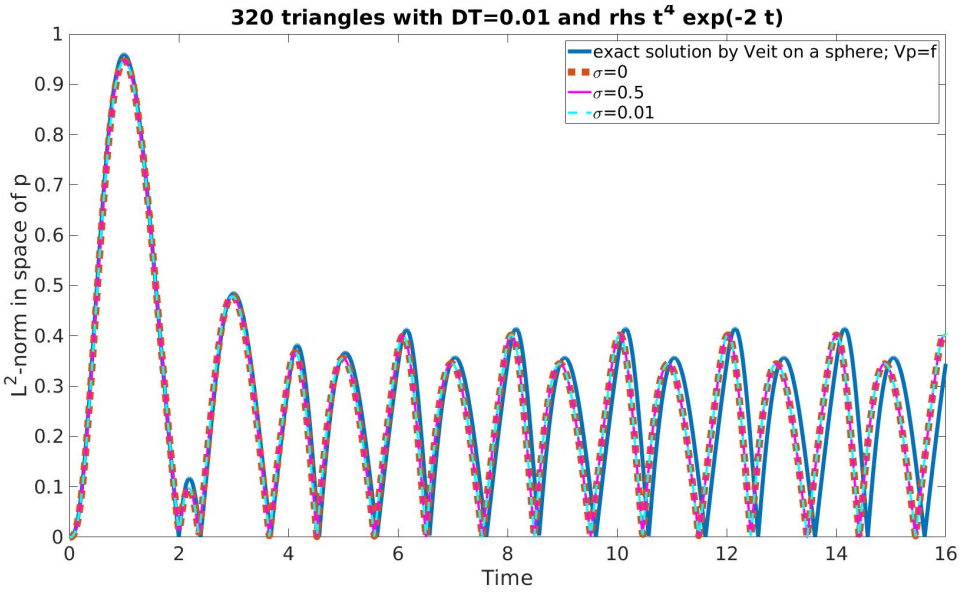

Figure 9.1: L2-Norm of the numerical solution of Example 9.1

9.5 A documentation of the operators used in maiprogs

In this section we write a listing of the scripts to run the computations with MAIPROGS. MAIPROGS is a batch control language (bcl). A bcl-script in MAIPROGS has commands, which are translated into Fortran90/95 commands. In order to implement our own code, we need to understand the syntax of Fortran90/95 and see [76]. In order to optimize the code an understanding of parallelization is very helpful. For details about MAIPROGS, see [76, 85, 77]. In our case the bcl-scipts are executed by typing in the corresponding folder in a console:⟨path to folder fo3c⟩/maicoup3 ⟨somebclscript⟩.coup3.

9.5.1 A bcl-script for the retarded single layer potential

```
!!!!!!!!!!!!!!!!!!!!!!!!!!!!!!!!!!!!!!!!!!!!!!!!!!!!!!!!!!!!!!!!!!!!!!!!!!!!
! RETARDED SINGLE LAYER POTENTIAL (RV)
!!!!!!!!!!!!!!!!!!!!!!!!!!!!!!!!!!!!!!!!!!!!!!!!!!!!!!!!!!!!!!!!!!!!!!!!!!!!

! here rhs = g(t) = t^4 * exp(-2 * t) ; R=8000

defproblem('Laplace','DTSRC15',315,'Dirichlet BEM, transient sound radiation',3)
setprob(spline='D',mat='D.RV.D',dat='D=u0')
setsp('D',(/2,3/),0,0,1,1,1)
defmatrix('RV','sparse-row','RV')
enddefproblem
```

```
!Set variables
I=1600 !number of time intervalls 1600
DT=0.01 !16.0/I !Time step size
MZERO=100
REF=2 ! is used later in icosahedron to get 320 triangles
K=1 !is later used in the loop for the right hand side
! ANZ=16 !number of subdivisions in space mesh (commented, may used for other meshes like a screen or a cube)
R=8000 ! a number which is later used to find the right hand side
QUADK=8 ! Amount of Gauss quadrature points for the matrices
QUAD=8

! geometry('Square',0,bmode=(/2,3/),gm='gm') defines a screen mesh (commented)

#ti
problem('Laplace',315)
icosahedron('uniform',refine=REF,p=0,spline='D')
timemesh(deltaT=DT,noint=I,ansatz=0,test=-1,ctyp=0)
setretoperator('RV',0,-1,0,0) !pw. constant vs pw. constant
elemsize('D')
! open(1) 'exdaten/mesh1.dat'
! #taf. 'D'
! #px. 'D'
! close(1)
open(2) 'l2normsinglelayerpwconstant.'//I//'_'//REF//'_.dat'
write(2) '# DOF, NoTimeIntervalls, hmax, DeltaT, CFL'
write(2) '#'//DOF,I,MYHMAX,DELTAT,CFL
write(2) '# Time, Timestep, Norm, Matrix-CPU, Matrix-WALL, Performance'
timediff(0)
settime(1)
setquadpara(quadpoints=QUADK,ijn_radius=5,ijn_angle=5,sigma=0.17)
matrix(quadrature='numeric',gqna=QUADK,gqnb=QUADK,ijn=5,sigma=0.17);
T=SEC;WT=WSEC
PER=T/WT
! open(1) 'exdaten/matrix_parallel0.dat'
! #fk. 'RV' 'thin'
! close(1)
! symch 'RV'
!show('sparse')
lft 24 R - R
solve(eps=1.0d-13,mdi='x=0',mit='CG',abrflag=1,quiet=1)
open(1) 'ddd'//1//'_'//REF//'.dat'
! #taf. 'D' ! #px. 'D' #cx. 'D'
```

```
close(1)
defspline('D[1]=Spline(D)')
eval('D[1]=D')
#no. 'L2' 'D[1]'
!#err. 16 R 'L2' 0 'D[1]'
TIME=1*DT
write(2) TIME,1,NORM,T,WT,PER
! write(2) TIME,1,NORM,T

do N=2,I
settime(N)
J=N-1
timediff(J)
!Test if lightcone passed body
! if (MZERO>0); then
defmatrix('RV[J]','sparse-row','RV')
! ZEIT1=SEC
setquadpara(quadpoints=QUAD,ijn_radius=5,ijn_angle=5,sigma=0.17)
matrix(quadrature='numeric',gqna=QUAD,gqnb=QUAD,ijn=5,sigma=0.17,
arg='D.RV[J].D');T=SEC;WT=WSEC
PER=T/WT
! open(1) 'exdaten/matrix_parallel2'//J//'.dat'
! #fk. 'RV[J]' 'thin'
! close(1)
! ZEIT2=SEC
zeromatrix('RV[J]')
! symch 'RV['//J//']'
! show('sparse')
! else
! K=K+1
! ZEIT1=0
! ZEIT2=0
! show('sparse')
! fi
lft 9 R - R
!Compute rhs (MOT-scheme)
do M=K,N-1
MN=N-M
eval('Rhs(D)=Rhs(D)-Matrix(RV[MN])*D[M]')
continue
solve(eps=1.0d-10,mdi='x=0',mit='CG',abrflag=1,quiet=1)
#rno.
defspline('D[N]=Spline(D)')
```

```
eval('D[N]=D')
#no. 'L2' 'D[N]'
! #err. 16 R 'L2' 0 'D[J]'
open(1) 'ddd'//N//'_'//REF//'.dat'
! #taf. 'D'
! #px. 'D'
#cx. 'D'
close(1)
TIME=N*DT
write(2) TIME,N,NORM,T,WT,PER
! write(2) TIME,N,NORM,T
continue
end
```

9.5.2 A bcl-script for the retarded double layer potential

```
!!!!!!!!!!!!!!!!!!!!!!!!!!!!!!!!!!!!!!!!!!!!!!!!!!!!!!!!!!!!!!!!!!!!!!!!!!!!
! RETARDED DOUBLE LAYER POTENTIAL (RI+RK)=(1/2 I + K)
!!!!!!!!!!!!!!!!!!!!!!!!!!!!!!!!!!!!!!!!!!!!!!!!!!!!!!!!!!!!!!!!!!!!!!!!!!!!

! hier: rhs= sin(2*t)^2 * t * exp(-t) ; R=8010

defproblem('Laplace','DTSRC15',330,'Dirichlet direct BEM, transient sound radiation',3)
setprob(spline='D',mat='D.RK.D:DT*D.RI.D',dat='D=u0')
setsp('D',(/2,3/),0,0,1,1,1,'D')

defmatrix('RK','sparse-row','RK')
defmatrix('RI','sparse-row','RI')
enddefproblem

!Set variables
I=1000 !number of time intervalls
DT=0.01 !Time step size
MZERO=100
K=1
L=1
QUAD=8
QUADK=8
R=8000

#ti
#time BEGINN WBEGINN
problem('Laplace',330)
```

```
icosahedron('uniform',refine=1,p=0,spline='D')

!open(1) 'mesh1.dat'
! #taf. 'D'
!#pnod. 'D'
!close(1)

timemesh(deltaT=DT,noint=I,ansatz=0,test=0,ctyp=0)

lft 24 R - R

setretoperator('RK',0,0,0,0)

elemsize('D')

open(4) 'setretoperator(0,0,0,0)_rhsgamma_monomials_pwconst'//DT:5//'.dat'
write(4) ' # DOF, NoTimeIntervalls, hmax, DeltaT, CFL '
write(4) ' #//DOF,I,MYHMAX,DELTAT,CFL '
write(4) ' # Time, Timestep, Norm, Error '
timediff(0)
settime(1)

setquadpara(quadpoints=QUADK,ijn_radius=5,ijn_angle=5,sigma=0.17)
matrix(quadrature='numeric',gqna=QUADK,gqnb=QUADK,ijn=5,sigma=0.17);
T=SEC;WT=WSEC

solve(eps=1.0d-10,mdi='x=0',mit='GMRES',abrflag=1,quiet=1)
#rno.
defspline('D[1]=Spline(D)')
eval('D[1]=D')

!open(1) 'indirect_discsol1.dat'
!#taf. 'D'
!#pnod. 'D'
!#rci. 'D'
!#cx. 'D'
!#cnod. 'D'
!close(1)

#no. 'L2' 'D[1]'

TIME=1*DT
```

```
write(4) TIME,1,NORM,T,WT

do F=2,I
! open(1) 'indirect_discsol'//F//'.dat'
settime(F)
J=F-1
timediff(J)
!Test if lightcone passed body
! if ( 100 > 0); then
defmatrix('RK[J]','sparse-row','RK')

setquadpara(quadpoints=QUAD,ijn_radius=5,ijn_angle=5,sigma=0.17)
matrix(quadrature='numeric',gqna=QUAD,gqnb=QUAD,ijn=5,sigma=0.17,
arg='D.RK[J].D');TRK=SEC;WTRK=WSEC

zeromatrix('RK[J]')

! else
! K=K+1
! fi

lft 24 R - R

!Compute rhs: add retarded double layer pot. to rhs
do M=K,F-1
MF=F-M
eval('Rhs(D)=Rhs(D)-Matrix(RK[MF])*D[M]')
continue

solve(eps=1.0d-10,mdi='x=0',mit='GMRES',abrflag=1,quiet=1)
#rno.
defspline('D[F]=Spline(D)')
eval('D[F]=D')

! open(1) 'indirect_discsol'//F//'.dat'
!#taf. 'D'
!#pnod. 'D'
!#rci. 'D'
! #cx. 'D'
! #cnod. 'D'
! close(1)

#no. 'L2' 'D[F]'
```

```
TIME=F*DT
write(4) TIME,F,NORM,WTRK,WTRKIM
continue
#time ENDE WENDE
print 'Dauer : '//ENDE-BEGINN
end
```

9.5.3 A bcl-scriot for the adjoint double layer potential

```
!!!!!!!!!!!!!!!!!!!!!!!!!!!!!!!!!!!!!!!!!!!!!!!!!!!!!!!!!!!!!!!!!!!!!!!!!!!
! RETARDED ADJOINT DOUBLE LAYER POTENTIAL (-RI+RK)=(-1/2 I + K')
!!!!!!!!!!!!!!!!!!!!!!!!!!!!!!!!!!!!!!!!!!!!!!!!!!!!!!!!!!!!!!!!!!!!!!!!!!!

!hier: rhs = t^4 * exp(-2*t) ; R=8000

defproblem('Laplace','DTSRC15',330,'Neumann direct BEM, transient sound radiation',3)
setprob(spline='D',mat='D.RKd.D:-DT*D.RI.D',dat='D=t0')
setsp('D',(/2,3/),0,0,1,1,1,'D')

defmatrix('RKd','sparse-row','RKd')
defmatrix('RI','sparse-row','RI')
enddefproblem

!Set variables
I=480 !number of time intervalls
DT=0.025 !Time step size
MZERO=100
K=1
L=1
QUAD=8
QUADK=8
R=8000

#ti
#time BEGINN WBEGINN
problem('Laplace',330)

icosahedron('uniform',refine=1,p=0,spline='D')

open(1) 'mesh1.dat'
! #taf. 'D'
! #taf. 'N'
#pnod. 'D'
```

```
close(1)
timemesh(deltaT=DT,noint=I,ansatz=1,test=0,ctyp=0)
lft 24 R - R
setretoperator('RKd',0,0,0,0)

elemsize('D')


open(4) 'indirect_neumann_sphere_openmp'//DT:5//'_4.dat'
write(4) '# DOF, NoTimeIntervalls, hmax, DeltaT, CFL'
write(4) '#'//DOF,I,MYHMAX,DELTAT,CFL
write(4) '# Time, Timestep, Norm, Error'
timediff(0)
settime(1)

setquadpara(quadpoints=QUADK,ijn_radius=5,ijn_angle=5,sigma=0.17)
matrix(quadrature='numeric',gqna=QUADK,gqnb=QUADK,ijn=5
,sigma=0.17);T=SEC;WT=WSEC

solve(eps=1.0d-10,mdi='x=0',mit='GMRES',abrflag=1,quiet=1)
#rno.
defspline('D[1]=Spline(D)')
eval('D[1]=D')

open(1) 'indirect_discsol1.dat'
#taf. 'D'; #pnod. 'D'; #rci. 'D'; #cx. 'D'; #cnod. 'D'; close(1)

#no. 'L2' 'D[1]'

TIME=1*DT
write(4) TIME,1,NORM,T,WT

do F=2,I
! open(1) 'indirect_discsol'//F//'.dat'
settime(F)
J=F-1
timediff(J)
!Test if lightcone passed body
! if ( 100>0); then
defmatrix('RKd[J]','sparse-row','RKd')
setquadpara(quadpoints=QUAD,ijn_radius=5,ijn_angle=5,sigma=0.17)
matrix(quadrature='numeric',gqna=QUAD,gqnb=QUAD,ijn=5,sigma=0.17,
arg='D.RKd[J].D');TRK=SEC;WTRK=WSEC
```

```
zeromatrix('RKd[J]')
!# else !# K=K+1 !# fi
lft 24 R - R


!Compute rhs: add retarded single layer pot. to rhs
do M=K,F-1
MF=F-M
eval('Rhs(D)=Rhs(D)-Matrix(RKd[MF])*D[M]')
continue

solve(eps=1.0d-10,mdi='x=0',mit='GMRES',abrflag=1,quiet=1)
#rno.
defspline('D[F]=Spline(D)')
eval('D[F]=D')

! #taf. 'D'; #pnod. 'D'; #rci. 'D'; #cx. 'D'; close(1)

#no. 'L2' 'D[F]'
TIME=F*DT
write(4) TIME,F,NORM,WTRK,WTRKIM
continue
#time ENDE WENDE
print 'Dauer : '//ENDE-BEGINN
end
```

9.5.4 A bcl-script for the retarded hypersingular integral operator

```
!!!!!!!!!!!!!!!!!!!!!!!!!!!!!!!!!!!!!!!!!!!!!!!!!!!!!!!!!!!!!!!!!!!!!!!!!!!!
! HYPERSINGULÄRER OPERATOR AUF DER KUGEL (RW)
!!!!!!!!!!!!!!!!!!!!!!!!!!!!!!!!!!!!!!!!!!!!!!!!!!!!!!!!!!!!!!!!!!!!!!!!!!!!

defproblem('Laplace','DTSRC15',330,'Neumann direct BEM, transient sound radiation',3)
setprob(spline='D',mat='D.RW.D',dat='D=t0')
setsp('D',(/2,3/),3,1,1,1,1,'D')
defmatrix('RW','sparse-row','RW')
enddefproblem

!Set variables
I=120 !number of time intervalls
DT=0.1 !Time step size
MZERO=100
K=1
```

```
R=8000 !Right hand side function
QUAD=8
QUADK=8
REF=1 ! 3

#ti
#time BEGINN WBEGINN
problem('Laplace',330)

icosahedron('uniform',refine=REF,p=1,spline='D')
timemesh(deltaT=DT,noint=I,ansatz=1,test=0,ctyp=1)
setretoperator('RW',1,0,1,0)
elemsize('D')
open(1) 'mesh_'//REF//'.dat'
#taf. 'D'
#px. 'D'
#pnod. 'D'
close(1)
pause
open(2) 'TEST_CCCC_CFL_Refine=1_indirect_neumann_sphere'//I//'_'//DT:5//'.dat'
write(2) '# DOF, NoTimeIntervalls, hmax, DeltaT, CFL'
write(2) '#'//DOF,I,MYHMAX,DELTAT,CFL,
write(2) '# Time, Timestep, Norm, Matrix-CPU, Matrix-WALL, Performance, Berech-
nungszeit'
timediff(0)
settime(1)
#time ZEITSTART
setquadpara(quadpoints=QUADK,ijn_radius=5,ijn_angle=5,sigma=0.17)
matrix(quadrature='numeric',gqna=QUADK,gqnb=QUADK,ijn=5,sigma=0.17)
T=SEC;WT=WSEC

lft 24 R - R
!open(1) 'rhs'//1//'.dat'
!#lx. 'D'
!close(1)

! ursprünglich 'thin'
!open(1) 'matrixWtest_'//I//'_'//DT:5//'_'//REF//'.dat'
! #fk. 'RW' 'dense'
!close(1)
show('sparse')
PER=1!T/WT
symch 'RW'
```

```
solve(eps=1.0d-13,mdi='x=0',mit='GMRES',abrflag=1,quiet=1)
defspline('D[1]=Spline(D)')
eval('D[1]=D')

open(1) 'indirect_hyper_sphere_discsol1.dat'
#taf. 'D'; #pnod. 'D'; #rci. 'D'; #cx. 'D'; #cnod. 'D' !; #c. 'D' same as #cx.
close(1)
#time ZEITENDE
#no. 'L2' 'D[1]'
TIME=1*DT
write(2) TIME,1,NORM,T,WT,PER,ZEITENDE-ZEITSTART

do F=2,I
settime(F)
J=F-1
timediff(J)
!Test if lightcone passed body
if (MZERO>0); then
defmatrix('RW[J]','sparse-row','RW')
#time ZEITSTART
setquadpara(quadpoints=QUAD,ijn_radius=1,ijn_angle=5,sigma=0.17)
matrix(quadrature= 'numeric',gqna=QUAD,gqnb=QUAD,ijn=5,sigma=0.17,
arg='D.RW[J].D');T=SEC;WT=WSEC

show('sparse')
PER=1!T/WT
zeromatrix('RW[J]')
symch 'RW['//J//']'
else
K=K+1
fi
lft 24 R - R
!rhs(gql=24,ltyp=R,ltypv=R)
!#lx. 'D'

F1=F-1

!Compute rhs: add retarded single layer pot. to rhs
do M=K,F-1
MF=F-M
eval('Rhs(D)=Rhs(D)-Matrix(RW[MF])*D[M]')
continue
```

```
solve(eps=1.0d-10,mdi='x=0',mit='GMRES',abrflag=1,quiet=1)
#time ZEITENDE
defspline('D[F]=Spline(D)')
eval('D[F]=D')
! open(1) 'indirect_hyper_shiftedsphere_discsol'//F//'.dat'
! #taf. 'D'; #pnod. 'D'; #rci. 'D'; #cx. 'D';
! close(1)

#no. 'L2' 'D[F]'
TIME=F*DT
write(2) TIME,F,NORM,T,WT,PER,ZEITENDE-ZEITSTART
continue
#time ENDE WENDE

print 'Dauer : '//ENDE-BEGINN
end
```

9.5.5 A bcl-script for the retarded Poincaré-Steklov operator

```
!!!!!!!!!!!!!!!!!!!!!!!!!!!!!!!!!!!!!!!!!!!!!!!!!!!!!!!!!!!!
!! POINCARE-STEKLOV OPERATOR (PS)
!!!!!!!!!!!!!!!!!!!!!!!!!!!!!!!!!!!!!!!!!!!!!!!!!!!!!!!!!!!!

defproblem('Laplace','DTSRC15',330,'Poincare-Steklov',3)
setprob(spline='D:v=D',mat='D.RW.D:(-1)*D.RKd.v:0.5*DT/2*D.RI.v:
(-1)*v.RK.D:(-1)*0.5*v.RI.D:(-1)*v.RV.v',dat='D=u0:v=0')
setsp('D',(/2,3/),3,1,1,1,1,'D')
setsp('v',(/2,3/),3,1,1,1,1,'v')
defmatrix('RW','sparse-row','RW')
defmatrix('RV','sparse-row','RV')
defmatrix('RK','sparse-row','RK')
defmatrix('RKd','sparse-row','RKd')
defmatrix('RI','sparse-row','RI')
enddefproblem

!Set variables
I=60 !number of time intervalls ursprünglich 200
DT=0.05 !Time step size ursprünglich 0.05
LT=DT/2
MZERO=100
K=1
R=9003 ! first row: f = t sin(2t)^2 exp(-t) in mydlapf; second row: g = 0 in mynlapf
```

```
QUAD=8
QUADK=8

#time ZEITSTART

problem('Laplace',330)
!icosahedron('uniform',refine=2,p=1,spline='D')
geometry('Cube',bmode=(/2,3/),gm='Dg');
mesh('uniform',n=4,p=1,elements='triangle',spline='D',gm='Dg')
!geometry('Cube',bmode=(/3,3/),gm='Dg')
!mesh('uniform',n=4,p=1,elements='tetrahedral',spline='D',gm='Dg')
!geometry('Cube',bmode=(/2,3/),gm='ug');
!mesh('uniform',n=4,p=1,elements='triangle',spline='u',gm='ug')
open(1) 'mesh_tracecube.dat'
#taf. 'D'
#px. 'D'
#pnod. 'D'
close(1)
timemesh(deltaT=DT,noint=I,ansatz=1,test=0,ctyp=0)

setretoperator('RW',1,0,1,0)

setretoperator('RV',1,-1,1,0)

setretoperator('RK',1,-1,1,0)

setretoperator('RKd',1,0,1,0)
timediff(0)
settime(1)
setquadpara(quadpoints=QUADK,ijn_radius=5,ijn_angle=5,sigma=0.17)

elemsize('D')

lft 24 R - R

matrix(quadrature='numeric',gqna=QUADK,gqnb=QUADK,ijn=5,sigma=0.17)

#ti
#time BEGINN WBEGINN

open(3) 'normV.dat'

!solve(eps=1.0d-13,mdi='x=0',mit='GMRES',abrflag=1,quiet=1)
```

```
solve(eps=1.0d-13,mdi='x=0',mit='GAUSS',abrflag=1,quiet=1)
defspline('D[1]=Spline(D)')
defspline('v[1]=Spline(v)')
eval('D[1]=D')
eval('v[1]=v')

open(2) 'TESTPS'//1//'_'//DT:5//'.dat'
write(2) '# DOF, NoTimeIntervalls, hmax, DeltaT, CFL'
write(2) '#'//DOF,I,MYHMIN,DELTAT,CFL,
write(2) '# Time, Timestep, Norm, Matrix-CPU, Matrix-WALL, Performance, Berech-
nungszeit'

open(1) 'leftMatrix.dat'
#fk. 'RV' 'sparse'
#fk. 'RW' 'sparse'
#fk. 'RK' 'sparse'
#fk. 'RKd' 'sparse'
#fk. 'RI' 'sparse'
close(1)
open(1) 'tno'//1//'.dat'
#taf. 'D'
#cx. 'D'
#cx. 'v'
#cnod. 'D'
#lx. 'D'
#lx. 'v'
#cnod. 'D'
close(1)

#no. 'L2' 'D[1]'
#err. 16 R 'L2' '0' 'D[1]' ; E[1]=ERR
#time ZEITENDE
TIME=1*DT
write(2) TIME,1,NORM,E[1],ZEITENDE-ZEITSTART
#no. 'L2' 'v[1]'
write(3) NORM

do F=2,I
settime(F)
J=F-1
timediff(J)

defmatrix('RW[J]','sparse-row','RW')
```

```
defmatrix('RV[J]','sparse-row','RV')

defmatrix('RK[J]','sparse-row','RK')

defmatrix('RKd[J]','sparse-row','RKd')

setquadpara(quadpoints=QUAD,ijn_radius=1,ijn_angle=5,sigma=0.17)

matrix(quadrature='numeric',gqna=QUAD,gqnb=QUAD,ijn=5,sigma=0.17,
arg='D.RW[J].D');
matrix(quadrature='numeric',gqna=QUAD,gqnb=QUAD,ijn=5,sigma=0.17,
arg='v.RV[J].v');
matrix(quadrature='numeric',gqna=QUAD,gqnb=QUAD,ijn=5,sigma=0.17,
arg='v.RK[J].D');
matrix(quadrature='numeric',gqna=QUAD,gqnb=QUAD,ijn=5,sigma=0.17,
arg='D.RKd[J].v');

open(1) 'motMatrix'//J//'.dat'
#fk. 'RV[J]' 'sparse'
#fk. 'RW[J]' 'sparse'
#fk. 'RK[J]' 'sparse'
#fk. 'RKd[J]' 'sparse'
#fk. 'RI' 'sparse'
close(1)

#time ZEITSTART

lft 24 R - R

do M=K,F-1
MF=F-M
if(M==F-1); then !Identitätsanteil für m=n-1
eval('Rhs(D)=Rhs(D)-Matrix(RW[MF])*D[M]+Matrix(RKd[MF])*v[M]
-0.5*LT*Matrix(RI)*v[M]')
eval('Rhs(v)=Rhs(v)+Matrix(RV[MF])*v[M]+Matrix(RK[MF])*D[M]
-0.5*Matrix(RI)*D[M]')
else
eval('Rhs(D)=Rhs(D)-Matrix(RW[MF])*D[M]+Matrix(RKd[MF])*v[M]')
eval('Rhs(v)=Rhs(v)+Matrix(RV[MF])*v[M]+Matrix(RK[MF])*D[M]')
fi
continue
```

```
!solve(eps=1.0d-13,mdi='x=0',mit='GMRES',abrflag=1,quiet=1)
solve(eps=1.0d-10,mdi='x=0',mit='GAUSS',abrflag=1,quiet=1)
#time ZEITENDE
defspline('D[F]=Spline(D)')
defspline('v[F]=Spline(v)')
eval('D[F]=D')
eval('v[F]=v')

open(1) 'tno'//F//'.dat'
#taf. 'D'
#cx. 'D'
#cnod. 'D'
#lx. 'D'
close(1)

#no. 'L2' 'D[F]'
#err. 16 R 'L2' '0' 'D[F]' ; E[F]=ERR
TIME=F*DT
write(2) TIME,F,NORM,E[F],ZEITENDE-ZEITSTART
#no. 'L2' 'v[F]'
write(3) NORM
continue
end
```

9.5.6 A bcl-script for the retarded inverse Poincaré-Steklov operator

```
!!!!!!!!!!!!!!!!!!!!!!!!!!!!!!!!!!!!!!!!!!!!!!!!!!!!!!!!!!!!
!! INVERSE POINCARE-STEKLOV OPERATOR (IPS)
!!!!!!!!!!!!!!!!!!!!!!!!!!!!!!!!!!!!!!!!!!!!!!!!!!!!!!!!!!!!

defproblem('Laplace','DTSRC15',330,'Poincare-Steklov',3)
setprob(spline='D:N=D',mat='(-1)*D.RW.D:(-1)*D.RKd.N:(-1)*DT*0.25*D.RI.N:
N.RK.D:(-1)*0.5*N.RI.D:(-1)*N.RV.N',dat='N=t0:D=0')
setsp('D',(/2,3/),3,1,1,1,1,'D')
setsp('N',(/2,3/),3,1,1,1,1,'N')
!setsp('u',(/3,3/),3,1,3,3,1,'u')
defmatrix('RW','sparse-row','RW')
defmatrix('RV','sparse-row','RV')
defmatrix('RK','sparse-row','RK')
defmatrix('RKd','sparse-row','RKd')
defmatrix('RI','sparse-row','RI')
enddefproblem
```

```
!Set variables
I=100 !number of time intervalls
DT=0.05 !Time step size ursprünglich 0.05
LT=DT/2
MZERO=100
K=1
R=9103 ! first row: f = t sin(2t)^2 exp(-t) in mydlapf second row: g = 0 in mynlapf
QUAD=8
QUADK=8

#time ZEITSTART

problem('Laplace',330)
!icosahedron('uniform',refine=2,p=1,spline='D')
geometry('Cube',bmode=(/2,3/),gm='Dg');
mesh('uniform',n=8,p=1,elements='triangle',spline='D',gm='Dg')
open(1) 'mesh_tracecube.dat'
#taf. 'D'
#px. 'D'
#pnod. 'D'
!#taf. 'u'
!#px. 'u'
!#pnod. 'u'
close(1)
timemesh(deltaT=DT,noint=I,ansatz=1,test=0,ctyp=0)

setretoperator('RW',1,0,1,0)

setretoperator('RV',1,-1,1,0)

setretoperator('RK',1,-1,1,0)

setretoperator('RKd',1,0,1,0)
timediff(0)
settime(1)
setquadpara(quadpoints=QUADK,ijn_radius=5,ijn_angle=5,sigma=0.17)

elemsize('D')

lft 24 R - R

matrix(quadrature='numeric',gqna=QUADK,gqnb=QUADK,ijn=5,sigma=0.17)
```

```
#ti
#time BEGINN WBEGINN

open(3) 'normV.dat'

solve(eps=1.0d-13,mdi='x=0',mit='GMRES',abrflag=1,quiet=1)
!solve(eps=1.0d-13,mdi='x=0',mit='GAUSS',abrflag=1,quiet=1)
defspline('D[1]=Spline(D)')
defspline('N[1]=Spline(N)')
eval('D[1]=D')
eval('N[1]=N')

open(2) 'TESTIPSCUBE'//R//'_'//DT:5//'.dat'
write(2) '# DOF, NoTimeIntervalls, hmax, DeltaT, CFL'
write(2) '#'//DOF,I,MYHMAX,DELTAT,CFL
write(2) '# Time, Timestep, L2-Norm, L2-Fehler, min. EW, max. EW, Kondition-
szahl, Berechnungszeit'

open(1) 'leftMatrix.dat'
#fk. 'RV'
#fk. 'RW'
#fk. 'RK' 'sparse'
#fk. 'RKd' 'sparse'
#fk. 'RI' 'sparse'
close(1)
!open(1) 'tno'//1//'.dat'
!#taf. 'D'
!#cx. 'D'
!#cx. 'N'
!#cnod. 'D'
!#lx. 'D'
!#lx. 'N'
!#cnod. 'D'
!close(1)

#no. 'L2' 'D[1]';K[1]=NORM
#no. 'L2' 'N[1]';K[2]=NORM
#err. 16 R 'L2' '0' 'N[1]' ; E[1]=ERR
#time ZEITENDE
TIME=1*DT
write(2) TIME,1,K[1],K[2],E[1],LMIN,LMAX,COND,ZEITENDE-ZEITSTART
!#no. 'L2' 'N[1]'
!write(3) NORM
```

```
do F=2,I
settime(F)
J=F-1
timediff(J)

defmatrix('RW[J]','sparse-row','RW')

defmatrix('RV[J]','sparse-row','RV')

defmatrix('RK[J]','sparse-row','RK')

defmatrix('RKd[J]','sparse-row','RKd')

setquadpara(quadpoints=QUAD,ijn_radius=1,ijn_angle=5,sigma=0.17)

!show('sparse')

matrix(quadrature='numeric',gqna=QUAD,gqnb=QUAD,ijn=5,sigma=0.17,
arg='D.RW[J].D');
matrix(quadrature='numeric',gqna=QUAD,gqnb=QUAD,ijn=5,sigma=0.17,
arg='N.RV[J].N');
matrix(quadrature='numeric',gqna=QUAD,gqnb=QUAD,ijn=5,sigma=0.17,
arg='N.RK[J].D');
matrix(quadrature='numeric',gqna=QUAD,gqnb=QUAD,ijn=5,sigma=0.17,
arg='D.RKd[J].N');

!open(1) 'motMatrix'//J//'.dat'
!#fk. 'RV[J]' 'sparse'
!#fk. 'RW[J]' 'sparse'
!#fk. 'RK[J]' 'sparse'
!#fk. 'RKd[J]' 'sparse'
!#fk. 'RI' 'sparse'
!close(1)

#time ZEITSTART

lft 24 R - R

do M=K,F-1
MF=F-M
if(M==F-1); then !Identitätsanteil für m=n-1
eval('Rhs(D)=Rhs(D)+Matrix(RW[MF])*D[M]+Matrix(RKd[MF])*N[M]
```

```
+DT*0.25*Matrix(RI)*N[M]')
eval('Rhs(N)=Rhs(N)+Matrix(RV[MF])*N[M]-Matrix(RK[MF])*D[M]
-0.5*Matrix(RI)*D[M]')
else
eval('Rhs(D)=Rhs(D)+Matrix(RW[MF])*D[M]+Matrix(RKd[MF])*N[M]')
eval('Rhs(N)=Rhs(N)+Matrix(RV[MF])*N[M]-Matrix(RK[MF])*D[M]')
fi
continue

solve(eps=1.0d-13,mdi='x=0',mit='GMRES',abrflag=1,quiet=1)
!solve(eps=1.0d-10,mdi='x=0',mit='GAUSS',abrflag=1,quiet=1)
#time ZEITENDE
defspline('D[F]=Spline(D)')
defspline('N[F]=Spline(N)')
eval('D[F]=D')
eval('N[F]=N')

!open(1) 'tno'//F//'.dat'
!#taf. 'D'
!#cx. 'D'
!#cnod. 'D'
!#lx. 'D'
!close(1)

#no. 'L2' 'D[F]' ; K[1]=NORM
#no. 'L2' 'N[F]' ; K[2]=NORM
#err. 16 R 'L2' '0' 'N[F]' ; E[F]=ERR
TIME=F*DT
write(2) TIME,F,K[1],K[2],E[F],LMIN,LMAX,COND,ZEITENDE-ZEITSTART
!#no. 'L2' 'N[F]'
!write(3) NORM
continue
end
```

9.5.7 A bcl-script for a time dependent Lame problem with finite elements

```
!!!!!!!!!!!!!!!!!!!!!!!!!!!!!!!!!!!!!!!!!!!!!!!!!!!!!!!!!!!!!!!!!!!!!!!
! Time dependent Lame-Operator with inhomogenous Dirichlet boundary
! conditions with homogenous initial conditions with piecewise linear
! ansatz and test functions in space and piecewise linear ansatz function
! in time with piecewise constant test function in space
!
! Similar to central differential coefficients in time
```

```
!
!!!!!!!!!!!!!!!!!!!!!!!!!!!!!!!!!!!!!!!!!!!!!!!!!!!!!!!!!!!!!!!!!!!!!!!
defproblem('Lame','FEMNHD',10,'FEM with non-homogenous Dirichlet-conditions',3)
setprob(spline='u:u_bd=Tu',mat='0.5*DT*u.A.u:1/DT*u.M.u',dat='u_bd=t0')
setsp('u',(/3,3/),3,1,3,3,1,'u')
setsp('u_bd',(/2,3/),3,1,3,3,1)
defmatrix('A','sparse-row')
defmatrix('M','sparse-row')
enddefproblem

open(2) 'solution_nonhom_Dirichlet64.dat'
geometry('Cube',0); #ti
problem('Lame',nickname='FEMNHD')

I=20 ! number of time elements
DT=0.2 ! Time Step size
LT=DT**2 ! DT**2
R=9006 ! rhs

!#ep 2000.0 0.3
#lm 2.0 1.0 ! Set Lame constants
J=2
mesh('uniform',n=J,p=1,elements='tetrahedral')
timemesh(deltaT=DT,noint=I,ansatz=1,test=0,ctyp=0)
elemsizetetrahedral('u')
write(2) '# DOF, NoTimeIntervalls, hmax, DeltaT, CFL'
write(2) '#'//DOF,I,MYHMAX,DELTAT,CFL
write(2) '# Time, Timestep, Norm, Matrix-CPU, Matrix-WALL, Performance'

settime(1)
!open(1) 'mesh1.dat'
! #taf. 'D'
!#taf. 'u'
!#pnod. 'u'
!close(1)

matrix('numeric',ijn=6,sigma=0.17,mu=1.0)
!open(1) 'matrixA.dat'
!#fk. 'A'
!close(1)
!open(1) 'matrixM.dat'
!#fk. 'M'
!close(1)
```

```
lft 16 R 0 R
!open(1) 'firstrhs1.dat'
!#lx. 'u'
!close(1)
solve(eps=1.0d-14,mit='CG'); T=SEC
#rno. defspline('u[1]=Spline(u)')
eval('u[1]=u')
#no. 'L2' 'u[1]'
TIME=1*DT
write(2) TIME,1,NORM,E[4],E[5],T

do N=2,I
settime(N)
J=N-1
timediff(J)
lft 9 R - R
if(N>=3); then
K=N-2
eval('Rhs(u)=Rhs(u)-1/DT*Matrix(M)*u[K]')
fi
eval('Rhs(u)=Rhs(u)+2/DT*Matrix(M)*u[J]-0.5*DT*Matrix(A)*u[J]')
solve(eps=1.0d-14,mit='CG'); T=SEC
#rno.

defspline('u[N]=Spline(u)')
eval('u[N]=u')
#no. 'L2' 'u[N]'
#err. 8 R 'L2' 0 'u' 'u' ; E[4]=ERR
TIME=N*DT
write(2) TIME,1,NORM,E[4],T
continue
close(2)
end
```

9.5.8 A bcl-script for a time dependent wave equation with finite elements

```
!!!!!!!!!!!!!!!!!!!!!!!!!!!!!!!!!!!!!!!!!!!!!!!!!!!!!!!!!!!!!!!!!!!!!!!!!!!
! Time dependent Wave-operator with inhomogenous Dirichlet boundary
! conditions with homogenous initial conditions with piecewise linear
! ansatz and test functions in space and piecewise linear ansatz function
! in time woth piecewise constant test function in space
!
! Similar to central differential coefficients in time
```

```
!
!!!!!!!!!!!!!!!!!!!!!!!!!!!!!!!!!!!!!!!!!!!!!!!!!!!!!!!!!!!!!!!!!!!!!!!
defproblem('Laplace','FEMNHD',10,'FEM with non-homogenous Dirichlet-conditions',3)
setprob(spline='u:u_bd=Tu',mat='0.5*DT*u.A.u:1/DT*u.M.u',dat='u_bd=u0')
setsp('u',(/3,3/),3,1,1,1,1,'u')
setsp('u_bd',(/2,3/),3,1,1,1,1)
defmatrix('A','sparse-row')
defmatrix('M','sparse-row')
enddefproblem

geometry('Cube',0); #ti
problem('Laplace',nickname='FEMNHD')

I=10 ! number of time elements
DT=0.4 ! Time Step size
LT=DT**2 ! DT**2
R=9006 ! rhs

J=2
open(2) 'solution_nonhom_Dirichletgaus'//DT//'.dat'
mesh('uniform',n=J,p=1,elements='tetrahedral')
timemesh(deltaT=DT,noint=I,ansatz=1,test=0,ctyp=0) ! set dt as timestep
elemsizetetrahedral('u')
write(2) '# DOF, NoTimeIntervalls, hmax, DeltaT, CFL'
write(2) '#'//DOF,I,MYHMAX,DELTAT,CFL
write(2) '# Time, Timestep, Norm, Matrix-CPU, Matrix-WALL, Performance'

settime(1)
open(1) 'mesh1.dat'
! #taf. 'D'
#taf. 'u'
#pnod. 'u'
close(1)

matrix('numeric',ijn=6,sigma=0.17,mu=1.0)
!open(1) 'matrixA.dat'
!#fk. 'A'
!close(1)
!open(1) 'matrixM.dat'
!#fk. 'M'
!close(1)
lft 16 R 0 R
!open(1) 'firstrhs1.dat'
```

```
!#lx. 'u'
!close(1)
solve(eps=1.0d-14,mit='GMRES'); T=SEC
#rno.
open(1) 'sol1.dat'
#cnod. 'u'
close(1)
defspline('u[1]=Spline(u)')
eval('u[1]=u')
#no. 'L2' 'u[1]'
#err. 8 R 'L2' 0 'u' 'u' ; E[4]=ERR
TIME=1*DT
write(2) TIME,1,NORM,E[4]


do N=2,I
settime(N)
J=N-1
timediff(J)
lft 9 R - R
!open(1) 'firstrhs'//N//'.dat'
!#lx. 'u'
!close(1)
if(N>=3); then
K=N-2
eval('Rhs(u)=Rhs(u)-1/DT*Matrix(M)*u[K]')
fi
eval('Rhs(u)=Rhs(u)+2/DT*Matrix(M)*u[J]-0.5*DT*Matrix(A)*u[J]')
solve(eps=1.0d-14,mit='GMRES'); T=SEC
defspline('u[N]=Spline(u)')
eval('u[N]=u')
#no. 'L2' 'u[N]'
#err. 8 R 'L2' 0 'u' 'u' ; E[4]=ERR
TIME=N*DT
write(2) TIME, N, NORM,E[4]
continue
close(2)
end
```

9.5.9 A bcl-script for the fluid-structure interaction problem with the retarded Poincare-Steklov operator

```
!!!!!!!!!!!!!!!!!!!!!!!!!!!!!!!!!!!!!!!!!!!!!!!!!!!!!!!!!!!!!!!!!!!!!!!
! Fluid-Structure Interaction (coupling of Lame with wave)
!!!!!!!!!!!!!!!!!!!!!!!!!!!!!!!!!!!!!!!!!!!!!!!!!!!!!!!!!!!!!!!!!!!!!!!

defproblem('FluidStructure','DTSRC15',330,'Poincare-Steklov',3)
setprob(spline='D<Tu:N=D:u:u_bd=Tu',&
mat='0.5*DT*u.ALame.u:1/DT*u.M.u:(-1)*D.RIn.u_bd:u_bd.nRI.D: &
& (-1)*D.RW.D:D.RKd.N:(-1)*0.5*DT/2*D.RI.N: &
& N.RK.D:0.5*N.RI.D:N.RV.N',dat='D=u0:N=0:u_bd=t0')
setsp('D',(/2,3/),3,1,1,1,1,'D')
setsp('N',(/2,3/),3,1,1,1,1,'N')
setsp('u',(/3,3/),3,1,3,3,1,'u')
setsp('u_bd',(/2,3/),3,1,3,3,1)
defmatrix('RW','sparse-row','RW')
defmatrix('RV','sparse-row','RV')
defmatrix('RK','sparse-row','RK')
defmatrix('RKd','sparse-row','RKd')
defmatrix('RI','sparse-row','RI')
defmatrix('RIn','dense','RIn') ! defined only for dense
defmatrix('nRI','dense','nRI') ! defined only for dense
defmatrix('ALame','sparse-row')
defmatrix('M','sparse-row')
enddefproblem

!Set variables
I=20 !number of time intervalls
DT=0.2 !Time step size
LT=DT/2
MZERO=100
K=1
R=9005 ! first row: f = t sin(2t)^2 exp(-t) in mydlapf second row: g = 0 in mynlapf
QUAD=8
QUADK=8
#lm 2.0 1.0 ! lambda and mu; Lame constants

#time ZEITSTART

problem('FluidStructure',330)
geometry('Cube',bmode=(/3,3/),gm='ug')
mesh('uniform',n=2,p=1,elements='tetrahedral',spline='u',gm='ug')
```

```
open(1) 'mesh_tracecube.dat'
#taf. 'D'
#px. 'D'
#pnod. 'D'
#taf. 'u'
#px. 'u'
#pnod. 'u'
close(1)
timemesh(deltaT=DT,noint=I,ansatz=1,test=0,ctyp=0)

setretoperator('RW',1,0,1,0)

setretoperator('RV',1,-1,1,0)

setretoperator('RK',1,-1,1,0)

setretoperator('RKd',1,0,1,0)
timediff(0)
settime(1)
setquadpara(quadpoints=QUADK,ijn_radius=5,ijn_angle=5,sigma=0.17)

elemsize('D')
elemsizetetrahedral('u')
lft 24 R - R

matrix(quadrature='numeric',gqna=QUADK,gqnb=QUADK,ijn=5,sigma=0.17)

#ti
#time BEGINN WBEGINN

open(3) 'normV.dat'

!solve(eps=1.0d-13,mdi='x=0',mit='GMRES',abrflag=1,quiet=1)
solve(eps=1.0d-13,mdi='x=0',mit='GAUSS',abrflag=1,quiet=1)
defspline('D[1]=Spline(D)')
defspline('N[1]=Spline(N)')
defspline('u[1]=Spline(u)')
defspline('u_bd[1]=Spline(u_bd)')
eval('D[1]=D')
eval('N[1]=N')
eval('u[1]=u')
eval('u_bd[1]=u_bd')
open(2) 'TESTPS'//1//'_'//DT:5//'.dat'
```

```
write(2) '# DOF, NoTimeIntervalls, hmax, DeltaT, CFL'
write(2) '#'//DOF,I,MYHMAX,DELTAT,CFL
write(2) '# Time, Timestep, Norm, Matrix-CPU, Matrix-WALL, Performance, Berechnungszeit'

open(1) 'leftMatrix.dat'
#fk. 'RV' 'sparse'
#fk. 'RW' 'sparse'
#fk. 'RK' 'sparse'
#fk. 'RKd' 'sparse'
#fk. 'RI' 'sparse'
#fk. 'ALame' 'sparse'
#fk. 'M' 'sparse'
#fk. 'RIn' 'dense'
#fk. 'nRI' 'dense'
close(1)

!open(1) 'tno'//1//'.dat'
!#taf. 'D'
!#cx. 'D'
!#cx. 'N'
!#cx. 'u_bd'
!#cx. 'u'
!#cnod. 'D'
!#cnod. 'N'
!#cnod. 'u_bd'
!#cnod. 'u'
!#lx. 'D'
!#lx. 'N'
!#lx. 'u_bd'
!#lx. 'u'
!close(1)

#no. 'L2' 'D[1]' ; K[1]=NORM
#no. 'L2' 'u[1]' ; K[2]=NORM
#no. 'L2' 'N[1]' ; K[3]=NORM
#time ZEITENDE
TIME=1*DT
!write(2) TIME,1,K[1],K[2] !,E[1],ZEITENDE-ZEITSTART
!#no. 'L2' 'N[1]'
!write(3) NORM
write(2) TIME,1,K[1],K[2],K[3],LMIN,LMAX,COND,ZEITENDE-ZEITSTART
```

```
do F=2,I
settime(F)
J=F-1
timediff(J)

defmatrix('RW[J]','sparse-row','RW')

defmatrix('RV[J]','sparse-row','RV')

defmatrix('RK[J]','sparse-row','RK')

defmatrix('RKd[J]','sparse-row','RKd')

setquadpara(quadpoints=QUAD,ijn_radius=1,ijn_angle=5,sigma=0.17)

!show('sparse')

matrix(quadrature='numeric',gqna=QUAD,gqnb=QUAD,ijn=5,sigma=0.17,
arg='D.RW[J].D');
matrix(quadrature='numeric',gqna=QUAD,gqnb=QUAD,ijn=5,sigma=0.17,
arg='N.RV[J].N');
matrix(quadrature='numeric',gqna=QUAD,gqnb=QUAD,ijn=5,sigma=0.17,
arg='N.RK[J].D');
matrix(quadrature='numeric',gqna=QUAD,gqnb=QUAD,ijn=5,sigma=0.17,
arg='D.RKd[J].N');

!open(1) 'motMatrix'//J//'.dat'
!#fk. 'RV[J]' 'sparse'
!#fk. 'RW[J]' 'sparse'
!#fk. 'RK[J]' 'sparse'
!#fk. 'RKd[J]' 'sparse'
!#fk. 'RI' 'sparse'
!close(1)

#time ZEITSTART

lft 24 R - R

do L=K,F-1
MF=F-L
if(L==F-1); then !Identitätsanteil für m=n-1
eval('Rhs(D)=Rhs(D)+Matrix(RW[MF])*D[L]-Matrix(RKd[MF])*N[L]
+LT*0.5*Matrix(RI)*N[L]')
```

```
eval('Rhs(D)=Rhs(D)-Matrix(RIn)*u_bd[L]')
eval('Rhs(N)=Rhs(N)-Matrix(RV[MF])*N[L]-Matrix(RK[MF])*D[L]
+0.5*Matrix(RI)*D[L]')
else
eval('Rhs(D)=Rhs(D)+Matrix(RW[MF])*D[L]-Matrix(RKd[MF])*N[L]')
eval('Rhs(N)=Rhs(N)-Matrix(RV[MF])*N[L]-Matrix(RK[MF])*D[L]')
fi
continue

if(F>=3); then
P=F-2
eval('Rhs(u)=Rhs(u)-1/DT*Matrix(M)*u[P]')
fi
eval('Rhs(u)=Rhs(u)+2/DT*Matrix(M)*u[J]-0.5*DT*Matrix(ALame)*u[J]')
eval('Rhs(u_bd)=Rhs(u_bd)+Matrix(nRI)*D[J]')

solve(eps=1.0d-13,mdi='x=0',mit='GMRES',abrflag=1,quiet=1)
!solve(eps=1.0d-10,mdi='x=0',mit='GAUSS',abrflag=1,quiet=1)
#time ZEITENDE
defspline('D[F]=Spline(D)')
defspline('N[F]=Spline(N)')
defspline('u[F]=Spline(u)')
defspline('u_bd[F]=Spline(u_bd)')
eval('D[F]=D')
eval('N[F]=N')
eval('u[F]=u')
eval('u_bd[F]=u_bd')

!open(1) 'tno'//F//'.dat'
!#taf. 'D'
!#cx. 'D'
!#cx. 'N'
!#cx. 'u_bd'
!#cx. 'u'
!#cnod. 'D'
!#cnod. 'N'
!#cnod. 'u_bd'
!#cnod. 'u'
!#lx. 'D'
!#lx. 'N'
!#lx. 'u_bd'
!#lx. 'u'
!close(1)
```

```
#no. 'L2' 'D[F]' ; K[1]=NORM
#no. 'L2' 'u[F]' ; K[2]=NORM
#no. 'L2' 'N[F]' ; K[3]=NORM
TIME=F*DT
write(2) TIME,F,K[1],K[2],K[3],LMIN,LMAX,COND,ZEITENDE-ZEITSTART
continue
end
```

9.6 Explanation of the Code for the hp-version

This section describes the way how the computations for the hp-version is done. The idea is to divide the implementation into 3 steps:

- Preprocessing
- Computation
- Postprocessing

The preprocessing and postprocessing are done in MATLAB, whereas the computation of the matrices are done in MAIPROGS.

In the preprocessing, we prepare everything in order to run the computation. We construct the space time mesh, where the timestep Δt is set and the space mesh is defined. Then we set the polynomial degree for each element and calculate the location of the time nodes on time intervals (t_{k-1}, t_k) for $k = 1, \ldots, N_t$ with $t_k = k\Delta t$ and N_t the amount of timesteps. We also define the indexing of the reference basis. Furthermore we compute the time coefficients for each element. Here our elements are triangles. At last we save these data in a file, which we load into MAIPROGS for the computation. The preprocessing step is executed with the MATLAB file monogeom2.m. The output is monogeom.dat.

Next is the computation step. This step is divided into 2 steps:

1. Computation of the light cone matrices
2. Computation of every block entries for the space time matrix.

Each step here is done in different MAIPROGS packages, since both use the same subroutine femcomp2x22 in a Fortran file called compfem22.f90 but with different goals. The first step is done in the folder CEYHUN5 while the second is done in PVersion/PCOMPRESS2, where each folder uses different compfem22.f90 Fortran code.

In the first step we compute only the matrices for each lightcone. This step requires the most computation time. It requires more time dependent on the refinement of the

space time mesh and the polynomial degree. This code is parallelized with OpenMP but could be faster, e.g. by using MPI in addition as well. We name the output matrices pre"j".dat with $j = 1, \ldots, N_t$.

In the second step we compute the block matrices of the space time matrix. We load the time coefficients together with pre"j".dat for $j = 1, \ldots, N_t$ into the program. By means of an index map we calculate the entries of each block matrix one by one. We save these matrices calling matrix"j".dat for $j = 1, \ldots, N_t$. We compute the right hand side for each timestep j with standard Gauss quadrature as well, denoting them as RHS"j".dat for $j = 1, \ldots, N_t$.

Finally in the postprocessing we load the block matrices matrix"j".dat and RHS"j".dat for $j = 1, \ldots, N_t$ into MATLAB. We build up the space time matrix and the corresponding right hand side. We solve this system with the Gauss algorithm. It is also possible to solve it with other solvers as well, e.g. a preconditioned GMRES (see [52]). We save the solution in a file called solvec.dat. Then we compute a discretized energy $\tilde{E}(t)$ like in (2.55) saving it in a file called outE.dat. Now we may evaluate the results.

Bibliography

[1] T. Abboud, P. Joly, J. Rodríguez, and I. Terrasse. Coupling discontinuous Galerkin methods and retarded potentials for transient wave propagation on unbounded domains. *J. Comput. Phys.*, 230(15):5877–5907, 2011.

[2] A. Aimi, L. Desiderio, M. Diligenti, and C. Guardasoni. A numerical study of energetic BEM-FEM applied to wave propagation in 2D multidomains. *Publ. Inst. Math. (Beograd) (N.S.)*, 96(110):5–22, 2014.

[3] A. Aimi, M. Diligenti, A. Frangi, and C. Guardasoni. A stable 3D energetic Galerkin BEM approach for wave propagation interior problems. *Eng. Anal. Bound. Elem.*, 36(12):1756–1765, 2012.

[4] A. Aimi, M. Diligenti, A. Frangi, and C. Guardasoni. Neumann exterior wave propagation problems: computational aspects of 3D energetic Galerkin BEM. *Comput. Mech.*, 51(4):475–493, 2013.

[5] A. Aimi, M. Diligenti, A. Frangi, and C. Guardasoni. Energetic BEM-FEM coupling for wave propagation in 3D multidomains. *Internat. J. Numer. Methods Engrg.*, 97(5):377–394, 2014.

[6] F. P. Andriulli, K. Cools, F. Olyslager, and E. Michielssen. Time domain Calderón identities and their application to the integral equation analysis of scattering by PEC objects. II. Stability. *IEEE Trans. Antennas and Propagation*, 57(8):2365–2375, 2009.

[7] I. Babuška. Finite element method for domains with corners. *Computing (Arch. Elektron. Rechnen)*, 6:264–273, 1970.

[8] I. Babuška, R. B. Kellogg, and J. Pitkäranta. Direct and inverse error estimates for finite elements with mesh refinements. *Numer. Math.*, 33(4):447–471, 1979.

[9] I. Babuška and M. Suri. The optimal convergence rate of the p-version of the finite element method. *SIAM J. Numer. Anal.*, 24(4):750–776, 1987.

[10] I. Babuška, B. A. Szabo, and I. N. Katz. The p-version of the finite element method. *SIAM J. Numer. Anal.*, 18(3):515–545, 1981.

[11] A. Bamberger and T. Ha-Duong. Formulation variationnelle espace-temps pour le calcul par potentiel retardé de la diffraction d'une onde acoustique. I. *Math.*

Methods Appl. Sci., 8(3):405–435, 1986.

[12] A. Bamberger and T. Ha-Duong. Formulation variationnelle pour le calcul de la diffraction d'une onde acoustique par une surface rigide. *Math. Methods Appl. Sci.*, 8(4):598–608, 1986.

[13] L. Banjai, C. Lubich, and F.-J. Sayas. Stable numerical coupling of exterior and interior problems for the wave equation. *Numer. Math.*, 129(4):611–646, 2015.

[14] L. Banjai and S. Sauter. Rapid solution of the wave equation in unbounded domains. *SIAM J. Numer. Anal.*, 47(1):227–249, 2008/09.

[15] L. Banz, H. Gimperlein, Z. Nezhi, and E. P. Stephan. Time domain BEM for sound radiation of tires. *Comput. Mech.*, 58(1):45–57, 2016.

[16] S. Barrelet, W. Kropp, and F. X. Becot. On the sound radiation from tyres. *Acta Acustica united with Acustica*, 86:769–779, 2000.

[17] E. Bécache. Equations intégrales pour l'équation des ondes. INRIA, Paris, janvier 1994.

[18] E. Becache and T. Ha-Duong. A space-time variational formulation for the boundary integral equation in a 2D elastic crack problem. *RAIRO Modél. Math. Anal. Numér.*, 28(2):141–176, 1994.

[19] R. Bernhard, R. L. Wayson, J. Haddock, N. Neithalath, A. El-Aassar, J. Olek, T. Pellinen, and W. J. Weiss. An introduction to tire/pavement noise of asphalt pavement. https://www.semanticscholar.org/paper/An-Introduction-to-Tire2004. Accessed: June 26, 2019.

[20] A. Bespalov. The *hp*-version of the BEM with quasi-uniform meshes for a three-dimensional crack problem: the case of a smooth crack having smooth boundary curve. *Numer. Methods Partial Differential Equations*, 24(4):1159–1180, 2008.

[21] A. Bespalov and N. Heuer. The *p*-version of the boundary element method for a three-dimensional crack problem. *J. Integral Equations Appl.*, 17(3):243–258, 2005.

[22] A. Bespalov and N. Heuer. The *p*-version of the boundary element method for hypersingular operators on piecewise plane open surfaces. *Numer. Math.*, 100(2):185–209, 2005.

[23] A. Bespalov and N. Heuer. The *p*-version of the boundary element method for weakly singular operators on piecewise plane open surfaces. *Numer. Math.*, 106(1):69–97, 2007.

[24] A. Bespalov and N. Heuer. The *hp*-version of the boundary element method with quasi-uniform meshes in three dimensions. *M2AN Math. Model. Numer. Anal.*,

42(5):821–849, 2008.

[25] J. Bielak, R. C. MacCamy, and X. Zeng. Stable coupling method for interface scattering problems by combined integral equations and finite elements. *J. Comput. Phys.*, 119(2):374–384, 1995.

[26] A. Bogomolnii, G. Èskin, and S. Zuchowizkii. Numerical solution of the stamp problem. *Comput. Methods Appl. Mech. Engrg.*, 15(2):149–159, 1978.

[27] M. Bonnet. *Boundary Integral Equation Methods for Solids and Fluids*. Wiley, 1999.

[28] D. Braess. *Finite elements*. Cambridge University Press, Cambridge, third edition, 2007. Theory, fast solvers, and applications in elasticity theory, Translated from the German by Larry L. Schumaker.

[29] C. Carstensen and E. P. Stephan. Adaptive coupling of boundary elements and finite elements. *RAIRO Modél. Math. Anal. Numér.*, 29(7):779–817, 1995.

[30] F. Chouly, M. Fabre, P. Hild, R. Mlika, J. Pousin, and Y. Renard. An overview of recent results on Nitsche's method for contact problems. In *Geometrically unfitted finite element methods and applications*, volume 121 of *Lect. Notes Comput. Sci. Eng.*, pages 93–141. Springer, Cham, 2017.

[31] M. Cocou. Existence of solutions of a dynamic Signorini's problem with nonlocal friction in viscoelasticity. *Z. Angew. Math. Phys.*, 53(6):1099–1109, 2002. Dedicated to Eugen Soós.

[32] K. Cools, F. P. Andriulli, F. Olyslager, and E. Michielssen. Time domain Calderón identities and their application to the integral equation analysis of scattering by PEC objects. I. Preconditioning. *IEEE Trans. Antennas and Propagation*, 57(8):2352–2364, 2009.

[33] R. G. III Jr. Cooper. Two variational inequality problems for the wave equation in a half-space. *J. Math. Anal. Appl.*, 232(2):434–460, 1999.

[34] C. Domínguez, M. Maischak, and E. P. Stephan. A FE-BE coupling for a fluid-structure interaction problem: hierarchical a posteriori error estimates. *Numer. Methods Partial Differential Equations*, 28(5):1417–1439, 2012.

[35] C. Domínguez, M. Maischak, and E. P. Stephan. FE/BE coupling for an acoustic fluid-structure interaction problem. Residual a posteriori error estimates. *Internat. J. Numer. Methods Engrg.*, 89(3):299–322, 2012.

[36] M. R. Dorr. The approximation theory for the p-version of the finite element method. *SIAM J. Numer. Anal.*, 21(6):1180–1207, 1984.

[37] M. R. Dorr. The approximation of solutions of elliptic boundary-value problems

via the p-version of the finite element method. *SIAM J. Numer. Anal.*, 23(1):58–77, 1986.

[38] D. Doyen and A. Ern. Analysis of the modified mass method for the dynamic Signorini problem with Coulomb friction. *SIAM J. Numer. Anal.*, 49(5):2039–2056, 2011.

[39] D. Doyen, A. Ern, and S. Piperno. Time-integration schemes for the finite element dynamic Signorini problem. *SIAM J. Sci. Comput.*, 33(1):223–249, 2011.

[40] C. Eck, J. Jarušek, and M. Krbec. *Unilateral contact problems*, volume 270 of *Pure and Applied Mathematics*. Chapman & Hall/CRC, Boca Raton, FL, 2005.

[41] V. J. Ervin, E. P. Stephan, and S. Abou El-Seoud. An improved boundary element method for the charge density of a thin electrified plate in $\mathbf{R}^3$. *Math. Methods Appl. Sci.*, 13(4):291–303, 1990.

[42] G. I. Eskin. *Boundary value problems for elliptic pseudodifferential equations*, volume 52 of *Translations of Mathematical Monographs*. American Mathematical Society, Providence, R.I., 1981.

[43] R. S. Falk. Error estimates for the approximation of a class of variational inequalities. *Math. Comput.*, 28:963–971, 1974.

[44] M. Filipe. *Etude mathematique et numerique d'un probleme d'interaction fluide - structure dependant du temps par la methode de couplage Elements Finis - Equations integrales*. PhD thesis, Ecole Polytechnique, 1994.

[45] H. Gimperlein, M. Maischak, and E. P. Stephan. Adaptive time domain boundary element methods with engineering applications. *J. Integral Equations Appl.*, 29(1):75–105, 2017.

[46] H. Gimperlein, F. Meyer, C. Özdemir, D. Stark, and E. P. Stephan. Boundary elements with mesh refinements for the wave equation. *Numer. Math.*, 139(4):867–912, 2018.

[47] H. Gimperlein, F. Meyer, C. Özdemir, and E. P. Stephan. Time domain boundary elements for dynamic contact problems. *Comput. Methods Appl. Mech. Engrg.*, 333:147–175, 2018.

[48] H. Gimperlein, Z. Nezhi, and E. P. Stephan. A priori error estimates for a time-dependent boundary element method for the acoustic wave equation in a half-space. *Math. Methods Appl. Sci.*, 40(2):448–462, 2017.

[49] H. Gimperlein, C. Özdemir, D. Stark, and E. P. Stephan. hp-version time domain boundary elements for the wave equation on quasi-uniform meshes. accepted for publication in Computer Methods in Applied Mechanics and Engineering, 2019.

[50] H. Gimperlein, C. Özdemir, D. Stark, and E. P. Stephan. A residual a posteriori error estimate for the time–domain boundary element method. submitted, Preprint 2019.

[51] H. Gimperlein, C. Özdemir, and E. P. Stephan. Time domain boundary element methods for the Neumann problem: error estimates and acoustic problems. *J. Comput. Math.*, 36(1):70–89, 2018.

[52] H. Gimperlein and D. Stark. On a preconditioner for time domain boundary element methods. *Eng. Anal. Bound. Elem.*, 96:109–114, 2018.

[53] M. Gläfke. *Adaptive Methods for Time Domain Boundary Integral Equations*. PhD thesis, Brunel University, London, 2012.

[54] J. Gwinner and E. P. Stephan. *Advanced boundary element methods*, volume 52 of *Springer Series in Computational Mathematics*. Springer, Cham, 2018. Treatment of boundary value, transmission and contact problems.

[55] T. Ha-Duong. *Equations integrales pour la resolution numerique des problemes de diffraction d'ondes acoustiques dans R^3*. PhD thesis, Paris VI, 1987.

[56] T. Ha-Duong. On the transient acoustic scattering by a flat object. *Japan J. Appl. Math.*, 7(3):489–513, 1990.

[57] T. Ha-Duong. On retarded potential boundary integral equations and their discretisation. In *Topics in computational wave propagation*, volume 31 of *Lect. Notes Comput. Sci. Eng.*, pages 301–336. Springer, Berlin, 2003.

[58] C. Hager, P. Hauret, P. Le Tallec, and B. I. Wohlmuth. Solving dynamic contact problems with local refinement in space and time. *Comput. Methods Appl. Mech. Engrg.*, 201/204:25–41, 2012.

[59] M. E. Hassell and F.-J. Sayas. A fully discrete BEM-FEM scheme for transient acoustic waves. *Comput. Methods Appl. Mech. Engrg.*, 309:106–130, 2016.

[60] P. Hauret. Mixed interpretation and extensions of the equivalent mass matrix approach for elastodynamics with contact. *Comput. Methods Appl. Mech. Engrg.*, 199(45-48):2941–2957, 2010.

[61] P. Hauret and P. Le Tallec. Energy-controlling time integration methods for nonlinear elastodynamics and low-velocity impact. *Comput. Methods Appl. Mech. Engrg.*, 195(37-40):4890–4916, 2006.

[62] C. Hoever. *The influence of modeling parameters on the simulation of car tyre rolling losses and rolling noise*. PhD thesis, Chalmers University of Technology, 2012.

[63] G. C. Hsiao, T. Sánchez-Vizuet, and F.-J. Sayas. Boundary and coupled

boundary–finite element methods for transient wave–structure interaction. *IMA J. Numer. Anal.*, 37(1):237–265, 2017.

[64] G. C. Hsiao, F.-J. Sayas, and R. J. Weinacht. Time-dependent fluid-structure interaction. *Math. Methods Appl. Sci.*, 40(2):486–500, 2017.

[65] G. C. Hsiao and W. L. Wendland. *Boundary integral equations*, volume 164 of *Applied Mathematical Sciences*. Springer-Verlag, Berlin, 2008.

[66] H. B. Khenous, P. Laborde, and Y. Renard. On the discretization of contact problems in elastodynamics. *Lect. Notes Appl. Comput. Mech.*, 27:31–38, 2006.

[67] N. Kikuchi and J. T. Oden. *Contact problems in elasticity: a study of variational inequalities and finite element methods*, volume 8 of *SIAM Studies in Applied Mathematics*. Society for Industrial and Applied Mathematics (SIAM), Philadelphia, PA, 1988.

[68] A. Yu. Kokotov, P. Neittaämaki, and B. A. Plamenevskii. The Neumann problem for the wave equation in a cone. *J. Math. Sci. (New York)*, 102(5):4400–4428, 2000. Function theory and applications.

[69] A. Yu. Kokotov and B. A. Plamenevskiĭ. On the asymptotic behavior of solutions of the Neumann problem for hyperbolic systems in domains with conical points. *Algebra i Analiz*, 16(3):56–98, 2004.

[70] A. R. Laliena and F.-J. Sayas. Theoretical aspects of the application of convolution quadrature to scattering of acoustic waves. *Numer. Math.*, 112(4):637–678, 2009.

[71] G. Lebeau and M. Schatzman. A wave problem in a half-space with a unilateral constraint at the boundary. *J. Differential Equations*, 53(3):309–361, 1984.

[72] J.-L. Lions and E. Magenes. *Problèmes aux limites non homogènes et applications. Vol. 2*. Travaux et Recherches Mathématiques, No. 18. Dunod, Paris, 1968.

[73] A. I. Luré. *Theory of Elasticity*. Nauka, Moscow, 1970.

[74] N. MacLaren. Nick maclaren's computing courses. http://people.ds.cam.ac.uk/nmm1/OpenMP/index.html. Accessed: February 17 2019.

[75] N. MacLaren. Nick maclaren's computing courses. http://people.ds.cam.ac.uk/nmm1/MPI/index.html. Accessed: February 17 2019.

[76] M. Maischak. *Manual of the software package maiprogs*, version 3.7.1 edition, August 22 2012.

[77] M. Maischak. *Technical Manual of the program system maiprogs*, August 23 2014.

[78] M. Maischak. B.o.n.e book of numerical experiments. http://people.brunel.ac.uk/~mastmmm/bone.pdf, November 5 2017. Accessed: April 11 2019.

[79] S. I. Matyukevich and B. A. Plamenevskiĭ. On dynamic problems in the theory of elasticity in domains with edges. *Algebra i Analiz*, 18(3):158–233, 2006.

[80] J. A. Morrison and J. A. Lewis. Charge singularity at the corner of a flat plate. *SIAM J. Appl. Math.*, 31(2):233–250, 1976.

[81] J. Nečas. *Introduction to the theory of nonlinear elliptic equations*, volume 52 of *Teubner-Texte zur Mathematik [Teubner Texts in Mathematics]*. BSB B. G. Teubner Verlagsgesellschaft, Leipzig, 1983. With German, French and Russian summaries.

[82] Z. Nezhi. *Adaptive time domain boundary element method for sound radiation of tyres*. PhD thesis, Leibniz University, Hanover, 2014.

[83] M. Ochmann. Closed form solutions for the acoustical impulse response over a masslike or an absorbing plane. *J. Acoust. Soc. Am.*, (129 (6)), 2011.

[84] E. Ostermann. *Numerical Methods for Space-Time Variational Formulations of Retarded Potential Boundary Integral Equations*. PhD thesis, Leibniz University, Hanover, 2009.

[85] E. Ostermann, M. Matthias, and M. Andres. *First Steps in MaiProgs*, Juni 26 2008.

[86] B. A. Plamenevskiĭ. On the Dirichlet problem for the wave equation in a cylinder with edges. *Algebra i Analiz*, 10(2):197–228, 1998.

[87] T. Qiu and F.-J. Sayas. The Costabel-Stephan system of boundary integral equations in the time domain. *Math. Comp.*, 85(301):2341–2364, 2016.

[88] B. Sako. *A Model for the Crack and Punch Problems in Elasticity*. PhD thesis, University of California, Los Angeles, 1986.

[89] S. Sauter and A. Veit. Adaptive time discretization for retarded potentials. *Numer. Math.*, 132(3):569–595, 2016.

[90] F.-J. Sayas. *Retarded potentials and time domain boundary integral equations*, volume 50 of *Springer Series in Computational Mathematics*. Springer, [Cham], 2016. A road map.

[91] D. Stark. *Adaptive and high order methods for time domain boundary elements*. PhD thesis, Heriot-Watt University, Edinburgh, 2018.

[92] E. P. Stephan. Coupling of boundary element methods and finite element methods. *Encyclopedia of Computational Mechanics, Fundamentals, E. Stein, R. de*

Borst, T. J. R. Hughes (eds.), vol. I:375–412, 2004.

[93] E. P. Stephan and M. Suri. On the convergence of the p-version of the boundary element Galerkin method. *Math. Comp.*, 52(185):31–48, 1989.

[94] E. P. Stephan and M. Suri. The h-p version of the boundary element method on polygonal domains with quasiuniform meshes. *RAIRO Modél. Math. Anal. Numér.*, 25(6):783–807, 1991.

[95] E. P. Stephan and T. von Petersdorff. Singularities of the solution of the Laplacian in domains with circular edges. *Appl. Anal.*, 45(1-4):281–294, 1992.

[96] M. Stephan, E. P.and Maischak and E. Ostermann. Transient boundary element method and numerical evaluation of retarded potentials. *Computational Science–ICCS 2008, LNCS 5102*, pages 321–330, 2008.

[97] I. Terrasse. *Résolution mathématique et numérique des équations de Maxwell instationnaires par une m éthode de potentiels retard és.* PhD thesis, Ecole Polytechnique, Palaiseau, 1993.

[98] F. Valdés, M. Ghaffari-Miab, F. P. Andriulli, K. Cools, and E. Michielssen. High-order Calderón preconditioned time domain integral equation solvers. *IEEE Trans. Antennas and Propagation*, 61(5):2570–2588, 2013.

[99] A. Veit. *Numerical methods for the time domain boundary integral equations.* PhD thesis, Universität Zürich, 2011.

[100] O. von Estorff, K. Sören, W. Kropp, E. P. Stephan, and T. Beckenbauer. Abschlussbericht speron 2020 – teil ii, entwicklung eines performanten rechenmodells zur berechnung und reduzierung der geräuschabstrahlung von reifen, 2014.

[101] T. von Petersdorff. *Randwertprobleme der Elastizitätstheorie für Polyeder - Singularitäten und Approximation mit Randelementmethoden.* PhD thesis, TU Darmstadt, 1989.

[102] T. von Petersdorff and E. P. Stephan. Regularity of mixed boundary value problems in $\mathbf{R}^3$ and boundary element methods on graded meshes. *Math. Methods Appl. Sci.*, 12:229–249, 1990.

[103] P. Wriggers. *Computational Contact Mechanics.* Wiley, New York, 2002.

[104] A. E. Yılmaz, J.-M. Jin, and E. Michielssen. Time domain adaptive integral method for surface integral equations. *IEEE Trans. Antennas and Propagation*, 52(10):2692–2708, 2004.

Curriculum Vitae

Personal Data:

Name:	Ceyhun Özdemir
Born:	21/07/1990, Hannover, Germany
Citizenship:	Turkish

Education:

since November 2015	PhD Student at the Institute of Applied Mathematics under the supervision of Prof. Dr. rer. nat. Ernst Peter Stephan (Leibniz Universität Hannover) and Dr. rer. nat. Heiko Gimperlein (Heriot-Watt-University, Edinburgh, UK) at the Leibniz Universität Hannover, Germany
2013-2015	Master of Science in Mathematics at Leibniz Universität Hannover
2009-2013	Bachelor of Science in Mathematics at Leibniz Universität Hannover
2002-2009	Secondary school, Lutherschule Gymnasium Hannover, Germany with university-entrance diploma (Abiturzeugnis)
2000-2002	Orientation Level, An der Uhlandstraße Hannover, Germany
1996-2000	Primary School, An der Uhlandstraße Hannover, Germany

Employment:

since October 2016	Receiving a scholarship of the Avicenna study agency (supported by BMBF, Germany)
since May 2012	Student assistant at the Institute of Applied Mathematics, Leibniz Universität Hannover, Germany

Publications:

Gimperlein, Heiko ; Özdemir, Ceyhun and Stephan, Ernst P.	Time domain boundary element methods for the Neumann problem: error estimates and acoustic problems. J. Comput. Math. 36 (2018), no. 1, 70–89.
Gimperlein, Heiko; Meyer, Fabian; Özdemir, Ceyhun and Stephan, Ernst P.	Time domain boundary elements for dynamic contact problems. Comput. Methods Appl. Mech. Engrg. 333 (2018), 147–175.
Gimperlein, Heiko; Meyer, Fabian; Özdemir, Ceyhun; Stark, David and Stephan, Ernst P.	Boundary elements with mesh refinements for the wave equation. Numer. Math. 139 (2018), no. 4, 867–912.
Gimperlein, Heiko; Özdemir, Ceyhun; Stark, David and Stephan, Ernst P.	hp-version time domain boundary elements for the wave equation on quasi-uniform meshes. has been accepted for publication in Computer Methods in Applied Mechanics and Engineering.